

# Pharmacological mechanisms of drugs affecting bone formation and bone resorption

**Edited by**

Xiaofeng Zhu, Alex Zhong and Dongwei Zhang

**Published in**

Frontiers in Pharmacology



## FRONTIERS EBOOK COPYRIGHT STATEMENT

The copyright in the text of individual articles in this ebook is the property of their respective authors or their respective institutions or funders. The copyright in graphics and images within each article may be subject to copyright of other parties. In both cases this is subject to a license granted to Frontiers.

The compilation of articles constituting this ebook is the property of Frontiers.

Each article within this ebook, and the ebook itself, are published under the most recent version of the Creative Commons CC-BY licence. The version current at the date of publication of this ebook is CC-BY 4.0. If the CC-BY licence is updated, the licence granted by Frontiers is automatically updated to the new version.

When exercising any right under the CC-BY licence, Frontiers must be attributed as the original publisher of the article or ebook, as applicable.

Authors have the responsibility of ensuring that any graphics or other materials which are the property of others may be included in the CC-BY licence, but this should be checked before relying on the CC-BY licence to reproduce those materials. Any copyright notices relating to those materials must be complied with.

Copyright and source acknowledgement notices may not be removed and must be displayed in any copy, derivative work or partial copy which includes the elements in question.

All copyright, and all rights therein, are protected by national and international copyright laws. The above represents a summary only. For further information please read Frontiers' Conditions for Website Use and Copyright Statement, and the applicable CC-BY licence.

ISSN 1664-8714  
ISBN 978-2-8325-2978-2  
DOI 10.3389/978-2-8325-2978-2

## About Frontiers

Frontiers is more than just an open access publisher of scholarly articles: it is a pioneering approach to the world of academia, radically improving the way scholarly research is managed. The grand vision of Frontiers is a world where all people have an equal opportunity to seek, share and generate knowledge. Frontiers provides immediate and permanent online open access to all its publications, but this alone is not enough to realize our grand goals.

## Frontiers journal series

The Frontiers journal series is a multi-tier and interdisciplinary set of open-access, online journals, promising a paradigm shift from the current review, selection and dissemination processes in academic publishing. All Frontiers journals are driven by researchers for researchers; therefore, they constitute a service to the scholarly community. At the same time, the *Frontiers journal series* operates on a revolutionary invention, the tiered publishing system, initially addressing specific communities of scholars, and gradually climbing up to broader public understanding, thus serving the interests of the lay society, too.

## Dedication to quality

Each Frontiers article is a landmark of the highest quality, thanks to genuinely collaborative interactions between authors and review editors, who include some of the world's best academicians. Research must be certified by peers before entering a stream of knowledge that may eventually reach the public - and shape society; therefore, Frontiers only applies the most rigorous and unbiased reviews. Frontiers revolutionizes research publishing by freely delivering the most outstanding research, evaluated with no bias from both the academic and social point of view. By applying the most advanced information technologies, Frontiers is catapulting scholarly publishing into a new generation.

## What are Frontiers Research Topics?

Frontiers Research Topics are very popular trademarks of the *Frontiers journals series*: they are collections of at least ten articles, all centered on a particular subject. With their unique mix of varied contributions from Original Research to Review Articles, Frontiers Research Topics unify the most influential researchers, the latest key findings and historical advances in a hot research area.

Find out more on how to host your own Frontiers Research Topic or contribute to one as an author by contacting the Frontiers editorial office: [frontiersin.org/about/contact](https://frontiersin.org/about/contact)



# Pharmacological mechanisms of drugs affecting bone formation and bone resorption

## Topic editors

Xiaofeng Zhu — Jinan University, China

Alex Zhong — Van Andel Institute, United States

Dongwei Zhang — Beijing University of Chinese Medicine, China

## Citation

Zhu, X., Zhong, A., Zhang, D., eds. (2023). *Pharmacological mechanisms of drugs affecting bone formation and bone resorption*. Lausanne: Frontiers Media SA.  
doi: 10.3389/978-2-8325-2978-2

# Table of contents

- 05 **Editorial: Pharmacological mechanisms of drugs affecting bone formation and bone resorption**  
Dongwei Zhang, Xiaofeng Zhu and Alex Zhong
- 08 **Advances in Our Understanding of the Mechanism of Action of Drugs (including Traditional Chinese Medicines) for the Intervention and Treatment of Osteoporosis**  
Junjie Lu, Desheng Hu, Chen Ma and Bo Shuai
- 26 **Monascin abrogates RANKL-mediated osteoclastogenesis in RAW264.7 cells via regulating MAPKs signaling pathways**  
Yin Cheng, Haixia Liu, Jing Li, Yujie Ma, Changheng Song, Yuhang Wang, Pei Li, Yanjing Chen and Zhiguo Zhang
- 35 **Effects of 6-Hydroxykaempferol: A Potential Natural Product for Amelioration of Tendon Impairment**  
Tsz Ngai Mok, Qiyu He, Xiaoxi Zhang, Tat Hang Sin, Huajun Wang, Huige Hou, Jinghua Pan, Xiaofei Zheng, Zhengang Zha and Jieruo Li
- 43 **Antiosteoporosis effect of tanshinol in osteoporosis animal models: A systematic review and meta-analysis**  
Shen Wang, Yifeng Yuan, Qian Lin, Hang Zhou, Binbin Tang, Yang Liu, Hai Huang, Bocheng Liang, Yingdelong Mao, Kang Liu and Xiaolin Shi
- 58 **Bu-Gu-Sheng-Sui decoction promotes osteogenesis via activating the ERK/Smad signaling pathways**  
Ning Liu, Baoyu Qi, Yili Zhang, Shengjie Fang, Chuanrui Sun, Qiuyue Li and Xu Wei
- 71 **Identification of a potential diagnostic signature for postmenopausal osteoporosis via transcriptome analysis**  
Rui Zeng, Tian-Cheng Ke, Mao-Ta Ou, Li-Liang Duan, Yi Li, Zhi-Jing Chen, Zhi-Bin Xing, Xiao-Chen Fu, Cheng-Yu Huang and Jing Wang
- 83 **Identification of kaempferol as an OSX upregulator by network pharmacology-based analysis of qianggu Capsule for osteoporosis**  
Ann Yehong Huang, Zhencheng Xiong, Kuankuan Liu, Yanan Chang, Li Shu, Guolan Gao and Chi Zhang
- 100 **BNTA alleviates inflammatory osteolysis by the SOD mediated anti-oxidation and anti-inflammation effect on inhibiting osteoclastogenesis**  
Huidong Wang, Xiankun Cao, Jiadong Guo, Xiao Yang, Xiaojiang Sun, Zhiyi Fu, An Qin, Yujie Wu and Jie Zhao
- 117 **Yi Shen Juan Bi Pill alleviates bone destruction in inflammatory arthritis under postmenopausal conditions by regulating ephrinB2 signaling**  
Huihui Xu, Li Tao, Jinfeng Cao, Peng Zhang, Hui Zeng and Hongyan Zhao

- 128 **Exploratory study of sea buckthorn enhancing QiangGuYin efficacy by inhibiting CKIP-1 and Notum activating the Wnt/ $\beta$ -catenin signaling pathway and analysis of active ingredients by molecular docking**  
Yi-Feng Yuan, Shen Wang, Hang Zhou, Bin-Bin Tang, Yang Liu, Hai Huang, Cai-Jian He, Tian-Peng Chen, Mou-Hao Fang, Bo-Cheng Liang, Ying-De-Long Mao, Feng-Qin Qie, Kang Liu and Xiao-Lin Shi
- 141 **A mechanistic review of chinese medicine polyphenols on bone formation and resorption**  
Yan Li, Lingyu Li, Xiaoyun Li, Bingjie Luo, Qianyun Ye, Haoyu Wang, Li Yang, Xiaofeng Zhu, Li Han, Ronghua Zhang, Huaqin Tian and Panpan Wang
- 154 **Ginsenoside Rg1 interferes with the progression of diabetic osteoporosis by promoting type H angiogenesis modulating vasculogenic and osteogenic coupling**  
Wenhui Chen, Xinyan Jin, Ting Wang, Rui Bai, Jun Shi, Yunxia Jiang, Simin Tan, Ruijie Wu, Shiqi Zeng, Hongxiang Zheng, Hongyang Jia and Shuanglei Li
- 170 **Autophagy: An important target for natural products in the treatment of bone metabolic diseases**  
Zhichao Li, Dandan Li, Hui Su, Haipeng Xue, Guoqing Tan and Zhanwang Xu
- 192 **Phosphatidyl Inositol 3-Kinase (PI3K)-Inhibitor CDZ173 protects against LPS-induced osteolysis**  
Zuoxing Wu, Xuedong Li, Xiaohui Chen, Xuemei He, Yu Chen, Long Zhang, Zan Li, Mengyu Yang, Guixin Yuan, Baohong Shi, Ning Chen, Na Li, Haotian Feng, Mengyu Zhou, Gang Rui, Feng Xu and Ren Xu
- 207 **Clinical application of the fracture risk assessment tool in the general population and its correlation with bone turnover markers**  
Zhi Yang, Shu Xuan, Weihong Li, Wan Hu, Ping Tu and Peng Duan



## OPEN ACCESS

EDITED AND REVIEWED BY  
Filippo Drago,  
University of Catania, Italy

## \*CORRESPONDENCE

Dongwei Zhang,  
✉ dongwei1006@gmail.com  
Xiaofeng Zhu,  
✉ zxiaof@jnu.edu.cn  
Alex Zhong,  
✉ alex.zhong@vai.org

RECEIVED 20 February 2023

ACCEPTED 23 June 2023

PUBLISHED 27 June 2023

## CITATION

Zhang D, Zhu X and Zhong A (2023),  
Editorial: Pharmacological mechanisms  
of drugs affecting bone formation and  
bone resorption.  
*Front. Pharmacol.* 14:1170340.  
doi: 10.3389/fphar.2023.1170340

## COPYRIGHT

© 2023 Zhang, Zhu and Zhong. This is an  
open-access article distributed under the  
terms of the [Creative Commons  
Attribution License \(CC BY\)](#). The use,  
distribution or reproduction in other  
forums is permitted, provided the original  
author(s) and the copyright owner(s) are  
credited and that the original publication  
in this journal is cited, in accordance with  
accepted academic practice. No use,  
distribution or reproduction is permitted  
which does not comply with these terms.

# Editorial: Pharmacological mechanisms of drugs affecting bone formation and bone resorption

Dongwei Zhang<sup>1\*</sup>, Xiaofeng Zhu<sup>2\*</sup> and Alex Zhong<sup>3\*</sup>

<sup>1</sup>Diabetes Research Center, School of Traditional Chinese Medicine, Beijing University of Chinese Medicine, Beijing, China, <sup>2</sup>Department of Chinese Medicine, The First Affiliated Hospital of Jinan University, Guangzhou, Guangdong, China, <sup>3</sup>Van Andel Institute, Grand Rapids, MI, United States

## KEYWORDS

bone metabolic diseases, bone remodeling, Chinese medicine, diabetic bone, energy metabolism

## Editorial on the Research Topic

[Pharmacological mechanisms of drugs affecting bone formation and bone resorption](#)

## 1 Introduction

Metabolic bone diseases are becoming a major health challenge in the aging population considering their high mortality and heavy economic burden on society (Shen et al., 2022). Ideally, osteoclastic resorption strives to keep pace with osteoblastic bone formation to maintain bone homeostasis (Chen et al., 2021). Disruption of the delicate balance between osteoblasts and osteoclasts leads to various bone diseases, such as osteoporosis, osteomalacia, osteogenesis imperfecta, osteopetrosis, and Paget's disease of bone (Kim et al., 2020). Scientists and clinicians are actively exploring the underlying pathological mechanisms of bone disorders and seeking novel effective countermeasures to promote healthy bone remodeling (Srivastava et al., 2022; Xia et al., 2022).

### 1.1 Drugs, natural products, and pathology for bone remodeling

In this special collection, Lu et al. comprehensively examined the applications and limitations of the marketed anti-osteoporosis agents, highlighting the directions of the future drug candidates for the management of bone disorders. Li et al. and Wang et al. critically reviewed the recent advances in polyphenols and tanshinol-derived from traditional Chinese medicine (TCM) in maintaining the balance of bone formation and resorption. However, strong evidence from multicenter randomized trials is required to lay the foundation for clinical applications. Li et al. reviewed the role of autophagy in the development of metabolic bone diseases and examined the actions and

challenges of natural products in the treatment of these diseases by targeting autophagy. Given that bone mineral density (BMD) examination may fail to provide a comprehensive profile of bone remodeling, Zeng et al. discovered that two differentially expressed genes—*METTL4* and *RAB2A*—are associated with BMD alterations, which contribute to accurate evaluation of the severity of osteoporosis and prediction of the risk of fracture.

## 1.2 Novel countermeasures to restore bone remodeling

New countermeasures, including synthetic compounds and TCM drugs, are emerging to restore bone remodeling. In this Research Topic, Wang et al. reported that N-[2-bromo-4-(phenylsulfonyl)-3-thienyl]-2-chlorobenzamide (BNTA), an artificially synthesized compound, can inhibit osteoclast formation and osteolytic resorption by suppressing the overaccumulation of intracellular reactive oxygen species (ROS) and receptor activator of nuclear factor kappa B ligand (RANKL)-stimulated proinflammatory cytokines to attenuate MARK signaling. In addition, Wu et al. reported that CDZ173, a selective PI3K inhibitor, might inhibit lipopolysaccharide-induced osteolysis by weakening the signal axis of PI3K-AKT/MAPK-NFATc1 in osteoclasts. Regarding the role of Chinese medicine in the regulation of bone homeostasis, several formulas and drugs have been extensively investigated, including Bu-Gu-Sheng-Sui decoction (Liu et al.), Yi Shen Juan Bi Pill (Xu et al.), QiangGuYin (Yuan et al.), monascin (Cheng et al.), and Shujin Huoxue Tablet (Sin et al.). The mechanisms of action of these TCM therapies in the promotion of healthy bone remodeling may be associated with the regulation of ERK/Smad, Ephrin B2, Wnt/ $\beta$ -catenin, JNK, and MAPK signaling cascades. Furthermore, we discuss the potential of monascin in preventing bone loss by inhibiting osteoclast activation. Interestingly, red yeast rice (RYR), one of the main sources of monascin, has been reported to maintain bone health (Wu et al., 2020), which highlights the potential of functional food for the management of chronic bone loss.

With the increasing prevalence of diabetes, the incidence of diabetic osteoporosis is also increasing every year (Ma et al., 2016). Currently, few drugs are available for managing this condition, sometimes termed “sweet and brittle bone disease.” (Ala et al., 2020). In this special collection, Chen et al. reported that ginsenoside Rg1 prevents the development of diabetic osteoporosis through the regulation of angiogenesis and osteogenesis coupling in Goto-Kakizaki rats. Emerging evidence suggests that ginseng attenuates the development of diabetic microvascular diseases (Liu et al., 2021; Zhang et al., 2022).

## References

- Ala, M., Jafari, R. M., and Dehpour, A. R. (2020). Diabetes mellitus and osteoporosis correlation: Challenges and hopes. *Curr. Diabetes Rev.* 16, 984–1001. doi:10.2174/1573399816666200324152517
- Chen, B., Wei, J., Zhu, R., Zhang, H., Xia, B., Liu, Y., et al. (2021). Fructus Ligustri Lucidi aqueous extract promotes calcium balance and short-chain fatty acids

## 1.3 Perspectives

In addition, it is recognized that bone remodeling is highly integrated with energy metabolism, which is in turn regulated by endocrine factors. This may highlight that the musculoskeletal system functions are highly influenced by interactions among the adipose tissues, muscles, and bones (Gomes et al., 2022). Therefore, further investigations are required to study the pharmacological effects of anti-osteoporotic drugs on energy metabolism.

In summary, phytochemicals with therapeutic and preventive effects on bone metabolism play a significant role in the prevention of bone disorders, including osteoporosis. Elucidating the pathological mechanisms and discovering more reliable diagnostic markers of osteoporosis continue to be research frontiers.

## Author contributions

All authors listed have made a substantial, direct, and intellectual contribution to the work and approved it for publication.

## Funding

This work was supported by grants from the National Natural Science Foundation of China (NSFC; grant numbers 82074235 and 82274335). The funding sources had no role in the study design, data analysis, interpretation, or paper submission.

## Acknowledgments

We deeply thank all the authors and reviewers who have participated in this Research Topic.

## Conflict of interest

The authors declare that the research was conducted in the absence of any commercial or financial relationships that could be construed as a potential conflict of interest.

## Publisher's note

All claims expressed in this article are solely those of the authors and do not necessarily represent those of their affiliated organizations, or those of the publisher, the editors and the reviewers. Any product that may be evaluated in this article, or claim that may be made by its manufacturer, is not guaranteed or endorsed by the publisher.

production in ovariectomized rats. *J. Ethnopharmacol.* 279, 114348. doi:10.1016/j.jep.2021.114348

Gomes, M. M., da Silva, M. M. R., de Araujo, I. M., and de Paula, F. J. A. (2022). Bone, fat, and muscle interactions in health and disease. *Arch. Endocrinol. Metab.* 66, 611–620. doi:10.20945/2359-3997000000550



- Kim, J. M., Lin, C., Stavre, Z., Greenblatt, M. B., and Shim, J. H. (2020). Osteoblast-osteoclast communication and bone homeostasis. *Cells* 9, 2073. doi:10.3390/cells9092073
- Liu, Y., Zhang, H., Dai, X., Zhu, R., Chen, B., Xia, B., et al. (2021). A comprehensive review on the phytochemistry, pharmacokinetics, and antidiabetic effect of Ginseng. *Phytomedicine* 92, 153717. doi:10.1016/j.phymed.2021.153717
- Ma, R., Zhu, R., Wang, L., Guo, Y., Liu, C., Liu, H., et al. (2016). Diabetic osteoporosis: A review of its traditional Chinese medicinal use and clinical and preclinical research. *Evid. Based Complement. Altern. Med.* 2016, 3218313. doi:10.1155/2016/3218313
- Shen, Y., Huang, X., Wu, J., Lin, X., Zhou, X., Zhu, Z., et al. (2022). The global burden of osteoporosis, low bone mass, and its related fracture in 204 countries and territories, 1990-2019. *Front. Endocrinol. (Lausanne)* 13, 882241. doi:10.3389/fendo.2022.882241
- Srivastava, R. K., Sapra, L., and Mishra, P. K. (2022). Osteometabolism: Metabolic alterations in bone pathologies. *Cells* 11, 3943. doi:10.3390/cells11233943
- Wu, B., Huang, J. F., He, B. J., Huang, C. W., and Lu, J. H. (2020). Promotion of Bone Formation by red yeast rice in experimental animals: A systematic review and meta-analysis. *Biomed. Res. Int.* 2020, 7231827. doi:10.1155/2020/7231827
- Xia, B., Zhu, R., Zhang, H., Chen, B., Liu, Y., Dai, X., et al. (2022). Lycopene improves bone quality and regulates AGE/RAGE/NF- $\kappa$ B signaling pathway in high-fat diet-induced obese mice. *Oxid. Med. Cell. Longev.* 2022, 3697067. doi:10.1155/2022/3697067
- Zhang, H., Hu, C., Xue, J., Jin, D., Tian, L., Zhao, D., et al. (2022). Ginseng in vascular dysfunction: A review of therapeutic potentials and molecular mechanisms. *Phytother. Res.* 36, 857–872. doi:10.1002/ptr.7369



# Advances in Our Understanding of the Mechanism of Action of Drugs (including Traditional Chinese Medicines) for the Intervention and Treatment of Osteoporosis

Junjie Lu<sup>†</sup>, Desheng Hu<sup>†</sup>, Chen Ma and Bo Shuai\*

Department of Integrated Traditional Chinese and Western Medicine, Union Hospital, Tongji Medical College, Huazhong University of Science and Technology, Wuhan, China

## OPEN ACCESS

### Edited by:

Dongwei Zhang,  
Beijing University of Chinese Medicine,  
China

### Reviewed by:

Yan Zhang,  
Shanghai University of Traditional  
Chinese Medicine, China  
Lili Wang,  
Beijing University of Chinese Medicine,  
China  
Yang Guo,  
Nanjing University of Chinese  
Medicine, China

### \*Correspondence:

Bo Shuai  
2011XH0899@hust.edu.cn

<sup>†</sup>These authors have contributed  
equally to this work

### Specialty section:

This article was submitted to  
Experimental Pharmacology and Drug  
Discovery,  
a section of the journal  
Frontiers in Pharmacology

**Received:** 07 May 2022

**Accepted:** 23 May 2022

**Published:** 14 June 2022

### Citation:

Lu J, Hu D, Ma C and Shuai B (2022)  
Advances in Our Understanding of the  
Mechanism of Action of Drugs  
(including Traditional Chinese  
Medicines) for the Intervention and  
Treatment of Osteoporosis.  
Front. Pharmacol. 13:938447.  
doi: 10.3389/fphar.2022.938447

Osteoporosis (OP) is known as a silent disease in which the loss of bone mass and bone density does not cause obvious symptoms, resulting in insufficient treatment and preventive measures. The losses of bone mass and bone density become more severe over time and an only small percentage of patients are diagnosed when OP-related fractures occur. The high disability and mortality rates of OP-related fractures cause great psychological and physical damage and impose a heavy economic burden on individuals and society. Therefore, early intervention and treatment must be emphasized to achieve the overall goal of reducing the fracture risk. Anti-OP drugs are currently divided into three classes: antiresorptive agents, anabolic agents, and drugs with other mechanisms. In this review, research progress related to common anti-OP drugs in these three classes as well as targeted therapies is summarized to help researchers and clinicians understand their mechanisms of action and to promote pharmacological research and novel drug development.

**Keywords:** bone, osteoporosis, fracture, osteoblast, osteoclast, antiresorptive agent, pharmacological mechanism

## INTRODUCTION

The World Population Prospects 2019 published by the United Nations states that the proportion of people over 65 years of age is expected to rise to 16% globally by 2050, and the incidence of osteoporosis (OP) is increasing exponentially with this rapid increase in aging. In addition to age-related OP, other factors, such as the inappropriate use of glucocorticoids, alcohol abuse, and malnutrition, are common causes of secondary OP. Fragility fractures due to OP result in long-term pain and impaired mobility, leading to physical and psychological damage and causing a heavy burden on society. Up to one-quarter of patients with hip fractures die within 1 year. The high rates of disability and mortality from OP-related fractures cannot be ignored and thus must be treated aggressively (Hoogendijk et al., 2019). Bone integrity is maintained by the processes of bone resorption and osteogenesis, which involve osteocytes, osteoblasts, and osteoclasts. A positive balance between osteogenesis and bone resorption maintains normal bone structure and function, while a negative balance results in bone loss (Figure 1). This balance is determined by the production and function of osteoblasts and osteoclasts, which are regulated by multiple factors (T. L. Yang et al., 2020).

Currently, anti-OP drugs are divided into three classes: antiresorptive agents, anabolic agents, and drugs with other mechanisms of action. Commonly used antiresorptive agents include bisphosphonates, hormone replacement therapy, and calcitonin. Anabolic agents include parathyroid hormone and parathyroid hormone-related protein analogs, fluoride, growth hormone, and statins. Other drugs include

strontium salts, vitamin D, vitamin K, and traditional Chinese medicines (TCM). Receptor Activator of Nuclear Factor- $\kappa$ B Ligand (RANKL) inhibitors, SOST inhibitors, and cathepsin K inhibitors are not included within the three major classes as targeted anti-OP agents (**Table1**). We systematically review common anti-OP drugs in each of these classes and discuss their molecular mechanisms of

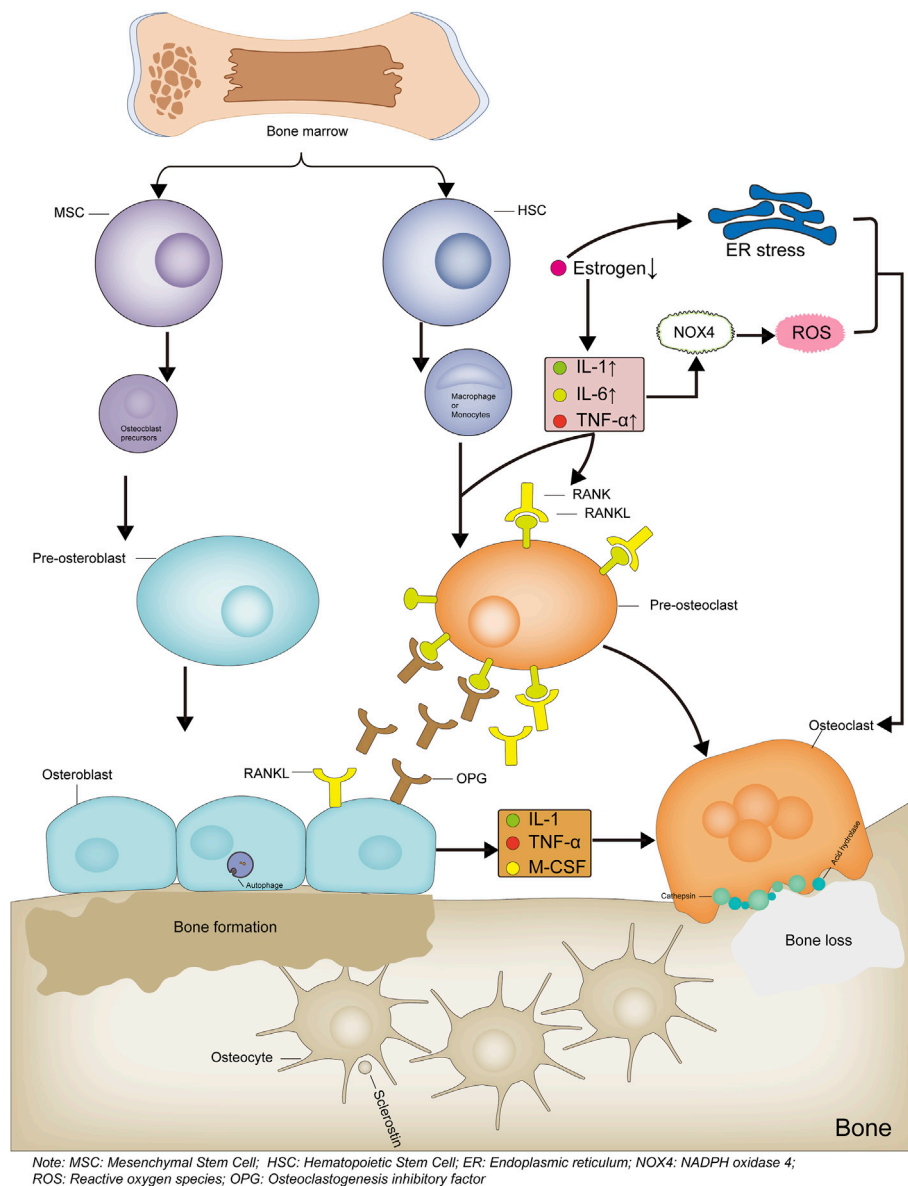


**FIGURE 1 |** Mechanism diagram of bone formation and loss. Bone marrow-derived hematopoietic stem cells differentiate into monocytes or macrophages, which then differentiate into osteoclast precursor cells, then differentiate into osteoclasts and participate in bone loss. When estrogen levels are reduced or inflammatory factors are activated, the RANKL/RANK signaling pathway is activated, leading to increased osteoclast differentiation. The increased ROS levels or endoplasmic reticulum stress also leads to increased osteoclast differentiation. Bone marrow-derived mesenchymal stem cells differentiate into osteoblast precursor cells, which then differentiate into osteoblasts and participate in bone formation. The Osteoblasts produce OPG, competitively bind RANKL and inhibit osteoclast differentiation, thereby reducing osteoclast production. Bone formation and bone loss are in dynamic balance to maintain bone integrity and normal bone structure and function. Bone formation and bone loss are in dynamic balance to maintain skeletal integrity, normal bone structure and function.

**TABLE 1 |** Some anti-osteoporosis drugs currently in use.

Types	Drugs	Administration pathways	Dosage for treatment	Brief function mechanism
Bisphosphonates	Alendronate	p.o.	10 mg Q.d or 70 mg Qw	Inhibit bone conversion;
	Zoledronic acid	p.o.	5 mg/year	Inhibit osteoclast recruitment on the bone surface;
	Risedronate	p.o.	5 mg Q.d or 35 mg Qw	Induce osteoclast apoptosis;
	Ibandronate	p.o.	2 mg/once/3 month	
	Etidronate disodium	p.o.	0.2 g Bid	
	Clodronate disodium	p.o.	0.4 g Bid or 0.8 g Q.d	
Hormone replacement therapy	Estrogen/progestogen	p.o.	customized	the inhibition of RANKL / rank activation;
	Raloxifene	p.o.	60 mg Q.d	the inhibition of oxidative stress; the inhibition of local inflammation
Calcitonin	Elcatonin	i.m.	20 U Qw or 10 U/twice/week	Inhibit osteoclast activity;
	Salmon calcitonin	i.m./Inhal	i.m.: 50 or 100 U Q.d/Inhal: 200 U Q.d	Inhibit acid hydrolase release; Reduce osteoclast adhesion on bone surface; Reduce blood calcium concentration
Parathyroid hormone and its analogs	Abaloptide	i.h.	80 ug Q.d	Regulation of serum calcium and phosphorus ion concentration
Vitamin D and its analogs	Teriparatide	i.h.	20 ug Q.d	
	$\alpha$ -calciferol	p.o.	0.25–1 ug Q.d	Regulation of calcium and phosphorus reabsorption
Strontium	Calcitriol	p.o.	0.25–0.5 ug Bid or 0.5 ug Q.d	
	Strontium ranelate	p.o.	2 g Q.d	Regulate Runx2; Activate non-classical Wnt pathway; Inhibit RANKL/RANK-induced osteoclastic differentiation
Vitamin K	Menatetrenone	p.o.	15 mg Tid	Enhanced cartilage protection
Traditional Chinese Medicine	customized	p.o.	customized	Multiple targets, multiple pathways and multiple mechanisms
Targeted agents for anti-osteoporosis	RANKL inhibitor-Denosumab	i.h.	60 mg/once/180 d	Specific targeting NF- $\kappa$ B receptor activator ligand
	Cat-K inhibitor-Odanacatib	p.o.	50 mg Qw	Selective inhibitor of Cathepsin K

action to guide their standardized clinical use, pharmacological research, and the development of novel targeted drugs. **Figure 2:** Targets and mechanisms of anti-osteoporosis drug action with different mechanisms.

## Antiresorptive Agents

### Bisphosphonates

Bisphosphonates are the most widely used drugs for the treatment of OP. They effectively reduce the risk of vertebral, non-vertebral, and hip fractures (Burr & Russell, 2011). The mainstream view is that bisphosphonates inhibit bone resorption by three principal mechanisms: 1) inhibition of bone turnover, 2) direct inhibition of osteoclasts and indirect promotion of osteoblast recruitment to the bone surface (Sato et al., 1991), and 3) induction of apoptosis in osteoclasts (Plotkin et al., 1999) (Plotkin, Aguirre, Kousteni, Manolagas, & Bellido, 2005) and inhibition of apoptosis in osteoblasts (Plotkin et al., 2008). The mechanism by which bisphosphonates inhibit bone resorption is related to their specific chemical structure. Bisphosphonates are derivatives of inorganic pyrophosphates, in which the central oxygen atom of the inorganic pyrophosphate molecule is replaced with a carbon atom, thus forming a P-C-P bond (Fleisch, Russell, & Francis, 1969). The presence of this chemical bond confers a strong affinity with calcium phosphate, leading to the inhibition of normal and ectopic mineralization. The structure of the two side chains: R1 and R2 on the central carbon atom determines the potency of the particular bisphosphonate; alendronate has a four-carbon

atom backbone and exhibits the best activity, while zoledronate is a cyclic bisphosphonate with a nitrogen ring and exhibits the highest relative potency (Luckman et al., 1998; E. van Beek, Pieterman, Cohen, Löwik, & Papapoulos, 1999a, 1999b) (Tafaro & Napoli, 2021). Simple bisphosphonates that closely resemble inorganic pyrophosphates bind to newly formed adenosine triphosphate (ATP) molecules via class II aminoacyl-tRNA synthetases, and these analogs accumulate within osteoclasts, thereby inducing apoptosis (Pelorgeas, Martin, & Satre, 1992; Sillero et al., 2009). A more clinically effective mechanism underlying the inhibition of osteoclast bone resorption is the inhibition of farnesyl pyrophosphate (FPP) synthase and/or isopentenyl pyrophosphate (IPP) isomerase activity using nitrogen-containing bisphosphonates. The inhibition of these essential enzymes in the mevalonate pathway decreases FPP and geranylgeranyl pyrophosphate (GGPP), resulting in reduced prenylation of the Rac, Ras, and Rho signal transduction proteins, in turn leading to a loss of osteoblast function (Dunford et al., 2001; E. R.; Van Beek, Löwik, & Papapoulos, 2002). These proteins may be intracellular targets of nitrogen-containing bisphosphonates (Kavanagh et al., 2006).

In addition to inhibiting osteoclast function and inducing osteoclast apoptosis, some studies have also shown that bisphosphonates have effects on osteoblast and osteocyte function. Bisphosphonates directly promote osteoblast proliferation and increase osteoblast differentiation. Additionally, bisphosphonates can directly promote osteoblast survival to exert anti-apoptotic effects (Igarashi, Hirafuji, Adachi,

Shinoda, & Mitani, 1997; Giuliani et al., 1998). This effect is dependent on the ability of bisphosphonates to rapidly induce ERK phosphorylation, and when ERK activation is inhibited, the anti-apoptotic effect of bisphosphonates is eliminated. Furthermore, bisphosphonates can also reduce RANKL expression in osteoblasts and increase osteoprotegerin (OPG) expression to exert anti-osteoporosis effects (Viereck et al., 2002; Pan et al., 2004). Similarly, bisphosphonates can maintain osteocyte activity and inhibit glucocorticoid-induced osteocyte apoptosis (Plotkin et al., 1999; Plotkin et al., 2005). Bisphosphonates also have a modulatory effect on bone marrow mesenchymal stem cells. Bisphosphonates could enhance the proliferation of bone marrow stromal cells and promoting osteogenic differentiation. Bisphosphonates promote the expression of the osteogenic genes *alkaline phosphatase (ALP)*, *bone morphogenetic protein-2 (BMP-2)* and *osteocalcin (OC)* in marrow mesenchymal stem cells (MSCs) (Ribeiro et al., 2014) and directly enhance osteoblast formation and subsequent mineral deposition, which may be another mechanism by which they exert anti-osteoporosis (Lindtner et al., 2014). MSC-like cells isolated from peripheral blood of osteoporotic patients with intervention with bisphosphonates showed significantly increased expression levels of the osteoblast marker gene *Runt-associated transcription factor 2 (RUNX2)*, *BMP-2* and bone turnover markers C-terminal telopeptide (CTX), pre-collagen type 1 N-terminal pro-peptide (PINP) and bone alkaline phosphatase (bALP) levels were significantly reduced (Dalle Carbonare et al., 2017; von Knoch et al., 2005).

Due to the effectiveness, safety, and affordability of bisphosphonates in preventing fractures, they have been used as the most common drug for postmenopausal osteoporosis and as a first-line agent (Black & Rosen, 2016; Ensrud & Crandall, 2019). Patients with postmenopausal osteoporosis who received annual intravenous infusions of zoledronic acid had a 70% reduction in the risk of lumbar vertebrae fracture and a 41% reduction in hip fracture over 3 years, with varying degrees of reduction in other fractures (Black et al., 2007). Treatment of postmenopausal women with osteopenia without osteoporosis with zoledronic acid also reduced the incidence of non-lumbar vertebrae or lumbar vertebrae fragility fractures, so zoledronic acid could be used to prevent fractures in older women with osteopenia. Zoledronic acid also has a better preventive effect on osteoporosis and secondary fractures caused by inappropriate glucocorticoid use, which increases lumbar spine bone mineral density (BMD) (D. M. Reid et al., 2009). After discontinuation of the drug, the effect of bisphosphonates gradually disappeared, and a decrease in BMD and a gradual increase in biochemical markers of bone turnover occurred within 5 years (Bone et al., 2004; Black et al., 2006). In the use of bisphosphonates, attention should be paid to their use characteristics and alert to the occurrence of adverse reactions. Differences exist between the injectable and oral forms of bisphosphonates. Gastrointestinal dysfunction and gastrointestinal reactions occur in about 20% of patients taking oral bisphosphonates, and transient acute allergy-like symptoms with fever, musculoskeletal pain, and flu-like symptoms are present in 20–30% of patients when the

injectable form is first used; most of these symptoms resolve within 3 days and can be effectively prevented with acetaminophen or ibuprofen for a short time after administration. In addition, intravenous administration of bisphosphonates can lead to renal impairment as evidenced by elevated blood creatinine levels or rare acute renal failure, and is therefore contraindicated in patients with creatinine clearance <35 ml/min. Appropriate rehydration should be administered prior to the use of intravenous dosage forms, and single doses and infusion rates should be controlled during use. Osteonecrosis of the jaw is a rare but serious complication of bisphosphonate use, but this is often seen in patients treated with bisphosphonates for myeloma or other bone tumors at doses more than 10 times the dose of osteoporosis treatment. (Maraka & Kennel, 2015; Eastell et al., 2016; Compston, McClung, & Leslie, 2019).

### Hormone Replacement Therapy

Women after menopause are over 50% more likely than men of the same age to experience OP-related fractures, with estrogen deficiency being the primary cause. Estrogen deficiency leads to increased bone turnover, with bone resorption increasing by 90% after menopause and osteogenesis increasing by only 45% (Garnero, Sornay-Rendu, Chapuy, & Delmas, 1996); this high level of bone turnover leads to bone loss during the bone remodeling cycle. Receptors with high affinity for estrogen are present in osteoblasts, osteoclasts, and osteocytes. An estrogen deficiency directly increases osteoclast formation and bone matrix degradation and decreases osteogenesis-related gene expression (Schiavi, Fodera, Brennan, & McNamara, 2021). It also decreases osteoblast autophagy, leading to increased osteoblast apoptosis (Schiavi et al., 2021) and the activation of endoplasmic reticulum stress, which results in reduced osteoblast formation and reduced matrix mineralization (Gavali et al., 2019; H.; Li et al., 2018). In addition, an estrogen deficiency induces increased activity of the osteoclastic cytokines IL-1, IL-6, and TNF- $\alpha$  (Pacifci et al., 1991; Kimble et al., 1994; Ammann et al., 1997). T cell activation also releases large amounts of TNF- $\alpha$  (Roggia et al., 2001), and the synergistic effects of these pathways lead to the activation of NF- $\kappa$ B (RANK) and NF- $\kappa$ B ligand (RANKL). This pathway induces osteoblasts to express NADPH oxidase 4 (NOX4), leading to increased levels of reactive oxygen species and subsequent increases in osteoclastogenesis (Goettsch et al., 2013). This leads to the formation of a pro-inflammatory environment locally in bone and exacerbates tissue damage. Theoretically, OP can be effectively intervened and treated with estrogen replacement therapy. The bone mineral density was increased and fracture risk was decreased in postmenopausal women after 3 years of estrogen use (Cauley et al., 2003). However, clinical estrogen supplementation for postmenopausal OP must be evaluated with caution owing to the potential for adverse cardiovascular and cerebrovascular events, thromboembolic disease, and an increased incidence of breast cancer in women (G. L. Anderson et al., 2004; LaCroix et al., 2011; Rozenberg, Vandromme, & Antoine, 2013). Thus, the prudent evaluation and rational short-term use of estrogen should be prioritized over long-term maintenance therapy.



One strategy that can be used as a long-term maintenance of estrogen replacement therapy is the use of selective estrogen receptor modulators (SERMs). SERM is different from endogenous estrogen in pharmacological action. It plays different roles in different tissues by binding with estrogen receptor and produces estrogen agonist effect on bone. Therefore, it can reduce bone resorption and increase bone mineral density (BMD) in postmenopausal women. In addition, the extraosseous effect of SERM is to regulate cholesterol metabolism and reduce the levels of total cholesterol and low-density lipoprotein cholesterol. The reduction of cholesterol level will lead to the nuclear condensation of osteoclasts, reduce the activity of osteoclasts and induce the activation of Caspase-3, so as to induce osteoclast apoptosis (Luegmayr et al., 2004), which may be similar to the mechanism of statins potentially reducing the risk of fracture. The only SERM recommended by JAMA for anti-osteoporosis treatment in 2019 is raloxifene (I. R. Reid & Billington, 2022). Among postmenopausal women with osteoporosis, raloxifene can increase the bone mineral density of spine and femoral neck and reduce the risk of vertebral fracture (Delmas et al., 1997; Walsh et al., 1998). While reducing the risk of fracture, raloxifene can also bring more clinical benefits. Raloxifene can reduce the concentration of serum total cholesterol and low-density lipoprotein cholesterol, and it can reduce the incidence rate of breast cancer in postmenopausal women with high levels of estradiol. Although it brings so many clinical benefits, its clinical application also has some problems. For example, it is only suitable for women and has poor effect in reducing non vertebral fractures. There is a significant increase in venous thrombosis and fatal stroke risk caused by the use of raloxifene, as well as the problem of intolerable vasomotor stability syndrome (hot flashes), which require clinicians to give comprehensive and careful consideration when using the drug (Ettinger et al., 1999; Cummings et al., 2002; Goldstein et al., 2009).

## Calcitonin

Calcitonin is a naturally occurring single-chain polypeptide consisting of 32 amino acids and a 7-amino-acid ring structure (Andreotti et al., 2006). Calcitonin has two types of receptors: calcitonin receptor (CTR) and calcitonin receptor-like receptor (CLR). Calcitonin inhibits osteoclast function by binding to specific receptors (Nicholson, Moseley, Sexton, Mendelsohn, & Martin, 1986). The NH<sub>2</sub>-terminal loop structure is a key structural domain for receptor activation (Barwell et al., 2012). Calcitonin is present in many species; in humans, calcitonin is secreted by parafollicular cells of the thyroid (C cells) and acts on bones. Calcitonin has a direct inhibitory effect on osteoclast activity (Chambers & Magnus, 1982). Calcitonin exerts anti-OP effects by preventing osteoclasts from secreting acid hydrolases to degrade and resorb bone (Horne, Shyu, Chakraborty, & Baron, 1994). Calcitonin also directly causes osteoclasts to detach from the resorption lacuna and reduces the number of osteoclasts adhering to the bone (Holtrop, Raisz, & Simmons, 1974; Delling, Schulz, & Ziegler, 1977). The extent of hypocalcemia is positively correlated with the rate of bone

resorption, and calcitonin antagonizes the increase in the blood calcium concentration by inhibiting the reabsorption of calcium and phosphorus ions by the renal tubules, thereby reducing the rate of bone resorption (Copp & Cheney, 1962; Hedlund, Hulth, & Johnell, 1983). Unlike other anti-OP drugs, calcitonin has the unique advantage of having analgesic effects and can relieve acute and chronic pain caused by OP-related vertebral compression fractures (Lyritis et al., 1997; Knopp-Sihota, Newburn-Cook, Homik, Cummings, & Voaklander, 2012; Terashima et al., 2019); the mechanism underlying this effect this remains unclear (Kaneb, Berardino, Hanukaai, Rooney, & Kaye, 2021). Previous studies have shown that calcitonin may exert analgesic effects by the modulation of the central nervous system as well as neurotransmitter release and neurophysiology (Pecile, Ferri, Braga, & Olgati, 1975; Yamamoto, Tachikawa, & Maeno, 1981; Laurian et al., 1986). Although the mechanism of action remains unclear, the analgesic effect of calcitonin has been confirmed. Structural differences in calcitonin among species correspond to large differences in its affinity for calcitonin receptors. Eel calcitonin derivatives in which NH<sub>2</sub>-terminal amino groups are replaced with hydrogen atoms and disulfide bonds with ethylene bonds have high stability with no differences in biological activity. Salmon calcitonin, the most widely used peptide in clinical practice (Chesnut et al., 2000), has high affinity and biological potency in humans and a long half-life due to its high sequence homology with human calcitonin. The specific properties of the calcitonin peptide limit its modes of administration. It was previously administered as a parenteral injection but is now available as an intranasal formulation, with improved convenience and tolerability (Reginster & Franchimont, 1985). The development of new dosage forms of calcitonin to improve its bioavailability is a focus of ongoing research, including oral and inhaled forms as well as allosteric calcitonin receptor activator dosage forms (Watkins, Rathbone, Barwell, Hay, & Poyner, 2013).

## Anabolic Agents

### Parathyroid Hormone and Parathyroid Hormone-Related Protein Analogs

Similar to calcitonin, PTH is a peptide consisting of 84 amino acids. PTH and its related protein analogs also act by binding to PTH 1 receptor (PTH1R), a class B G protein-coupled receptor with an important role in maintaining calcium ion homeostasis. Functionally, PTH and its related protein analogs function with calcitonin in the regulation of calcium and phosphorus ion metabolism in the blood and bone cell activity (Beutner & Munson, 1960; Felsenfeld, Levine, & Rodriguez, 2015) (Raisz, 1963; Bingham, Brazell, & Owen, 1969). The N-terminal sequence of PTH is highly conserved in many mammals; accordingly, the main biological activities of PTH are mediated by the binding of the N-terminal to PTH1R (Martin et al., 1983), while the C-terminal region is mainly involved in the regulation of bone resorption and serum calcium ions. In addition, mutations in the C-terminal sequence affects its affinity to the receptor and its own metabolic degradation rate (Potts et al., 1971). Animal studies have shown that the continuous administration of PTH leads to bone loss (Cosman, Shen,

Herrington, & Lindsay, 1991), whereas intermittent administration leads to increased osteoblast numbers and osteogenesis (Frolik et al., 2003). Currently, JAMA lists two PTH analogs for the treatment of OP: teriparatide and abaloparatide (I. R. Reid & Billington, 2022). Teriparatide induces bone formation by stimulating the proliferation and activity of osteoblasts. This stimulation peaks at 6–12 months and decreases thereafter, even after a second course of treatment administered 1 year after discontinuation. Abaloparatide binds highly selectively to the R0 and RG conformations of PTH1R, resulting in a shorter cAMP response, and exhibits greater osteogenic effects than those of teriparatide (Hattersley, Dean, Corbin, Bahar, & Gardella, 2016). Toxicological studies of PTH and its related protein analogs in animals have shown that the lifetime use of PTH and its related protein analogs in excess of equivalent human doses of PTH results in an increased risk of osteosclerosis and osteosarcoma (Sato et al., 2002; Vahle et al., 2004). However, based on the stimulatory effects of PTH and its related protein analogs described above, teriparatide and abaloparatide are not used for the long-term treatment of OP.

### Fluoride

Fluorine is an essential trace element in the human body and is particularly important for bone growth, development, and calcification. Fluorine promotes osteoblast proliferation and activation by stimulating the differentiation of mesenchymal stem cells into osteoblasts and inhibiting acid phosphatase activity in osteoblasts, leading to increased osteogenesis (Hall, 1987; Lau, Farley, Freeman, & Baylink, 1989). However, caution must be exercised in the use of fluoride to treat OP, as excessive fluorine intake can lead to decreased bone strength and toughness, increased insulin resistance, elevated inflammatory factor levels, and disturbances of lipid metabolism, all of which can lead to adverse events (de Cássia Alves Nunes et al., 2016; Pereira et al., 2017). In addition, the development of gastrointestinal disturbances in a large proportion of patients (34%) due to the use of fluoride and a variety of adverse effects, such as fluorosis, have limited its application (Franke, 1988).

### Growth Hormone

A growth hormone deficiency in adults leads to a decreased bone mineral density; however, it is not clear whether growth hormone supplementation is beneficial for aging-related bone loss. Clinical studies have shown that growth hormone activates osteoblasts and stimulates bone remodeling in older men, women, and postmenopausal patients with OP but has no long-term effects on the spine and proximal femur bone density (Brixen, Nielsen, Mosekilde, & Flyvbjerg, 1990; Rudman et al., 1990; Ghiron et al., 1995). A meta-analysis has shown that the incidence of adverse events in patients treated with growth hormone was  $24.8 \pm 28.6\%$  compared to  $6.1 \pm 7.8\%$  in the control group. Both meta-analyses have shown that the most common adverse effects of growth hormone use were pain and edema due to fluid retention and carpal tunnel syndrome (Atkinson, Moyer, Yacoub, Coughlin, & Birmingham, 2017; Barake et al., 2018).

### Statins

Statins are frequently used and have been found to regulate lipids and to reduce the incidence of fractures. Some studies have shown that the statin compactin promotes osteoblast differentiation and bone nodule formation (Phillips, Belmonte, Vernochet, Ailhaud, & Dani, 2001), which may be associated with the activation of the Ras/Smad/Erk/BMP-2 pathway (P. Y. Chen et al., 2010). However, clinical observations have yielded mixed findings. For example, comparative study published in the Lancet in 2020 showed that 13 or more doses of statins reduced the risk of pathological bone fracture in women over 60 years of age (Chan et al., 2000). A systematic evaluation and meta-analysis of the efficacy of statins for OP by Zou *et al.* revealed that statins reduced the overall fracture risk, increased hip BMD, and increased osteocalcin expression, with no significant effects on the femoral neck BMD and bone-specific alkaline phosphatase (BALP) and serum collagen type I telopeptide (S-CTX). In addition, statins had greater therapeutic effects against OP in male patients than in female patients (An et al., 2017). However, other clinical studies have reported the opposite results. In a clinical observation of 93,716 postmenopausal women aged 50–79 years, statin use did not improve the BMD or fracture risk (LaCroix et al., 2003). Therefore, definitive conclusions cannot be drawn about the relationship between statin use and OP and more molecular biological and clinical studies are needed.

### Drugs With Other Mechanisms of Action

#### Vitamin D

Vitamin D is obtained through dietary sources and exposure to sunlight. Upon exposure to sunlight (especially wavelengths of 280–320 nm), 7-dehydrocholesterol is converted to a previtamin, which is then slowly isomerized to vitamin D<sub>3</sub>, and ergosterol is converted to vitamin D<sub>2</sub>. Vitamin D is metabolized in three major steps: 25-hydroxylation, 1 $\alpha$ -hydroxylation, and 24-hydroxylation (Bikle, 2014). Vitamin D is first hydroxylated to 25-hydroxyvitamin D by CYP27A1 and CYP2R1, with CYP27A1 acting only on vitamin D<sub>2</sub> and CYP2R1 acting on both vitamins D<sub>2</sub> and D<sub>3</sub>. Other enzymes, such as CYP3A4, which is primarily involved in drug metabolism, also have 25-hydroxylation activity; however, CYP27A1 and CYP2R1 are the primary enzymes involved in the 25-hydroxylation process. 25-Hydroxyvitamin D produced in the liver undergoes 1 $\alpha$ -hydroxylation catalyzed by CYP27B1 (1 $\alpha$ -hydroxylase) into 1 $\alpha$ -25-dihydroxyvitamin D, which in turn undergoes 23-hydroxylation catalyzed by CYP24A1 (23-hydroxylase) into the biologically active 1, 25–26,23 lactone. It also undergoes 24-hydroxylation catalyzed by CYP24A1 (24-hydroxylase), forming 1,24,25-trihydroxyvitamin D, which binds to the vitamin D receptor and performs a variety of functions, including calcium absorption, intestinal phosphate absorption, bone calcium mobilization, and renal calcium reabsorption (Meyer, Goetsch, & Pike, 2010; Jones, Prosser, & Kaufmann, 2012). Of these steps, 25-hydroxylation occurs primarily in the liver, while 1 $\alpha$ -hydroxylation and 24-hydroxylation occur primarily in the kidney. 25-Hydroxylase in the liver is regulated by several factors; therefore, the double deletion of CYP27A1 and

CYP2R1 does not completely block 25-hydroxylation in the liver. Renal 1 $\alpha$ -hydroxylase is primarily regulated by PTH, fibroblast growth factor 23 (FGF23), and 1 $\alpha$ ,25-dihydroxyvitamin D itself (Armbrecht et al., 1998; Bacchetta et al., 2013). PTH stimulation promotes CYP27B1 production, while FGF23 and high calcium (Ca) and phosphorus (P) inhibit CYP27B1 production; CYP24A1 is regulated in the opposite direction. 1, 25 (OH) $_2$ D $_3$  also directly regulates its own synthesis by inhibiting PTH production, stimulating FGF23 production, and inducing CYP24A1 production.

Currently, the effect of vitamin D supplementation on the risk of fracture is controversial. Chapuy *et al.* reported a 43% reduction in the risk of hip fracture and a 32% reduction in the risk of non-vertebral fractures in 3,270 elderly French women who took 1,200 mg of calcium and 800 units of vitamin D $_3$  daily for 3 years (Chapuy et al., 1992). However, many recent studies have questioned this finding, and a 2017 meta-analysis found that neither calcium, vitamin D, nor a combination of the two reduced the fracture risk in older adults, controlling for calcium and vitamin D dose, gender, and baseline serum 25-hydroxyvitamin D concentrations (Zhao, Zeng, Wang, & Liu, 2017). Similarly, a 2019 study found that even 3 years of treatment with high doses (10,000 IU) of vitamin D daily did not produce significant changes in radial or tibial bone strength (Burt et al., 2019). These findings suggest the importance of individualized vitamin D supplementation based on baseline 25-hydroxyvitamin D concentrations and patient conditions, such as exposure to outdoor light levels and differences in joint loading due to differences in body weights and activity levels, rather than the universal use of vitamin D to prevent OP and bone fracture across all populations. Several analyses have shown that adjusting serum 25-hydroxyvitamin D concentrations to 90–100 nmol/L (36–40 ng/ml) effectively reduces the fracture risk (Bischoff-Ferrari, Giovannucci, Willett, Dietrich, & Dawson-Hughes, 2006; Leidig-Bruckner et al., 2011; Bischoff-Ferrari, 2014).

A major cause of fracture in some elderly people is the increased risk of falls due to a lack of muscle strength and muscle fatigue due to a vitamin D deficiency, as skeletal muscles contain many vitamin D receptors (Dawson-Hughes, 2017). With increasing age, vitamin D receptor expression decreases (Bischoff-Ferrari et al., 2004), and if vitamin D is deficient, the risk of muscle fatigue may be exacerbated. Appropriate vitamin D supplementation is effective in improving muscle strength and movement speed, which can reduce the risk of falls in the elderly (Bouillon et al., 2019). This may explain the inconsistent results of clinical trials, which did not consider differences in muscle levels between samples.

### Strontium Salts

Strontium is a trace element with similar physical and chemical properties to those of calcium ions, enabling it to partially replace their function (Kołodziejska, Stępień, & Kolmas, 2021). Strontium has a unique anti-OP mechanism that affects both bone resorption and osteogenesis (Peng et al., 2011). On one hand, it promotes

the differentiation of bone marrow mesenchymal stem cells (BMSCs) into osteoblasts by regulating Runx2, a key transcription factor for osteoblast differentiation, and activating NFATc1/Maf via the canonical and non-canonical Wnt pathways (Cui et al., 2020). On the other hand, it inhibits the expression of RANKL and AP-1 by interacting with calcium-sensing receptor (CaSR) and antagonizes the NF- $\kappa$ B-mediated differentiation of bone marrow MSCs into osteoblasts (Brennan et al., 2009; Saidak, Haÿ, Marty, Barbara, & Marie, 2012). Strontium ranelate is one of a few drugs currently available for the treatment of postmenopausal OP. In 2013, the European Medicines Agency recommended the discontinuation of strontium ranelate because it increases the risk of cardiovascular disease and venous thrombosis and thus its risks outweigh its benefits. In addition, the FDA has not approved the drug for clinical use; therefore, it is not detailed further in this review.

### Vitamin K

Vitamin K (VK) is a fat-soluble vitamin that has effects on bone in addition to activating prothrombin to promote coagulation (Tsugawa & Shiraki, 2020). VK is a coenzyme necessary for the synthesis of  $\gamma$ -carboxyglutamate and can facilitate the transition from inactive low carboxylation levels to fully functional active carboxylation levels. Skeletal malformations have been found in patients using the VK antagonist warfarin, suggesting that VK is associated with bone and bone metabolism (Palermo et al., 2017). A number of studies have shown that VK regulates bone metabolism via both VK-dependent and non-VK-dependent protein pathways. Since studies of non-VK-dependent protein pathways have focused on osteoarthritis, we focus here on the relationship between VK-dependent proteins and OP. There are six VK-dependent proteins in bone tissues: osteocalcin, matrix GLA protein (MGP), upper zone of growth plate and cartilage matrix-associated protein (UCMA), also known as GLA-rich protein (GRP), periostin, protein S, and growth arrest-specific 6 protein (Gas6) (Hauschka, Lian, Cole, & Gundersen, 1989; Shearer, 2000). These proteins regulate bone metabolism by promoting osteoblast differentiation and inhibiting osteoclastogenesis (Stock & Schett, 2021).

VK acts as a coenzyme for carboxylase to promote osteocalcin carboxylation levels and increase calcium ion and hydroxyapatite binding activity for hydroxyapatite crystal formation (Atkins, Welldon, Wijenayaka, Bonewald, & Findlay, 2009). The GLA residue-rich structure of MGP results in a high affinity for calcium ions and hydroxyapatite. UCMA and GRP have multiple functions, including a well-established protective effect on cartilage and the ability to bind to types II, I, and XI collagen with high affinity (Wallin, Schurgers, & Loeser, 2010; Theuvsen, Smit, & Vermeer, 2012). However, their roles in osteoblast differentiation are not clear. There is some evidence that UCMA/GRP inhibits osteoblast differentiation, while other studies have shown that UCMA/GRP overexpression in osteoblasts promotes

osteogenic differentiation (Houtman et al., 2021). These results were based on transcript-level analyses, and differences in levels of  $\gamma$ -carboxylation and post-translational modification require further study. Relatively few studies have evaluated periostin, Gas6, and protein S and therefore they are not reviewed here for the sake of brevity. Some clinical studies of VK and OP have been reported, and a systematic review and meta-analysis has shown that patients using VK antagonists had a greater risk of fracture, but VK antagonists were not associated with BMD (Veronese et al., 2015). Clinical evidence for VK supplementation in patients with OP is lacking, and long-term follow-up studies are required to elucidate the short- and long-term effects of VK on bone.

### Traditional Chinese Medicines

China has over 2000 years of rich history and experience in the use of herbal medicines. The use of TCM for the intervention and treatment of OP has been included in the latest Chinese clinical guidelines. However, most TCM use involves the personal experience of clinicians and their lineage, without specific indications, scope of use, documentation of adverse reactions and contraindications, modern pharmacological studies, and standardized clinical phase III trials. The complex composition and multi-pathway and multi-target mechanisms of TCM pose great difficulties for research. Research on modern pharmacological and molecular mechanisms of action of TCM is being promoted (Shuai, Shen, Zhu, & Zhou, 2015). We need to standardize their scientific application, elucidate their pharmacological effects and mechanisms, define their safety and toxic side effects, and accelerate the innovation of drug formulations and absorption methods.

Anti-OP components in TCM are diverse and include flavonoids, lignans, saponins, and iridoid glycosides (Sun et al., 2021). They function via multiple pathways, such as the Wnt/ $\beta$ -catenin, BMP/Smad, PI3K/AKT, MAPK, and RANKL/OPG pathways (Stock & Schett, 2021; Yang et al., 2020). Their therapeutic mechanisms are similar to those of the drugs described earlier and they can regulate bone turnover and exert other anti-OP effects via the signaling pathways described earlier (He et al., 2019). However, TCM has the characteristics of multi-components and multi-targets. *Psoralea corylifolia*.

For example, the compound bakuchiol isolated from *Psoralea corylifolia* Linn (PCL), PCL, and Modified Qing' E Formula (MQEF) with PCL as the monarch drug, both of them can show promising anti-osteoporosis effect. Bakuchiol (BAK) is a compound isolated from PCL that inhibits M-CSF and RANKL co-stimulation-induced osteoclast differentiation and bone resorption via AKT and AP-1 pathways (Chai et al., 2018). In addition, BAK also acts on osteoblasts to induce osteoclast differentiation through upregulation of transcription factors Runx2, Collagen-I, ALP, osteocalcin (OCN) and activation of Wnt3a, LRP5 and  $\beta$ -catenin on the Wnt pathway (Weng et al., 2015). Furthermore, BAK is a natural estrogen receptor  $\alpha$  (ER $\alpha$ ) agonist that reduces

postmenopausal bone loss by increasing ALP, calcium ion concentration, and serum estradiol concentration (S. H. Lim et al., 2009). BAK also has good anti-inflammatory and antioxidant effects and inhibits LPS stimulation-induced elevation of iNOS, COX-2, and TNF- $\alpha$  by inhibiting the p38 MAPK/ERK signaling pathway (H. S. Lim, Kim, Kim, & Jeong, 2019). In addition, BAK also has various effects such as inhibiting nitric oxide (NO) production and reducing oxidative stress damage (Liu et al., 2020; Xu, Lv, Liu, Zhang, & Yang, 2021). Inflammatory factor activation, NO production and oxidative stress damage are all important pathological changes of OP, but there is a lack of relevant studies and further exploration is needed in the future. The herb PCL also has the same effect of promoting osteoblast proliferative activity, improving BMD, reducing serum osteocalcin and promoting bone formation as BAK (W. D. Li et al., 2014; S. H. Lim et al., 2009). PCL attenuates pro-inflammatory cytokine expression (Pai et al., 2021). MQEF, which consists of PCL as the monarch drug, also improves bone biomechanics in osteoporotic ovariectomized mice by enhancing the expression of  $\beta$ -catenin on the Wnt pathway (Shuai et al., 2019). MQEF also increases the expression levels of adiponectin, BMP2 and OPG in patients with non-traumatic osteonecrosis, thus exerting a clinical protective effect (C. G. Li et al., 2017). In addition, MQEF was able to increase serum estradiol levels and reduce luteinizing hormone release, showing significant estrogenic activity in animals (Y. Xu et al., 2010) and the MQEF combination had more potent estrogen-like effects compared to the individual components, and the use of the formula alleviated the loss of appetite in animals caused by the use of PCL alone, which could explain the synergistic effect of MQEF with efficacy enhancing and toxicity reducing compared with PCL alone **Figure 3: TCM for the treatment of osteoporosis** (Xiong et al., 2022). In China, MQEF is recommended as a drug in the primary osteoporosis treatment guidelines, and the existence of MQEF-related Chinese patent drug also provides more convenience for patients. However, the lack of phase III clinical trials has prevented it from being used globally.

The screening of active ingredients from herbal medicines and herbal compounds, and studies of proximal mechanisms of action, specification of safety ranges by toxicological methods, standardized phase III clinical trials to determine efficacy and indications, and application of modern technologies to establish quality control and standardized testing of herbal medicines are required.

### Novel Biological Therapeutics Targeted to OP

#### RANKL Inhibitors

RANKL was initially identified as a novel member of the tumor necrosis factor receptor (TNFR) family expressed on dendritic cells and involved in dendritic cell-mediated T cell proliferation and the activation of RANK + T cells (D. M. Anderson et al., 1997). RANKL and bone metabolism have



been studied extensively owing to the important role of the RANK/RANKL signaling pathway in osteoclast formation (Hsu et al., 1999; McDonald et al., 2021). RANKL, a homotrimeric transmembrane protein, exists as three isoforms. RANKL-1 and RANKL-2 have transmembrane structural domains, but RANKL-2 has a shorter intracellular structural domain and RANKL-3 has no transmembrane structural domain and is therefore soluble (Ikeda, Kasai, Utsuyama, & Hirokawa, 2001). Nuclear factor of activated T cells c1 (NFATc1) is the most potent transcription factor induced by RANKL and is essential for osteoclast activation, and activation of the calcium-NFATc1 pathway is essential for osteoclastogenesis and differentiation (Ikeda et al., 2001; Negishi-Koga & Takayanagi, 2009). RANKL induces *NFATc1* gene expression primarily by various mechanisms. RANK activates NF- $\kappa$ B by interacting with TNF receptor-associated factors (TRAFs). RANK contains two independent TRAF binding domains: the TRAF1, 2, 3, 5, and 6 binding regions (amino acids 544–616) and the TRAF6 binding region (amino acids 340–421). RANK-mediated NF- $\kappa$ B signaling is completely inhibited by the deletion of the TRAF6-binding region, indicating that the RANK-TRAF interaction is required for RANK activation (Jules et al., 2015). RANK-specific activation mediated by TRAF6 leads to the activation of NFATc1, a key transcription factor for osteoclast differentiation. In addition, in conjunction with RANK and co-stimulatory receptors, immunoreceptor tyrosine-based activation motif (ITAM) is phosphorylated by tyrosine kinase, leading to the

activation of spleen tyrosine kinase (Syk) and phospholipase C $\gamma$  (PLC $\gamma$ ) (Koga et al., 2004). This forms an osteoclastogenic signaling complex, in turn activating calcium ion signaling, which is required for the induction and activation of NFATc1. c-fms is a receptor for macrophage colony-stimulating factor (M-CSF), and their binding leads to the upregulation of c-Fos, a component of the AP-1 transcription factor dimer complex, which is essential for osteoclast differentiation (Feng & Teitelbaum, 2013). c-Fos upregulation leads to the expression of RANKL and its receptor RANK, and the loss of c-Fos leads to a complete lack of osteoclast differentiation and the development of severe osteopetrosis (Wagner & Eferl, 2005). The AP-1 complex also plays a major role in NFATc1 amplification (Takayanagi et al., 2002). Therefore, inhibiting osteoclast production and differentiation by inhibiting RANKL activity, thus inhibiting bone resorption, may be an efficient strategy for the treatment of OP (**Figure 4**: Mechanism diagram of RANKL/RANK/OPG signaling pathway cascade in osteoclastogenesis). A clinical study of denosumab, an anti-RANKL monoclonal antibody, in postmenopausal patients with OP showed that 12 months of treatment resulted in a lower risk of fracture and lower incidence of reported adverse reactions, such as osteoarthritis, than those in the placebo control group (Cosman et al., 2016). Ten years of denosumab treatment had even greater benefits, including a sustained reduction in the fracture incidence and sustained increases in BMD (Bone et al., 2017). Based on the significant loss of antiresorptive effects within 7 months after a single injection of denosumab,

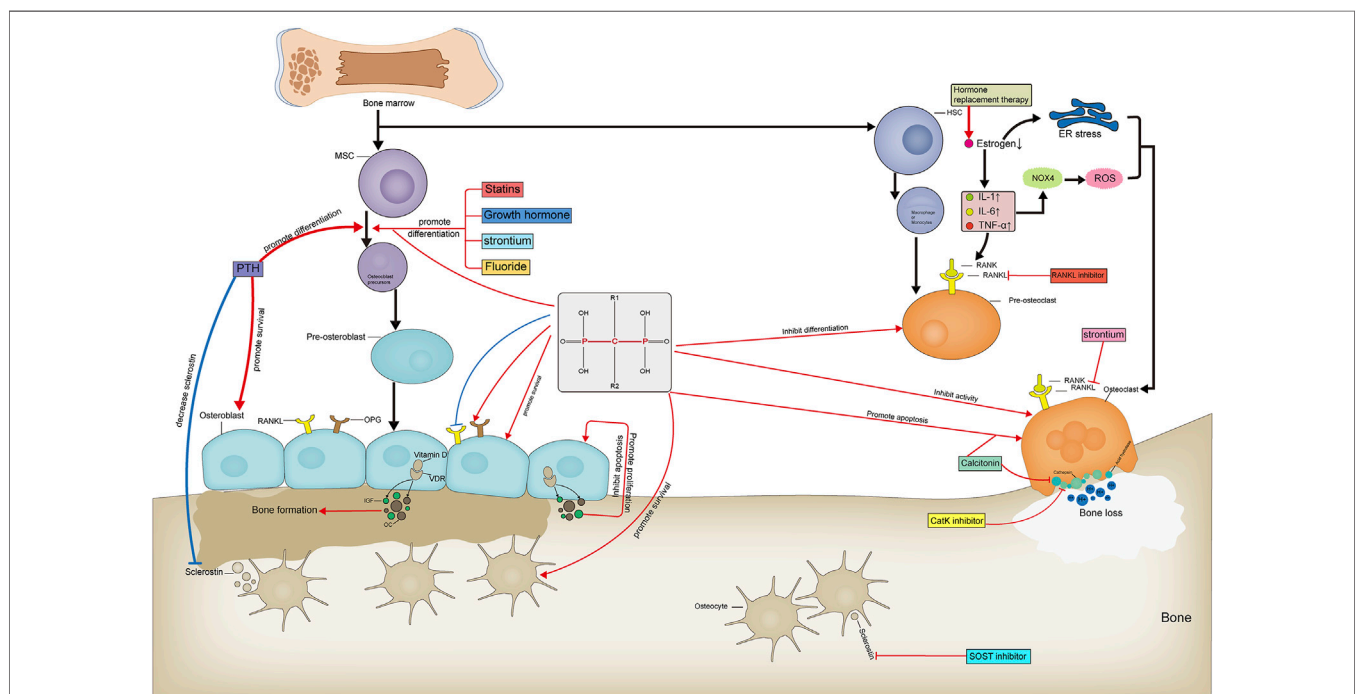
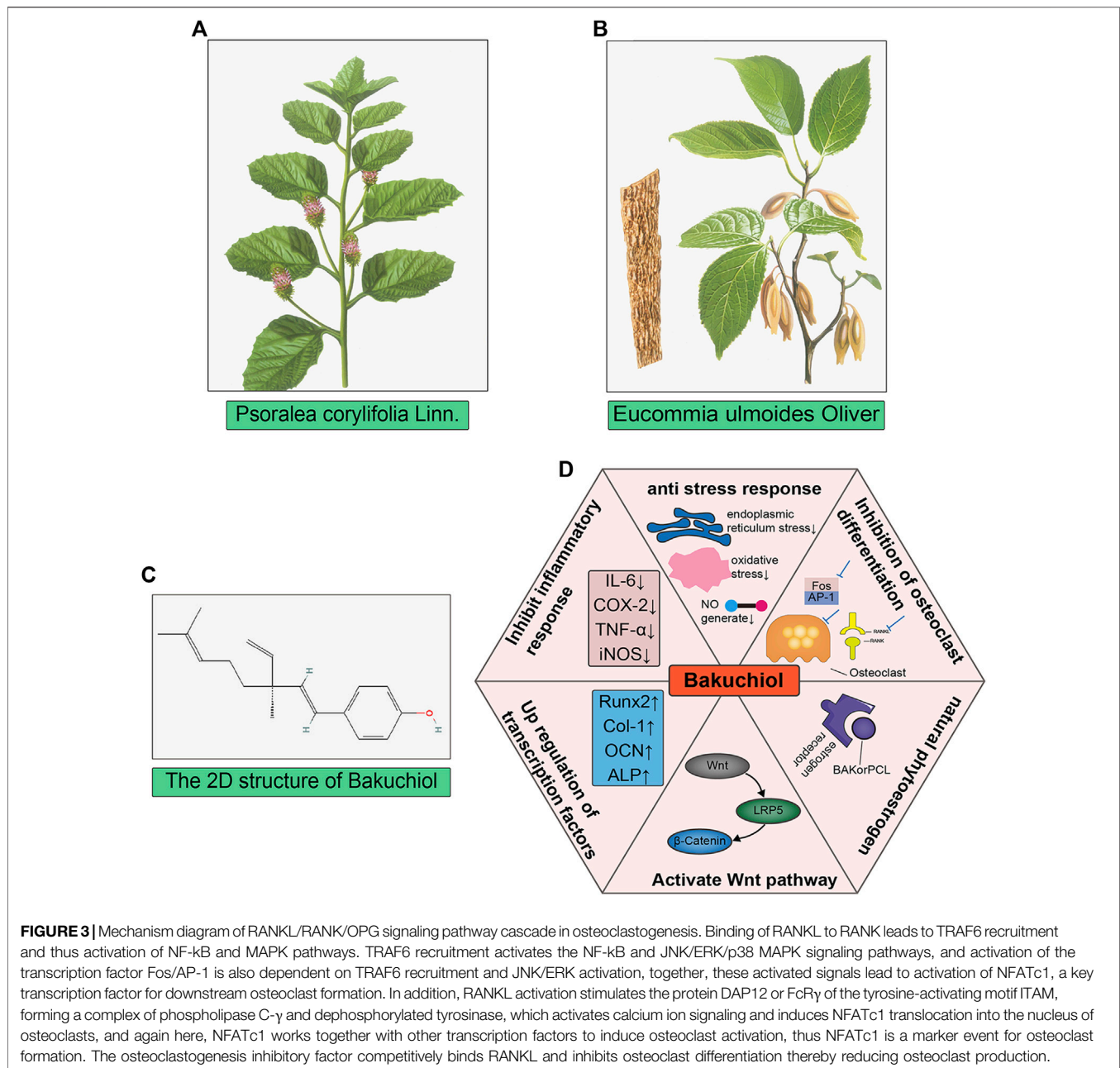


**FIGURE 2 |** Targets and mechanisms of anti-osteoporosis drug action with different mechanisms. Pharmacological mechanism of anti-osteoporosis drugs affecting bone formation and bone resorption.





which may lead to an increased risk of rebound-associated vertebral fractures, injections must be administered every 6 months (Lyu et al., 2020).

### Romsozumab

Sclerostin, encoded by the *SOST* gene and secreted by osteoblasts, inhibits osteoblast differentiation and reduces osteogenesis. In mice, sclerostin (Tg-Sost) overexpression inhibits osteoblast activity, increases osteoclast proliferation, decreases serum 1α, 25-hydroxyvitamin D concentrations, increases FGF23, and decreases calcium and phosphorus levels (Winkler et al., 2003), whereas *Sost* knockout (*Sost*<sup>-/-</sup>) mice exhibit the opposite phenotypes, with an increased relative polysaccharide

content in bone, decreased organic salt maturation and crystallization, and decreased bone matrix mineralization (X. Li et al., 2008; Sebastian & Loots, 2018). Thus, sclerostin, the product of the *Sost* gene, is a key negative regulator of bone formation, and *Sost* inhibitors are expected to be effective targets for the treatment of OP (Dai et al., 2021). Sclerostin antagonizes Wnt signaling in osteoblasts (Kim et al., 2020). Activation of the Wnt pathway not only induces osteogenic differentiation of MSCs and the expression of osteoprotegerin by osteoblasts to inhibit bone resorption by osteoclasts but also acts directly on osteoclasts to inhibit their differentiation (van Bezooijen et al., 2007). Sclerostin promotes β-catenin phosphorylation and proteasomal degradation by binding to the nuclear Wnt

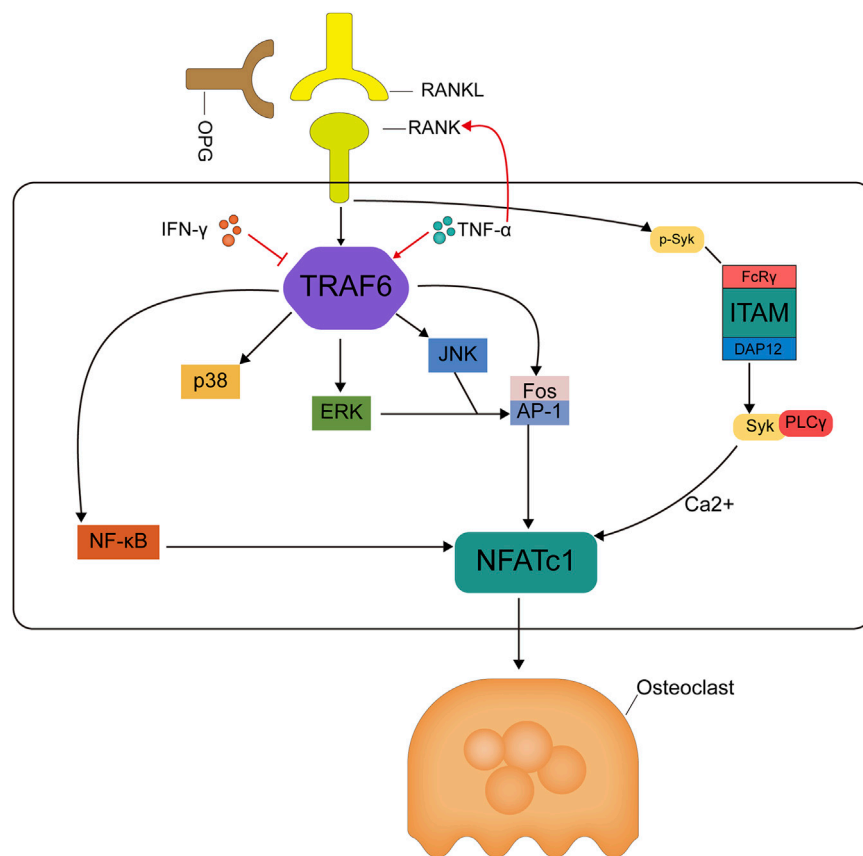


**FIGURE 4** | TCM for the treatment of osteoporosis. **(A,B)** The image of *Psoralea corylifolia* Linn and *Eucommia ulmoides* Oliver, both of them are the monarch drugs of Qing' E formula; **(C)** The 2D chemical structure of bakuchiol, which is one of the main components in *Psoralea corylifolia* Linn. **(D)** showed the six main mechanisms that bakuchiol exerts anti-osteoporosis.

receptor and also inhibits low-density lipoprotein receptor-related proteins 5 and 6 (LRP5/6) binding to DKK by binding competitively to LRP5/6, together antagonizing canonical Wnt signaling activation to promote osteogenesis (Little, Recker, & Johnson, 2002; Mao et al., 2002; Clevers, 2006; Bhat et al., 2007). Clinical studies have shown that romosozumab improves trabecular and cortical bone architecture and is more effective in increasing spine and hip BMD compared to teriparatide (McClung et al., 2014; Ishibashi et al., 2017). Romosozumab resulted in greater increases in lumbar, hip, and femoral neck BMD than those observed for denosumab (Miyachi et al., 2019). However, romosozumab may carry a potential risk of cardiovascular mortality and stroke (Tankó et al., 2005; Saag et al., 2017), thus limiting its use in patients with OP and concomitant cardiovascular disease, in which the benefits and risks must be weighed to maximize the clinical benefit.

### Odanacatib (Cathepsin K Inhibitor)

Cathepsins are a class of cysteine proteases that degrade proteins in a variety of tissues. Cathepsin K (Cat K) is highly expressed in osteoclasts and is primarily responsible for the degradation of type I collagen. The inhibition of cathepsin K activity effectively inhibits bone resorption, as inorganic bone minerals are primarily

degraded by the release of acidic ions, whereas organic bone matrix is primarily degraded by cathepsin K (Dodds et al., 2001). In mice with *CatK* gene knockout, osteoclasts have normal survival but bone resorption is inhibited (Gentile et al., 2014). In contrast, *CatK* transgenic mice exhibit increased bone resorption and bone turnover (Saftig et al., 1998; Kiviranta et al., 2001; Leung, Pickarski, Zhuo, Masarachia, & Duong, 2011); these processes are reversible (Zhuo, Gauthier, Black, Percival, & Duong, 2014). Based on these studies, odanacatib was developed and entered in a phase III clinical trial, demonstrating better or similar effects in increasing BMD and reducing fracture risk compared to those of denosumab (Harris et al., 1999; Black et al., 2007). Adverse events include cerebrovascular events, which may be related to molecular and cellular alterations in the central nervous system caused by low levels of cathepsin K in response to odanacatib, thereby affecting tissue homeostasis (Dauth et al., 2011; Drake, Clarke, Oursler, & Khosla, 2017).

In addition to these targeted anti-OP drugs, other targeted drugs are in development and in pre-clinical trials, such as the Src inhibitor saracatinib and the anti-DKK-1 antibody BHQ-880. Given the important role of these targets in OP, these drugs have great potential for clinical use and offer an encouraging strategy for the treatment of OP in the future (Heath et al., 2009; Rachner, Khosla, & Hofbauer, 2011).

## DISCUSSION

Recent advances in our understanding of bone biology have revealed new options and have prompted unprecedented progress in the treatment of OP. The clinical use of denosumab and romosozumab is a good example. In this review, we provide an overview of commonly used anti-OP drugs, their pharmacological and molecular mechanisms, and promising targeted anti-OP therapeutics.

Bone remodeling is mediated by both osteoblasts and osteoclasts. Osteoblast differentiation is regulated by three key transcription factors, Runx2, Osterix, and  $\beta$ -catenin, which are essential for the induction of the differentiation of bone marrow MSCs into osteoblasts (Koga et al., 2005; Long, 2011). Osteoclast regulation is affected by the M-CSF/c-Fos and RANKL/RANK/OPG pathways. The Wnt pathway is the most important in the regulation of bone remodeling and bone metabolism (Gori, Superti-Furga, & Baron, 2016), and members of the Wnt family are indispensable for the processes of osteogenic differentiation, bone metabolism balance, and bone remodeling. DKK-1 secreted by osteoblasts binds to the BP1 and BP3 structural domains of LRP5/6 receptors in the Wnt signaling pathway, and secreted SOST binds to the BP1 structural domain of LRP5/6 and LRP4 receptors in the Wnt signaling pathway (Patel & Karsenty, 2002). This competitive binding enhances the inhibitory effects on the canonical Wnt pathway, and the knockout of Dkk1 or Sost significantly increases the bone content. The canonical Wnt pathway induces osteogenic differentiation via  $\beta$ -catenin by increasing the expression of target genes, including *Runx2*, *Osterix*, and *OPG*, increasing OPG protein expression, and inhibiting RANKL/RANK interactions to inhibit bone resorption (Baron & Kneissel, 2013). The non-canonical Wnt pathway regulates osteogenesis and bone resorption by the regulation of Wnt ligands, such as Wnt5a, the most strongly expressed of all Wnt ligands, and activates non-canonical Wnt signaling via the receptor tyrosine kinase-like orphan receptor (Ror) protein. Wnt5a is expressed by cells in the osteoblast lineage, whereas Ror2 is expressed by osteoclast precursors. The knockout of Wnt5a in osteoblasts or knockout of Ror2 in osteoclasts leads to reduced osteoclast formation and inhibits Wnt5a-induced osteoblast differentiation. Wnt5a ligands bind to Wnt receptors, leading to the activation of the Ror2 signaling cascade, which in turn activates the JNK/c-Jun pathway and enhances RANKL/RANK-induced osteoclastogenesis (Maeda et al., 2012; Hasegawa et al., 2018). Similar to conventional anti-OP therapeutics, novel targeted anti-OP drugs exert anti-OP effects by regulating the RANKL/RANK/OPG axis and the Wnt pathway. However, unlike the broad-spectrum targeting effects of conventional anti-OP drugs, targeted anti-OP drugs bind specifically and selectively to a receptor to affect osteoblast and osteoclast functions in bone remodeling. Despite their promise, some issues in the clinical use of targeted drugs remain, such as difficulties in development, high prices, and the presence of side effects that potentially outweigh the benefits. Therefore, conventional anti-OP drugs cannot be ignored and novel, effective, targeted anti-OP drugs with fewer side effects should be developed. Clinical observation studies and systematic evaluations and meta-analyses are needed to help these drugs reach the clinic more quickly. For conventional anti-OP drugs, in-depth

research on their molecular mechanisms and pharmacological effects should be conducted along with toxicological and safety studies to guide the rational use of these drugs, eliminate drugs with few benefits and high risks, and improve and update our conceptual understanding of these drugs.

The safety of combinations of anti-OP drugs is also a concern. Different anti-OP drugs have different mechanisms of action, and the combination of drugs that inhibit bone resorption and drugs that promote bone formation may be an effective strategy for the treatment of OP. Some combinations may be effective, such as the combination of teriparatide and denosumab or zoledronate to increase BMD, whereas other combinations either show lower efficacies than those of single agents or lack sufficient clinical evidence (Eastell & Walsh, 2013; Tsai et al., 2013). It may be reasonable to consider the sequential use of drugs, which avoids the increased risk of specific diseases and minimizes resistance and peak effects caused by the long-term use of a single drug. Drug safety is directly related to patient safety issues, and some anti-OP drugs have been restricted or even withdrawn owing to inherent defects or clinical risks that far exceed the benefits. For example, fluoride ions are rarely used in conventional anti-OP therapies owing to the high incidence of gastrointestinal reactions and a tendency to cause fluorosis. The risk of heart disease and venous thrombosis associated with strontium salts is gradually being recognized and their use is decreasing. Novel anti-OP targets are rapidly moving into the clinic; however, their adverse events are unclear, which poses a challenge for drug safety studies.

In summary, anti-OP drugs are developing rapidly, and a comprehensive understanding of OP therapeutic agents and their molecular mechanisms of action is necessary. This review introduces anti-OP drug therapy and its pharmacological mechanisms from four major categories and 14 subcategories. We hope to help clinicians and researchers understand the past and future of anti-OP drugs, update their concepts and keep up with the frontier to achieve standardized clinical use, pharmacological and toxicological studies of drugs and the development of new drugs. Only through joint efforts can we gain an advantage in the fight against OP, a potentially devastating disease of aging.

## AUTHOR CONTRIBUTIONS

BS, DH and JLL conceived the idea for the study and provided critical revision of the manuscript. CM collected the information. BS and JL participated in study design, supervising, writing and drafting of the manuscript. All authors read and approved the final manuscript.

## FUNDING

This study was partially funded by the National Natural Science Foundation of China (Project Number: 82174182, 81974546, 81974249, and 82004201).

## ACKNOWLEDGMENTS

The authors would like to thank Editage ([www.editage.cn](http://www.editage.cn)) for English language editing.

## REFERENCES

- Ammann, P., Rizzoli, R., Bonjour, J. P., Bourrin, S., Meyer, J. M., Vassalli, P., et al. (1997). Transgenic Mice Expressing Soluble Tumor Necrosis Factor-Receptor Are Protected against Bone Loss Caused by Estrogen Deficiency. *J. Clin. Invest.* 99 (7), 1699–1703. doi:10.1172/jci119333
- An, T., Hao, J., Sun, S., Li, R., Yang, M., Cheng, G., et al. (2017). Efficacy of Statins for Osteoporosis: a Systematic Review and Meta-Analysis. *Osteoporos. Int.* 28 (1), 47–57. doi:10.1007/s00198-016-3844-8
- Anderson, D. M., Maraskovsky, E., Billingsley, W. L., Dougall, W. C., Tometsko, M. E., Roux, E. R., et al. (1997). A Homologue of the TNF Receptor and its Ligand Enhance T-Cell Growth and Dendritic-Cell Function. *Nature* 390 (6656), 175–179. doi:10.1038/36593
- Anderson, G. L., Limacher, M., Assaf, A. R., Bassford, T., Beresford, S. A., Black, H., et al. (2004). Effects of Conjugated Equine Estrogen in Postmenopausal Women with Hysterectomy: the Women's Health Initiative Randomized Controlled Trial. *Jama* 291 (14), 1701–1712. doi:10.1001/jama.291.14.1701
- Andreotti, G., Méndez, B. L., Amodeo, P., Morelli, M. A., Nakamuta, H., and Motta, A. (2006). Structural Determinants of Salmon Calcitonin Bioactivity: the Role of the Leu-Based Amphipathic Alpha-Helix. *J. Biol. Chem.* 281 (34), 24193–24203. doi:10.1074/jbc.M603528200
- Armbricht, H. J., Hodam, T. L., Boltz, M. A., Partridge, N. C., Brown, A. J., and Kumar, V. B. (1998). Induction of the Vitamin D 24-hydroxylase (CYP24) by 1,25-dihydroxyvitamin D3 Is Regulated by Parathyroid Hormone in UMR106 Osteoblastic Cells. *Endocrinology* 139 (8), 3375–3381. doi:10.1210/endo.139.8.6134
- Atkins, G. J., Weldon, K. J., Wijenayaka, A. R., Bonewald, L. F., and Findlay, D. M. (2009). Vitamin K Promotes Mineralization, Osteoblast-To-Osteocyte Transition, and an Anticatabolic Phenotype by  $\gamma$ -carboxylation-dependent and -independent Mechanisms. *Am. J. Physiol. Cell. Physiol.* 297 (6), C1358–C1367. doi:10.1152/ajpcell.00216.2009
- Atkinson, H. F., Moyer, R. F., Yacoub, D., Coughlin, D., and Birmingham, T. B. (2017). Effects of Recombinant Human Growth Hormone for Osteoporosis: Systematic Review and Meta-Analysis. *Can. J. Aging* 36 (1), 41–54. doi:10.1017/s0714980816000696
- Bacchetta, J., Sea, J. L., Chun, R. F., Lisse, T. S., Wesseling-Perry, K., Gales, B., et al. (2013). Fibroblast Growth Factor 23 Inhibits Extrarenal Synthesis of 1,25-dihydroxyvitamin D in Human Monocytes. *J. Bone Min. Res.* 28 (1), 46–55. doi:10.1002/jbmr.1740
- Barake, M., Arabi, A., Nakhoul, N., El-Hajj Fuleihan, G., El Ghandour, S., Klibanski, A., et al. (2018). Effects of Growth Hormone Therapy on Bone Density and Fracture Risk in Age-Related Osteoporosis in the Absence of Growth Hormone Deficiency: a Systematic Review and Meta-Analysis. *Endocrine* 59 (1), 39–49. doi:10.1007/s12020-017-1440-0
- Baron, R., and Kneissel, M. (2013). WNT Signaling in Bone Homeostasis and Disease: from Human Mutations to Treatments. *Nat. Med.* 19 (2), 179–192. doi:10.1038/nm.3074
- Barwell, J., Gingell, J. J., Watkins, H. A., Archbold, J. K., Poyner, D. R., and Hay, D. L. (2012). Calcitonin and Calcitonin Receptor-like Receptors: Common Themes with Family B GPCRs? *Br. J. Pharmacol.* 166 (1), 51–65. doi:10.1111/j.1476-5381.2011.01525.x
- Beutner, E. H., and Munson, P. L. (1960). Time Course of Urinary Excretion of Inorganic Phosphate by Rats after Parathyroidectomy and after Injection of Parathyroid Extract. *Endocrinology* 66, 610–616. doi:10.1210/endo-66-4-610
- Bhat, B. M., Allen, K. M., Liu, W., Graham, J., Morales, A., Anisowicz, A., et al. (2007). Structure-based Mutation Analysis Shows the Importance of LRP5 Beta-Propeller 1 in Modulating Dkk1-Mediated Inhibition of Wnt Signaling. *Gene* 391 (1–2), 103–112. doi:10.1016/j.gene.2006.12.014
- Bikle, D. D. (2014). Vitamin D Metabolism, Mechanism of Action, and Clinical Applications. *Chem. Biol.* 21 (3), 319–329. doi:10.1016/j.chembiol.2013.12.016
- Bingham, P. J., Brazell, I. A., and Owen, M. (1969). The Effect of Parathyroid Extract on Cellular Activity and Plasma Calcium Levels *In Vivo*. *J. Endocrinol.* 45 (3), 387–400. doi:10.1677/joe.0.0450387
- Bischoff-Ferrari, H. A., Borchers, M., Gudat, F., Dürmüller, U., Stähelin, H. B., and Dick, W. (2004). Vitamin D Receptor Expression in Human Muscle Tissue Decreases with Age. *J. Bone Min. Res.* 19 (2), 265–269. doi:10.1359/jbmr.2004.19.2.265
- Bischoff-Ferrari, H. A., Giovannucci, E., Willett, W. C., Dietrich, T., and Dawson-Hughes, B. (2006). Estimation of Optimal Serum Concentrations of 25-hydroxyvitamin D for Multiple Health Outcomes. *Am. J. Clin. Nutr.* 84 (1), 18–28. doi:10.1093/ajcn/84.1.18
- Bischoff-Ferrari, H. A. (2014). Optimal Serum 25-hydroxyvitamin D Levels for Multiple Health Outcomes. *Adv. Exp. Med. Biol.* 810, 500–525. doi:10.1007/978-1-4939-0437-2\_28
- Black, D. M., Delmas, P. D., Eastell, R., Reid, I. R., Boonen, S., Cauley, J. A., et al. (2007). Once-yearly Zoledronic Acid for Treatment of Postmenopausal Osteoporosis. *N. Engl. J. Med.* 356 (18), 1809–1822. doi:10.1056/NEJMoa067312
- Black, D. M., and Rosen, C. J. (2016). Clinical Practice. Postmenopausal Osteoporosis. *N. Engl. J. Med.* 374 (3), 254–262. doi:10.1056/NEJMcp1513724
- Black, D. M., Schwartz, A. V., Ensrud, K. E., Cauley, J. A., Levis, S., Quandt, S. A., et al. (2006). Effects of Continuing or Stopping Alendronate after 5 Years of Treatment: the Fracture Intervention Trial Long-Term Extension (FLEX): a Randomized Trial. *Jama* 296 (24), 2927–2938. doi:10.1001/jama.296.24.2927
- Bone, H. G., Hosking, D., Devogelaer, J. P., Tucci, J. R., Emkey, R. D., Tonino, R. P., et al. (2004). Ten Years' Experience with Alendronate for Osteoporosis in Postmenopausal Women. *N. Engl. J. Med.* 350 (12), 1189–1199. doi:10.1056/NEJMoa030897
- Bone, H. G., Wagman, R. B., Brandi, M. L., Brown, J. P., Chapurlat, R., Cummings, S. R., et al. (2017). 10 Years of Denosumab Treatment in Postmenopausal Women with Osteoporosis: Results from the Phase 3 Randomised FREEDOM Trial and Open-Label Extension. *Lancet Diabetes Endocrinol.* 5 (7), 513–523. doi:10.1016/s2213-8587(17)30138-9
- Bouillon, R., Marcocci, C., Carmeliet, G., Bikle, D., White, J. H., Dawson-Hughes, B., et al. (2019). Skeletal and Extraskelatal Actions of Vitamin D: Current Evidence and Outstanding Questions. *Endocr. Rev.* 40 (4), 1109–1151. doi:10.1210/er.2018-00126
- Brennan, T. C., Rybchyn, M. S., Green, W., Atwa, S., Conigrave, A. D., and Mason, R. S. (2009). Osteoblasts Play Key Roles in the Mechanisms of Action of Strontium Ranelate. *Br. J. Pharmacol.* 157 (7), 1291–1300. doi:10.1111/j.1476-5381.2009.00305.x
- Brixen, K., Nielsen, H. K., Mosekilde, L., and Flyvbjerg, A. (1990). A Short Course of Recombinant Human Growth Hormone Treatment Stimulates Osteoblasts and Activates Bone Remodeling in Normal Human Volunteers. *J. Bone Min. Res.* 5 (6), 609–618. doi:10.1002/jbmr.5650050610
- Burr, D., and Russell, G. (2011). Foreword: Bisphosphonates. *Bone* 49 (1), 1. doi:10.1016/j.bone.2011.05.019
- Burt, L. A., Billington, E. O., Rose, M. S., Raymond, D. A., Hanley, D. A., and Boyd, S. K. (2019). Effect of High-Dose Vitamin D Supplementation on Volumetric Bone Density and Bone Strength: A Randomized Clinical Trial. *Jama* 322 (8), 736–745. doi:10.1001/jama.2019.11889
- Cauley, J. A., Robbins, J., Chen, Z., Cummings, S. R., Jackson, R. D., LaCroix, A. Z., et al. (2003). Effects of Estrogen Plus Progestin on Risk of Fracture and Bone Mineral Density: the Women's Health Initiative Randomized Trial. *Jama* 290 (13), 1729–1738. doi:10.1001/jama.290.13.1729
- Chai, L., Zhou, K., Wang, S., Zhang, H., Fan, N., Li, J., et al. (2018). Psoralen and Bakuchiol Ameliorate M-CSF Plus RANKL-Induced Osteoclast Differentiation and Bone Resorption via Inhibition of AKT and AP-1 Pathways *In Vitro*. *Cell. Physiol. Biochem.* 48 (5), 2123–2133. doi:10.1159/000492554
- Chambers, T. J., and Magnus, C. J. (1982). Calcitonin Alters Behaviour of Isolated Osteoclasts. *J. Pathol.* 136 (1), 27–39. doi:10.1002/path.1711360104
- Chan, K. A., Andrade, S. E., Boles, M., Buist, D. S., Chase, G. A., Donahue, J. G., et al. (2000). Inhibitors of Hydroxymethylglutaryl-Coenzyme A Reductase and Risk of Fracture Among Older Women. *Lancet* 355 (9222), 2185–2188. doi:10.1016/s0140-6736(00)02400-4
- Chapuy, M. C., Arlot, M. E., Duboeuf, F., Brun, J., Crouzet, B., Arnaud, S., et al. (1992). Vitamin D3 and Calcium to Prevent Hip Fractures in Elderly Women. *N. Engl. J. Med.* 327 (23), 1637–1642. doi:10.1056/nejm199212033272305
- Chen, C. H., Hwang, T. L., Chen, L. C., Chang, T. H., Wei, C. S., and Chen, J. J. (2017). Isoflavones and Anti-inflammatory Constituents from the Fruits of *Psoralea Corylifolia*. *Phytochemistry* 143, 186–193. doi:10.1016/j.phytochem.2017.08.004
- Chen, P. Y., Sun, J. S., Tsuang, Y. H., Chen, M. H., Weng, P. W., and Lin, F. H. (2010). Simvastatin Promotes Osteoblast Viability and Differentiation via



- Ras/Smad/Erk/BMP-2 Signaling Pathway. *Nutr. Res.* 30 (3), 191–199. doi:10.1016/j.nutres.2010.03.004
- Chesnut, C. H., 3rd, Silverman, S., Andriano, K., Genant, H., Gimona, A., Harris, S., et al. (2000). A Randomized Trial of Nasal Spray Salmon Calcitonin in Postmenopausal Women with Established Osteoporosis: the Prevent Recurrence of Osteoporotic Fractures Study. PROOF Study Group. *Am. J. Med.* 109 (4), 267–276. doi:10.1016/s0002-9343(00)00490-3
- Clevers, H. (2006). Wnt/beta-catenin Signaling in Development and Disease. *Cell.* 127 (3), 469–480. doi:10.1016/j.cell.2006.10.018
- Compston, J. E., McClung, M. R., and Leslie, W. D. (2019). Osteoporosis. *Lancet* 393 (10169), 364–376. doi:10.1016/s0140-6736(18)32112-3
- Copp, D. H., and Cheney, B. (1962). Calcitonin-a Hormone from the Parathyroid Which Lowers the Calcium-Level of the Blood. *Nature* 193, 381–382. doi:10.1038/193381a0
- Cosman, F., Crittenden, D. B., Adachi, J. D., Binkley, N., Czerwinski, E., Ferrari, S., et al. (2016). Romosozumab Treatment in Postmenopausal Women with Osteoporosis. *N. Engl. J. Med.* 375 (16), 1532–1543. doi:10.1056/NEJMoa1607948
- Cosman, F., Shen, V., Herrington, B., and Lindsay, R. (1991). Response of the Parathyroid Gland to Infusion of Human Parathyroid Hormone-(1-34) [PTH-(1-34)]: Demonstration of Suppression of Endogenous Secretion Using Immunoradiometric Intact PTH-(1-84) Assay. *J. Clin. Endocrinol. Metab.* 73 (6), 1345–1351. doi:10.1210/jcem-73-6-1345
- Cui, X., Zhang, Y., Wang, J., Huang, C., Wang, Y., Yang, H., et al. (2020). Strontium Modulates Osteogenic Activity of Bone Cement Composed of Bioactive Borosilicate Glass Particles by Activating Wnt/ $\beta$ -Catenin Signaling Pathway. *Bioact. Mater.* 5 (2), 334–347. doi:10.1016/j.bioactmat.2020.02.016
- Cummings, S. R., Duong, T., Kenyon, E., Cauley, J. A., Whitehead, M., and Krueger, K. A. (2002). Serum Estradiol Level and Risk of Breast Cancer during Treatment with Raloxifene. *Jama* 287 (2), 216–220. doi:10.1001/jama.287.2.216
- Dai, Z., Fang, P., Yan, X., Zhu, R., Feng, Q., Yan, Q., et al. (2021). Single Dose of SHR-1222, a Sclerostin Monoclonal Antibody, in Healthy Men and Postmenopausal Women with Low Bone Mass: A Randomized, Double-Blind, Placebo-Controlled, Dose-Escalation, Phase I Study. *Front. Pharmacol.* 12, 770073. doi:10.3389/fphar.2021.770073
- Dalle Carbonare, L., Mottes, M., Malerba, G., Mori, A., Zaninotto, M., Plebani, M., et al. (2017). Enhanced Osteogenic Differentiation in Zoledronate-Treated Osteoporotic Patients. *Int. J. Mol. Sci.* 18 (6). doi:10.3390/ijms18061261
- Dauth, S., Sirbulescu, R. F., Jordans, S., Rehders, M., Avena, L., Oswald, J., et al. (2011). Cathepsin K Deficiency in Mice Induces Structural and Metabolic Changes in the Central Nervous System that Are Associated with Learning and Memory Deficits. *BMC Neurosci.* 12, 74. doi:10.1186/1471-2202-12-74
- Dawson-Hughes, B. (2017). Vitamin D and Muscle Function. *J. Steroid Biochem. Mol. Biol.* 173, 313–316. doi:10.1016/j.jsbmb.2017.03.018
- de Cássia Alves Nunes, R., Chiba, F. Y., Pereira, A. G., Pereira, R. F., de Lima Coutinho Mattered, M. S., Ervolino, E., et al. (2016). Effect of Sodium Fluoride on Bone Biomechanical and Histomorphometric Parameters and on Insulin Signaling and Insulin Sensitivity in Ovariectomized Rats. *Biol. Trace Elem. Res.* 173 (1), 144–153. doi:10.1007/s12011-016-0642-2
- Delling, G. R., Schulz, A., and Ziegler, R. (1977). Changes of Bone Remodelling Surfaces and Bone Structure in Paget's Disease Following Long-Term Treatment with Calcitonin. *Calcif. Tissue Res.* 22 Suppl (Suppl. 1), 359–361. doi:10.1007/bf02064100
- Delmas, P. D., Bjarnason, N. H., Mitlak, B. H., Ravoux, A. C., Shah, A. S., Huster, W. J., et al. (1997). Effects of Raloxifene on Bone Mineral Density, Serum Cholesterol Concentrations, and Uterine Endometrium in Postmenopausal Women. *N. Engl. J. Med.* 337 (23), 1641–1647. doi:10.1056/nejm199712043372301
- Dodds, R. A., James, I. E., Riemann, D., Ahern, R., Hwang, S. M., Connor, J. R., et al. (2001). Human Osteoclast Cathepsin K Is Processed Intracellularly Prior to Attachment and Bone Resorption. *J. Bone Min. Res.* 16 (3), 478–486. doi:10.1359/jbmr.2001.16.3.478
- Drake, M. T., Clarke, B. L., Oursler, M. J., and Khosla, S. (2017). Cathepsin K Inhibitors for Osteoporosis: Biology, Potential Clinical Utility, and Lessons Learned. *Endocr. Rev.* 38 (4), 325–350. doi:10.1210/er.2015-1114
- Dunford, J. E., Thompson, K., Coxon, F. P., Luckman, S. P., Hahn, F. M., Poulter, C. D., et al. (2001). Structure-activity Relationships for Inhibition of Farnesyl Diphosphate Synthase *In Vitro* and Inhibition of Bone Resorption *In Vivo* by Nitrogen-Containing Bisphosphonates. *J. Pharmacol. Exp. Ther.* 296 (2), 235–242.
- Eastell, R., O'Neill, T. W., Hofbauer, L. C., Langdahl, B., Reid, I. R., Gold, D. T., et al. (2016). Postmenopausal Osteoporosis. *Nat. Rev. Dis. Prim.* 2, 16069. doi:10.1038/nrdp.2016.69
- Eastell, R., and Walsh, J. S. (2013). Is it Time to Combine Osteoporosis Therapies? *Lancet* 382 (9886), 5–7. doi:10.1016/s0140-6736(13)60984-8
- Ensrud, K. E., and Crandall, C. J. (2019). Bisphosphonates for Postmenopausal Osteoporosis. *Jama* 322 (20), 2017–2018. doi:10.1001/jama.2019.15781
- Ettinger, B., Black, D. M., Mitlak, B. H., Knickerbocker, R. K., Nickelsen, T., Genant, H. K., et al. (1999). Reduction of Vertebral Fracture Risk in Postmenopausal Women with Osteoporosis Treated with Raloxifene: Results from a 3-year Randomized Clinical Trial. Multiple Outcomes of Raloxifene Evaluation (MORE) Investigators. *Jama* 282 (7), 637–645. doi:10.1001/jama.282.7.637
- Felsenfeld, A. J., Levine, B. S., and Rodriguez, M. (2015). Pathophysiology of Calcium, Phosphorus, and Magnesium Dysregulation in Chronic Kidney Disease. *Semin. Dial.* 28 (6), 564–577. doi:10.1111/sdi.12411
- Feng, X., and Teitelbaum, S. L. (2013). Osteoclasts: New Insights. *Bone Res.* 1 (1), 11–26. doi:10.4242/br201301003
- Fleisch, H., Russell, R. G., and Francis, M. D. (1969). Diphosphonates Inhibit Hydroxyapatite Dissolution *In Vitro* and Bone Resorption in Tissue Culture and *In Vivo*. *Science* 165 (3899), 1262–1264. doi:10.1126/science.165.3899.1262
- Franke, J. (1988). Fluoride and Osteoporosis. *Ann. Chir. Gynaecol.* 77 (5-6), 235–245.
- Frolik, C. A., Black, E. C., Cain, R. L., Satterwhite, J. H., Brown-Augsburger, P. L., Sato, M., et al. (2003). Anabolic and Catabolic Bone Effects of Human Parathyroid Hormone (1-34) Are Predicted by Duration of Hormone Exposure. *Bone* 33 (3), 372–379. doi:10.1016/s8756-3282(03)00202-3
- Garnero, P., Sornay-Rendu, E., Chapuy, M. C., and Delmas, P. D. (1996). Increased Bone Turnover in Late Postmenopausal Women Is a Major Determinant of Osteoporosis. *J. Bone Min. Res.* 11 (3), 337–349. doi:10.1002/jbmr.5650110307
- Gavali, S., Gupta, M. K., Daswani, B., Wani, M. R., Sirdeshmukh, R., and Khatkhatay, M. I. (2019). Estrogen Enhances Human Osteoblast Survival and Function via Promotion of Autophagy. *Biochim. Biophys. Acta Mol. Cell. Res.* 1866 (9), 1498–1507. doi:10.1016/j.bbmc.2019.06.014
- Gentile, M. A., Soung, D. Y., Horrell, C., Samadifam, R., Drissi, H., and Duong, L. T. (2014). Increased Fracture Callus Mineralization and Strength in Cathepsin K Knockout Mice. *Bone* 66, 72–81. doi:10.1016/j.bone.2014.04.032
- Ghiron, L. J., Thompson, J. L., Holloway, L., Hintz, R. L., Butterfield, G. E., Hoffman, A. R., et al. (1995). Effects of Recombinant Insulin-like Growth Factor-I and Growth Hormone on Bone Turnover in Elderly Women. *J. Bone Min. Res.* 10 (12), 1844–1852. doi:10.1002/jbmr.5650101203
- Giuliani, N., Pedrazzoni, M., Negri, G., Passeri, G., Impicciatore, M., and Girasole, G. (1998). Bisphosphonates Stimulate Formation of Osteoblast Precursors and Mineralized Nodules in Murine and Human Bone Marrow Cultures *In Vitro* and Promote Early Osteoblastogenesis in Young and Aged Mice *In Vivo*. *Bone* 22 (5), 455–461. doi:10.1016/s8756-3282(98)00033-7
- Goettsch, C., Babelova, A., Trummer, O., Erben, R. G., Rauner, M., Rammelt, S., et al. (2013). NADPH Oxidase 4 Limits Bone Mass by Promoting Osteoclastogenesis. *J. Clin. Invest.* 123 (11), 4731–4738. doi:10.1172/jci67603
- Goldstein, S. R., Duvernoy, C. S., Calaf, J., Adachi, J. D., Mershon, J. L., Dowsett, S. A., et al. (2009). Raloxifene Use in Clinical Practice: Efficacy and Safety. *Menopause* 16 (2), 413–421. doi:10.1097/gme.0b013e3181883dae
- Gori, F., Superti-Furga, A., and Baron, R. (2016). Bone Formation and the Wnt Signaling Pathway. *N. Engl. J. Med.* 375 (19), 1902–1903. doi:10.1056/NEJMc1609768
- Hall, B. K. (1987). Sodium Fluoride as an Initiator of Osteogenesis from Embryonic Mesenchyme *In Vitro*. *Bone* 8 (2), 111–116. doi:10.1016/8756-3282(87)90079-2
- Harris, S. T., Watts, N. B., Genant, H. K., McKeever, C. D., Hangartner, T., Keller, M., et al. (1999). Effects of Risedronate Treatment on Vertebral and Nonvertebral Fractures in Women with Postmenopausal Osteoporosis: a Randomized Controlled Trial. Vertebral Efficacy with Risedronate Therapy (VERT) Study Group. *Jama* 282 (14), 1344–1352. doi:10.1001/jama.282.14.1344
- Hasegawa, D., Wada, N., Yoshida, S., Mitarai, H., Arima, M., Tomokiyo, A., et al. (2018). Wnt5a Suppresses Osteoblastic Differentiation of Human Periodontal



- Ligament Stem Cell-like Cells via Ror2/JNK Signaling. *J. Cell. Physiol.* 233 (2), 1752–1762. doi:10.1002/jcp.26086
- Hattersley, G., Dean, T., Corbin, B. A., Bahar, H., and Gardella, T. J. (2016). Binding Selectivity of Abaloparatide for PTH-Type-1-Receptor Conformations and Effects on Downstream Signaling. *Endocrinology* 157 (1), 141–149. doi:10.1210/en.2015-1726
- Hauschka, P. V., Lian, J. B., Cole, D. E., and Gundberg, C. M. (1989). Osteocalcin and Matrix Gla Protein: Vitamin K-dependent Proteins in Bone. *Physiol. Rev.* 69 (3), 990–1047. doi:10.1152/physrev.1989.69.3.990
- He, J., Li, X., Wang, Z., Bennett, S., Chen, K., Xiao, Z., et al. (2019). Therapeutic Anabolic and Anticatabolic Benefits of Natural Chinese Medicines for the Treatment of Osteoporosis. *Front. Pharmacol.* 10, 1344. doi:10.3389/fphar.2019.01344
- Heath, D. J., Chantry, A. D., Buckle, C. H., Coulton, L., Shaughnessy, J. D., Jr., Evans, H. R., et al. (2009). Inhibiting Dickkopf-1 (Dkk1) Removes Suppression of Bone Formation and Prevents the Development of Osteolytic Bone Disease in Multiple Myeloma. *J. Bone Min. Res.* 24 (3), 425–436. doi:10.1359/jbmr.081104
- Hedlund, T., Hulth, A., and Johnell, O. (1983). Early Effects of Parathormone and Calcitonin on the Number of Osteoclasts and on Serum-Calcium in Rats. *Acta Orthop. Scand.* 54 (6), 802–804. doi:10.3109/17453678308992912
- Holtrop, M. E., Raisz, L. G., and Simmons, H. A. (1974). The Effects of Parathyroid Hormone, Colchicine, and Calcitonin on the Ultrastructure and the Activity of Osteoclasts in Organ Culture. *J. Cell. Biol.* 60 (2), 346–355. doi:10.1083/jcb.60.2.346
- Hoogendijk, E. O., Afilalo, J., Ensrud, K. E., Kowal, P., Onder, G., and Fried, L. P. (2019). Frailty: Implications for Clinical Practice and Public Health. *Lancet* 394 (10206), 1365–1375. doi:10.1016/s0140-6736(19)31786-6
- Horne, W. C., Shyu, J. F., Chakraborty, M., and Baron, R. (1994). Signal Transduction by Calcitonin Multiple Ligands, Receptors, and Signaling Pathways. *Trends Endocrinol. Metab.* 5 (10), 395–401. doi:10.1016/1043-2760(95)92521-j
- Houtman, E., Coutinho de Almeida, R., Tuerlings, M., Suchiman, H. E. D., Broekhuis, D., Nelissen, R. G. H. H., et al. (2021). Characterization of Dynamic Changes in Matrix Gla Protein (MGP) Gene Expression as Function of Genetic Risk Alleles, Osteoarthritis Relevant Stimuli, and the Vitamin K Inhibitor Warfarin. *Osteoarthr. Cartil.* 29 (8), 1193–1202. doi:10.1016/j.joca.2021.05.001
- Hsu, H., Lacey, D. L., Dunstan, C. R., Solovyev, I., Colombero, A., Timms, E., et al. (1999). Tumor Necrosis Factor Receptor Family Member RANK Mediates Osteoclast Differentiation and Activation Induced by Osteoprotegerin Ligand. *Proc. Natl. Acad. Sci. U. S. A.* 96 (7), 3540–3545. doi:10.1073/pnas.96.7.3540
- Huang, Y., Liao, L., Su, H., Chen, X., Jiang, T., Liu, J., et al. (2021). Psoralen Accelerates Osteogenic Differentiation of Human Bone Marrow Mesenchymal Stem Cells by Activating the TGF- $\beta$ /Smad3 Pathway. *Exp. Ther. Med.* 22 (3), 940. doi:10.3892/etm.2021.10372
- Igarashi, K., Hirafuji, M., Adachi, H., Shinoda, H., and Mitani, H. (1997). Effects of Bisphosphonates on Alkaline Phosphatase Activity, Mineralization, and Prostaglandin E2 Synthesis in the Clonal Osteoblast-like Cell Line MC3T3-E1. *Prostagl. Leukot. Essent. Fat. Acids* 56 (2), 121–125. doi:10.1016/s0952-3278(97)90508-1
- Ikedo, T., Kasai, M., Utsuyama, M., and Hirokawa, K. (2001). Determination of Three Isoforms of the Receptor Activator of Nuclear Factor- $\kappa$ B Ligand and Their Differential Expression in Bone and Thymus. *Endocrinology* 142 (4), 1419–1426. doi:10.1210/endo.142.4.8070
- Ishibashi, H., Crittenden, D. B., Miyauchi, A., Libanati, C., Maddox, J., Fan, M., et al. (2017). Romosozumab Increases Bone Mineral Density in Postmenopausal Japanese Women with Osteoporosis: A Phase 2 Study. *Bone* 103, 209–215. doi:10.1016/j.bone.2017.07.005
- Jones, G., Prosser, D. E., and Kaufmann, M. (2012). 25-Hydroxyvitamin D-24-Hydroxylase (CYP24A1): its Important Role in the Degradation of Vitamin D. *Arch. Biochem. Biophys.* 523 (1), 9–18. doi:10.1016/j.abb.2011.11.003
- Jules, J., Wang, S., Shi, Z., Liu, J., Wei, S., and Feng, X. (2015). The IVVY Motif and Tumor Necrosis Factor Receptor-Associated Factor (TRAF) Sites in the Cytoplasmic Domain of the Receptor Activator of Nuclear Factor  $\kappa$ B (RANK) Cooperate to Induce Osteoclastogenesis. *J. Biol. Chem.* 290 (39), 23738–23750. doi:10.1074/jbc.M115.667535
- Kaneb, A., Berardino, K., Hanukaai, J. S., Rooney, K., and Kaye, A. D. (2021). Calcitonin (FORTICAL, MICALCIN) for the Treatment of Vertebral Compression Fractures. *Orthop. Rev. (Pavia)* 13 (2), 24976. doi:10.52965/001c.24976
- Kavanagh, K. L., Guo, K., Dunford, J. E., Wu, X., Knapp, S., Ebetino, F. H., et al. (2006). The Molecular Mechanism of Nitrogen-Containing Bisphosphonates as Antiosteoporosis Drugs. *Proc. Natl. Acad. Sci. U. S. A.* 103 (20), 7829–7834. doi:10.1073/pnas.0601643103
- Kim, J., Han, W., Park, T., Kim, E. J., Bang, I., Lee, H. S., et al. (2020). Sclerostin Inhibits Wnt Signaling through Tandem Interaction with Two LRP6 Ectodomains. *Nat. Commun.* 11 (1), 5357. doi:10.1038/s41467-020-19155-4
- Kimble, R. B., Vannice, J. L., Bloedow, D. C., Thompson, R. C., Hopfer, W., Kung, V. T., et al. (1994). Interleukin-1 Receptor Antagonist Decreases Bone Loss and Bone Resorption in Ovariectomized Rats. *J. Clin. Investig.* 93 (5), 1959–1967. doi:10.1172/jci117187
- Kiviranta, R., Morko, J., Uusitalo, H., Aro, H. T., Vuorio, E., and Rantakokko, J. (2001). Accelerated Turnover of Metaphyseal Trabecular Bone in Mice Overexpressing Cathepsin K. *J. Bone Min. Res.* 16 (8), 1444–1452. doi:10.1359/jbmr.2001.16.8.1444
- Knopp-Sihota, J. A., Newburn-Cook, C. V., Homik, J., Cummings, G. G., and Voaklander, D. (2012). Calcitonin for Treating Acute and Chronic Pain of Recent and Remote Osteoporotic Vertebral Compression Fractures: a Systematic Review and Meta-Analysis. *Osteoporos. Int.* 23 (1), 17–38. doi:10.1007/s00198-011-1676-0
- Koga, T., Inui, M., Inoue, K., Kim, S., Suematsu, A., Kobayashi, E., et al. (2004). Costimulatory Signals Mediated by the ITAM Motif Cooperate with RANKL for Bone Homeostasis. *Nature* 428 (6984), 758–763. doi:10.1038/nature02444
- Koga, T., Matsui, Y., Asagiri, M., Kodama, T., de Crombrugge, B., Nakashima, K., et al. (2005). NFAT and Osterix Cooperatively Regulate Bone Formation. *Nat. Med.* 11 (8), 880–885. doi:10.1038/nm1270
- Kołodziejka, B., Stepień, N., and Kolmas, J. (2021). The Influence of Strontium on Bone Tissue Metabolism and its Application in Osteoporosis Treatment. *Int. J. Mol. Sci.* 22 (12). doi:10.3390/ijms22126564
- LaCroix, A. Z., Cauley, J. A., Pettinger, M., Hsia, J., Bauer, D. C., McGowan, J., et al. (2003). Statin Use, Clinical Fracture, and Bone Density in Postmenopausal Women: Results from the Women's Health Initiative Observational Study. *Ann. Intern. Med.* 139 (2), 97–104. doi:10.7326/0003-4819-139-2-200307150-00009
- LaCroix, A. Z., Chlebowski, R. T., Manson, J. E., Aragaki, A. K., Johnson, K. C., Martin, L., et al. (2011). Health Outcomes after Stopping Conjugated Equine Estrogens Among Postmenopausal Women with Prior Hysterectomy: a Randomized Controlled Trial. *Jama* 305 (13), 1305–1314. doi:10.1001/jama.2011.382
- Lau, K. H., Farley, J. R., Freeman, T. K., and Baylink, D. J. (1989). A Proposed Mechanism of the Mitogenic Action of Fluoride on Bone Cells: Inhibition of the Activity of an Osteoblastic Acid Phosphatase. *Metabolism* 38 (9), 858–868. doi:10.1016/0026-0495(89)90232-1
- Laurian, L., Oberman, Z., Graf, E., Gilad, S., Hoerer, E., and Simantov, R. (1986). Calcitonin Induced Increase in ACTH, Beta-Endorphin and Cortisol Secretion. *Horm. Metab. Res.* 18 (4), 268–271. doi:10.1055/s-2007-1012291
- Leidig-Bruckner, G., Roth, H. J., Bruckner, T., Lorenz, A., Raue, F., and Frank-Raue, K. (2011). Are Commonly Recommended Dosages for Vitamin D Supplementation Too Low? Vitamin D Status and Effects of Supplementation on Serum 25-hydroxyvitamin D Levels-Aan Observational Study during Clinical Practice Conditions. *Osteoporos. Int.* 22 (1), 231–240. doi:10.1007/s00198-010-1214-5
- Leung, P., Pickarski, M., Zhuo, Y., Masarachia, P. J., and Duong, L. T. (2011). The Effects of the Cathepsin K Inhibitor Odanacatib on Osteoclastic Bone Resorption and Vesicular Trafficking. *Bone* 49 (4), 623–635. doi:10.1016/j.bone.2011.06.014
- Li, C. G., Shen, L., Yang, Y. P., Xu, X. J., Shuai, B., and Ma, C. (2017). Effects of Modified Qing'e Pill ( ) on expression of adiponectin, bone morphogenetic protein 2 and coagulation-related factors in patients with nontraumatic osteonecrosis of femoral head. *Chin. J. Integr. Med.* 23 (3), 183–189. doi:10.1007/s11655-016-2407-3
- Li, H., Li, D., Ma, Z., Qian, Z., Kang, X., Jin, X., et al. (2018). Defective Autophagy in Osteoblasts Induces Endoplasmic Reticulum Stress and Causes Remarkable Bone Loss. *Autophagy* 14 (10), 1726–1741. doi:10.1080/15548627.2018.1483807

- Li, W. D., Yan, C. P., Wu, Y., Weng, Z. B., Yin, F. Z., Yang, G. M., et al. (2014). Osteoblasts Proliferation and Differentiation Stimulating Activities of the Main Components of Fructus Psoraleae Corylifoliae. *Phytomedicine* 21 (4), 400–405. doi:10.1016/j.phymed.2013.09.015
- Li, X., Ominsky, M. S., Niu, Q. T., Sun, N., Daugherty, B., D'Agostin, D., et al. (2008). Targeted Deletion of the Sclerostin Gene in Mice Results in Increased Bone Formation and Bone Strength. *J. Bone Min. Res.* 23 (6), 860–869. doi:10.1359/jbmr.080216
- Lim, H. S., Kim, Y. J., Kim, B. Y., and Jeong, S. J. (2019). Bakuchiol Suppresses Inflammatory Responses via the Downregulation of the P38 MAPK/ERK Signaling Pathway. *Int. J. Mol. Sci.* 20 (14). doi:10.3390/ijms20143574
- Lim, S. H., Ha, T. Y., Kim, S. R., Ahn, J., Park, H. J., and Kim, S. (2009). Ethanol Extract of Psoralea Corylifolia L. And its Main Constituent, Bakuchiol, Reduce Bone Loss in Ovariectomized Sprague-Dawley Rats. *Br. J. Nutr.* 101 (7), 1031–1039. doi:10.1017/s0007114508066750
- Lindtner, R. A., Tiaden, A. N., Genelin, K., Ebner, H. L., Manzl, C., Klawitter, M., et al. (2014). Osteoanabolic Effect of Alendronate and Zoledronate on Bone Marrow Stromal Cells (BMSCs) Isolated from Aged Female Osteoporotic Patients and its Implications for Their Mode of Action in the Treatment of Age-Related Bone Loss. *Osteoporos. Int.* 25 (3), 1151–1161. doi:10.1007/s00198-013-2494-3
- Little, R. D., Recker, R. R., and Johnson, M. L. (2002). High Bone Density Due to a Mutation in LDL-Receptor-Related Protein 5. *N. Engl. J. Med.* 347 (12), 943–944. doi:10.1056/NEJM200209193471216
- Liu, H., Guo, W., Guo, H., Zhao, L., Yue, L., Li, X., et al. (2020). Bakuchiol Attenuates Oxidative Stress and Neuron Damage by Regulating Trx1/TXNIP and the Phosphorylation of AMPK after Subarachnoid Hemorrhage in Mice. *Front. Pharmacol.* 11, 712. doi:10.3389/fphar.2020.00712
- Long, F. (2011). Building Strong Bones: Molecular Regulation of the Osteoblast Lineage. *Nat. Rev. Mol. Cell. Biol.* 13 (1), 27–38. doi:10.1038/nrm3254
- Luckman, S. P., Hughes, D. E., Coxon, F. P., Graham, R., Russell, G., and Rogers, M. J. (1998). Nitrogen-containing Bisphosphonates Inhibit the Mevalonate Pathway and Prevent Post-translational Prenylation of GTP-Binding Proteins, Including Ras. *J. Bone Min. Res.* 13 (4), 581–589. doi:10.1359/jbmr.1998.13.4.581
- Luegmayr, E., Glantschnig, H., Wesolowski, G. A., Gentile, M. A., Fisher, J. E., Rodan, G. A., et al. (2004). Osteoclast Formation, Survival and Morphology Are Highly Dependent on Exogenous Cholesterol/lipoproteins. *Cell. Death Differ.* 11 (Suppl. 1), S108–S118. doi:10.1038/sj.cdd.4401399
- Lyrakis, G. P., Paspati, I., Karachalios, T., Ioakimidis, D., Skarantavos, G., and Lyrakis, P. G. (1997). Pain Relief from Nasal Salmon Calcitonin in Osteoporotic Vertebral Crush Fractures. A Double Blind, Placebo-Controlled Clinical Study. *Acta Orthop. Scand. Suppl.* 275, 112–114. doi:10.1080/17453674.1997.11744761
- Lyu, H., Yoshida, K., Zhao, S. S., Wei, J., Zeng, C., Tedeschi, S. K., et al. (2020). Delayed Denosumab Injections and Fracture Risk Among Patients with Osteoporosis : A Population-Based Cohort Study. *Ann. Intern. Med.* 173 (7), 516–526. doi:10.7326/m20-0882
- Maeda, K., Kobayashi, Y., Udagawa, N., Uehara, S., Ishihara, A., Mizoguchi, T., et al. (2012). Wnt5a-Ror2 Signaling between Osteoblast-Lineage Cells and Osteoclast Precursors Enhances Osteoclastogenesis. *Nat. Med.* 18 (3), 405–412. doi:10.1038/nm.2653
- Mao, B., Wu, W., Davidson, G., Marhold, J., Li, M., Mechler, B. M., et al. (2002). Kremen Proteins Are Dickkopf Receptors that Regulate Wnt/beta-Catenin Signalling. *Nature* 417 (6889), 664–667. doi:10.1038/nature756
- Maraka, S., and Kennel, K. A. (2015). Bisphosphonates for the Prevention and Treatment of Osteoporosis. *Bmj* 351, h3783. doi:10.1136/bmj.h3783
- Martin, K. J., Bellorin-Font, E., Morrissey, J. J., Jilka, R. L., MacGregor, R. R., and Cohn, D. V. (1983). Relative Sensitivity of Kidney and Bone to the Amino-Terminal Fragment B-PTH (1–30) of Native Bovine Parathyroid Hormone: Implications for Assessment of Bioactivity of Parathyroid Hormone Fragments *In Vivo* and *In Vitro*. *Calcif. Tissue Int.* 35 (4–5), 520–525. doi:10.1007/bf02405087
- McClung, M. R., Grauer, A., Boonen, S., Bolognese, M. A., Brown, J. P., Diez-Perez, A., et al. (2014). Romosozumab in Postmenopausal Women with Low Bone Mineral Density. *N. Engl. J. Med.* 370 (5), 412–420. doi:10.1056/NEJMoa1305224
- McDonald, M. M., Khoo, W. H., Ng, P. Y., Xiao, Y., Zamerli, J., Thatcher, P., et al. (2021). Osteoclasts Recycle via Osteomorphs during RANKL-Stimulated Bone Resorption. *Cell* 184 (5), 1330–e13. e1313. doi:10.1016/j.cell.2021.02.002
- Meyer, M. B., Goetsch, P. D., and Pike, J. W. (2010). A Downstream Intergenic Cluster of Regulatory Enhancers Contributes to the Induction of CYP24A1 Expression by 1alpha,25-Dihydroxyvitamin D3. *J. Biol. Chem.* 285 (20), 15599–15610. doi:10.1074/jbc.M110.119958
- Miyauchi, A., Dinavahi, R. V., Crittenden, D. B., Yang, W., Maddox, J. C., Hamaya, E., et al. (2019). Increased Bone Mineral Density for 1 Year of Romosozumab, vs Placebo, Followed by 2 Years of Denosumab in the Japanese Subgroup of the Pivotal FRAME Trial and Extension. *Arch. Osteoporos.* 14 (1), 59. doi:10.1007/s11657-019-0608-z
- Negishi-Koga, T., and Takayanagi, H. (2009). Ca<sup>2+</sup>-NFATc1 Signaling Is an Essential axis of Osteoclast Differentiation. *Immunol. Rev.* 231 (1), 241–256. doi:10.1111/j.1600-065X.2009.00821.x
- Nicholson, G. C., Moseley, J. M., Sexton, P. M., Mendelsohn, F. A., and Martin, T. J. (1986). Abundant Calcitonin Receptors in Isolated Rat Osteoclasts. Biochemical and Autoradiographic Characterization. *J. Clin. Invest.* 78 (2), 355–360. doi:10.1172/jci.112584
- Pacifici, R., Brown, C., Puschek, E., Friedrich, E., Slatopolsky, E., Maggio, D., et al. (1991). Effect of Surgical Menopause and Estrogen Replacement on Cytokine Release from Human Blood Mononuclear Cells. *Proc. Natl. Acad. Sci. U. S. A.* 88 (12), 5134–5138. doi:10.1073/pnas.88.12.5134
- Pai, F. T., Lu, C. Y., Lin, C. H., Wang, J., Huang, M. C., Liu, C. T., et al. (2021). Psoralea Corylifolia L. Ameliorates Collagen-Induced Arthritis by Reducing Proinflammatory Cytokines and Upregulating Myeloid-Derived Suppressor Cells. *Life (Basel)* 11 (6). doi:10.3390/life11060587
- Palermo, A., Tuccinardi, D., D'Onofrio, L., Watanabe, M., Maggi, D., Maurizi, A. R., et al. (2017). Vitamin K and Osteoporosis: Myth or Reality? *Metabolism* 70, 57–71. doi:10.1016/j.metabol.2017.01.032
- Pan, B., Farrugia, A. N., To, L. B., Findlay, D. M., Green, J., Lynch, K., et al. (2004). The Nitrogen-Containing Bisphosphonate, Zoledronic Acid, Influences RANKL Expression in Human Osteoblast-like Cells by Activating TNF-Alpha Converting Enzyme (TACE). *J. Bone Min. Res.* 19 (1), 147–154. doi:10.1359/jbmr.2004.19.1.147
- Patel, M. S., and Karsenty, G. (2002). Regulation of Bone Formation and Vision by LRP5. *N. Engl. J. Med.* 346 (20), 1572–1574. doi:10.1056/nejm200205163462011
- Pecile, A., Ferri, S., Braga, P. C., and Olgati, V. R. (1975). Effects of Intracerebroventricular Calcitonin in the Conscious Rabbit. *Experientia* 31 (3), 332–333. doi:10.1007/bf01922569
- Pelorgeas, S., Martin, J. B., and Satre, M. (1992). Cytotoxicity of Dichloromethane Diphosphonate and of 1-Hydroxyethane-1,1-Diphosphonate in the Amoebae of the Slime Mould *Dictyostelium discoideum*. A 31P NMR Study. *Biochem. Pharmacol.* 44 (11), 2157–2163. doi:10.1016/0006-2952(92)90342-g
- Peng, S., Liu, X. S., Huang, S., Li, Z., Pan, H., Zhen, W., et al. (2011). The Cross-Talk between Osteoclasts and Osteoblasts in Response to Strontium Treatment: Involvement of Osteoprotegerin. *Bone* 49 (6), 1290–1298. doi:10.1016/j.bone.2011.08.031
- Pereira, A. G., Chiba, F. Y., de Lima Coutinho Mattered, M. S., Pereira, R. F., de Cássia Alves Nunes, R., Tsosura, T. V. S., et al. (2017). Effects of Fluoride on Insulin Signaling and Bone Metabolism in Ovariectomized Rats. *J. Trace Elem. Med. Biol.* 39, 140–146. doi:10.1016/j.jtemb.2016.09.007
- Phillips, B. W., Belmonte, N., Vernochet, C., Ailhaud, G., and Dani, C. (2001). Compactin Enhances Osteogenesis in Murine Embryonic Stem Cells. *Biochem. Biophys. Res. Commun.* 284 (2), 478–484. doi:10.1006/bbrc.2001.4987
- Plotkin, L. I., Aguirre, J. I., Kousteni, S., Manolagas, S. C., and Bellido, T. (2005). Bisphosphonates and Estrogens Inhibit Osteocyte Apoptosis via Distinct Molecular Mechanisms Downstream of Extracellular Signal-Regulated Kinase Activation. *J. Biol. Chem.* 280 (8), 7317–7325. doi:10.1074/jbc.M412817200
- Plotkin, L. I., Lezcano, V., Thostenson, J., Weinstein, R. S., Manolagas, S. C., and Bellido, T. (2008). Connexin 43 Is Required for the Anti-apoptotic Effect of Bisphosphonates on Osteocytes and Osteoblasts *In Vivo*. *J. Bone Min. Res.* 23 (11), 1712–1721. doi:10.1359/jbmr.080617
- Plotkin, L. I., Weinstein, R. S., Parfitt, A. M., Roberson, P. K., Manolagas, S. C., and Bellido, T. (1999). Prevention of Osteocyte and Osteoblast Apoptosis by Bisphosphonates and Calcitonin. *J. Clin. Invest.* 104 (10), 1363–1374. doi:10.1172/jci6800
- Potts, J. T., Jr., Tregear, G. W., Keutmann, H. T., Niall, H. D., Sauer, R., Deftos, L. J., et al. (1971). Synthesis of a Biologically Active N-Terminal

- Tetrapentapeptide of Parathyroid Hormone. *Proc. Natl. Acad. Sci. U. S. A.* 68 (1), 63–67. doi:10.1073/pnas.68.1.63
- Rachner, T. D., Khosla, S., and Hofbauer, L. C. (2011). Osteoporosis: Now and the Future. *Lancet* 377 (9773), 1276–1287. doi:10.1016/s0140-6736(10)62349-5
- Raisz, L. G. (1963). Stimulation of Bone Resorption by Parathyroid Hormone in Tissue Culture. *Nature* 197, 1015–1016. doi:10.1038/1971015a0
- Reginster, J. Y., and Franchimont, P. (1985). Side Effects of Synthetic Salmon Calcitonin Given by Intranasal Spray Compared with Intramuscular Injection. *Clin. Exp. Rheumatol.* 3 (2), 155–157.
- Reid, D. M., Devogelaer, J. P., Saag, K., Roux, C., Lau, C. S., Reginster, J. Y., et al. (2009). Zoledronic Acid and Risedronate in the Prevention and Treatment of Glucocorticoid-Induced Osteoporosis (HORIZON): a Multicentre, Double-Blind, Double-Dummy, Randomised Controlled Trial. *Lancet* 373 (9671), 1253–1263. doi:10.1016/s0140-6736(09)60250-6
- Reid, I. R., and Billington, E. O. (2022). Drug Therapy for Osteoporosis in Older Adults. *Lancet* 399 (10329), 1080–1092. doi:10.1016/s0140-6736(21)02646-5
- Ribeiro, V., Garcia, M., Oliveira, R., Gomes, P. S., Colaço, B., and Fernandes, M. H. (2014). Bisphosphonates Induce the Osteogenic Gene Expression in Co-cultured Human Endothelial and Mesenchymal Stem Cells. *J. Cell. Mol. Med.* 18 (1), 27–37. doi:10.1111/jcmm.12154
- Roggia, C., Gao, Y., Cenci, S., Weitzmann, M. N., Toraldo, G., Isaia, G., et al. (2001). Up-regulation of TNF-Producing T Cells in the Bone Marrow: a Key Mechanism by Which Estrogen Deficiency Induces Bone Loss *In Vivo*. *Proc. Natl. Acad. Sci. U. S. A.* 98 (24), 13960–13965. doi:10.1073/pnas.251534698
- Rozenberg, S., Vandromme, J., and Antoine, C. (2013). Postmenopausal Hormone Therapy: Risks and Benefits. *Nat. Rev. Endocrinol.* 9 (4), 216–227. doi:10.1038/nrendo.2013.17
- Rudman, D., Feller, A. G., Nagraj, H. S., Gergans, G. A., Lalitha, P. Y., Goldberg, A. F., et al. (1990). Effects of Human Growth Hormone in Men over 60 Years Old. *N. Engl. J. Med.* 323 (1), 1–6. doi:10.1056/nejm199007053230101
- Saag, K. G., Petersen, J., Brandi, M. L., Karaplis, A. C., Lorentzen, M., Thomas, T., et al. (2017). Romosozumab or Alendronate for Fracture Prevention in Women with Osteoporosis. *N. Engl. J. Med.* 377 (15), 1417–1427. doi:10.1056/NEJMoa1708322
- Saftig, P., Hunziker, E., Wehmeyer, O., Jones, S., Boyde, A., Rommerskirch, W., et al. (1998). Impaired Osteoclastic Bone Resorption Leads to Osteopetrosis in Cathepsin-K-Deficient Mice. *Proc. Natl. Acad. Sci. U. S. A.* 95 (23), 13453–13458. doi:10.1073/pnas.95.23.13453
- Saidak, Z., Hay, E., Marty, C., Barbara, A., and Marie, P. J. (2012). Strontium Ranelate Rebalances Bone Marrow Adipogenesis and Osteoblastogenesis in Senescent Osteopenic Mice through NFATc/Maf and Wnt Signaling. *Aging Cell.* 11 (3), 467–474. doi:10.1111/j.1474-9726.2012.00804.x
- Sato, M., Grasser, W., Endo, N., Akins, R., Simmons, H., Thompson, D. D., et al. (1991). Bisphosphonate Action. Alendronate Localization in Rat Bone and Effects on Osteoclast Ultrastructure. *J. Clin. Invest.* 88 (6), 2095–2105. doi:10.1172/jci115539
- Sato, M., Vahle, J., Schmidt, A., Westmore, M., Smith, S., Rowley, E., et al. (2002). Abnormal Bone Architecture and Biomechanical Properties with Near-Lifetime Treatment of Rats with PTH. *Endocrinology* 143 (9), 3230–3242. doi:10.1210/en.2002-220149
- Schiavi, J., Fodera, D. M., Brennan, M. A., and McNamara, L. M. (2021). Estrogen Depletion Alters Osteogenic Differentiation and Matrix Production by Osteoblasts *In Vitro*. *Exp. Cell. Res.* 408 (1), 112814. doi:10.1016/j.yexcr.2021.112814
- Sebastian, A., and Loots, G. G. (2018). Genetics of Sost/SOST in Sclerosteosis and Van Buchem Disease Animal Models. *Metabolism* 80, 38–47. doi:10.1016/j.metabol.2017.10.005
- Shearer, M. J. (2000). Role of Vitamin K and Gla Proteins in the Pathophysiology of Osteoporosis and Vascular Calcification. *Curr. Opin. Clin. Nutr. Metab. Care* 3 (6), 433–438. doi:10.1097/00075197-200011000-00004
- Sheng, L., Wu, C. Y., and Chen, X. F. (2011). Inhibitory Acting Mechanism of Psoralen-Osthole on Bone Metastasis of Breast Cancer-Aan Expatiation Viewing from OPG/RANKL/RANK System. *Zhongguo Zhong Xi Yi Jie He Za Zhi* 31 (5), 684–689.
- Shuai, B., Shen, L., Zhu, R., and Zhou, P. (2015). Effect of Qing'e formula on the *In Vitro* differentiation of bone marrow-derived mesenchymal stem cells from proximal femurs of postmenopausal osteoporotic mice. *BMC Complement. Altern. Med.* 15, 250. doi:10.1186/s12906-015-0777-2
- Shuai, B., Zhu, R., Yang, Y. P., Shen, L., Xu, X. J., Ma, C., et al. (2019). Positive Effects of Qing'e Pill ( ) on Trabecular Microarchitecture and its Mechanical Properties in Osteopenic Ovariectomised Mice. *Chin. J. Integr. Med.* 25 (4), 270–277. doi:10.1007/s11655-016-2604-0
- Sillero, M. A., de Diego, A., Tavares, J. E., Silva, J. A., Pérez-Zúñiga, F. J., and Sillero, A. (2009). Synthesis of ATP Derivatives of Compounds of the Mevalonate Pathway (Isopentenyl Di- and Triphosphate; Geranyl Di- and Triphosphate, Farnesyl Di- and Triphosphate, and Dimethylallyl Diphosphate) Catalyzed by T4 RNA Ligase, T4 DNA Ligase and Other Ligases Potential Relationship with the Effect of Bisphosphonates on Osteoclasts. *Biochem. Pharmacol.* 78 (4), 335–343. doi:10.1016/j.bcp.2009.04.028
- Stock, M., and Schett, G. (2021). Vitamin K-dependent Proteins in Skeletal Development and Disease. *Int. J. Mol. Sci.* 22 (17). doi:10.3390/ijms22179328
- Sun, W., Li, M., Xie, L., Mai, Z., Zhang, Y., Luo, L., et al. (2021). Exploring the Mechanism of Total Flavonoids of *Drynariae Rhizoma* to Improve Large Bone Defects by Network Pharmacology and Experimental Assessment. *Front. Pharmacol.* 12, 603734. doi:10.3389/fphar.2021.603734
- Tafaro, L., and Napoli, N. (2021). “Current and Emerging Treatment of Osteoporosis,” in *Orthogeriatrics: The Management of Older Patients with Fragility Fractures*. Editors P. Falaschi and D. Marsh (Cham (CH: Springer), 257–272. doi:10.1007/978-3-030-48126-1\_15
- Takayanagi, H., Kim, S., Koga, T., Nishina, H., Ishiki, M., Yoshida, H., et al. (2002). Induction and Activation of the Transcription Factor NFATc1 (NFAT2) Integrate RANKL Signaling in Terminal Differentiation of Osteoclasts. *Dev. Cell.* 3 (6), 889–901. doi:10.1016/s1534-5807(02)00369-6
- Tankó, L. B., Christiansen, C., Cox, D. A., Geiger, M. J., McNabb, M. A., and Cummings, S. R. (2005). Relationship between Osteoporosis and Cardiovascular Disease in Postmenopausal Women. *J. Bone Min. Res.* 20 (11), 1912–1920. doi:10.1359/jbmr.050711
- Terashima, Y., Takebayashi, T., Jimbo, S., Ogon, I., Sato, T., Ichise, N., et al. (2019). Analgesic Effects of Calcitonin on Radicular Pain in Male Rats. *J. Pain Res.* 12, 223–230. doi:10.2147/jpr.S185233
- Theuvsen, E., Smit, E., and Vermeer, C. (2012). The Role of Vitamin K in Soft-Tissue Calcification. *Adv. Nutr.* 3 (2), 166–173. doi:10.3945/an.111.001628
- Tsai, J. N., Uihlein, A. V., Lee, H., Kumbhani, R., Siwila-Sackman, E., McKay, E. A., et al. (2013). Teriparatide and Denosumab, Alone or Combined, in Women with Postmenopausal Osteoporosis: the DATA Study Randomised Trial. *Lancet* 382 (9886), 50–56. doi:10.1016/s0140-6736(13)60856-9
- Tsugawa, N., and Shiraki, M. (2020). Vitamin K Nutrition and Bone Health. *Nutrients* 12 (7). doi:10.3390/nu12071909
- Vahle, J. L., Long, G. G., Sandusky, G., Westmore, M., Ma, Y. L., and Sato, M. (2004). Bone Neoplasms in F344 Rats Given Teriparatide [rPTH(1-34)] Are Dependent on Duration of Treatment and Dose. *Toxicol. Pathol.* 32 (4), 426–438. doi:10.1080/01926230490462138
- van Beek, E., Pieterman, E., Cohen, L., Löwik, C., and Papapoulos, S. (1999a). Farnesyl Pyrophosphate Synthase Is the Molecular Target of Nitrogen-Containing Bisphosphonates. *Biochem. Biophys. Res. Commun.* 264 (1), 108–111. doi:10.1006/bbrc.1999.1499
- van Beek, E., Pieterman, E., Cohen, L., Löwik, C., and Papapoulos, S. (1999b). Nitrogen-containing Bisphosphonates Inhibit Isopentenyl Pyrophosphate Isomerase/farnesyl Pyrophosphate Synthase Activity with Relative Potencies Corresponding to Their Antiresorptive Potencies *In Vitro* and *In Vivo*. *Biochem. Biophys. Res. Commun.* 255 (2), 491–494. doi:10.1006/bbrc.1999.0224
- Van Beek, E. R., Löwik, C. W., and Papapoulos, S. E. (2002). Bisphosphonates Suppress Bone Resorption by a Direct Effect on Early Osteoclast Precursors without Affecting the Osteoclastogenic Capacity of Osteogenic Cells: the Role of Protein Geranylgeranylation in the Action of Nitrogen-Containing Bisphosphonates on Osteoclast Precursors. *Bone* 30 (1), 64–70. doi:10.1016/s8756-3282(01)00655-x
- van Bezooijen, R. L., Svensson, J. P., Eefting, D., Visser, A., van der Horst, G., Karperien, M., et al. (2007). Wnt but Not BMP Signaling Is Involved in the Inhibitory Action of Sclerostin on BMP-Stimulated Bone Formation. *J. Bone Min. Res.* 22 (1), 19–28. doi:10.1359/jbmr.061002
- Veronese, N., Bano, G., Bertozzo, G., Granziera, S., Solmi, M., Manzato, E., et al. (2015). Vitamin K Antagonists' Use and Fracture Risk: Results from a

- Systematic Review and Meta-Analysis. *J. Thromb. Haemost.* 13 (9), 1665–1675. doi:10.1111/jth.13052
- Viereck, V., Emons, G., Lauck, V., Frosch, K. H., Blaschke, S., Gründker, C., et al. (2002). Bisphosphonates Pamidronate and Zoledronic Acid Stimulate Osteoprotegerin Production by Primary Human Osteoblasts. *Biochem. Biophys. Res. Commun.* 291 (3), 680–686. doi:10.1006/bbrc.2002.6510
- von Knoch, F., Jaquiere, C., Kowalsky, M., Schaeren, S., Alabre, C., Martin, I., et al. (2005). Effects of Bisphosphonates on Proliferation and Osteoblast Differentiation of Human Bone Marrow Stromal Cells. *Biomaterials* 26 (34), 6941–6949. doi:10.1016/j.biomaterials.2005.04.059
- Wagner, E. F., and Eferl, R. (2005). Fos/AP-1 Proteins in Bone and the Immune System. *Immunol. Rev.* 208, 126–140. doi:10.1111/j.0105-2896.2005.00332.x
- Wallin, R., Schurgers, L. J., and Loeser, R. F. (2010). Biosynthesis of the Vitamin K-dependent Matrix Gla Protein (MGP) in Chondrocytes: a Fetuin-MGP Protein Complex Is Assembled in Vesicles Shed from Normal but Not from Osteoarthritic Chondrocytes. *Osteoarthr. Cartil.* 18 (8), 1096–1103. doi:10.1016/j.joca.2010.05.013
- Walsh, B. W., Kuller, L. H., Wild, R. A., Paul, S., Farmer, M., Lawrence, J. B., et al. (1998). Effects of Raloxifene on Serum Lipids and Coagulation Factors in Healthy Postmenopausal Women. *Jama* 279 (18), 1445–1451. doi:10.1001/jama.279.18.1445
- Watkins, H. A., Rathbone, D. L., Barwell, J., Hay, D. L., and Poyner, D. R. (2013). Structure-activity Relationships for  $\alpha$ -calcitonin Gene-Related Peptide. *Br. J. Pharmacol.* 170 (7), 1308–1322. doi:10.1111/bph.12072
- Weng, Z. B., Gao, Q. Q., Wang, F., Zhao, G. H., Yin, F. Z., Cai, B. C., et al. (2015). Positive Skeletal Effect of Two Ingredients of *Psoralea Corylifolia* L. On Estrogen Deficiency-Induced Osteoporosis and the Possible Mechanisms of Action. *Mol. Cell. Endocrinol.* 417, 103–113. doi:10.1016/j.mce.2015.09.025
- Winkler, D. G., Sutherland, M. K., Geoghegan, J. C., Yu, C., Hayes, T., Skonier, J. E., et al. (2003). Osteocyte Control of Bone Formation via Sclerostin, a Novel BMP Antagonist. *Embo J.* 22 (23), 6267–6276. doi:10.1093/emboj/cdg599
- Xiong, J. L., Cai, X. Y., Zhang, Z. J., Li, Q., Zhou, Q., and Wang, Z. T. (2022). Elucidating the Estrogen-like Effects and Biocompatibility of the Herbal Components in the Qing' E Formula. *J. Ethnopharmacol.* 283, 114735. doi:10.1016/j.jep.2021.114735
- Xu, Q., Lv, Q., Liu, L., Zhang, Y., and Yang, X. (2021). New Bakuchiol Dimers from *Psoralea Fructus* and Their Inhibitory Activities on Nitric Oxide Production. *Chin. Med.* 16 (1), 98. doi:10.1186/s13020-021-00499-y
- Xu, Q., Zhang, Y., He, Z., Liu, Z., Zhang, Y., Xu, W., et al. (2022). Constituents Promoting Osteogenesis from the Fruits of *Psoralea Corylifolia* and Their Structure-Activity Relationship Study. *Phytochemistry* 196, 113085. doi:10.1016/j.phytochem.2022.113085
- Xu, Y., Zhang, Z. J., Geng, F., Su, S. B., White, K. N., Bligh, S. W., et al. (2010). Treatment with Qing'E, a Kidney-Invigorating Chinese Herbal Formula, Antagonizes the Estrogen Decline in Ovariectomized Mice. *Rejuvenation Res.* 13 (4), 479–488. doi:10.1089/rej.2009.1000
- Yamamoto, M., Tachikawa, S., and Maeno, H. (1981). Evoked Potential Studies of Porcine Calcitonin in Rabbits. *Neuropharmacology* 20 (1), 83–86. doi:10.1016/0028-3908(81)90047-2
- Yang, T. L., Shen, H., Liu, A., Dong, S. S., Zhang, L., Deng, F. Y., et al. (2020). A Road Map for Understanding Molecular and Genetic Determinants of Osteoporosis. *Nat. Rev. Endocrinol.* 16 (2), 91–103. doi:10.1038/s41574-019-0282-7
- Yang, Y., Yu, T., Tang, H., Ren, Z., Li, Q., Jia, J., et al. (2020). Ganoderma Lucidum Immune Modulator Protein rLZ-8 Could Prevent and Reverse Bone Loss in Glucocorticoids-Induced Osteoporosis Rat Model. *Front. Pharmacol.* 11, 731. doi:10.3389/fphar.2020.00731
- Zhao, J. G., Zeng, X. T., Wang, J., and Liu, L. (2017). Association between Calcium or Vitamin D Supplementation and Fracture Incidence in Community-Dwelling Older Adults: A Systematic Review and Meta-Analysis. *Jama* 318 (24), 2466–2482. doi:10.1001/jama.2017.19344
- Zhuo, Y., Gauthier, J. Y., Black, W. C., Percival, M. D., and Duong, L. T. (2014). Inhibition of Bone Resorption by the Cathepsin K Inhibitor Odanacatib Is Fully Reversible. *Bone* 67, 269–280. doi:10.1016/j.bone.2014.07.013

**Conflict of Interest:** The authors declare that the research was conducted in the absence of any commercial or financial relationships that could be construed as a potential conflict of interest.

**Publisher's Note:** All claims expressed in this article are solely those of the authors and do not necessarily represent those of their affiliated organizations, or those of the publisher, the editors and the reviewers. Any product that may be evaluated in this article, or claim that may be made by its manufacturer, is not guaranteed or endorsed by the publisher.

Copyright © 2022 Lu, Hu, Ma and Shuai. This is an open-access article distributed under the terms of the Creative Commons Attribution License (CC BY). The use, distribution or reproduction in other forums is permitted, provided the original author(s) and the copyright owner(s) are credited and that the original publication in this journal is cited, in accordance with accepted academic practice. No use, distribution or reproduction is permitted which does not comply with these terms.





## OPEN ACCESS

## EDITED BY

Dongwei Zhang,  
Beijing University of Chinese Medicine,  
China

## REVIEWED BY

Cheng Xiao,  
China-Japan Friendship Hospital, China  
Liming Xue,  
Shanghai Municipal Center for Disease  
Control and Prevention (SCDC), China  
Gary Xiao,  
Dalian University of Technology, China

## \*CORRESPONDENCE

Yanjing Chen,  
chenyj010@163.com  
Zhiguo Zhang,  
zzgtcm@163.com

<sup>†</sup>These authors have contributed equally  
to this work

## SPECIALTY SECTION

This article was submitted to  
Experimental Pharmacology and Drug  
Discovery,  
a section of the journal  
Frontiers in Pharmacology

RECEIVED 22 May 2022

ACCEPTED 28 June 2022

PUBLISHED 15 July 2022

## CITATION

Cheng Y, Liu H, Li J, Ma Y, Song C,  
Wang Y, Li P, Chen Y and Zhang Z (2022),  
Monascin abrogates RANKL-mediated  
osteoclastogenesis in RAW264.7 cells  
via regulating MAPKs  
signaling pathways.  
*Front. Pharmacol.* 13:950122.  
doi: 10.3389/fphar.2022.950122

## COPYRIGHT

© 2022 Cheng, Liu, Li, Ma, Song, Wang,  
Li, Chen and Zhang. This is an open-  
access article distributed under the  
terms of the [Creative Commons  
Attribution License \(CC BY\)](#). The use,  
distribution or reproduction in other  
forums is permitted, provided the  
original author(s) and the copyright  
owner(s) are credited and that the  
original publication in this journal is  
cited, in accordance with accepted  
academic practice. No use, distribution  
or reproduction is permitted which does  
not comply with these terms.

# Monascin abrogates RANKL-mediated osteoclastogenesis in RAW264.7 cells via regulating MAPKs signaling pathways

Yin Cheng<sup>1†</sup>, Haixia Liu<sup>1†</sup>, Jing Li<sup>2</sup>, Yujie Ma<sup>1</sup>, Changheng Song<sup>1</sup>,  
Yuhan Wang<sup>1</sup>, Pei Li<sup>1</sup>, Yanjing Chen<sup>1\*</sup> and Zhiguo Zhang<sup>1\*</sup>

<sup>1</sup>Institute of Basic Theory, China Academy of Chinese Medical Sciences, Beijing, China, <sup>2</sup>Institute of Basic Medical Sciences Chinese Academy of Medical Sciences, School of Basic Medicine Peking Union Medical College, Center of Excellence in Tissue Engineering, Chinese Academy of Medical Sciences; Beijing Key Laboratory of New Drug Development and Clinical Trial of Stem Cell Therapy (BZ0381), Beijing, China

Osteoclasts (OCs) are multinucleated cells that play a major role in osteolytic diseases such as osteoporosis. Monascin (Ms) is one of the active substances in the traditional Chinese medicine red yeast rice. Studies have found that red yeast rice can maintain bone health. In this study, the anti-osteoclastogenesis effects of Ms on RANKL-induced RAW264.7 cells were assessed, and the underlying mechanism was investigated. Ms exhibited inhibitory effects on OC differentiation and formation in a dose-dependent manner and suppressed the bone-resorbing activity of mature OCs. Ms blocked OCs-typical genes (c-Fos, NFATc1, CSTK, MMP-9, TRAP, ITG- $\beta$ 3, OSCAR and DC-STAMP). Furthermore, Ms treatment considerably inhibited the activation of MAPKs, JNK and p38. Taken together, Ms suppresses RANKL-induced osteoclastogenesis of RAW264.7 cells by restraining MAPKs signaling pathways and is a potential therapeutic option as a novel OC inhibitor to mitigate bone erosion.

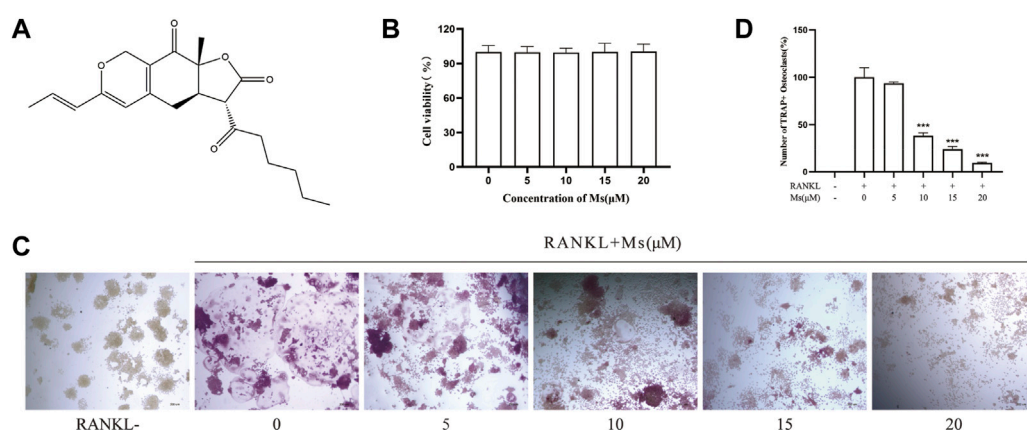
## KEYWORDS

monascin, osteoclast, RAW264.7, bone resorption, mapks, osteoporosis

## Introduction

The bones of human body provide surprisingly sophisticated support for the entire body as they protect the internal organs and are involved in metabolism (Karsenty and Ferron, 2012; Wang et al., 2021). As a mineralized connective tissue, bones are dynamically remodeled throughout life, consisting of three consecutive and cyclic phases: resorption, reversal and formation (Siddiqui and Partridge, 2016; Chen et al., 2018). Several bone diseases result from the disruption of the balance between osteoclasts (OCs) and osteoblasts. Excessive OC bone resorption results in osteoporosis and rheumatoid arthritis, characterized by low bone density, whereas the contrary may



**FIGURE 1**

Inhibitory effect of Ms on RANKL-induced osteoclast formation *in vitro*. **(A)** Chemical structure of Ms. **(B)** Viability of RAW264.7 cells. RAW264.7 cells exposed to 5, 10, 15 and 20 μM Ms were assessed by CCK-8 kits after 72 h. **(C)** The osteoclast morphology after incubation with RANKL and Ms at 5, 10, 15 and 20 μM for 5 days. TRAP-positive cells (TRAP+) (nuclei ≥ 3) were photographed by a light microscope, original magnification x200 (Scale bar = 200 μm). **(D)** Quantitative assessment of TRAP-positive cells. The results represent the mean ± SD of three independent samples. \* $p < 0.05$ , \*\* $p < 0.01$ , \*\*\* $p < 0.001$  vs. Control (RANKL+, Ms-).

contribute to osteopetrosis, marked by high bone density (Jacome-Galarza et al., 2019; Blangy et al., 2020). Inhibiting OC formation and function is a viable strategy for treating low bone density diseases.

OCs are terminally differentiated macrophage multinucleated cells tightly attached to the bone surface, derived from myeloid mononuclear cells. Their differentiation depends on multiple factors (Asagiri and Takayanagi, 2007). Previous research reported the essential roles of the macrophage colony-stimulating factor (M-CSF) and the receptor activator of nuclear factor kappa-B ligand (RANKL) in OC differentiation, formation and function (Song et al., 2019; Zhao et al., 2019; Kitauro et al., 2020). M-CSF not only stimulates the proliferation and survival of the OC precursor cells but also upregulates RANK expression (Asagiri and Takayanagi, 2007). The RANKL-induced osteoclastogenesis is a sequential process comprising three stages: integration to its receptor RANK to recruit the adaptor molecule TNF receptor-associated factor 6 (TRAF6), resulting in mitogen-activated protein kinases (MAPKs) and nuclear factor-kappa B (NF-κB) activation, and promoting the expression of OCs-typical genes (Sun et al., 2021).

MAPKs signal pathways are indispensable in OC differentiation and bone resorption, including extracellular signal-regulated kinase (ERK), c-Jun N-terminal kinase (JNK), and p38 signaling (Lee et al., 2018). ERKs regulate the transcription factors c-Fos and nuclear factor of activated T-cells, cytoplasmic (NFATc) 1, which are involved in the differentiation, migration and function of OCs (He et al., 2011). JNK signaling is activated by RANKL through

inflammatory cytokines such as TRAF6, mainly affecting the fusion and tartrate-resistant acid phosphatase (TRAP) activity of OC precursors (Chang et al., 2008; Ikeda et al., 2008). RANKL-RANK signaling induces p38 phosphorylation and NF-κB activation (Matsumoto et al., 2000), which directly influences the fusion factors such as dendrocyte-expressed seven-transmembrane protein (DC-STAMP) and ITG-β3, as well as function factors, including TRAP, cathepsin K (CTSK) and matrix metalloproteinase 9 (MMP-9) (Mansky et al., 2002; Herbert et al., 2015).

Red yeast rice (RYR) has been used in East Asian countries for thousands of years as a food supplement or herbal medicine and is produced by the fermentation of rice with *Monascus purpureus* (Nguyen et al., 2017). According to numerous previous researches, RYR has been reported to maintain bone health (Wong and Rabie, 2008; Wang et al., 2015; Wu et al., 2020) and be effective against a variety of diseases such as hyperlipidemia, osteoporosis and cardiovascular disease (Wang et al., 2015; Liu et al., 2017; Xiong et al., 2017; Wang et al., 2019; Wu et al., 2020). Notably, *Monascus purpureus* has been shown to produce many functional monascus pigments, applied as a food colorant, functional foods or treatment for some diseases (Patakova, 2013). Yellow pigments monascin (Ms, Figure 1A) has a potential role in alleviating metabolic syndrome (Lin et al., 2017). It has anti-inflammatory, antioxidant and other properties (Lin et al., 2017; Zhang et al., 2020). The effect of Ms on OCs has not been investigated yet.

This study explores the role of Ms in RANKL-induced OC differentiation and bone resorption *in vitro* and investigates its

potential mechanism. Ms may provide a treatment strategy for osteoporosis.

## Materials and methods

### Materials

RAW264.7 cells were purchased from the Institute of Basic Medicine of Peking Union Medical College (Beijing, China). High glucose Dulbecco minimum essential medium (DMEM) and fetal bovine serum (FBS) were sourced from Gibco Company (Rockford, IL, United States). Recombinant Mouse RANKL (462-TEC-010/CF) was obtained from R&D Systems (R&D, Minneapolis, United States). Leukocyte Acid Phosphatase (TRAP) Kits (G1492), bovine bone slices (IDS, Jelling, Denmark), 1% toluidine blue O solution in sodium borate (G3663) were obtained from the Solarbio company (Beijing, China). Monascin (Ms, CAS: 21,516-68-7, purity>98% by HPLC) was purchased from Chengdu Desite Bio-Technology Company (Chengdu, China). All cell culture plasticware was supplied by Corning (NY, United States). Primary antibodies of p-p38(Thr180/Tyr182), p-ERK (Thr202/Tyr204), p-JNK(Thr183/Tyr185) and NFATc1 were products of Cell Signaling Technology (Beverly, MA, United States). Primary antibodies of c-Fos and secondary antibodies were purchased from the Proteintech group (Rocky Hill, United States).

### Cell culture and viability assay

RAW264.7 cells were cultured in DMEM supplemented with 10% FBS (complete DMEM) at 37 °C in a 5% CO<sub>2</sub> incubator with humidified air.

To determine the effect of Ms on the viability of RAW264.7 cells, Cell Counting Kit-8 (CCK-8) assays were used. The cells at a density of  $8 \times 10^3$  cells per well were seeded into a sterile 96-well plate, and incubated for 24 h to allow the cells to attach to the plate. After incubation with Ms at concentrations of 0–20  $\mu$ M for 72 h, 100  $\mu$ L 10% CCK-8 solution was added to replace the original medium, followed by 4 h of incubation at 37°C, and the absorbance at 450 nm was measured using a microplate reader.

### TRAP staining assay

TRAP staining was conducted to identify the morphology of mature OCs. RAW264.7 cells were cultured overnight in a 24-well plate at a density of  $1 \times 10^4$  cells per well for adherence and then stimulated with 0, 5, 10, 15 and 20  $\mu$ M Ms respectively in combination with RANKL 50 ng/ml. After

5 days, the cells were fixed with 4% paraformaldehyde for 5 min at 4°C and then stained with the TRAP staining kit according to the manufacturer's instructions. Cells with more than three nuclei were identified as TRAP-positive multinucleated cells (TRAP (+)), which were counted and photographed using a light microscope.

### Bone resorption assay

RAW264.7 cells ( $8 \times 10^3$  cells per well) were seeded in a 96-well plate containing a sterile bovine bone slice, using the same methods of stimulation and cultivation as described previously. After a 7-days incubation period, all slices were washed in an ultrasonic instrument with 0.1% aqueous ammonia to remove the cells adhered to the surface. Subsequently, the bone slices were stained with 1% toluidine blue solution as described in the previous experiment described. Resorption pits were photographed using a microscope, and the percentage resorption was analyzed using Image-Pro Plus.

### F-actin ring formation assay

RAW264.7 cells at a density of  $1 \times 10^4$  cells per well were induced in 24-well plates in a complete medium with RANKL (50 ng/ml) and Ms (0, 5, 10, 15 and 20  $\mu$ M) for 5 days. The cells were fixed in 4% paraformaldehyde for 20 min, permeabilized with 0.1% TritonX-100 for 10 min, and stained with rhodamine-conjugated phalloidin for 40 min at 4°C to visualize F-actin cytoskeleton. Finally, the actin rings of mature OCs were captured using a fluorescence microscope. The fluorescence images were processed by Image-Pro Plus software.

### Quantitative real-time PCR (RT-qPCR)

RAW264.7 cells ( $4 \times 10^4$  cells per well) were seeded in 12-well plates using the same methods. Total RNA was extracted from cells by TRIzol reagent. After isolation, 3  $\mu$ g total RNA from each sample was reverse transcribed into cDNA by Oligo (dT) and M-MLV reverse transcriptase. Thereafter, using SYBR Green detection and specific primers (listed in Table 1), the RT-generated DNA (0.5  $\mu$ L) was amplified by a Bio-rad real-time PCR detection system. On completion of the reaction, gene expression values were calculated following the relative quantification method ( $2^{-\Delta\Delta CT}$ ; means  $\pm$  SD of triplicate determination).

### Western blot analysis

The cells were washed three times with ice-cold PBS, and lysed in radioimmunoprecipitation assay (RIPA) buffer

TABLE 1 RT-qPCR related primers.

Gene Names	Forward primer sequence (5'-3')	Reverse primer sequence (5'-3')
<i>β-actin</i>	GGCTGTATTCCCTCCATCG	CCAGTTGGTAACAATGCCATGT
<i>c-Fos</i>	CGGGTTTCAACGCCGACTA	TGGCACTAGAGACGGACAGAT
<i>NFATc1</i>	GCCTTTTGCAGCAGTATCTG	GCTGCACCTCGATCCGAAG
<i>MMP-9</i>	GGACCCGAAGCGGACATTG	CGTCGTCGAAATGGGCATCT
<i>CTSK</i>	CTCGGCGTTTAATTGGGAGA	TCGAGAGGGAGGTATTCTGAGT
<i>TRAP</i>	CACTCCACCCCTGAGATTTGT	CATCGTCTGCACGGTTCTG
<i>ITG-β3</i>	CCTCTTCGGCTACTCGGTG	CCAGTCCGGTTGGTATAGTCATC
<i>OSCAR</i>	CCGTGCTGACTTCACACCAA	GGGGTGACAAGGCCACTTTT
<i>DC-STAMP</i>	CTGTGTCCTCCGCTGAATAA	AGCCGATACAGCAGATAGTCC

supplemented with Protease Inhibitor Cocktail and phenylmethylsulfonyl fluoride (PMSF) to obtain total protein. Proteins were quantitated using a bicinchoninic acid protein assay kit, separated on a 10% polyacrylamide gel, and transferred to a polyvinylidene difluoride membrane. Subsequently, the membranes were blocked with 5% skimmed milk for 1 h at room temperature, and then incubated with the indicated primary antibodies including c-Fos (1:500), NFATc1 (1:1,000), p-p38 (1:1,000), p-JNK (1:1,000), p-ERK (1:1,000) and GAPDH (1:1,000) at 4 °C overnight. Then, the membranes were incubated with the corresponding horseradish peroxidase-conjugated secondary antibodies for 2 h, visualized with the ECL system, and analyzed by ImageJ software.

## Statistical analysis

Statistical analysis was performed with SPSS 25.0 software. The data are expressed as mean ± standard deviation (SD). Two-group comparisons were conducted using the Students' *t*-test, multiple-group comparisons were conducted using one-way ANOVA, and any two-group comparisons were conducted by SNK-q test. Differences were considered to be statistically significant if  $p < 0.05$ .

## Results

### Ms inhibited RANKL-induced osteoclastogenesis

Ms treatment at concentrations of 0–20 μM for 72 h did not affect the viability of OC precursors (Figure 1B). TRAP is considered a histochemical marker of OCs (Lv et al., 2015). A TRAP staining assay was used to explore whether Ms suppressed RANKL-induced OC formation. As shown in Figures 1C,D, the number of TRAP-positive multinuclear cells increased

substantially in response to RANKL stimulation. Still, Ms treatment suppressed the purple giant multinucleated cells induced by RANKL in a dose-dependent manner. Collectively, these results indicate that Ms inhibits the OC formation and differentiation of RANKL-stimulated RAW264.7 cells.

### Ms affected OC morphology and bone resorption *in vitro*

Mature OCs play an essential role in polarization and adherence in bone resorption due to their unique morphological characteristics, consisting of an actin ring structure and a ruffled border membrane (Garbe et al., 2012; Georgess et al., 2014). In this study, F-actin rings were visualized by phalloidin staining and bone resorption pits were identified by toluidine blue staining. As illustrated in Figures 2A–D, numerous F-actin rings and bone resorption pits were generated in RANKL-induced RAW264.7-OCs, which were significantly reduced following Ms treatment in a dose-dependent manner. These results indicate that Ms inhibits the OC bone resorption.

### Ms reduced the expression of OC-related genes

Western blot analysis was carried out to investigate whether Ms inhibited c-Fos and NFATc1. As shown in Figures 3A,C, Ms significantly inhibited c-Fos and NFATc1 protein levels. Furthermore, RT-qPCR was performed to analyze expression levels of OC-specific genes in the absence or presence of Ms. As shown in Figures 3B,D, Ms had a strong inhibitory effect on c-Fos and NFATc1 genes, essential transcription factors and master regulators of osteoclastogenesis. In addition, we found that several NFATc1-regulated genes, including MMP-9, CTSK, TRAP, ITG-β3, OSCAR and DC-STAMP, were upregulated in RANKL-induced RAW264.7-OCs, but downregulated by Ms in a

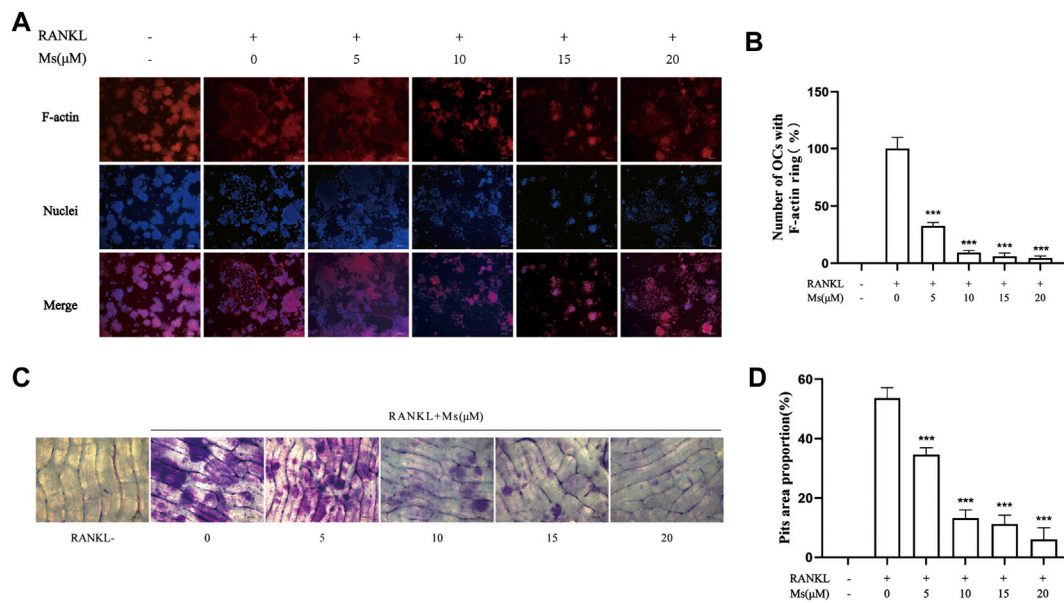


FIGURE 2

Ms inhibits formation of the F-actin ring and osteoclast resorptive function induced by RANKL *in vitro*. RAW264.7 macrophages were cultured in 24-well plates with or without Ms (5, 10, 15 and 20  $\mu$ M) in the presence of 50 ng/ml RANKL for 5 days. **(A)** Representative images of F-actin rings; F-actin: red, nuclei: blue, original magnification  $\times 200$  (Scale bar = 200  $\mu$ m) **(B)** Quantitative analyses of osteoclast numbers with intact F-actin ring. RAW264.7 macrophages were cultured on a bone slice in 96-well plates with or without Ms (5, 10, 15 and 20  $\mu$ M) in the presence of 50 ng/ml RANKL for 7 days. **(C)** Resorption pits of osteoclasts were captured by a light microscope. Original magnification  $\times 200$  (Scale bar = 200  $\mu$ m) **(D)** The resorbed areas were calculated using Image (J). The results represent the mean  $\pm$  SD of three independent samples. \* $p < 0.05$ , \*\* $p < 0.01$ , \*\*\* $p < 0.001$  vs. Control (RANKL+, Ms-).

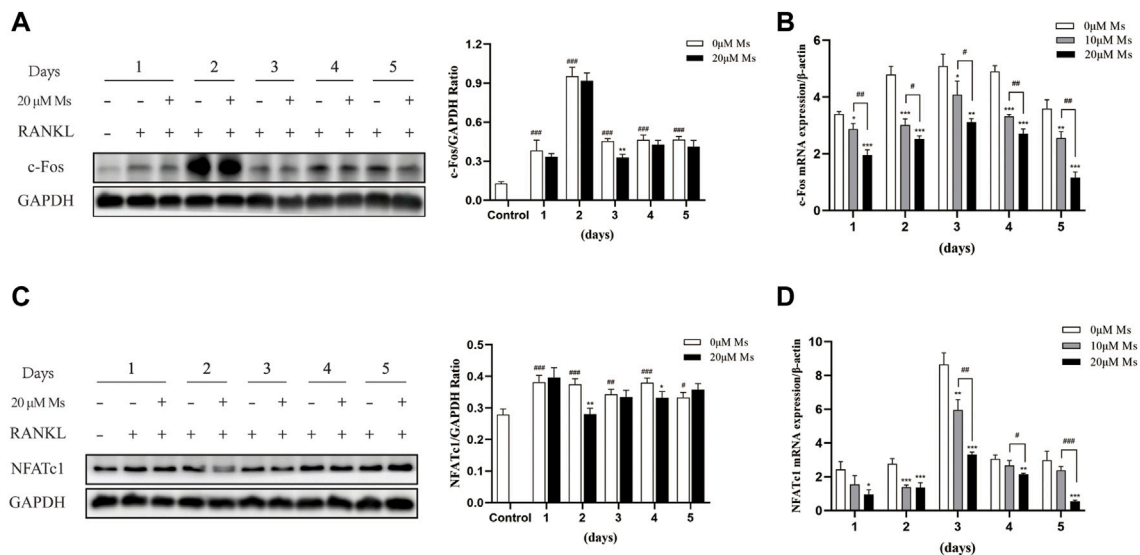


FIGURE 3

Effect of Ms on NFATc1 and c-Fos expression in RANKL-induced RAW264.7 cells. RAW264.7 cells were treated with varying concentrations of Ms with RANKL (50 ng/ml) for 5 days. The proteins were extracted to analyze c-Fos and NFATc1 expression by Western blot per day (A and C). The mRNA expression levels of c-Fos and NFATc1 genes were analyzed using RT-qPCR per day (B and D). Each point represents the mean  $\pm$  SD. The experiments were repeated three times. # $p < 0.05$ , ## $p < 0.01$  and ### $p < 0.001$  vs. Control group (RANKL-, Ms-); \* $p < 0.05$ , \*\* $p < 0.01$  vs. \*\*\* $p < 0.001$  vs. corresponding time 0  $\mu$ M Ms group (RANKL+, Ms-).

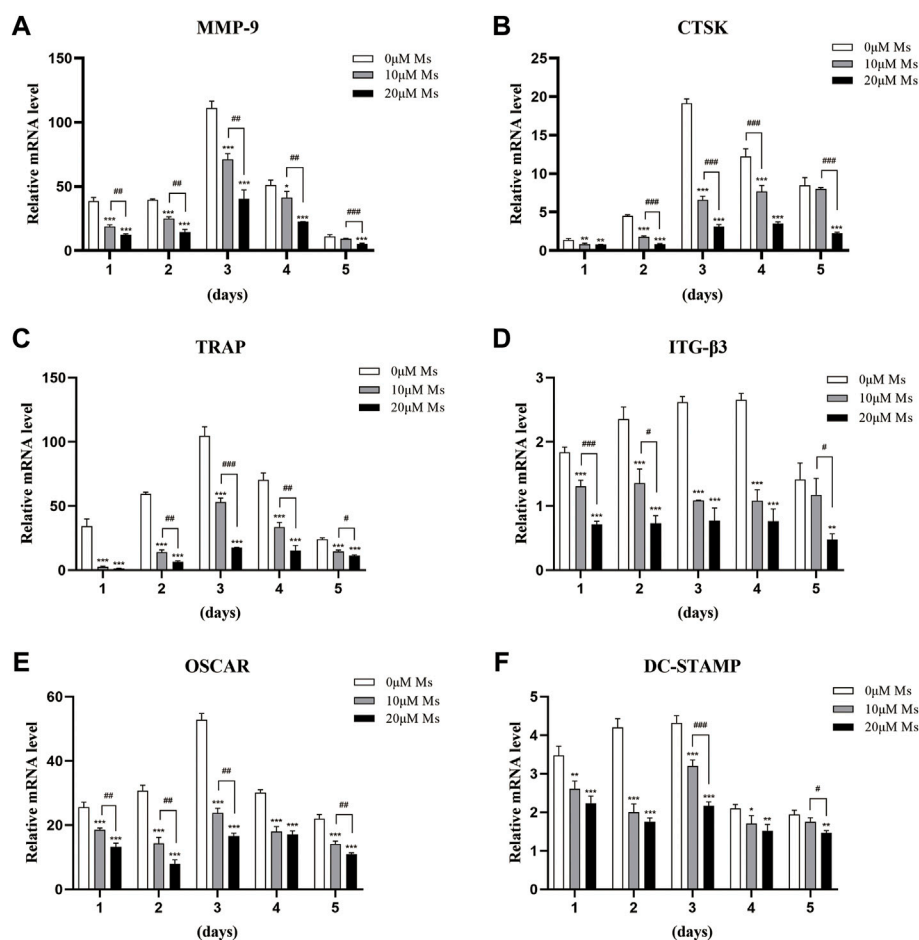


FIGURE 4

Ms inhibits the RANKL-induced expression of osteoclast marker genes. RAW264.7 cells were treated with or without Ms (10 and 20  $\mu$ M) in the presence of RANKL (50 ng/ml) after a 1–5 days culture period. The mRNA expression levels of osteoclast-specific genes, such as MMP-9 (A), CTSK (B), TRAP (C), ITG- $\beta$ 3 (D), OSCAR (E), and DC-STAMP (F), were analyzed using RT-qPCR. \* $p < 0.05$ , \*\* $p < 0.01$  vs. \*\*\* $p < 0.001$  vs. corresponding time 0  $\mu$ M Ms group (RANKL+, Ms-); # $p < 0.05$ , ## $p < 0.01$  and ### $p < 0.001$  vs. corresponding time 10  $\mu$ M Ms group (RANKL+, Ms+).

dose-dependent manner (Figure 4). These results suggest that Ms inhibits osteoclastogenesis via suppressing the expression of these genes.

## Ms suppressed the activation of the MAPKs pathways

RANKL bind to its receptor RANK to activate a series of intracellular signaling pathways involved in OC differentiation, proliferation and survival (Leibbrandt and Penninger, 2009), including MAPKs pathways, which activate various transcription factors through phosphorylation (Ono and Nakashima, 2018). Firstly, western blot analysis was carried out to investigate whether Ms inhibited the activation and phosphorylation

of MAPKs. Treatment with RANKL significantly increased the phosphorylation of JNK and p38 within 60 min, except ERK (Figure 5). Treatment with Ms for 15 min attenuated the phosphorylation of p38, JNK and ERK (Figure 5). These findings suggest that Ms inhibits RANKL induced osteoclastogenesis and bone resorption by suppressing MAPKs signal pathways in OCs.

## Discussion

Osteoclasts are essential in the complex process of bone remodeling and are related to lytic bone disorders, including osteoporosis and bone tumor metastasis, according to previous studies (Novack and Teitelbaum, 2008). Inhibiting OC formation is a promising strategy for these diseases. However, synthetic



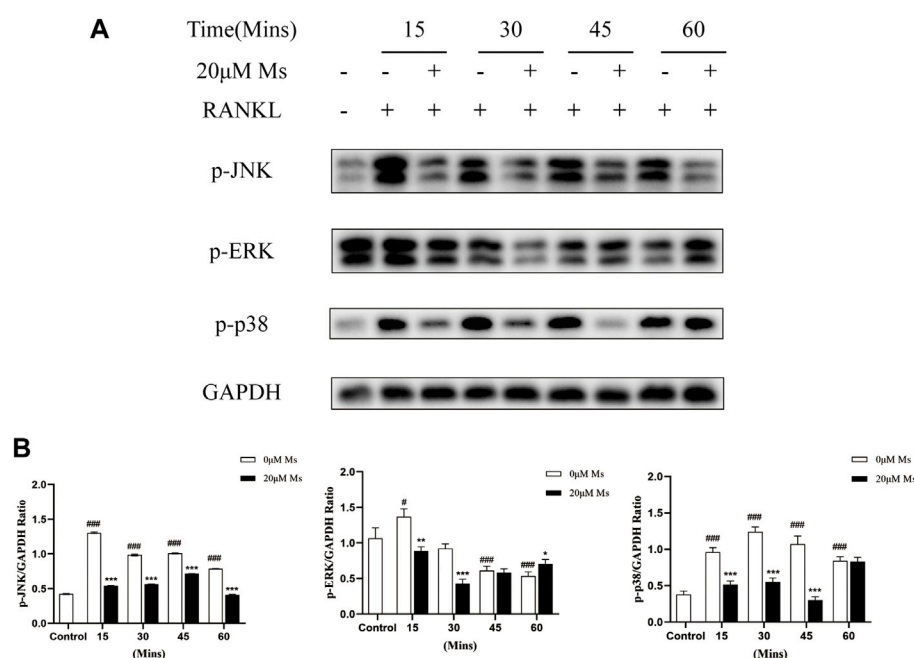


FIGURE 5

Ms inhibits RANKL-induced osteoclast differentiation by suppressing MAPKs signaling pathways. RAW264.7 cells were treated with or without Ms (20 μM) in the presence of RANKL. Protein levels of MAPKs activation, including JNK, ERK and p38, were detected by western blot at 0, 15, 30, 45 and 60 min. The results were expressed as means ± SD from three independent experiments. # $p < 0.05$ , ## $p < 0.01$  and ### $p < 0.001$  vs. Control group (RANKL-, Ms-); \* $p < 0.05$ , \*\* $p < 0.01$  vs. \*\*\* $p < 0.001$  vs. corresponding time 0 μM Ms group (RANKL+, Ms-).

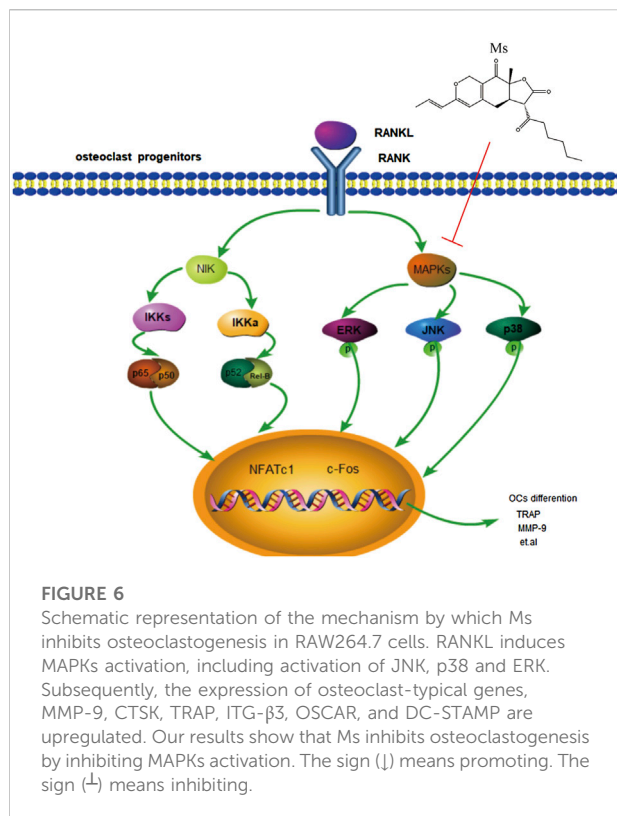
drugs usually cause severe side effects relative to natural components from herbal medicine. In this study, we performed a TRAP staining assay and observed that Ms inhibited RANKL-induced osteoclastogenesis. In addition, bone resorption was suppressed by Ms *in vitro*. Ms also suppressed OCs-typical genes in a dose-dependent manner. Furthermore, Ms inhibited the RANKL-induced phosphorylation of p38, JNK and ERK, and activation of c-Fos and NFATc1 in RANKL-induced RAW264.7-OCs.

The RAW264.7 cell lineage is well-accepted and vastly used as a cellular model in osteoclastogenic research, supporting the exploration of the biological mechanisms of osteoclastogenesis (Collin-Osdoby and Osdoby, 2012). Mature OCs are giant, multinuclear, and polarized cells characterized by rearrangements of the actin cytoskeleton and a sealed compartment between the bone surface and basal membrane. Mature OCs are responsible for the digestion of the bone matrix (Boyle et al., 2003). In the first stage of this study, we defined TRAP-positive OCs and bone resorption area as indicators. The results revealed that Ms treatment significantly decreased the number of TRAP (+) cells, bone resorption area and F-actin rings compared to the RANKL-induced RAW264.7-OCs group. The findings suggest that Ms inhibits RANKL-mediated osteoclastogenesis and bone resorption. The underlying

mechanisms of the inhibitory properties of Ms were investigated in subsequent experiments.

NFATc1 is a common target gene of both NF-κB and AP-1 in the early phase of RANKL-stimulated osteoclastogenesis. The former is recruited by the NFATc1 promoter, and the latter, containing c-Fos, assists NFATc1 (Ishida et al., 2002; Asagiri and Takayanagi, 2007). Cumulative evidence also indicates that c-Fos activation is a prerequisite for NFATc1 because RANKL-induced NFATc1 is completely abrogated in c-Fos-deficient cells (Takayanagi et al., 2002; Matsuo et al., 2004). In the second stage of our study, the essential transcription factors of c-Fos and NFATc1 were measured. Subsequently, we detected the OC-specific gene expression regulated by NFATc1, including TRAP, CTSK, MMP-9, OSCAR, DC-STAMP, and ITG-β3. Ms suppressed the activation of c-Fos and NFATc1 and reduced the expression of OC formation/function-related genes in a dose-dependent manner.

The stimuli of extracellular signaling transmission to coordinated intracellular molecules by MAPKs activation has been demonstrated to be significant for osteoclastogenesis (Lee et al., 2018; Qu et al., 2021). Both M-CSF and RANKL act through MAPKs, including ERK, JNK, and p38 signaling as cultured bone marrow/RAW264.7 cells differentiate into OCs (Ross, 2006; Lee et al., 2016). In the third stage of our study, we



explored the inhibitory effect of Ms on the MAPKs signaling pathway. A series of experiments indicated that Ms attenuated the phosphorylation of p38, JNK and ERK. These results suggest that Ms inhibited RANKL-induced RAW264.7-OCs via blocking the MAPKs signaling pathways.

Taken together, this study was shown that Ms has potential anti-osteoclastogenic effects by inhibiting the MAPKs signaling pathways activation (Figure 6). Furthermore, Ms inhibits the transcription factors NFATc1 and c-Fos, resulting in decreased expression of OC-specific genes such as TRAP, CTSK, MMP-9, OSCAR, DC-STAMP, and ITG-β3. This study provides fundamental knowledge about the effects of Ms on osteoclastogenesis and insight into the therapeutic potential for diseases such as osteoporosis. In the future, animal studies will be performed to determine whether Ms retains its anti-

osteoclastogenic effects and its impact on the MAPKs pathways *in vivo*.

## Data availability statement

The raw data supporting the conclusions of this article will be made available by the authors, without undue reservation.

## Author contributions

ZZ, YC and HL conceived the idea, drafted the manuscript and revised the manuscript. HL and JL conducted experimental guidance. YC performed the experiments and organized the manuscript. YM, CS, YW and PL helped to perform experiments.

## Funding

This work was supported by the CACMS Innovation Fund (grant number CI2021A00107), the National Natural Science Foundation of China (grant number 82074297) and the Fundamental Research Funds for the Central Public Welfare Research Institutes (grant numbers YZ-202147, YZ-202108).

## Conflict of interest

The authors declare that the research was conducted in the absence of any commercial or financial relationships that could be construed as a potential conflict of interest.

## Publisher's note

All claims expressed in this article are solely those of the authors and do not necessarily represent those of their affiliated organizations, or those of the publisher, the editors and the reviewers. Any product that may be evaluated in this article, or claim that may be made by its manufacturer, is not guaranteed or endorsed by the publisher.

## References

- Asagiri, M., and Takayanagi, H. (2007). The molecular understanding of osteoclast differentiation. *Bone* 40 (2), 251–264. doi:10.1016/j.bone.2006.09.023
- Blangy, A., Bompard, G., Guerit, D., Marie, P., Maurin, J., Morel, A., et al. (2020). The osteoclast cytoskeleton - Current understanding and therapeutic perspectives for osteoporosis. *J. Cell Sci.* 133 (13), jcs244798. doi:10.1242/jcs.244798
- Boyle, W. J., Simonet, W. S., and Lacey, D. L. (2003). Osteoclast differentiation and activation. *Nature* 423 (6937), 337–342. doi:10.1038/nature01658
- Chang, E. J., Ha, J., Huang, H., Kim, H. J., Woo, J. H., Lee, Y., et al. (2008). The JNK-dependent CaMK pathway restrains the reversion of committed cells during osteoclast differentiation. *J. Cell Sci.* 121 (15), 2555–2564. doi:10.1242/jcs.028217
- Chen, X., Wang, Z., Duan, N., Zhu, G., Schwarz, E. M., Xie, C., et al. (2018). Osteoblast-osteoclast interactions. *Connect. Tissue Res.* 59 (2), 99–107. doi:10.1080/03008207.2017.1290085
- Collin-Osdoby, P., and Osdoby, P. (2012). RANKL-mediated osteoclast formation from murine RAW 264.7 cells. *Methods Mol. Biol.* 816, 187–202. doi:10.1007/978-1-61779-415-5\_13

- Garbe, A. I., Roscher, A., Schüler, C., Lutter, A. H., Glösmann, M., Bernhardt, R., et al. (2012). Regulation of bone mass and osteoclast function depend on the F-actin modulator SWAP-70. *J. Bone Min. Res.* 27 (10), 2085–2096. doi:10.1002/jbmr.1670
- Georgess, D., Machuca-Gayet, I., Blangy, A., and Jurdic, P. (2014). Podosome organization drives osteoclast-mediated bone resorption. *Cell adh. Migr.* 8 (3), 191–204. doi:10.4161/cam.27840
- He, Y., Staser, K., Rhodes, S. D., Liu, Y., Wu, X., Park, S. J., et al. (2011). Erk1 positively regulates osteoclast differentiation and bone resorptive activity. *PLoS One* 6 (9), e24780. doi:10.1371/journal.pone.0024780
- Herbert, B. A., Valerio, M. S., Gaestel, M., and Kirkwood, K. L. (2015). Sexual dimorphism in MAPK-activated protein kinase-2 (MK2) regulation of RANKL-induced osteoclastogenesis in osteoclast progenitor subpopulations. *PLoS One* 10 (5), e0125387. doi:10.1371/journal.pone.0125387
- Ikeda, F., Matsubara, T., Tsurukai, T., Hata, K., Nishimura, R., Yoneda, T., et al. (2008). JNK/c-Jun signaling mediates an anti-apoptotic effect of RANKL in osteoclasts. *J. Bone Min. Res.* 23 (6), 907–914. doi:10.1359/jbmr.080211
- Ishida, N., Hayashi, K., Hoshijima, M., Ogawa, T., Koga, S., Miyatake, Y., et al. (2002). Large scale gene expression analysis of osteoclastogenesis *in vitro* and elucidation of NFAT2 as a key regulator. *J. Biol. Chem.* 277 (43), 41147–41156. doi:10.1074/jbc.M205063200
- Jacome-Galarza, C. E., Percin, G. I., Muller, J. T., Mass, E., Lazarov, T., Eitler, J., et al. (2019). Developmental origin, functional maintenance and genetic rescue of osteoclasts. *Nature* 568 (7753), 541–545. doi:10.1038/s41586-019-1105-7
- Karsenty, G., and Ferron, M. (2012). The contribution of bone to whole-organism physiology. *Nature* 481 (7381), 314–320. doi:10.1038/nature10763
- Kitaura, H., Marahleh, A., Ohori, F., Noguchi, T., Shen, W. R., Qi, J., et al. (2020). Osteocyte-related cytokines regulate osteoclast formation and bone resorption. *Int. J. Mol. Sci.* 21 (14), E5169. doi:10.3390/ijms21145169
- Lee, K., Chung, Y. H., Ahn, H., Kim, H., Rho, J., Jeong, D., et al. (2016). Selective regulation of MAPK signaling mediates RANKL-dependent osteoclast differentiation. *Int. J. Biol. Sci.* 12 (2), 235–245. doi:10.7150/ijbs.13814
- Lee, K., Seo, I., Choi, M. H., and Jeong, D. (2018). Roles of mitogen-activated protein kinases in osteoclast biology. *Int. J. Mol. Sci.* 19 (10), E3004. doi:10.3390/ijms19103004
- Leibbrandt, A., and Penninger, J. M. (2009). RANKL/RANK as key factors for osteoclast development and bone loss in arthropathies. *Adv. Exp. Med. Biol.* 649, 100–113. doi:10.1007/978-1-4419-0298-6\_7
- Lin, C. H., Lin, T. H., and Pan, T. M. (2017). Alleviation of metabolic syndrome by monascin and ankaflavin: The perspective of monascus functional foods. *Food Funct.* 8 (6), 2102–2109. doi:10.1039/c7fo00406k
- Liu, J. T., Chen, H. Y., Chen, W. C., Man, K. M., and Chen, Y. H. (2017). Red yeast rice protects circulating bone marrow-derived proangiogenic cells against high-glucose-induced senescence and oxidative stress: The role of heme oxygenase-1. *Oxid. Med. Cell. Longev.* 2017, 3831750. doi:10.1155/2017/3831750
- Lv, Y. D., Wang, G. H., Xu, W. H., Tao, P. H., Lv, X. L., Wang, Y. Z., et al. (2015). Tartrate-resistant acid phosphatase 5b is a marker of osteoclast number and volume in RAW 264.7 cells treated with receptor-activated nuclear  $\kappa$ B ligand. *Exp. Ther. Med.* 9 (1), 143–146. doi:10.3892/etm.2014.2071
- Mansky, K. C., Sankar, U., Han, J. H., and Ostrowski, M. C. (2002). Microphthalmia transcription factor is a target of the p38 MAPK pathway in response to receptor activator of NF- $\kappa$ B ligand signaling. *J. Biol. Chem.* 277 (13), 11077–11083. doi:10.1074/jbc.M111696200
- Matsumoto, M., Sudo, T., Saito, T., Osada, H., and Tsujimoto, M. (2000). Involvement of p38 mitogen-activated protein kinase signaling pathway in osteoclastogenesis mediated by receptor activator of NF- $\kappa$ B ligand (RANKL). *J. Biol. Chem.* 275 (40), 31155–31161. doi:10.1074/jbc.M001229200
- Matsuo, K., Galson, D. L., Zhao, C., Peng, L., Laplace, C., Wang, K. Z., et al. (2004). Nuclear factor of activated T-cells (NFAT) rescues osteoclastogenesis in precursors lacking c-Fos. *J. Biol. Chem.* 279 (25), 26475–26480. doi:10.1074/jbc.M313973200
- Nguyen, T., Karl, M., and Santini, A. (2017). Red yeast rice. *Foods* 6 (3), E19. doi:10.3390/foods6030019
- Novack, D. V., and Teitelbaum, S. L. (2008). The osteoclast: Friend or foe? *Annu. Rev. Pathol.* 3, 457–484. doi:10.1146/annurev.pathmechdis.3.121806.151431
- Ono, T., and Nakashima, T. (2018). Recent advances in osteoclast biology. *Histochem. Cell Biol.* 149 (4), 325–341. doi:10.1007/s00418-018-1636-2
- Patakova, P. (2013). Monascus secondary metabolites: Production and biological activity. *J. Ind. Microbiol. Biotechnol.* 40 (2), 169–181. doi:10.1007/s10295-012-1216-8
- Qu, Y. Y., Liu, X., Zong, S., Sun, H. X., Liu, S., Zhao, Y. R., et al. (2021). Protocatechualdehyde inhibits the osteoclast differentiation of RAW264.7 and BMM cells by regulating NF- $\kappa$ B and MAPK activity. *Biomed Res. Int.* 2021, 1–11. doi:10.1155/2021/6108999
- Ross, F. P. (2006). M-CSF, c-Fms, and signaling in osteoclasts and their precursors. *Ann. N. Y. Acad. Sci.* 1068, 110–116. doi:10.1196/annals.1346.014
- Siddiqui, J. A., and Partridge, N. C. (2016). Physiological bone remodeling: Systemic regulation and growth factor involvement. *Physiol. (Bethesda)* 31 (3), 233–245. doi:10.1152/physiol.00061.2014
- Song, C., Yang, X., Lei, Y., Zhang, Z., Smith, W., Yan, J., et al. (2019). Evaluation of efficacy on RANKL induced osteoclast from RAW264.7 cells. *J. Cell. Physiol.* 234 (7), 11969–11975. doi:10.1002/jcp.27852
- Sun, Y., Li, J., Xie, X., Gu, F., Sui, Z., Zhang, K., et al. (2021). Recent advances in osteoclast biological behavior. *Front. Cell Dev. Biol.* 9, 788680. doi:10.3389/fcell.2021.788680
- Takayanagi, H., Kim, S., Koga, T., Nishina, H., Isshiki, M., Yoshida, H., et al. (2002). Induction and activation of the transcription factor NFATc1 (NFAT2) integrate RANKL signaling in terminal differentiation of osteoclasts. *Dev. Cell* 3 (6), 889–901. doi:10.1016/s1534-5807(02)00369-6
- Wang, Y. F., Liu, W. T., Chen, C. Y., Ke, H. P., Jiang, H. L., Chen, X. L., et al. (2015). Anti-osteoporosis activity of red yeast rice extract on ovariectomy-induced bone loss in rats. *Genet. Mol. Res.* 14 (3), 8137–8146. doi:10.4238/2015.July.27.2
- Wang, T. J., Lien, A. S., Chen, J. L., Lin, C. H., Yang, Y. S., Yang, S. H., et al. (2019). A randomized clinical efficacy trial of red yeast rice (*monascus pilosus*) against hyperlipidemia. *Am. J. Chin. Med.* 47 (2), 323–335. doi:10.1142/S0192415X19500150
- Wang, H., Zheng, X., Zhang, Y., Huang, J., Zhou, W., Li, X., et al. (2021). The endocrine role of bone: Novel functions of bone-derived cytokines. *Biochem. Pharmacol.* 183, 114308. doi:10.1016/j.bcp.2020.114308
- Wong, R. W., and Rabie, B. (2008). Chinese red yeast rice (*Monascus purpureus*-fermented rice) promotes bone formation. *Chin. Med.* 3, 4. doi:10.1186/1749-8546-3-4
- Wu, B., Huang, J. F., He, B. J., Huang, C. W., and Lu, J. H. (2020). Promotion of bone formation by red yeast rice in experimental animals: A systematic review and meta-analysis. *Biomed. Res. Int.* 2020, 7231827. doi:10.1155/2020/7231827
- Xiong, X., Wang, P., Li, X., Zhang, Y., and Li, S. (2017). The effects of red yeast rice dietary supplement on blood pressure, lipid profile, and C-reactive protein in hypertension: A systematic review. *Crit. Rev. Food Sci. Nutr.* 57 (9), 1831–1851. doi:10.1080/10408398.2015.1018987
- Zhang, X., Liu, C., Tian, W., Zhang, H., Li, P., Wang, J., et al. (2020). Theoretical and experimental investigation of the antioxidative activity of monascin. *Food Funct.* 11 (7), 5915–5923. doi:10.1039/c9fo02410g
- Zhao, J., Huang, M., Zhang, X., Xu, J., Hu, G., Zhao, X., et al. (2019). MiR-146a deletion protects from bone loss in OVX mice by suppressing RANKL/OPG and M-CSF in bone microenvironment. *J. Bone Min. Res.* 34 (11), 2149–2161. doi:10.1002/jbmr.3832



# Effects of 6-Hydroxykaempferol: A Potential Natural Product for Amelioration of Tendon Impairment

Tsz Ngai Mok<sup>1†</sup>, Qiyu He<sup>2†</sup>, Xiaoxi Zhang<sup>1</sup>, Tat Hang Sin<sup>3</sup>, Huajun Wang<sup>1</sup>, Huige Hou<sup>1</sup>, Jinghua Pan<sup>1,4</sup>, Xiaofei Zheng<sup>1</sup>, Zhengang Zha<sup>1</sup> and Jieruo Li<sup>1\*</sup>

<sup>1</sup>Department of Orthopedic Surgery and Sports Medicine Center, The First Affiliated Hospital and The First Clinical College, Jinan University, Guangzhou, China, <sup>2</sup>Pediatric Cardiac Surgery Center, National Center for Cardiovascular Disease and Fuwai Hospital, Chinese Academy of Medical Sciences, Peking Union Medical, Beijing, China, <sup>3</sup>Department of Breast Surgery, Peking Union Medical College Hospital, Chinese Academy of Medical Science and Peking Union Medical College, Beijing, China, <sup>4</sup>Department of General Surgery, The First Affiliated Hospital of Jinan University, Guangzhou, China

## OPEN ACCESS

### Edited by:

Xiaofeng Zhu,  
Jinan University, China

### Reviewed by:

Qiu Xinguang,  
First Affiliated Hospital of Zhengzhou  
University, China  
Fan Pan,  
German Cancer Research Center  
(DKFZ), Germany

### \*Correspondence:

Jieruo Li  
lijieruo@jnu.edu.cn

<sup>†</sup>These authors have contributed  
equally to this work

### Specialty section:

This article was submitted to  
Experimental Pharmacology and Drug  
Discovery,  
a section of the journal  
Frontiers in Pharmacology

**Received:** 13 April 2022

**Accepted:** 10 June 2022

**Published:** 22 July 2022

### Citation:

Mok TN, He Q, Zhang X, Sin TH,  
Wang H, Hou H, Pan J, Zheng X, Zha Z  
and Li J (2022) Effects of 6-  
Hydroxykaempferol: A Potential  
Natural Product for Amelioration of  
Tendon Impairment.  
Front. Pharmacol. 13:919104.  
doi: 10.3389/fphar.2022.919104

Tendon impairment is a common injury associated with impairment of range of motion and pain. Currently, evidence has confirmed that natural herbs contribute to orthopedics and have shown excellent results in the clinical management of tendon impairment. Shujin Huoxue tablet (SHT) and its complex prescriptions are regularly used in tendon rupture therapy with positive results. This study aimed to discover the potential molecules that promote tendon healing. The Chinese traditional medicine system pharmacological database analysis platform (TCMSP) is the primary resource. The Traditional Chinese Medicine Integrated Database and Encyclopedia of Traditional Chinese Medicine database were used as secondary databases. The GeneCards database was used to search for reported tendinopathy-related genes by keywords. Functions of the targeted genes were analyzed using Gene Ontology enrichment analysis and Kyoto Encyclopedia of Genes and Genomes. Protein-protein interaction information was extracted from the STRING database. Docking study, MTT assay, quantitative real-time PCR, and migration assays were performed to obtain a better understanding of the herbs according to cell function to test the basic pharmacological action *in vitro*. A total of 104 disease nodes, 496 target gene nodes, 35 ingredient nodes, and one drug node were extracted. According to the TCMSP database, 6-hydroxykaempferol, which reportedly promotes the proliferation of microvascular endothelial cells, is a molecule found in SHT. We found that it promoted the proliferation and migration of tendon fibroblasts and elevated tendon repair-related gene expression. Purified 6-hydroxykaempferol promoted the proliferation and migration of tendon fibroblasts and increased their mRNA expression in tendon proliferation.

**Keywords:** pharmacological mechanisms, tendon injury, tendon rupture, tendon healing, tendon adhesion, Shujin Huoxue tablet

## INTRODUCTION

Tendon injuries, such as pain and lack of mobility, are common in both athletes and nonathletes (Watts et al., 2017). In modern medicine, oral nonsteroidal anti-inflammatory drugs (NSAIDs) are regularly used to manage tendon injuries (Jones et al., 2015). However, NSAIDs injure the mucosa of the stomach and duodenum. The primary mechanism of gastrointestinal mucosal injury theory is NSAID-induced inhibition of mucosal prostaglandin synthesis (Shim and Kim, 2016).

Currently, evidence confirms that natural herbs contribute to orthopedics with excellent results in clinical management (Lo et al., 2019). Shujin Huoxue tablet (SHT) and its complex prescriptions are frequently used in tendon rupture therapy, with promising results (Guosen and Washing, 2014; Tseng et al., 2018). Network pharmacology combines various biological and drug databases as an up-to-date model for drug research. It constructs a network prediction model of drug–gene–target protein–disease, resulting from bioinformatics analyses, to predict drug action targets and analyze drug action mechanisms from the perspective of biological network balance (Zhao et al., 2015; Fang et al., 2017; Lyu et al., 2017). However, research on purified molecules of SHT compound prescriptions is limited. This study aimed to discover the potential molecules that promote tendon healing. Furthermore, this study aimed to deliver a theoretical basis for further experimental studies and rational clinical applications of SHT based on pharmacological validation.

## MATERIALS AND METHODS

### Major Chemical Components of Shujin Huoxue Tablet

The Chinese traditional medicine system pharmacological database analysis platform (TCMSP) was used as the primary database in this study. Moreover, the Traditional Chinese Medicine Integrated Database (TCMID) and Encyclopedia of Traditional Chinese Medicine (ETCM) database were used as secondary databases. These databases were used in combination to bridge any gaps in key information, such as the name or number of ingredients. Even with the same database and screening strategy, the components included in the analysis vary (Ming, 2021). Therefore, all the data from the databases were integrated. Literature mining and the GoPubMed platform were used to confirm the molecular structure, using the mol2 file format for the components (Figure 1). The database uses the HIT database prediction algorithm, SysDT, to identify the relationship between drug targets. Disease information in this database was obtained from the TTD and PharmGKB databases. The value of TCMSP is that it provides pharmacokinetic information for each compound, such as drug product similarity (DL), oral bioavailability (OB), potential to cross the blood–brain barrier (BBB), intestinal epithelial permeability (Caco-2), lipid–water partition coefficient (ALogP), and the number of H-bond donor/acceptor (Hdon/Hacc). Therefore, users can select compounds with desirable absorption, distribution, metabolism, and excretion (ADME) characteristics for further studies (Ru et al., 2014).

TCMID collects TCM-related information from different sources through text mining. Furthermore, it links common drug and disease databases, including DrugBank, OMIM, and PubChem. Chemical changes may occur during the torment of prescriptions, resulting in the generation of new ingredients. Data containing prescription ingredients were collected from the website, and 778 herbal mass spectra (MS) related to 170 herbs were added. Spectral data were analyzed to show the variation in the quality of herbal medicines from different sources and to differentiate between genuine medicinal materials and common medicinal materials. A massive increase in website analysis data will facilitate the study of combination therapy and the understanding of the underlying mechanisms of TCM at the molecular level (Huang et al., 2018).

ETCM data on 402 herbs, 3,959 TCM compounds, 7,284 TCM chemical constituents, 2,266 drug targets, and 4,323 related diseases were collected. Data collected on herbal medicines included details of their origin, medicinal taste (sour, bitter, sweet, pungent, and salty), medicinal properties (cold, hot, warm, cool, and flat), return meridians (lung meridian and liver meridian), indications, ingredients, and quality control standards. Furthermore, other information such as compound name, dosage form, composition, indications, and ingredients, including the molecular formula, molecular weight, various physical and chemical indicators, ADME parameters, and drug-like properties at the compound level, was collected. Quantitative standards were set according to the Pharmacopoeia of the People's Republic of China (2015 version) which are the official TCM quality evaluation standards in China (Xu et al., 2019).

The absorption, distribution, metabolism, and excretion (ADME) processes of the active compounds are examined. In this process, the oral bioavailability (OB), drug similarity (DL), and half-life (HL) were the crucial parameters of ADME. The active compounds are indicated with  $OB \geq 30\%$  and  $DL \geq 0.18$  (Figure 1).

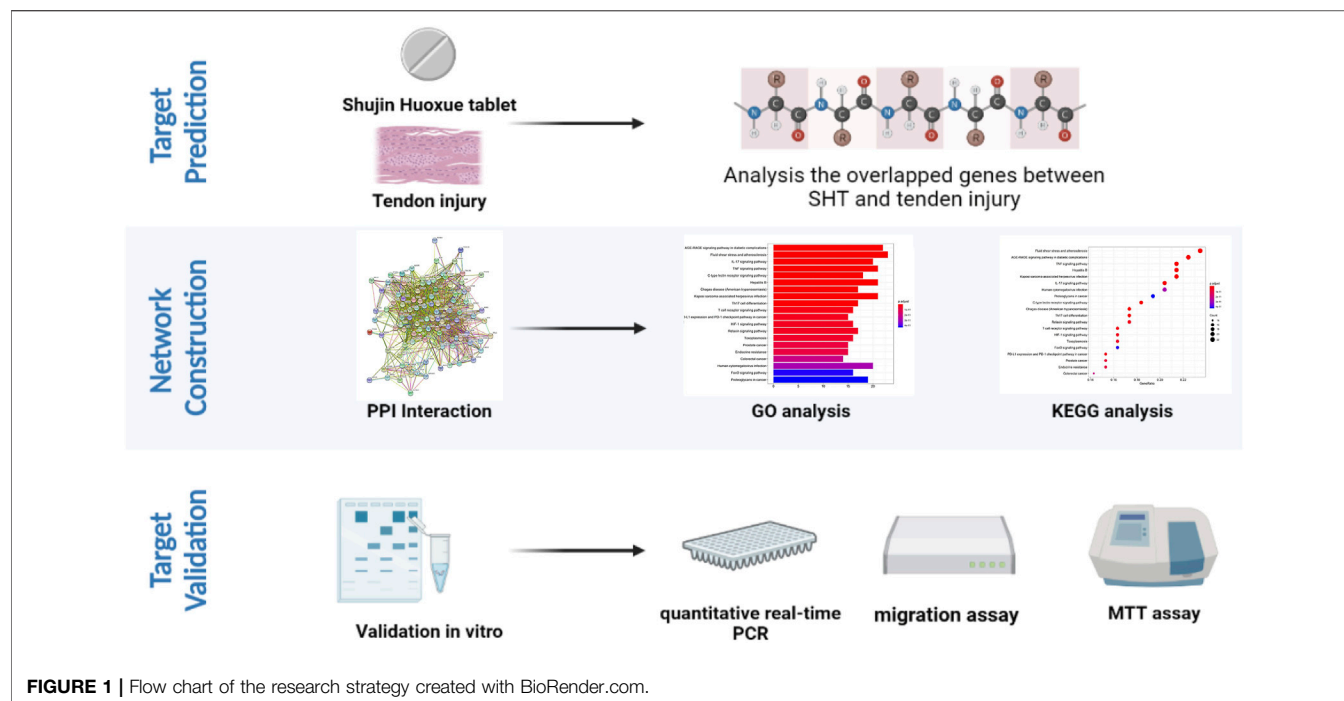
### Prediction of Potential Targets

The GeneCards (RRID:SCR\_002773) database was used to search for reported tendinopathy-related genes by entering keywords of tendon injuries, tendon rupture, tendon healing, and tendon adhesion for target-based drug applications. The potential tendon-healing targets of the active components of SHT matched the potential gene targets of the active ingredients of SHT. According to the UniProt database (<https://www.uniprot.org/>), the full names of the target proteins were transformed into gene symbols based on the UniProt ID (The UniProt Consortium, 2017) (Figure 1). The database leverages the unique rich combinatorial annotations of GeneCards. The GeneCards database provides direct links to gene-related research reagents, such as antibodies, recombinant proteins, DNA clones, and inhibitory RNAs, and lists of gene-related drugs and compounds. GeneCards was used to depict the GeneCards Inferred Functionality Score annotation landscape tool for scoring the functional status of genes (Fishilevich et al., 2016).

### Analysis of Functional Enrichment

Various biological processes and molecular functions were provided through the Database for Annotation, Visualization, and Integrated Discovery (DAVID, <https://david.ncifcrf.gov/>) v6.8. The examination of the function target genes based on DAVID was carried out through the Gene Ontology (RRID:SCR\_002811) biological process (GOBP).





enrichment analysis and Kyoto Encyclopedia of Genes and Genomes (KEGG) pathway enrichment analysis. A *p*-value of 0.05 or less represents importance in the analysis. The capabilities provided by DAVID accelerate the analysis of genome-scale datasets by facilitating the transition from data collection to biological meaning, and the analysis results and graphical displays remain dynamically linked to raw data and external data repositories, providing in-depth and extensive data cover.

## Network Pharmacology Evaluations

In network pharmacology, it is necessary to evaluate the reliability, normativeness, and rationality of the data collected. The specific requirements include three steps. First, in the reliability evaluation, the reliability of acquisition of main data and its associated information, the design of software algorithms and analysis methods, and the selection of verification methods and model building were evaluated according to their ability to meet the analysis requirements. Second, in the normative evaluation, the process of data information extraction and conversion, software/algorithm development, network construction, and analysis were evaluated. Moreover, the experimental verification is standardized, and the accuracy of relevant technical methods is evaluated to ensure the accuracy of the analysis results and reproducibility. Finally, during rationality evaluation data screening and filtering, selection of network analysis indicators and determination of thresholds, and selection of verification models and detection indicators were evaluated for reasonability (Li, 2021).

## Docking Study

The molecular structure of active ingredients in the mol2 format was obtained from the TCMSP database. The PDB format of the 3D molecular structure of the corresponding target (protein) gene was

obtained from the PDB (<https://www.rcsb.org>) database. The molecular structure documents of active ingredients and key target genes were imported into AutoDock (RRID:SCR\_012746) Tools 1.5.6 software for molecular docking, and the documents in the PDBQT format were imported into Open Babel software and converted them into the PDB format. PyMOL 2.5.0 software was used for visual analysis of the target protein and the compound with a high docking score and relatively stable conformation.

## Cell Culture

Primary rat tendon fibroblasts were purchased from ProCell in Wuhan, China (CP-R237). According to the manufacturer's instructions, cells were digested with 0.25% trypsin and seeded in six-well plates, with 2 ml culture medium made of Dulbecco's modified Eagle's medium with 10% fetal bovine serum (FBS), 100 U/ml penicillin, and 100 mg/ml streptomycin in each well and incubated at 37°C in a humidified atmosphere of 5% CO<sub>2</sub>: 95% air. When cell confluence reached 90%, the cells were subcultured by trypsinization at a 1:6 dilution ratio. Cells from passage 3 were used for subsequent experiments.

## MTT Assay

Tendon fibroblasts ( $3 \times 10^3$ ) were seeded in each well of a 96-well culture plate with culture medium containing DMEM (0.1 ml of DMEM), 10% FBS, 100 U/ml penicillin, and 100 mg/ml streptomycin in each well. Then, 6-hydroxykaempferol (Shanghai Yuanye Bio-Technology Co., Ltd., B50362) was added to each well at concentrations of 50, 100, 200, and 500 µg/ml. After incubation at 37°C for 24 h, cells were washed once with 1× phosphate-buffered saline (PBS), followed by adding 0.1 ml DMEM with 0.1 ml 3-(4,5-dimethyl-2-thiazolyl)-2,5-diphenyl-2-H-tetrazolium bromide (MTT, Servicebio, G4101-200T). After incubation at 37°C for 30 min, the media were removed, and formazan crystals in the cells were solubilized in 0.2 ml

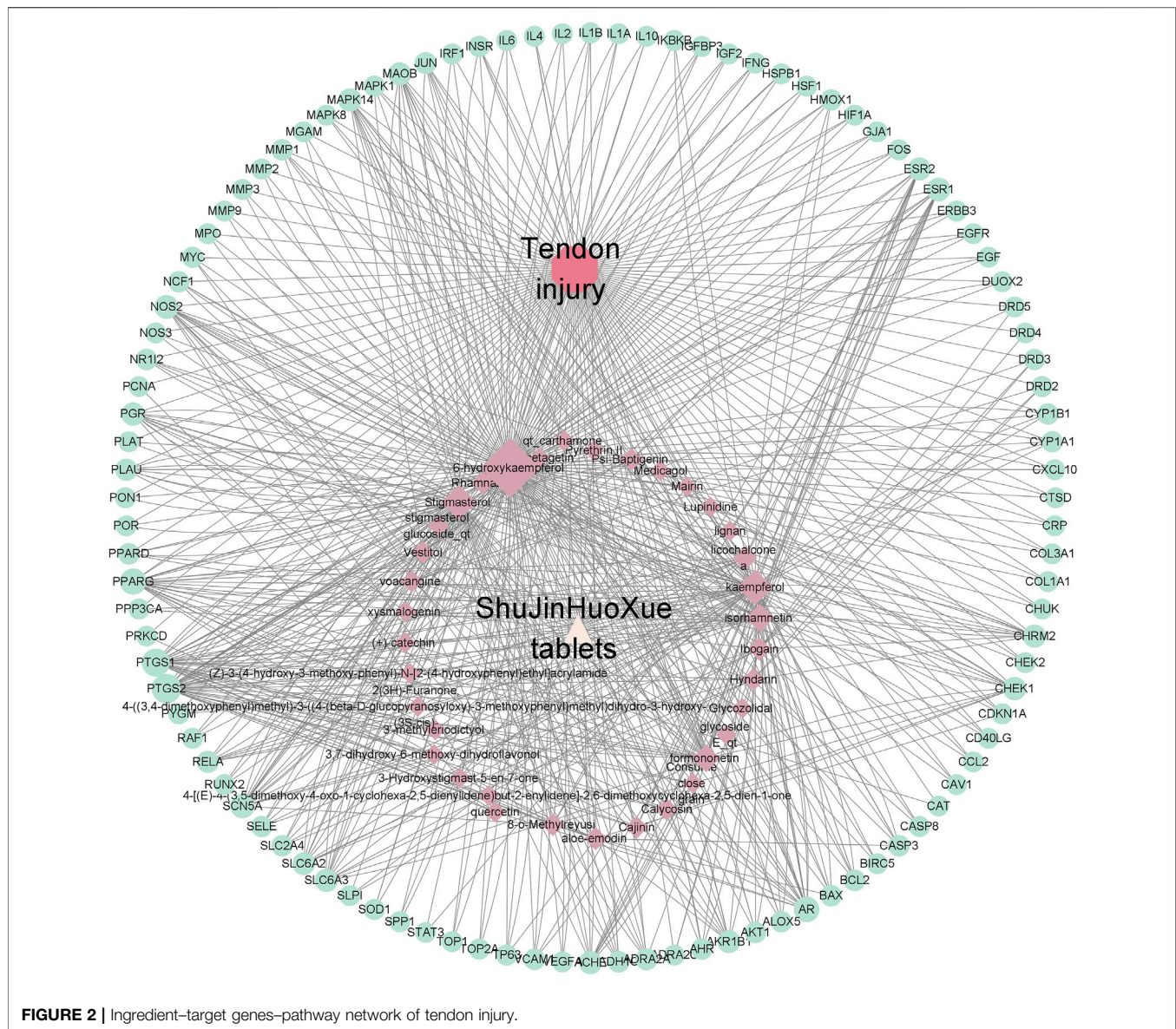


FIGURE 2 | Ingredient-target genes-pathway network of tendon injury.

DMSO and processed for OD reading at 570 nm using a spectrophotometer. Five wells were used for each concentration for each experiment, and the entire experiment was repeated three times.

## RNA Extraction, RT-PCR, and Quantitative Real-Time PCR

Total cellular RNA was extracted using a miRNeasy Mini Kit (Qiagen, 217004) according to the manufacturer's instructions. Total RNA (2 µg of total RNA) was reverse-transcribed to cDNA using the PrimeScript reverse transcription system (TaKaRa, 2680A). Quantification of the RNA levels of *Colla1* and *Tenascin C* (*TNC*) was achieved by quantitative real-time PCR using an ABI ViiA7 system and PowerUp SYBR Green Master Mix (Applied Biosystems, A25742). The data were normalized to the GAPDH expression. The PCR program consisted of 95°C for

5 min, 40 cycles of 95°C for 30 s, 56–58°C for 30 s, and 72°C for 30 s, followed by a final extension step at 72°C for 10 min. All reactions were conducted in triplicate. The data were analyzed using the threshold cycle (Ct) method. The primer sequences for the target genes were as follows: *Colla1* forward primer, 5'-CCC AGCGGTGGTTATGACTT-3'; *Colla1* reverse primer, 5'- TCG ATCCAGTACTCTCCGCT-3'; *TNC* forward primer, 5'- CAG AGTTGCCACCTACTTGCC-3'; *TNC* reverse primer, 5'-TCT CTCCTCATCTTCTTTGTTCA-3'; *GAPDH* forward primer, 5'-CTGGAGAAACCTGCCAAGTATG -3'; and *GAPDH* reverse primer, 5'-GGTGAAGAATGGGAGTTGCT-3'.

## Migration Assay

A scratch wound assay was performed to test the migration of tendon fibroblasts. Tendon fibroblasts ( $1 \times 10^6$ ) were seeded in each well of a six-well culture plate with culture medium containing 2 ml

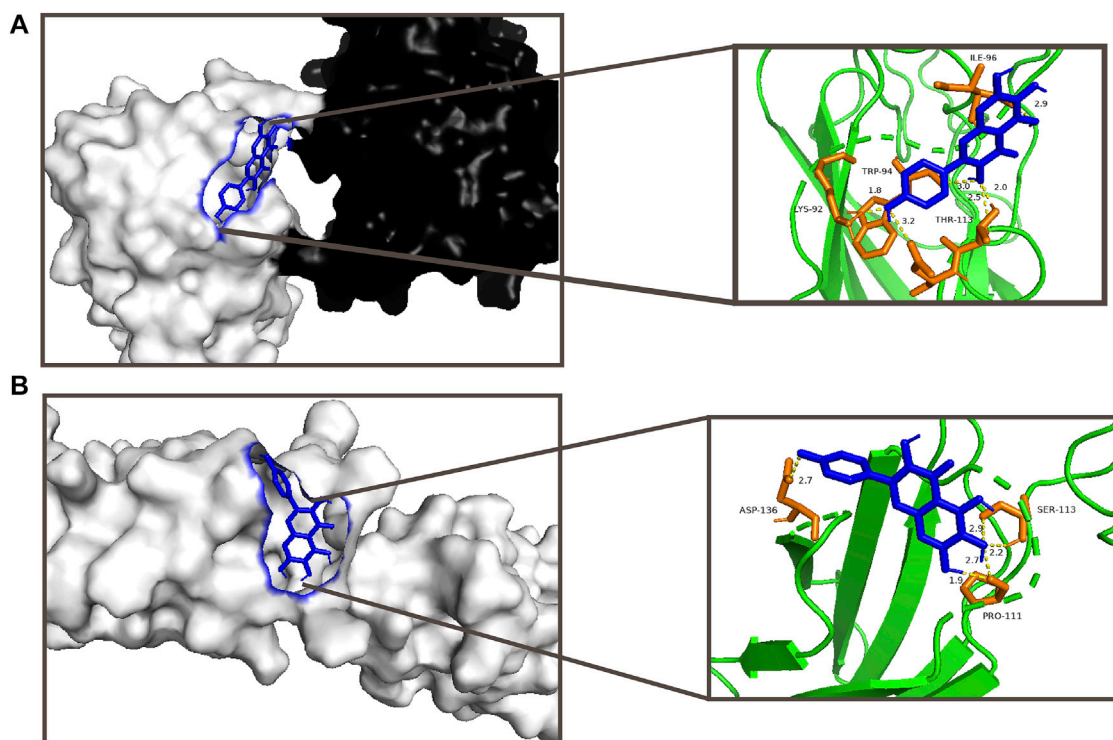


**FIGURE 3** | Visual analysis of compounds with higher scores and more stable conformation and target proteins by the docking study; **(A)** interaction between 6-hydroxykaempferol and *Col1a1* with an affinity of  $-4.63$  kcal/mol; **(B)** interaction between 6-hydroxykaempferol and *TNC* with an affinity of  $-5.21$  kcal/mol.

of DMEM with 10% FBS, 100 U/ml penicillin, and 100 mg/ml streptomycin in each well and cultured overnight at  $37^{\circ}\text{C}$ . After cell confluency reached over 95%, the medium was removed, and the cells were washed once with  $1\times$  PBS. Then, a linear scratch within the cell monolayer was generated using a sterile 1,000- $\mu\text{l}$  plastic pipette tip. The cellular debris was washed with  $1\times$  PBS. Next, 2 ml starvation medium composed of DMEM with 1% FBS, 100 U/ml penicillin, and 100 mg/ml streptomycin was added to each well, followed by treatment with 400  $\mu\text{g}$  of 6-hydroxykaempferol in three wells, and the cells were incubated at  $37^{\circ}\text{C}$  to allow migration. At 0 and 3 h, the images were photographed ( $10\times$  magnification). The percentage of the open wound area (3 h relative to 0 h) was calculated using ImageJ software.

### Statistical Analysis

Data are the mean  $\pm$  SD. The significance of the results was determined based on one-way analysis of variance using Prism 8.0.1 (GraphPad Prism (RRID:SCR\_002798), San Diego, CA, United States).  $p < 0.05$  was considered significant and presented with \* in the figure.

## RESULTS

### Network Pharmacology Evaluation

The evaluation group was established with a clear analysis of objects and goals. The evaluation content was then determined.

The evaluation implementation achieved a general and scalable evaluation. The results indicated that the evaluation was qualified.

### Target Genes of Shujin Huoxue Tablet Prescription

According to the TCMSP, TCMID, and ETCM databases, the SHT contains a total of 104 species. Species that could be identified include *Carthami flos* with 22 species, *Cyperi Rhizoma* with 18 species, *Cortex Periplocae Radicis* with 17 species, *Trachelospermum jasminoides* with 9 species, *Rhizome of whiteback greenbrier* with 5 species, *Lycopi Herba* with 2 species, *Viscum angulatum heyne* with 7 species, and *Spatholobus suberectus* Dunn with 24 species.

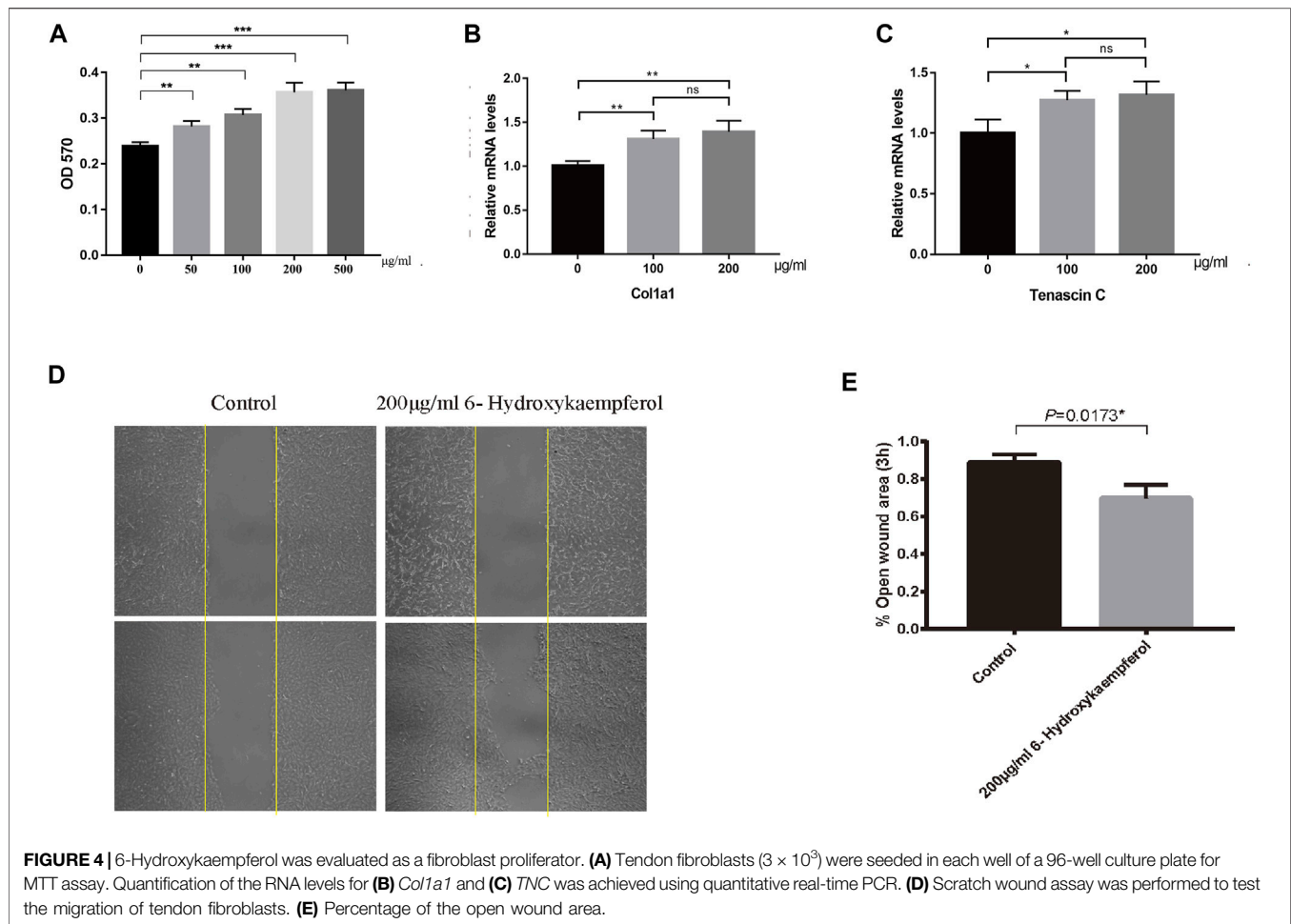
### Disease-Related Gene Extraction

Considering that the SHT prescription is used for killing pain, setting bone, and alleviating arthritis, the disease is related to the tendon injury, adhesion, and healing. The genes overlapped the disease-related genes, and the target genes of active compounds were pooled. Then, 104 genes were covered from tendon injury.

### Validation of Purified Molecules

In terms of tendon injury, 673 genes were in total in the network. Then, 104 disease nodes, 496 target gene nodes, 35 ingredient nodes, and 1 drug node were extracted. According to the result, the data processed by STRING (version 11.0) were used to produce a PPI network. It shows the protein-protein





interaction between the disease, including tendon injury, tendon adhesion and tendon healing, and the target gene of the active compound. The simple tabular text is extracted from the graphic to run the R program (version 3.6.2). From **Figure 4**, AKT 1 showed a high degree of coreness with 79 times interaction. IL6, CASP3, and VEGFA followed AKT 1 with 71, 68, and 68 times of interaction, respectively. The more interaction indicated the higher chance to become core proteins (**Figure 2**).

## Functional Annotation Analysis

The overlapped genes were further studied through GO-BP and KEGG (RRID:SCR\_012773) enrichment analysis. As shown in **Figure 1**, those genes were significantly related with KEGG pathway of “AGE-RAGE signaling pathway in diabetic complications” ( $p = 2.88\text{E-}22$ ), “fluid shear stress and atherosclerosis” ( $p = 2.94\text{E-}20$ ), “IL-17 signaling pathway” ( $p = 5.69\text{E-}20$ ), and “TNF signaling pathway” ( $p = 1.02\text{E-}19$ ) in the healing process (**Supplementary Table S2**). In terms of GO-BP analysis, “nuclear receptor activity” ( $p = 2.63\text{E-}12$ ), “transcription factor activity, direct ligand-regulated sequence-specific DNA binding” ( $p = 2.63\text{E-}12$ ), “cytokine receptor binding” ( $p = 3.31\text{E-}10$ ), “tetrapyrrole binding” ( $p = 5.01\text{E-}09$ ), “cytokine activity” ( $p = 1.97\text{E-}09$ ), “heme binding” ( $p = 2.50\text{E-}09$ ), “steroid hormone receptor activity” ( $p = 1.78\text{E-}08$ ), “receptor ligand activity” ( $p = 2.43\text{E-}07$ ),

“DNA-binding transcription activator activity, RNA polymerase II-specific” ( $p = 5.48\text{E-}07$ ), “growth factor receptor binding” ( $p = 5.64\text{E-}07$ ), and “scaffold protein binding” ( $p = 6.86\text{E-}07$ ) were significantly enriched in the healing process (**Supplementary Table S3**).

## Validation of Purified Molecules

According to the TCMSP database, 6-hydroxykaempferol is a molecule found in SHT (Ru et al., 2014). Several studies have shown that 6-hydroxykaempferol promotes the proliferation of microvascular endothelial cells (Yao et al., 2016; Liao et al., 2018). The positive results include the highest DC values among 6-hydroxykaempferol for docking study affinity values of  $-4.63$  kcal/mol in *Col1a1* and  $-5.21$  kcal/mol in *TNC* (**Figure 3**). Then, 6-hydroxykaempferol was therefore chosen for validation. This is the first study to explore the effects of this particular molecule on tendon fibroblasts. Since tendon repair is highly related to fibroblast proliferation, migration, and differentiation, the following molecular analyses were carried out to establish the potential relationship between 6-hydroxykaempferol and tendon repair (Chang et al., 2011; Guo et al., 2019). Analysis of its effects on cell viability showed that the herb improved proliferation in a concentration-dependent manner. Hierarchically organized collagen fibrils in the extracellular matrix (ECM) form tendons. The gene *Col1a1* encodes type I collagen, which has the highest percentage of collagen fibrils (Guerquin et al., 2013). In

contrast, *TNC* participates in the regulation of tendon repair (Xu et al., 2021), and its expression significantly increases during tendon-derived stem cell-mediated tendon repair. Therefore, these two genes were chosen for expression analyses, and positive results were obtained for both *Col1a1* and *TNC*. Furthermore, a migration assay showed that 6-hydroxykaempferol at a concentration of 200 µg/ml promoted tendon fibroblast migration. The percentage of open wound area significantly decreased at 3 h after treatment ( $p = 0.0173$ ). Our results showed that treatment with 6-hydroxykaempferol was able to promote tendon fibroblast proliferation, highly related gene expression, and migration (Figure 4).

## DISCUSSION

The treatment strategy for tendon injury is a clinical challenge. Furthermore, the basic mechanisms of intratendinous and tendon-to-bone healing remain only partially understood (Thomopoulos et al., 2015). Full coordination between the intrinsic tendon core tissue and surrounding extrinsic synovial tissues is needed for tendon tissue repair. According to a recent study, metabolic demands on resident tendon cells may be crucial for the regulation of tissue compartments involved in tendon recovery. SHT, a Chinese medicine consisting of herbal prescriptions widely used in clinical practice in China, can relax muscles and stimulate blood circulation (Tong et al., 2012), which may help metabolic demands in tendon repair. Our study provides evidence consistent with this theory. Moreover, 6-hydroxykaempferol is a competitive inhibitor of tyrosinase (Information NCIB, 2022). Naturally occurring flavonoids from a set of 14 hydroxy-flavones tested were previously shown to exhibit high inhibitory effects on tyrosinase compared to L-DOPA (Gao et al., 2007). However, this has never been studied in tendon reconstructions.

Previous studies have reported the anti-platelet aggregation, anticoagulation, and antioxidation effects of 6-hydroxykaempferol (Yao et al., 2016). Moreover, it has been reported to promote blood circulation to remove blood stasis, which may explain its anti-inflammatory effects, pain relief, muscle relaxation, and increased blood flow. Therefore, it advances the tendon repair process, which is consistent with the experimental results. This effect is believed to be achieved by cumulative biological exposure to antioxidants, which can quench the proliferation of radical oxygen and reactive nitrogen species, which are implicated in the pathology of fibroblasts (Wootton-Beard et al., 2011).

## STRENGTHS AND LIMITATIONS

This is the first study to explore the characteristics of 6-hydroxykaempferol on tendon repair. To prove this variability, MTT assays, quantitative real-time PCR, and migration assays were performed to test the basic pharmacological action. Network pharmacology mainly relies on the integrated analysis of data from different sources, and the emergence of massive data has brought new challenges to the development of network pharmacology. Specifically, it has three main aspects. First, the data sources are scattered, and integration is difficult. Databases are the main data

sources of network pharmacology, but there are challenges, such as large differences in data collection in different databases and relatively independent data. Second, the data usage has not been standardized. Owing to the lack of systematic research on the impact of data from different sources on the analysis results and the applicability of different databases, irregularities in the use of various types of data are inevitable. Third, *in vitro* cell verification was performed, but the cell experiments did not fully reflect the overall effect of the compound. However, different verification methods have certain limitations. According to the guidelines, the overall efficacy of the drug was clinically verified. Subsequently, the specific mechanism of action or target was further verified (Li, 2021).

Clinically, SHT has been used to treat tendon injury. However, a molecular validation of its effects has not previously been conducted. Based on *ex vivo* experiments, 6-hydroxykaempferol is able to promote tendon fibroblast proliferation, high mRNA expression (in *Col1A1* and *TNC*), and migration in tendon proliferation. Further studies should be conducted to determine the potential characteristics of 6-hydroxykaempferol.

## DATA AVAILABILITY STATEMENT

The original contributions presented in the study are included in the article/Supplementary Materials; further inquiries can be directed to the corresponding author.

## AUTHOR CONTRIBUTIONS

TM, QH, and JL contributed to the conception and design of the study. TS organized the database. JP performed the statistical analysis. TM and XZ (Zhang) wrote the first draft of the manuscript. HW and HH wrote sections of the manuscript. JL, XZ (Zheng), and ZZ supervised the research. All authors contributed to manuscript revision and read and approved the submitted version.

## FUNDING

The authors disclose receipt of the following support for the research, authorship, and/or publication of this article: Scientific Research Project of Guangdong Provincial Bureau of Traditional Chinese Medicine in (No. 20212044), Fundamental Research Funds for the Central Universities (No. 21620109), and Science and Technology Projects in Guangzhou (No. 202201020056).

## SUPPLEMENTARY MATERIAL

The Supplementary Material for this article can be found online at: <https://www.frontiersin.org/articles/10.3389/fphar.2022.919104/full#supplementary-material>



## REFERENCES

- Chang, C.-H., Tsai, W.-C., Lin, M.-S., Hsu, Y.-H., and Pang, J.-H. S. (2011). The Promoting Effect of Pentadecapeptide BPC 157 on Tendon Healing Involves Tendon Outgrowth, Cell Survival, and Cell Migration. *J. Appl. Physiology* 110, 774–780. doi:10.1152/japplphysiol.00945.2010
- Fang, H. Y., Zeng, H. W., Lin, L. M., Chen, X., Shen, X. N., Fu, P., et al. (2017). A Network-Based Method for Mechanistic Investigation of Shexiang Baoxin Pill's Treatment of Cardiovascular Diseases. *Sci. Rep.* 7, 43632. doi:10.1038/srep43632
- Fishilevich, S., Zimmerman, S., Kohn, A., Iny Stein, T., Olender, T., Kolker, E., et al. (2016). *Genic Insights from Integrated Human Proteomics in GeneCards Database* (2016).
- Gao, H., Nishida, J., Saito, S., and Kawabata, J. (2007). Inhibitory Effects of 5,6,7-trihydroxyflavones on Tyrosinase. *Molecules* 12, 86–97. doi:10.3390/12010086
- Guerquin, M.-J., Charvet, B., Nourissat, G., Havis, E., Ronsin, O., Bonnin, M.-A., et al. (2013). Transcription Factor EGR1 Directs Tendon Differentiation and Promotes Tendon Repair. *J. Clin. Invest.* 123, 3564–3576. doi:10.1172/jci67521
- Guo, W., Huang, J., Wang, N., Tan, H. Y., Cheung, F., Chen, F., et al. (2019). Integrating Network Pharmacology and Pharmacological Evaluation for Deciphering the Action Mechanism of Herbal Formula Zuojin Pill in Suppressing Hepatocellular Carcinoma. *Front. Pharmacol.* 10, 1185. doi:10.3389/fphar.2019.01185
- Guosen, L., and Washing, S. (2014). Treatment Efficacy Supination External Rotation Ankle Fracture with Deltoid Ligament Injury. *Yiyao Qianyan* 2014, 1. doi:10.3969/j.issn.2095-1752.2014.20.089
- Huang, L., Xie, D., Yu, Y., Liu, H., Shi, Y., Shi, T., et al. (2018). TCMID 2.0: a Comprehensive Resource for TCM. *Nucleic Acids Res.* 46, D1117–D1120d1120. doi:10.1093/nar/gkx1028
- Information NCfB (2022). *Pubchem. Compd Summ. CID. 2022*, 6. Hydroxykaempferol. <https://pubchem.ncbi.nlm.nih.gov/compound/6-Hydroxykaempferol>.
- Jones, P., Dalziel, S. R., Lamdin, R., Miles-Chan, J. L., and Frampton, C. (2015). Oral Non-steroidal Anti-inflammatory Drugs versus Other Oral Analgesic Agents for Acute Soft Tissue Injury. *Cochrane Database Syst. Rev.* 7, CD007789. doi:10.1002/14651858.CD007789.pub2
- Li, S. (2021). Network Pharmacology Evaluation Method Guidance - Draft [Guidelines]. *World J. Trad. Chin. Med.* 7, 21. doi:10.4103/wjtc.wjtc\_11\_21
- Liao, F., Meng, Y., Zheng, H., He, D., Shen, X., Yu, J., et al. (2018). Biospecific Isolation and Characterization of Angiogenesis-Promoting Ingredients in Buyang Huanwu Decoction Using Affinity Chromatography on Rat Brain Microvascular Endothelial Cells Combined with Solid-phase Extraction, and HPLC-MS/MS. *Talanta* 179, 490–500. doi:10.1016/j.talanta.2017.11.018
- Lo, P.-C., Lin, F.-C., Tsai, Y.-C., and Lin, S.-K. (2019). Traditional Chinese Medicine Therapy Reduces the Risk of Total Knee Replacement in Patients with Knee Osteoarthritis. *Med. (Baltim.)* 98, e15964. doi:10.1097/md.00000000000015964
- Lyu, M., Yan, C.-L., Liu, H.-X., Wang, T.-Y., Shi, X.-H., Liu, J.-P., et al. (2017). Network Pharmacology Exploration Reveals Endothelial Inflammation as a Common Mechanism for Stroke and Coronary Artery Disease Treatment of Danhong Injection. *Sci. Rep.* 7, 15427. doi:10.1038/s41598-017-14692-3
- Niu, M., Zhang, S. Q., Zhang, B., Yang, K., and Li, Z. (2021). "Interpretation of "Guideline for Web-Based Pharmacologic Evaluation methods," in *Chin. Trad. Herb. Drugs. LI Shao* (Interpretation of Network Pharmacology Evaluation Method Guidance), 52 (14), 4119–4129.
- Ru, J., Li, P., Wang, J., Zhou, W., Li, B., Huang, C., et al. (2014). TCMSP: a Database of Systems Pharmacology for Drug Discovery from Herbal Medicines. *J. Cheminform.* 6, 13. doi:10.1186/1758-2946-6-13
- Shim, Y. K., and Kim, N. (2016). Nonsteroidal Anti-inflammatory Drug and Aspirin-Induced Peptic Ulcer Disease. *Korean J. Gastroenterol.* 67, 300–312. doi:10.4166/kjg.2016.67.6.300
- Thomopoulos, S., Parks, W. C., Rifkin, D. B., and Derwin, K. A. (2015). Mechanisms of Tendon Injury and Repair. *J. Orthop. Res.* 33, 832–839. doi:10.1002/jor.22806
- Tong, Z., Yu, F., Liu, Z., and Liang, H. (2012). Influence of ShujinHuoXue Tablets on Ischemia Reperfusion Injury of Animals' Skeletal Muscle. *Molecules* 17, 8494–8505. doi:10.3390/molecules17078494
- Tseng, C. Y., Huang, C. W., Huang, H. C., and Tseng, W. C. (2018). Utilization Pattern of Traditional Chinese Medicine Among Fracture Patients: A Taiwan Hospital-Based Cross-Sectional Study. *Evid. Based Complement. Altern. Med.* 2018, 1706517. doi:10.1155/2018/1706517
- UniProt Consortium, The (2017). UniProt: the Universal Protein knowledgeBase. *Nucleic Acids Res.* 45, D158–D169. doi:10.1093/nar/gkw1099
- Watts, A. E., Millar, N. L., Platt, J., Kitson, S. M., Akbar, M., Rech, R., et al. (2017). MicroRNA29a Treatment Improves Early Tendon Injury. *Mol. Ther.* 25, 2415–2426. doi:10.1016/j.ymthe.2017.07.015
- Wootton-Beard, P. C., Moran, A., and Ryan, L. (2011). Stability of the Total Antioxidant Capacity and Total Polyphenol Content of 23 Commercially Available Vegetable Juices before and after *In Vitro* Digestion Measured by FRAP, DPPH, ABTS and Folin-Ciocalteu Methods. *Food Res. Int.* 44, 217–224. doi:10.1016/j.foodres.2010.10.033
- Xu, H.-Y., Zhang, Y.-Q., Liu, Z.-M., Chen, T., Lv, C.-Y., Tang, S.-H., et al. (2019). ETCM: an Encyclopaedia of Traditional Chinese Medicine. *Nucleic Acids Res.* 47, D976–D982. doi:10.1093/nar/gky987
- Xu, K., Shao, Y., Xia, Y., Qian, Y., Jiang, N., Liu, X., et al. (2021). Tenascin-C Regulates Migration of SOX10 Tendon Stem Cells via Integrin- $\alpha$ 9 for Promoting Patellar Tendon Remodeling. *BioFactors* 47, 768–777. doi:10.1002/biof.1759
- Yao, D., Wang, Z., Miao, L., and Wang, L. (2016). Effects of Extracts and Isolated Compounds from Safflower on Some Index of Promoting Blood Circulation and Regulating Menstruation. *J. Ethnopharmacol.* 191, 264–327. doi:10.1016/j.jep.2016.06.009
- Zhao, F., Guochun, L., Yang, Y., Shi, L., Xu, L., and Yin, L. (2015). A Network Pharmacology Approach to Determine Active Ingredients and Rationality of Herb Combinations of Modified-Simiaoan for Treatment of Gout. *J. Ethnopharmacol.* 168, 1–16. doi:10.1016/j.jep.2015.03.035

**Conflict of Interest:** The authors declare that the research was conducted in the absence of any commercial or financial relationships that could be construed as a potential conflict of interest.

**Publisher's Note:** All claims expressed in this article are solely those of the authors and do not necessarily represent those of their affiliated organizations, or those of the publisher, the editors, and the reviewers. Any product that may be evaluated in this article, or claim that may be made by its manufacturer, is not guaranteed or endorsed by the publisher.

Copyright © 2022 Mok, He, Zhang, Sin, Wang, Hou, Pan, Zheng, Zha and Li. This is an open-access article distributed under the terms of the Creative Commons Attribution License (CC BY). The use, distribution or reproduction in other forums is permitted, provided the original author(s) and the copyright owner(s) are credited and that the original publication in this journal is cited, in accordance with accepted academic practice. No use, distribution or reproduction is permitted which does not comply with these terms.



## OPEN ACCESS

## EDITED BY

Xiaofeng Zhu,  
Jinan University, China

## REVIEWED BY

Bing Shu,  
Shanghai University of Traditional  
Chinese Medicine, China  
Lili Wang,  
Beijing University of Chinese Medicine,  
China

## \*CORRESPONDENCE

Xiaolin Shi,  
xlshi-2002@163.com  
Kang Liu,  
liukang1982@163.com

<sup>†</sup>These authors have contributed equally  
to this work and share first authorship

## SPECIALTY SECTION

This article was submitted to  
Experimental Pharmacology and Drug  
Discovery,  
a section of the journal  
Frontiers in Pharmacology

RECEIVED 06 May 2022

ACCEPTED 12 July 2022

PUBLISHED 10 August 2022

## CITATION

Wang S, Yuan Y, Lin Q, Zhou H, Tang B,  
Liu Y, Huang H, Liang B, Mao Y, Liu K and  
Shi X (2022), Antiosteoporosis effect of  
tanshinol in osteoporosis animal  
models: A systematic review and meta-  
analysis.  
*Front. Pharmacol.* 13:937538.  
doi: 10.3389/fphar.2022.937538

## COPYRIGHT

© 2022 Wang, Yuan, Lin, Zhou, Tang,  
Liu, Huang, Liang, Mao, Liu and Shi. This  
is an open-access article distributed  
under the terms of the [Creative  
Commons Attribution License \(CC BY\)](#).  
The use, distribution or reproduction in  
other forums is permitted, provided the  
original author(s) and the copyright  
owner(s) are credited and that the  
original publication in this journal is  
cited, in accordance with accepted  
academic practice. No use, distribution  
or reproduction is permitted which does  
not comply with these terms.

# Antiosteoporosis effect of tanshinol in osteoporosis animal models: A systematic review and meta-analysis

Shen Wang<sup>1†</sup>, Yifeng Yuan<sup>1†</sup>, Qian Lin<sup>2†</sup>, Hang Zhou<sup>1†</sup>,  
Binbin Tang<sup>1,3</sup>, Yang Liu<sup>1</sup>, Hai Huang<sup>1</sup>, Bocheng Liang<sup>3</sup>,  
Yingdelong Mao<sup>3</sup>, Kang Liu<sup>3\*</sup> and Xiaolin Shi<sup>3\*</sup>

<sup>1</sup>The Second School of Clinical Medicine, Zhejiang Chinese Medical University, Hangzhou, China,

<sup>2</sup>Changping District Hospital of Integrated Traditional Chinese and Western Medicine, Beijing, China,

<sup>3</sup>The Second Affiliated Hospital of Zhejiang Chinese Medical University (Xinhua Hospital of Zhejiang Province), Hangzhou, China

**Background:** Osteoporosis (OP) is an age-related bone disease that has emerged as a worldwide public health concern due to its increasing incidence and high disability rate. Tanshinol [D (+)  $\beta$ -3,4-dihydroxyphenyl lactic acid, TS], a water-soluble component extracted from *Salvia miltiorrhiza*, has proven to be effective in attenuating OP *in vitro* and *in vivo*. However, there is insufficient evidence to support its clinical application.

**Objective:** This meta-analysis aimed to investigate available OP animal model studies to demonstrate the antiosteoporosis effects of TS in a systematic manner.

**Methods:** Electronic searches of related studies were conducted in the following databases: EMBASE, PubMed, Web of Science, Cochrane Library, Chinese National Knowledge Infrastructure, Chinese VIP Database, Chinese Biomedical Literature Database, and Wanfang. The retrieval date was January 2022, and there were no time or language restrictions. The CAMARADES 10-item quality checklist was utilized to test the risk of potential bias for each study, and modifications were performed accordingly. The primary outcome was bone mineral density (BMD, which included the femur and lumbar spine); and secondary outcomes were parameters for trabecular bone such as bone volume over total volume (BV/TV), trabecular number (Tb.N), trabecular thickness (Tb.Th), trabecular separation (Tb.Sp), conditions of the femur (including bone maximum load and bone elastic load), and markers of bone metabolism (serum osteocalcin, S-OCN).

**Results:** A total of nine studies including 176 rats were chosen for this analysis. Egger's test revealed the presence of publication bias in various studies regarding the primary outcome. According to this systematic review, TS significantly increased the BMD of the femur (BMD-femur) (SMD = 4.40; 95% CI = 1.61 to 7.19;  $p = 0.002$ ,  $I^2 = 94.6\%$ ), BMD of the lumbar spine (BMD-lumbar) (SMD = 6.390; 95% CI = 2.036 to 10.744;  $p = 0.004$ ,  $I^2 = 95.9\%$ ), BV/TV (SMD = 0.790; 95% CI = 0.376 to 1.204;  $p = 0.000$ ,  $I^2 = 10.8$ ),

Tb.N (SMD = 0.690; 95% CI = 0.309 to 1.071;  $p = 0.000$ ,  $I^2 = 12\%$ ), Tb.Th (SMD = 0.772; 95% CI = 0.410 to 1.134;  $p = 0.000$ ,  $I^2 = 32.2\%$ ), and S-OCN (SMD = 3.13; 95% CI = 0.617 to 5.65;  $p = 0.015$ ,  $I^2 = 92.3\%$ ), while the Tb.Sp level was markedly decreased in OP models in comparison to the controls (SMD =  $-0.822$ ; 95% CI =  $-1.207$  to  $-0.437$ ;  $p = 0.000$ ,  $I^2 = 0\%$ ). Moreover, TS treatment was associated with a significant improvement of the bone biomechanical indicators, including bone maximum load (SMD = 0.912; 95% CI = 0.370 to 1.455;  $p = 0.001$ ,  $I^2 = 40\%$ ) and elasticity load (SMD = 0.821; 95% CI = 0.290 to 1.351;  $p = 0.002$ ,  $I^2 = 0\%$ ).

**Conclusion:** Collectively, our findings suggest that TS can improve BMD, bone microarchitecture, bone biomechanics, and S-OCN expression in rats, implying that it could be used clinically in the future.

**Systematic Review Registration:** <https://inplasy.com/inplasy-2022-3-0053/>, identifier [INPLASY202230053].

#### KEYWORDS

osteoporosis, tanshinol, systematic review, meta-analysis, animal model

## Introduction

Osteoporosis (OP) is a disease characterized by low bone mass and structural degeneration that is becoming more prevalent globally as the elderly population grows. OP can be induced by various factors, including diet, diabetes, and medication-associated side effects. Many complications, such as fractures and chronic pain, have been proven to be associated with osteoporosis and are a considerable burden on the healthcare system. In the United States, it is reported that over 40 million women are diagnosed with low bone density, and 300,000 suffer from hip fractures each year (Black and Rosen, 2016). In addition, the annual osteoporosis-related costs in China have been estimated at \$25.43 (95% CI = 23.92–26.95) billion by 2050 (Si et al., 2015).

Several treatments for OP have been shown to be effective, including diet modifications, rehabilitation exercises, and medication. Medication is the most effective treatment option, with others serving as adjuvant therapy. On the other hand, calcium supplements and active vitamin D can only increase bone calcium content while having a limited regulatory effect on bone metabolic balance. Although some medications have been shown to reduce fracture incidence, they are frequently associated with some potential side effects. For instance, bisphosphonates can lead to jaw osteonecrosis (Drake et al., 2008) and severe musculoskeletal pain, while disuzumab use often leads to back and limb pain (Deeks, 2018). In addition, teriparatide use may impair the cardiovascular, central nervous, and endocrine systems and induce other systemic diseases (Lindsay et al., 2016). Therefore, exploring alternative treatment options with a better safety profile is important.

Traditional Chinese medicine (TCM) has been used to treat many diseases in China for a long time. *Salvia miltiorrhiza* is known to improve blood circulation, remove blood stasis, and relieve pain; as a result, it has been widely used in the treatment of vascular diseases,

coronary heart diseases, and musculoskeletal diseases. Tanshinol [D (+)- $\beta$ -3,4-dihydroxyphenyl lactic acid, TS] is a water-soluble component extracted from *Salvia miltiorrhiza* (Liu, 2019; Wang, 2015). Several *in vivo* and *in vitro* studies indicated that tanshinol has anti-OP effects (Cui et al., 2009; Luo et al., 2016; Yang et al., 2016; Chen et al., 2017; Han and Wang, 2017). However, its clinical application has been limited due to insufficient evidence. Meta-analysis of *in vivo* studies has been found to be useful in determining the efficacy and safety of drugs. To that end, we included animal studies that previously examined the potential effect of TS in OP treatment in our analysis to provide a scientific basis for future clinical trials.

## Materials and methods

### Literature retrieval

Electronic study search was conducted in the following databases: EMBASE, PubMed, Web of Science, Cochrane Library, Chinese National Knowledge Infrastructure, Chinese VIP Database, Chinese Biomedical Literature Database, and Wanfang Database. No time or language restrictions were set, and the retrieval date was January 2022. The search algorithm was adapted according to the different database requirements. For instance, the retrieval strategy for Web of Science was (((TS=(“Tanshinol”)) OR TS=(Danshensu)) OR TS=(“dan shen su a”)) OR TS=(“Salvianic acid A”)) AND TS=(osteoporosis).

### Inclusion criteria

Animal studies that fulfilled the following conditions were included in our study: 1) experimental groups received tanshinol

as monotherapy, while the corresponding control groups were treated with a vehicle or received a placebo such as saline solution; 2) studies with conclusive results; and 3) animals models established using different methods, regardless of species, age, weight, or gender.

## Exclusion criteria

Studies with the following conditions were excluded from the analysis: 1) *in vitro* studies, case reports, clinical trials, reviews, abstracts, comments, and editorials, 2) studies that did not use an acceptable established osteoporosis model, 3) studies with missing data, 4) duplicate publications, and 5) studies in which no outcome indicators were used.

## Outcome measurements

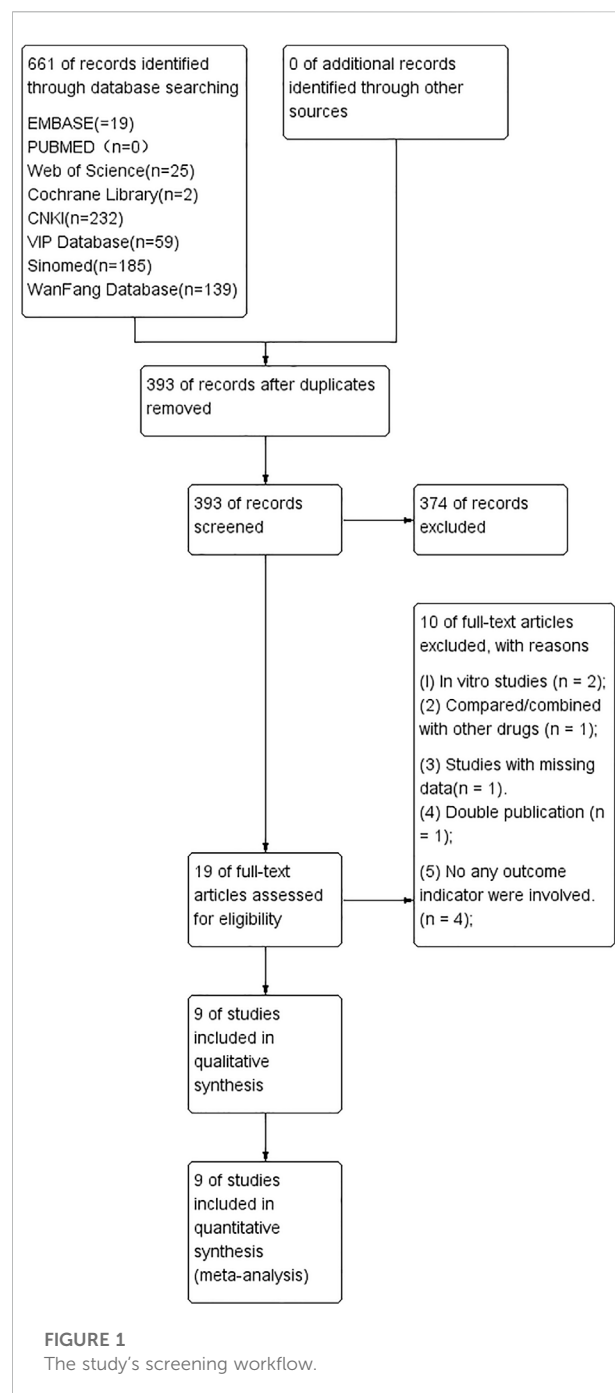
The primary outcome of this study was bone mineral density (BMD, including the femur and lumbar spine), and the secondary outcomes were the static parameters for trabecular bone: bone volume over total volume (BV/TV), trabecular number (Tb.N), trabecular thickness (Tb.Th), trabecular separation (Tb.Sp), biomechanical quality of the femur: bone maximum load, bone elastic load, and serum osteocalcin (S-OCN).

## Data extraction

Data were extracted by two authors independently and reviewed by a third author. The following information was extracted from each study: author name, date of publication, animal species, age, sex, body weight, sample size, OP modeling methods, anesthetics method used, the treatment protocol for control and experimental groups, and primary and secondary outcomes. We extracted the mean and standard deviation (SD) for continuous variables. If different doses of tanshinol were used, only data with the highest dose were collected. Authors of these publications were contacted to obtain relevant data where necessary.

## Data analysis

Data analyses were performed using the Stata software (Stata SE, version 16). When significant heterogeneity ( $I^2 \geq 50\%$ ) was detected, sensitivity analysis was performed to identify the possible cause. A fixed-effects model was used when heterogeneity was not detected ( $I^2 < 50\%$ ) or when the effects of significant clinical heterogeneity were excluded. Moreover, Egger's test was conducted to investigate the effect of publication bias. We calculated the pooled estimate as a standard mean difference (SMD) with a 95% confidence interval (CI) for continuous outcomes.



## Results

### Literature selection

A total of 661 articles were identified after searching eight databases, and 268 were excluded due to duplication. After reviewing the abstract, another 374 studies were eliminated. The remaining 19 studies were read in full, and ten reports were excluded because of the following: TS was compared/

TABLE 1 The details of included studies.

Study (year)	Animals	Weight	Age	Anesthetic	Sample size (n = experimental/control group)	Experimental group	Control group	Outcome indicators	Duration
Zhang et al. (2011)	Female SD rats	299 ± 20 g	6 months	NG	8/8	TS (12.5 mg/kg.d P.O)+OVX	Distilled water + OVX	(4) (5) (6)	90 days
Chen (2015)	Female SD rats	300 ± 20 g	7 months	NG	10/10	TS (50 mg/kg.d,P.O)+PA (6 mg/kg.d,qd,P.O)	PA (6 mg/kg.d,qd,P.O)<	(3) (4) (5) (6)	14 weeks
Luo SY (2016)	Female SD rats	300 ± 10 g	7 months	Peritoneal injection of sodium pentobarbital	10/10	TS (50 mg/kg.d,P.O)+PA (6 mg/kg.d,qd,P.O)	Distilled water + PA (6 mg/kg.d,qd,P.O)	(1) (2) (3) (4) (5) (6) (7) (8) (9)	14 weeks
Qu et al. (2016)	Female SD rats	300 ± 20 g	5 months	Peritoneal injection of sodium pentobarbital	10/10	TS 12.5 mg/kg.d P.O + OVX (2 weeks after modeling)	Distilled water + OVX (2 weeks after modeling)	(1) (2) (7) (9)	90 days
Yang YJ et al. (2016)	Female SD rats	200–250 g	4 months	Peritoneal injection of sodium pentobarbital	8/8	TS (16 mg/kg.d,P.O)+PA (5 mg/kg.d,qd,P.O)	PA (5 mg/kg.d,qd,P.O)	(3) (4) (5) (6) (8) (9)	14 weeks
Wang (2017)	Female SD rats	240 ± 10 g	4 months	NG	10/10	TS (30 mg/kg.d,P.O)+PA (5 mg/kg.d,qd,P.O)	PA (5 mg/kg.d,qd,P.O)	(1) (2)	14 weeks
Du (2018)	Male SD rats	325 ± 25 g	3 months	Peritoneal injection of sodium pentobarbital	8/8	TS (25 mg/kg.d,P.O)+levothyroxine (0.25mg/k g.d,qd,P.O)	Levothyroxine (0.25mg/k g.d,qd,P.O) +NS(5 ml/kg.d,qd,P.O)for 12 weeks	(1) (3) (4) (5) (6) (7) (8) (9)	3 months
Sang (2019)	Female SD rats	220–260 g	16 weeks	Peritoneal injection of chloral hydrate	12/12	TS (30 mg/kg.d,P.O) after Modeling (tretinoin 70 mg/kg/d,qd,P.O) for 2 weeks)	5%CMC-Na (5 ml/kg.d,qd,P.O) after modeling (tretinoin 70 mg/kg/d,qd,P.O) for 2 weeks)	(1) (2)	14 weeks
Lai WX et al. (2021)	Male SD rats	396.4 ± 28.55 g	4 months	Peritoneal injection of chloral hydrate	12/12	TS (25 mg/kg.d,qd,P.O)+PA (6 mg/kg.d,qd,P.O)	PA (6 mg/kg.d,qd,P.O)	(3) (4) (5) (6) (7) (8) (9)	16 weeks

(1) BMD-femur, (2) BMD-lumbar, (3) BV/TV, (4) Tb.N, (5) Tb.Th, (6) Tb.Sp, (7) bone maximum load, (8) bone elastic load, and (9) S-OCN.

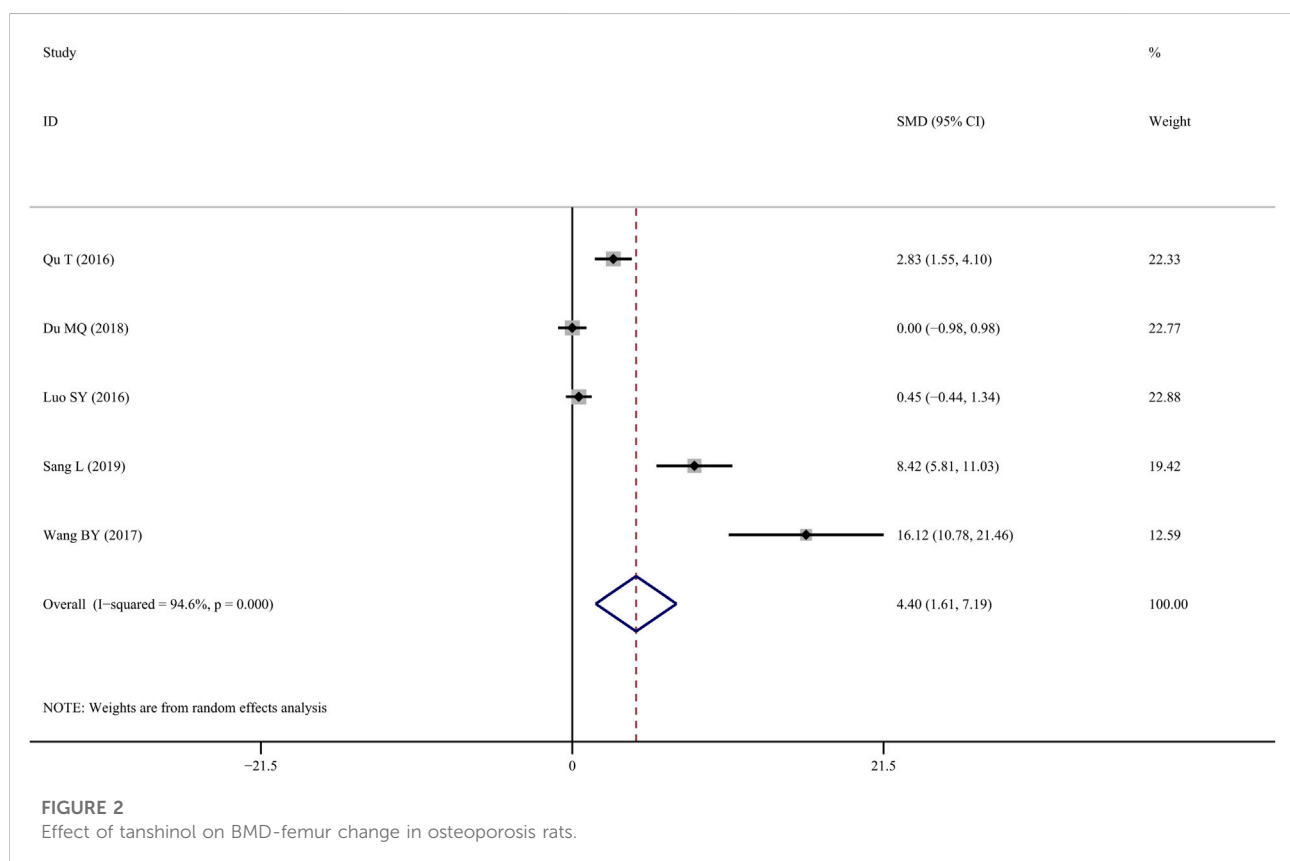
NG, not given the specific name of anesthetics; OVX, ovariectomized; SD, Sprague–Dawley; PA, prednisone acetate.



TABLE 2 Risk of bias of the included studies.

Study (year)	(1)	(2)	(3)	(4)	(5)	(6)	(7)	(8)	(9)	(10)	Total
Zhang et al. (2011)	✓	✓	✓						✓		4
Chen (2015)	✓	✓	✓						✓		4
Luo SY (2016)		✓	✓			✓			✓		4
Qu et al. (2016)	✓	✓	✓			✓			✓		5
Yang YJ et al. (2016)	✓	✓	✓			✓			✓	✓	6
Wang (2017)	✓	✓	✓						✓		4
Du (2018)		✓	✓			✓			✓		4
Sang (2019)	✓		✓			✓					3
Lai WX et al. (2021)	✓	✓	✓			✓			✓		5

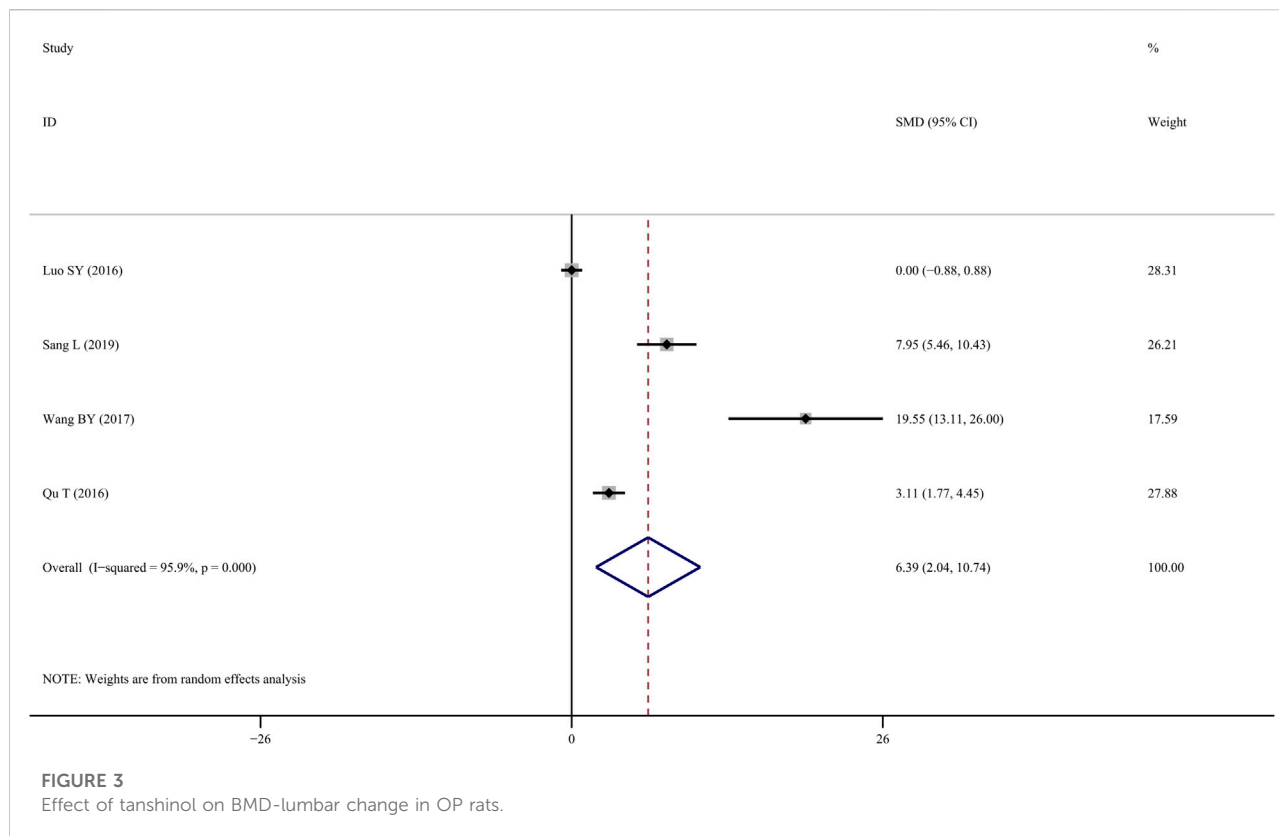
(1) publication in a peer-reviewed journal; (2) statement of control of temperature; (3) randomization of treatment or control; (4) blinded induction of model; (5) blinding of outcome assessment; (6) use of anesthetic without proven protective measures that may have toxic effects on bones; (7) appropriate animal model (aged, diabetic, or hypertensive); (8) sample size estimation; (9) compliance with animal welfare regulations; (10) declaration of any potential conflict of interest.



combined with other drugs; there was no control group; and/or there was data duplication. Eventually, nine studies were selected for this meta-analysis, including two published in English (Yang et al., 2016; Lai et al., 2021) and seven published in Chinese (Zhang et al., 2011; Chen J, 2015; Qu et al., 2016; SY, 2016; Wang, 2017; Du, 2018; Sang, 2019) (Figure 1).

## Basic information of the included studies

Table 1 shows the specifics of the nine studies that were selected. All studies were published between 2011 and 2021, and a total of 176 subjects were enrolled, with 88 in the experimental group and 88 in the control group. Sample sizes of enrolled studies ranged from 16 to 24 (median = 20). Sprague-Dawley (SD) rats were used for all



studies, and seven studies used female (75%) murine models (Zhang et al., 2011; Chen J, 2015; Qu et al., 2016; SY, 2016; Yang et al., 2016; Wang, 2017; Sang, 2019), while two studies used male (25%) murine models (Du, 2018; Lai et al., 2021). Rats in five studies were treated with oral prednisone acetate (PA, 5 mg–6 mg/kg.d, 14–16 weeks) (Chen J, 2015; SY, 2016; Yang et al., 2016; Wang B, 2017; Lai et al., 2021), two with bilateral oophorectomy (Zhang et al., 2011; Qu T, 2016), one with oral levothyroxine (0.25 mg/kg.d, 12 weeks) (Du, 2018), and one with oral retinoic acid (70 mg/kg.d, 2 weeks) (Sang, 2019). The rats in all of the enrolled studies received intragastrical tanshinol at doses ranging from 12.5 mg/kg.d to 50 mg/kg.d (Zhang et al., 2011; Chen J, 2015; Qu T, 2016; SY, 2016; Yang et al., 2016; Wang B, 2017; Du, 2018; Sang, 2019; Lai et al., 2021). In terms of the primary outcome, BMD-femur was measured in five studies (Qu T, 2016; SY, 2016; Wang B, 2017; Du, 2018; Sang L, 2019), while four studies quantified BMD-lumbar (SY, 2016; Sang L, 2019; Wang B, 2017; Qu T, 2016). In addition, the BV/TV value was measured in five studies (Chen J, 2015; Yang et al., 2016; SY, 2016; Du, 2018; Lai et al., 2021), Tb.N in six studies (Zhang et al., 2011; Chen J, 2015; SY, 2016; Yang et al., 2016; Du, 2018; Lai et al., 2021), Tb.Th in six studies (Zhang et al., 2011; Chen J, 2015; SY, 2016; Yang et al., 2016; Du, 2018; Lai et al., 2021), Tb.Sp in six studies (Zhang et al., 2011; Chen J, 2015; SY, 2016; Yang et al., 2016; Du, 2018; Lai et al., 2021), bone maximum load in four studies (Qu et al., 2016; SY, 2016; Du, 2018; Lai et al., 2021), bone elastic load in four studies (SY, 2016; Yang et al.,

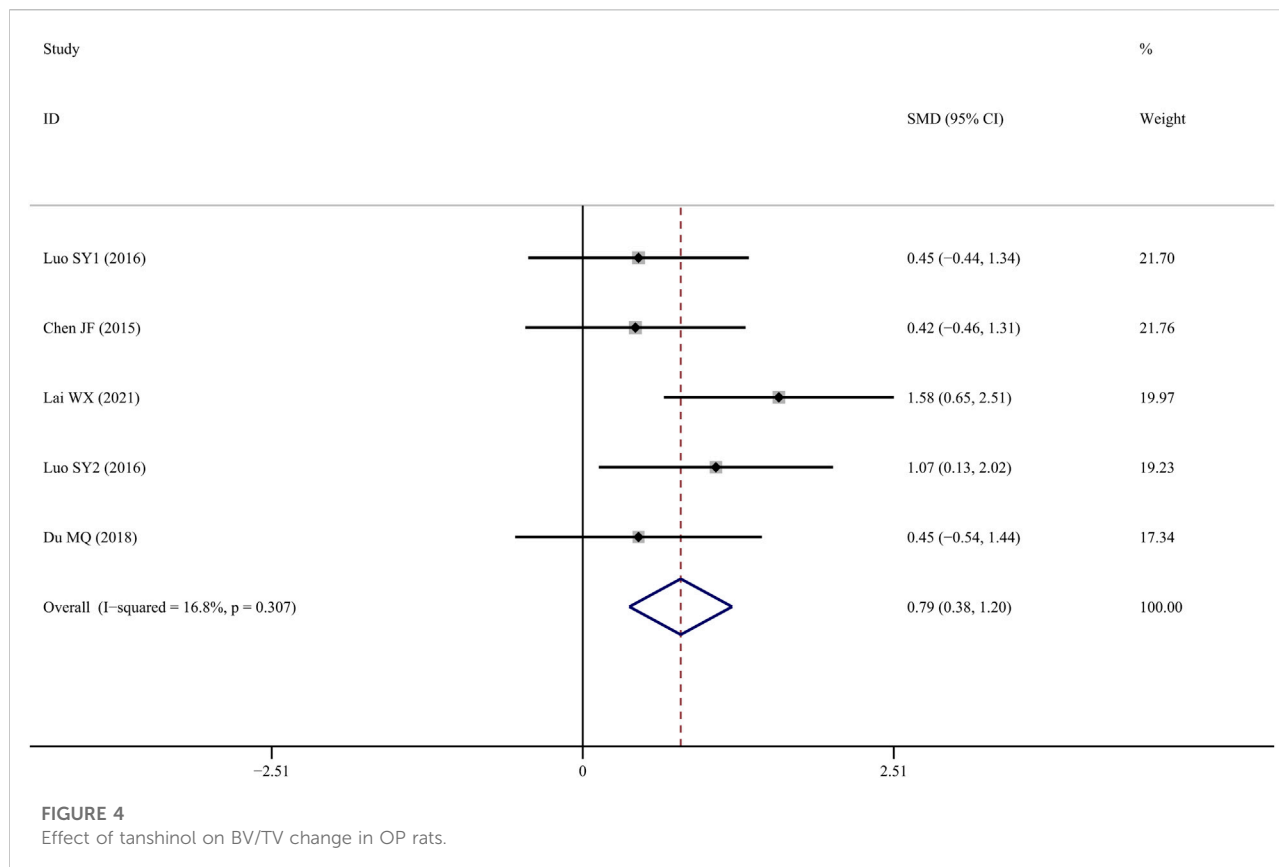
2016; Du, 2018; Lai et al., 2021), and serum osteocalcin (S-OCN) in four studies (Qu et al., 2016; SY, 2016; Yang et al., 2016; Du, 2018).

## Risk of bias

The risk of bias for each study was tested using the CAMARADES 10-item quality checklist (Macleod et al., 2004) (Table 2). Modifications were implemented where needed (Bao et al., 2018): 1) blinded induction of model, 2) use of anesthetic without significant protective and toxic effects on bones. The quality score of studies ranged from 3 to 6 (mean  $\pm$  SD: 4.5  $\pm$  0.83).

## BMD-femur

Five studies (Qu et al., 2016; SY, 2016; Wang, 2017; Du, 2018; Sang, 2019) reported on BMD-femur and revealed that TS treatment was significantly associated with improved BMD values when compared to controls ( $SMD = 4.40$ ; 95% CI = 1.61 to 7.19;  $p = 0.002$ , heterogeneity  $\chi^2 = 73.92$ ,  $df = 4$ ,  $p = 0.000$ ,  $I^2 = 94.6\%$ , Figure 2). The random-effect model was chosen given the significant heterogeneity among the included studies. Metaregression was not performed because only a small number of studies were included.



### 3.5 BMD-lumbar

Four studies (SY, 2016; Du, 2018; Lai et al., 2021) investigated the efficacy of TS treatment on BMD-lumbar and discovered that TS could significantly enhance BMD values when compared to the control group ( $SMD = 6.390$ ; 95% CI = 2.036 to 10.744;  $p = 0.004$ , heterogeneity  $\chi^2 = 72.51$ ,  $df = 3$ ,  $p = 0.0001$ ,  $I^2 = 95.9\%$ , Figure 3). Similarly, the random-effect model was applied due to notable heterogeneity, while metaregression was not performed due to the small sample size.

## The BMD-Related index of femur and tibia under Micro-CT

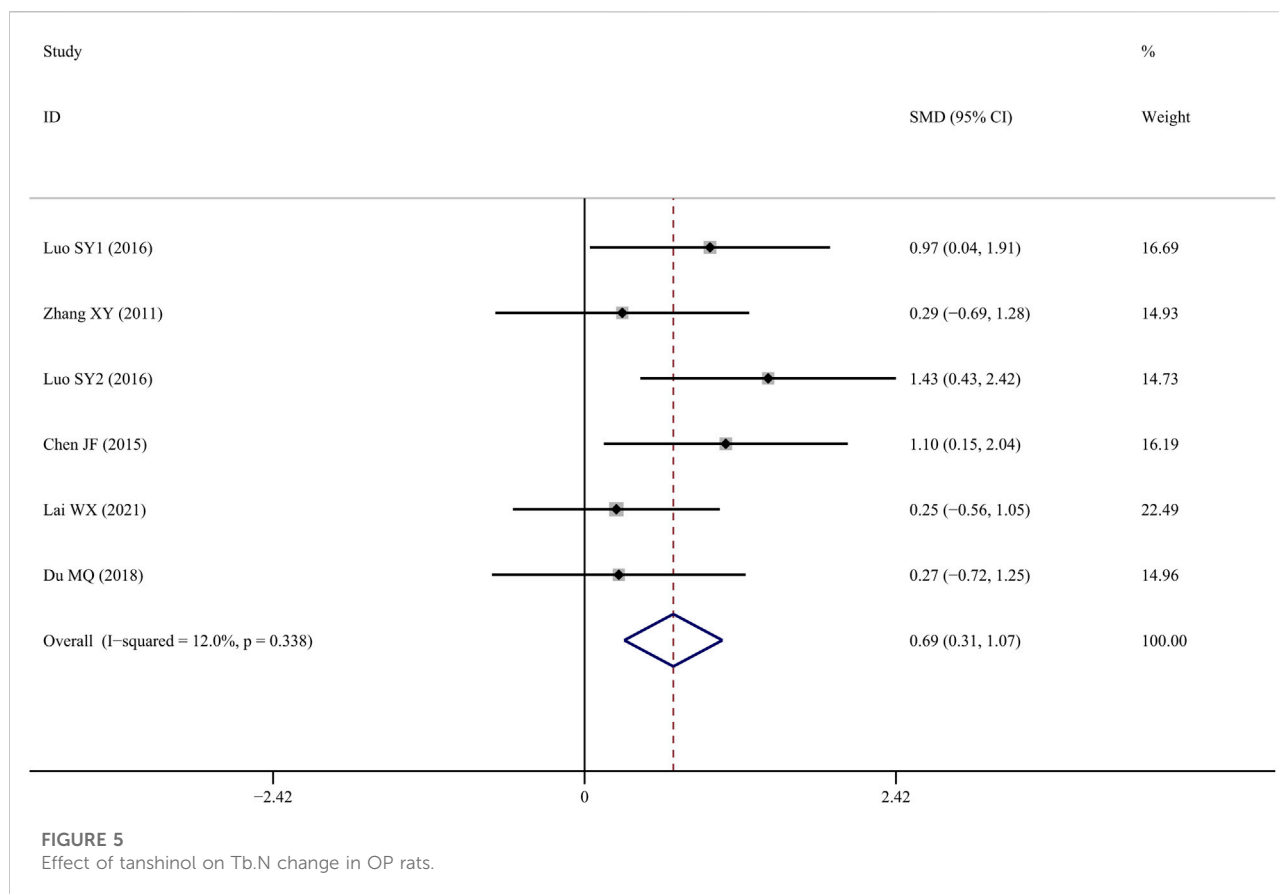
### BV/TV

Five studies (Chen J, 2015; SY, 2016; Yang et al., 2016; Du, 2018; Lai et al., 2021) measured BV/TV following TS administration, and the results indicated that the TS treatment group showed a significant improvement compared to the control group ( $SMD = 1.192$ ; 95% CI = 0.357 to 2.027;  $p = 0.005$ , heterogeneity  $\chi^2 = 19.71$ ,  $df = 5$ ,  $p = 0.001$ ,  $I^2 = 74.6\%$ ). Sensitivity analyses identified that the

source of the heterogeneity was mainly from one study (Yang et al., 2016), and the  $I^2$  value was reduced to 10.8% when this study was eliminated. The fixed-effects model revealed that TS treatment increased BV/TV significantly more than control intervention ( $SMD = 0.790$ ; 95% CI = 0.376 to 1.204;  $p = 0.000$ , heterogeneity  $\chi^2 = 4.81$ ,  $df = 4$ ,  $p = 0.307$ , Figure 4).

### Tb.N

Tb.N was reported in six studies (Zhang et al., 2011; Chen J, 2015; SY, 2016; Yang et al., 2016; Du, 2018; Lai et al., 2021), and the results indicated that TS treatment could significantly improve Tb.N values when compared to the control group ( $SMD = 1.096$ ; 95% CI = 0.253 to 1.938;  $p = 0.011$ , heterogeneity  $\chi^2 = 26.90$ ,  $df = 6$ ,  $p = 0.000$ ,  $I^2 = 77.7\%$ ). Similarly, the source of the heterogeneity originated from one study (Yang et al., 2016), and the  $I^2$  value was reduced to 12% after removing that article. According to the fixed-effects model, TS significantly increased Tb.N values when compared to controls ( $SMD = 0.690$ ; 95% CI = 0.309 to 1.071;  $p = 0.000$ , heterogeneity  $\chi^2 = 5.68$ ,  $df = 5$ ,  $p = 0.338$ , Figure 5).



## Tb.Th

Tb.Th data reported from six studies (Zhang et al., 2011; Chen J, 2015; SY, 2016; Yang et al., 2016; Du, 2018; Lai et al., 2021) indicated that TS treatment was associated with a significant improvement when compared to controls ( $SMD = 0.772$ ; 95% CI = 0.410 to 1.134;  $p = 0.000$ , heterogeneity  $\chi^2 = 8.85$ ,  $df = 6$ ,  $p = 0.182$ ,  $I^2 = 32.2\%$ , Figure 6).

## Tb.Sp

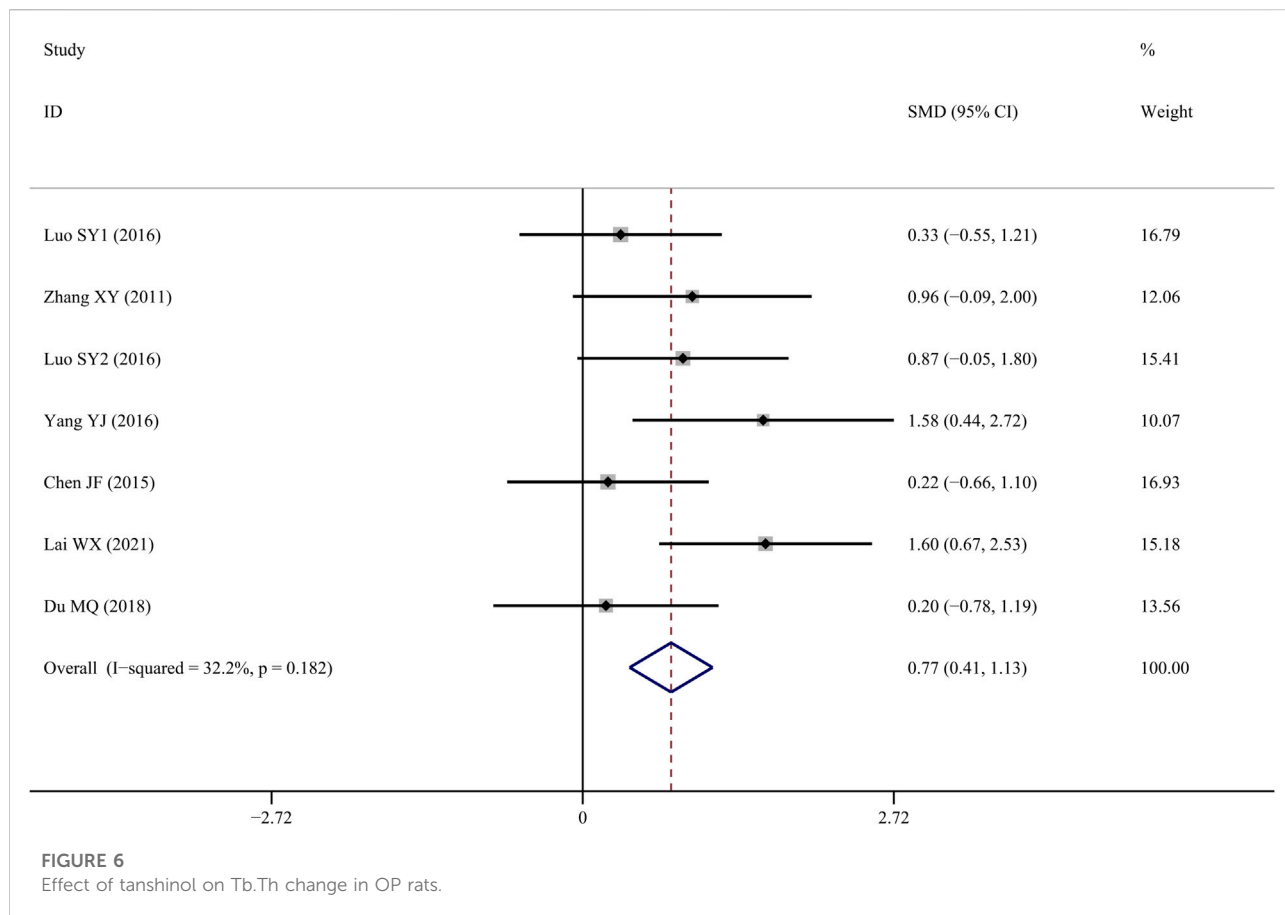
Tb.Sp results from six studies (Zhang et al., 2011; Chen J, 2015; SY, 2016; Yang et al., 2016; Du, 2018; Lai et al., 2021) suggested that TS treatment was associated with a significant decline when compared to the control group ( $SMD = -1.137$ ; 95% CI = -1.834 to -0.441;  $p = 0.001$ , heterogeneity  $\chi^2 = 19.11$ ,  $df = 6$ ,  $p = 0.04$ ,  $I^2 = 68.6\%$ ). Sensitivity analyses revealed that the source of the heterogeneity was primarily from one study (Yang et al., 2016), with the  $I^2$  value dropping to 0% when that study was removed. According to the fixed-effect model, TS administration significantly reduced Tb.Sp

when compared to the control group ( $SMD = -0.822$ ; 95% CI = -1.207 to -0.437;  $p = 0.000$ , heterogeneity  $\chi^2 = 4.59$ ,  $df = 5$ ,  $p = 0.467$ , Figure 7).

## Bone biomechanical indicator

### Bone maximum load

Four studies (Chen J, 2015; Qu et al., 2016; Yang et al., 2016; Du, 2018) examined femur bone maximum load, and the results indicated that TS treatment could significantly improve it in comparison to the control group ( $SMD = 1.292$ ; 95% CI = 0.360 to 2.224;  $p = 0.007$ , heterogeneity  $\chi^2 = 10.27$ ,  $df = 3$ ,  $p = 0.016$ ,  $I^2 = 70.8\%$ ). The source of the heterogeneity was mainly from one study (Qu et al., 2016), and the  $I^2$  value was reduced to 40% when this study was removed. The fixed-effects model indicated that TS treatment could significantly increase femur bone maximum load compared to the control group ( $SMD = 0.912$ ; 95% CI = 0.370 to 1.455;  $p = 0.001$ , heterogeneity  $\chi^2 = 3.33$ ,  $df = 2$ ,  $p = 0.189$ , Figure 8).



## Bone elastic load

Four studies (SY, 2016; Du, 2018; Lai et al., 2021) reported findings on femur bone elastic load, indicating that TS treatment was associated with a significant improvement compared to the control group ( $SMD = 1.496$ ; 95% CI = 0.332 to 2.660;  $p = 0.01$ , heterogeneity  $\chi^2 = 13.68$ ,  $df = 3$ ,  $p = 0.003$ ,  $I^2 = 78.1\%$ ). The source of the heterogeneity was mainly generated by one study (Yang et al., 2016), and the  $I^2$  value was reduced to 0% when this article was removed. The fixed-effects model indicated that TS significantly increased femur bone elastic load compared to the controls ( $SMD = 0.821$ ; 95% CI = 0.290 to 1.351;  $p = 0.002$ , heterogeneity  $\chi^2 = 0.63$ ,  $df = 2$ ,  $p = 0.729$ , Figure 9).

## S-OCN

Four studies (Qu et al., 2016; SY, 2016; Yang et al., 2016; Du, 2018) reported S-OCN results in the femur, and results indicated that TS treatment was associated with a significant improvement compared with the control group ( $SMD = 3.13$ ; 95% CI = 0.617 to 5.65;  $p = 0.015$ , heterogeneity  $\chi^2 = 39.1$ ,  $df = 3$ ,  $p = 0.000$ ,  $I^2 = 92.3\%$ , Figure 10).

## Publication bias and sensitivity analysis

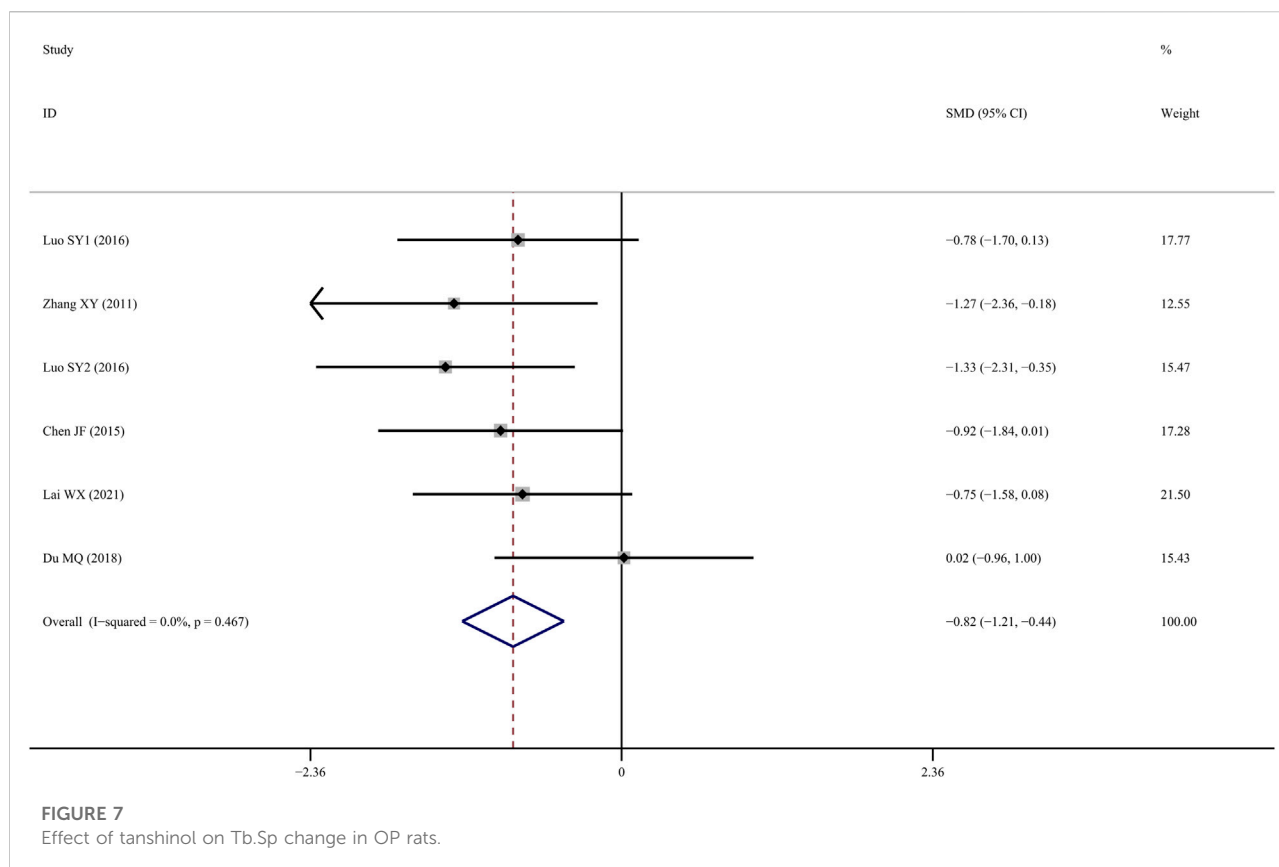
Egger's test was applied to assess the potential publication bias in this meta-analysis and identified several publication biases (BMD-femur,  $p = 0.009$ ; BMD-lumbar,  $p = 0.028$ ) (Figure 11). Sensitivity analyses were also conducted by omitting each study, and no obvious effect was found (supplemental material, Figure 12).

## Discussion

To the best of our knowledge, this is the first preclinical systematic review and meta-analysis examining TS's efficacy on osteoporosis. Nine studies with 168 rats were included in this analysis and indicated that the TS treatment significantly increased BMD, BV/TV, Tb.N, Tb.Th, and S-OCN, while reducing Tb.Sp in OP animal models. Moreover, TS treatment was associated with significantly improved bone biomechanical indicators, including bone maximum load and elasticity load.

Notably, the majority of previous meta-analyses examining the effect of TCM herbal components focused on serological indicators and BMD measurements using dual-energy X-ray



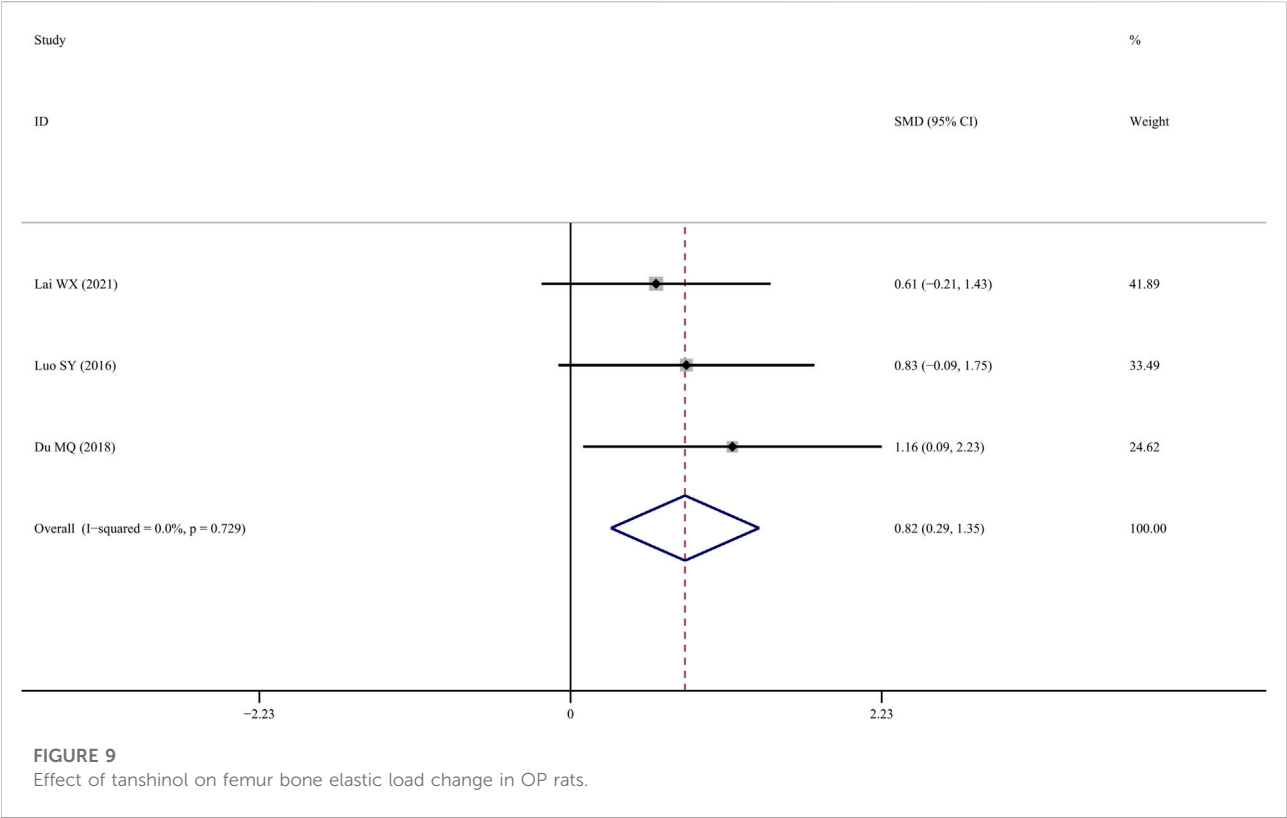
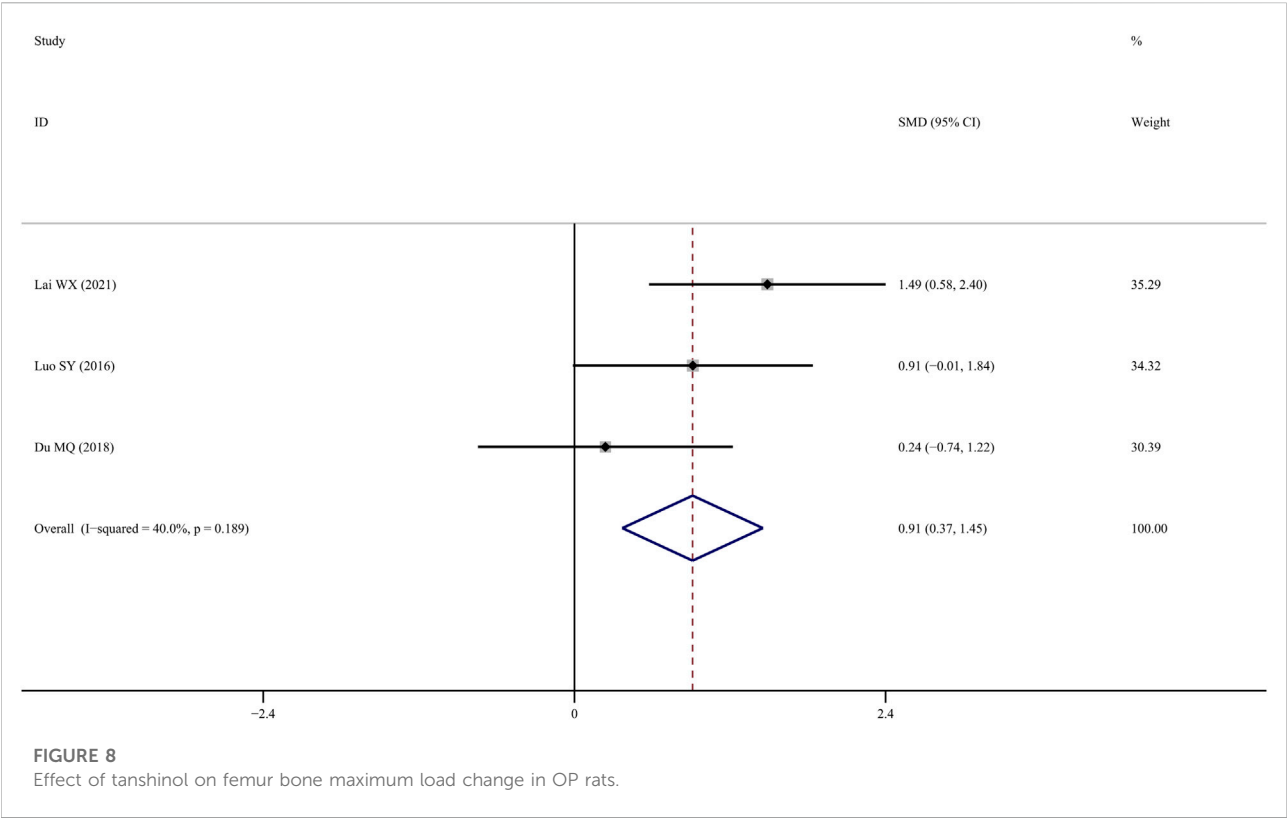


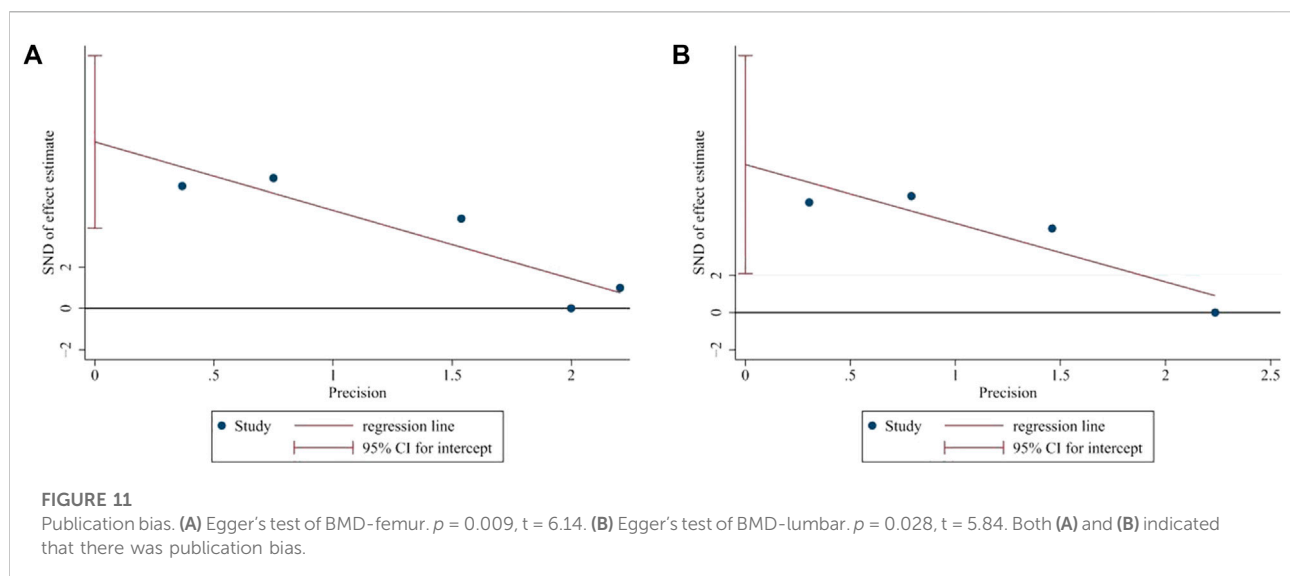
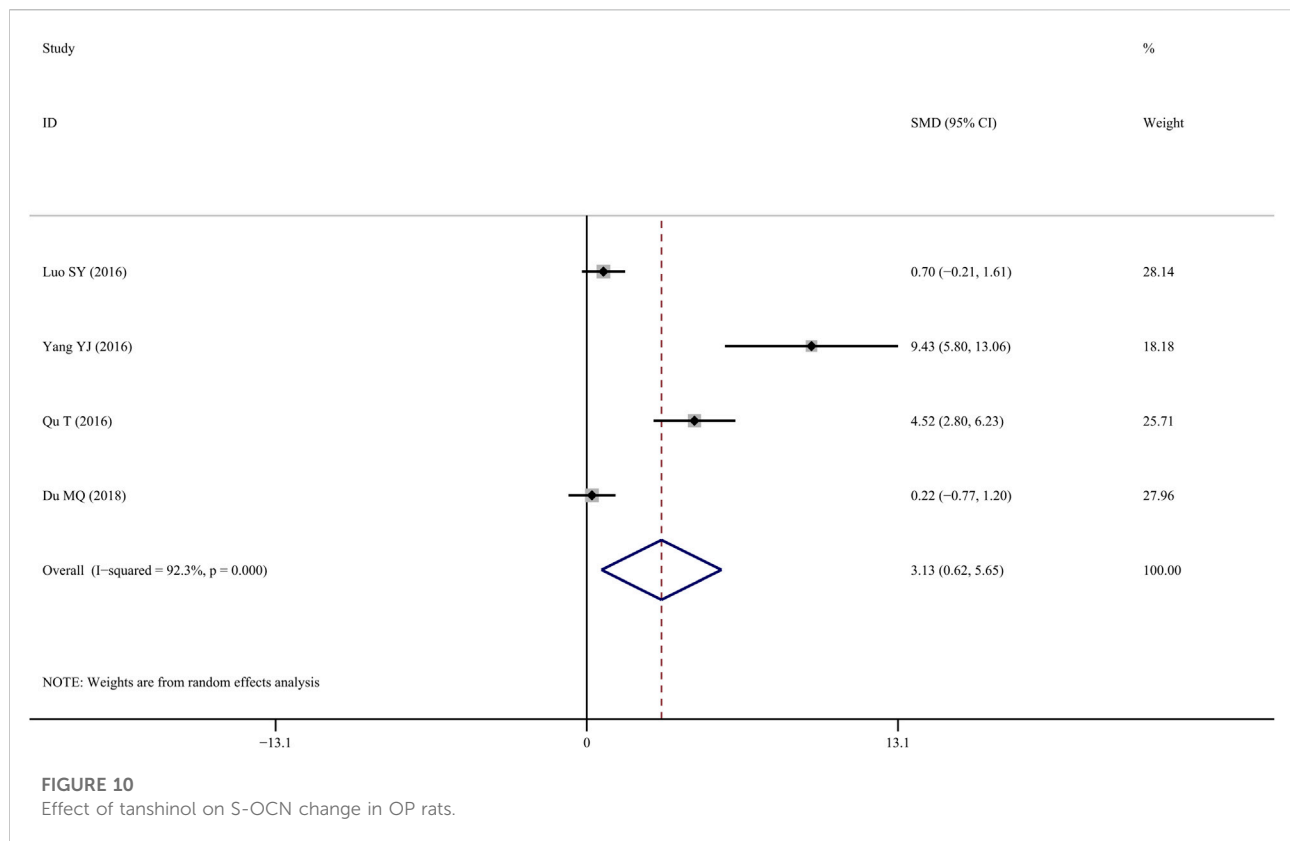
absorptiometry (DXA) (Fu et al., 2014; Xu et al., 2016; Wu et al., 2020; Yang et al., 2020), while relatively few studies examined the bone structure under micro-CT (Lin et al., 2021; Zhu et al., 2021). Increasing evidence suggests that DXA has some limitations (Hahn et al., 1992). For instance, when measuring low-density bone, such as osteoporotic bone or osteophyte tissue, the DXA approach is associated with errors as high as 30% (Bolotin and Sievänen, 2001, 2001; Warden et al., 2005). However, such shortcomings can be avoided using micro-CT (Laib et al., 2000; Mittra et al., 2005). Furthermore, this technique enables quantitative analysis, which allows for multifaceted comparisons, particularly in small animals (Du et al., 2007; Brouwers et al., 2008). Taken together, using a micro-CT-based technique in BMD measurements can help reveal the geometric features of the trabecular bone and allow for more accurate data analysis.

S-OCN plays an important role in regulating calcium homeostasis and bone metabolism (Seibel, 2000). The level of S-OCN was measured in most animal studies. Several studies have revealed that there are factors that can influence OC values in blood serum, particularly oxalate and fluoride, which are present in anticoagulants (Power and Fottrell, 1991). OCN is highly unstable *in vitro* and should be separated immediately after collection and stored at  $-70^{\circ}\text{C}$  without repeated freezing and thawing since OCN immunoreactivity can be reduced by

40% after repeated freeze-thaw cycles (Power and Fottrell, 1991; Woitge and Seibel, 1999). Moreover, some studies have shown that serum OCN levels are susceptible to many factors, such as circadian rhythm, menstrual cycle, age, ethanol intake, season, and hormone replacement therapy (Gundberg et al., 1985; Thomsen et al., 1989; Nielsen et al., 1990). The large difference in S-OCN levels among enrolled studies may be attributed to the aforementioned factors, which suggest the need to strengthen the training of experimental operators.

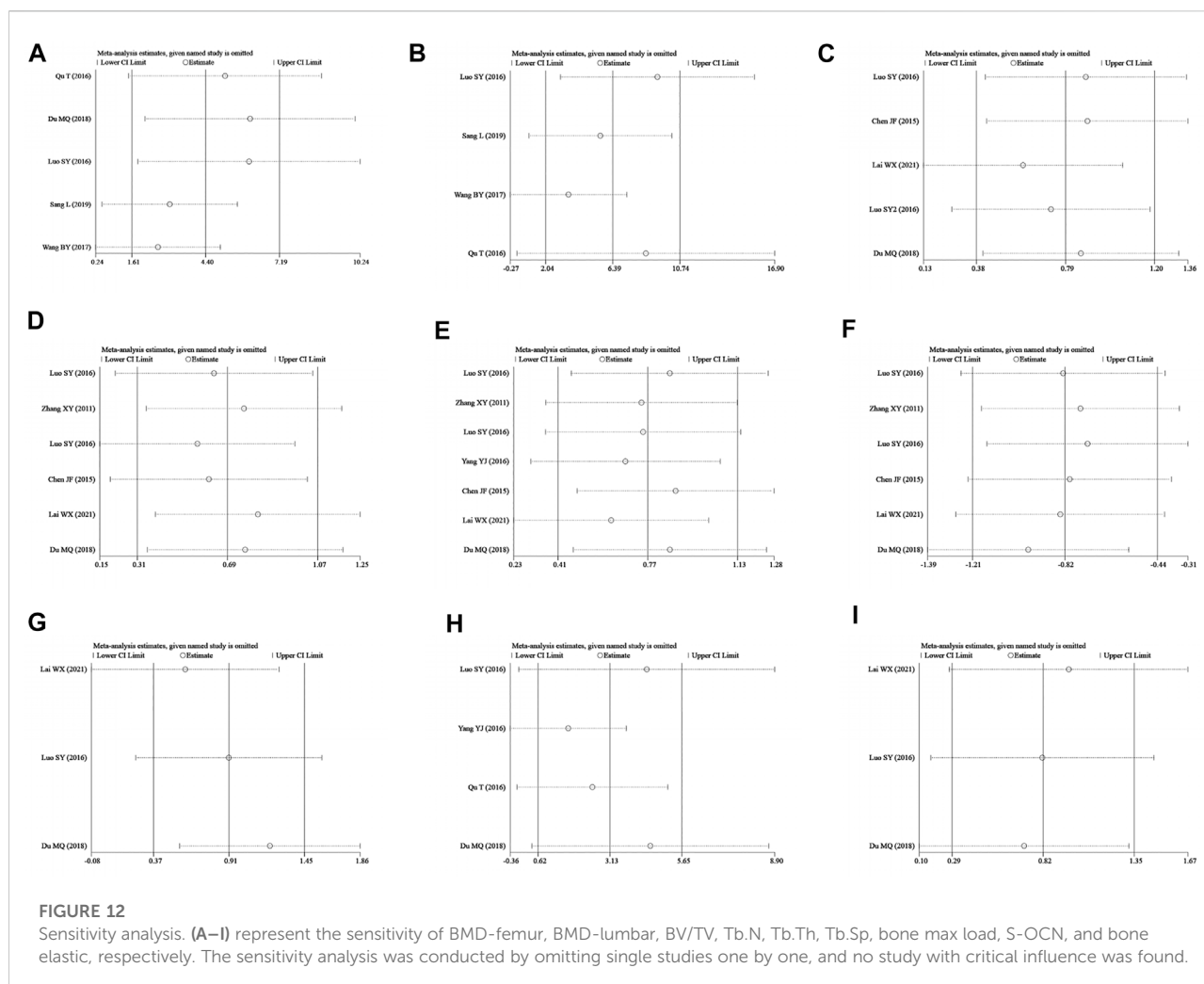
As we all know, OP has become a major public health concern, particularly in recent years, due to its rising incidence and disability rates. Bone homeostasis is delicately maintained by a dynamic balance of osteoblasts and osteoclasts. The pathogenic factors of OP are frequently caused by excessive osteoclast activity, which destroys the structure of the trabecular bone and reduces the biomechanical properties of bone tissues. Mounting evidence demonstrates that active ingredients extracted from natural plants could influence these processes and exert a protective role. Existing studies have proven that TS can reduce the loss of bone components and stimulate the expression of osteoblast-specific genes by eliminating reactive oxygen species (ROS) and inhibiting glucocorticoid (GC) treatment-associated side effects (Yang et al., 2016). In addition, TS can increase the expression of





osteoprotegerin (OPG) mRNA and type I collagen (ColI-I) mRNA, enhance the activity of alkaline phosphatase (ALP), upregulate the expression level of runt-related transcription factor 2 (Runx2), and promote the formation of calcified

nodules (Cui et al., 2009; Han and Wang, 2017). Moreover, TS could suppress oxidative stress-induced osteoporosis and reduce osteoblasts' apoptosis through the PI3k/Akt pathway (Wang, 2017). In addition, TS can block the NF- $\kappa$ B pathway and



inhibit bone cell turnover rates (Han and Wang, 2017). Meanwhile, TS can also regulate osteoclast differentiation and reduce bone resorption through the NF- $\kappa$ B–RANKL signal transduction pathway (Sang, 2019). Additionally, according to evidence from microvascular perfusion imaging of the cancellous bone in GIO rats, as well as the migration capacity of human endothelial cells, TS has a significant protective effect on bone microcirculation. In addition, tanshinol also attenuated GC-elicited the activation of the thioredoxin-interacting protein (TXNIP) signaling pathway and reversed the down-regulation of the Wnt and vascular endothelial growth factor (VEGF) pathways (Lai et al., 2021). Furthermore, another study on glucocorticoid-induced osteoporosis (GIOP) has uncovered that TS could alleviate impaired bone formation. Similarly, co-treatment with TS can effectively offset the impaired bone formation and adipogenesis mechanism caused by oral GC and restore the expression of signal molecules in GIO rats to normal (Yang et al., 2018).

## Limitations

Nonetheless, this study has several limitations. First, although we searched eight databases without any preset restriction on language, it is possible that we may have omitted some relevant studies. Second, given that negative outcomes are not always reported or published, the studies we selected might be biased (supplemental material, Figures 1 and 2). Third, the heterogeneity of tanshinol source and purity cannot be overlooked, as this could jeopardize the validity of our findings. Therefore, additional prospective studies with large sample sizes are warranted to validate our conclusion.

## Conclusion

The study's main finding indicated that TS treatment could promote BMD, bone microarchitecture, bone biomechanics, and

S-OCN expression in rats and that tanshinol, an active component of *Salvia miltiorrhiza*, has therapeutic potential for treating human OP.

## Data availability statement

The original contributions presented in the study are included in the article/Supplementary Material; further inquiries can be directed to the corresponding authors.

## Author contributions

Conceptualization: KL and XS. Data curation: SW and YY. Formal analysis: SW and YY. Funding acquisition: XS. Investigation: QL. Methodology: HZ, YL, HH, BL, and YM. Software: BT. Supervision: SW and YY. Validation: SW and YY. Writing—original draft: SW.

## References

- Bao, X., Zheng, Q., Tong, Q., Zhu, P., Zhuang, Z., Zheng, G., et al. (2018). Danshensu for myocardial ischemic injury: Preclinical evidence and novel methodology of quality assessment tool. *Front. Pharmacol.* 9, 1445. doi:10.3389/fphar.2018.01445
- Black, D. M., and Rosen, C. J. (2016). Clinical practice postmenopausal osteoporosis. *N. Engl. J. Med.* 374, 254–262. [WWW Document]. doi:10.1056/NEJMcp1513724
- Bolotin, H. H., and Sievänen, H. (2001). Inaccuracies inherent in dual-energy X-ray absorptiometry *in vivo* bone mineral density can seriously mislead diagnostic/prognostic interpretations of patient-specific bone fragility. *J. Bone Min. Res.* 16, 799–805. doi:10.1359/jbmr.2001.16.5.799
- Brouwers, J., Lambers, F. M., Gasser, J. A., Van Rietbergen, B., and Huiskes, R. (2008). Bone degeneration and recovery after early and late bisphosphonate treatment of ovariectomized wistar rats assessed by *in vivo* micro-computed tomography. *Calcif. Tissue Int.* 82, 202–211. doi:10.1007/s00223-007-9084-3
- Chen, G., Zhang, X., Lin, H., Huang, G., Chen, Y., Cui, L., et al. (2017). Tanshinol alleviates osteoporosis and myopathy in glucocorticoid-treated rats. *Planta Med.* 83, 1264–1273. doi:10.1055/s-0043-108761
- Chen, J. L. S. C. L. (2015). Effect of tanshinol on bone mineral density and microstructure of proximal tibias in rats with bone loss induced by glucocorticoid. *Chin. Pharmacol. Bull.* 31, 1681–1687. doi:10.3969/j.issn.1001-1978.2015.12.011
- Cui, L., Liu, Y., Wu, T., Ai, C., and Chen, H. (2009). Osteogenic effects of D+beta-3, 4-dihydroxyphenyl lactic acid (salvianic acid A, SAA) on osteoblasts and bone marrow stromal cells of intact and prednisone-treated rats. *Acta Pharmacol. Sin.* 30, 321–332. doi:10.1038/aps.2009.9
- Deeks, E. D. (2018). Denosumab: A review in postmenopausal osteoporosis. *Drugs Aging* 35, 163–173. doi:10.1007/s40266-018-0525-7
- Du, L. Y., Umoh, J., Nikolov, H. N., Pollmann, S. I., Lee, T.-Y., Holdsworth, D. W., et al. (2007). A quality assurance phantom for the performance evaluation of volumetric micro-CT systems. *Phys. Med. Biol.* 52, 7087–7108. doi:10.1088/0031-9155/52/23/021
- Du, M. Q. (2018). *An intervention study of Danshensu combined with fructose on hyperthyroidism-induced osteoporosis in rats*. Zhanjiang, China: Guangdong Medical University.
- Fu, S., Zeng, G., Zong, S., Zhang, Z., Zou, B., Fang, Y., et al. (2014). Systematic review and meta-analysis of the bone protective effect of phytoestrogens on osteoporosis in ovariectomized rats. *Nutr. Res.* 34, 467–477. doi:10.1016/j.nutres.2014.05.003
- Gundberg, C. M., Markowitz, M. E., Mizuchi, M., and Rosen, J. F. (1985). Osteocalcin in human serum: A circadian rhythm. *J. Clin. Endocrinol. Metab.* 60, 736–739. doi:10.1210/jcem-60-4-736
- Hahn, M., Vogel, M., Pompesius-Kempa, M., and Delling, G. (1992). Trabecular bone pattern factor—a new parameter for simple quantification of bone microarchitecture. *Bone* 13, 327–330. doi:10.1016/8756-3282(92)90078-b
- Han, J., and Wang, W. (2017). Effects of tanshinol on markers of bone turnover in ovariectomized rats and osteoblast cultures. *PLoS ONE* 12, e0181175. doi:10.1371/journal.pone.0181175
- Lai, W., Mo, Y., Wang, D., Zhong, Y., Lu, L., Wang, J., et al. (2021). Tanshinol alleviates microcirculation disturbance and impaired bone formation by attenuating TXNIP signaling in GIO rats. *Front. Pharmacol.* 12, 722175. doi:10.3389/fphar.2021.722175
- Laib, A., Barou, O., Vico, L., Lafage-Proust, M. H., Alexandre, C., and Rüsgesser, P. (2000). 3D micro-computed tomography of trabecular and cortical bone architecture with application to a rat model of immobilisation osteoporosis. *Med. Biol. Eng. Comput.* 38, 326–332. doi:10.1007/BF02347054
- Lin, Z., Zheng, J., Chen, J., Chen, M., and Dong, S. (2021). Antiosteoporosis effect and possible mechanisms of the ingredients of fructus psoraleae in animal models of osteoporosis: A preclinical systematic review and meta-analysis. *Oxid. Med. Cell. Longev.* 2021, 2098820. doi:10.1155/2021/2098820
- Lindsay, R., Krege, J. H., Marin, F., Jin, L., and Stepan, J. J. (2016). Teriparatide for osteoporosis: Importance of the full course. *Osteoporos. Int.* 27, 2395–2410. doi:10.1007/s00198-016-3534-6
- Liu, S. C. Z. L. T. (2019). Research Progress on the influence of traditional Chinese medicine on the quality of life of patients with coronary heart disease and angina pectoris. *Hubei J. Trad. Chin. Med.* 14, 60–63.
- Luo, S., Yang, Y., Chen, J., Zhong, Z., Huang, H., Zhang, J., et al. (2016). Tanshinol stimulates bone formation and attenuates dexamethasone-induced inhibition of osteogenesis in larval zebrafish. *J. Orthop. Transl.* 4, 35–45. doi:10.1016/j.jot.2015.07.002
- Macleod, M. R., O'Collins, T., Howells, D. W., and Donnan, G. A. (2004). Pooling of animal experimental data reveals influence of study design and publication bias. *Stroke* 35, 1203–1208. doi:10.1161/01.STR.0000125719.25853.20
- Mittra, E., Rubin, C., and Qin, Y.-X. (2005). Interrelationship of trabecular mechanical and microstructural properties in sheep trabecular bone. *J. Biomech.* 38, 1229–1237. doi:10.1016/j.jbiomech.2004.06.007

## Funding

This work was supported by the National Natural Science Foundation of China (No: 82074183 and No:81873129).

## Conflict of interest

The authors declare that the research was conducted in the absence of any commercial or financial relationships that could be construed as a potential conflict of interest.

## Publisher's note

All claims expressed in this article are solely those of the authors and do not necessarily represent those of their affiliated organizations, or those of the publisher, the editors, and the reviewers. Any product that may be evaluated in this article, or claim that may be made by its manufacturer, is not guaranteed or endorsed by the publisher.



- Nielsen, H. K., Brixen, K., and Mosekilde, L. (1990). Diurnal rhythm and 24-hour integrated concentrations of serum osteocalcin in normals: Influence of age, sex, season, and smoking habits. *Calcif. Tissue Int.* 47, 284–290. doi:10.1007/BF02555910
- Power, M. J., and Fottrell, P. F. (1991). Osteocalcin: diagnostic methods and clinical applications. *Crit. Rev. Clin. Lab. Sci.* 28, 287–335. doi:10.3109/10408369109106867
- Qu, T., Z. P. Y. C., Zheng, P., Yang, C., Lan, X., Zhang, T., Liu, H., et al. (2016). Effects of Danshensu on bone formation in ovariectomized rats. *J. Zhejiang Univ. Med. Sci.* 45, 587–591. doi:10.3785/j.issn.1008-9292.2016.11.05
- Sang, L., H. H. D. K.-D. (2019). Inhibition of Danshensu on osteoclast differentiation by inhibiting nuclear factor- $\kappa$ B receptor activator ligand pathway in the treatment of osteoporosis in rats. *Chin. J. Clin. Pharmacol.* 35, 3072–3076. doi:10.13699/j.cnki.1001-6821.2019.23.033
- Seibel, M. J. (2000). Molecular markers of bone turnover: biochemical, technical and analytical aspects. *Osteoporos. Int.* 11, S18–S29. doi:10.1007/s001980070003
- Si, L., Winzenberg, T. M., Jiang, Q., Chen, M., and Palmer, A. J. (2015). Projection of osteoporosis-related fractures and costs in China: 2010–2050. *Osteoporos. Int.* 26, 1929–1937. doi:10.1007/s00198-015-3093-2
- Sy, L. (2016). *Effects of tanshinol and salivianolic acid B on glucocorticoid-induced osteoporosis in zebrafish and in rats*. Guangzhou, China: Southern Medical University.
- Thomsen, K., Eriksen, E. F., Jørgensen, J., Charles, P., and Mosekilde, L. (1989). Seasonal variation of serum bone GLA protein. *Scand. J. Clin. Lab. Invest.* 49, 605–611. doi:10.1080/00365518909091535
- Wang, B. P. J. (2017). Tanshinol attenuates oxidative stress-induced osteoporosis and reduces apoptosis of osteoblasts via PI3/Akt signal pathway. *Chin. J. Osteoporos.* 23, 1–511. doi:10.3969/j.issn.1006-7108.2017.01.001
- Wang, Y. L., Y. W. U. (2015). Progress on effect and mechanism of Danhong injection in treatment of coronary heart disease. *Chin. J. Biochem. Pharm.* 35, 186–188.
- Warden, S. J., Hurst, J. A., Sanders, M. S., Turner, C. H., Burr, D. B., Li, J., et al. (2005). Bone adaptation to a mechanical loading program significantly increases skeletal fatigue resistance. *J. Bone Min. Res.* 20, 809–816. doi:10.1359/JBMR.041222
- Woitte, H. W., and Seibel, M. J. (1999). Molecular markers of bone and cartilage metabolism. *Curr. Opin. Rheumatol.* 11, 218–225. doi:10.1097/00002281-199905000-00011
- Wu, B., Huang, J.-F., He, B.-J., Huang, C.-W., and Lu, J.-H. (2020). Promotion of bone formation by red yeast rice in experimental animals: A systematic review and meta-analysis. *Biomed. Res. Int.* 2020, 7231827. doi:10.1155/2020/7231827
- Xu, J., Yao, M., Ye, J., Wang, G., Wang, J., Cui, X., et al. (2016). Bone mass improved effect of icariin for postmenopausal osteoporosis in ovariectomy-induced rats: A meta-analysis and systematic review. *Menopause* 23, 1152–1157. doi:10.1097/GME.0000000000000673
- Yang, X., Zheng, H., Liu, Y., Hao, D., He, B., Kong, L., et al. (2020). Puerarin for OVX-induced postmenopausal osteoporosis in murine model: systematic review and meta-analysis. *Curr. Stem Cell Res. Ther.* 15, 37–42. doi:10.2174/1574888X14666190703143946
- Yang, Y., Su, Y., Wang, D., Chen, Y., Liu, Y., Luo, S., et al. (2016). Tanshinol rescues the impaired bone formation elicited by glucocorticoid involved in KLF15 pathway. *Oxid. Med. Cell. Longev.* 2016, 1092746. doi:10.1155/2016/1092746
- Yang, Y., Zhu, Z., Wang, D., Zhang, X., Liu, Y., Lai, W., et al. (2018). Tanshinol alleviates impaired bone formation by inhibiting adipogenesis via KLF15/PPAR $\gamma$ 2 signaling in GIO rats. *Acta Pharmacol. Sin.* 39, 633–641. doi:10.1038/aps.2017.134
- Zhang, X.-Y., Liao, C., Tie, W., and Yun-Xin, L. (2011). Effects of tanshinol on alveolar bone metabolism in rats. *J. Clin. Rehabilitative Tissue Eng. Res.* 15 (33), 6203–6206. doi:10.3969/j.issn.1673-8225.2011.33.030
- Zhu, Zhu, Xie, W., Li, Y., Zhu, Zaiou, and Zhang, W. (2021). Effect of naringin treatment on postmenopausal osteoporosis in ovariectomized rats: A meta-analysis and systematic review. *Evid. Based. Complement. Altern. Med.* 2021, 6016874. doi:10.1155/2021/6016874



## OPEN ACCESS

## EDITED BY

Xiaofeng Zhu,  
Jinan University, China

## REVIEWED BY

Aifeng Liu,  
First Teaching Hospital of Tianjin  
University of Traditional Chinese  
Medicine, China  
Hao Yue,  
Changchun University of Chinese  
Medicine, China  
Shi Wei,  
Affiliated Hospital of Shandong  
University of Traditional Chinese  
Medicine, China

## \*CORRESPONDENCE

Xu Wei,  
weixu.007@163.com

<sup>†</sup>These authors share first authorship

## SPECIALTY SECTION

This article was submitted to  
Experimental Pharmacology and Drug  
Discovery,  
a section of the journal  
Frontiers in Pharmacology

RECEIVED 23 June 2022

ACCEPTED 29 July 2022

PUBLISHED 25 August 2022

## CITATION

Liu N, Qi B, Zhang Y, Fang S, Sun C, Li Q  
and Wei X (2022), Bu-Gu-Sheng-Sui  
decoction promotes osteogenesis via  
activating the ERK/Smad  
signaling pathways.  
*Front. Pharmacol.* 13:976121.  
doi: 10.3389/fphar.2022.976121

## COPYRIGHT

© 2022 Liu, Qi, Zhang, Fang, Sun, Li and  
Wei. This is an open-access article  
distributed under the terms of the  
[Creative Commons Attribution License](https://creativecommons.org/licenses/by/4.0/)  
(CC BY). The use, distribution or  
reproduction in other forums is  
permitted, provided the original  
author(s) and the copyright owner(s) are  
credited and that the original  
publication in this journal is cited, in  
accordance with accepted academic  
practice. No use, distribution or  
reproduction is permitted which does  
not comply with these terms.

# Bu-Gu-Sheng-Sui decoction promotes osteogenesis via activating the ERK/Smad signaling pathways

Ning Liu<sup>1†</sup>, Baoyu Qi<sup>1†</sup>, Yili Zhang<sup>2†</sup>, Shengjie Fang<sup>1</sup>,  
Chuanrui Sun<sup>1</sup>, Qiuyue Li<sup>1</sup> and Xu Wei<sup>1\*</sup>

<sup>1</sup>Wangjing Hospital, China Academy of Chinese Medical Sciences, Beijing, China, <sup>2</sup>School of Traditional Chinese Medicine and School of Integrated Chinese and Western Medicine, Nanjing University of Chinese Medicine, Nanjing, China

Osteoporosis is a systemic metabolic skeletal disease, which becomes a common public health problem that seriously endangers people's health. Bu-Gu-Sheng-Sui decoction (BGSSD) is a safe and effective Chinese medicine formulation for the treatment of osteoporosis. Numerous studies have indicated that it played a significant role in bone anabolism. However, the underlying mechanism remains unclear. Herein, we selected senescence-accelerated mice prone 6 (SAMP6) and MC3T3-E1 cells to study the effects of BGSSD on osteogenesis and then investigated the potential mechanism of BGSSD. Our research found that BGSSD protected the bone mass in SAMP6, increased the expression of osteogenic specific factor Runx2, and improved bone trabecular structure. *In vitro*, BGSSD accelerated the proliferation and differentiation of MC3T3-E1 cells, which was characterized by stimulating the activity of Alkaline phosphatase (ALP) and raising the expression of Runx2. Moreover, BGSSD could effectively boost the expression levels of ERK and Smad in SAMP6 and MC3T3-E1. Therefore, we speculate that BGSSD may promote bone formation through ERK/Smad pathways. Collectively, our results highlight the importance of BGSSD as a compound in promoting osteogenic differentiation and osteogenesis, demonstrating that BGSSD may become a latent drug to prevent and treat osteoporosis.

## KEYWORDS

Bu-Gu-Sheng-Sui decoction, osteogenesis, mechanism, ERK/Smad, osteoporosis

## Introduction

Osteoporosis (OP) is a systemic metabolic skeletal disease characterized by decreased bone mineral density (BMD), bone mass loss, and destructed microstructure of bones, easily leading to bone fragility and a high probability of fracture (Johnston and Dagar, 2020). OP is one of the age-related bone diseases in which bone loss progresses with advancing age. With the advent of an aging society, OP has become a common public health problem that seriously endangers people's health in various countries (Noh et al.,

2020). Especially fractures caused by OP seriously affect the patient's quality of life and increase the mortality rate (Compston et al., 2019). The pathogenesis of OP is complicated, yet more bone resorption than formation is the primary pathological manifestation (Wong et al., 2019). The current clinical treatment of OP mainly focuses on inhibiting bone resorption, yet with many side effects. Although many researchers have demonstrated that the multilevel processes of bone formation are essential for maintaining bone mass, effective drugs are still lacking (Chang et al., 2019). Therefore, looking for potential drugs for the treatment of OP, which stimulate bone formation, is an urgent problem to be solved.

Traditional Chinese medicine (TCM) has unique advantages in treating OP due to its multi-component and multi-target characteristics, especially in promoting bone formation (Zhang et al., 2016). Bu-Gu-Sheng-Sui decoction (BGSSD) is composed of eight herbs (Drynaria, Fructus Psoraleae, Rhizoma cibotii, Wolfberry, Raw Oysters, Ginseng, Panax Notoginseng, and Fructus Amomi), which has exact efficacy in treating OP. A randomized controlled trial of 80 cases manifested that the significant and overall effective rates of BGSSD in treating OP were 46% and 82%, respectively. BGSSD raised BMD, ameliorated clinical symptoms, and had reliable safety in the treatment process (Xie et al., 1997a). On the premise of good clinical efficacy, many basic studies were conducted, and the results testified that BGSSD could increase the BMD and bone biomechanical properties of ovariectomized rats (Xie et al., 1997b), modify microcirculation disorders (Liu et al., 1997) and relieve inflammation and pain (Ji et al., 1997). These results attested that BGSSD could promote osteogenesis effectively. However, the detailed mechanism of BGSSD is still unclear.

The extracellular regulated protein kinases (ERK) pathway acted a prominent role in enhancing osteoblast differentiation and promoting bone formation (Catalano et al., 2017; Mizumachi et al., 2017; Kim et al., 2018). It was the most critical event in bone development and bone mass maintenance (Bhaskar et al., 2014; Park et al., 2019). The Smad protein family also played an integral part in regulating bone metabolism (Kopf et al., 2014; Cheng et al., 2019; Feng et al., 2020). The down-regulation of Smad mRNA expression and protein level may be one of the momentous mechanisms of OP (Donoso et al., 2015; Durbano et al., 2020). Inhibition and defect of Smad signal transduction may down-regulate the expression of Runx2 and Osterix, affecting the activity of osteoblasts, leading to reduced osteogenesis and bone mass, and ultimately to the occurrence of OP (Dineen and Gaudet, 2014; Li et al., 2014; Liu et al., 2017). Studies showed that the main extracts of herbs in BGSSD affected the differentiation of osteoblasts by modifying the ERK or Smad pathway (Zhu et al., 2012; Zhang et al., 2019; Sun et al., 2021b; Huang et al.,

2021). Moreover, many kinds of research have shown a mutual crosstalk relationship between ERK and Smad (Zhou et al., 2007; Park et al., 2011; Lee et al., 2018; Tashima et al., 2020). Therefore, we hypothesize that BGSSD may enhance osteoblast differentiation through ERK/Smad pathway to exert an anti-osteoporosis effect.

Based on the above, the osteogenic functions of BGSSD will be verified in SAMP6 and MC3T3-E1 cells. Furthermore, potential mechanisms of BGSSD in boosting osteogenesis through ERK/Smad will be investigated in the rat model and osteoblastic cells. The above research results may provide new pharmacological evidence for BGSSD in clinically treating or preventing osteoporosis.

## Materials and methods

### Experimental animal

The animals were purchased from the Laboratory Animal Science Department of Peking University Health Science Center, with the license number SCXK (Jing) 2020-0002. SAMP6 were randomly divided into the model group (Model,  $n = 6$ ), high-dose BGSSD-treated group (H-BGSSD,  $n = 6$ ), middle-dose BGSSD-treated group (M-BGSSD,  $n = 6$ ), low-dose BGSSD-treated group (L-BGSSD,  $n = 6$ ), and alendronate (Shi Yao, Hebei, China)-treated group (Alendronate,  $n = 6$ ). Six senescence-accelerated mice resistant 1 (SAMR1) were used as the control group (Control,  $n = 6$ ), alendronate was given at 1.517 mg/kg, and the low-, medium-, and high-dose of BGSSD groups were respectively given the crude drug at 10.16 g/kg, 20.32 g/kg, and 40.64 g/kg intragastrically. All animals were housed at 1 per cage in the Animal Experiment Center of the Acupuncture Institute, China Academy of Chinese Medical Sciences, with humidity of 48% and temperature of 25°C, and freed access to food and water. Two weeks of adaptive feeding were adjusted before the gavage.

### Drug preparation

Chinese herbal medicine was purchased from Wangjing Hospital of China Academy of Chinese Medical Sciences, and administered dosages were converted according to the clinically effective dose. We referenced the procedure of drug preparation by Jiang et al. (2021). All medicinal plants of BGSSD were decocted 40 min twice with boiling purified water (1:10 and then 1: 5, w/v). After filtering, the solution was concentrated using a vacuum evaporator (70°C). The solution was stored at 4°C and diluted with ultrapure water to the desired concentrations before use.

## Tissue collection

After 12 weeks, all animals were anesthetized by intraperitoneal injection of 0.3% sodium pentobarbital (Haling, Shanghai, China). Obtained the left femurs and immediately placed them in PBS (Solarbio, Beijing, China) for BMD detection. The right femurs were stored in paraformaldehyde solution (Solarbio, Beijing, China) for fixation, and the distal femoral metaphysis was selected for Hematoxylin-eosin (HE) staining. The right tibias were determined by immunohistochemistry (IHC) Staining, and the left tibias were quick-frozen with liquid nitrogen and stored at  $-80^{\circ}\text{C}$ , which were used for Western Blotting (WB) and Real-time PCR (RT-PCR) detection.

## Dual-energy X-ray absorptiometry test

The skeletal imaging was performed via a dual-energy X-ray scanner (Osteocore, Medilink, France). It can automatically aim at the induction area and control quality and periosteum calibration. Cross-sectional images of the samples were collected, and the range of the femur was framed. Bone mineral mass and bone area were analyzed and calculated by Osteocore3.7.0.0.5 software. Finally, the BMD was calculated.

## Hematoxylin-eosin staining assay

Right femurs were fixed with 4% paraformaldehyde (Solarbio, Beijing, China) for 7 days, and decalcified, dehydrated, embedded in paraffin, cut into 5- $\mu\text{m}$  sections, and then deparaffinized by xylene (Solarbio, Beijing, China) together with ethanol (in the following order: 100, 95, 90, 80, 70%). The sections were immersed in distilled water, and hematoxylin-eosin staining (Baso, Zhuhai, China) was performed according to the protocol. Bone trabeculae were observed under a microscope (Carl Zeiss, Germany), and bone cavity volume ratio was measured by Image-Proplus5 (IPP).

## Immunohistochemical staining assay

Tibias were fixed in 4% paraformaldehyde solution at  $4^{\circ}\text{C}$  for 24 h, and then they were placed in 10% ethylene diamine tetraacetic acid solution (Solarbio, Beijing, China) and decalcified for 21 days. Next, the bones were embedded in paraffin (Guoyao, Shanghai, China). Paraffin wax blocks were sliced into longitudinally oriented bone sections with a thickness of 4  $\mu\text{m}$ . After retrieval of antigens, quenching of endogenous peroxidase, and blocking of nonspecific binding, the sections were incubated with the corresponding primary antibodies at  $4^{\circ}\text{C}$ . After washing, the tissue sections were incubated with a

secondary antibody linked to horseradish peroxidase (Zymed, San Francisco, United States). After rinsing in PBS, the sections were stained with DAB (DAKO, Glostrup, Denmark) and counterstained with hematoxylin, and then images were captured by a fluorescence microscope.

## MC3T3-E1 cell culture and treatment

MC3T3-E1 cells were purchased from the Institute of Basic Medical Sciences, Chinese Academy of Medical Sciences, and cultured in alpha-modified minimum essential medium eagle ( $\alpha$ -MEM, Shanghai BasalMedia Technologies Co., LTD., China) containing 10% fetal bovine serum (FBS, Gibco, United States) and 1% penicillin-streptomycin (Gibco, United States), incubated at  $37^{\circ}\text{C}$  and 5%  $\text{CO}_2$ . The medium was changed every 2 days. MC3T3-E1 was modeled by the method of serum starvation as a control group for subsequent experiments. Firstly different concentrations of BGSSD medicated serum were used to intervene MC3T3-E1 to find the optimal medicated serum concentration. Then the further experiment was performed. The Control, Epidermal growth factor (EGF), and BGSSD groups were treated for 48 h, 72 h, or 7 days with blank serum, EGF (10 ng/ml, Proteintech, United States), and optimal concentration of BGSSD containing serum, respectively.

## Preparation of drug-containing serum

When the BGSSD-Containing Serum was prepared, the intragastric dose of rats was the equivalent dose (5.87 g/kg). After the last intragastric administration, the blood of rats was collected and placed at  $4^{\circ}\text{C}$  for 1 h, then centrifuged for 10 min ( $4^{\circ}\text{C}$ , 3000 rpm). The supernatant was collected, and anhydrous ethanol of 4 times the volume of serum was added to precipitate proteins. The suspension was centrifuged for 10 min ( $4^{\circ}\text{C}$ , 5000 rpm), and the supernatant was dried in a vacuum centrifuge concentrator ( $45^{\circ}\text{C}$ , 1,600 rpm, 300 min). The powder was stored separately at  $-80^{\circ}\text{C}$ . To eliminate individual differences, the drug-containing serum of each group was premixed and concentrated. The quality control (QC) of BGSSD medicated serum has been previously examined by high-performance liquid chromatography (HPLC), which ensured the experimental stability and controllability (Supplementary Figure S1).

## Cell counting kit 8 assay

The cell viability was tested via Cell counting kit 8 assay (CCK-8; Bioson, Beijing, China). MC3T3-E1 cells were inoculated into 96-well plates at  $5 \times 10^3$  per well and



TABLE 1 Sequences of primers used for RT-PCR.

Gene	Primer sequences (5'→3')	
ERK1	F:TGTTCCCAAATGCTGACT	R:GGGTCGTAATACTGCTCC
Runx2	F:TCCCTCCATCCTCCCTTATTT	R:CCTCATTCCCTAACCTGAAACC
Smad4	F:ACCTTTTACACTCCAACCTGC	R:AACTTCCCCAACATTCTCT
β-actin	F:ACTGCCGCATCCTCTTCCTC	R:ACTCCTGCTTGCTGATCCACAT

F, forward; R, reverse.

incubated overnight to adhere. After 8 h, the cells were treated with different treatments. CCK-8 reagent (10%, v/v) was added after 48 h, 72 h, or 7 days of administration, and the optical density (OD) was detected at 450 nm to analyze the cells' proliferation.

## Alkaline phosphatase activity assay

MC3T3-E1 cells were seeded into 6-well plates at  $5 \times 10^4$  cells per well and incubated with a 3 ml medium to adherence. Serum-free medium containing corresponding drugs was added for different groups, 5% CO<sub>2</sub>, 37°C incubating for 72 h. In the end, cells were washed once with PBS, and 100 μL 0.1% Triton X-100 (v/v, PBS) was added, transferring them to 1.5 ml Eppendorf tubes, and the cells were sufficiently lysed by 40% intensity sonication (ice bath operation), centrifuged at 3000 rpm, 4°C for 15 min, collecting the supernatant. BCA protein assay kit (MA, United States) was used to determine the concentration at 3 mg/ml (w/v, PBS). Samples were tested for ALP contents following the enzyme-linked immunosorbent assay (ELISA) kit operating instructions.

## Western blotting

The proteins of animal bone tissue and osteoblasts were quantified using a BCA protein assay kit and separated by electrophoresis in 10% sodium dodecyl sulphate-polyacrylamide gel before being transferred to PVDF membranes (Millipore, United States). PVDF membrane was combined with antibodies of β-actin, ERK1/2 (Proteintech, United States), Smad4 (Proteintech, United States), Runx2 (Bioss, Beijing, China), incubating overnight at 4°C, then shaken with secondary antibody at room temperature for 1 h. Exposure was taken in a TANON gel imager.

## Real-time PCR

Trizol reagent (Solarbio, Beijing, China) was used to extract total RNA from MC3T3-E1 cells and bone tissue of SAMP6.

Then TransScript II All-in-One First-Strand cDNA Synthesis SuperMix Kit (Crenscene, China) was used to synthesize the first-strand cDNA templates. According to the manufacturer's protocol, RT-PCR was carried out by RT-PCR testing equipment (Roche LightCycler® 480II, Switzerland), and the results were analyzed by Applied Biosystems 7500 Fast System SDS software. Using the expression levels of β-actin and calculated by the  $2^{-\Delta\Delta C_t}$  method. The primer gene sequences used are listed in Table 1.

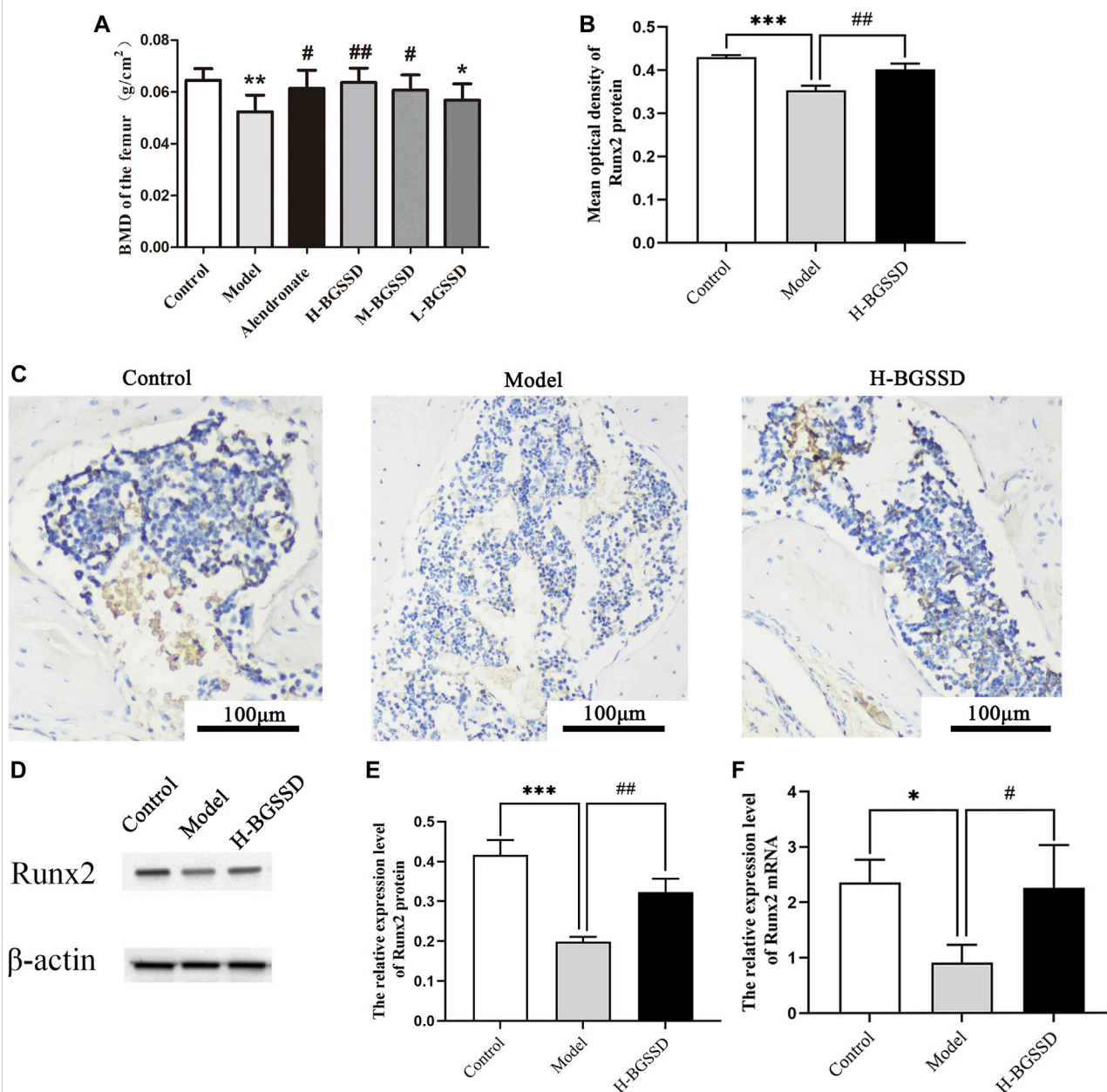
## Statistical analysis

SPSS 24.0 statistical software was used to check the data normality and homogeneity of variance of experimental data. Statistical analysis was performed by one-way ANOVA. All data were presented as mean ± SD.  $p < 0.05$  is considered to be statistically significant.

## Results

### Effects of Bu-Gu-Sheng-Sui decoction on femoral bone mass in SAMP6

To identify the pharmacodynamic effects of BGSSD in age-related osteoporosis, we adopted SAMP6, a model of senile osteoporosis, as the subjects, and manifested that the BMD of SAMP6 was significantly lower than SAMR1. It was altered by using BGSSD. The BGSSD-treated groups had higher BMD than the model group, and the H-BGSSD-treated group was the best versus the other two administration groups (Figure 1A;  $p < 0.05$ ). To better compare and analyze the changes in femoral bone mass, we performed HE staining to investigate whether BGSSD affected skeletal histomorphometry in SAMP6. The results demonstrated that the bone trabeculae in the control group were numerous, closely arranged, relatively evenly distributed, and interconnected into a dense network structure. However, the bone trabeculae of SAMP6 were extremely damaged, with few in number, sparse arrangement and interrupted connectivity, and non-reticular structure. Compared with the model group, the trabecular bone structure improved after the intervention of

**FIGURE 1**

BGSSD promoted bone formation of SAMP6. Control: control group (SAMR1), Model: model group (SAMP6), H-BGSSD: High-dose BGSSD-treated group, M-BGSSD: middle-dose BGSSD-treated group, L-BGSSD: low-dose BGSSD-treated group, Alendronate: positive control, alendronate-treated group. First, BGSSD raised the BMD of the femoral in SAMP6. **(A)** X-ray imaging was performed on the femurs collected from the above groups. BMD of each group was measured by dual-energy X-ray absorptiometry. Data are expressed as mean  $\pm$  SD, \* $p$  < 0.05, \*\* $p$  < 0.01 compared with the control group; # $p$  < 0.05, ## $p$  < 0.01 versus the model group. Furthermore, BGSSD promoted overexpression of osteogenic specific factor Runx2 in SAMP6. **(C)** Immunohistochemical staining was carried out to evaluate the expression of Runx2 protein in bone tissue. Scale bar = 100 μm. **(B)** The mean optical density of Runx2 protein was quantified by ImageJ. Values were expressed as mean  $\pm$  SD, \*\*\* $p$  < 0.001 the model group versus the control group; ## $p$  < 0.01, the group of H-BGSSD versus the model group. WB was carried out to assess the expression of Runx2 protein in bone tissue. **(D)** Representative images of WB. **(E)** The quantification of the protein expression level of Runx2, samples were collected from the bone tissue. Values were expressed as mean  $\pm$  SD, \*\*\* $p$  < 0.001, versus the control group; ## $p$  < 0.01, versus the model group. **(F)** The mRNA expression of Runx2 in bone tissue was assessed by RT-PCR. Values were expressed as mean  $\pm$  SD, \* $p$  < 0.05, versus the control group; # $p$  < 0.05, versus the model group. All the assays were repeated more than three times.

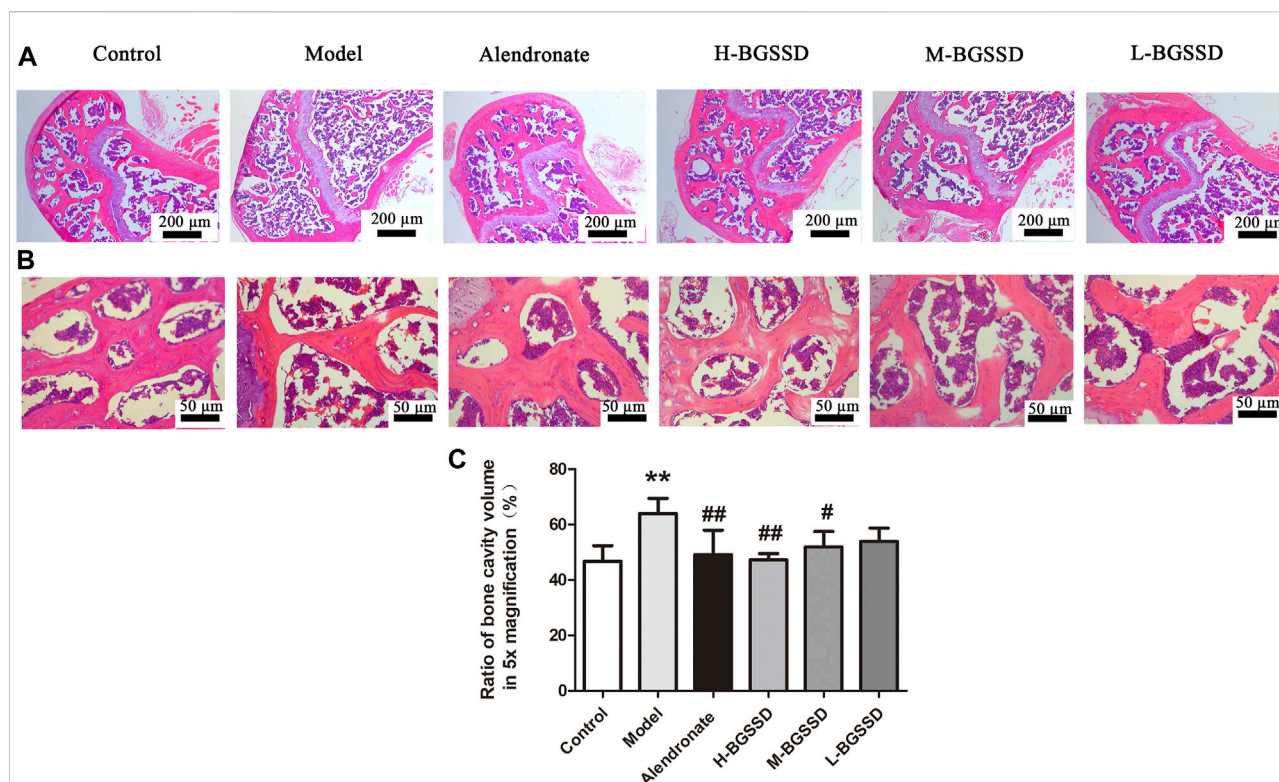


**FIGURE 2**

BGSSD ameliorated the bone tissue morphology of SAMP6. The femurs gathered from the above groups were performed by HE staining, the images of trabecular bone structure were selected from blow the growth plates, magnification is  $\times 5$  (A) and  $\times 20$  (B). (C) Ratio of bone cavity volume regarding representative HE staining of femoral sections from different groups in  $\times 5$  magnification, the site of choice was selected from blow the growth plates. Data are expressed as mean  $\pm$  SD, \*\* $p < 0.01$ , compared with the control group; # $p < 0.05$ , ## $p < 0.01$ , versus the model group. All assays were repeated more than three times.

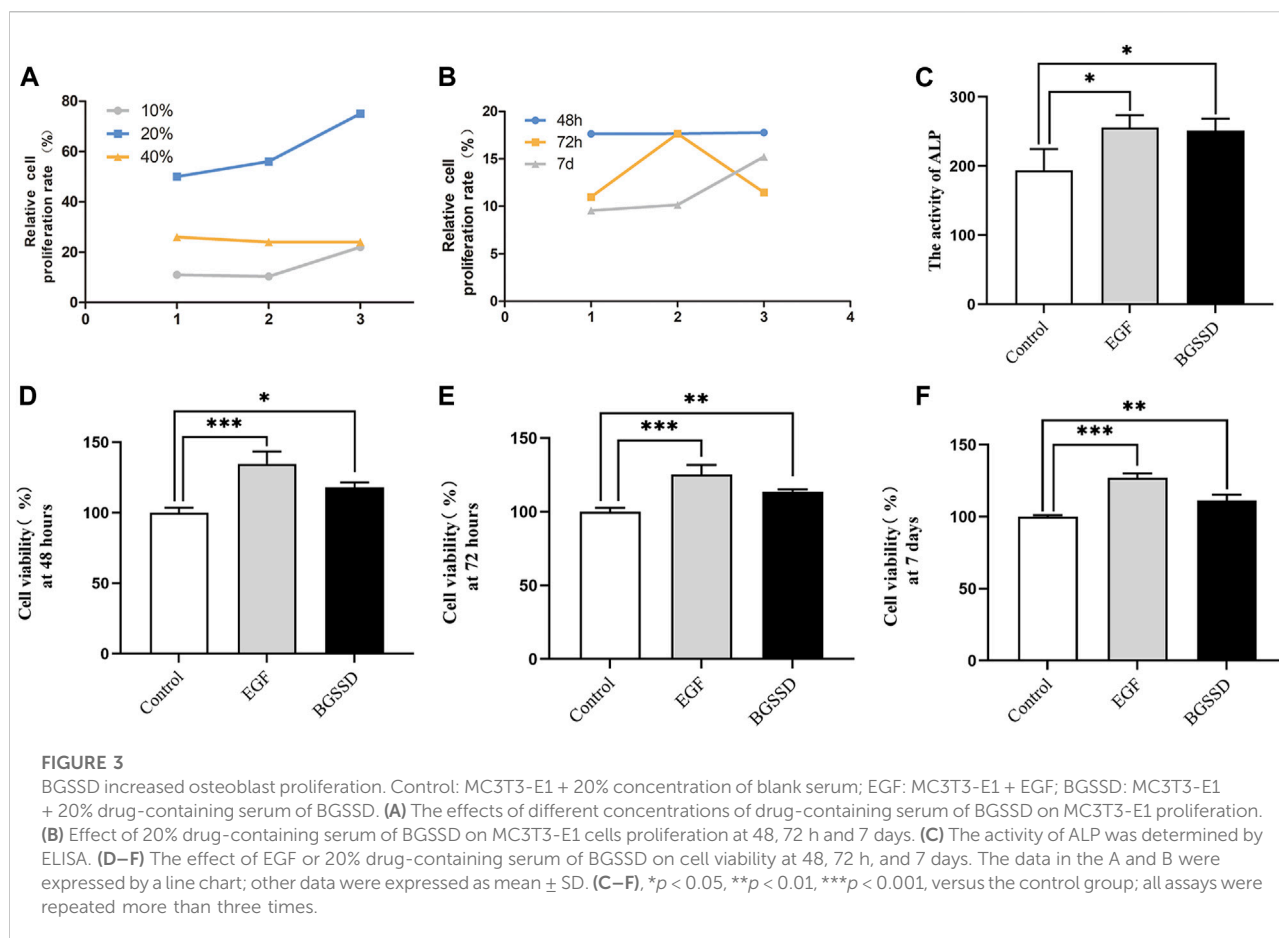
BGSSD. The most apparent performance was the H-BGSSD group (Figures 2A,B); meanwhile, the ratio of bone cavity volume regarding representative HE staining of femoral sections showed that the model group was the largest, improved after BGSSD treatment, and the H-BGSSD group had the best effect (Figure 2C;  $p < 0.05$ ), which were consistent with BMD results. These results indicated that the impact of BGSSD on preventing bone mass loss presented as a dose-dependent trend. H-BGSSD group showed the best therapeutic effect, which was the optimal dosing group for this experiment, so it was selected for IHC, WB, and RT-PCR detection.

Furthermore, Runx2 is a marker for initiating osteoblast differentiation and is the earliest and most specific marker gene during bone formation (Komori, 2020). Meanwhile, Runx2 is the central control gene of the osteoblast phenotype (Franceschi et al., 2009). Therefore, we examined Runx2 expression in bone tissue. Our IHC, WB, and RT-PCR indicated that H-BGSSD increased the expression of osteogenic specific factor Runx2 (Figures 1B–F;  $p < 0.05$ ). Overall, our findings demonstrate that

BGSSD treatment could actively protect the bone structure and prevent bone loss.

## Effects of Bu-Gu-Sheng-Sui decoction on the proliferation of osteoblasts

To confirm whether BGSSD affects the proliferation of MC3T3-E1 cells, we used different concentrations of drug-containing serum of BGSSD to treat MC3T3-E1 cells. The CCK-8 assay was applied for determination. The results showed that different concentrations of drug-containing serum of BGSSD promoted osteoblasts proliferation, and the 20% drug-containing serum of the BGSSD group performed the best effect (Figure 3A). Then, we used EGF or 20% drug-containing serum of BGSSD to intervene in MC3T3-E1 cells. The consequences revealed that EGF and 20% drug-containing serum of BGSSD elevated the viability of MC3T3-E1 cells after 48 h, 72 h, and 7 days, compared with untreated cells (Figures 3D–F;  $p < 0.05$ ). Furthermore, after being treated with 20% drug-containing serum of BGSSD, the differentiation of MC3T3-E1



cells had the most significant effect at the 48-h time point (Figure 3B). Therefore, the cells treated for 48 h were selected as the samples for further detection. Altogether, our data suggest that BGSSD could promote the proliferation of osteoblasts.

### Bu-Gu-Sheng-Sui decoction upregulated osteoblast alkaline phosphatase activity

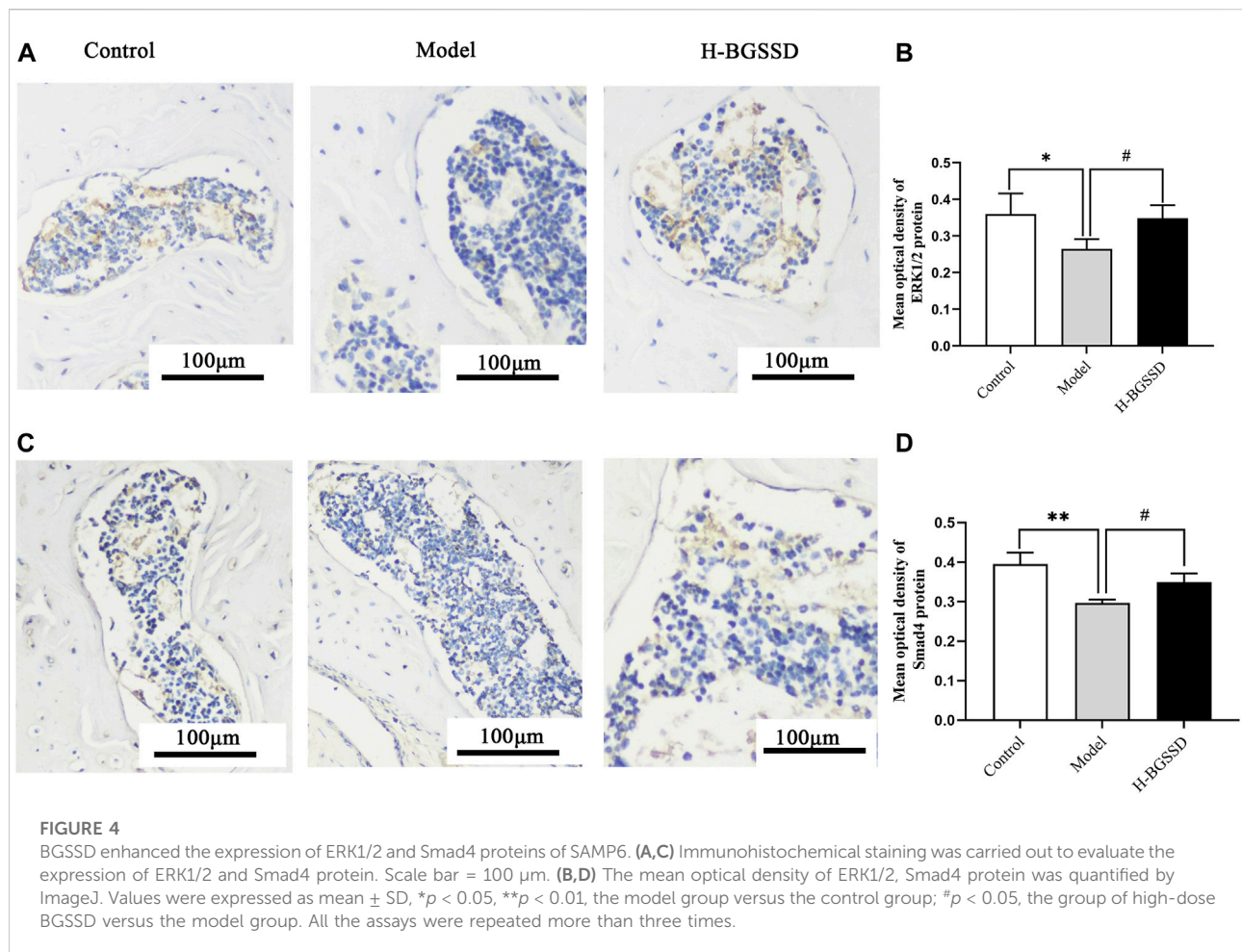
To determine whether BGSSD increases bone mass by affecting the process of osteoblastogenesis, we applied 20% drug-containing serum of BGSSD and EGF to intervene MC3T3-E1 *in vitro* and measured the activity of ALP. The results demonstrated that the levels of ALP enhanced after intervention in both the EGF group and the BGSSD group versus the control group (Figure 3C;  $p$  < 0.05). Since ALP starts to be secreted during the phase of bone matrix synthesis, which can stimulate processes such as inorganic phosphorus release and matrix mineralization (Sunden et al., 2017), the elevation of ALP is currently the most widely recognized marker of osteoblast differentiation (Lee et al., 2011). All these demonstrated that the activity of ALP affects

the differentiation of osteoblasts. Thus, our findings prove that BGSSD may stimulate osteoblast differentiation by upregulating ALP activity in MC3T3-E1 cells.

### Bu-Gu-Sheng-Sui decoction promoted the expression of osteogenic specific factor Runx2

Runx2 is essential for regulating the expression of genes responsible for osteogenic specific matrix proteins (including ALP, Col I, BSP, OCN, and OPN), and it has a significant effect on the development, proliferation, differentiation, and mineralization of osteoblasts (Yang et al., 2011). To observe the effect of BGSSD-containing serum on osteoblast, we examined Runx2 expression in osteoblasts. The *in vitro* experiments results showed that drug-containing serum of BGSSD and EGF increased the protein and mRNA levels of Runx2 compared with the control (Figures 5D,G, 6E;  $p$  < 0.05). These results suggested that BGSSD may promote osteoblast proliferation, differentiation, and mineralization.





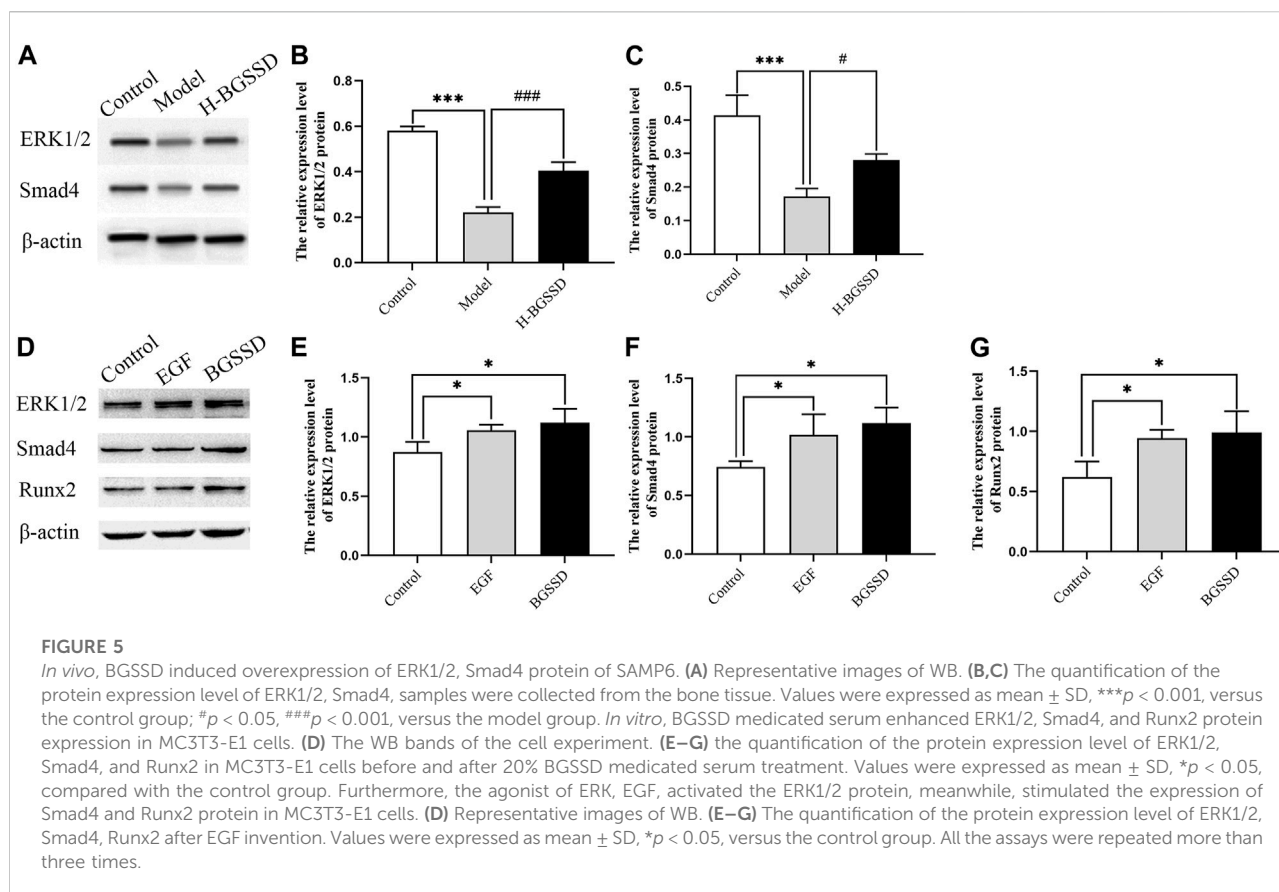
## Bu-Gu-Sheng-Sui decoction regulated osteoblast differentiation by activating ERK/Smad

To investigate the mechanisms involved in regulating BGSSD-induced osteoblast proliferation, we assayed the expressions of ERK and Smad *in vivo* and *in vitro*. *In vivo*, IHC and WB were performed to assess the protein levels of ERK1/2 and Smad4. IHC staining demonstrated that the levels of ERK1/2 and Smad4 were lower in the model group than those in the control group; after H-BGSSD treatment, the expression of these proteins significantly increased compared with the model group (Figures 4A,C). The mean optical density of ERK1/2 and Smad4 also illustrated this point (Figures 4B,D;  $p$  < 0.05). This observation was subsequently confirmed in the results of WB bands (Figure 5A) and the relative expression levels of proteins (Figures 5B,C;  $p$  < 0.05). *In vitro*, 20% drug-containing serum of BGSSD promoted the expression of ERK1/2 and Smad4 protein compared with the control (Figures 5D–F;  $p$  < 0.05). Moreover, RT-PCR was also performed. *In vivo*, RT-PCR manifested that the mRNA expression levels of ERK1 and Smad4 in the model

group were lower versus the control group, which were reversed by H-BGSSD, and the expression of ERK1 and Smad4 mRNA significantly increased (Figures 6A,B;  $p$  < 0.05). *In vitro*, 20% drug-containing serum of BGSSD promoted the expression of ERK1 and Smad4 mRNA versus the control group (Figures 6C,D;  $p$  < 0.05). Thus, our results indicated that BGSSD could boost the expression levels of ERK and Smad.

To further verify the existence of crosstalk between the ERK and Smad pathways, we overexpressed ERK by using EGF, an agonist of ERK. WB and RT-PCR were performed to detect the expression of ERK, Smad-related proteins, and mRNA. EGF overexpressed the expression of ERK1/2 protein (Figures 5D,E;  $p$  < 0.05) and, meanwhile, increased the protein level of Smad4 (Figures 5D,F;  $p$  < 0.05) compared with the control group. Moreover, the result of RT-PCR indicated that EGF stimulated the overexpression of ERK1 (Figure 6C;  $p$  < 0.05), at the same time, raised the level of Smad4 mRNA (Figure 6D;  $p$  < 0.05), versus the control group. Thus, we demonstrated that there was crosstalk between ERK and Smad signaling pathways. From all these results, we conclude that BGSSD may activate the ERK/Smad signal transduction pathway to promote bone formation.





## Discussion

We have previously confirmed that the BGSSD is influential in the treatment of OP clinically, and it enhances the BMD of the lumbar spine and femur in ovariectomized rats and improves bone biomechanical indexes. However, its molecular mechanism for osteogenesis is still unclear. In the present study, we discovered that BGSSD could accelerate bone formation in SAMP6 and positively affect MC3T3-E1. At the same time, we investigated the underlying mechanism of BGSSD, and our study demonstrated that BGSSD could promote osteoblast proliferation and osteogenesis by regulating the ERK/Smad pathway.

In the animal experiments, we chose SAMP6 as the model. SAMP6 was developed by Japanese scholars from AKR/J strains is a valuable mouse model of senile osteoporosis. They are characterized by peak bone mass at 4 months, but their peak bone mass is lower than SAMR1 (Chawalitpong et al., 2018). The osteoblastic hypoplasia of SAMP6 leads to degradation in the number of bone trabeculae, thinning of cortical bone, and decrease in bone formation, and eventually decline in bone density, bone calcium, and bone phosphorus (Oda et al., 2018). These features are similar to the changes in the bones of the elderly (Kasai et al., 2004) and show the characteristics of

low turnover rate osteoporosis, so it is widely used in animal models of senile osteoporosis (Antika et al., 2017; Kim et al., 2019). To verify the pharmacodynamic effect of BGSSD on SAMP6, we evaluated the bone density and bone tissue morphology of SAMP6. Our results showed that BGSSD ameliorated the morphology and microstructure of trabecular bone in SAMP6, raised bone mass, and elevated bone density. Thus, we confirm that BGSSD can stimulate bone formation.

In cellular models, we selected MC3T3-E1. MC3T3-E1 cells are osteoblastic precursor cells that can be further differentiated into mature osteoblasts under the induction and stimulation of osteogenic signals (Long, 2011). It has osteoblast characteristics, strong proliferation ability, and stable cell biology. So, it is a good osteoblast differentiation research model (Chaves Neto et al., 2011). Currently, the most widely recognized biochemical marker of osteoblast differentiation is increasable in ALP activity, and the level of ALP activity reflects the degree of osteogenic differentiation (Lee et al., 2011). Studies showed that kidney-tonifying herbs could upregulate ALP activity and osteogenic differentiation of MC3T3-E1 cells (Zhang et al., 2016). Ge et al. (2018) demonstrated, that is, opsores promoted the ossification of MC3T3-E1 cells and the activity of ALP. In Li et al. (2016) study, Bu Shen Huo Xue Gu Chi decoction promoted the development of MC3T3-E1 cells to osteoblast-like phenotype,

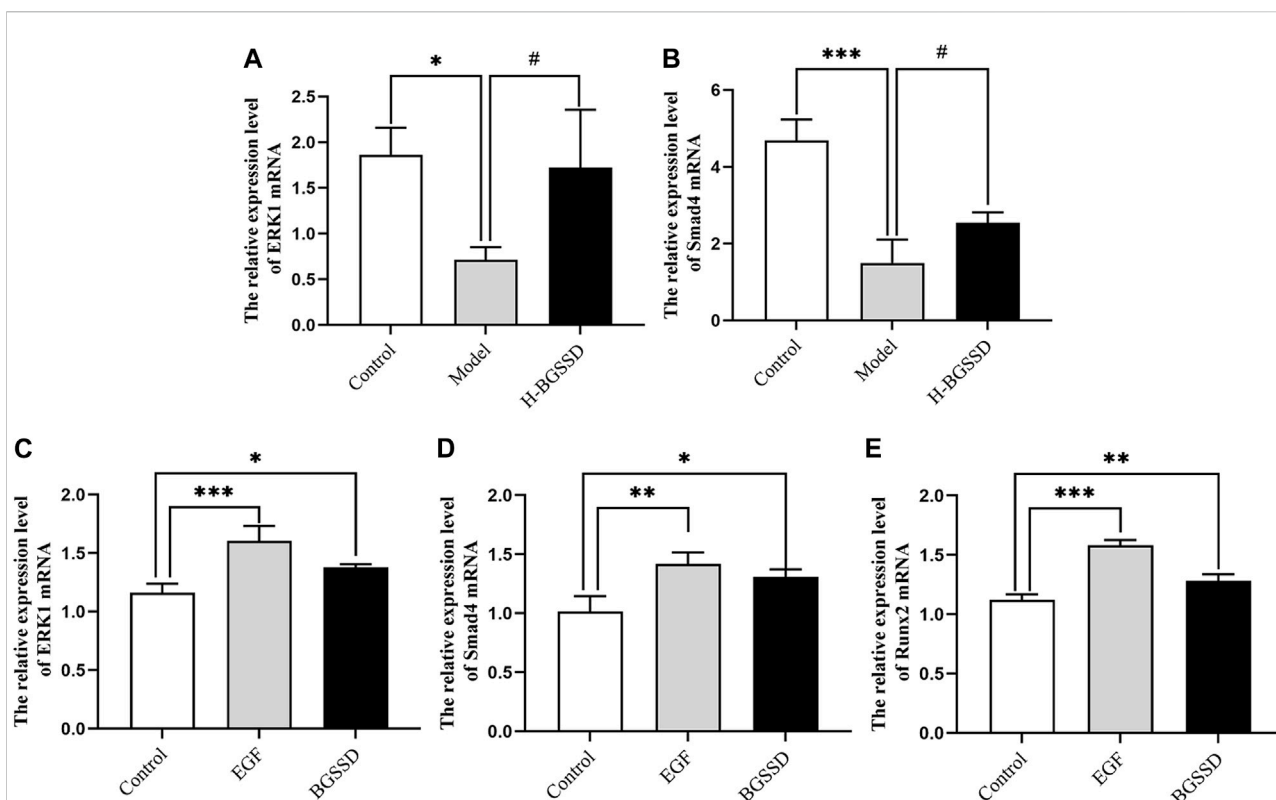


FIGURE 6

BGSSD stimulated the expression of ERK1 and Smad4 mRNA *in vivo*. (A,B) The mRNA expression of ERK1 and Smad4 in SAMP6 were assessed by RT-PCR. Values were expressed as mean  $\pm$  SD, \* $p$  < 0.05, \*\*\* $p$  < 0.001, versus the control group; # $p$  < 0.05, versus the model group. And BGSSD medicated serum enhanced expression of ERK1, Smad4, and Runx2 mRNA *in vitro*. (C–E) The quantification of ERK1, Smad4, and Runx2 mRNA in MC3T3-E1 cells before and after 20% BGSSD medicated serum treatment. Values were expressed as mean  $\pm$  SD, \* $p$  < 0.05, \*\* $p$  < 0.01, compared with control group. (C–E) The expression of ERK1, Smad4, and Runx2 mRNA after EGF intervention. Values were expressed as mean  $\pm$  SD, \*\* $p$  < 0.01, \*\*\* $p$  < 0.001, compared with the control group. All the assays were repeated more than three times.

increased the ALP activity of MC3T3-E1 cells, accelerated the differentiation and maturation of MC3T3-E1 cells, and stimulated the formation of bone tissue. We checked the ALP activity in MC3T3-E1 cells and tested the effect of BGSSD-containing serum on the differentiation of MC3T3-E1 cells. We discovered that BGSSD increased ALP's activity and promoted osteoblasts' proliferation. Therefore, our findings prove that BGSSD can promote osteoblast differentiation.

Runx2 is the earliest and most specific marker gene in bone formation (Komori, 2020). It is essential for regulating the expression of genes responsible for osteogenic specific matrix proteins, and it significantly affects the development, proliferation, differentiation, and mineralization of osteoblasts (Yang et al., 2011; Komori, 2019). Deleting runt in osteoblasts results in no bone phenotype, lower transcription activation capacity, and bone loss (Adhami et al., 2014). Thus, Runx2 plays a crucial part in osteoblast differentiation and osteogenesis (Li et al., 2017; Kim et al., 2020). Studies confirmed that the recipe of Osteoking stimulated the proliferation and differentiation of MC3T3-E1 by regulating

the expression of bone-specific factor Runx2 (Qin et al., 2019). Sun et al. (2021a) proved that the total flavonoids of Rhizoma Drynariae upregulated the expression of Runx2 and accelerated bone formation in rats. We examined Runx2 protein and mRNA expression in SAMP6 and MC3T3-E1 cells. The results showed that the expression of Runx2 was enhanced. These data reveal that BGSSD may induce bone formation by promoting osteoblast differentiation and mineralization.

Based on these, we explored the potential molecular mechanism of BGSSD in promoting osteogenesis. As we all know, there are many mechanisms for the regulation of bone remodeling. ERK and Smad played momentous roles in the modulation of osteoblasts and could participate in the proliferation and differentiation of osteoblasts (Lee et al., 2018). According to reports, the activation of the ERK signaling pathway was crucial to the proliferation and differentiation of osteoblasts, and it can upregulate the expression of bone formation-related genes, promote the differentiation and mineralization of osteoblasts, and play an essential role in bone formation and bone homeostasis (Miao

et al., 2018; Sun et al., 2018; Zhang et al., 2019). Liu et al. (2018) reported that lactoferrin modulated the ERK signaling pathway to stimulate osteogenesis *in vivo*; Wang et al. (2019) revealed that Melatonin can alleviate bone loss in retinoic acid-induced OP model mice, repair trabecular bone microstructure, and promote bone formation by regulating the ERK/Smad pathway. Vitro experiments revealed that the proliferation of osteoblasts and primary osteoblasts was enhanced under the action of ERK protein (Peng et al., 2018; Assefa et al., 2022). Studies found that Longan fruit extract upregulated ALP activity of MC3T3-E1 cells, induced mineralization, and promoted Runx2 expression. In addition, it activated the ERK1/2 pathway (Park et al., 2016); Wang et al. (2017) indicated that Naringin could significantly promote the proliferation and osteogenic differentiation of bone marrow mesenchymal stem cells and increase the protein and mRNA expression levels in a dose-dependent manner, such as Runx-2, OCN. They revealed that Naringin enhanced osteogenic differentiation was related to the activation of ERK. Moreover, SPRY as a receptor tyrosine kinase (RTK)-associated signaling protein reduced osteogenic differentiation and bone formation when the ERK signaling pathway was restrained (Park et al., 2019). As well the Smad pathway also plays a significant role in bone formation. The expression of Smad is closely related to the number of osteoblasts, bone formation, and BMD (Jin et al., 2020). It was found that *Prunella vulgaris* could relieve glucocorticoid-induced osteogenesis inhibition by activating the Smad pathway and prevented the deterioration of OP (Xi et al., 2020), which was also supported by Cui et al. (2019) result. Our study verified that BGSSD upregulated the protein and mRNA levels of ERK and Smad in SAMP6 and MC3T3-E1 cells. We conclude that the molecular mechanism of BGSSD seems to depend partly on ERK and Smad signaling pathways.

The crosstalk between ERK and Smad signaling was described more than a decade ago (Zhou et al., 2007; Park et al., 2011), and recent studies showed (Park et al., 2016; Liu and Yang, 2020) that the ERK activity increased Smad-mediated transcription. Others indicated that ERK inhibitors could down-regulate the expression of Smad-related proteins and affected bone formation (Mei et al., 2013). In our study, we used the EGF to promote the expression of ERK and found that Smad's expression also increased, agreeing with the results in BGSSD. Therefore, we deduce that the BGSSD may activate ERK and Smad to upregulate osteogenesis, and the two signal pathways communicate through signal crosstalk.

However, some limitations of this study should be noted. Firstly, we detected the trabecular bone morphology and structure by HE. Although it indicated that BGSSD could improve the bone trabecular structure and promote bone formation, it is obviously not as intuitive and accurate as Micro-CT for observing bone microstructure. Secondly, we have not verified the exact mechanism of BGSSD through inhibitor or RNAi, which we will further investigate.

## Conclusion

Taken together, BGSSD has a positive effect on osteoblast differentiation and bone formation. Such responsiveness may predominantly be associated with ERK/Smad signaling pathways. Therefore, this study provides experimental evidence of BGSSD as a treatment for osteoporosis, and it suggests that BGSSD is an effective drug for the prevention and treatment of osteoporosis.

## Data availability statement

The original contributions presented in the study are included in the article/Supplementary Materials, further inquiries can be directed to the corresponding author.

## Ethics statement

The animal study was reviewed and approved by Ethics Committee of longan, Beijing/Laboratory animal culture center, longan, Beijing, China.

## Author contributions

The concept of the research was provided by XW and YZ. Animal experiments were carried out by NL, QL, and CS, cell experiments were performed by BQ and SF. Statistical analysis was done by NL and BQ. The manuscript was drafted by NL. All authors read and approved the final manuscript.

## Funding

This work were supported by the General Project of the National Natural Science Foundation of China (No.81704102) and the Fundamental Research Funds for the Central Public Welfare Research Institutes (No.ZZ13-YQ-039).

## Conflict of interest

The authors declare that the research was conducted in the absence of any commercial or financial relationships that could be construed as a potential conflict of interest.

## Publisher's note

All claims expressed in this article are solely those of the authors and do not necessarily represent those of their

affiliated organizations, or those of the publisher, the editors and the reviewers. Any product that may be evaluated in this article, or claim that may be made by its manufacturer, is not guaranteed or endorsed by the publisher.

## References

- Adhami, M. D., Rashid, H., Chen, H., and Javed, A. (2014). Runx2 activity in committed osteoblasts is not essential for embryonic skeletogenesis. *Connect. Tissue Res.* 55 (1), 102–106. doi:10.3109/03080207.2014.923873
- Antika, L. D., Lee, E. J., Kim, Y. H., Kang, M. K., Park, S. H., Kim, D. Y., et al. (2017). Dietary phlorizin enhances osteoblastogenic bone formation through enhancing  $\beta$ -catenin activity via GSK-3 $\beta$  inhibition in a model of senile osteoporosis. *J. Nutr. Biochem.* 49, 42–52. doi:10.1016/j.jnutbio.2017.07.014
- Assefa, F., Kim, J. A., Lim, J., Nam, S. H., Shin, H. I., and Park, E. K. (2022). The neuropeptide spexin promotes the osteoblast differentiation of mc3t3-E1 cells via the MEK/ERK pathway and bone regeneration in a mouse calvarial defect model. *Tissue Eng. Regen. Med.* 19 (1), 189–202. doi:10.1007/s13770-021-00408-2
- Bhaskar, B., Mekala, N. K., Baadhe, R. R., and Rao, P. S. (2014). Role of signaling pathways in mesenchymal stem cell differentiation. *Curr. Stem Cell Res. Ther.* 9 (6), 508–512. doi:10.2174/1574888x09666140812112002
- Catalano, M. G., Marano, F., Rinella, L., de Girolamo, L., Bosco, O., Fortunati, N., et al. (2017). Extracorporeal shockwaves (ESWs) enhance the osteogenic medium-induced differentiation of adipose-derived stem cells into osteoblast-like cells. *J. Tissue Eng. Regen. Med.* 11 (2), 390–399. doi:10.1002/term.1922
- Chang, Y. Y., Zhang, J. W., Liu, Z. Q., Chu, W. X., and Li, H. W. (2019). Andrographolide stimulates osteoblastogenesis and bone formation by inhibiting nuclear factor-kappa-B signaling both *in vivo* and *in vitro*. *J. Orthop. Transl.* 19, 47–57. doi:10.1016/j.jot.2019.02.001
- Chaves Neto, A. H., Machado, D., Yano, C. L., and Ferreira, C. V. (2011). Antioxidant defense and apoptotic effectors in ascorbic acid and  $\beta$ -glycerophosphate-induced osteoblastic differentiation. *Dev. Growth Differ.* 53 (1), 88–96. doi:10.1111/j.1440-169X.2010.01232.x
- Chawalitpong, S., Chokchaisiri, R., Suksamrarn, A., Katayama, S., Mitani, T., Nakamura, S., et al. (2018). Cyperenoic acid suppresses osteoclast differentiation and delays bone loss in a senile osteoporosis mouse model by inhibiting non-canonical NF- $\kappa$ B pathway. *Sci. Rep.* 8 (1), 5625. doi:10.1038/s41598-018-23912-3
- Cheng, W., Yang, S., Liang, F., Wang, W., Zhou, R., Li, Y., et al. (2019). Low-dose exposure to triclosan disrupted osteogenic differentiation of mouse embryonic stem cells via BMP/ERK/Smad/Runx-2 signalling pathway. *Food Chem. Toxicol.* 127, 1–10. doi:10.1016/j.fct.2019.02.038
- Compston, J. E., McClung, M. R., and Leslie, W. D. (2019). Osteoporosis. *Lancet (London, Engl.)* 393 (10169), 364–376. doi:10.1016/S0140-6736(18)32112-3
- Cui, Q., Xing, J., Yu, M., Wang, Y., Xu, J., Gu, Y., et al. (2019). Mmu-miR-185 depletion promotes osteogenic differentiation and suppresses bone loss in osteoporosis through the Bgn-mediated BMP/Smad pathway. *Cell Death Dis.* 10 (3), 172. doi:10.1038/s41419-019-1428-1
- Dineen, A., and Gaudet, J. (2014). TGF- $\beta$  signaling can act from multiple tissues to regulate *C. elegans* body size. *BMC Dev. Biol.* 14, 43. doi:10.1186/s12861-014-0043-8
- Donoso, O., Pino, A. M., Seitz, G., Osses, N., and Rodríguez, J. P. (2015). Osteoporosis-associated alteration in the signalling status of BMP-2 in human MSCs under adipogenic conditions. *J. Cell. Biochem.* 116 (7), 1267–1277. doi:10.1002/jcb.25082
- Durbano, H. W., Halloran, D., Nguyen, J., Stone, V., McTague, S., Eskander, M., et al. (2020). Aberrant BMP2 signaling in patients diagnosed with osteoporosis. *Int. J. Mol. Sci.* 21 (18), 6909. doi:10.3390/ijms21186909
- Feng, C., Xiao, L., Yu, J. C., Li, D. Y., Tang, T. Y., Liao, W., et al. (2020). Simvastatin promotes osteogenic differentiation of mesenchymal stem cells in rat model of osteoporosis through BMP-2/Smads signaling pathway. *Eur. Rev. Med. Pharmacol. Sci.* 24 (1), 434–443. doi:10.26355/eurrev\_202001\_19943
- Franceschi, R. T., Ge, C., Xiao, G., Roca, H., and Jiang, D. (2009). Transcriptional regulation of osteoblasts. *Cells tissues organs* 189 (1–4), 144–152. doi:10.1159/000151747
- Ge, L., Cui, Y., Cheng, K., and Han, J. (2018). Isopsoralen enhanced osteogenesis by targeting AhR/era. *Mol. (Basel, Switz.)* 23 (10), 2600. doi:10.3390/molecules23102600
- Huang, Y., Liao, L., Su, H., Chen, X., Jiang, T., Liu, J., et al. (2021). Psoralen accelerates osteogenic differentiation of human bone marrow mesenchymal stem cells by activating the TGF- $\beta$ /Smad3 pathway. *Exp. Ther. Med.* 22 (3), 940. doi:10.3892/etm.2021.10372
- Ji, Y., Liu, J. G., Xu, X. S., Zhang, F. Z., and Xie, Y. M. (1997). Experimental study on anti-inflammatory and analgesic effects of Bu Gu Sheng Sui capsule. *Zhong Guo Zhong Xi Yi Jie He Za Zhi* 17, 253–255.
- Jiang, Y. H., Zhang, P., Tao, Y., Liu, Y., Cao, G., Zhou, L., et al. (2021). Banxia Baizhu Tianma decoction attenuates obesity-related hypertension. *J. Ethnopharmacol.* 266, 113453. doi:10.1016/j.jep.2020.113453
- Jin, S. L., Bai, Y. M., Zhao, B. Y., Wang, Q. H., and Zhang, H. S. (2020). Silencing of miR-330-5p stimulates osteogenesis in bone marrow mesenchymal stem cells and inhibits bone loss in osteoporosis by activating Bgn-mediated BMP/Smad pathway. *Eur. Rev. Med. Pharmacol. Sci.* 24 (8), 4095–4102. doi:10.26355/eurrev\_202004\_20987
- Johnston, C. B., and Dagar, M. (2020). Osteoporosis in older adults. *Med. Clin. North Am.* 104, 873–884. doi:10.1016/j.mcna.2020.06.004
- Kasai, S., Shimizu, M., Matsumura, T., Okudaira, S., Matsushita, M., Tsuboyama, T., et al. (2004). Consistency of low bone density across bone sites in SAMP6 laboratory mice. *J. Bone Min. Metab.* 22 (3), 207–214. doi:10.1007/s00774-003-0471-1
- Kim, H. Y., Park, S. Y., and Choung, S. Y. (2018). Enhancing effects of myricetin on the osteogenic differentiation of human periodontal ligament stem cells via BMP-2/Smad and ERK/JNK/p38 mitogen-activated protein kinase signaling pathway. *Eur. J. Pharmacol.* 834, 84–91. doi:10.1016/j.ejphar.2018.07.012
- Kim, J. S., Lee, H., Nirmala, F. S., Jung, C. H., Jang, Y. J., Ha, T. Y., et al. (2019). Dry-fermented soybean food (cheonggukjang) ameliorates senile osteoporosis in the senescence-accelerated mouse prone 6 model. *J. Med. Food* 22 (10), 1047–1057. doi:10.1089/jmf.2018.4335
- Kim, J. M., Yang, Y. S., Park, K. H., Ge, X., Xu, R., Li, N., et al. (2020). A RUNX2 stabilization pathway mediates physiologic and pathologic bone formation. *Nat. Commun.* 11 (1), 2289. doi:10.1038/s41467-020-16038-6
- Komori, T. (2019). Regulation of proliferation, differentiation and functions of osteoblasts by Runx2. *Int. J. Mol. Sci.* 20 (7), 1694. doi:10.3390/ijms20071694
- Komori, T. (2020). Molecular mechanism of runx2-dependent bone development. *Mol. Cells* 43 (2), 168–175. doi:10.14348/molcells.2019.0244
- Kopf, J., Paarmann, P., Hiepen, C., Horbelt, D., and Knaus, P. (2014). BMP growth factor signaling in a biomechanical context. *BioFactors Oxf. Engl.* 40 (2), 171–187. doi:10.1002/biof.1137
- Lee, C. H., Huang, Y. L., Liao, J. F., and Chiou, W. F. (2011). Ugonin K promotes osteoblastic differentiation and mineralization by activation of p38 MAPK- and ERK-mediated expression of Runx2 and osterix. *Eur. J. Pharmacol.* 668 (3), 383–389. doi:10.1016/j.ejphar.2011.06.059
- Lee, J. S., Kim, M. E., Seon, J. K., Kang, J. Y., Yoon, T. R., Park, Y. D., et al. (2018). Bone-forming peptide-3 induces osteogenic differentiation of bone marrow stromal cells via regulation of the ERK1/2 and Smad1/5/8 pathways. *Stem Cell Res.* 26, 28–35. doi:10.1016/j.scr.2017.11.016
- Li, N., Lee, W. Y., Lin, S. E., Ni, M., Zhang, T., Huang, X. R., et al. (2014). Partial loss of Smad7 function impairs bone remodeling, osteogenesis and enhances osteoclastogenesis in mice. *Bone* 67, 46–55. doi:10.1016/j.bone.2014.06.033
- Li, L. F., Li, M., Diao, Z. H., Gao, Y., and Wang, S. S. (2016). Effects of Bu shen Huo Xue Gu Chi recipe on BMP2 expression and ultrastructure of rat mc3t3-E1 cells. *Zhong Hua Zhong Yi Yao Xue Gan Za Zhi* 34 (07), 1663–1665. doi:10.13193/j.issn.1673-7717.2016.07.036
- Li, Y., Ge, C., and Franceschi, R. T. (2017). MAP kinase-dependent RUNX2 phosphorylation is necessary for epigenetic modification of chromatin during osteoblast differentiation. *J. Cell. Physiol.* 232 (9), 2427–2435. doi:10.1002/jcp.25517
- Liu, Z., and Yang, J. (2020). Uncarboxylated osteocalcin promotes osteogenic differentiation of mouse bone marrow-derived mesenchymal stem cells by

## Supplementary material

The Supplementary Material for this article can be found online at: <https://www.frontiersin.org/articles/10.3389/fphar.2022.976121/full#supplementary-material>



activating the Erk-Smad/ $\beta$ -catenin signalling pathways. *Cell Biochem. Funct.* 38 (1), 87–96. doi:10.1002/cbf.3457

Liu, J. G., Xu, X. S., Ji, Y., Zhang, F. Z., and Xie, Y. M. (1997). Effect of Bu Gu Sheng Sui Capsule on promoting blood circulation and removing blood stasis and experimental microcirculation disorder. *Zhong Guo Zhong Xi Yi Jie He Za Zhi* 17, 255–257.

Liu, J., Liang, C., Guo, B., Wu, X., Li, D., Zhang, Z., et al. (2017). Increased PLEKHO1 within osteoblasts suppresses Smad-dependent BMP signaling to inhibit bone formation during aging. *Aging cell* 16 (2), 360–376. doi:10.1111/acle.12566

Liu, M., Fan, F., Shi, P., Tu, M., Yu, C., Yu, C., et al. (2018). Lactoferrin promotes MC3T3-E1 osteoblast cells proliferation via MAPK signaling pathways. *Int. J. Biol. Macromol.* 107, 137–143. doi:10.1016/j.ijbiomac.2017.08.151

Long, F. (2011). Building strong bones: Molecular regulation of the osteoblast lineage. *Nat. Rev. Mol. Cell Biol.* 13 (1), 27–38. doi:10.1038/nrm3254

Mei, Y., Bian, C., Li, J., Du, Z., Zhou, H., Yang, Z., et al. (2013). miR-21 modulates the ERK-MAPK signaling pathway by regulating SPRY2 expression during human mesenchymal stem cell differentiation. *J. Cell. Biochem.* 114 (6), 1374–1384. doi:10.1002/jcb.24479

Miao, C., Qin, D., Cao, P., Lu, P., Xia, Y., Li, M., et al. (2018). BMP2/7 heterodimer enhances osteogenic differentiation of rat BMSCs via ERK signaling compared with respective homodimers. *J. Cell. Biochem.* 120, 28162. Advance online publication. doi:10.1002/jcb.28162

Mizumachi, H., Yoshida, S., Tomokiyo, A., Hasegawa, D., Hamano, S., Yuda, A., et al. (2017). Calcium-sensing receptor-ERK signaling promotes odontoblastic differentiation of human dental pulp cells. *Bone* 101, 191–201. doi:10.1016/j.bone.2017.05.012

Noh, J. Y., Yang, Y., and Jung, H. (2020). Molecular mechanisms and emerging therapeutics for osteoporosis. *Int. J. Mol. Sci.* 21 (20), 7623. doi:10.3390/ijms21207623

Oda, Y., Sasaki, H., Miura, T., Takanashi, T., Furuya, Y., Yoshinari, M., et al. (2018). Bone marrow stromal cells from low-turnover osteoporotic mouse model are less sensitive to the osteogenic effects of fluvastatin. *PLoS one* 13 (8), e0202857. doi:10.1371/journal.pone.0202857

Park, K. H., Kang, J. W., Lee, E. M., Kim, J. S., Rhee, Y. H., Kim, M., et al. (2011). Melatonin promotes osteoblastic differentiation through the BMP/ERK/Wnt signaling pathways. *J. Pineal Res.* 51 (2), 187–194. doi:10.1111/j.1600-079X.2011.00875.x

Park, S., Kim, J. H., Son, Y., Goh, S. H., and Oh, S. (2016). Longan (dimocarpus longan lour.) fruit extract stimulates osteoblast differentiation via erk1/2-dependent RUNX2 activation. *J. Microbiol. Biotechnol.* 26 (6), 1063–1066. doi:10.4014/jmb.1601.01092

Park, S., Arai, Y., Kim, B. J., Bello, A., Ashraf, S., Park, H., et al. (2019). Suppression of SPRY4 promotes osteogenic differentiation and bone formation of mesenchymal stem cell. *Tissue Eng. Part A* 25 (23–24), 1646–1657. doi:10.1089/ten.TEA.2019.0056

Peng, X., He, J., Zhao, J., Wu, Y., Shi, X., Du, L., et al. (2018). Polygonatum sibiricum polysaccharide promotes osteoblastic differentiation through the ERK/GSK-3 $\beta$ -Catenin signaling pathway *in vitro*. *Rejuvenation Res.* 21 (1), 44–52. doi:10.1089/rej.2017.1956

Qin, D., Zhang, H., Zhang, H., Sun, T., Zhao, H., and Lee, W. H. (2019). Anti-osteoporosis effects of osteoking via reducing reactive oxygen species. *J. Ethnopharmacol.* 244, 112045. doi:10.1016/j.jep.2019.112045

Sun, X., Xie, Z., Ma, Y., Pan, X., Wang, J., Chen, Z., et al. (2018). TGF- $\beta$  inhibits osteogenesis by upregulating the expression of ubiquitin ligase SMURF1 via MAPK-ERK signaling. *J. Cell. Physiol.* 233 (1), 596–606. doi:10.1002/jcp.25920

Sun, W., Li, M., Xie, L., Mai, Z., Zhang, Y., Luo, L., et al. (2021a). Exploring the mechanism of total flavonoids of drynariae rhizoma to improve large bone defects

by network Pharmacology and experimental assessment. *Front. Pharmacol.* 12, 603734. doi:10.3389/fphar.2021.603734

Sun, W., Li, M., Zhang, Y., Huang, Y., Zhan, Q., Ren, Y., et al. (2021b). Total flavonoids of rhizoma drynariae ameliorates bone formation and mineralization in BMP-Smad signaling pathway induced large tibial defect rats. *Biomed. Pharmacother. = Biomedicine Pharmacother.* 138, 111480. doi:10.1016/j.biopha.2021.111480

Sunden, F., AlSadhan, I., Lyubimov, A., Doukov, T., Swan, J., and Herschlag, D. (2017). Differential catalytic promiscuity of the alkaline phosphatase superfamily bimetallo core reveals mechanistic features underlying enzyme evolution. *J. Biol. Chem.* 292 (51), 20960–20974. doi:10.1074/jbc.M117.788240

Tashima, Y., He, H., Cui, J. Z., Pedroza, A. J., Nakamura, K., Yokoyama, N., et al. (2020). Androgens accentuate TGF- $\beta$  dependent erk/smad activation during thoracic aortic aneurysm formation in marfan syndrome male mice. *J. Am. Heart Assoc.* 9 (20), e015773. doi:10.1161/JAHA.119.015773

Wang, H., Li, C., Li, J., Zhu, Y., Jia, Y., Zhang, Y., et al. (2017). Naringin enhances osteogenic differentiation through the activation of ERK signaling in human bone marrow mesenchymal stem cells. *Iran. J. Basic Med. Sci.* 20 (4), 408–414. doi:10.22038/IJBMS.2017.8582

Wang, X., Liang, T., Zhu, Y., Qiu, J., Qiu, X., Lian, C., et al. (2019). Melatonin prevents bone destruction in mice with retinoic acid-induced osteoporosis. *Mol. Med.* 25 (1), 43. doi:10.1186/s10020-019-0107-0

Wong, S. K., Mohamad, N. V., Ibrahim, N., Chin, K. Y., Shuid, A. N., and Ima-Nirwana, S. (2019). The molecular mechanism of vitamin E as a bone-protecting agent: A review on current evidence. *Int. J. Mol. Sci.* 20 (6), 1453. doi:10.3390/ijms20061453

Xi, L., Zhang, Y. F., Zhao, Z. J., Pan, D. S., and Liang, W. (2020). Prunella vulgaris L protects glucocorticoids-induced osteogenesis inhibition in bone marrow mesenchymal stem cells through activating the Smad pathway. *Eur. Rev. Med. Pharmacol. Sci.* 24 (10), 5691–5696. doi:10.26355/eurrev\_202005\_21360

Xie, Y. M., Zhang, F. Z., Zhou, W. Q., Gao, P., Fu, Y. J., Zhao, T. Z., et al. (1997a). [Clinical study of bugu shengsui capsule in treating primary osteoporosis with kidney-yang deficiency syndrome]. *Zhong Guo Zhong Xi Yi Jie He Za Zhi* 17 (9), 526–530.

Xie, Y. M., Zhang, F. Z., Cheng, J. L., Zhou, W. Q., Cui, W., and He, Y. X. (1997b). Effects of Bu Gu sheng sui capsules on osteoporosis in castrated rats. *Zhong Yao Xin Yao Yu Lin. Chuang Yao Li Za Zhi* 8 (4), 210–213.

Yang, D. C., Yang, M. H., Tsai, C. C., Huang, T. F., Chen, Y. H., and Hung, S. C. (2011). Hypoxia inhibits osteogenesis in human mesenchymal stem cells through direct regulation of RUNX2 by TWIST. *PLoS One* 6 (9), e23965. doi:10.1371/journal.pone.0023965

Zhang, N. D., Han, T., Huang, B. K., Rahman, K., Jiang, Y. P., Xu, H. T., et al. (2016). Traditional Chinese medicine formulas for the treatment of osteoporosis: Implication for antiosteoporotic drug discovery. *J. Ethnopharmacol.* 189, 61–80. doi:10.1016/j.jep.2016.05.025

Zhang, T., Han, W., Zhao, K., Yang, W., Lu, X., Jia, Y., et al. (2019). Psoralen accelerates bone fracture healing by activating both osteoclasts and osteoblasts. *FASEB J. official Publ. Fed. Am. Soc. Exp. Biol.* 33 (4), 5399–5410. doi:10.1096/fj.201801797R

Zhou, Q., Heinke, J., Vargas, A., Winnik, S., Krauss, T., Bode, C., et al. (2007). ERK signaling is a central regulator for BMP-4 dependent capillary sprouting. *Cardiovasc. Res.* 76 (3), 390–399. doi:10.1016/j.cardiores.2007.08.003

Zhu, X. F., Wang, T. C., Zhang, R. H., Sun, S. Y., Wang, P. P., Yang, L., et al. (2012). [Effects of total flavonoids in Drynaria fortunei on osteoblasts differentiation and the expression of ERK1/2 and p38 MAPK after treatment by high glucose *in vitro*]. *Zhong Yao Cai* 35 (03), 424–429.





## OPEN ACCESS

## EDITED BY

Dongwei Zhang,  
Beijing University of Chinese Medicine,  
China

## REVIEWED BY

Daniele Mercatelli, University of  
Bologna, Italy  
Xiaofan Ding,  
The Chinese University of Hong Kong,  
China

## \*CORRESPONDENCE

Jing Wang,  
wangjing11277@126.com

<sup>†</sup>These authors have contributed equally  
to this work and share first authorship

## SPECIALTY SECTION

This article was submitted to  
Experimental Pharmacology and Drug  
Discovery,  
a section of the journal  
Frontiers in Pharmacology

RECEIVED 15 May 2022

ACCEPTED 25 July 2022

PUBLISHED 29 August 2022

## CITATION

Zeng R, Ke T-C, Ou M-T, Duan L-L, Li Y,  
Chen Z-J, Xing Z-B, Fu X-C, Huang C-Y  
and Wang J (2022), Identification of a  
potential diagnostic signature for  
postmenopausal osteoporosis via  
transcriptome analysis.  
*Front. Pharmacol.* 13:944735.  
doi: 10.3389/fphar.2022.944735

## COPYRIGHT

© 2022 Zeng, Ke, Ou, Duan, Li, Chen,  
Xing, Fu, Huang and Wang. This is an  
open-access article distributed under  
the terms of the [Creative Commons  
Attribution License \(CC BY\)](https://creativecommons.org/licenses/by/4.0/). The use,  
distribution or reproduction in other  
forums is permitted, provided the  
original author(s) and the copyright  
owner(s) are credited and that the  
original publication in this journal is  
cited, in accordance with accepted  
academic practice. No use, distribution  
or reproduction is permitted which does  
not comply with these terms.

# Identification of a potential diagnostic signature for postmenopausal osteoporosis via transcriptome analysis

Rui Zeng<sup>1†</sup>, Tian-Cheng Ke<sup>2†</sup>, Mao-Ta Ou<sup>2</sup>, Li-Liang Duan<sup>2</sup>, Yi Li<sup>3</sup>,  
Zhi-Jing Chen<sup>4</sup>, Zhi-Bin Xing<sup>2</sup>, Xiao-Chen Fu<sup>2</sup>,  
Cheng-Yu Huang<sup>2</sup> and Jing Wang<sup>2\*</sup>

<sup>1</sup>Department of Physiology, School of Medicine, Jinan University, Guangzhou, China, <sup>2</sup>Department of Orthopedics, The First Affiliated Hospital of Jinan University, Guangzhou, China, <sup>3</sup>Department of Radiology, The First Affiliated Hospital of Jinan University, Guangzhou, China, <sup>4</sup>Department of Plastic Surgery, The First Affiliated Hospital of Jinan University, Guangzhou, China

**Purpose:** We aimed to establish the transcriptome diagnostic signature of postmenopausal osteoporosis (PMOP) to identify diagnostic biomarkers and score patient risk to prevent and treat PMOP.

**Methods:** Peripheral blood mononuclear cell (PBMC) expression data from PMOP patients were retrieved from the Gene Expression Omnibus (GEO) database. Differentially expressed genes (DEGs) were screened using the “limma” package. The “WGCNA” package was used for a weighted gene co-expression network analysis to identify the gene modules associated with bone mineral density (BMD). Least absolute shrinkage and selection operator (LASSO) regression was used to construct a diagnostic signature, and its predictive ability was verified in the discovery cohort. The diagnostic values of potential biomarkers were evaluated by receiver operating characteristic curve (ROC) and coefficient analysis. Network pharmacology was used to predict the candidate therapeutic molecules. PBMCs from 14 postmenopausal women with normal BMD and 14 with low BMD were collected, and RNA was extracted for RT-qPCR validation.

**Results:** We screened 2420 differentially expressed genes (DEGs) from the pilot cohort, and WGCNA showed that the blue module was most closely related to BMD. Based on the genes in the blue module, we constructed a diagnostic signature with 15 genes, and its ability to predict the risk of osteoporosis was verified in the discovery cohort. RT-qPCR verified the expression of potential biomarkers and showed a strong correlation with BMD. The functional annotation results of the DEGs showed that the diagnostic signature might affect the occurrence and development of PMOP through multiple biological pathways. In addition, 5 candidate molecules related to diagnostic signatures were screened out.

**Conclusion:** Our diagnostic signature can effectively predict the risk of PMOP, with potential application for clinical decisions and drug candidate selection.

## KEYWORDS

postmenopausal osteoporosis (PMOP), biomarkers, diagnostic signature, WGCNA, network pharmacology

## Introduction

Osteoporosis is the most common systemic bone disease in postmenopausal women (PMOP). This condition is characterized by decreased bone mineral density (BMD) and destruction of the bone tissue microstructure, resulting in decreased bone strength and increased fracture risk (Yao et al., 2019). The latest data show that the prevalence of osteoporosis in women over 50 years old in China is 29.1%, and the total number of patients is approximately 49 million. With the increase in the aging of society, by 2050, there will be 5.99 million cases of osteoporosis-related fractures in China every year (Cheng et al., 2021). Hip fracture is a common osteoporotic fracture in older postmenopausal women. Approximately 33% of women aged 90 years will experience a hip fracture, and these patients are older and have multiple comorbidities, leading to a poor prognosis (Ensrud et al., 2019). Osteoporosis has become a major public health problem worldwide, placing a heavy financial burden on patients and healthcare systems. Osteoporosis includes primary and secondary osteoporosis. The occurrence of primary osteoporosis is related to estrogen deficiency in women, decreased testosterone levels in men, and changes in hormone levels such as parathyroid hormone and calcitonin. Secondary osteoporosis is mainly caused by endocrine and metabolic diseases, connective tissue diseases, kidney diseases, digestive tract diseases, and drugs.

Most patients have no apparent symptoms in the early stage of osteoporosis, and the main clinical manifestations include pain, reduced height, limited activities, stooped posture, and respiratory system involvement. Most people lack awareness of osteoporosis and fail to detect the symptoms. Even when a brittle fracture occurs, there is no clear history of trauma or only a slight history of trauma (Glaser and Kaplan, 1976). Osteoporosis can be characterized by sparse trabecular bone and decreased BMD on imaging, but these imaging manifestations are affected by subjective factors and are not sensitive to early bone loss. Dual-energy X-ray absorptiometry (DXA) testing of BMD is strongly recommended by the World Health Organization (WHO). However, DXA cannot detect early bone loss, and studies of many clinical cases have suggested that DXA does not accurately assess the severity of osteoporosis and the risk of fracture. For example, in one report, the individuals who had the highest risk of future fractures among those who had bone density tests were rarely diagnosed with osteoporosis ( $T < -2.5$ ) but were often diagnosed with reduced bone mass ( $-2.5 < T < -1$ ) (Siris et al., 2014).

Therefore, transcriptome analysis may be helpful for the early diagnosis and prevention of osteoporosis. Based on the Gene Expression Omnibus (GEO) database, we used WGCNA to identify the top gene modules related to osteoporosis and conducted least absolute shrinkage and selection operator (LASSO) regression to build a diagnostic signature composed of 15 genes. The two most representative genes, *METTL4* and *RAB2A*, were subjected to RT-qPCR to verify the correlation between their expression and BMD. In addition, we explored the potential molecular mechanism of osteoporosis, which will contribute to the early diagnosis, treatment, and prevention of this disease. To discover novel osteoporosis drugs from our research, we explored the molecular targets of the diagnostic signature through network pharmacology.

## Materials and methods

### Microarray data collection and processing

The datasets were downloaded from the GEO database (<https://www.ncbi.nlm.nih.gov/geo/>) (Barrett et al., 2013), and the pilot cohort and discovery cohort were analyzed on the Affymetrix Human Genome U133A Array platform. As the pilot cohort, GSE56815 included 80 Caucasian females, 40 of whom had high BMD and 40 of whom had low BMD. In addition, we selected 20 postmenopausal subjects from the GSE13850 dataset as a discovery cohort: 10 women with high BMD and 10 women with low BMD. Raw data were read through the “affy” package (Gautier et al., 2004), and the RMA algorithm was used for background correction and data normalization. To verify the purity of peripheral blood mononuclear cells (PBMCs) in the pilot cohort, we used the “Cibersort” package.

### Identification of differentially expressed genes (DEGs)

Patients are classified into high- and low-BMD groups based on clinical information provided by uploaders in the pilot cohort. The “limma” package (Ritchie et al., 2015) was used to compare samples from the high- and low-BMD groups. Genes with adjusted  $p$ -value  $< 0.05$  were defined as DEGs, DEGs with  $\log_2FC > 0$  were defined as up-regulated DEGs, while those with  $\log_2FC < 0$  were down-regulated DEGs. The “ggplot2” package (Ito and Murphy, 2013) was used to visualize the DEGs.

# Weighted gene coexpression network analysis

WGCNA is an algorithm to mine module information from high-throughput data. In this method, the module is defined as genes with similar expression trends. If these genes always have similar expression changes in a physiological or pathological process, it is reasonable to believe that they are functionally related and can be defined as a module. In this study, the “WGCNA” package (Langfelder and Horvath, 2008) was used to construct the weighted adjacency matrix by selecting appropriate thresholds, and the weighted adjacency matrix was transformed into a topological overlap matrix (TOM). The hierarchical clustering method was used to cluster the TOM matrix, and the dynamic tree-cutting algorithm was adopted to divide modules, each corresponding to a color, merge similar modules to find the module with the highest correlation with BMD, and extract the most significant genes associated with BMD in the module.

# Construction and validation of a genetic diagnostic signature of osteoporosis

LASSO logistic regression was used to reduce the dimensionality of genes in the BMD association module to construct a genetic diagnostic signature, which was generated by using the “glmnet” package (Friedman et al., 2010). Then, the signature was used to calculate the risk score of each patient. The corresponding coefficient of the gene weighted the expression values of these genes in each patient, and then, the weighted

expression values were added to obtain the risk score of the patient, which was calculated as follows:

$$\text{Risk score} = \sum_{i=1}^n \text{Exp}_i * \text{Coef}_i$$

where  $n$  is the number of genes included in the signature,  $\text{Exp}_i$  is the expression value of this gene of the patient, and  $\text{Coef}_i$  is the coefficient of this gene in the signature. Finally, patients were classified into a high-risk group or a low-risk group according to the median value of the risk score.

Next, the “pROC” package (Robin et al., 2011) was used to draw the receiver operating characteristic curve (ROC) and determine the area under the curve (AUC). If the AUC was  $>0.8$ , the diagnostic effect was defined as good. In addition, we obtained another independent dataset, GSE13850, as the discovery cohort, applied the genetic diagnostic signature to the discovery cohort and defined its diagnostic effect in the discovery cohort according to the AUC.

# Functional annotation analysis

For determination of the potential biological pathways of osteoporosis, “clusterProfiler” package (Yu et al., 2012) was used to perform Kyoto Encyclopedia of Genes (KEGG), Gene Ontology (GO), Disease Ontology (DO) on the up- and down-regulated DEGs, the results for which adjust  $p\text{-value} < 0.05$  were considered statistically significant. Gene Set Enrichment Analysis (GSEA) on the up- and down-regulated DEGs was performed by “fgsea” package.

# Gene-miRNA interaction analysis, molecular docking, and network visualization

TargetScan (McGeary et al., 2019) was used to predict the interacting miRNAs of the genes in the genetic diagnostic signature and explore whether potential miRNAs are involved in the process of osteoporosis by targeting genes. Subsequently, miRPath was used for pathway enrichment analysis of miRNAs (Vlachos et al., 2012).

Firstly, we screened potential small molecule substances and drugs from the CTD database (Davis et al., 2021) and DGIdb database. Cytoscape was used to construct the miRNA-gene-molecule network. Secondly, we downloaded the protein 3D structures from the PDB database (Burley et al., 2021) and used PyMOL software to remove the water molecules of the protein. Then, we collected the 3D structures of these potential small-molecule substances and drugs from PubChem. Next, the SwissDock (Grosdidier et al., 2011) database was used for protein-molecule docking. Finally, PyMOL software was used to modify the docking results.

TABLE 1 Patient characteristics (n = 28).

Characteristic	Mean ± SD (Range)	
	High bone density	Low bone density
Patients (n)	14	14
Age (years)	61.9 ± 9.5	66.2 ± 8.4
Height (cm)	156.8 ± 6.7	158.6 ± 5.6
Weight (kg)	58.4 ± 6.3	61.1 ± 7.6
T-score	0.7 ± 0.9	-2.4 ± 0.8
Menstrual condition		
Menopause	14	14
Premenopausal	0	0
Smoking status		
Smoking	0	0
No history of smoking	14	14
Surgery situation		
Have vertebroplasty	0	0
No vertebroplasty	14	14

## RNA extraction and quantitative real-time polymerase chain reaction

Fourteen women with PMOP and 14 healthy postmenopausal-matched women controls were selected, and PBMCs were obtained from them. The characteristics of the patients are summarized in Table 1. This study was approved by the Ethics Committee of the First Affiliated Hospital of Jinan University. Both patients and controls provided written informed consent.

PBMCs were extracted with Histopaque-1077 (Sigma, United States). According to the manufacturer's protocol, the total RNA of PBMCs from all samples was extracted using an EZ-Press RNA Purification Kit (EZBioscience, United States). cDNA was obtained by reverse transcription using a PrimeScript RT Kit (TaKaRa, Japan). Based on the SYBR Green method (ChamQ Universal SYBR qPCR Master Mix, Vazyme Biotech, China), The CFX96 Real-Time PCR System (Bio-Rad, United States) was used for RT-qPCR detection. The mRNA-specific primer sequences are shown in Table 2. After the expression level of GAPDH was used for normalization, the relative expression level of mRNA was determined.

## Statistical analysis

Statistical analyses were conducted using RStudio version 1.3.1093 (RStudio Inc.) and GraphPad Prism 8 (GraphPad Software, Inc.). All data are expressed as the mean  $\pm$  SD. A paired difference test between Low BMD samples and normal control samples in two groups by the "limma" package was used to determine the DEGs. Analysis with one-way ANOVA followed by the Student–Newman–Keuls multiple comparison test was used for the comparison of three or more experimental groups. For qPCR data, Student's t test was used for analysis.

## Results

### Quality control of microarray data and DEG screening

First, cell purity analysis was performed on the pilot cohort (GSE56815), and the results are shown in Figure 1A, indicating

TABLE 2 mRNA-specific primer sequences.

Gene	Primer sequence	Tm
METTL4	F: GCTGTTCTATAAAGAATGCCAGCAA	57
	R: CAGCTCCCTGATCTTTGTATGGT	56
RAB2A	F: TCCATCACAAAGGTCGTATTACAGA	55
	R: TGGTTGAATGTATCTCTCCGTGTA	55
GAPDH	F: ACAGTTGCCATGTAGACC	56
	R: TTTTGGTTGAGCACAGG	60

that PBMCs accounted for the majority of the pilot cohort, consistent with the description in NCBI. DEG analysis was performed on the pilot cohort, and patients were divided into two groups according to BMD. DEGs were identified by "limma" package analysis, and 2,420 DEGs were screened out, as shown in Figure 1B.

### Weighted coexpression network and identification of bone mineral density-related modules

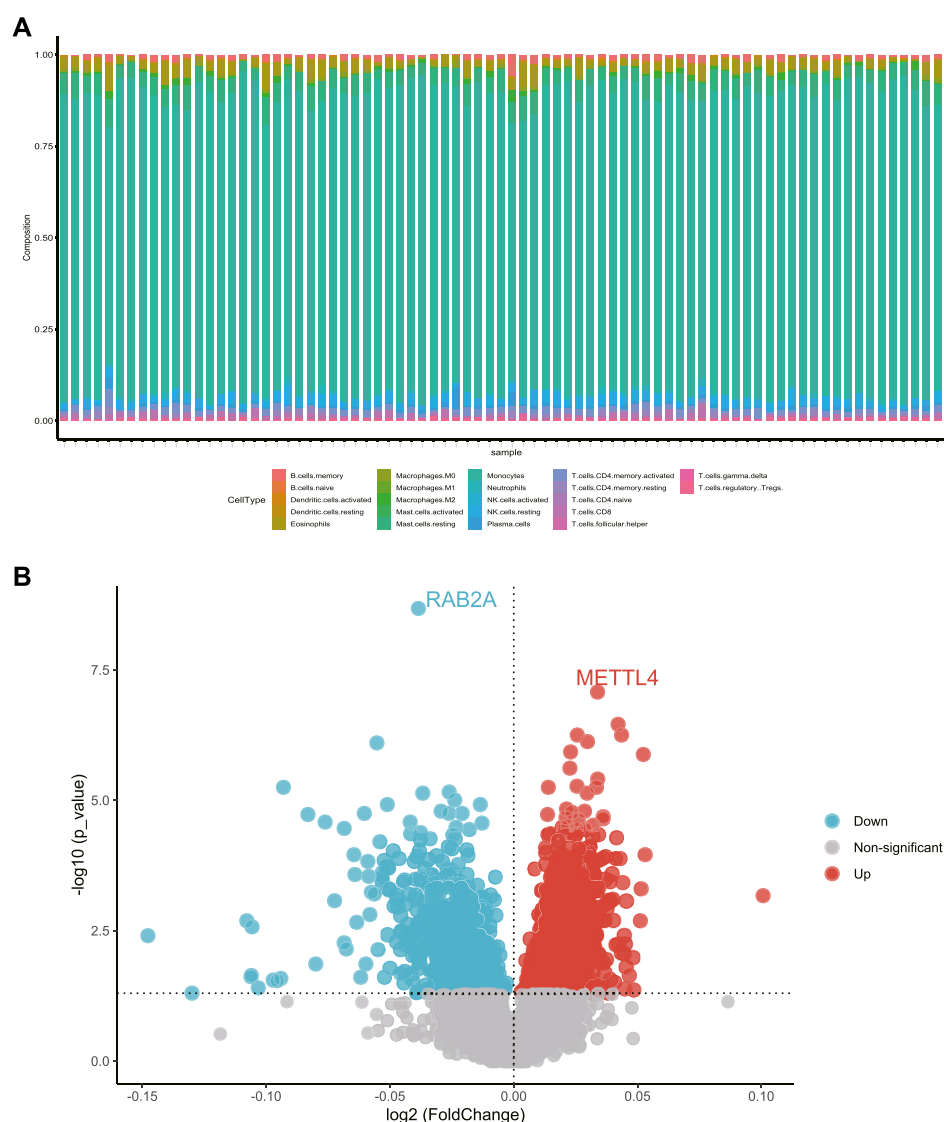
In this study, the "WGCNA" package was used to construct a weighted gene coexpression network in the pilot cohort. According to several iterations,  $\beta = 6$  was selected as the optimal soft threshold to construct a scale-free network (Figure 2A). After exclusion of the MEgrey module, which contains all genes not involved in clustering, a total of 7 modules were identified. The interaction between modules was analyzed, and the heatmap showed that the gene expression of each module was relatively independent (Figure 2B). Then, correlation analysis between these modules and BMD was carried out, and the results showed that the MEblue module, which consisted of 396 genes, had the highest correlation with BMD ( $\text{cor} = 0.51$ ,  $p < 0.001$ ) (Figure 2C).

### Construction and testing of the diagnostic signature

The LASSO algorithm was used to determine  $\lambda = 0.09$  (Figure 2D), and a diagnostic signature consisting of 15 genes

TABLE 3 Genes and their coefficients that constitute the diagnostic signature.

Gene	Coefficient
RAB2A	−0.69559
VSIG4	0.005073
ADAM7	0.014223
AMBP	0.018658
PAFAH1B2	0.031496
AOC3	0.050969
KLK3	0.088715
KRTAP1.3	0.100,972
LPO	0.13443
SLC41A3	0.144,549
NKX3.1	0.208,241
GLT8D2	0.231,434
LAMB1	0.338,636
SEC14L1P1	0.394,242
METTL4	1.089913

**FIGURE 1**

(A) Cell abundance of the pilot cohort. (B) Volcano plot of DEGs between the individuals with a high BMD and a low BMD in the pilot cohort.

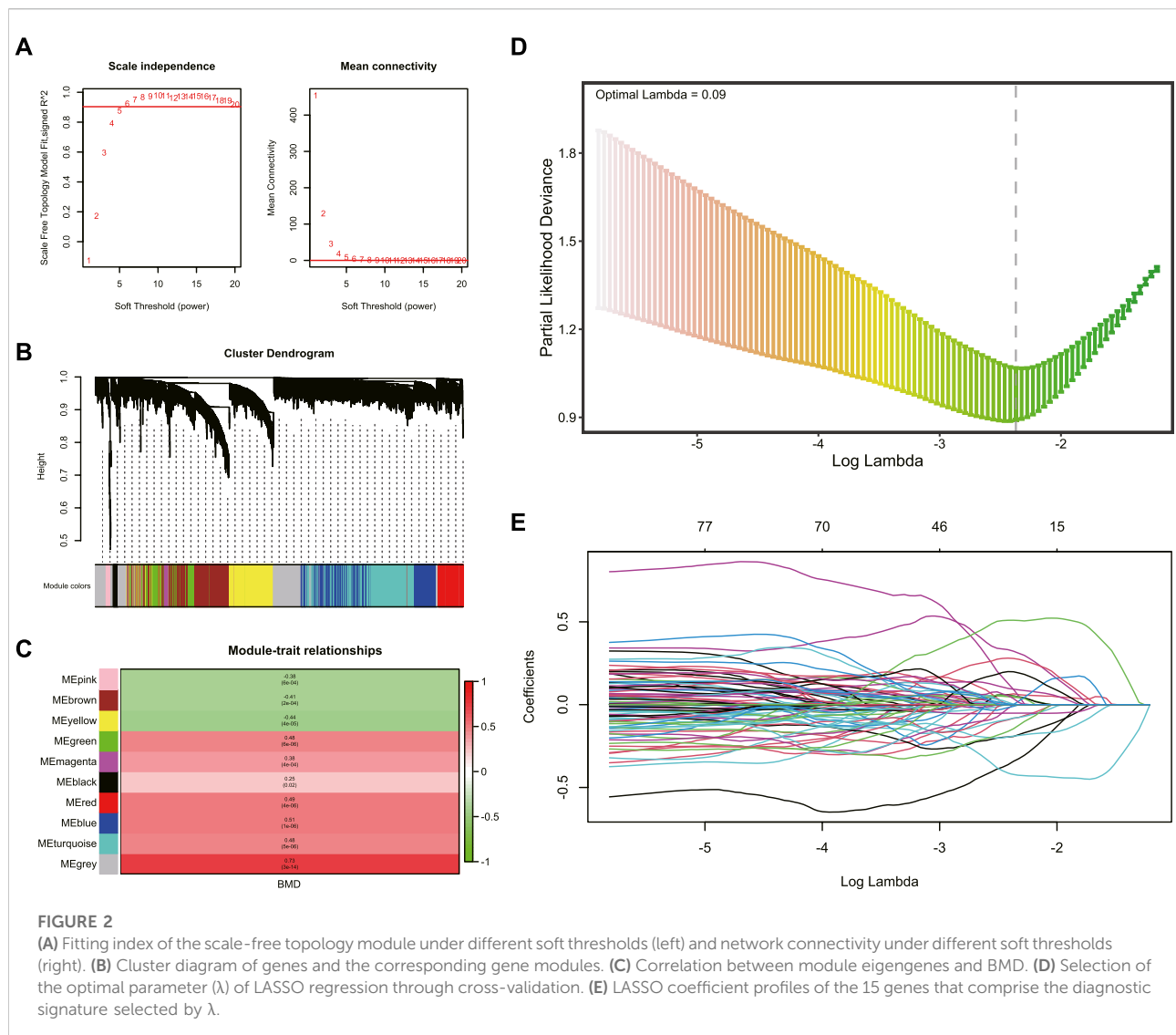
(Figure 2E) was established. The specific gene composition and coefficient of each gene are shown in Table 3. The diagnostic signature calculated the patients' risk scores and divided them into high-risk and low-risk groups (Figure 3A). Principal component analysis (PCA) showed that risk scores could categorize patients with different BMDs in the pilot cohort into two groups (Figure 3B). Moreover, verification was carried out in this study, and the results showed that the AUC value of the diagnostic signature was 0.993 in the pilot cohort and 0.980 in the discovery cohort (Figure 3C). The expression patterns of the 15 genes that constituted the signature (Figure 3D) and all the DEGs (Figure 3E) in the high-risk and low-risk groups are shown. Heatmap results showed that the gene expression

patterns of the high-risk and low-risk groups were different, especially those of the 15 genes that constituted the signature. All the above results showed that this signature has an excellent ability to predict the risk of osteoporosis. In addition, we explored the interactions of these 15 genes (Figure 3F).

## Functional annotation and Gene Set Enrichment Analysis

KEGG functional annotation analysis (Figure 4A) showed that cytokine receptor interaction, neural activity





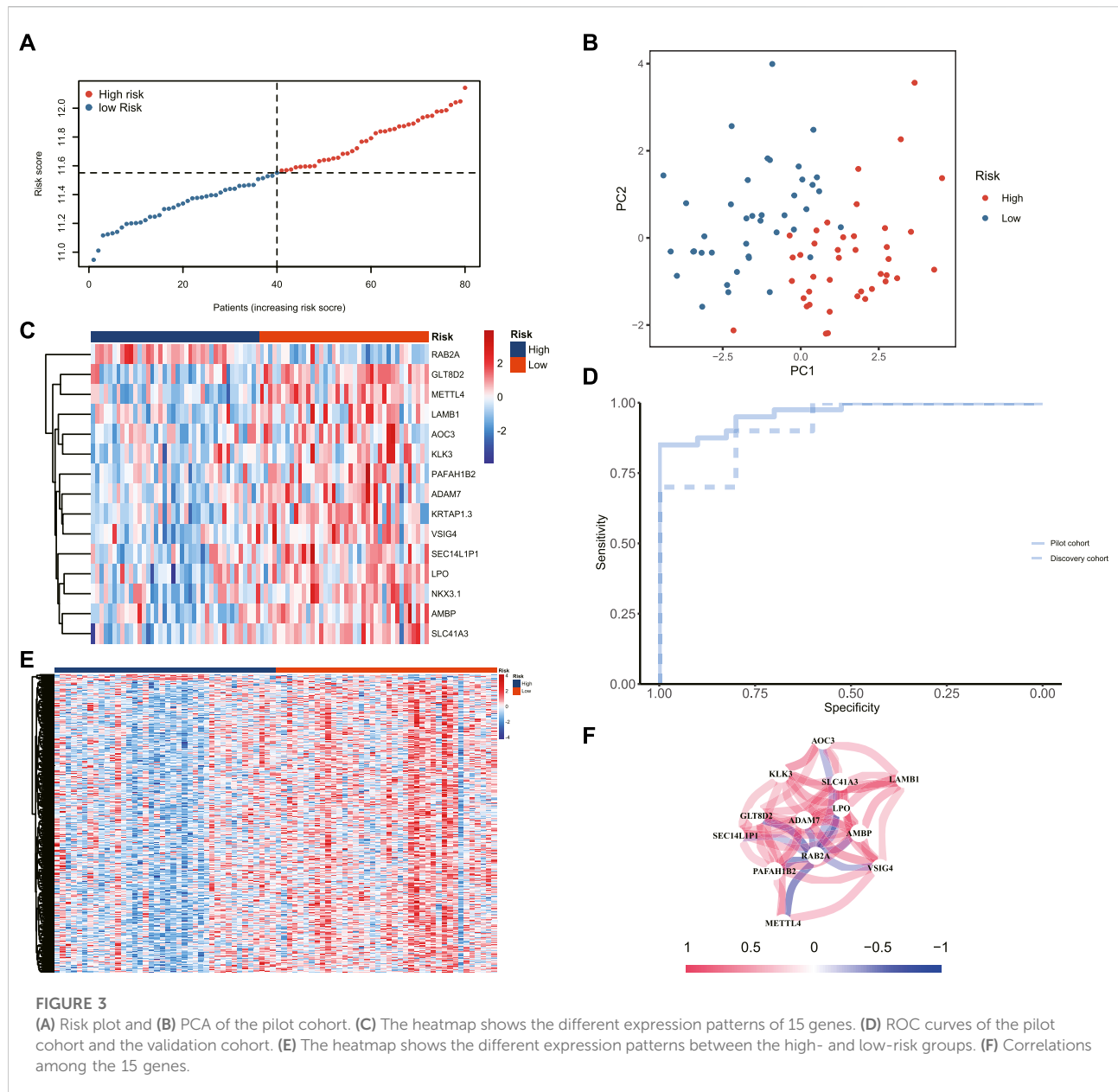
ligand–receptor interaction, Rap1 signaling pathway, autoimmune thyroid disease, natural killer cell-mediated cytotoxicity, PI3K-Akt signaling pathway, gap junction, calcium signaling pathway, and oxytocin signaling pathway were up-regulated. Combining the above results with previous studies, we found that the calcium activator calcimycin can activate the RAF/MEK/ERK pathway through Ras (Li et al., 2005), and increased calcium concentrations have also been shown to modulate Ras-dependent Raf1 activation (Yoshiki et al., 2010). Moreover, lactoferrin-induced PI3K-Akt pathway activation and Ras phosphorylation can promote osteoblast proliferation (Hou et al., 2015). DO analysis (Figure 4B) showed that gynecological and aging diseases were up-regulated, such as female reproductive system disease, ovarian disease, bone remodeling disease, osteoporosis, and bone

resorption diseases. GO analysis (Figure 4C) showed that ion channel complex activity, bone development, bone morphogenesis were up-regulated, and odontogenesis, GTPase activity, GDP binding were down-regulated.

According to the GSEA results (Figure 4D), we suggest that androgen response, late estrogen response, the P53 pathway, and TNF- $\alpha$  signaling *via* NF- $\kappa$ B are down-regulated in the DEGs of osteoporosis.

## miRNA interaction identification and candidate molecule prediction

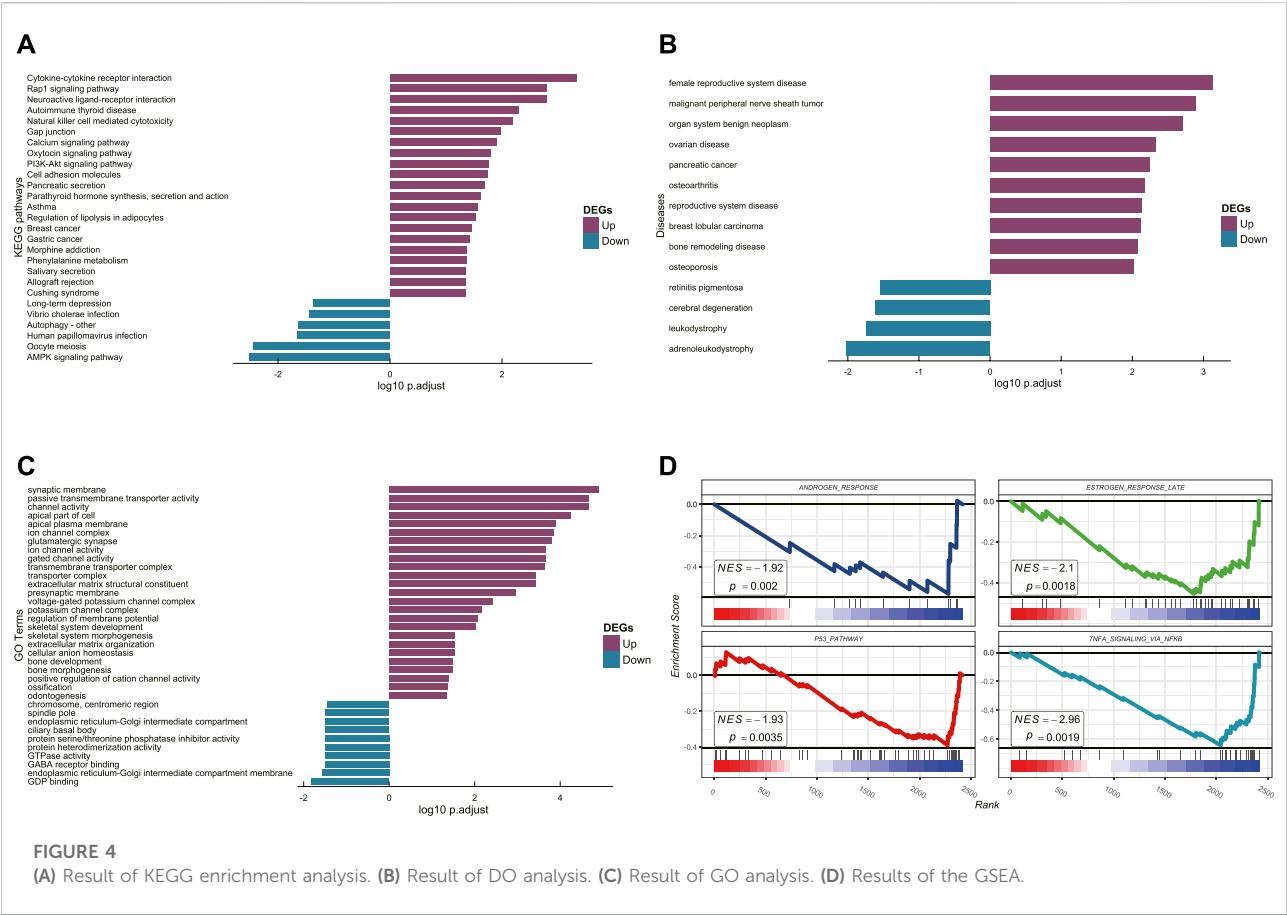
Thirty-eight miRNAs were expected to interact with the genes constituting the diagnostic signature and were used to construct the



miRNA-Gene-Molecule network (Figure 5A). The result of KEGG (Figure 5B) enrichment analysis showed that miRNA pathway enrichment overlapped with DEG pathways, such as the Rap1 signaling pathway, suggesting that overlapping pathways play a potentially important role in the occurrence and development of PMOP. We selected the molecules connected to at least two genes as the candidate molecules. Five candidate molecules were screened out, including bisphenol A (BPA), fulvestrant, bicalutamide, mifepristone, and valproic acid (VPA). RAF, an essential protein in the Rap1 signaling pathway, was selected for docking with the candidate molecules to explore their possible binding locations (Supplementary Figure S1).

## Validation by real-time polymerase chain reaction

To verify the authenticity of the diagnostic signature, we collected PBMCs from 14 postmenopausal healthy controls (Figure 6A) and 14 postmenopausal women with low BMD (Figure 6B) in this study. RNA was extracted for RT-qPCR to verify the diagnostic signature. The gene with the most significant coefficient had the strongest contribution to the risk score, and the gene with the largest AUC showed the strongest relationship to BMD. Interestingly, *METTL4* and *RAB2A* had the largest positive and negative coefficients, respectively, and they also had



the most significant AUC values (Table 4). Therefore, these two genes were further investigated, and the results were consistent with the bioinformatics results. The expression of *METTL4* in the low BMD group was significantly higher than that in the normal BMD group (Figure 6C), while the expression of *RAB2A* in the normal BMD group was significantly higher than that in the low BMD group (Figure 6D), suggesting that these two genes play an essential role in the occurrence and development of osteoporosis.

## Discussion

Osteoporosis is a systemic bone disease that mainly involves decreased bone mass and increased bone brittleness caused by degeneration of the bone tissue microstructure, resulting in susceptibility to fracture (Wang et al., 2020). DXA is widely used in clinical practice as a diagnostic standard for osteoporosis. However, only a small number of postmenopausal women are tested for BMD, and many of them have already suffered from brittle fractures when BMD is found to be reduced (Siris et al., 2014).

TABLE 4 Genes and their AUCs that constitute the diagnostic signature.

Gene	AUC
<i>RAB2A</i>	0.8638
<i>VSIG4</i>	0.7431
<i>ADAM7</i>	0.7219
<i>AMBP</i>	0.72
<i>PAFAH1B2</i>	0.725
<i>AOC3</i>	0.6444
<i>KLK3</i>	0.6444
<i>KRTAP1.3</i>	0.7375
<i>LPO</i>	0.7141
<i>SLC41A3</i>	0.7338
<i>NKX3.1</i>	0.7075
<i>GLT8D2</i>	0.7819
<i>LAMB1</i>	0.6481
<i>SEC14L1P1</i>	0.7038
<i>METTL4</i>	0.8306

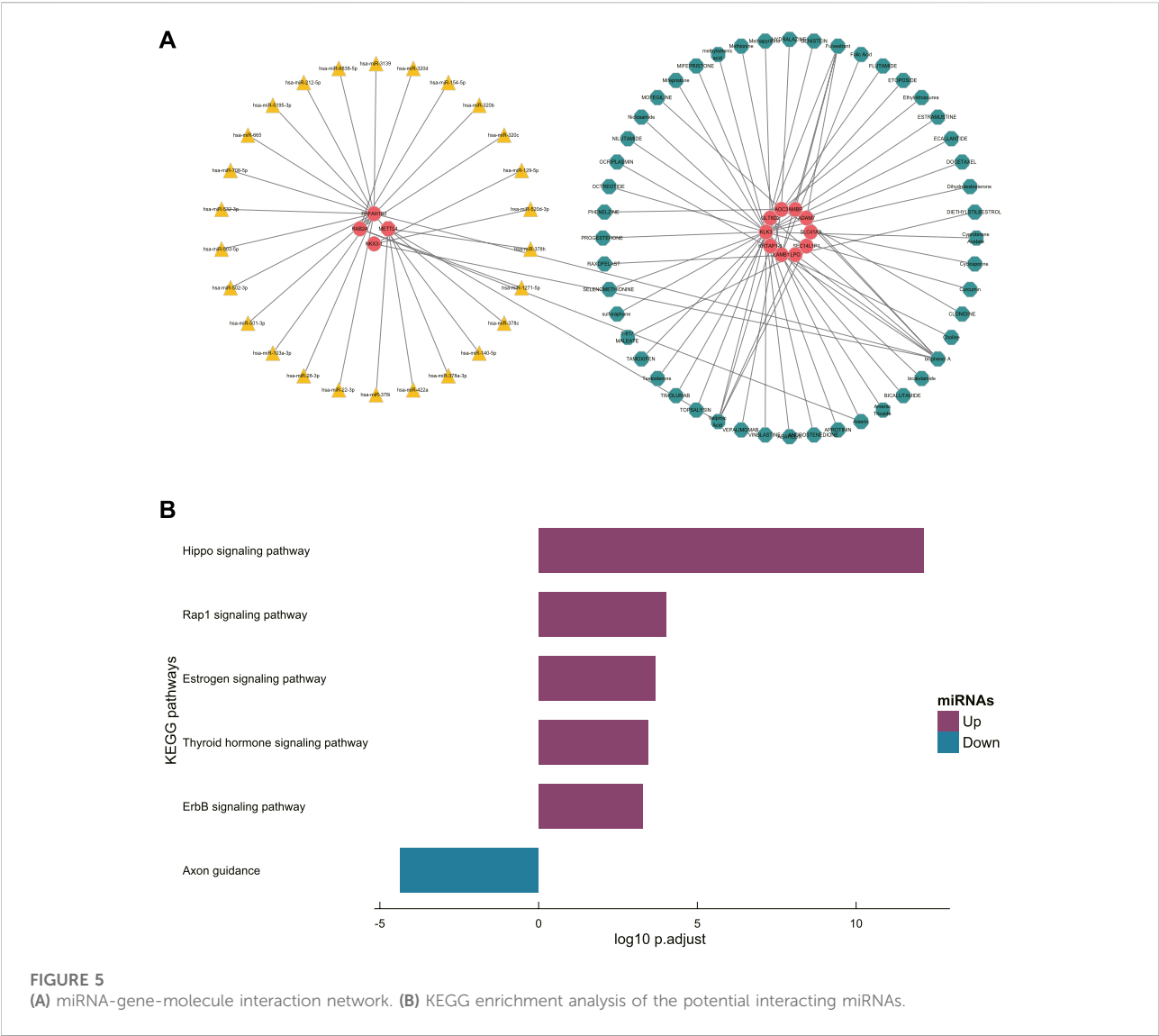


**FIGURE 5**  
(A) miRNA-gene-molecule interaction network. (B) KEGG enrichment analysis of the potential interacting miRNAs.

BMD examination results may be affected by body weight, lumbar curvature, osteophytes, vertebral fractures, and vascular calcification. Studies have shown that vertebral osteoarthropathy and aortic calcification can cause false BMD increases and decrease diagnostic sensitivity (Orwoll et al., 1990; Frohn et al., 1991).

Relying solely on BMD testing will lead to the failure of clinicians and patients to correctly evaluate the severity of osteoporosis, thus affecting clinical treatment strategies. In addition, the radiation of DXA is very low, with each scan receiving only 1/60 to 1/10 of the radiation dose of a conventional X-ray. However, repeated exposure to ionizing radiation over a long period can have long-term health effects, including cancer (Hill and Einstein, 2016; Howard et al., 2020), suggesting that frequent imaging detection is still not advisable.

Due to the difficulty in the extraction and separation of osteoblasts and osteoclasts, on the contrary, the isolation and

extraction technology of PBMCs has become increasingly mature, and its extraction and purification rate can reach more than 90%. PBMCs are the most likely precursors of osteoclasts, especially in adult peripheral bone, and are the only precursors of osteoclasts (Fujikawa et al., 1996). Secondly, PBMCs can secrete cytokines such as IL-1B, IL-6, and TNF- $\alpha$ , which play an essential role in osteoclast differentiation, activation, and apoptosis (Custer and Ahlfeldt, 1932). The decrease of PBMCs cytokines is the primary mechanism by which sex hormones inhibit osteoclast formation and bone resorption. Therefore, PBMCs are widely used as an ideal cell model for osteoporosis study (Zhou et al., 2015).

Previous studies have shown that osteoporosis is a polygenic disease, and genetic factors play an essential role in the occurrence and development of this condition. However, there are few relevant studies at present, and few candidate genes have been identified (Andrew and

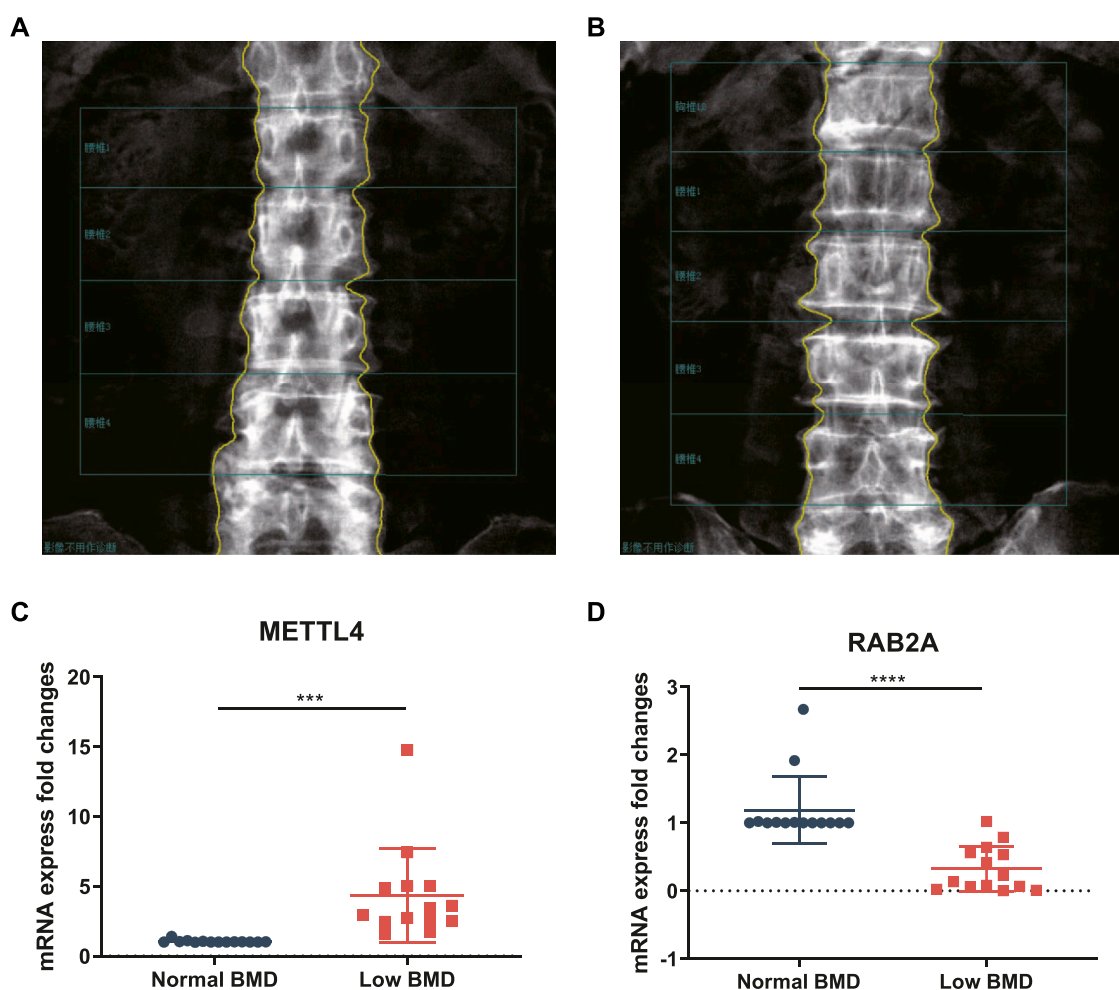


FIGURE 6

DXA images of the lumbar spine L1-L4 of women with a normal BMD (A) and low BMD (B). The overall expression of *METTL4* (C) and *RAB2A* (D) in PBMCs from 14 low BMD patients and healthy controls.

Macgregor, 2004; Cai et al., 2018). Thus, we used public databases to construct a transcriptome-based diagnostic signature, which is expected to be applied in clinical practice in the future to assess the risk of osteoporosis in the potential population and help doctors diagnose this disease. In this study, the GEO dataset GSE56815 was first used to identify DEGs between patients with osteoporosis and healthy controls, and then WGCNA was performed on these DEGs. The results showed that the blue module was most closely related to osteoporosis. Then, the genes in the blue module were extracted, and a diagnostic signature composed of 15 genes was constructed through LASSO regression. Subsequently, the independent dataset GSE13850 was used to verify the classification ability of the signature. We found that the AUC values of the signature in the pilot cohort and the discovery cohort were 0.993 and 0.920, respectively, showing good prediction of the risk of osteoporosis in different patients.

To further explore the potential pathogenesis of osteoporosis, we conducted the functional enrichment analysis of DEGs between the high- and low-BMD groups and interacting miRNAs of the diagnostic signature. We found that both were involved with the Rap1 signaling pathway, suggesting that, compared with other mechanisms, the Rap1 signaling pathway may be more closely related to our diagnostic signature. The calcium activator calcimycin can activate the RAF-MEK-ERK pathway through the RAS signaling pathway (Li et al., 2005). An increased calcium concentration has also been shown to modulate RAS-dependent RAF1 activation (Yoshiki et al., 2010), and lactoferrin-induced PI3K-Akt pathway activation and Ras phosphorylation can promote osteoblast proliferation (Hou et al., 2015). According to previous studies, osteoclasts are specialized macrophage/monocyte lineage-derived cells that resorb bone, and neurofibromatosis type I (NF1) haploinsufficient osteoclasts have abnormal Ras-dependent bone resorption. (Yan et al., 2008).



Our study found that the two genes with the most significant positive and negative coefficients in the diagnostic signature, *METTL4* and *RAB2A*, were also the two genes with the most significant AUC values among the 15 genes. Therefore, we selected these two genes as representative molecules that were validated by RT-qPCR. We collected PBMCs from 14 patients with normal BMD and 14 patients with low BMD for RNA extraction. The results showed that *METTL4* expression was significantly lower in patients with normal BMD than in patients with low BMD, while *RAB2A* expression was significantly higher in healthy controls than in patients with low BMD, which was consistent with our bioinformatics results and the results of other studies. *RAB2A* is a member of the Ras gene family. When it binds to GTP, the Ras protein can phosphorylate and activate downstream proteins, thus regulating the proliferation and differentiation of osteoblasts (Ge et al., 2007). The Ras gene family regulates anterograde transport from the endoplasmic reticulum to the Golgi complex, inhibits the proliferation and differentiation of osteoprogenitor MC3T3-E1 cells and promotes apoptosis by reducing the membrane transport process. During this process, the protein expression of *RAB2A* was inhibited (Hong et al., 2011). *METTL4*, as an m6A methyltransferase, can lead to increased m6A modification. As a new extranuclear marker, m6A modification is involved in bone development and metabolism and plays an essential role in osteoporosis. A previous study showed that both m6A levels and methyltransferase expression are increased during osteoclast differentiation, and methyltransferase knockdown led to increased osteoclast volume and decreased bone resorption capacity (Li et al., 2020). Another study also showed that inhibition of mRNA methyltransferase reversed osteoclast differentiation and bone resorption (Wang et al., 2021).

Another vital function of diagnostic signatures is to provide evidence for candidate drugs. RAF is a crucial component of the Rap1 signaling pathway, and RAF has also been shown to affect the proliferation and function of osteoblasts (Meng et al., 2015). Therefore, it is necessary to develop effective new osteoporosis drugs that target RAF. This study screened out five medications with high affinity for the diagnostic signature: BPA, fulvestrant, mifepristone, bicalutamide, and VPA. Although the specific mechanisms of action of these small compounds remain to be further elucidated, our results suggest that they have therapeutic potential for osteoporosis, especially in patients with PMOP.

We speculated that using transcriptome analysis to detect gene expression might be a complementary method for the diagnosis of osteoporosis, and the genes can be used as biomarkers to evaluate the effect of osteoporosis treatment to avoid frequent radiation examinations in patients.

## Data availability statement

The original contributions presented in the study are included in the article/supplementary materials, further inquiries can be directed to the corresponding author.

## Ethics statement

This study was approved by the Ethics Committee of the First Affiliated Hospital of Jinan University. Both patients and controls provided written informed consent.

## Author contributions

All persons who meet authorship criteria are listed as authors, and all authors certify that they have participated sufficiently in the work to take public responsibility for the content, including participation in the concept, design, analysis, writing, or revision of the manuscript. Conception and design of study: RZ, T-CK, and JW Acquisition of data: RZ, T-CK, and M-TO Analysis and/or interpretation of data: RZ, T-CK, Drafting the manuscript: RZ, T-CK, L-LD, Z-JC, and JW Revising the manuscript critically for important intellectual content: YL, Z-BX, X-CF, and C-YH.

## Acknowledgments

This study was funded by Science and Technology Program of Guangzhou (No. 202102010107) and Clinical Research Project of the First Clinical Medical College of Jinan University (No. 2018005). Experimental instrument support from the Medical Experimental Center, School of Medicine, Jinan University is gratefully acknowledged.

## Conflict of interest

The authors declare that the research was conducted in the absence of any commercial or financial relationships that could be construed as a potential conflict of interest.

## Publisher's note

All claims expressed in this article are solely those of the authors and do not necessarily represent those of their affiliated organizations, or those of the publisher, the editors and the reviewers. Any product that may be evaluated in this article, or claim that may be made by its manufacturer, is not guaranteed or endorsed by the publisher.

## Supplementary material

The Supplementary Material for this article can be found online at: <https://www.frontiersin.org/articles/10.3389/fphar.2022.944735/full#supplementary-material>

## References

- Andrew, T., and Macgregor, A. J. (2004). Genes and osteoporosis. *Curr. Osteoporos. Rep.* 2 (3), 79–89. Epub 2005/07/23. doi:10.1007/s11914-004-0015-1
- Barrett, T., Wilhite, S. E., Ledoux, P., Evangelista, C., Kim, I. F., Tomashevsky, M., et al. (2013). Ncbi geo: Archive for functional genomics data sets—update. *Nucleic Acids Res.* 41, D991–D995. Database issue Epub 2012/11/30. doi:10.1093/nar/gks1193
- Burley, S. K., Bhikadiya, C., Bi, C., Bittrich, S., Chen, L., Crichlow, G. V., et al. (2021). Rcsb protein data bank: Powerful new tools for exploring 3d structures of biological macromolecules for basic and applied research and education in fundamental biology, biomedicine, Biotechnology, bioengineering and energy sciences. *Nucleic Acids Res.* 49 (D1), D437–D451. Epub 2020/11/20. doi:10.1093/nar/gkaa1038
- Cai, X., Yi, X., Zhang, Y., Zhang, D., Zhi, L., and Liu, H. (2018). Genetic susceptibility of postmenopausal osteoporosis on sulfide quinone reductase-like gene. *Osteoporos. Int.* 29 (9), 2041–2047. Epub 2018/06/02. doi:10.1007/s00198-018-4575-9
- Cheng, X., Zhao, K., Zha, X., Du, X., Li, Y., Chen, S., et al. (2021). Opportunistic screening using low-dose ct and the prevalence of osteoporosis in China: A nationwide, multicenter study. *J. Bone Min. Res.* 36 (3), 427–435. Epub 2020/11/05. doi:10.1002/jbmr.4187
- Custer, R., and Ahlfeldt, F. E. (1932). Studies on the structure and function of bone marrow: II. Variations in cellularity in various bones with advancing years of life and their relative response to stimuli. *J. Laboratory Clin. Med.* 17 (10), 960–962.
- Davis, A. P., Grondin, C. J., Johnson, R. J., Sciaky, D., Wiegiers, J., Wiegiers, T. C., et al. (2021). Comparative toxicogenomics database (ctd): Update 2021. *Nucleic Acids Res.* 49 (D1), D1138–D1143. Epub 2020/10/18. doi:10.1093/nar/gkaa891
- Ensrud, K. E., Kats, A. M., Boyd, C. M., Diem, S. J., Schousboe, J. T., Taylor, B. C., et al. (2019). Association of disease definition, comorbidity burden, and prognosis with hip fracture probability among late-life women. *JAMA Intern. Med.* 179 (8), 1095–1103. Epub 2019/06/18. doi:10.1001/jamainternmed.2019.0682
- Friedman, J., Hastie, T., and Tibshirani, R. (2010). Regularization paths for generalized linear models via coordinate descent. *J. Stat. Softw.* 33 (1), 1–22. Epub 2010/09/03. doi:10.18637/jss.v033.i01
- Frohn, J., Wilken, T., Falk, S., Stutte, H. J., Kollath, J., and Hör, G. (1991). Effect of aortic sclerosis on bone mineral measurements by dual-photon absorptiometry. *J. Nucl. Med.* 32 (2), 259–262. Epub 1991/02/01.
- Fujikawa, Y., Quinn, J. M., Sabokbar, A., McGee, J. O., and Athanasou, N. A. (1996). The human osteoclast precursor circulates in the monocyte fraction. *Endocrinology* 137 (9), 4058–4060. Epub 1996/09/01. doi:10.1210/endo.137.9.8756585
- Gautier, L., Cope, L., Bolstad, B. M., and Irizarry, R. A. (2004). Affy—Analysis of Affymetrix genechip data at the probe level. *Bioinformatics* 20 (3), 307–315. Epub 2004/02/13. doi:10.1093/bioinformatics/btg405
- Ge, C., Xiao, G., Jiang, D., and Franceschi, R. T. (2007). Critical role of the extracellular signal-regulated kinase-mapk pathway in osteoblast differentiation and skeletal development. *J. Cell Biol.* 176 (5), 709–718. Epub 2007/02/28. doi:10.1083/jcb.200610046
- Glaser, D. L., and Kaplan, F. S. (1976). Osteoporosis. Definition and clinical presentation. *Spine* 22 (24), 12S–16S. Epub 1998/02/07. doi:10.1097/00007632-199712151-00003
- Grosdidier, A., Zoete, V., and Michielin, O. (2011). Swissdock, a protein-small molecule docking web service based on eadock dss. *Nucleic Acids Res.* 39, W270–W277. Web Server issue Epub 2011/06/01. doi:10.1093/nar/gkr366
- Hill, K. D., and Einstein, A. J. (2016). New approaches to reduce radiation exposure. *Trends Cardiovasc. Med.* 26 (1), 55–65. Epub 2015/05/13. doi:10.1016/j.tcm.2015.04.005
- Hong, D., Chen, H. X., Yu, H. Q., Wang, C., Deng, H. T., Lian, Q. Q., et al. (2011). Quantitative proteomic analysis of dexamethasone-induced effects on osteoblast differentiation, proliferation, and apoptosis in mc3t3-E1 cells using silac. *Osteoporos. Int.* 22 (7), 2175–2186. Epub 2010/11/10. doi:10.1007/s00198-010-1434-8
- Hou, J. M., Chen, E. Y., Lin, F., Lin, Q. M., Xue, Y., Lan, X. H., et al. (2015). Lactoferrin induces osteoblast growth through igf-1r. *Int. J. Endocrinol.* 2015, 282806. Epub 2015/08/21. doi:10.1155/2015/282806
- Howard, A., West, R. M., Iball, G., Panteli, M., Baskshi, M. S., Pandit, H., et al. (2020). Should radiation exposure Be an issue of concern in children with multiple trauma? *Ann. Surg.* 275, 596–601. Epub 2020/08/03. doi:10.1097/sla.0000000000004204
- Ito, K., and Murphy, D. (2013). Application of Ggplot2 to pharmacometric graphics. *CPT. Pharmacometrics Syst. Pharmacol.* 2 (10), e79. Epub 2013/10/18. doi:10.1038/psp.2013.56
- Langfelder, P., and Horvath, S. (2008). Wgcna: An R package for weighted correlation network analysis. *BMC Bioinforma.* 9, 559. Epub 2008/12/31. doi:10.1186/1471-2105-9-559
- Li, D., Cai, L., Meng, R., Feng, Z., and Xu, Q. (2020). Mettl3 modulates osteoclast differentiation and function by controlling rna stability and nuclear export. *Int. J. Mol. Sci.* 21 (5), E1660. Epub 2020/03/04. doi:10.3390/ijms21051660
- Li, D. W., Liu, J. P., Mao, Y. W., Xiang, H., Wang, J., Ma, W. Y., et al. (2005). Calcium-activated raf/mek/erk signaling pathway mediates P53-dependent apoptosis and is abrogated by alpha B-crystallin through inhibition of Ras activation. *Mol. Biol. Cell* 16 (9), 4437–4453. Epub 2005/07/08. doi:10.1091/mbc.e05-01-0010
- McGeary, S. E., Lin, K. S., Shi, C. Y., Pham, T. M., Bisaria, N., Kelley, G. M., et al. (2019). The biochemical basis of microrna targeting efficacy. *Science* 366 (6472), eaav1741. Epub 2019/12/07. doi:10.1126/science.aav1741
- Meng, H. Z., Zhang, W. L., Liu, F., and Yang, M. W. (2015). Advanced glycation end products affect osteoblast proliferation and function by modulating autophagy via the receptor of advanced glycation end products/raf protein/mitogen-activated protein kinase/extracellular signal-regulated kinase kinase/extracellular signal-regulated kinase (Raf/Mek/Erk) pathway. *J. Biol. Chem.* 290 (47), 28189–28199. Epub 2015/10/17. doi:10.1074/jbc.M115.669499
- Orwoll, E. S., Oviatt, S. K., and Mann, T. (1990). The impact of osteophytic and vascular calcifications on vertebral mineral density measurements in men. *J. Clin. Endocrinol. Metab.* 70 (4), 1202–1207. Epub 1990/04/01. doi:10.1210/jcem-70-4-1202
- Ritchie, M. E., Phipson, B., Wu, D., Hu, Y., Law, C. W., Shi, W., et al. (2015). Limma powers differential expression analyses for rna-sequencing and microarray studies. *Nucleic Acids Res.* 43 (7), e47. Epub 2015/01/22. doi:10.1093/nar/gkv007
- Robin, X., Turck, N., Hainard, A., Tiberti, N., Lisacek, F., Sanchez, J. C., et al. (2011). Proc: An open-source package for R and S+ to analyze and compare roc curves. *BMC Bioinforma.* 12, 77. Epub 2011/03/19. doi:10.1186/1471-2105-12-77
- Siris, E. S., Adler, R., Bilezikian, J., Bolognese, M., Dawson-Hughes, B., Favus, M. J., et al. (2014). The clinical diagnosis of osteoporosis: A position statement from the national bone health alliance working group. *Osteoporos. Int.* 25 (5), 1439–1443. Epub 2014/03/01. doi:10.1007/s00198-014-2655-z
- Vlachos, I. S., Kostoulas, N., Vergoulis, T., Georgakilas, G., Reczko, M., Maragkakis, M., et al. (2012). Diana mirpath V2.0: Investigating the combinatorial effect of micromas in pathways. *Nucleic Acids Res.* 40, W498–W504. Web Server issue Epub 2012/06/01. doi:10.1093/nar/gks494
- Wang, H., Zhao, W., Tian, Q. J., Xin, L., Cui, M., and Li, Y. K. (2020). Effect of Incrna Ak023948 on rats with postmenopausal osteoporosis via pi3k/akt signaling pathway. *Eur. Rev. Med. Pharmacol. Sci.* 24 (5), 2181–2188. Epub 2020/03/21. doi:10.26355/eurrev-202003\_20483
- Wang, W., Qiao, S. C., Wu, X. B., Sun, B., Yang, J. G., Li, X., et al. (2021). Circ\_0008542 in osteoblast exosomes promotes osteoclast-induced bone resorption through M6a methylation. *Cell Death Dis.* 12 (7), 628. Epub 2021/06/20. doi:10.1038/s41419-021-03915-1
- Yan, J., Chen, S., Zhang, Y., Li, X., Li, Y., Wu, X., et al. (2008). Rac1 mediates the osteoclast gains-in-function induced by haploinsufficiency of Nf1. *Hum. Mol. Genet.* 17 (7), 936–948. Epub 2007/12/20. doi:10.1093/hmg/ddm366
- Yao, P., Bennett, D., Mafham, M., Lin, X., Chen, Z., Armitage, J., et al. (2019). Vitamin D and calcium for the prevention of fracture: A systematic review and meta-analysis. *JAMA Netw. Open* 2 (12), e1917789. Epub 2019/12/21. doi:10.1001/jamanetworkopen.2019.17789
- Yoshiki, S., Matsunaga-Udagawa, R., Aoki, K., Kamioka, Y., Kiyokawa, E., and Matsuda, M. (2010). Ras and calcium signaling pathways converge at Raf1 via the Shoc2 scaffold protein. *Mol. Biol. Cell* 21 (6), 1088–1096. Epub 2010/01/15. doi:10.1091/mbc.e09-06-0455
- Yu, G., Wang, L. G., Han, Y., and He, Q. Y. (2012). Clusterprofiler: An R package for comparing biological themes among gene clusters. *Omics* 16 (5), 284–287. Epub 2012/03/30. doi:10.1089/omi.2011.0118
- Zhou, Y., Deng, H. W., and Shen, H. (2015). Circulating monocytes: An appropriate model for bone-related study. *Osteoporos. Int.* 26 (11), 2561–2572. Epub 2015/07/22. doi:10.1007/s00198-015-3250-7



## OPEN ACCESS

## EDITED BY

Xiaofeng Zhu,  
Jinan University, China

## REVIEWED BY

Liusheng Huang,  
University of California, San Francisco,  
United States  
Xuenong Zou,  
The First Affiliated Hospital of Sun  
Yat-sen University, China

## \*CORRESPONDENCE

Chi Zhang,  
chi.zhang@case.edu

## SPECIALTY SECTION

This article was submitted to  
Experimental Pharmacology and  
Drug Discovery,  
a section of the journal  
Frontiers in Pharmacology

RECEIVED 04 August 2022

ACCEPTED 31 August 2022

PUBLISHED 23 September 2022

## CITATION

Huang AY, Xiong Z, Liu K, Chang Y,  
Shu L, Gao G and Zhang C (2022),  
Identification of kaempferol as an OSX  
upregulator by network pharmacology-  
based analysis of qianggu Capsule  
for osteoporosis.  
*Front. Pharmacol.* 13:1011561.  
doi: 10.3389/fphar.2022.1011561

## COPYRIGHT

© 2022 Huang, Xiong, Liu, Chang, Shu,  
Gao and Zhang. This is an open-access  
article distributed under the terms of the  
[Creative Commons Attribution License](https://creativecommons.org/licenses/by/4.0/)  
(CC BY). The use, distribution or  
reproduction in other forums is  
permitted, provided the original  
author(s) and the copyright owner(s) are  
credited and that the original  
publication in this journal is cited, in  
accordance with accepted academic  
practice. No use, distribution or  
reproduction is permitted which does  
not comply with these terms.

# Identification of kaempferol as an OSX upregulator by network pharmacology-based analysis of qianggu Capsule for osteoporosis

Ann Yehong Huang<sup>1</sup>, Zhencheng Xiong<sup>2</sup>, Kuankuan Liu<sup>2</sup>,  
Yanan Chang<sup>2</sup>, Li Shu<sup>2</sup>, Guolan Gao<sup>3</sup> and Chi Zhang<sup>2,4,5\*</sup>

<sup>1</sup>Department of Biochemistry, University of Texas Southwestern Medical Center, Dallas, TX, United States, <sup>2</sup>Central Laboratory, Peking University International Hospital, Beijing, China,

<sup>3</sup>Department of Obstetrics and Gynecology, Peking University International Hospital, Beijing, China,

<sup>4</sup>Department of Orthopedics, Peking University International Hospital, Beijing, China, <sup>5</sup>Biomedical Engineering Department, Peking University, Beijing, China

Osteoporosis is the most common metabolic disease of skeleton with reduced bone density and weaker bone. Qianggu Capsule as a traditional Chinese medicine has been widely used to treat osteoporosis. The potential pharmacological mechanism of its active ingredient Gusuibu is not well understood. The purpose of this work is to analyze the anti-osteoporosis function of Gusuibu based on network pharmacology, and further explore the potential mechanism of Qianggu Capsule. The active compounds and their corresponding targets of Gusuibu were obtained from TCMSP, TCMID, and BATMAN-TCM databases. Potential therapeutic targets for osteoporosis were obtained through DisGeNET, TTD, GeneCards, MalaCards, CTD, and OMIM databases. The overlapping targets of Gusuibu and osteoporosis were obtained. GO and KEGG pathway enrichment analysis were performed. The “Gusuibu-active compounds-target genes-osteoporosis” network and protein-protein interaction (PPI) network were constructed, and the top hub genes were screened by using the plug-in CytoHubba. Molecular docking was used to verify the binding activity of hub genes and key compounds. We identified 21 active compounds and 140 potential therapeutic targets that may be related to Gusuibu and 10 hub genes (AKT1, IL6, JUN, TNF, MAPK3, VEGFA, EGFR, MAPK1, CASP3, PTGS2). Molecular docking analysis demonstrated that four key active small molecules in Gusuibu (including Luteolin, Naringenin, Kaempferol, and Beta-sitosterol) have excellent binding affinity to the target proteins encoded by the top 10 hub genes. Our new findings indicated that one key active compound kaempferol activated the expression of osteoblast specific transcription factor OSX through JNK kinase pathway.

## KEYWORDS

kaempferol, osteoporosis, qianggu capsule, gusuibu, OSX, network pharmacology

## Introduction

Osteoporosis is the most common metabolic disease of skeleton with reduced bone density and weaker bone structure. Patients are more likely to have fractures with the pain and other complications, and the quality of life is dramatically affected (Zheng et al., 2020). Postmenopausal osteoporosis is one common form of primary osteoporosis. Osteoporosis is classified into the categories of “Gu Bi” and “Gu Lou” in the “Huang Di Nei Jing” of Traditional Chinese Medicine (TCM) theory (CSOaBM, 2019). Bone metabolism is a continuous process, and bone mass will be gradually lost after the age of 35. People especially postmenopausal women and the elderly should pay more attention to osteoporosis prevention (Li et al., 2020a; Saul and Kosinsky, 2021). The fragility fractures induced by osteoporosis will lead to increased disability and mortality, resulting in a heavy family, social and economic burden (Kanis, 2002; Xiong et al., 2021). The commonly used anti-osteoporosis drugs include estrogen, calcium, vitamin D, bisphosphonates, and denosumab; however, the consequent adverse effects are still a challenge to be solved due to the increased duration of use and dose (Jackson and Mysiw, 2014). Therefore, it is needed to explore potential anti-osteoporosis drugs with high efficacy and safety.

It is well known that TCM has a long history of practice in China and other Asian countries to treat a wide range of diseases, including osteoporosis (Li et al., 2017a; Wei et al., 2017; Wu et al., 2017; Zhang et al., 2017; Ge et al., 2018; Li et al., 2020a; Li et al., 2020b; Liu et al., 2020; Zheng et al., 2020). Among those to treat osteoporosis, the clinically commonly used Traditional Chinese Medicine prescriptions include Qianggu Capsule, XianlingGubao Capsule, DuhuoJisheng Decoction, LiuweiDihuang Pill, and Erxian Decoction (Li et al., 2017a; Wei et al., 2017; Wu et al., 2017; Ge et al., 2018; Li et al., 2020a). Qianggu Capsule (Drug approval number: Z20030007, Qi-Huang Pharmaceutical CO. LTD., Beijing, China) is a China Food and Drug Administration (CFDA)-approved TCM for the treatment of osteoporosis and bone loss. The active ingredients in Qianggu Capsule are total flavonoids extracted from *Rhizoma Drynariae* (English name is Fortune's *Drynaria Rhizome*, and Chinese name is Gusuibu), the dried rhizome of *Drynaria fortunei* (Kunze) J. SM. (Wang et al., 2008; CSOaBM, 2019). The active ingredient of Qianggu Capsules is the herbal Gusuibu. Gusuibu is still a kind of raw material, and there are many compounds in Gusuibu, including flavonoids. Studies have shown that the flavonoids in Gusuibu may treat osteoporosis by improving bone density and reducing bone loss (Zhang et al., 2017; Shen et al., 2020). However, the mechanism of function of many TCM cannot be elucidated due to the complexity of the ingredients in TCM.

In recent years, many researchers have started to use bioinformatics and network pharmacology to analyze the

multi-component, multi-target and multi-pathway characteristics of TCM in order to elucidate mechanisms of its action, thus providing directions for further research (Shuai et al., 2020). Gusuibu contains a variety of components. Although some studies have suggested that total flavonoids play a key role in anti-osteoporosis (Wang et al., 2008; Zhang et al., 2017), the molecular mechanism has not been elucidated yet.

In this study we used a network pharmacology approach to analyze the key genes, active compounds and pathways in the anti-osteoporosis of Gusuibu, and further explored possible underlying molecular mechanisms. We identified one key active compound kaempferol in Gusuibu as an upregulator of osteoblast specific transcription factor OSX.

## Materials and methods

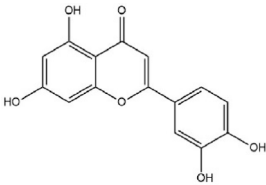
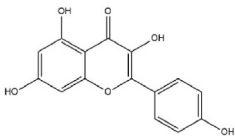
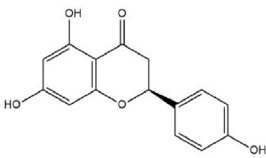
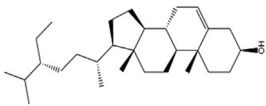
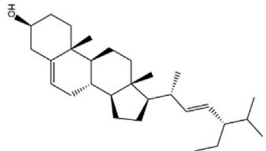
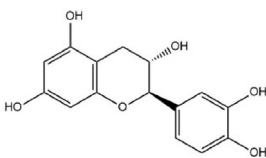
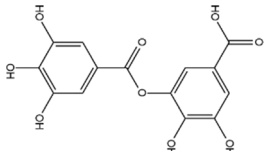
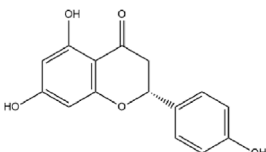
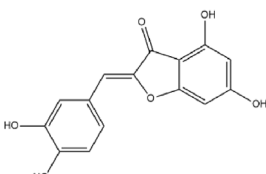
### Exploring potential pharmacodynamic compounds and relevant targets of gusuibu

Using TCM Systems Pharmacology (TCMSP, Version: 2.3, <https://tcmssp.com/tcmssp.php>) database (Ru et al., 2014), BATMAN-TCM platform (<http://bionet.ncpsb.org/batman-tcm/>) (Liu et al., 2016) and TCM Integrated Database (TCMID, <http://www.megabionet.org/tcmid/>) (Huang et al., 2018), the corresponding compounds of Gusuibu and related information were obtained. The compounds retrieved in the previous step were screened for active compounds according to the absorption, distribution, metabolism and excretion (ADME) protocol (oral bioavailability (OB)  $\geq 30$  and drug-likeness (DL)  $\geq 0.18$ ) (Tsaoun et al., 2016; Sheng et al., 2020). The databases were then used to mine potential targets corresponding to the active compounds. The target proteins were then converted to the corresponding gene names and UniProt ID using the UniProt database (<https://www.uniprot.org/>) for “*Homo sapiens*” (UniProt Consortium, 2018).

### Exploring the relevant targets of osteoporosis

The targets related to osteoporosis were obtained through retrieving GeneCards (<https://www.genecards.org/>) (Relevance score  $\geq 10$ ) (Stelzer et al., 2016), MalaCards (<https://www.malacards.org/>) (Rappaport et al., 2017), DisGeNet database (<https://www.disgenet.org/>, v7.0) (Score  $\geq 0.01$ ) (Piñero et al., 2020), Therapeutic Target Database (TTD) (<http://db.idrblab.net/ttd/>, Last update by 1 June 2020) (Wang et al., 2020), Comparative Toxicogenomics Database (CTD) (<http://ctdbase.org/>, Last update by June 2020) (Inference score  $\geq 15$ ) (Davis et al., 2020), and Online Mendelian Inheritance in Man (OMIM)

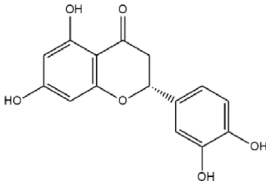
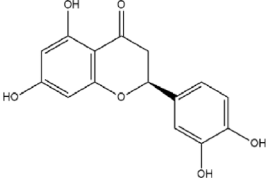
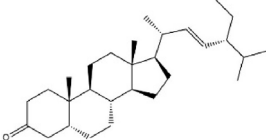
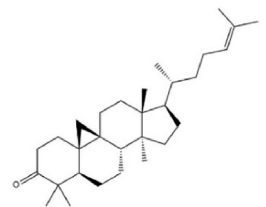
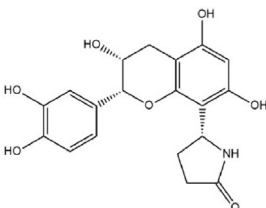
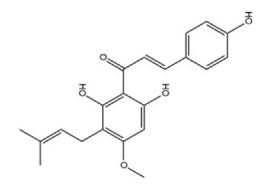
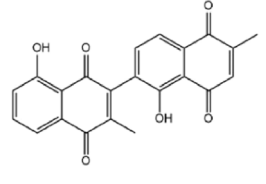
TABLE 1 Basic information of active compounds in Gusuibu.

Molecule ID	Molecule name	OB (%)	DL	2D structure	InChI key	PubChem CID
MOL000006	Luteolin	36.16	0.25		IQPNAANSBPBGFQ-UHFFFAOYSA-N	5280445
MOL000422	Kaempferol	41.88	0.24		IYRMWYBZSQPKC-UHFFFAOYSA-N	5280863
MOL004328	Naringenin	59.29	0.21		FTVWIRXFELQLPI-ZDUSSCGKSA-N	439246
MOL000358	Beta-sitosterol	36.91	0.75		KZJWDPNRJALLNS-VJSFXLFSA-N	222284
MOL000449	Stigmasterol	43.83	0.76		HCXVJBMSMIARIN-PHZDYDNGSA-N	5280794
MOL000492	(+)-catechin	54.83	0.24		PFTAWBLQPZVEMU-DZGCQCFKSA-N	9064
MOL000569	Digallate	61.85	0.26		COVFEVWNJUOYRL-UHFFFAOYSA-N	341
MOL001040	(2R)-5,7-dihydroxy-2-(4-hydroxyphenyl)chroman-4-one	42.36	0.21		FTVWIRXFELQLPI-CYBMUJFWSA-N	667495
MOL001978	Aureusidin	53.42	0.24		WBEFUVAYFSOUEA-PQMHYQBVSA-N	5281220

(Continued on following page)

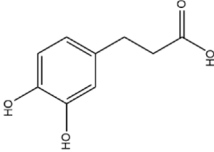
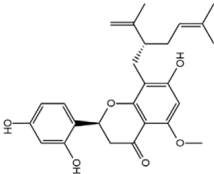
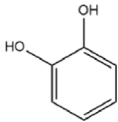
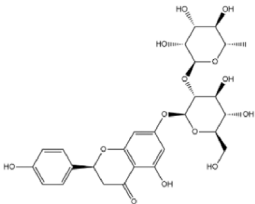
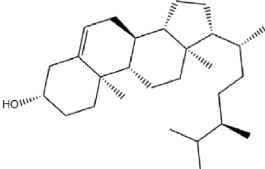
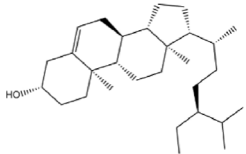
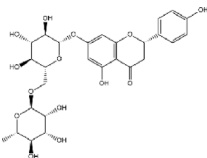
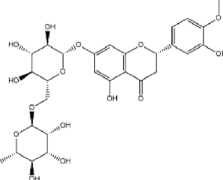


TABLE 1 (Continued) Basic information of active compounds in Gusuibu.

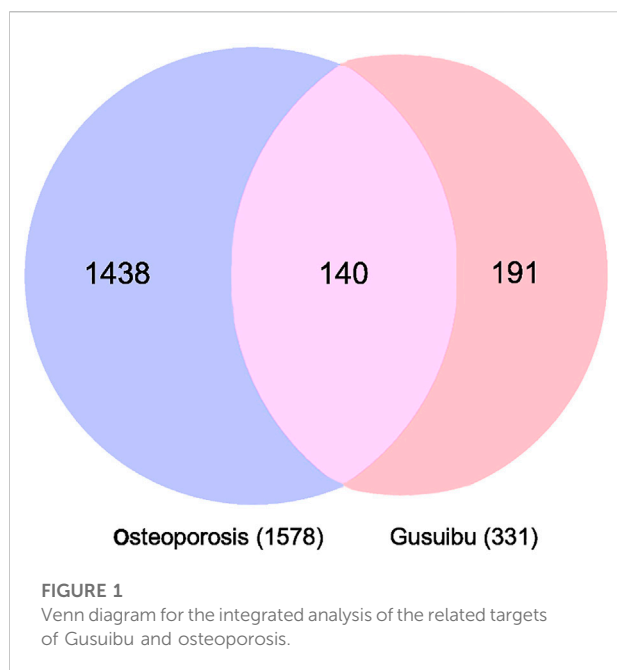
Molecule ID	Molecule name	OB (%)	DL	2D structure	InChI key	PubChem CID
MOL002914	Eriodyctiol (flavanone)	41.35	0.24		SBHXYTNGIZCORG-CYBMUJFWSA-N	373261
MOL005190	Eriodictyol	71.79	0.24		SBHXYTNGIZCORG-ZDUSSCGKSA-N	440735
MOL009061	22-Stigmasten-3-one	39.25	0.76		RTLUSWHIKFIQFU-ZBWVUXHASA-N	91692436
MOL009075	Cycloartenone	40.57	0.79		NAJCQAAOHKVCES-ZZOQNIIDSA-N	12305360
MOL009078	DavalliosideA_qt	62.65	0.51		ZGIKMQUZZSYOY-QEIWDELWSA-N	NR
MOL009091	Xanthogalenol	41.08	0.32		ALGFNVZQNNGHPA-YRNVUSSQSA-N	14309735
	Chitranone				ITGPISXKMZIRAV-UHFFFAOYSA-N	633072

(Continued on following page)

TABLE 1 (Continued) Basic information of active compounds in Gusuibu.

Molecule ID	Molecule name	OB (%)	DL	2D structure	InChI key	PubChem CID
	Dihydrocaffeic acid				DZAUWHJDUNRCTF-UHFFFAOYSA-N	348154
	Kurarinone				LTTQKYMNTNISSZ-MWTRTKDXSA-N	11982640
	Catechol				YCIMNLLNPGFGHC-UHFFFAOYSA-N	289
	Naringin				DFPMSGMNTNDNHN-ZPHOTFPESA-N	442428
	Campesterol				SGNBVLSWZMBQTH-PODYLTMSA-N	173183
	Gamma-Sitosterol				KZJWDPNRJALLNS-FBZNIEFRSA-N	457801
	Narirutin				HXTFHSYLYXVTHC-AJHDJQPGSA-N	442431
	Hesperidin				QUQPHWDTPGMPEX-QJBIFVCTSA-N	10621

Abbreviations: OB, Oral bioavailability; DL, Drug-likeness; NR, not reported.



(<https://omim.org/>, updated 25 November 2020) (Amberger and Hamosh, 2017) using the keyword “osteoporosis or postmenopausal osteoporosis”. The potential targets obtained from these 6 databases were integrated and deduplicated to generate the osteoporosis-related target set.

## Network construction and protein-protein interaction analysis

Gusuibu-related targets and osteoporosis-related targets were input to the Vennonline tool (<http://www.bioinformatics.com.cn/>) to obtain the common targets. These were the candidate targets of Gusuibu to treat osteoporosis. Cytoscape software (version 3.7.2) was used to construct the network diagram of “Gusuibu-active compounds-target genes-osteoporosis” (Shannon et al., 2003).

PPI is the basis of most biological processes and is important to understand cell physiology in both normal and disease states (Xiao et al., 2020). The STRING database (<http://string-db.org/>; version 11) was used to perform a PPI network analysis on the common targets (Szkłarczyk et al., 2017). The species is limited to “*Homo sapiens*” with a confidence level greater than 0.4. Cytoscape software (version 3.7.2) was used to construct the PPI network, and the plug-in 12 CytoHubba algorithms [Degree, Maximal Clique Centrality (MCC), Clustering Coefficient, Density of Maximum Neighborhood Component (DMNC), BottleNeck, Maximum Neighborhood Component (MNC), Radiality, Edge Percolated Component (EPC), Eccentricity, Closeness, Betweenness, Stress] were used to find the top 10 hub genes (Chin et al., 2014; Xu et al., 2020).

## Enrichment analysis of GO and KEGG pathway

The cluster Profiler package in R (R 4.0.2 for Windows) was used to perform Gene Ontology (GO) and Kyoto Encyclopedia of Genes and Genomes (KEGG) analysis to explore biological processes and signaling pathways in Gusuibu for osteoporosis (Kanehisa et al., 2008; Yu et al., 2012; Consortium, 2015). An adjusted *p*-value of less than 0.05 was used to determine the enrichment term.

## Implementation of molecular docking

The Sankey diagram (<http://sankeymatic.com/>) reveals the correspondence between herbs, components, and targets by constructing the interrelationship between the active compounds of Gusuibu and the top 10 hub genes. AutoDock Vina was used to perform molecular docking between the top 10 hub genes and key active ingredients to predict their binding affinity (Trott and Olson, 2010). The PDB format of the target proteins and the MOL2 format of active compounds could be obtained from the RCSB protein data (<http://www.rcsb.org/>) and the PubChem database (<https://pubchem.ncbi.nlm.nih.gov/>) (Kanis, 2002). The smaller the molecular docking score, the more stable the binding affinity between target proteins and active compounds (Chang et al., 2020).

## Cell culture

C2C12 mesenchymal stem cells (ATCC) were cultured in DMEM with 10% fetal bovine serum (FBS, Gibco), 100U/mL penicillin G sodium and 100 µg/ml streptomycin sulfate in a humidified atmosphere at 37°C. Cells were plated in 6-well plates, cultured to 60–80% confluence and treated with kaempferol.

## Reverse transcription-quantitative PCR

Kaempferol (1,000 ng/ml; Sigma) was used to stimulate C2C12 cells for 24 h before harvest. TRIzol (Invitrogen Life Technologies, Carlsbad, CA, United States) was used to extract total RNA from cultured cells as previously described (Tang et al., 2012). RNA purity and integrity were determined by the RNA 6000 Nano assay with an Agilent Bioanalyzer 2,100 (Agilent Technologies, Santa Clara, CA). 1 µg total RNA was reverse transcribed into cDNA using the GoScript Reverse Transcription System (Promega Corp., Madison, WI, United States) based on the manufacturer protocol. qPCR was performed in triplicate.

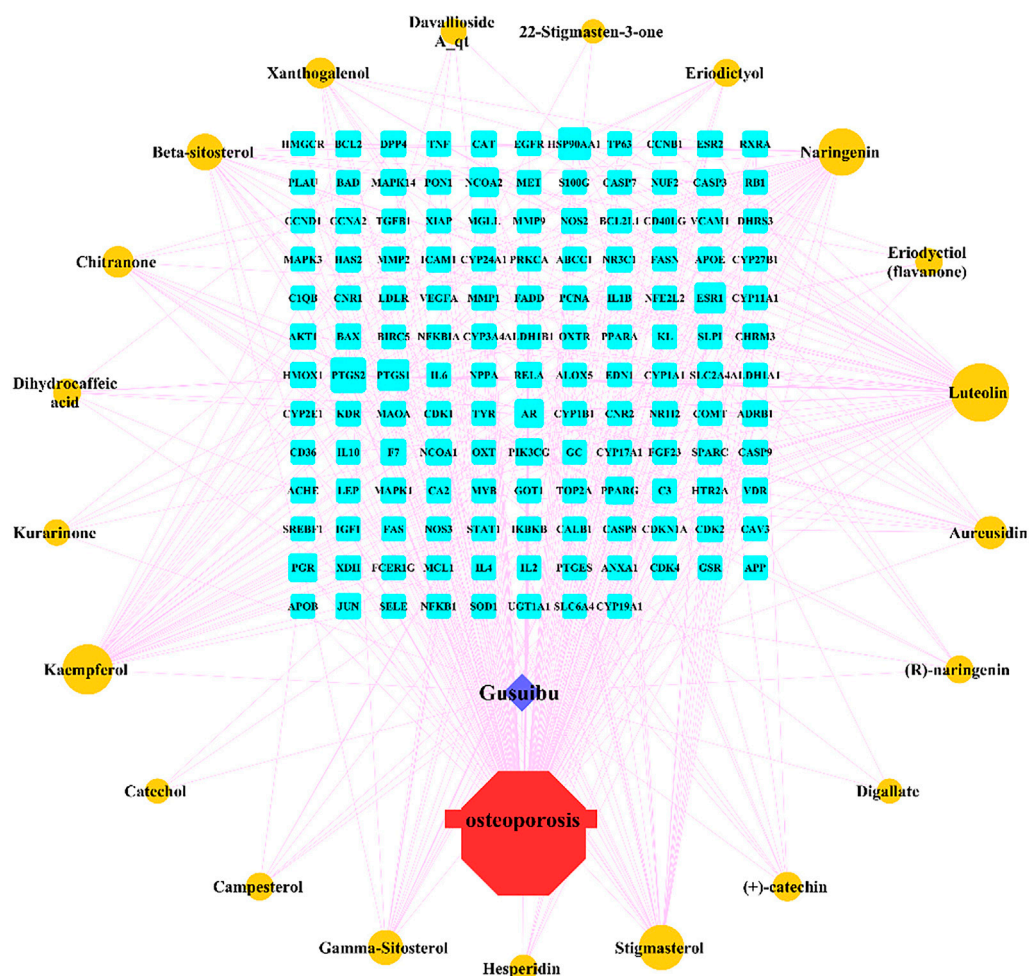


FIGURE 2

"Gusuibu-active compounds-target genes-osteoporosis" network. The red octagon represents osteoporosis; the blue diamond represents Gusuibu; the cyan rectangle represents the potential target; the brown ellipse represents the active compound contained in Gusuibu. The line between two nodes indicates that there is a relationship, and the size of each node indicates the number of relationships.

using SYBR-Green SuperReal PreMix Plus [Tiangen Biotech (Beijing) Co., Ltd., China] and the iQ5 PCR system (Bio-Rad Laboratories, Inc., Hercules, CA, United States). The reaction conditions were as follows: 95°C for 30 s, and 40 cycles of 95°C for 10 s and 60°C for 30 s. Data were reported as cycle threshold (Ct) values. The  $2^{-\Delta\Delta Ct}$  method was used to compare the RNA expressions. RNA levels were normalized to glyceraldehyde-3-phosphate dehydrogenase (GAPDH) levels.

## Statistical analysis

All qPCR experiments were performed in triplicate. Data were expressed as the mean  $\pm$  SD. Comparisons were made between groups by Student's *t* test with  $p < 0.05$  being considered as statistically significant.

## Results

### Pharmacodynamic compounds and potential target genes of gusuibu

A total of 131 compounds in Gusuibu (*Rhizoma Drynariae*) were obtained through the TCMSP database (Number: 71), TCMID database (Number: 53), and BATMAN-TCM platform (Number: 7). Based on the respective standards of TCMSP database (OB  $\geq$  30% and DL  $\geq$  0.18) and BATMAN-TCM platform (Score cutoff  $> 20$ , adjusted  $p$ -value  $< 0.05$ ) along with the existence of target proteins, a total of 24 active compounds of Gusuibu were screened. The corresponding target proteins were deduplicated, and a total of 331 target proteins were obtained. The UniProt database was used to convert the target proteins predicted by Gusuibu's bioactive compounds into gene names. Table 1 includes the basic information of active compounds in Gusuibu.



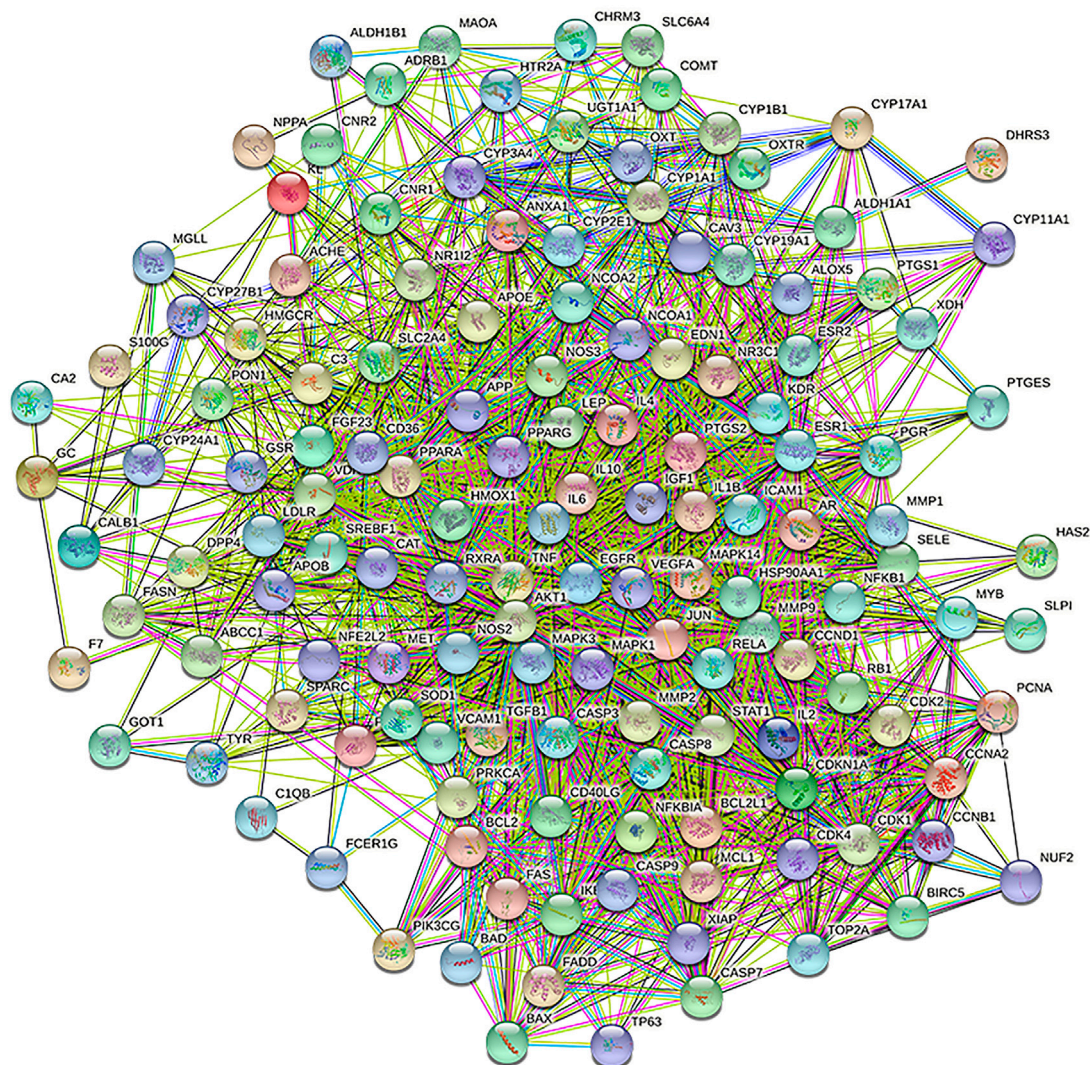


**FIGURE 3**  
PPI network based on STRING database.

## Potential therapeutic targets of gusuibu in the treatment of osteoporosis

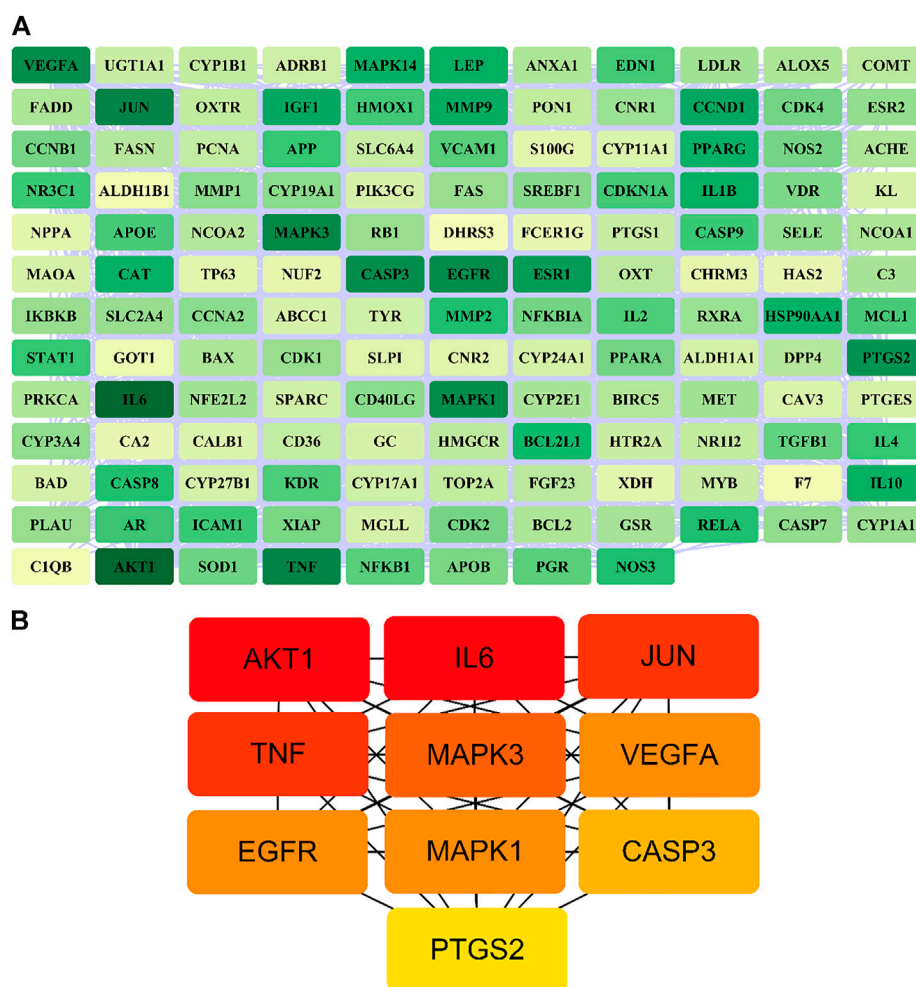
By searching the GeneCard, TTD, MalaCard, CTD, DisGeNET, and OMIM databases, a total of 1,578 potential therapeutic targets for osteoporosis were obtained. By constructing the Venn diagram of the targets regulated by Gusuibu's active ingredients and the potential targets of osteoporosis, a total of 140 intersection targets were obtained, which are potential therapeutic targets of Gusuibu against osteoporosis as shown in [Figure 1](#). Cytoscape software was used to construct the “Gusuibu-active compounds-target genes-osteoporosis” network for Gusuibu against osteoporosis as shown in [Figure 2](#). There are three compounds (Cycloartenone,

Narirutin, Naringin) corresponding to targets that are not intersecting genes, so there are 21 active compounds in the network.

## PPI network construction and exploration of potential hub genes for gusuibu against osteoporosis

A total of 140 potential target genes of Gusuibu for treating osteoporosis were entered into the STRING database to obtain a PPI network, which involved 140 nodes and 2,199 edges (Figure 3). The data obtained was imported into Cytoscape software (version 3.7.2) for further visualization (Figure 4A). According to the 12 CytoHubba algorithms of Cytoscape software, the top 10 hub



**FIGURE 4**

PPI network of potential target genes and top 10 hub genes for Gusuibu against osteoporosis. **(A)** PPI network constructed by using Cytoscape software. **(B)** The top 10 hub genes was identified by the Degree algorithm.

genes of Gusuibu for the treatment of osteoporosis were screened. A total of 37 different genes and the number of algorithms to which these genes belong were sorted in Table 2. The top 10 hub genes were consistent with the results of the Degree algorithm (Figure 4B). The Sankey diagram was constructed by using the top 10 ranked hub genes (AKT1, IL6, JUN, TNF, MAPK3, VEGFA, EGFR, MAPK1, CASP3, PTGS2) and the corresponding active compounds of Gusuibu. Luteolin targeted most of the hub genes while PTGS2 targeted most of the active compounds (Figure 5).

## Enrichment analysis of GO and KEGG pathway

The Cluster Profiler package in R was used to perform GO enrichment analysis on 140 potential targets of Gusuibu in the

treatment of osteoporosis. 2601 GO items (adjusted,  $p < 0.05$ ) were obtained, including 2,398 biological process (BP) items, 75 cellular component (CC) terms and 128 molecular function (MF) items. As shown in Figure 6, the top 10 enrichment results of GO-BP, GO-CC, and GO-MF were visualized by bubble chart.

A total of 166 KEGG enriched pathways (adjusted,  $p < 0.05$ ) were obtained through the above R package. As shown in Figure 7, the top 20 KEGG pathway enrichment terms were visualized by bubble chart.

We searched for osteoporosis in the KEGG database, and compared the retrieved relevant pathways with the enriched 166 pathways. A total of 50 pathways that may be related to osteoporosis were obtained, and we used Cytoscape software to construct a network diagram of potential target genes and pathways as shown in Figure 8.

TABLE 2 Basic information of top 10 hub genes by 12 CytoHubba algorithms.

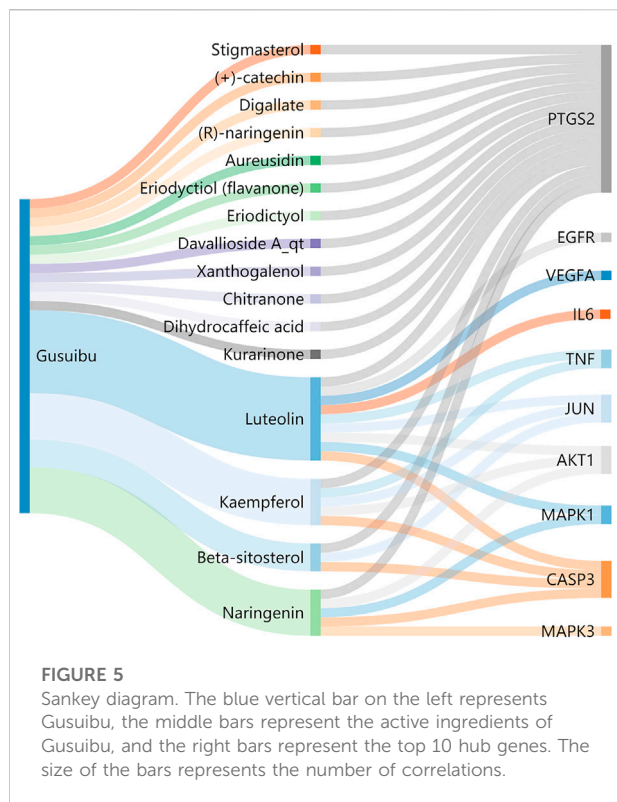
UniProt ID	Gene symbol	Protein names	Algorithms
P31749	AKT1	RAC-alpha serine/threonine-protein kinase	A, B, C, D, E, G, H, J, K, L
P05231	IL6	Interleukin-6	A, B, C, D, E, G, J, K, L
P05412	JUN	Transcription factor AP-1	A, B, C, D, G, H, J, K, L
P01375	TNF	Tumor necrosis factor	A, B, C, D, E, G, J, K, L
P42574	CASP3	Caspase-3	A, B, D, E, G, J, K, L
P28482	MAPK1	Mitogen-activated protein kinase 1	A, B, C, D, G, J, K, L
P27361	MAPK3	Mitogen-activated protein kinase 3	A, B, C, D, G, J, K, L
P35354	PTGS2	Prostaglandin G/H synthase 2	A, B, C, D, E, G, J, K
P15692	VEGFA	Vascular endothelial growth factor A	A, B, D, E, G, J, K
P00533	EGFR	Epidermal growth factor receptor	A, C, D, J, K, L
P03372	ESR1	Estrogen receptor	C, E, G, L
P14780	MMP9	Matrix metalloproteinase-9	B, E, H
P10275	AR	Androgen receptor	E, H
P04040	CAT	Catalase	C, L
P29965	CD40LG	CD40 ligand	I, H
P03956	MMP1	Interstitial collagenase	I, F
P16581	SELE	E-selectin	I, F
P98170	XIAP	E3 ubiquitin-protein ligase XIAP	I, H
P09917	ALOX5	Polyunsaturated fatty acid 5-lipoxygenase	H
Q92934	BAD	Bcl2-associated agonist of cell death	F
P55210	CASP7	Caspase-7	H
Q14790	CASP8	Caspase-8	I
P20309	CHRM3	Muscarinic acetylcholine receptor M3	F
P05108	CYP11A1	Cholesterol side-chain cleavage enzyme, mitochondrial	H
Q92819	HAS2	Hyaluronan synthase 2	F
P05362	ICAM1	Intercellular adhesion molecule 1	I
P22301	IL10	Interleukin-10	E
P60568	IL2	Interleukin-2	I
Q07820	MCL1	Induced myeloid leukemia cell differentiation protein Mcl-1	I
P10242	MYB	Transcriptional activator Myb	F
P25963	NFKBIA	NF-kappa-B inhibitor alpha	I
Q9BZD4	NUF2	Kinetochore protein Nuf2	F
P00749	PLAU	Urokinase-type plasminogen activator	H
O14684	PTGES	Prostaglandin E synthase	F
P03973	SLPI	Antileukoproteinase	F
P09486	SPARC	SPARC	F
P01137	TGFB1	Transforming growth factor beta-1 proprotein	I

A: Degree, B: Maximal Clique Centrality (MCC), C: Betweenness, D: closeness, E: BottleNeck, F: ClusteringCoefficient, G: Edge Percolated Component (EPC), H: Eccentricity, I: Density of Maximum Neighborhood Component (DMNC), J: Maximum Neighborhood Component (MNC), K: radiality, L: stress.

## Molecular docking

Based on the Sankey diagram results, molecular docking was performed between the top 10 target proteins (AKT1, IL6, JUN, TNF, MAPK3, VEGFA, EGFR, MAPK1, CASP3, PTGS2) and four key active compounds (Luteolin, Naringenin, Kaempferol, and Beta-sitosterol) using AutoDock Vina. As

shown in Figure 9, a heatmap was used to visualize the strongest affinity docking scores of top 10 target proteins and 4 key active compounds. The binding energy between the top 10 target proteins and the active compound is about  $-6.4$  to  $-10.8$  kcal mol<sup>-1</sup>, indicating that the key active compounds in Gusuibu bind well to the top 10 target proteins.



## Kaempferol induced the expression of osteoblast genes

To explore the possible role of one key active compound kaempferol in osteoblast genes, we examined the effect of kaempferol on osteoblast differentiation related gene expressions. C2C12 cells were cultured and treated as indicated with kaempferol (1,000 ng/ml, Sigma) for 24 h. Total RNA was isolated and measured by real time RT-PCR. As shown in Figure 10, after kaempferol stimulation osteoblast specific transcription factor Osterix (OSX) expression was upregulated by about 6.1 folds, while the expression of OSX downstream osteoblastic gene osteocalcin (OCN) increased by 5.9 fold. These observations demonstrated that kaempferol induced OSX gene expression.

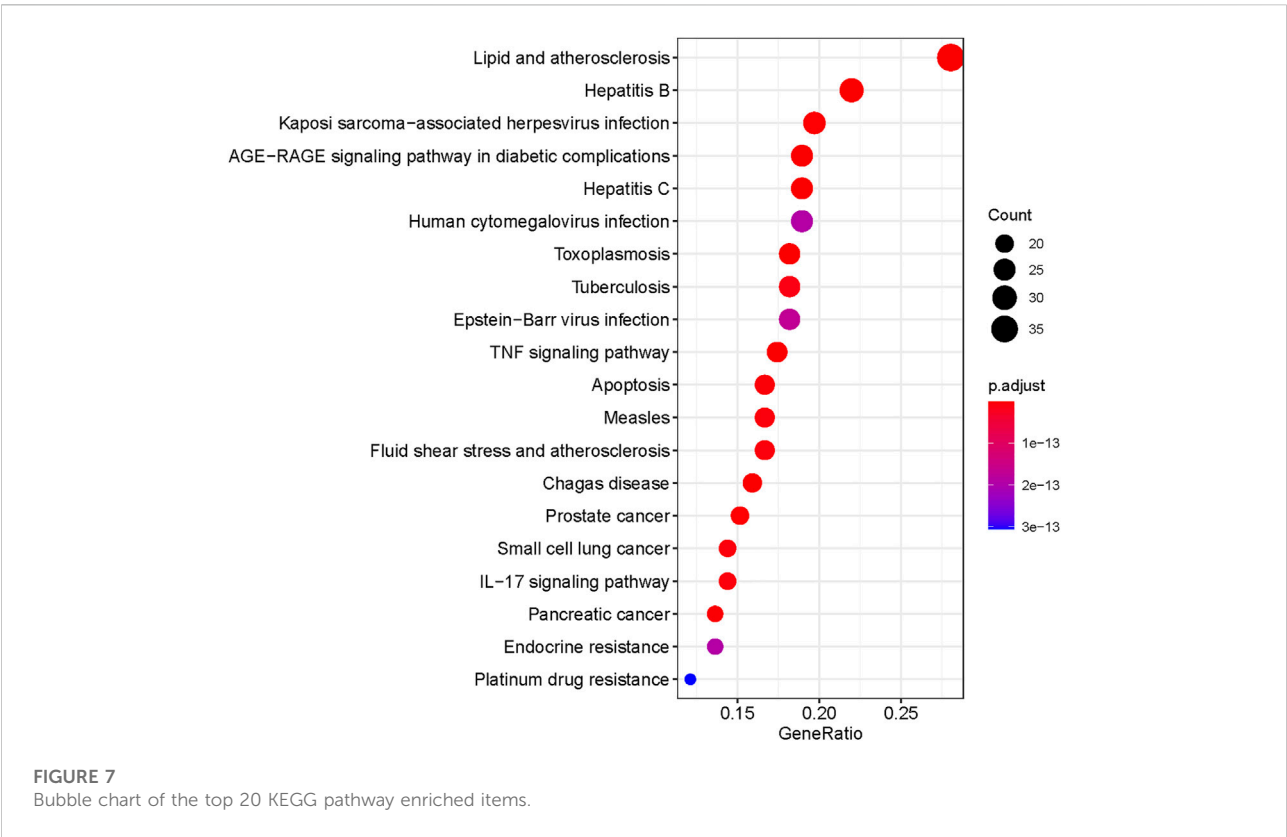
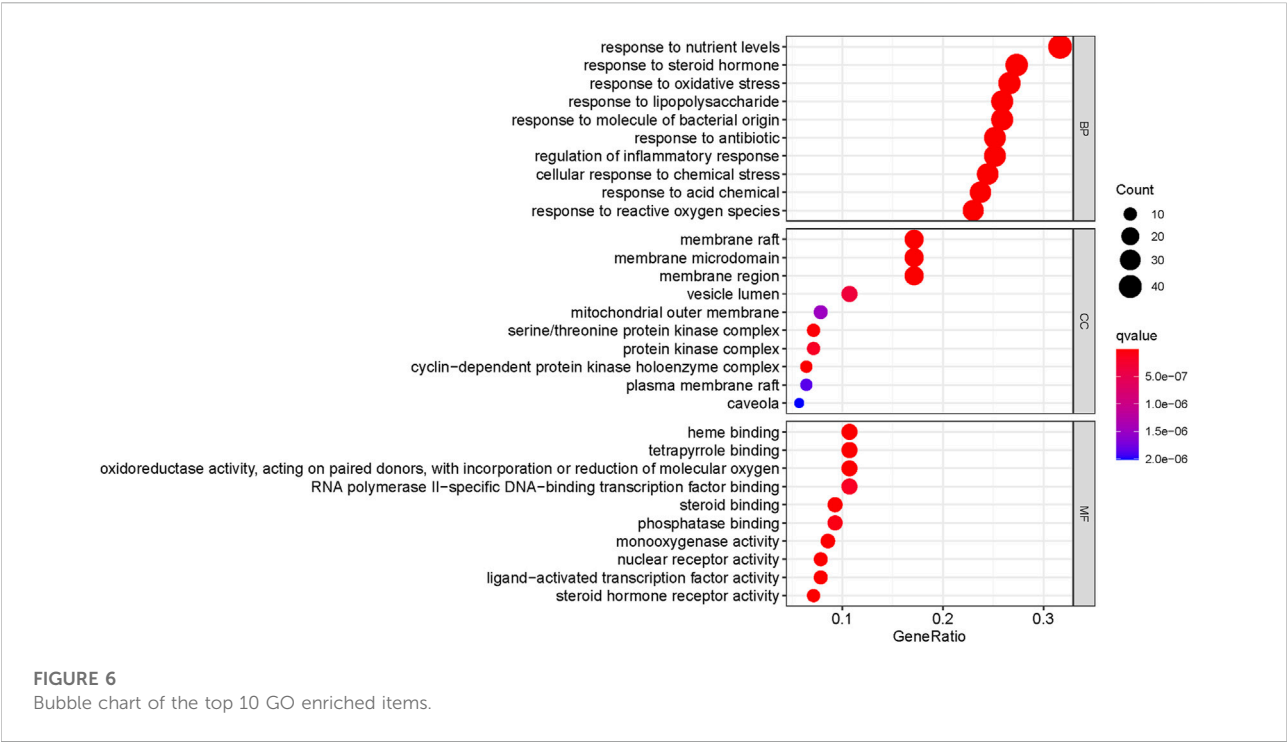
We asked which pathway was involved in kaempferol induced OSX gene expression. To explore molecular mechanisms of kaempferol effect on OSX expression, we used a loss-of-function approach to examine possible pathways involved. The selective inhibitors were used: SB203580 as a specific inhibitor for p38 MAPK pathway, and SP600125 is a specific inhibitor for JNK kinase pathway. C2C12 cells were treated with kaempferol. Different inhibitors were added in the culture medium. As shown in Figure 11, kaempferol treatment led to OSX expression increase by 10.8-fold. Addition of 50  $\mu$ M SP600125 almost abolished the increment

of OSX expression induced by kaempferol. Kaempferol-induced OSX activation remained unchanged after treatment with 10  $\mu$ M SB203580. The data indicate that kaempferol-induced OSX activation is mediated through JNK kinase pathway.

## Discussion

Osteoporosis has become an important health issue with aging (Zheng et al., 2020). For example, postmenopausal osteoporosis as a very common form of primary osteoporosis affects most postmenopausal women (Jackson and Mysiw, 2014). Due to severe side effects of current clinical osteoporosis drugs, more and more attention has been paid to possible drugs for the prevention and treatment of osteoporosis from natural products (Li et al., 2020a). Qianggu Capsule is a proprietary Traditional Chinese Medicine approved by CFDA to treat osteoporosis, and its active ingredient is total flavonoids of *Rhizoma Drynariae* (Gusuibu) (CSOaBM, 2019). Studies have shown that Qianggu Capsule may prevent and treat osteoporosis by improving bone density and reducing bone loss (Wei et al., 2017). The raw material of Qianggu Capsules is the flavonoids of the herbal Gusuibu, but the mixture is not a single compound at all, and the underlying mechanism is not clear yet. Based on the network pharmacological approaches such as databases mining, PPI network construction, GO and KEGG enrichment analysis and molecular docking validation, this study aims to analyze the active ingredients and potential targets of Gusuibu for osteoporosis treatment and to explore possible mechanisms of Qianggu Capsule active ingredients.

Based on the principle of ADME (setting OB  $\geq$  30 and DL  $\geq$  0.18) (Tsaïoun et al., 2016), we searched three herbal databases, including TCMSP, TCMID and BATMAN-TCM platform, and screened 24 active compounds from Gusuibu (131 initially, after removing duplicates and null targets), and finally 331 corresponding target proteins were found. The protein name of the target protein obtained was converted into a gene ID through the UniProt database. Subsequently, we searched 6 disease-related databases (GeneCards, MalaCards, DisGeNET, TTD, CTD, and OMIM) and obtained a total of 1,578 potential therapeutic targets for osteoporosis. After constructing Venn diagrams with potential targets of Gusuibu, we obtained 140 potential target genes of Gusuibu for osteoporosis treatment. “Gusuibu-active compounds-target genes-osteoporosis” network was established, which involved 163 nodes and 432 interactions. The PPI network of potential therapeutic targets had also been constructed, involving 140 nodes and 2,199 edges. Based on the CytoHubba 12 algorithms of Cytoscape software (Degree, Clustering Coefficient, DMNC, Bottle Neck, MCC, MNC, Radiality, EPC, EcCentricity, Closeness, Betweenness, Stress), the top 10 hub genes were obtained, including AKT1, IL6, JUN, TNF, MAPK3,





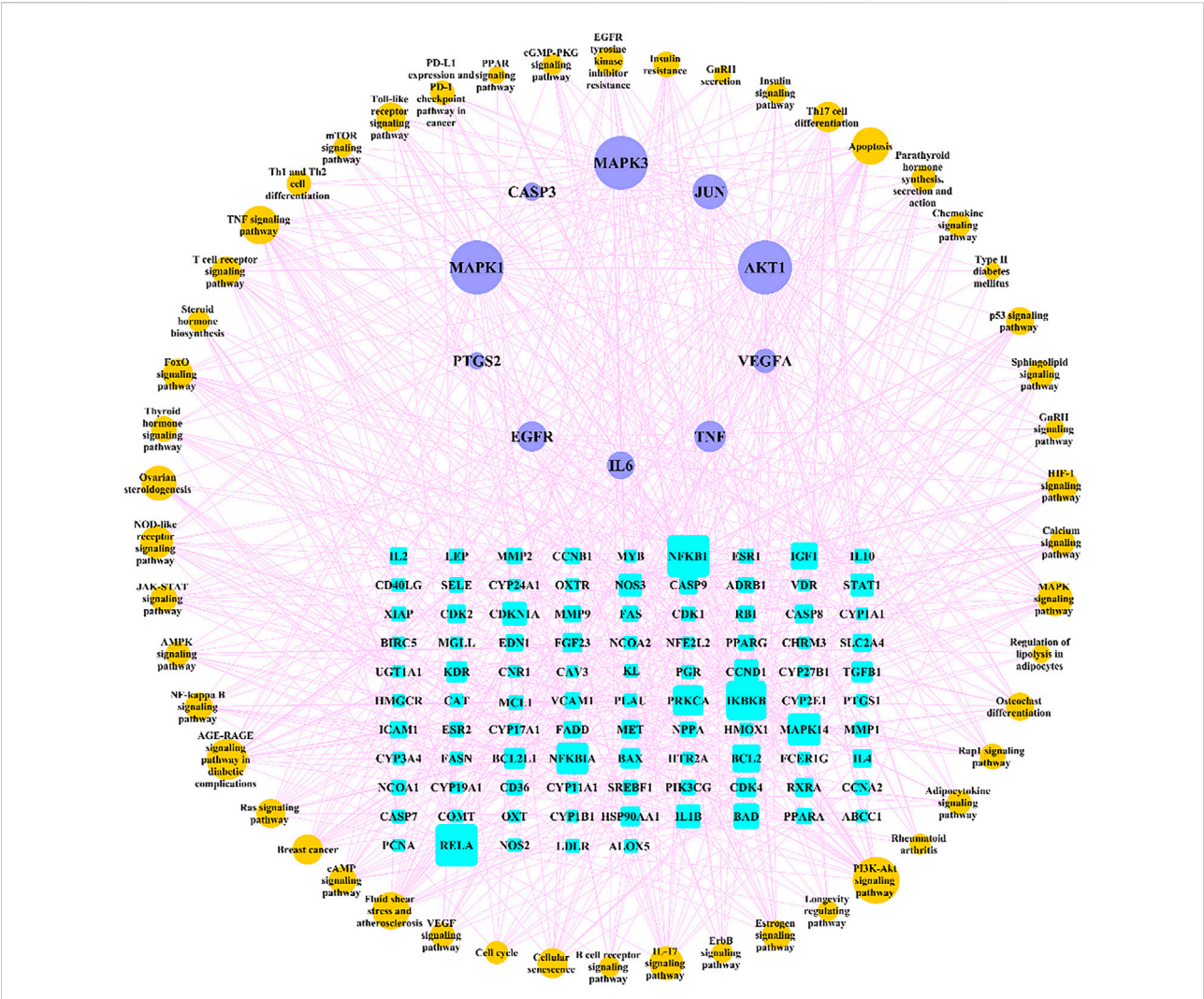


**FIGURE 8** “Target genes-pathways” network. The cyan rectangle represents the potential target genes of Gusuibu against osteoporosis; the light blue ellipse represents the top 10 hub genes; the brown ellipse represents potential osteoporosis-related pathways.

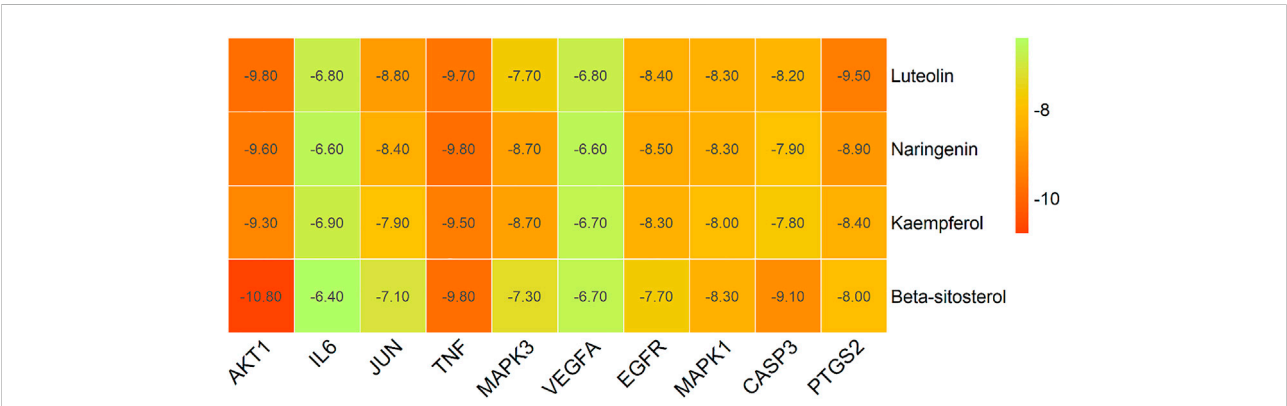


**FIGURE 9** Heatmap of molecular docking scores.



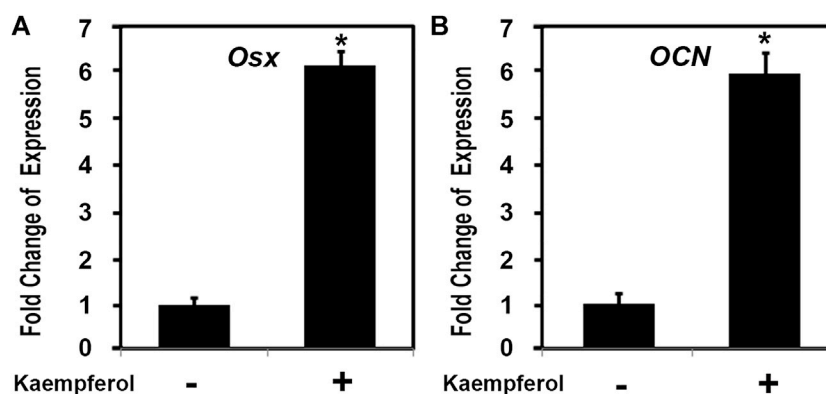


FIGURE 10

Kaempferol induced the expression of osteoblast genes. C2C12 cells were treated with 1,000 ng/ml kaempferol for 24 h. Total RNA was isolated and measured by real time RT-PCR. The RNA level from the control group was normalized to a value of 1. Values were presented as the mean  $\pm$  S.D. \*: A star indicates statistical significance compared to control group with  $p < 0.05$ . (A) Effect of kaempferol on *OSX* expression; (B) Effect of kaempferol on *OCN* expression.

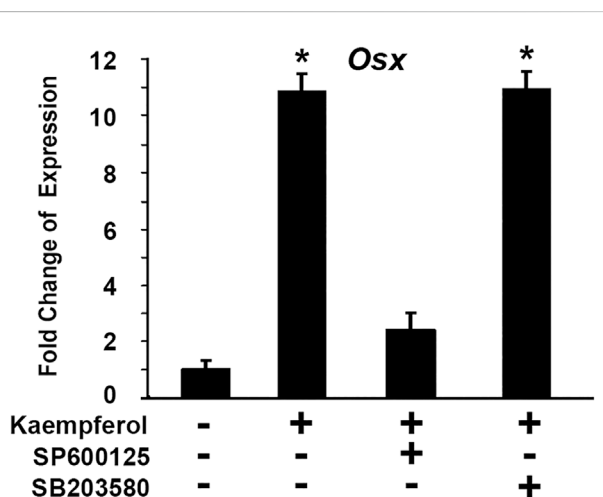


FIGURE 11

Kaempferol-induced *OSX* activation is mediated through JNK kinase pathway. Gene expressions were determined via qRT-PCR with or without kaempferol stimulation. The RNA level from the control group was normalized to a value of 1. \*: A star indicates statistical significance compared to control group with  $p < 0.05$ . Specific inhibitors (50  $\mu$ M SP600125 or 10  $\mu$ M SB203580) were added as indicated.

VEGFA, EGFR, MAPK1, CASP3, PTGS2. The physiological processes regulated by the proteins encoded by these core target genes mainly include inflammatory response, cell proliferation and differentiation, apoptosis, migration, cell cycle progression, angiogenesis, immune response, endocrine metabolism, bone metabolism, reproductive function, growth and nutrition. Therefore, based on these results, it may be speculated that Gusuibu may play a role in resisting osteoporosis through the multiple processes.

Sankey diagram showed the one-to-one correspondence between the top 10 hub genes and the corresponding active compounds contained in Gusuibu [Luteolin, Naringenin, Kaempferol, Beta-sitosterol, (+)-catechin, (R)-naringenin, Aureusidin, Digallate, Eriodictiol (flavanone), Eriodictyol, DavalliosideA\_qt, Dihydrocaffeic acid, Kurarinone, Chitranone, Stigmasterol, Xanthogalenol]. Among them, Luteolin targeted nine hub genes, Naringenin targeted five hub genes, Kaempferol targeted five hub genes, Beta-sitosterol targeted three hub genes, and the others targeted one hub gene each. Luteolin is a flavonoid found in many herbal extracts with antioxidant, anti-inflammatory and anti-tumor activities, and has been shown to reduce glucocorticoid-induced osteoporosis by modulating the ERK/Lrp-5/GSK-3 $\beta$  signaling pathway *in vitro* and *in vivo* (Jing et al., 2019). We summarized the relevant literature exploring the possible mechanisms of Qianggu Capsule and its compounds for osteoporosis treatment (Liu et al., 2001; Wong et al., 2007; Wang et al., 2008; Chen et al., 2009; Hung et al., 2010; Guo et al., 2011; Huang et al., 2011; Ouyang et al., 2012; Li et al., 2017b; Wei et al., 2017; Zhang et al., 2017; Jing et al., 2019; Dong et al., 2020; Ruangsuriya et al., 2020; Shen et al., 2020; Liu et al., 2021) in Table 3.

We further analyzed the potential therapeutic genes of Gusuibu against osteoporosis by GO and KEGG pathway enrichment analysis. We used osteoporosis as a search term in the KEGG database and obtained ten directly related pathways, including osteoclast differentiation (hsa04380), AGE-RAGE signaling pathway in diabetic complications (hsa04933), Endocrine and other factor-regulated calcium reabsorption (hsa04961), Mineral absorption (hsa04978), Wnt pathway (hsa04310), MAPK pathway (hsa04010), Apoptosis (hsa04210), Chemokine pathway (hsa04062), T cell receptor pathway (hsa04660), and B cell receptor pathway (hsa04662).

TABLE 3 Studies related to the regulation of bone metabolism by Qianggu Capsule and its active compounds.

Chinese herbal medicine or compounds	Study	Organism	Possible pharmacological mechanisms	References
Qianggu Capsule (total flavonoids of <i>Rhizoma Drynariae</i> )	Wei et al. (2017)	Human	Improving BMD	Wei et al. (2017)
	Zhang et al. (2017)	Human	Improving BMD	Zhang et al. (2017)
	Li et al. (2017b)	Rat	Enhancing the expression of TGF-β1 and promoting bone metabolism	Li et al. (2017b)
	Ouyang et al. (2012)	Human	Improving BMD	Ouyang et al. (2012)
	Huang et al. (2011)	Rat	Promoting the proliferation and decrease the apoptosis of osteoblasts by improving the ratio of Bcl-2 mRNA to Bax mRNA	Huang et al. (2011)
	Chen et al. (2009)	Rat	Promoting bone metabolism	Chen et al. (2009)
Gusuibu ( <i>Rhizoma Drynariae</i> )	Shen et al. (2020)	Rat	Enhancing angiogenic-osteogenic coupling during distraction osteogenesis by promoting type H vessel formation through PDGF-BB/PDGFR-β instead of HIF-1α/VEGF axis	Shen et al. (2020)
	Hung et al. (2010)	Rat	Promoting osteoblast maturation by regulating bone differentiation-related gene expression	Hung et al. (2010)
	Wang et al. (2008)	Rat	Promoting bone healing	Wang et al. (2008)
	Wong et al. (2007)	Mouse	Promoting bone healing	Wong et al. (2007)
	Liu et al. (2001)	Rat	Promoting bone healing	Liu et al. (2001)
Luteolin	Jing et al. (2019)	Mouse	Luteolin reduced glucocorticoid-induced osteoporosis by modulating the ERK/Lrp-5/GSK-3β signaling pathway	Jing et al. (2019)
Naringin	Dong et al. (2020)	Rabbit	Naringin may be good natural BMP regulator in bone tissue engineering	Dong et al. (2020)
Naringin and Naringenin	Guo et al. (2011)	Mouse	Naringin and Naringenin revealed a double directional adjusting function of estrogenic and anti-estrogenic activities	Guo et al. (2011)
Kaempferol	Liu et al. (2021)	Rat	Kaempferol promotes BMSC osteogenic differentiation and improves osteoporosis by downregulating miR-10a-3p and upregulating CXCL12	Liu et al. (2021)
Beta-sitosterol	Ruangsuriya et al. (2020)	Human	Beta-sitosterol triggered the molecules involved in bone formation and the molecules inhibiting bone resorption	Ruangsuriya et al. (2020)

Abbreviations: BMD, bone mineral density; BMSC, bone marrow mesenchymal stem cell.

Five of the top 10 hub genes (AKT1, TNF, MAPK3, JUN, MAPK1) are enriched in osteoclast differentiation. Eight of the top 10 hub genes (AKT1, IL6, CASP3, TNF, VEGFA, MAPK3, JUN, MAPK1) are enriched in AGE-RAGE pathway in diabetic complications. Eight of the top 10 hub genes (AKT1, CASP3, TNF, VEGFA, MAPK3, JUN, EGFR, MAPK1) are enriched in MAPK pathway. Six of the top 10 hub genes (AKT1, CASP3, TNF, MAPK3, JUN, MAPK1) are enriched in Apoptosis. Three of the top 10 hub genes (AKT1, MAPK3, MAPK1) are enriched in Chemokine pathway. Five of the top 10 hub genes (AKT1, TNF, MAPK3, JUN, MAPK1) are enriched in T cell receptor pathway. Four of the top 10 hub genes (AKT1, MAPK3, JUN, MAPK1) are enriched in B cell receptor pathway. The three pathways are not enriched including Endocrine and other factor-regulated calcium reabsorption, Mineral absorption, and Wnt pathway.

To search for potentially relevant pathways, we obtained 50 enriched pathways as osteoporosis-related pathways and used Cytoscape software to construct the “pathway-gene” network. Studies have shown that there are many pathways associated with osteoporosis, which are mainly related to bone metabolism, inflammatory response, immune response, endocrine

metabolism and apoptosis (Liu et al., 2020). Based on these analyses, Gusuibu may exert anti-osteoporosis effects through many pathways and hub genes.

As an osteoblast-specific transcription factor OSX is required for bone formation and osteoblast differentiation (Nakashima et al., 2002; Zhang et al., 2008). OSX was originally discovered as a BMP2 inducible gene in C2C12 mesenchymal stem cells, and OSX knock-out mice lack bone formation (Nakashima et al., 2002). OCN is a well-known downstream osteoblastic gene of OSX. There are three critical transcription factors required for osteoblast differentiation and bone formation: IHH, RUNX2 and OSX. OSX is the only osteoblast-specific transcription factor identified so far, and it is only expressed in cells in the bone matrix and the inner (endosteum) and outer (periosteum) bone surfaces. OSX discovery as a master regulator of bone formation and osteoblast differentiation opens a new window to bone biology. As far as we know, this is the first study to discover that one active compound kaempferol in Gusuibu activated the expression of osteoblast specific transcription factor OSX through JNK kinase pathway.

In summary, through network pharmacology, we explored the potential mechanisms by which Gusuibu exerts its anti-osteoporosis effects with a multi-component, multi-target, and multi-pathway profile. Potential therapeutic targets for Gusuibu to exert anti-osteoporosis effects include AKT1, IL6, JUN, TNF, MAPK3, VEGFA, EGFR, MAPK1, CASP3, PTGS2. Most of the key active compounds in Gusuibu are flavonoids, mainly including Luteolin, Naringenin, Kaempferol, and Beta-sitosterol. Interestingly, kaempferol was identified as an upregulator of OSX.

## Data availability statement

The original contributions presented in the study are included in the article/Supplementary Material, further inquiries can be directed to the corresponding author.

## Author contributions

CZ designed the study. AH, ZX, KL, YC, and LS performed the experiments. GG and CZ analyzed the data. CZ supervised the study. AH and ZX drafted the text. CZ corrected the manuscript.

## References

- Amberger, J., and Hamosh, A. (2017). Searching online mendelian inheritance in man (OMIM): A knowledgebase of human genes and genetic phenotypes. *Curr. Protoc. Bioinforma.* 581, 1–2. doi:10.1002/cpbi.27
- Chang, J., Liu, L., Wang, Y., Sui, Y., Li, H., and Feng, L. (2020). Investigating the multitarget mechanism of traditional Chinese medicine prescription for cancer-related pain by using network pharmacology and molecular docking approach. *Evid. Based. Complement. Altern. Med.* 2020, 7617261. doi:10.1155/2020/7617261
- Chen, L., Chen, L., Chen, H., Guo, X., Xu, H., Zhang, G., et al. (2009). Skeletal biomechanical effectiveness of retinoic acid on induction of osteoporotic rats treated by alendronate and qianggu capsules. *Zhonghua yi xue za zhi* 89 (27), 1930–1933.
- Chin, C., Chen, S., Wu, H., Ho, C., Ko, M., and Lin, C. (2014). cytoHubba: identifying hub objects and sub-networks from complex interactome. *BMC Syst. Biol.* S11, S11. doi:10.1186/1752-0509-8-S4-S11
- Consortium, T. G. O. (2015). Gene Ontology Consortium: Going forward. *Nucleic Acids Res.* 43, D1049–D1056. doi:10.1093/nar/gku1179
- CSOaBM, Research (2019). Guidelines for the diagnosis and management of primary osteoporosis (2017). *Chin. J. Osteoporos.* 25 (3), 281.
- Davis, A., Grondin, C., Johnson, R., Sciaky, D., Wieggers, J., Wieggers, T., et al. (2020). Comparative Toxicogenomics database (CTD): Update 2021. *Nucleic acids Res.* 49, D1138–D1143. doi:10.1093/nar/gkaa891
- Dong, G., Ma, T., Li, C., Chi, C., Su, C., Huang, C., et al. (2020). A study of *Drynaria fortunei* in modulation of BMP-2 signalling by bone tissue engineering. *Turk. J. Med. Sci.* 50 (5), 1444–1453. doi:10.3906/sag-2001-148
- Ge, J., Xie, L., Chen, J., Li, S., Xu, H., Lai, Y., et al. (2018). Liuwei dihuang Pill treats postmenopausal osteoporosis with shen (kidney) yin deficiency via janus kinase/signal transducer and activator of transcription signal pathway by up-regulating cardiotrophin-like cytokine factor 1 expression. *Chin. J. Integr. Med.* 24 (6), 415–422. doi:10.1007/s11655-016-2744-2
- Guo, D., Wang, J., Wang, X., Luo, H., Zhang, H., Cao, D., et al. (2011). Double directional adjusting estrogenic effect of naringin from *Rhizoma drynariae* (Gusuibu). *J. Ethnopharmacol.* 138 (2), 451–457. doi:10.1016/j.jep.2011.09.034
- Huang, L., Xie, D., Yu, Y., Liu, H., Shi, Y., Shi, T., et al. (2018). Tcmid 2.0: A comprehensive resource for TCM. *Nucleic Acids Res.* 46, D1117–D1120. doi:10.1093/nar/gkx1028
- Huang, Z., Ouyang, G., Xiao, L., Li, N., Gao, H., He, Y., et al. (2011). Effects of *Drynaria* total flavonoids on apoptosis of osteoblasts mediated by tumor necrosis factor- $\alpha$ . *Zhong xi yi jie he xue bao* 9 (2), 173–178. doi:10.3736/jcim20110210
- Hung, T., Chen, T., Liao, M., Ho, W., Liu, D., Chuang, W., et al. (2010). *Drynaria fortunei* J. Sm. promotes osteoblast maturation by inducing differentiation-related gene expression and protecting against oxidative stress-induced apoptotic insults. *J. Ethnopharmacol.* 131 (1), 70–77. doi:10.1016/j.jep.2010.05.063
- Jackson, R., and Mysiw, W. (2014). Insights into the epidemiology of postmenopausal osteoporosis: The women's health initiative. *Semin. Reprod. Med.* 32 (6), 454–462. doi:10.1055/s-0034-1384629
- Jing, Z., Wang, C., Yang, Q., Wei, X., Jin, Y., Meng, Q., et al. (2019). Luteolin attenuates glucocorticoid-induced osteoporosis by regulating ERK/Lrp-5/GSK-3 $\beta$  signaling pathway *in vivo* and *in vitro*. *J. Cell. Physiol.* 234 (4), 4472–4490. doi:10.1002/jcp.27252
- Kanehisa, M., Araki, M., Goto, S., Hattori, M., Hirakawa, M., Itoh, M., et al. (2008). KEGG for linking genomes to life and the environment. *Nucleic Acids Res.* 36, D480–D484. doi:10.1093/nar/gkm882
- Kanis, J. A. (2002). Diagnosis of osteoporosis and assessment of fracture risk. *Lancet (London, Engl.)* 359–1936. doi:10.1016/S0140-6736(02)08761-5
- Li, G., Xu, Q., Han, K., Yan, W., and Huang, C. (2020). Experimental evidence and network pharmacology-based analysis reveal the molecular mechanism of Tongxinluo capsule administered in coronary heart diseases. *Biosci. Rep.* 40 (10), BSR20201349. doi:10.1042/BSR20201349
- Li, J., Jia, Y., Chai, L., Mu, X., Ma, S., Xu, L., et al. (2017). Effects of Chinese herbal formula *erxian* decoction for treating osteoporosis: A systematic review. *Clin. Interv. Aging* 12, 45–53. doi:10.2147/CIA.S117597
- Li, J., Wang, W., Feng, G., Du, J., Kang, S., Li, Z., et al. (2020). Efficacy and safety of *duhuo jisheng* decoction for postmenopausal osteoporosis: A systematic review and meta-analysis. *Evid. Based. Complement. Altern. Med.* 2020, 6957825. doi:10.1155/2020/6957825
- Li, M., Wang, Y., Liao, N., Li, J., and Dong, Q. (2017). Changes of TGF- $\beta$ 1 expression during orthodontic tooth movement in rats with osteoporosis. *Shanghai kou qiang yi xue* 26 (1), 17–20.

## Funding

This work was supported by the Beijing Municipal Science and Technology Commission (Grant Number: Z181100001818006).

## Conflict of interest

The authors declare that the research was conducted in the absence of any commercial or financial relationships that could be construed as a potential conflict of interest.

## Publisher's note

All claims expressed in this article are solely those of the authors and do not necessarily represent those of their affiliated organizations, or those of the publisher, the editors and the reviewers. Any product that may be evaluated in this article, or claim that may be made by its manufacturer, is not guaranteed or endorsed by the publisher.

- Liu, H., Chen, R., Jian, W., and Lin, Y. (2001). Cytotoxic and antioxidant effects of the water extract of the traditional Chinese herb gusuibu (*Drynaria fortunei*) on rat osteoblasts. *J. Formos. Med. Assoc. = Taiwan yi zhi* 100 (6), 383–388.
- Liu, H., Yi, X., Tu, S., Cheng, C., and Luo, J. (2021). Kaempferol promotes BMSC osteogenic differentiation and improves osteoporosis by downregulating miR-10a-3p and upregulating CXCL12. *Mol. Cell. Endocrinol.* 520, 111074. doi:10.1016/j.mce.2020.111074
- Liu, W., Jiang, Z., Chen, Y., Xiao, P., Wang, Z., Huang, T., et al. (2020). Network pharmacology approach to elucidate possible action mechanisms of *Sinomenium Caulis* for treating osteoporosis. *J. Ethnopharmacol.* 257, 112871. doi:10.1016/j.jep.2020.112871
- Liu, Z., Guo, F., Wang, Y., Li, C., Zhang, X., Li, H., et al. (2016). BATMAN-TCM: A bioinformatics analysis tool for molecular mechanism of traditional Chinese medicine. *Sci. Rep.* 6, 21146. doi:10.1038/srep21146
- Nakashima, K., Zhou, X., Kunkel, G., Zhang, Z., Deng, J. M., Behringer, R. R., et al. (2002). The novel zinc finger-containing transcription factor osterix is required for osteoblast differentiation and bone formation. *Cell* 108, 17–29. doi:10.1016/s0092-8674(01)00622-5
- Ouyang, G., Feng, X., Xiao, L., Huang, Z., Xia, Q., and Zhu, F. (2012). Effects of Chinese herbal medicine qianggu capsule on patients with rheumatoid arthritis-induced osteoporosis: A report of 82 cases. *Zhong Xi Yi Jie He Xue Bao* 10 (12), 1394–1399. doi:10.3736/jcim20121210
- Piñero, J., Ramírez-Anguita, J., Saüch-Pitarch, J., Ronzano, F., Centeno, E., Sanz, F., et al. (2020). The DisGeNET knowledge platform for disease genomics: 2019 update. *Nucleic Acids Res.* 48, D845–D855. doi:10.1093/nar/gkz1021
- Rappaport, N., Twik, M., Plaschkes, I., Nudel, R., Iny Stein, T., Levitt, J., et al. (2017). MalaCards: An amalgamated human disease compendium with diverse clinical and genetic annotation and structured search. *Nucleic Acids Res.* 45, D877–D887. doi:10.1093/nar/gkw1012
- Ru, J., Li, P., Wang, J., Zhou, W., Li, B., Huang, C., et al. (2014). Tcmsp: A database of systems pharmacology for drug discovery from herbal medicines. *J. Cheminform.* 6 (13). doi:10.1186/1758-2946-6-13
- Ruangsurinya, J., Charumane, S., Jiranusornkul, S., Sirisa-Ard, P., Sirithunyalug, B., Sirithunyalug, J., et al. (2020). Depletion of  $\beta$ -sitosterol and enrichment of quercetin and rutin in *Cissus quadrangularis* Linn fraction enhanced osteogenic but reduced osteoclastogenic marker expression. *BMC Complement. Med. Ther.* 20 (1), 105. doi:10.1186/s12906-020-02892-w
- Saul, D., and Kosinsky, R. (2021). Epigenetics of aging and aging-associated diseases. *Int. J. Mol. Sci.* 22 (1), E401. doi:10.3390/ijms22010401
- Shannon, P., Markiel, A., Ozier, O., Baliga, N., Wang, J., Ramage, D., et al. (2003). Cytoscape: A software environment for integrated models of biomolecular interaction networks. *Genome Res.* 13 (11), 2498–2504. doi:10.1101/gr.1239303
- Shen, Z., Chen, Z., Li, Z., Zhang, Y., Jiang, T., Lin, H., et al. (2020). Total flavonoids of rhizoma *drynariae* enhances angiogenic-osteogenic coupling during distraction osteogenesis by promoting type H vessel formation through PDGF-BB/PDGF- $\beta$  instead of HIF-1 $\alpha$ /VEGF Axis. *Front. Pharmacol.* 11, 503524. doi:10.3389/fphar.2020.503524
- Sheng, S., Yang, Z., Xu, F., and Huang, Y. (2020). Network pharmacology-based exploration of synergistic mechanism of guanxin II formula (II) for coronary heart disease. *Chin. J. Integr. Med.* 27, 106–114. doi:10.1007/s11655-020-3199-z
- Shuai, Y., Jiang, Z., Yuan, Q., Tu, S., and Zeng, F. (2020). Deciphering the underlying mechanism of eucommia cortex against osteoporotic fracture by network pharmacology. *Evid. Based. Complement. Altern. Med.* 2020, 7049812. doi:10.1155/2020/7049812
- Stelzer, G., Rosen, N., Plaschkes, I., Zimmerman, S., Twik, M., Fishilevich, S., et al. (2016). The GeneCards suite: From gene data mining to disease genome sequence analyses. *Curr. Protoc. Bioinforma.* 541, 1–30. doi:10.1002/cpbi.5
- Szklarczyk, D., Morris, J., Cook, H., Kuhn, M., Wyder, S., Simonovic, M., et al. (2017). The STRING database in 2017: Quality-controlled protein-protein association networks, made broadly accessible. *Nucleic Acids Res.* 45, D362–D368. doi:10.1093/nar/gkw937
- Tang, W., Yang, F., Li, Y., de Crombrughe, B., Jiao, H., Xiao, G., et al. (2012). Transcriptional regulation of vascular endothelial growth factor (VEGF) by osteoblast-specific transcription factor osterix (osx) in osteoblasts. *J. Biol. Chem.* 287, 1671–1678. doi:10.1074/jbc.M111.288472
- Trott, O., and Olson, A. (2010). AutoDock Vina: Improving the speed and accuracy of docking with a new scoring function, efficient optimization, and multithreading. *J. Comput. Chem.* 31 (2), 455–461. doi:10.1002/jcc.21334
- Tsaioun, K., Blaauboer, B., and Hartung, T. (2016). Evidence-based absorption, distribution, metabolism, excretion (ADME) and its interplay with alternative toxicity methods. *ALTEX* 33 (4), 343–358. doi:10.14573/altex.1610101
- UniProt Consortium, T. (2018). UniProt: The universal protein knowledgebase. *Nucleic Acids Res.* 46 (5), 2699. doi:10.1093/nar/gky092
- Wang, X., Wang, N., Zhang, Y., Gao, H., Pang, W., Wong, M., et al. (2008). Effects of eleven flavonoids from the osteoprotective fraction of *Drynaria fortunei* (KUNZE) J. SM. on osteoblastic proliferation using an osteoblast-like cell line. *Chem. Pharm. Bull.* 56 (1), 46–51. doi:10.1248/cpb.56.46
- Wang, Y., Zhang, S., Li, F., Zhou, Y., Zhang, Y., Wang, Z., et al. (2020). Therapeutic target database 2020: Enriched resource for facilitating research and early development of targeted therapeutics. *Nucleic Acids Res.* 48, D1031–D1041. doi:10.1093/nar/gkz981
- Wei, X., Xu, A., Shen, H., and Xie, Y. (2017). Qianggu capsule for the treatment of primary osteoporosis: Evidence from a Chinese patent medicine. *BMC Complement. Altern. Med.* 17 (1), 108. doi:10.1186/s12906-017-1617-3
- Wong, R., Rabie, B., Bendeus, M., and Hägg, U. (2007). The effects of rhizoma curculiginis and rhizoma *drynariae* extracts on bones. *Chin. Med.* 2, 13. doi:10.1186/1749-8546-2-13
- Wu, Z., Zhu, X., Xu, C., Chen, Y., Zhang, L., and Zhang, C. (2017). Effect of Xianling Gubao capsules on bone mineral density in osteoporosis patients. *J. Biol. Regul. Homeost. Agents* 31 (2), 359–363.
- Xiao, W., Sun, W., Lian, H., and Shen, J. (2020). Integrated network and experimental pharmacology for deciphering the medicinal substances and multiple mechanisms of duhuo jisheng decoction in osteoarthritis therapy. *Evid. Based. Complement. Altern. Med.* 2020, 7275057. doi:10.1155/2020/7275057
- Xiong, Z., Zheng, C., Chang, Y., Liu, K., Shu, L., and Zhang, C. (2021). Exploring the pharmacological mechanism of duhuo jisheng decoction in treating osteoporosis based on network pharmacology. *Evidence-based complementary Altern. Med.* 5510290, 2021–21. doi:10.1155/2021/5510290
- Xu, C., Li, R., and Wu, J. (2020). Effects of Yuanhu- Zhitong tablets on alcohol-induced conditioned place preference in mice. *Biomed. Pharmacother. = Biomedecine Pharmacother.* 133, 110962. doi:10.1016/j.biopha.2020.110962
- Yu, G., Wang, L., Han, Y., and He, Q. (2012). clusterProfiler: an R package for comparing biological themes among gene clusters. *Omic a J. Integr. Biol.* 16 (5), 284–287. doi:10.1089/omi.2011.0118
- Zhang, C., Cho, K., Huang, Y., Lyons, J. P., Zhou, X., Sinha, K., et al. (2008). Inhibition of Wnt signaling by the osteoblast-specific transcription factor Osterix. *Proc. Natl. Acad. Sci. U. S. A.* 105, 6936–6941. doi:10.1073/pnas.0710831105
- Zhang, Y., Jiang, J., Shen, H., Chai, Y., Wei, X., and Xie, Y. (2017). Total flavonoids from rhizoma *drynariae* (gusuibu) for treating osteoporotic fractures: Implication in clinical practice. *Drug Des. devel. Ther.* 11–1890. doi:10.2147/DDDT.S139804
- Zheng, H., Feng, H., Zhang, W., Han, Y., and Zhao, W. (2020). Targeting autophagy by natural product Ursolic acid for prevention and treatment of osteoporosis. *Toxicol. Appl. Pharmacol.* 115271, 115271. doi:10.1016/j.taap.2020.115271



## OPEN ACCESS

## EDITED BY

Alex Zhong,  
Van Andel Institute, United States

## REVIEWED BY

Fan He,  
Soochow University, China  
Jiao Zhai,  
City University of Hong Kong, Hong  
Kong, SAR China

## \*CORRESPONDENCE

Yujie Wu,  
yujwu0414@163.com  
Jie Zhao,  
Profzhaojie@126.com

<sup>†</sup>These authors have contributed equally  
to this work

## SPECIALTY SECTION

This article was submitted to  
Experimental Pharmacology and Drug  
Discovery,  
a section of the journal  
Frontiers in Pharmacology

RECEIVED 09 May 2022

ACCEPTED 09 September 2022

PUBLISHED 29 September 2022

## CITATION

Wang H, Cao X, Guo J, Yang X, Sun X,  
Fu Z, Qin A, Wu Y and Zhao J (2022),  
BNTA alleviates inflammatory osteolysis  
by the SOD mediated anti-oxidation and  
anti-inflammation effect on  
inhibiting osteoclastogenesis.  
*Front. Pharmacol.* 13:939929.  
doi: 10.3389/fphar.2022.939929

## COPYRIGHT

© 2022 Wang, Cao, Guo, Yang, Sun, Fu,  
Qin, Wu and Zhao. This is an open-  
access article distributed under the  
terms of the [Creative Commons  
Attribution License \(CC BY\)](#). The use,  
distribution or reproduction in other  
forums is permitted, provided the  
original author(s) and the copyright  
owner(s) are credited and that the  
original publication in this journal is  
cited, in accordance with accepted  
academic practice. No use, distribution  
or reproduction is permitted which does  
not comply with these terms.

# BNTA alleviates inflammatory osteolysis by the SOD mediated anti-oxidation and anti-inflammation effect on inhibiting osteoclastogenesis

Huidong Wang<sup>†</sup>, Xiankun Cao<sup>†</sup>, Jiadong Guo, Xiao Yang,  
Xiaojiang Sun, Zhiyi Fu, An Qin, Yujie Wu\* and Jie Zhao\*

Shanghai Key Laboratory of Orthopedic Implants, Department of Orthopaedics Surgery, Shanghai  
Ninth People's Hospital, Shanghai Jiao Tong University School of Medicine, Shanghai, China

Abnormal activation and overproliferation of osteoclast in inflammatory bone diseases lead to osteolysis and bone mass loss. Although current pharmacological treatments have made extensive advances, limitations still exist. N-[2-bromo-4-(phenylsulfonyl)-3-thienyl]-2-chlorobenzamide (BNTA) is an artificially synthesized molecule compound that has antioxidant and anti-inflammatory properties. In this study, we presented that BNTA can suppress intracellular ROS levels through increasing ROS scavenging enzymes SOD1 and SOD2, subsequently attenuating the MARK signaling pathway and the transcription of NFATc1, leading to the inhibition of osteoclast formation and osteolytic resorption. Moreover, the results also showed an obvious restrained effect of BNTA on RANKL-stimulated proinflammatory cytokines, which indirectly mediated osteoclastogenesis. In line with the *in vitro* results, BNTA protected LPS-induced severe bone loss *in vivo* by enhancing scavenging enzymes, reducing proinflammatory cytokines, and decreasing osteoclast formation. Taken together, all of the results demonstrate that BNTA effectively represses oxidation, regulates inflammatory activity, and inhibits osteolytic bone resorption, and it may be a potential and exploitable drug to prevent inflammatory osteolytic bone diseases.

## KEYWORDS

BNTA, MAPK, SOD, osteolysis, inflammatory osteolysis, bone loss

## Introduction

The homeostasis of bone metabolism is finely regulated and maintained based on the balance of osteogenesis by osteoblasts and osteolysis by osteoclasts. Inflammatory bone diseases, usually caused by some infectious bone diseases, such as purulent spondylitis, purulent osteomyelitis, and periprosthetic infection, induce abnormal activation and overproliferation of osteoclasts and eventually lead to osteolysis and bone mass loss (Kim



et al., 2013). Current studies have found that the release of endogenous products of bacteria can activate immune cells, cause excessive proliferation of osteoclasts and enhance bone resorption (Mbalaviele et al., 2017; Yang et al., 2021). Over the past few decades, there have been some advances in the treatment of inflammatory osteolytic bone diseases, but some limitations remain. Estrogen is mainly used to treat osteoporosis in postmenopausal women, but it carries a risk of breast cancer (Clemons and Goss, 2001; Lobo, 2017); bisphosphonates are used to inhibit osteoclastic bone resorption, but they are increasingly reported to be associated with the occurrence of aseptic necrosis of the mandible and local fractures (Woo et al., 2006; Shane et al., 2014); parathyroid hormone increases bone formation by promoting osteoblast activity, but it cannot be taken orally and cannot be used for a long time because it risks causing bone tumors (Nikitovic et al., 2016; Al-Khan et al., 2021). Therefore, there is still a great need to develop more effective and safe anti-osteolytic drugs.

Osteoclasts, acting with a vital role in osteolytic bone diseases, are large multinucleated phagocytes that originate from mononuclear-macrophage lines. The differentiation and maturity from bone marrow monocyte/macrophage to osteoclasts are dependent on the receptor activator of nuclear factor kappa B ligand (RANKL), a direct regulatory factor that controls the dynamic differentiation processes of osteoclasts (Lagasse and Weissman, 1997; Theill et al., 2002). The macrophage colony-stimulating factor (M-CSF), a cytokine for the proliferation and survival of osteoclast precursor cells, also plays an essential role in osteoclastogenesis (Wiktor-Jedrzejczak et al., 1990; Lagasse and Weissman, 1997). The binding of RANKL with its receptor the receptor activator of nuclear factor kappa B (RANK) initiates the recruitment of TNF receptor-associated factor 6 (TRAF6), which then activates multiple downstream signaling including mitogen-activated protein kinases (MAPKs) and NF- $\kappa$ B pathways, leading to the activation of c-fos and nuclear factor of activated T cells 1 (NFATc1). These signaling cascades enable the expression of osteoclast-related genes which administrate osteoclast fusion, cytoskeletal reorganization, and resorptive function (Chen X. et al., 2019). Among the cytokines regulating osteoclast activation and formation, RANKL is the most important one (Lee et al., 2019). Thus, interrupting the interaction between RANK and RANKL is an efficient and feasible strategy for suppressing osteoclast differentiation and maturation (Xu et al., 2021).

Reactive oxygen species (ROS), including hydroxyl radicals or superoxide anions, play a very important role in regulating the differentiation of osteoclasts. Previous research has suggested that the target molecule ROS stimulated and facilitated osteoclast differentiation and osteolytic resorption through activating the downstream MAPKs pathway and subsequently switching on the crucial NFATc1 signals (Lee et al., 2005; Zhan et al., 2019; Zhang et al., 2019). Under normal physiological conditions, ROS in osteoclasts activate osteoclastogenesis and facilitate bone

resorption (Agidigbi and Kim, 2019). However, excessive ROS in osteoclasts, not only causes direct or indirect oxidative damage, impairing DNA and proteins but also leads to osteolysis and bone destruction (Wells et al., 2009; Kanzaki et al., 2017). The ROS physiological homeostasis depends on the balance between ROS generation and removal rate by scavenging (Maciag et al., 2013; He et al., 2021). The SODs are the first and most important antioxidant enzyme defense system, which are against ROS, especially superoxide anion radicals (Zelko et al., 2002). There have three distinct isoforms of SODs been identified in mammals at present, including SOD1 (CuZn-SOD, located in the cytoplasm), SOD2 (Mn-SOD, located in the mitochondrial), and SOD3 (EC-SOD, located in the extracellular spaces) (Zelko et al., 2002). SOD3 is the most recently discovered member of the SOD family, which exhibited high expression in selected tissues, particularly in blood vessels, lungs, kidneys, and heart (Fattman et al., 2003; Nozik-Grayck et al., 2005). It can regulate proinflammatory factor expression and affect the inflammatory response, but there is almost no report on the effect of SOD3 on osteoclastogenesis (Kemp et al., 2010; Hu et al., 2019). Unlike SOD3, SOD1 and SOD2 express practically in all cells (Wang et al., 2018). Several researches have focused on the possible role of SODs on osteolytic disease. The deficiency of SOD1 or SOD2 lead to increased osteoclastogenesis *in vitro* and decreased bone volume *in vivo*, while the upregulation of SOD1 or SOD2 reduced osteoclastogenesis by reducing ROS level (Lee et al., 2014; Kobayashi et al., 2015; Lee and Jang, 2015; Kim et al., 2017; He et al., 2021).

BNTA is a small artificial synthesized molecule compound. It was firstly reported that BNTA not only effectively activates the SOD3-mediated dismutation reaction of superoxide anions but also obviously inhibited the expression of inflammatory factors in osteoarthritis (OA) (Shi et al., 2019). Given its significant bioactivation and the pivotal role of inflammation and oxidation on osteolytic bone diseases, we hypothesized that BNTA may affect the osteoclastic formation and osteolytic resorption, similar to the effect on chondrocyte and OA, by regulating the SOD (SOD1 and SOD2)-ROS-MAPK signaling pathways axis and SOD-ROS-inflammation axis. In this study, we evaluated the therapeutic effects of BNTA on RANKL-induced osteoclastogenesis *in vitro* and lipopolysaccharides (LPS)-induced inflammatory osteolysis in mice calvaria *in vivo*, focusing on clarifying the antioxidant capacity of BNTA and elaborating its underlying mechanisms.

## Materials and methods

### Chemicals and reagents

The synthetic small molecule compound BNTA (CAS: 685119-25-9), purchased from National Compound Resource

Center (Shanghai, China) and Maybridge (Cornwall, Cornwall, United Kingdom), was dissolved by Dimethyl sulfoxide (DMSO) and stored at  $-20^{\circ}\text{C}$ . It was diluted in a cell culture medium so that the final concentrations of DMSO were less than 0.1%.

## Bone marrow macrophage preparation and *in vitro* osteoclast differentiation

Primary bone marrow-derived monocytes/macrophages (BMMs) were isolated from the femoral and tibial bone marrow of 4-weeks-old C57BL/6J mice. Isolated cells were then cultured in  $\alpha$ -minimum essential medium ( $\alpha$ -MEM) supplemented with 10% fetal bovine serum (FBS), 1% penicillin/streptomycin (Gibco, Thermo Fisher Scientific, Waltham, MA, United States), and 30 ng/ml M-CSF (R&D, Systems MN, United States) in an incubator with 5%  $\text{CO}_2$  and 95% air at  $37^{\circ}\text{C}$  until cells reached 90% confluence. BMMs were seeded into a 96-wells plate at a density of 8,000 cells/well, and cultured in a complete  $\alpha$ -MEM medium with 30 ng/ml M-CSF, 50 ng/ml RANKL (R&D, Systems MN, United States), and different concentrations of BNTA (10, 20, and 40  $\mu\text{M}$ ). Untreated BMM cells were also included as positive controls and each concentration had three replications. The culture medium was replaced every 2 days. Mature, large, multinucleated osteoclasts were formed after incubation for a total of 5–7 days. Cells were gently washed twice, fixed with 4% paraformaldehyde (PFA) for 15 min, and then stained for tartrate-resistant acid phosphatase (TRAP). The number and size of TRAP-positive multinucleated osteoclasts with at least three nuclei were scored.

## Cytotoxicity assay

The cytotoxic and proliferated effect of BNTA on BMMs was assessed using the Cell Counting Kit-8 (CCK-8) assay (Dojindo, Kumamoto, Japan). To determine toxicity, BMMs were seeded into a 96-well plate at a density of  $8 \times 10^3$  cells/well and cultured with different concentrations of BNTA (0, 1, 10, 20, 40, 80, and 160  $\mu\text{M}$ ) for 24 h. To determine proliferation, BMMs at a density of  $3 \times 10^3$  cells/well were cultured with BNTA for 24, 48, 72, and 96 h. After being seeded into a 96-well plate for 24 h to allow them to adhere, BMMs were then treated with different concentrations of BNTA (0, 1, 10, 20, and 40  $\mu\text{M}$ ). The cultural medium was changed every second day. At the end of the experimental period, 10  $\mu\text{L}$  CCK-8 buffer was added to each well, and the plate was incubated for an additional 2 h. The absorbances were read at a wavelength of 450 nm by a spectrophotometer on an Infinite M200 Pro multimode microplate reader (Tecan Life Sciences, Männedorf, Switzerland).

## *In vitro* osteoclast bone absorption assay

Bone resorption effects of osteoclasts were measured with a hydroxyapatite-coated plate (Corning Inc. NY, United States). BMMs were seeded onto hydroxyapatite-coated plates in triplicates with a concentration of  $5 \times 10^3$ /well. Cells were cultured for 24 h to allow adherence and then induced to osteoclasts with 50 ng/ml RANKL, with or without different concentrations of BNTA (10, 20, and 40  $\mu\text{M}$ ). Culture medium was replaced every 2 days. After 7 days, the cells were brushed off the plates, and resorption pits were pictured with a light microscope (OLYMPUS, IX71). The area of resorption pits was measured using ImageJ software.

## RNA extraction and quantitative real-time PCR

Quantitative real-time PCR was used to measure the gene expression levels during osteoclast formation. Mouse BMMs were cultured in six-well plates at a concentration of  $5 \times 10^3$ /well with complete  $\alpha$ -MEM including 30 ng/ml M-CSF and 50 ng/ml RANKL. During the RANKL-induced osteoclastogenesis, BMMs were treated with different concentrations of BNTA (10, 20, and 40  $\mu\text{M}$ ). Untreated samples were used as controls. The total RNA of each sample was extracted using a TRIzol reagent (Thermo Fisher Scientific, Waltham, MA, United States) after BNTA treatment for 5 days. Complementary DNA (cDNA) was synthesized with 1  $\mu\text{g}$  of RNA extracted from each sample, 4  $\mu\text{L}$  of  $5 \times$  PrimeScript RT Master Mix (TaKaRa Bio, Otsu, Japan) and RNase-free distilled water ( $\text{dH}_2\text{O}$ ) in a total volume of 20  $\mu\text{L}$ . The real-time qPCR was performed using the TB Green Premix Ex Taq kit (TaKaRa Bio, Otsu, Japan) on an SYBR Green-Based Real-Time Quantitative Reverse Transcription PCR System (Thermo Fisher Scientific, Waltham, MA, United States). Primers were shown in Table 1. Target gene expression levels were determined using the  $2^{-\Delta\Delta\text{CT}}$  method and normalized to the expression of GAPDH.

## Western blot analysis

To assess the effect of BNTA on the signaling pathway, BMMs were seeded into six-well plates. They were starved with serum-free  $\alpha$ -MEM medium with or without 40  $\mu\text{M}$  BNTA for 2 h. After that, cells of each group were stimulated with 50 ng/ml RANKL for 10 min. To determine the influence of BNTA on c-fos and NFATc1 expression, BMMs were cultured in a complete  $\alpha$ -MEM medium including 30 ng/ml M-CSF and 50 ng/ml RANKL, with or without 40  $\mu\text{M}$  BNTA for 1, 3, or 5 days, or with different

TABLE 1 Gene primer sequences used in qPCR.

Target genes	Accession number	Primer sequences 5'→3'
CTSK	NM_007802.4	F: TAGCCACGCTTCCTATCCGA R: CCTCCGGAGACAGAGCAAAG
NFATc1	NM_001164112.1	F: CTTTCGAGTTTCGATCAGAGCGG R: AGGGTCGAGGTGACACTAGG
ACP5	NM_001102405.1	F: CACTCCCACCTGAGATTTGT R: CATCGTCTGCACGGTCTG
D2	NM_175406.3	F: GCAGAGCTGTACTTCAATGTGG R: TAGTCCGTGGTCTGGAGATG
c-Fos	NM_010234.3	F: TGTTCCTGGCAATAGCGTGT R: TCAGACCACCTCGACAATGC
MMP9	NM_013599.5	F: CCCTGGAACCTCACACGACAT R: TGGTTCACCTCATGGTCCAC
SOD1	NM_011434.2	F: TCTCGTCTGTCTCTCTCTGG R: CTTGCCTTCTGCTCGAAGTG
SOD2	NM_013671.3	F: CTGTCCGATGATGTACGCCA R: AACCCATTGCGCTACTGA
SOD3	NM_011435.3	F: GAGAAGATAGGCGACACGCA R: GAGAACCAAGCCGTGATCT
TNF- $\alpha$	NM_001278601.1	F: GCCTCTTCTCATTCTGCTTGTGG R: TGGTTTGTGAGTGTGAGGGTCTG
IL-1 $\beta$	NM_008361.4	F: TCGCAGCAGCACATCAACAAGAG R: AGGTCCACGGGAAAGACACAGG
IL-6	NM_001314054.1	F: CTGGTCTTCTGGAGTACCATAGC R: GTGACTCCAGCTTATCTCTTGGT
IL-4	NM_021283.2	F: ATGGATGTGCCAAACGTCCT R: AAGCCCGAAAGAGTCTCTGC
GAPDH	NM_008084.3	F: ACCCAGAAGACTGTGGATGG R: CACATTGGGGGTAGGAACAC

concentrations of BNTA (0, 10, 20, 40  $\mu$ M) for 5 days. Total protein was extracted from cultured cells using the radioimmunoprecipitation assay (RIPA) lysis buffer with phosphatase and protease inhibitor cocktail (Roche, Basel, Switzerland). The proteins were separated using 4%–20% SDS-polyacrylamide gel electrophoresis (PAGE) gel (GenScript Laboratories, Piscataway, NJ, United States) electrophoresis, and were then transferred onto a polyvinylidene fluoride (PVDF) membrane (Merck Millipore, CA, United States). The membranes were blocked with 5% skim milk-TBST at RT for 1 h. After being washed 3 times for 15 min, the membranes were incubated overnight at 4°C with primary antibodies (Cell Signal Technology, Danvers, MA, United States) against the following proteins: p38 MAPK (D13E1), phospho-p38 MAPK (Thr180/Tyr182; D3F9), p44/42 MAPK (ERK1/2; 137F5), phospho-p44/42 MAPK (ERK1/2; Thr202/Tyr204; D13.14.4E), SAPK/c-Jun N-terminal kinase (JNK;), phospho-SAPK/JNK (Thr183/Tyr185; 81E11), NFAT2

(D15F1); c-Fos (9F6);  $\beta$ -actin (D6A8). The membranes were washed by TBST 3 times and then incubated with anti-rabbit or anti-mouse IgG secondary antibody (H + L; DyLight™800 4×PEG conjugate; Cell Signaling Technology, Danvers, MA, United States) for 1 h in dark. Finally, the membranes were washed another 3 times for 15 min, and the protein bands were visualized by the LI-COR Odyssey fluorescence imaging system (LI-COR Biosciences, Lincoln, NE, United States). The gray value of each protein band was quantified by ImageJ software.

## Intracellular ROS generation assay

The intracellular production of ROS was quantified using DCFDA cellular ROS Assay Kit (Beyotime, Shanghai, China) following the manufacturer's instruction and as described previously (Lee et al., 2005). BMs were cultured in 96-well plates at a concentration of  $8 \times 10^3$ /well with complete

$\alpha$ -MEM supplementing with 30 ng/ml M-CSF, 50 ng/ml RANKL, and different concentrations of BNTA (0, 10, 20, 40  $\mu$ M) for 72 h. Cells were then washed and incubated in DCFH-DA solution (5 mM) diluted with Hank's buffer for 1 h. Subsequently, the digital images of each well were taken by fluorescence microscopy (Nikon Eclipse C1, NIKON, Japan). The number of ROS-positive cells per well was analyzed with ImageJ software.

## LPS-induced calvarial osteolysis model

The animal experiments were consented to by the Animal Care and Experiment Committee of Shanghai Jiao Tong University of Medicine. Procedures of all experiments were performed in strict accordance with the guidelines for Ethical Conduct in the Care and Use of Nonhuman Animals in Research by the American Psychological Association. Twenty-four 7-weeks-old C57BL/6J male mice were randomized into four groups: 1) sham-operated control group (PBS-treated); 2) LPS control group (LPS 5 mg/kg); 3) low dose BNTA group (LPS 5 mg/kg and BNTA 0.15 mg/kg); 4) high dose BNTA group (LPS 5 mg/kg and BNTA 1.5 mg/kg). Gelatin sponges (4 mm  $\times$  4 mm  $\times$  2 mm) soaked with PBS or LPS were implanted on the midline suture of the skull surfaces to induce osteolysis. Next, PBS or LPS was injected into the gelatin sponges on the surfaces of the skulls, and BNTA was administered by abdominal injections every second day for 10 days. When arrived the deadline, all groups of mice were euthanized and then their calvarial bones were separated.

## $\mu$ CT scanning

A high-resolution Micro-CT instrument (Skyscan; Burker, Kontich, Belgium; resolution 10  $\mu$ m; X-ray source 46 kv/75  $\mu$ A; exposure time 80 ms applied; conducted in 75% ethanol) was used for calvarias scanning. A square around the osteolytic area was defined as an interesting region for bone volume analysis. Trabecular morphometry was analyzed by measuring the bone volume fraction (BV/TV), trabecular thickness (Tb.Th), trabecular number (Tb.N), and trabecular spacing (Tb.Sp).

## Histomorphometry and immunofluorescence assay

The calvarial bones were then fixed with 4% polyformaldehyde and decalcified with 10% EDTA, buried in paraffin, and cut into 4 mm thick slices. Slices were used to make HE and TRAP staining. After taking pictures with Axio ScopeA1 light microscope (ZEISS, Germany), quantitative analysis was performed using ImageJ

software. Furthermore, we detected redox-related and inflammation-related proteins using immunofluorescence assays. The tissue slices were incubated with primary antibodies overnight against the proteins as follows: SOD1 (10269-1-AP, Proteintech, United States), SOD2 (24127-1-AP, Proteintech, United States), SOD3 (DF7753, Affinity, United States), TNF- $\alpha$  (ab183218, Abcam, United Kingdom), IL-1 $\beta$  (ab216995, Abcam, United Kingdom), IL-4 (AF5142, Affinity, United States), and IL-6 (66146-1-Ig, Proteintech, United States). After being washed with PBS, slices were incubated with FITC-conjugated secondary antibodies (Proteintech, Chicago, Illinois, United States) for 1 h, and subsequently with DAPI (ab285390, Abcam, Cambridge, United Kingdom) for 15 min at room temperature. Digital fluorescence images were taken with fluorescence microscopy (Nikon Eclipse C1, NIKON, Japan). The fluorescence images were analyzed by ImageJ software. Besides, the main organs (heart, liver, spleens, lungs, and kidneys) of groups of mice were excised and histologically analyzed *via* hematoxylin and eosin (H&E) to evaluate the toxicity of BNTA *in vivo*.

## Statistical analysis

GraphPad Prism 8 (GraphPad Software, San Diego, CA, United States) was used to analyze the data. Results were presented as mean  $\pm$  standard deviation (SD) with at least three replications. Statistical differences were conducted with two-tailed, unpaired Student's *t*-test or one-way ANOVA followed by Turkey's post hoc. \**p* value less than 0.05, \*\**p* value less than 0.01, \*\*\**p* value less than 0.001 and \*\*\*\**p* value less than 0.0001 were defined as statistically significant.

## Results

### Effects of BNTA on viability and proliferation of BMMs

The chemical structure of BNTA is presented in Figure 1A. Effects of BNTA on viability and proliferation of BMMs were analyzed by CCK-8 assay. Treatment of BMMs with BNTA of 0, 1, 10, 20, and 40  $\mu$ M showed that BNTA had no significant effect on the viability and proliferation of BMM (Figures 1B–F). Based on the results, 40  $\mu$ M of BNTA was used in the subsequent experiments.

### BNTA inhibited RANKL-induced osteoclast differentiation and impaired osteoclastic bone resorption *in vitro*

First, the effects of BNTA on RANKL-induced osteoclastogenesis *in vitro* were analyzed. As is shown in Figure 2A that BMMs of the

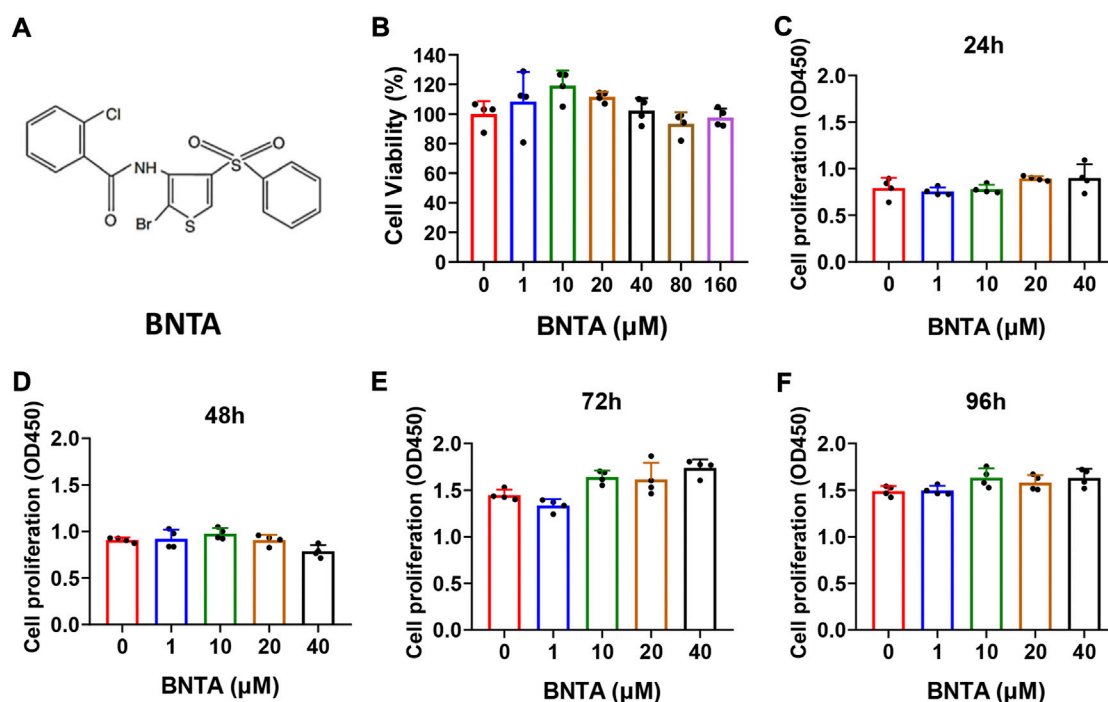


FIGURE 1

Effects of N-[2-bromo-4-(phenylsulfonyl)-3-thienyl]-2-chlorobenzamide (BNTA) on the cytotoxicity and proliferation of bone marrow-derived monocytes (BMMs). (A) The chemical structure of BNTA. (B) Viability of BMMs treated by indicated concentrations of BNTA at 24 h ( $n = 4$  per group). (C–F) The proliferation of BMMs treated by indicated concentrations of BNTA at 24, 48, 72, and 96 h ( $n = 4$  per group). All data are presented as mean  $\pm$  SD.

control group formed typical “pancake” shaped and highly TRAP-positive multinucleated osteoclasts, as was described in the previous report (Chen X. et al., 2019). The number of osteoclasts in the control group was presented to be  $429.75 \pm 48.20$  cells per well. However, the number of osteoclasts in the 40  $\mu$ M group decreased to  $6.75 \pm 1.71$  cells per well and typical “pancake” shaped multinucleated osteoclasts almost didn’t form. The formation of osteoclasts was significantly inhibited by BNTA in a concentration-dependent mode (Figures 2B,C). Subsequently, the bone resorption function of osteoclasts was evaluated *via* Hydroxyapatite resorption experiments. Compared to the control group, the bone resorption area of groups treated with 10, 20, and 40  $\mu$ M BNTA showed reductions of 94.3%, 97.3%, and 99.9%, respectively (Figures 2D,E). Thus, these data suggested that BNTA can effectively inhibit osteoclast differentiation and impair bone resorption *in vitro*.

## BNTA inhibited osteoclastogenesis and osteoclast-related genes expression

The effects of BNTA on osteoclastogenesis and bone resorption were next determined by investigating the mRNA expression levels of osteoclastic marker genes. The quantification of osteoclastic marker genes was conducted by qPCR. The expression of genes,

including *c-fos*, *NFATc1*, *CTSK*, *D2*, *MMP9*, and *ACP5* was remarkably suppressed in 20 or 40  $\mu$ M BNTA treated groups compared to the control group (Figures 3A–F). We further investigated *c-fos* and *NFATc1* gene expressions during RANKL-induced osteoclast formation using western blot analysis. The results demonstrated that BMMs reduced *c-fos* and *NFATc1* protein translation during the treatment of BNTA for 1, 3, or 5 days (Figures 3G,I,J). The protein reduction was also observed in a dose-dependent manner (Figures 3H,K,L), which was in line with the downregulation of gene expression of *c-fos* and *NFATc1* observed in our qPCR analysis (Figures 3A,B). All these results further indicated that BNTA inhibited osteoclastogenesis *in vitro*.

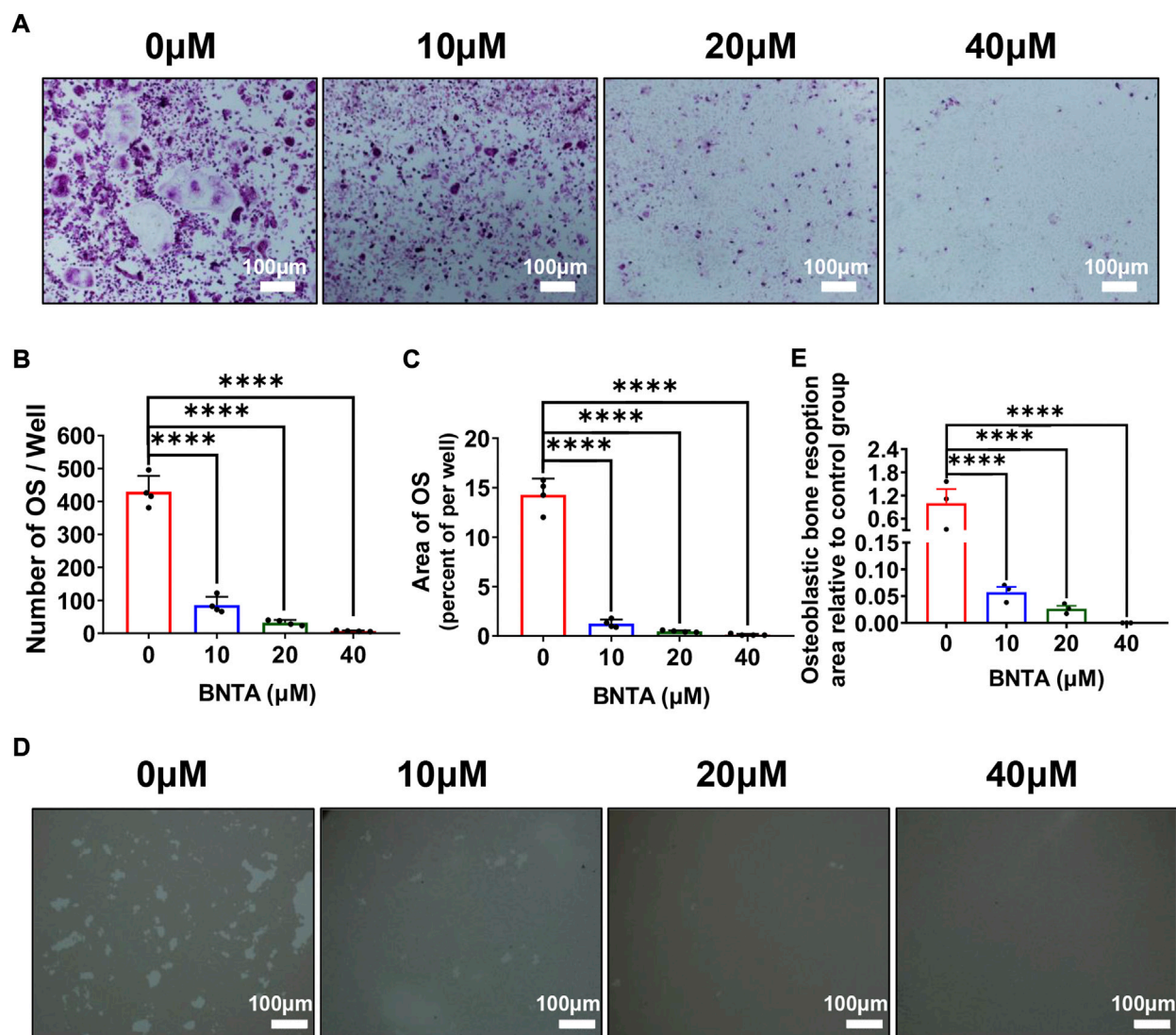
## BNTA inhibited ROS generation induced by RANKL *in vitro* and upregulated SOD1/SOD2 expression both *in vitro* and *in vivo*

To understand the potential mechanism of BNTA-dependent of osteoclastogenesis inhibition, we evaluated the effect of BNTA on RANKL-induced intracellular ROS generation and SODs expression. Intracellular ROS was detected as a fluorescent signal derived from the



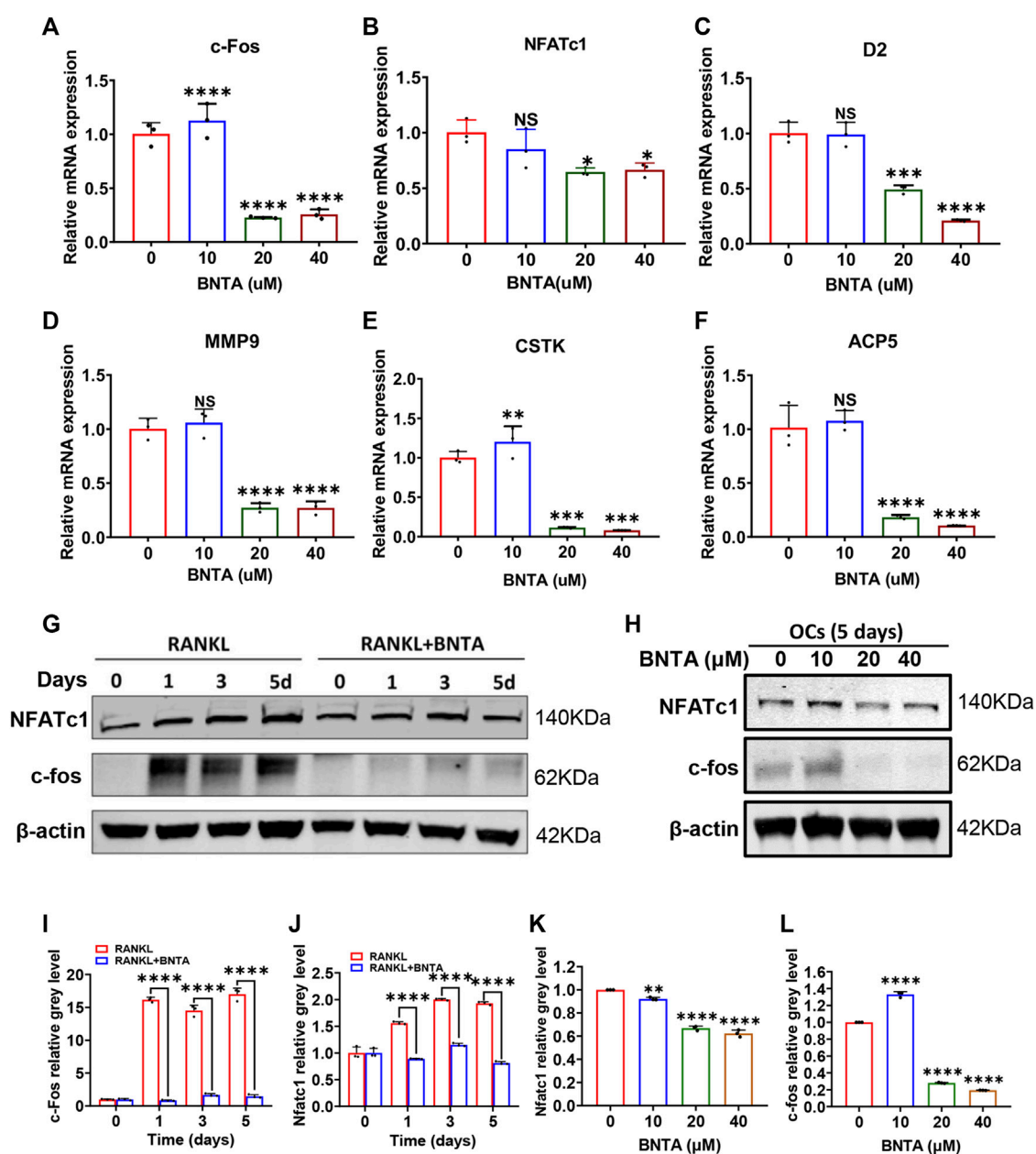
oxidative-sensitive fluorescent probe DCF using fluorescent microscopy. The number of ROS-positive cells was significantly reduced in a dose-dependent manner by BNTA treatment (Figures 4A,B). Additionally, known as ROS scavengers, SODs were found to be involved in the inhibition of ROS-stimulated osteoclastogenesis in this study. The results of qPCR exhibited that SOD1 and SOD2 were enhanced dose-dependently in BMMs induced by RANKL with the treatment of BNTA (Figures 4D,E). But SOD3, another member of the superoxide dismutase family usually highly expressed in specific cells or tissues, did not

show noticeable expression variation in BMMs regardless induced by RANKL or treated by BNTA (Figures 4C,F). Furthermore, we investigated the generation of SODs in the LPS-induced inflammatory osteolytic model of the mice calvarias. The immunofluorescence assays were applied to analyze the expression levels of oxidative-related proteins, including SOD1, SOD2, and SOD3. It was noted that BNTA observably enhanced the generation of SOD1 and SOD2 in LPS-induced bone tissue (Figures 4G–I, Supplementary Figure S1A,B). The expression level of



**FIGURE 2**

BNTA inhibited RANKL-induced osteoclastogenesis and osteolysis *in vitro*. **(A)** Representative images of BMMs stained for TRAP showed BNTA inhibited osteoclastogenesis in a dose-dependent manner. BMMs were stimulated by RANKL for 5 days with or without indicated concentrations of BNTA. **(B,C)** Quantification of TRAP-positive multinucleated cells (nuclei  $\geq 3$ ) ( $n = 4$  per group). All data are presented as mean  $\pm$  SD. \*\*\*\* $p < 0.0001$  compared with control group. **(D)** Representative images of hydroxyapatite resorption in each group presented BNTA inhibited osteolysis dose-dependently. BMMs were stimulated by RANKL for 5 days with or without indicated concentrations of BNTA. **(E)** Quantification of resorbed hydroxyapatite area per well. ( $n = 3$  per group). All data are presented as mean  $\pm$  SD. \*\*\*\* $p < 0.0001$  compared with control group.

**FIGURE 3**

BNTA attenuated osteoclast-related gene expression and inhibited NFATc1 activation. (A–F) qPCR analysis of osteoclast-related gene expression of c-fos, NFATc1, D2, MMP9, CSTK, and ACP5 relative to Control in BMMs stimulated by RANKL for 5 days with or without an indicated dose of BNTA ( $n = 3$  per group). All data are presented as mean  $\pm$  SD. \* $p < 0.05$ , \*\* $p < 0.01$ , \*\*\* $p < 0.001$ , \*\*\*\* $p < 0.0001$  compared with control group. (G) Representative Western Blot images of the effect of BNTA on the protein expression of NFATc1 and c-fos on days 0, 1, 3, and 5 with the stimulation of RANKL. (H) Representative Western Blot images of the effect of BNTA on the protein expression of NFATc1 and c-fos at day 5 stimulated by RANKL with or without an indicated dose of BNTA. (I–L) Quantitative analysis of the ratio of band intensity of NFATc1 and c-fos relative to  $\beta$ -actin ( $n = 3$  per group). \*\* $p < 0.01$ , \*\*\*\* $p < 0.0001$  relative to control group.

SOD3 in bone tissue was very low even induced by LPS (Figures 4G,J, Supplementary Figure S1C). These findings indicate that BNTA is able to upregulate the expression of SOD1 and SOD2 and enhance the scavenging ability of ROS.

## BNTA inhibited osteoclastogenesis via suppressing the MAPK pathway

To further explore the underlying molecular mechanisms of the impact of BNTA on osteoclastogenesis, we investigated the

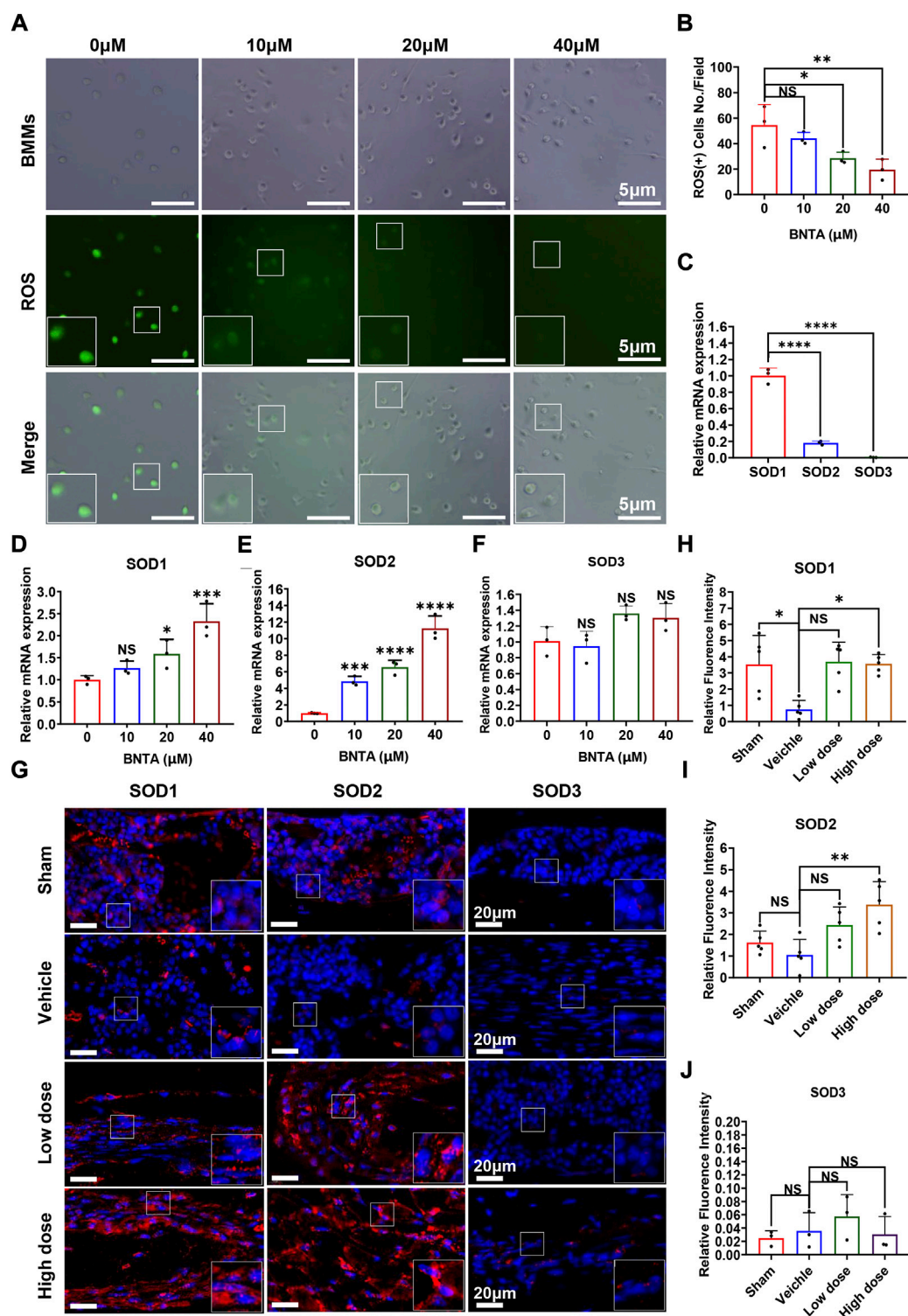
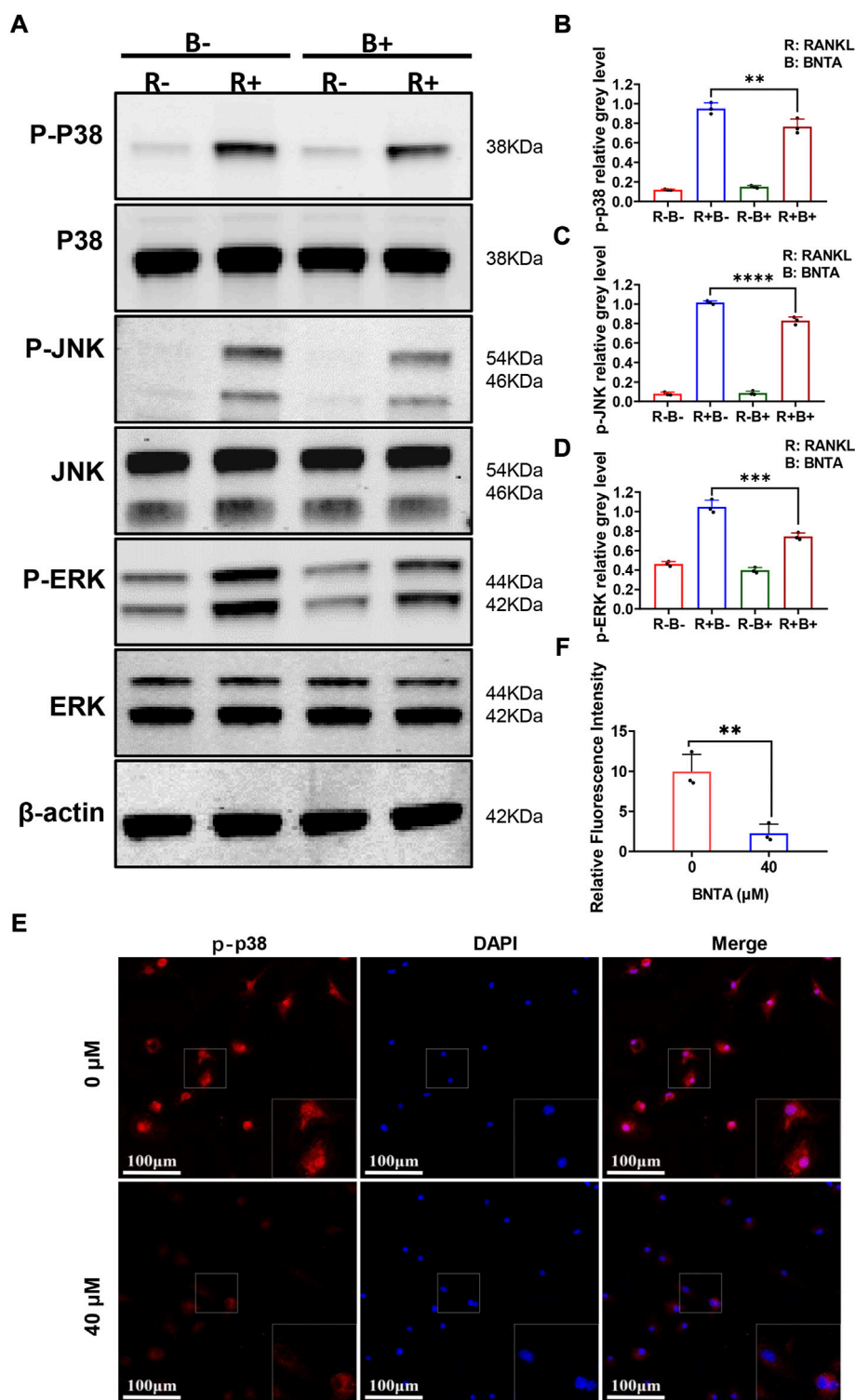


FIGURE 4

BNTA regulated Redox-related gene expression and inhibited intracellular ROS generation. **(A)** Representative fluorescence images of RANKL-stimulated ROS production in BMMs with or without pre-treatment of indicated dose of BNTA. **(B)** Quantification of the number of ROS positive cells per field ( $n = 3$  per group). All data are presented as mean  $\pm$  SD.  $*p < 0.05$ ,  $**p < 0.01$ . **(C)** qPCR analysis of mRNA expression of SOD1, SOD2, and SOD3 relative to GAPDH in BMMs stimulated by RANKL for 5 days without stimulation of BNTA ( $n = 3$  per group). All data are presented as mean  $\pm$  SD.  $****p < 0.0001$  compared with control group. **(D–F)** qPCR analysis of redox-related genes expression of SOD1, SOD2, and SOD3 relative to GAPDH in BMMs stimulated by RANKL for 5 days with or without an indicated dose of BNTA ( $n = 3$  per group). All data are presented as mean  $\pm$  SD.  $*p < 0.05$ ,  $***p < 0.001$ ,  $****p < 0.0001$  compared with control group. **(G)** Representative immunofluorescence staining images of decalcified bone sections for protein expression of SOD1, SOD2, and SOD3. **(H–J)** Quantitative analysis of protein expression of SOD1, SOD2, and SOD3 *in vivo*.  $*p < 0.05$ ,  $**p < 0.01$  compared with control group.



**FIGURE 5**  
BNTA inhibited osteoclastogenesis via the MAPK signaling pathway. **(A)** Representative Western Blot images of BNTA on the MAPKs pathway, including p38, ERK, and JNK. **(B–D)** Quantification of the ratio of band intensity of p-p38/p38, p-JNK/JNK, p-ERK/ERK ( $n = 3$  per group). All data are presented as mean  $\pm$  SD.  $**p < 0.01$ ,  $***p < 0.001$ ,  $****p < 0.0001$  compared with control group. **(E)** Representative immunofluorescence images of the effect of BNTA on the phosphorylation and nucleus translocation of p-p38 with stimulation of RANKL. **(F)** Quantification of the ratio of fluorescence intensity ( $n = 3$  per group). All data are presented as mean  $\pm$  SD.  $**p < 0.01$  compared with control group.



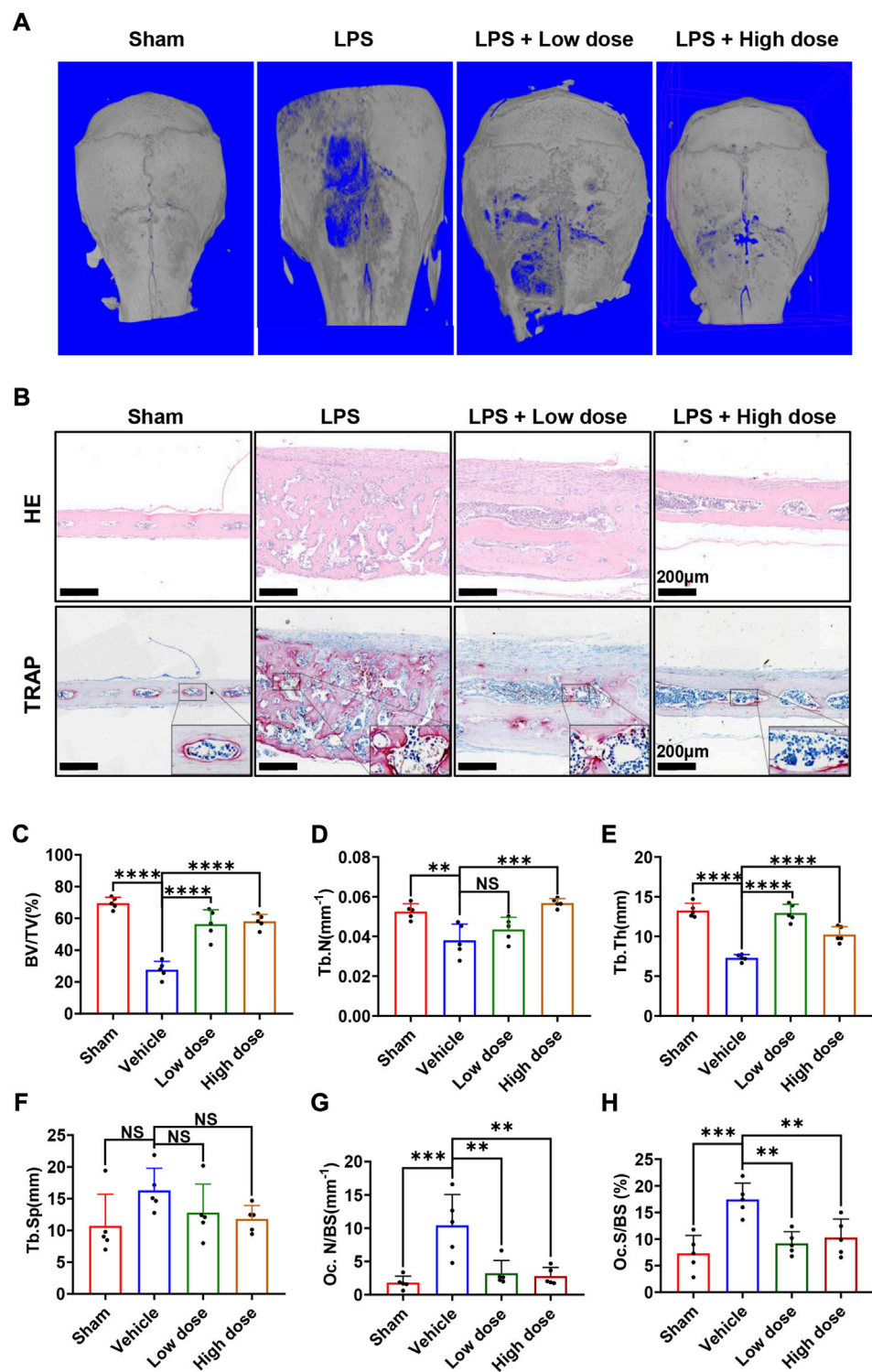


**FIGURE 6**  
BNTA attenuated LPS-induced bone loss in murine calvaria. **(A)** Micro-CT and 3-dimensional reconstruction of murine calvaria from sham group (PBS), vehicle group (LPS 5 mg/kg body weight), low dose group (LPS 5 mg/kg and BNTA 0.15 mg/kg) and high dose group (LPS 5 mg/kg and BNTA 1.5 mg/kg). **(B)** Representative images of decalcified bone sections stained with H&E and TRAP from each group. **(C–H)** Quantitative analysis of BV/TV, Tb.N, Tb.Th, Tb.sp, Oc. N/BS and Oc. S/BS in tissue sections. (*n* = 5). All data are presented as mean ± SD. \*\**p* < 0.01, \*\*\**p* < 0.001 \*\*\*\**p* < 0.0001. TRAP, tartrate resistant acid phosphatase; HE, hematoxylin and eosin; BV/TV, bone volume per tissue volume; Tb.N, trabecular number; Tb.Th, trabecular thickness; Tb.sp, trabecular space; Oc. N/BS, osteoclast number/bone surface; Oc. S/BS, osteoclast surface/bone surface.



RANKL-stimulated signaling pathways by western blot assay. BMMs were pretreated with 40  $\mu$ M BNTA for 2 h and then stimulated with RANKL for another 10 min. We observed that phosphorylation of p38, ERK, JNK was upregulated as a result of stimulation of RANKL. However, the phosphorylation could be suppressed obviously by BNTA (Figures 5A–D). Additionally, the immunofluorescence staining revealed that BNTA could significantly inhibit the translocation of phosphorylated p38 from the cytosol to the nucleus (Figures 5E,F). Collectively, these data indicated that BNTA inhibited RANKL-induced osteoclast formation *via* attenuating the activation of the MAPK signaling pathway and subsequent nucleus translocation of p38.

## BNTA attenuated LPS-induced osteolysis and bone loss via modulating osteoclast activity *in vivo*

Subsequently, the mouse calvarial model of LPS-induced inflammatory osteolysis was used to further evaluate the potential therapeutic application of BNTA toward osteolytic bone loss. The 3D  $\mu$ CT reconstructive images revealed severe osteolysis and widespread bone erosion of varying sizes on the surface of the calvaries in the LPS control group. In contrast, treatment with high-dose BNTA significantly reduced LPS-induced bone destruction in mice (Figure 6A). Quantitative morphometric analysis suggested that BV/TV, Tb.N, Tb.Th in the LPS group were presented to be significantly decreased compared with those in the sham group, while BV/TV, Tb.N and Tb.Th in the high dose treatment group were remarkably ameliorated relative to those in the LPS group (Figures 6C–F). Moreover, histologic and histomorphometry analyses of calvaries further verified the protective effect of BNTA against LPS-induced bone loss. The TRAP-staining assay exhibited that the number of TRAP-positive osteoclasts in the LPS group increased relative to the control group. The formation of osteoclasts and their recruitment to the bone surface was suppressed obviously with the treatment of BNTA (Figures 6B,G,H). Besides, H&E staining showed no significant damage, and toxicity was caused to the normal anatomical structure of main organs including the heart, liver, spleen, lung, and kidney during the treatment with BNTA (Supplementary Figure S3). These data illustrate that BNTA is a potentially effective and safe agent that can prevent bone osteolysis induced by LPS.

## BNTA also regulated the production of proinflammatory cytokines *in vitro* and *in vivo*

Moreover, we inspected the impact of BNTA on inflammatory cytokines in BMMs induced by RANKL. The

results found that BNTA markedly suppressed the expression of proinflammatory cytokines, including TNF- $\alpha$ , IL-1 $\beta$ , and IL-6 (Figures 7A,B,D), while increasing the expression of inflammatory inhibitory factors, such as IL-4 (Figure 7C). In addition, these inflammatory cytokines were investigated using immunofluorescence assays as well *in vivo*. The results showed that BNTA significantly inhibited the production of proinflammatory cytokines, including TNF- $\alpha$ , IL-1 $\beta$ , and IL-6, while no influence on the expression of IL-4 (Figures 7E–I, Supplementary Figure S2). These findings indicate that besides promoting the generation of SOD1 and SOD2 and enhancing the scavenging ability of ROS, BNTA is also able to regulate the levels of the inflammatory factors *in vitro* induced by RANKL or *in vivo* stimulated by LPS.

## Discussion

Human bone remodeling is a continuous process throughout life, which is tightly and delicately regulated based on a balance between bone formation by osteoblasts and bone resorption by osteoclasts. Overactivated osteoclastogenesis and excessive bone resorption during the bone remodeling process occur in a variety of inflammatory osteolytic bone diseases, such as osteoarthritis, inflammatory aseptic prosthetic loosening, periprosthetic infection, and osteomyelitis (Roux and Richette, 2012; Gallo et al., 2013; Loi et al., 2016). Current clinically available therapeutic agents for inflammatory osteolysis like estrogen, bisphosphonates, and parathyroid hormone are effective, but still have some limitations and side effects including increased cancer risks, aseptic jaw osteonecrosis, and atypical femur fracture (Clemons and Goss, 2001; Woo et al., 2006; Shane et al., 2014; Nikitovic et al., 2016; Lobo, 2017; Al-Khan et al., 2021). Therefore, the pursuit of novel and effective drug candidates that can safely treat osteolytic bone disorders is always required.

As an artificially synthesized small molecular chemical compound, BNTA identified antioxidative and anti-inflammatory activities in the treatment of OA by enhancing SOD3 expression (Shi et al., 2019). As a result, we consider it might be an effective candidate to treat inflammatory osteolytic bone diseases. In this study, the cytotoxicity assay found that BNTA exhibited no influence on the viability and proliferation of BMM cells, even if the concentration was up to 40  $\mu$ M. Treated with 40  $\mu$ M BNTA, the number and area of TRAP-positive osteoclasts were decreased and the resorption area was noticeably reduced, which indicated that BNTA significantly inhibited osteoclastogenesis and osteoclastic resorption. Furthermore, we focused on the expression of osteoclast-related genes. As is suggested, NFATc1 is a key target gene in the phase of osteoclastogenesis stimulated by RANKL (Negishi-Koga and Takayanagi, 2009; Zhao et al., 2010). C-fos, a critical component of the activator protein-1 (AP-1), cooperates with

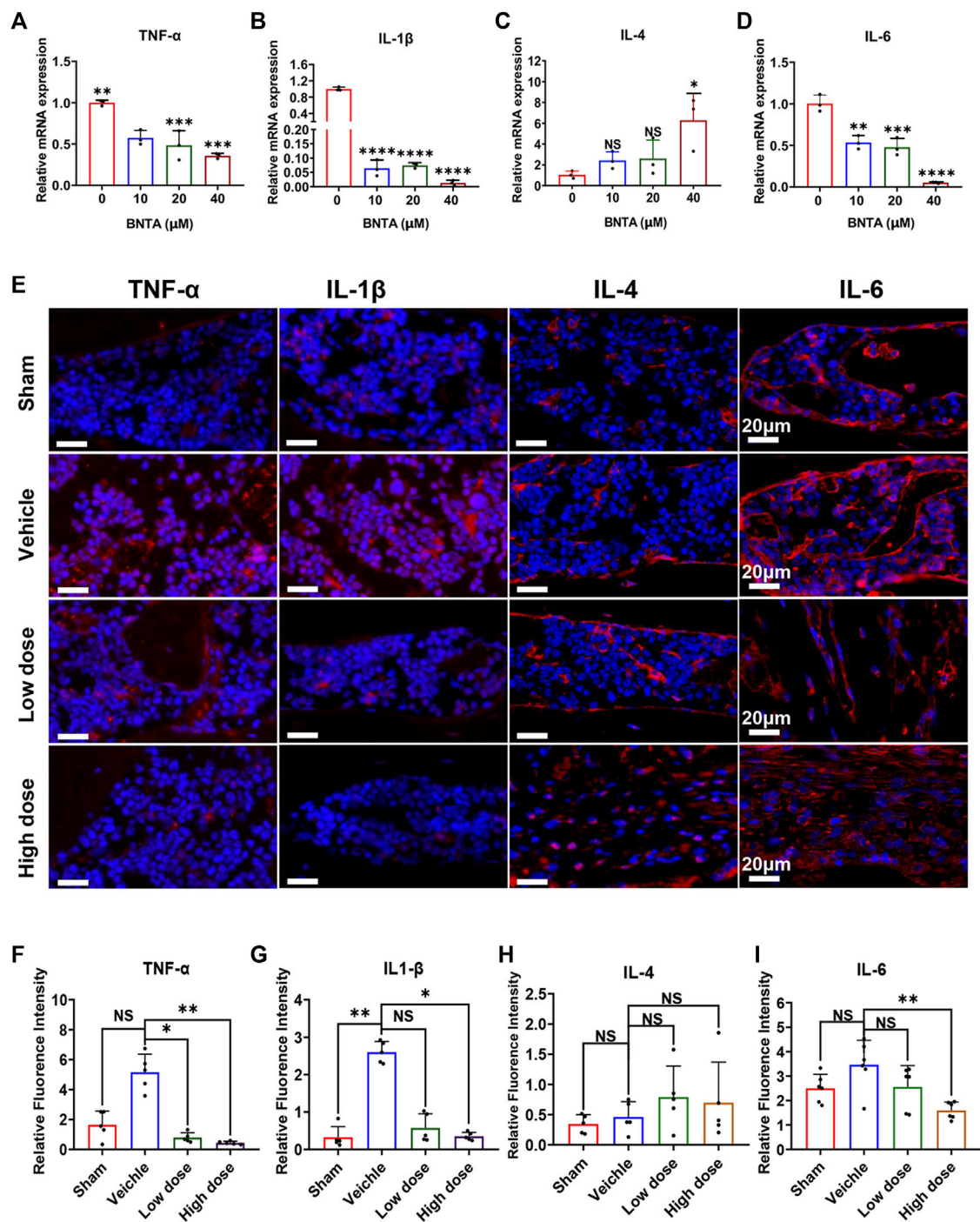
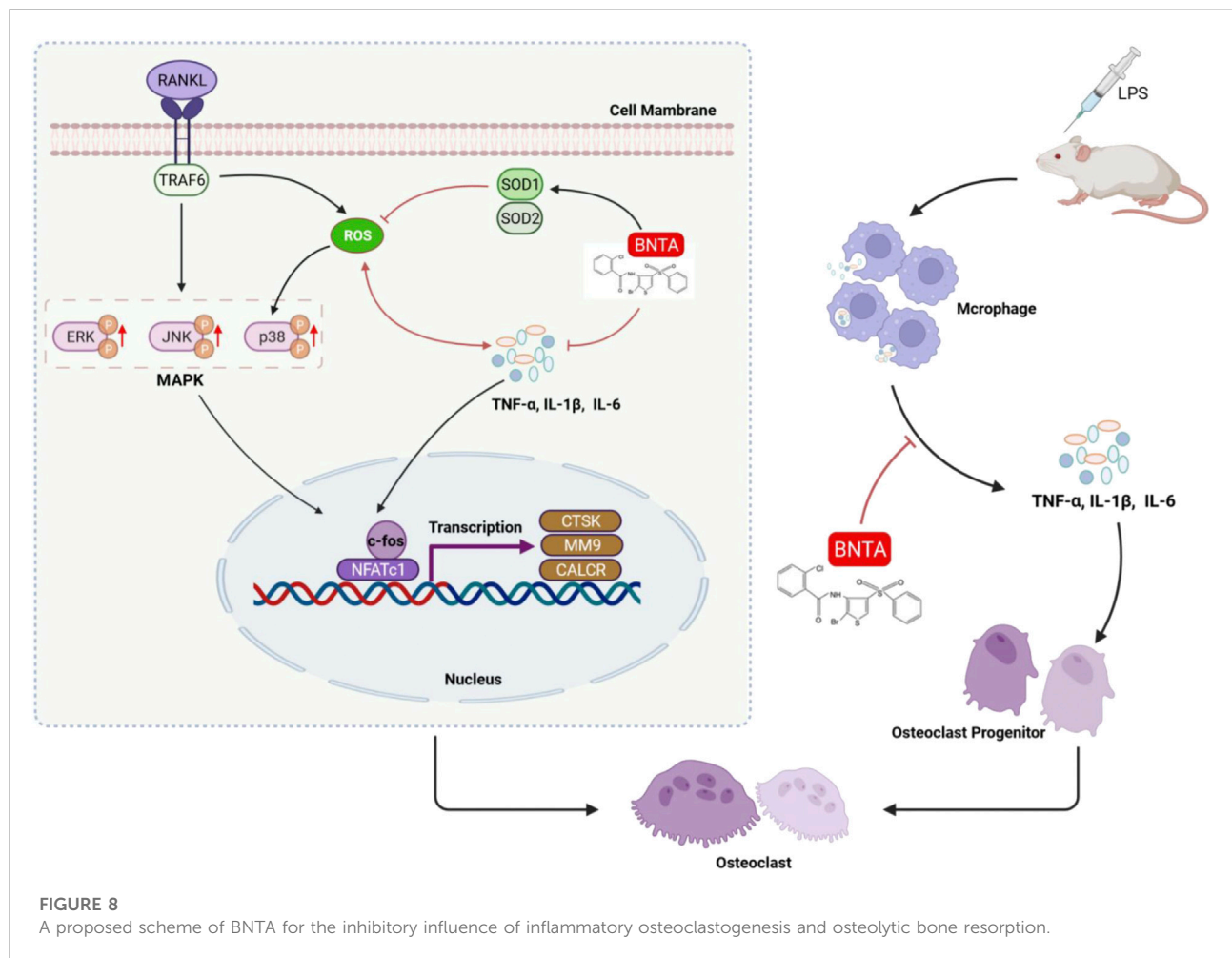


**FIGURE 7**  
BNTA regulated inflammation-related gene expression. (A–D) qPCR analysis of inflammation-related genes expression of TNF-α, IL1-β, IL-4, and IL-6 relative to GAPDH in BMMS stimulated by RANKL for 5 days with or without an indicated dose of BNTA ( $n = 3$  per group). All data are presented as mean  $\pm$  SD. \* $p < 0.05$ , \*\* $p < 0.01$ , \*\*\* $p < 0.001$ , \*\*\*\* $p < 0.0001$  compared with control group. (E) Representative immunofluorescence staining images of decalcified bone sections for protein expression of TNF-α, IL1-β, IL-4, and IL-6. (F–I) Quantitative analysis of protein expression of TNF-α, IL1-β, IL-4, and IL-6 *in vivo* ( $n = 5$  per group). All data are presented as mean  $\pm$  SD. \* $p < 0.05$ , \*\* $p < 0.01$  compared with control group.



NFATc1 to promote osteoclastic differentiation (Takayanagi et al., 2002; Wagner and Eferl, 2005). This study found that BNTA significantly reduced the expression of c-fos and NFATc1, which further led to the downregulation of associated osteoclast-specific gene expressions including CTSK, D2, MMP9, and ACP5. These findings indicated that BNTA was involved in NFATc1-mediated mechanisms that inhibited osteoclastogenesis and osteoclast resorption.

Next, this study then explored the mechanisms for the anti-oxidative and anti-osteoclastic effects of BNTA. SODs, including SOD1, SOD2, and SOD3, are peroxide catalysts that can catalyze ROS into hydrogen peroxide and then into water, avoiding producing nitrogen oxides, and other toxic substances (Zelko et al., 2002; Shi et al., 2019). Interestingly, we found that BNTA treatment significantly augmented the expression both of SOD1 and SOD2 in BMMs, which attenuated the production of ROS and subsequently inhibited osteoclastic formation. *In vivo* study results also showed upregulation of SOD1 and SOD2 expression with the treatment of BNTA also inhibited osteolytic bone loss. Thus, SOD1 and SOD2 are possibly more

important in protecting bone tissue against ROS-mediated osteolytic bone resorption. Additionally, we further explored the underlying signaling pathway. As a physiologic second messenger, ROS can oxidize cysteine residues of proteins, including protein tyrosine phosphatases, and make them inactive. Therefore, ROS may activate MAPKs, which contain threonine and tyrosine residues in their conserved TXY motifs (Lee et al., 2005; Chen K. et al., 2019). The MAPK pathway, including three major family members (p38, JNKs, and ERKs), serves an important role in osteoclast differentiation activated by RANKL (Boyle et al., 2003; Chen K. et al., 2019; He et al., 2021). As signal mediators in osteoclast metabolism, p38, JNKs, and ERKs exhibit differences in the duration of activation. P38 predominantly facilitates osteoclast differentiation and function, whereas JNK and ERK primarily mediate osteoclastic apoptosis and promote osteoclast precursor proliferation, respectively, which indicates that p38 signaling is more tightly connected to the control of osteoclastogenesis and osteoclastic resorption than ERK and JNK signaling (Lee et al., 2018). P38-MAPK signaling is activated by MAPK kinases

via phosphorylation of tyrosine and threonine, and subsequently promotes the expression of NFATc1 and osteoclast-related genes, whereas inactivated by MAPK phosphatases (MKPs) through dephosphorylation (Lee et al., 2018). Our research showed that BNTA significantly attenuated the activation of the MAPK signaling pathway and subsequent nucleus translocation of p38. So, BNTA-SOD1/2-ROS-MAPK signaling pathway axis was demonstrated to be involved in regulating osteoclastogenesis.

Furthermore, this study found that BNTA regulated the levels of many inflammatory cytokines during osteoclastogenesis *in vitro* and *in vivo*. Known as a highly conserved important constituent almost of all Gram-negative bacteria, Lipopolysaccharide (LPS) can promote the release of inflammatory factors such as TNF- $\alpha$  and IL-1 $\beta$ , increase the secretion of RANKL, and enhance osteoclast formation and osteolysis (Islam et al., 2007; Guo et al., 2014). Thus, LPS is extensively used in the investigation of inflammatory osteolysis (Islam et al., 2007; Yang et al., 2019; Yang et al., 2021). In our study, LPS was injected on the surfaces of mice's calvarias to create inflammatory bone erosion models. We inspected that several osteoclasts generated on the inflammatory bone surface, accompanying large amounts of inflammatory cytokines produced and released by multiple immune cells, which was in line with the previous study (Kumar and Roger, 2019). The evidence is clear that some proinflammatory cytokines, like TNF and IL-1, regulate the activation of calcium signaling and NFATc1, which subsequently activate genes related to osteoclastogenesis and osteoclast function (Kim et al., 2013; Terkawi et al., 2022). It is obvious that inflammatory stimulation induces bone resorption and leads to bone loss. As a signaling molecule and a mediator of inflammation, ROS acts a central role in the progression of many inflammatory disorders (Mittal et al., 2014). The nucleotide-binding oligomerization domain (NOD)-like receptor containing pyrin domain 3 (NLRP3) is an inflammasome which was found playing an important role in inflammatory response (Sho and Xu, 2019). Many researchers have confirmed that once it is assembled and activated, the NLRP3 will convert some inflammatory factors precursors such as pro-IL-1 $\beta$  and pro-IL-18 into mature cytokines, leading to inflammatory response in bodies (Pellegrini et al., 2017; Sho and Xu, 2019). ROS has already been detected involving in activation of NLRP3 inflammasome through regulating Caspase-11 (Lupfer et al., 2014), (Martinon et al., 2002)). In this study we found BNTA significantly promoted the generation of SOD1/SOD2 and then reduced ROS levels in LPS-induced inflammatory wounds. These results suggest that the BNTA-SOD1/2-ROS-inflammatory axis is involved in down-regulating inflammatory activity and attenuating inflammatory osteolysis.

Our study demonstrated that BNTA exerts an effective inhibitory effect on osteoclastogenesis and osteoclastic

resorption through SOD1/2-ROS- MAPK signaling pathway axis and SODs-ROS-inflammation axis (Figure 8). However, there are still two limitations. First, although we detected and elucidated the potential mechanism between SOD1/2 and osteoclastogenesis and osteoclastic resorption and inflammation, the details of the interaction between BNTA and SOD1/2 upregulation still need to be further investigated in our following study. Second, although we confirmed the anti-osteolytic and anti-inflammatory effects of BNTA *in vitro* partially, and further confirmed these effects in mouse models, we still lack a rat model to further elucidate the therapeutic effects of BNTA and we will do further studies in the next experiments.

In summary, this study provides a less cytotoxicity and side effects small molecule compound BNTA, and we confirmed that it acts as an anti-osteoclastic and anti-inflammatory agent in inflammatory osteolytic bone diseases. Moreover, given the advantage of simple chemical structure of BNTA, high yields may be more available if used clinically in the future, which is another benefit. Therefore, the BNTA may be considered as a potential and therapeutic candidate for the prevention and treatment of inflammatory osteoclast-related bone diseases.

## Data availability statement

The original contributions presented in the study are included in the article/Supplementary Material, further inquiries can be directed to the corresponding authors.

## Ethics statement

The animal study was reviewed and approved by Institutional Animal Ethics Review Board of Shanghai Ninth People's Hospital, Shanghai Jiao Tong University School of Medicine.

## Author contributions

JZ and YW guided all the experiments. HW, XC, JG, and XY performed the experiments, organized the data, and drafted the manuscript. JZ and XS performed the statistical analysis and reviewed the manuscript critically for important intellectual content. ZF, AQ, and JZ analyzed the data, confirmed the authenticity of all the raw data, and helped to write the manuscript. All authors read and approved the final manuscript.

## Funding

The present study was supported by grants from The National Natural Science Foundation of China (Grant nos.



82130073, 81871790, 81572768, and 81972136), and Shanghai Ninth People's Hospital, Shanghai Jiao Tong University School of Medicine "Multi-Disciplinary Team" Clinical Research Project (grant nos. 201701010).

## Conflict of interest

The authors declare that the research was conducted in the absence of any commercial or financial relationships that could be construed as a potential conflict of interest.

## Publisher's note

All claims expressed in this article are solely those of the authors and do not necessarily represent those of their affiliated organizations, or those of the publisher, the editors and the reviewers. Any product that may be evaluated in this article, or claim that may be made by its manufacturer, is not guaranteed or endorsed by the publisher.

## References

- Agidigbi, T. S., and Kim, C. (2019). Reactive oxygen species in osteoclast differentiation and possible pharmaceutical targets of ROS-mediated osteoclast diseases. *Int. J. Mol. Sci.* 20 (14), E3576. doi:10.3390/ijms20143576
- Al-Khan, A. A., Al Balushi, N. R., Richardson, S. J., and Danks, J. A. (2021). Roles of parathyroid hormone-related protein (PTHrP) and its receptor (PTHR1) in normal and tumor tissues: Focus on their roles in osteosarcoma. *Front. Vet. Sci.* 8, 637614. doi:10.3389/fvets.2021.637614
- Boyle, W. J., Simonet, W. S., and Lacey, D. L. (2003). Osteoclast differentiation and activation. *Nature* 423 (6937), 337–342. doi:10.1038/nature01658
- Chen, K., Qiu, P., Yuan, Y., Zheng, L., He, J., Wang, C., et al. (2019). Pseurotin A inhibits osteoclastogenesis and prevents ovariectomized-induced bone loss by suppressing reactive oxygen species. *Theranostics* 9 (6), 1634–1650. doi:10.7150/thno.30206
- Chen, X., Chen, X., Zhou, Z., Qin, A., Wang, Y., Fan, B., et al. (2019). LY411575, a potent gamma-secretase inhibitor, suppresses osteoclastogenesis *in vitro* and LPS-induced calvarial osteolysis *in vivo*. *J. Cell. Physiol.* 234 (11), 20944–20956. doi:10.1002/jcp.28699
- Clemons, M., and Goss, P. (2001). Estrogen and the risk of breast cancer. *N. Engl. J. Med.* 344 (4), 276–285. doi:10.1056/NEJM200101253440407
- Fattman, C. L., Schaefer, L. M., and Oury, T. D. (2003). Extracellular superoxide dismutase in biology and medicine. *Free Radic. Biol. Med.* 35 (3), 236–256. doi:10.1016/s0891-5849(03)00275-2
- Gallo, J., Goodman, S. B., Kontinen, Y. T., Wimmer, M. A., and Holinka, M. (2013). Osteolysis around total knee arthroplasty: A review of pathogenetic mechanisms. *Acta Biomater.* 9 (9), 8046–8058. doi:10.1016/j.actbio.2013.05.005
- Guo, C., Yuan, L., Wang, J. G., Wang, F., Yang, X. K., Zhang, F. H., et al. (2014). Lipopolysaccharide (LPS) induces the apoptosis and inhibits osteoblast differentiation through JNK pathway in MC3T3-E1 cells. *Inflammation* 37 (2), 621–631. doi:10.1007/s10753-013-9778-9
- He, J., Chen, K., Deng, T., Xie, J., Zhong, K., Yuan, J., et al. (2021). Inhibitory effects of rhaponticin on osteoclast formation and resorption by targeting RANKL-induced NFATc1 and ROS activity. *Front. Pharmacol.* 12, 645140. doi:10.3389/fphar.2021.645140
- Hu, L., Zachariae, E. D., Larsen, U. G., Vilhardt, F., and Petersen, S. V. (2019). The dynamic uptake and release of SOD3 from intracellular stores in macrophages modulates the inflammatory response. *Redox Biol.* 26, 101268. doi:10.1016/j.redox.2019.101268
- Islam, S., Hassan, F., Tumurkhuu, G., Dagvadorj, J., Koide, N., Naiki, Y., et al. (2007). Bacterial lipopolysaccharide induces osteoclast formation in RAW 264.7 macrophage cells. *Biochem. Biophys. Res. Commun.* 360 (2), 346–351. doi:10.1016/j.bbrc.2007.06.023
- Kanzaki, H., Wada, S., Narimiya, T., Yamaguchi, Y., Katsumata, Y., Itohiya, K., et al. (2017). Pathways that regulate ROS scavenging enzymes, and their role in defense against tissue destruction in periodontitis. *Front. Physiol.* 8, 351. doi:10.3389/fphys.2017.00351
- Kemp, K., Gray, E., Mallam, E., Scolding, N., and Wilkins, A. (2010). Inflammatory cytokine induced regulation of superoxide dismutase 3 expression by human mesenchymal stem cells. *Stem Cell Rev. Rep.* 6 (4), 548–559. doi:10.1007/s12015-010-9178-6
- Kim, J., Yang, J., Park, O. J., Kang, S. S., Kim, W. S., Kurokawa, K., et al. (2013). Lipoproteins are an important bacterial component responsible for bone destruction through the induction of osteoclast differentiation and activation. *J. Bone Min. Res.* 28 (11), 2381–2391. doi:10.1002/jbmr.1973
- Kim, H., Lee, Y. D., Kim, H. J., Lee, Z. H., and Kim, H. H. (2017). SOD2 and Sirt3 control osteoclastogenesis by regulating mitochondrial ROS. *J. Bone Min. Res.* 32 (2), 397–406. doi:10.1002/jbmr.2974
- Kobayashi, K., Nojiri, H., Saita, Y., Morikawa, D., Ozawa, Y., Watanabe, K., et al. (2015). Mitochondrial superoxide in osteocytes perturbs canalicular networks in the setting of age-related osteoporosis. *Sci. Rep.* 5, 9148. doi:10.1038/srep09148
- Kumar, G., and Roger, P. M. (2019). From crosstalk between immune and bone cells to bone erosion in infection. *Int. J. Mol. Sci.* 20 (20), E5154. doi:10.3390/ijms20205154
- Lagasse, E., and Weissman, I. L. (1997). Enforced expression of Bcl-2 in monocytes rescues macrophages and partially reverses osteopetrosis in op/op mice. *Cell* 89 (7), 1021–1031. doi:10.1016/s0092-8674(00)80290-1
- Lee, S. H., and Jang, H. D. (2015). Scoparone attenuates RANKL-induced osteoclastic differentiation through controlling reactive oxygen species production and scavenging. *Exp. Cell Res.* 331 (2), 267–277. doi:10.1016/j.yexcr.2014.12.018
- Lee, N. K., Choi, Y. G., Baik, J. Y., Han, S. Y., Jeong, D. W., Bae, Y. S., et al. (2005). A crucial role for reactive oxygen species in RANKL-induced osteoclast differentiation. *Blood* 106 (3), 852–859. doi:10.1182/blood-2004-09-3662
- Lee, S. H., Kim, J. K., and Jang, H. D. (2014). Genistein inhibits osteoclastic differentiation of RAW 264.7 cells via regulation of ROS production and scavenging. *Int. J. Mol. Sci.* 15 (6), 10605–10621. doi:10.3390/ijms150610605

## Supplementary material

The Supplementary Material for this article can be found online at: <https://www.frontiersin.org/articles/10.3389/fphar.2022.939929/full#supplementary-material>

### SUPPLEMENTARY FIGURE S1

Representative images of immunofluorescence for SOD1, SOD2, and SOD3 in murine calvaria. (A,B) BNTA upregulated protein expression of SOD1 and SOD2. (C) The protein expression of SOD3 in murine calvaria was at a low level. Red fluorescence represents marked protein expression. Blue fluorescence represents the cell nucleus.

### SUPPLEMENTARY FIGURE S2

Representative images of immunofluorescence for inflammatory factors in murine calvaria. (A–C) The protein expression of pro-inflammatory factors of TNF- $\alpha$ , IL1- $\beta$ , and IL-6 was stimulated by LPS while downregulated by BNTA. (D) The protein expression of inflammatory inhibitory factors of IL-4 did not present significant change with the stimulation of LPS or treatment of BNTA. Red fluorescence represents marked protein expression. Blue fluorescence represents the cell nucleus.

### SUPPLEMENTARY FIGURE S3

Toxicity analysis in major organs of mice. H&E staining of heart, liver, spleen, lung, and kidney after 10-days treatment of each group.



- Lee, K., Seo, I., Choi, M. H., and Jeong, D. (2018). Roles of mitogen-activated protein kinases in osteoclast biology. *Int. J. Mol. Sci.* 19 (10), E3004. doi:10.3390/ijms19103004
- Lee, H. I., Lee, J., Hwang, D., Lee, G. R., Kim, N., Kwon, M., et al. (2019). Dehydrocostus lactone suppresses osteoclast differentiation by regulating NFATc1 and inhibits osteoclast activation through modulating migration and lysosome function. *FASEB J.* 33 (8), 9685–9694. doi:10.1096/fj.201900862R
- Lobo, R. A. (2017). Hormone-replacement therapy: Current thinking. *Nat. Rev. Endocrinol.* 13 (4), 220–231. doi:10.1038/nrendo.2016.164
- Loi, F., Cordova, L. A., Pajarinen, J., Lin, T. H., Yao, Z., and Goodman, S. B. (2016). Inflammation, fracture and bone repair. *Bone* 86, 119–130. doi:10.1016/j.bone.2016.02.020
- Lupfer, C. R., Anand, P. K., Liu, Z., Stokes, K. L., Vogel, P., Lamkanfi, M., et al. (2014). Reactive oxygen species regulate caspase-11 expression and activation of the non-canonical NLRP3 inflammasome during enteric pathogen infection. *PLoS Pathog.* 10 (9), e1004410. doi:10.1371/journal.ppat.1004410
- Maciag, A. E., Holland, R. J., Robert Cheng, Y. S., Rodriguez, L. G., Saavedra, J. E., Anderson, L. M., et al. (2013). Nitric oxide-releasing prodrug triggers cancer cell death through deregulation of cellular redox balance. *Redox Biol.* 1, 115–124. doi:10.1016/j.redox.2012.12.002
- Martinon, F., Burns, K., and Tschopp, J. (2002). The inflammasome: A molecular platform triggering activation of inflammatory caspases and processing of proIL-beta. *Mol. Cell* 10 (2), 417–426. doi:10.1016/s1097-2765(02)00599-3
- Mbalaviele, G., Novack, D. V., Schett, G., and Teitelbaum, S. L. (2017). Inflammatory osteolysis: A conspiracy against bone. *J. Clin. Invest.* 127 (6), 2030–2039. doi:10.1172/JCI93356
- Mittal, M., Siddiqui, M. R., Tran, K., Reddy, S. P., and Malik, A. B. (2014). Reactive oxygen species in inflammation and tissue injury. *Antioxid. Redox Signal.* 20 (7), 1126–1167. doi:10.1089/ars.2012.5149
- Negishi-Koga, T., and Takayanagi, H. (2009). Ca<sup>2+</sup>-NFATc1 signaling is an essential axis of osteoclast differentiation. *Immunol. Rev.* 231 (1), 241–256. doi:10.1111/j.1600-065X.2009.00821.x
- Nikitovic, D., Kavasi, R. M., Berdiaki, A., Papachristou, D. J., Tsiaoussis, J., Spandidos, D. A., et al. (2016). Parathyroid hormone/parathyroid hormone-related peptide regulate osteosarcoma cell functions: Focus on the extracellular matrix (Review). *Oncol. Rep.* 36 (4), 1787–1792. doi:10.3892/or.2016.4986
- Nozik-Grayck, E., Suliman, H. B., and Piantadosi, C. A. (2005). Extracellular superoxide dismutase. *Int. J. Biochem. Cell Biol.* 37 (12), 2466–2471. doi:10.1016/j.biocel.2005.06.012
- Pellegrini, C., Antonioli, L., Lopez-Castejon, G., Blandizzi, C., and Fornai, M. (2017). Canonical and non-canonical activation of NLRP3 inflammasome at the crossroad between immune tolerance and intestinal inflammation. *Front. Immunol.* 8, 36. doi:10.3389/fimmu.2017.00036
- Roux, C., and Richette, P. (2012). Impact of treatments for osteoporosis on osteoarthritis progression. *Osteoporos. Int.* 23 (8), S881–S883. doi:10.1007/s00198-012-2168-6
- Shane, E., Burr, D., Abrahamsen, B., Adler, R. A., Brown, T. D., Cheung, A. M., et al. (2014). Atypical subtrochanteric and diaphyseal femoral fractures: Second report of a task force of the American society for bone and mineral research. *J. Bone Min. Res.* 29 (1), 1–23. doi:10.1002/jbmr.1998
- Shi, Y., Hu, X., Cheng, J., Zhang, X., Zhao, F., Shi, W., et al. (2019). A small molecule promotes cartilage extracellular matrix generation and inhibits osteoarthritis development. *Nat. Commun.* 10 (1), 1914. doi:10.1038/s41467-019-09839-x
- Sho, T., and Xu, J. (2019). Role and mechanism of ROS scavengers in alleviating NLRP3-mediated inflammation. *Biotechnol. Appl. Biochem.* 66 (1), 4–13. doi:10.1002/bab.1700
- Takayanagi, H., Kim, S., Koga, T., Nishina, H., Isshiki, M., Yoshida, H., et al. (2002). Induction and activation of the transcription factor NFATc1 (NFAT2) integrate RANKL signaling in terminal differentiation of osteoclasts. *Dev. Cell* 3 (6), 889–901. doi:10.1016/s1534-5807(02)00369-6
- Terkawi, M. A., Matsumae, G., Shimizu, T., Takahashi, D., Kadoya, K., and Iwasaki, N. (2022). Interplay between inflammation and pathological bone resorption: Insights into recent mechanisms and pathways in related diseases for future perspectives. *Int. J. Mol. Sci.* 23 (3), 1786. doi:10.3390/ijms23031786
- Theill, L. E., Boyle, W. J., and Penninger, J. M. (2002). RANK-L and RANK: T cells, bone loss, and mammalian evolution. *Annu. Rev. Immunol.* 20, 795–823. doi:10.1146/annurev.immunol.20.100301.064753
- Wagner, E. F., and Eferl, R. (2005). Fos/AP-1 proteins in bone and the immune system. *Immunol. Rev.* 208, 126–140. doi:10.1111/j.0105-2896.2005.00332.x
- Wang, Y., Branicky, R., Noe, A., and Hekimi, S. (2018). Superoxide dismutases: Dual roles in controlling ROS damage and regulating ROS signaling. *J. Cell Biol.* 217 (6), 1915–1928. doi:10.1083/jcb.201708007
- Wells, P. G., McCallum, G. P., Chen, C. S., Henderson, J. T., Lee, C. J., Perstin, J., et al. (2009). Oxidative stress in developmental origins of disease: Teratogenesis, neurodevelopmental deficits, and cancer. *Toxicol. Sci.* 108 (1), 4–18. doi:10.1093/toxsci/kfn263
- Wiktor-Jedrzejczak, W., Bartocci, A., Ferrante, A. W., Jr., Ahmed-Ansari, A., Sell, K. W., Pollard, J. W., et al. (1990). Total absence of colony-stimulating factor 1 in the macrophage-deficient osteopetrotic (op/op) mouse. *Proc. Natl. Acad. Sci. U. S. A.* 87 (12), 4828–4832. doi:10.1073/pnas.87.12.4828
- Woo, S. B., Hellstein, J. W., and Kalmar, J. R. (2006). Narrative [corrected] review: Bisphosphonates and osteonecrosis of the jaws. *Ann. Intern. Med.* 144 (10), 753–761. doi:10.7326/0003-4819-144-10-200605160-00009
- Xu, H., Liu, T., Jia, Y., Li, J., Jiang, L., Hu, C., et al. (2021). (-)-Epigallocatechin-3-gallate inhibits osteoclastogenesis by blocking RANKL-RANK interaction and suppressing NF- $\kappa$ B and MAPK signaling pathways. *Int. Immunopharmacol.* 95, 107464. doi:10.1016/j.intimp.2021.107464
- Yang, J., Tang, R., Yi, J., Chen, Y., Li, X., Yu, T., et al. (2019). Diallyl disulfide alleviates inflammatory osteolysis by suppressing osteoclastogenesis via NF- $\kappa$ B-NFATc1 signal pathway. *FASEB J.* 33 (6), 7261–7273. doi:10.1096/fj.201802172R
- Yang, J., Qin, L., Huang, J., Li, Y., Xu, S., Wang, H., et al. (2021). Astragalus polysaccharide attenuates LPS-related inflammatory osteolysis by suppressing osteoclastogenesis by reducing the MAPK signalling pathway. *J. Cell. Mol. Med.* 25 (14), 6800–6814. doi:10.1111/jcmm.16683
- Zelko, I. N., Mariani, T. J., and Folz, R. J. (2002). Superoxide dismutase multigene family a comparison of the CuZn-SOD (SOD1), Mn-SOD (SOD2), and EC-SOD (SOD3) gene structures, evolution, and expression. *Free Radic. Biol. Med.* 33 (3), 337–349. doi:10.1016/s0891-5849(02)00905-x
- Zhan, Y., Liang, J., Tian, K., Che, Z., Wang, Z., Yang, X., et al. (2019). Vindoline inhibits RANKL-induced osteoclastogenesis and prevents ovariectomy-induced bone loss in mice. *Front. Pharmacol.* 10, 1587. doi:10.3389/fphar.2019.01587
- Zhang, J., Hu, W., Ding, C., Yao, G., Zhao, H., and Wu, S. (2019). Deferoxamine inhibits iron-uptake stimulated osteoclast differentiation by suppressing electron transport chain and MAPKs signaling. *Toxicol. Lett.* 313, 50–59. doi:10.1016/j.toxlet.2019.06.007
- Zhao, Q., Wang, X., Liu, Y., He, A., and Jia, R. (2010). NFATc1: Functions in osteoclasts. *Int. J. Biochem. Cell Biol.* 42 (5), 576–579. doi:10.1016/j.biocel.2009.12.018



## OPEN ACCESS

## EDITED BY

Dongwei Zhang,  
Beijing University of Chinese Medicine,  
China

## REVIEWED BY

Yuan Xu,  
China-Japan Friendship Hospital, China  
Wang Hailong,  
Dongzhimen Hospital, Beijing University  
of Chinese Medicine, China

## \*CORRESPONDENCE

Peng Zhang,  
peng.zhang@siat.ac.cn  
Hui Zeng,  
zenghui\_36@163.com  
Hongyan Zhao,  
zhaohongyan1997@163.com

## SPECIALTY SECTION

This article was submitted to  
Experimental Pharmacology and Drug  
Discovery,  
a section of the journal  
Frontiers in Pharmacology

RECEIVED 03 August 2022

ACCEPTED 16 September 2022

PUBLISHED 30 September 2022

## CITATION

Xu H, Tao L, Cao J, Zhang P, Zeng H and  
Zhao H (2022), Yi Shen Juan Bi Pill  
alleviates bone destruction in  
inflammatory arthritis under  
postmenopausal conditions by  
regulating ephrinB2 signaling.  
*Front. Pharmacol.* 13:1010640.  
doi: 10.3389/fphar.2022.1010640

## COPYRIGHT

© 2022 Xu, Tao, Cao, Zhang, Zeng and  
Zhao. This is an open-access article  
distributed under the terms of the  
[Creative Commons Attribution License](#)  
(CC BY). The use, distribution or  
reproduction in other forums is  
permitted, provided the original  
author(s) and the copyright owner(s) are  
credited and that the original  
publication in this journal is cited, in  
accordance with accepted academic  
practice. No use, distribution or  
reproduction is permitted which does  
not comply with these terms.

# Yi Shen Juan Bi Pill alleviates bone destruction in inflammatory arthritis under postmenopausal conditions by regulating ephrinB2 signaling

Huihui Xu<sup>1,2,3</sup>, Li Tao<sup>3</sup>, Jinfeng Cao<sup>3</sup>, Peng Zhang<sup>2\*</sup>, Hui Zeng<sup>1\*</sup>  
and Hongyan Zhao<sup>3\*</sup>

<sup>1</sup>Department of Bone & Joint Surgery and National & Local Joint Engineering Research Center of Orthopaedic Biomaterials, Peking University Shenzhen Hospital, Shenzhen, China, <sup>2</sup>Center for Translational Medicine Research and Development, Shenzhen Institutes of Advanced Technology, Chinese Academy of Sciences, Shenzhen, China, <sup>3</sup>Beijing Key Laboratory of Research of Chinese Medicine on Prevention and Treatment for Major Diseases, Experimental Research Center, China Academy of Chinese Medical Science, Beijing, China

Yi Shen Juan Bi Pill (YSJB) is a traditional Chinese medicine (TCM) formulation that has a therapeutic effect upon rheumatoid arthritis (RA), but how YSJB affects bone destruction in arthritis under postmenopausal conditions is not known. We evaluated the therapeutic role of YSJB in bone destruction in postmenopausal arthritis. We used collagen-induced arthritis (CIA) rats who had been ovariectomized (OVX) as models and explored the possible mechanism from the synovium and bone marrow (BM). Arthritis was generated after ovariectomy or sham surgery for 12 weeks. After 14 days of primary immunization, rats were administered YSJB or estradiol valerate (EV) for 28 days. YSJB could prevent bone destruction in the inflamed joints of rats in the OVX + CIA group. CIA promoted osteoclast differentiation significantly in the synovial membrane according to tartrate resistant acid phosphatase (TRACP) staining, and OVX tended to aggravate the inflammatory reaction of CIA rats according to hematoxylin-and-eosin staining. Immunohistochemistry revealed that the synovium did not have significant changes in erythropoietin-producing hepatocellular interactor (ephrin)B2 or erythropoietin-producing hepatocellular (eph) B4 expression after YSJB treatment, but YSJB treatment reduced nuclear factor of activated T cells (NFATc1) expression. The BM of rats in the OVX + CIA exhibited remarkable increases in the number of osteoclasts and NFATc1 expression, as well as significantly reduced expression of ephrinB2 and ephB4 compared with the CIA group and sham group. YSJB treatment reduced NFATc1 expression significantly but also increased ephrinB2 expression in the BM markedly. These data suggest that YSJB exhibit a bone-protective effect, it may be a promising therapeutic strategy for alleviating bone destruction in arthritis under postmenopausal conditions, and one of the mechanisms is associated with the modulation of ephrinB2 signaling.

## KEYWORDS

collagen-induced arthritis, ovariectomy, bone destruction, Yi Shen Juan Bi Pill, ephrinB2

## Introduction

Rheumatoid arthritis (RA) is a systemic autoimmune disease characterized by inflammatory synovitis, cartilage erosion, and bone destruction. RA prevalence worldwide is ~1% (van der Woude and van der Helm-van Mil, 2018). RA prevalence in women is higher than that in men, and the former experience increased disability and greater functional decline than men (Kvien et al., 2006; Wallenius et al., 2009). Changes in gonadal hormones may participate in these differential immune responses in RA (Pennell et al., 2012). For instance, estrogen deficiency (which is attributed to aging and menopause) is related to RA progression (Shah et al., 2020). Menopause has a significant impact on worsening progression of functional decline in women with RA, which is not observed in premenopausal women compared with postmenopausal women (Mollard et al., 2018). Postmenopausal RA patients are susceptible to considerable bone damage and disability (Sammaritano, 2012). Therefore, discovering new targets for RA treatment after menopause are crucial.

In traditional Chinese medicine (TCM) theory, kidney deficiency syndrome is one of the most common syndromes of RA and corresponds (at least in part) to low levels of gonadal hormones. Yi Shen Juan Bi Pill (YSJB) is a TCM formulation which is used to treat RA patients with kidney deficiency syndrome. Previously, we demonstrated that YSJB protected against collagen-induced arthritis (CIA) in rats with a castration-induced kidney-deficiency pattern (Zhao et al., 2012). Moreover, we showed that YSJB ameliorated systemic bone loss/destruction in CIA rats, which affected the activation of osteoclasts and regulated osteoclast-mediated bone resorption by inhibiting expression of receptor activator of nuclear factor- $\kappa$ B (RANK), nuclear factor of activated T cells (NFATc) 1, and c-fos (Zhao et al., 2018; Xia et al., 2021).

Bone destruction and general bone loss in RA are considered to be related to abnormal activation of osteoclasts (Kim et al., 2020; Liu et al., 2020). Interactions between osteoclasts and osteoblasts by erythropoietin-producing hepatocellular interactor (ephrin) ligands and erythropoietin-producing hepatocellular (eph) receptors have crucial roles in maintaining bone homeostasis (Tazaki et al., 2018), and they also participate in RA pathogenesis (Romanovsky, 2006). EphrinB2 is expressed on the membrane of mature osteoclasts. Interestingly, the osteoblast membrane expresses ephrinB2 and ephB4 simultaneously (Matsuo, 2010). The bidirectional signaling between osteoclastic ephrinB2 and osteoblastic ephB4 suppresses the bone resorption of osteoclasts and enhances the bone formation of osteoblasts (Zhao et al., 2006). Reverse signaling through ephrinB2 can inhibit NFATc1 transcription and thereby suppress osteoclast activity (Matsuo and Otaki, 2012). Enhancing

ephrinB2-ephB4 signaling can inhibit osteoclastogenesis and prevent bone loss in ovariectomized (OVX) rats (Zhang et al., 2022).

Studies have found that inflammatory infiltrates are present in the deep part of the bone marrow (BM), far from the synovium–BM junction. Data from animal experiments have shown that the cortical-bone canaliculi connecting BM and synovium increase, which may help osteoclastic precursor cells migrate directly from the BM to the synovium, thus stimulating the “extraarticular” pathologic process of RA centered on the BM. According to the TCM theory “kidney governs bone and generates marrow” in many clinical and experimental studies, kidney-tonifying TCM formulations can inhibit bone absorption or promote bone formation.

We explored how YSJB influences bone destruction in arthritis under postmenopausal conditions with modulation of ephrinB2-ephB4 signaling from the synovium and BM.

## Materials and methods

### Ethical approval of the study protocol

The experimental protocol was approved (2016-030) by the Institute of Basic Theory of Traditional Chinese Medicine within the China Academy of Chinese Medical Sciences (Beijing, China).

### Animals

Seventy female adult Sprague–Dawley rats (10 weeks) were purchased from the National Institutes for Food and Drug Control (animal license number: SCXK (Beijing) 2014-0013). Rats were kept in plastic cages (545 × 395 × 200 mm) with a maximum of five animals per cage under specific pathogen-free conditions in the Experimental Animal Center of the Institute of Basic Theory of Traditional Chinese Medicine [Experimental Animal Center license number: SYXK (Beijing) 2016-0021]. They were allowed to adapt to their environment for 7 days before experimentation initiation. Rats were housed in a room at 22°C ± 1°C with 45%–65% humidity under a 12-h light–dark cycle. They were provided with a normal chow diet and water *ad libitum*. The bodyweight of rats, water intake, and food consumption were assessed every week.

### Drugs

YSJB was provided by Nantong Liangchun Hospital of Traditional Chinese Medicine (Nantong, Jiangsu, China).

Estradiol valerate (EV) was obtained from Bayer Delpharm Lille (Lys-lez-Lannoy, France).

## Ovariectomy

Rats were divided randomly into a sham group and OVX group by body weight. Rats were anesthetized using pentobarbital sodium (45 mg/kg, i.p.) and bilateral ovaries were removed from rats in the OVX group. Through flank incisions, only the adipose tissue near the ovaries was cut in rats in the sham group. Regrettably, two rats died during ovariectomy. After 11 weeks, OVX rats were subjected to collection of vaginal secretions (from which atrophic patterns were noted upon creation of vaginal smears).

## Collagen-induced arthritis induction

Twelve weeks after ovariectomy, an emulsion for primary injection was prepared, as reported previously (Xiao et al., 2009). Briefly, bovine type-II collagen (Chondrex, Woodinville, WA, United States) was emulsified with an equal amount of incomplete Freund's adjuvant (Chondrex, Woodinville, WA, United States). Then, the emulsion (100 µg) was injected subcutaneously at the base of the tail of each rat. After 1 week, a secondary booster dose of 100 µg was given as the same preparation. The sham group received a subcutaneous injection of physiologic saline at the base of the tail. Arthritis severity was expressed as the arthritic index from 0 to four according to the following scale: 0, no signs of disease; 1, detectable arthritis with erythema in at least some digits; 2, significant redness and swelling; 3, severe redness and swelling from joint to digit; 4, maximal swelling with arthrokinesis. The maximum arthritic index score per rat was 8 (4 points × 2 hind paws).

## Experimental grouping

Fifteen days after primary immunization or the sham procedure, rats were divided randomly into five groups by the arthritic index score: sham ( $n = 12$ ); CIA ( $n = 15$ ); OVX + CIA ( $n = 13$ ); OVX + CIA + EV ( $n = 14$ ); OVX + CIA + YSJB ( $n = 14$ ).

Rats in the OVX + CIA + YSJB group and OVX + CIA + EV group were administered 1.29 g/kg d and 0.11 mg/kg d, respectively, of the drug *via* the oral route. The other groups were administered an equal volume of pure water (1 ml/100 g).

## Histology

Rats were killed under anesthesia by cervical dislocation 4 weeks after drug administration. The right ankle and knee

joints were dissected and fixed immediately in formalin for 7 days. The right joints were decalcified in 12.5% EDTA and embedded in paraffin. Tissue sections were stained with hematoxylin and eosin. The infiltration of cells into synovial tissue, cartilage, and bone damage was scored on a scale of 0–3 (0: absent; 1: weak; 2: moderate; 3: severe).

## Micro-computed tomography

The left hind paws and ankle joints were imaged and reconstructed into a three-dimensional (3D) structure using a micro-CT system (Skyscan 1174; Bruker, Billerica, MA, United States). The bone volume (BV) and bone surface (BS) of tarsal bones were analyzed to evaluate microstructural changes in bone. The BS/BV ratio was calculated to evaluate the surface density and focal erosion of periarticular bone.

## Tartrate resistant acid phosphatase staining

Sections of ankle joints were subjected to TRACP staining to identify osteoclastogenesis according to the instructions of a TRACP staining kit (MilliporeSigma, Burlington, MA, United States). TRACP<sup>+</sup> multinucleated cells containing ≥3 nuclei were counted as osteoclasts. Specimens were evaluated by Qwin<sup>TM</sup> (Leica Microsystems, Wetzlar, Germany).

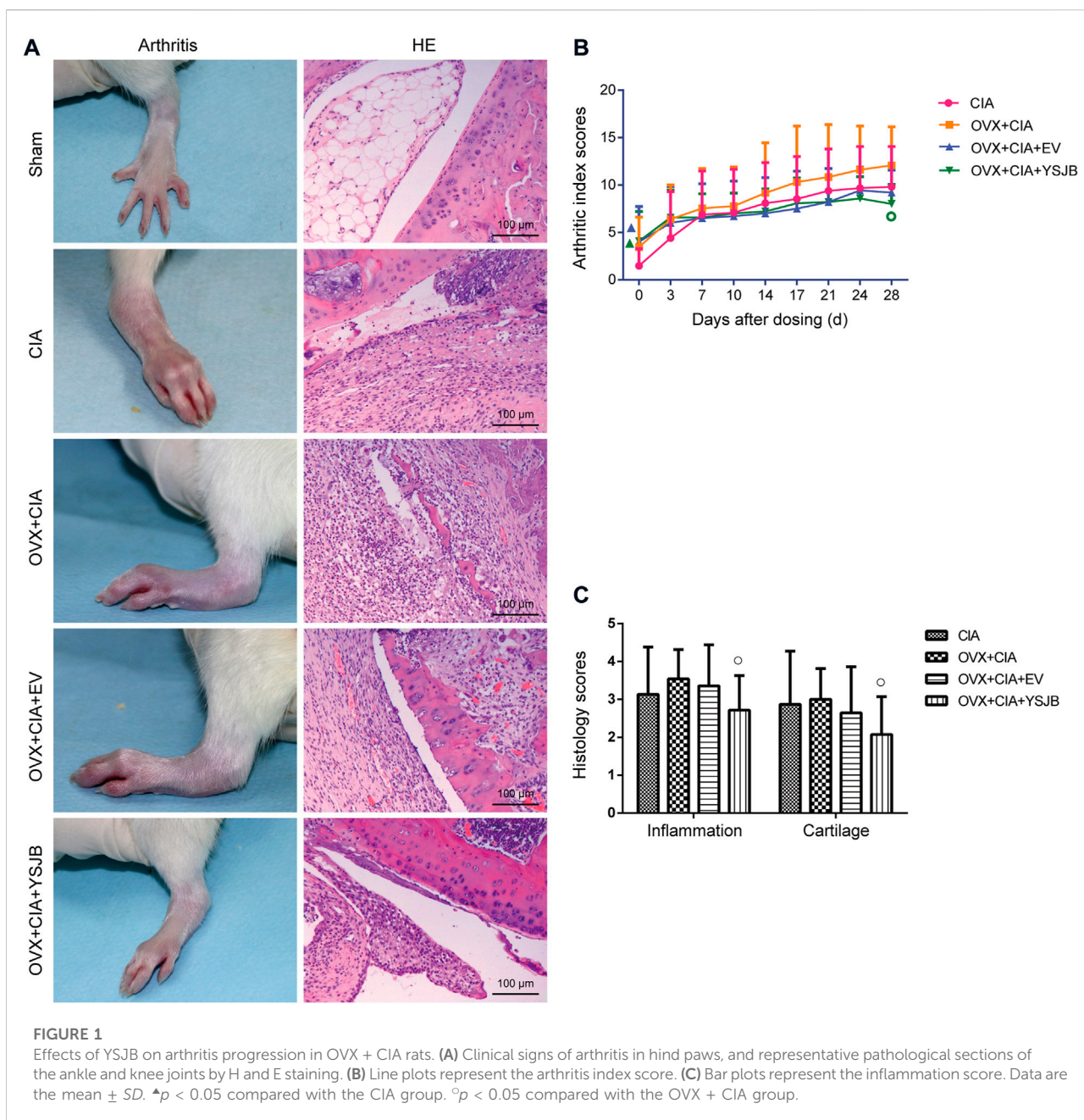
## Immunohistochemistry

EphrinB2, ephB4, and NFATc1 (Abcam, Cambridge, UK) were localized in ankle joints according to manufacturer's instructions. Paraffin sections were dewaxed using routine methods and treated overnight with primary antibodies against ephrinB2, ephB4, and NFATc1 for rats at 4°C. Then, specimens were incubated with poly-horseradish peroxidase anti-rabbit immunoglobulin (IgG) for 10 min at room temperature, stained with 3,3'-diaminobenzidine, and counterstained with hematoxylin. As a control, rabbit IgG isotype (1:100 dilution) was used instead of primary antibodies. Specimens were analyzed, and positive cells were counted using Qwin<sup>TM</sup> (Leica Microsystems).

## Statistical analyses

Data were analyzed using SPSS 20.0 (IBM, Armonk, NY, United States). Data are the mean ± SD. Results were compared using one-way ANOVA.  $p < 0.05$  was considered significant.





## Results

### YSJB reduces the arthritis index scores in OVX + CIA rats to prevent arthritis progression

CIA induced inflammation and swelling in the hind paws of rats. The sham group did not show an increasing arthritis index scores for paws. Ovariectomy tended to enhance the mean arthritis index scores for paws and aggravate the clinical signs of arthritis in comparison with CIA induction in rats [Figure 1A (left)]. YSJB

treatment lowered the arthritis index scores significantly compared with that in the OVX + CIA group [Figures 1A (left) and B].

Histology of the knee joints in the CIA group showed synovial hyperplasia, inflammatory-cell infiltration, cartilage damage, and bone erosion [Figure 1A (right)]. Ovariectomy tended to aggravate inflammatory-cell infiltration and damage to cartilage and bone compared with the CIA model (Figure 1C). We used semiquantitative grading scales to evaluate the influence of YSJB in inflamed joints: the histology scores were reduced significantly in comparison with those in the OVX + CIA group ( $p < 0.05$ ) (Figure 1C).



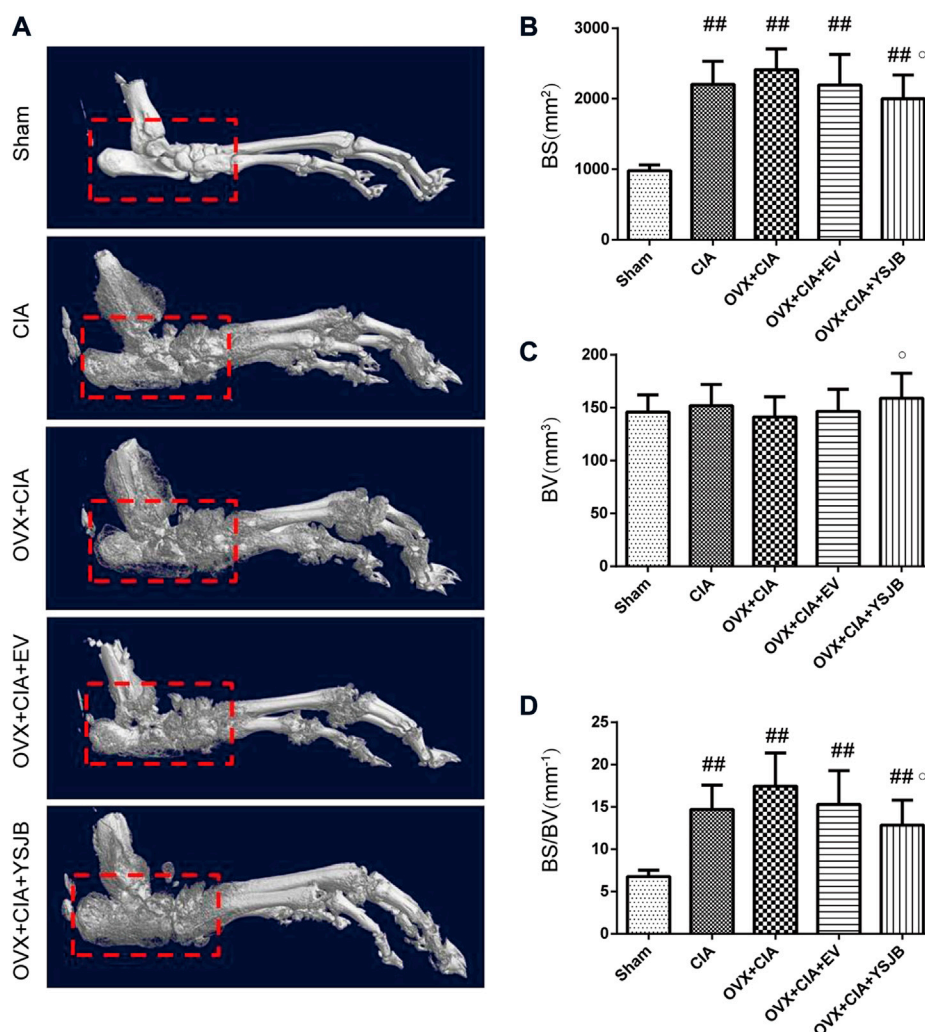


**FIGURE 2**

Micro-CT demonstrated that YSJB had a bone-protective effect on ankle joints. (A) Representative three-dimensional renditions of the ankle joint. (B–D) Bar plots of the bone surface, bone volume, and bone surface: bone volume ratio (BS/BV). Data are the mean  $\pm$  SD. <sup>#</sup> $p < 0.05$ , <sup>##</sup> $p < 0.01$  compared with the sham group. <sup>○</sup> $p < 0.05$  compared with the OVX + CIA group.

## YSJB ameliorates bone destruction in OVX + CIA rats

3D reconstructions based on micro-CT revealed the bone parameters of the hind paws and ankle joints. CIA induced bone destruction as quantified by BS (mm<sup>2</sup>), BV (mm<sup>3</sup>), and the BS/BV ratio (mm<sup>-1</sup>). The CIA, OVX + CIA, OVX + CIA + EV, and OVX + CIA + YSJB groups presented more severe bone damage than that in the sham group (Figure 2A), with significantly higher BS and the BS/BV ratio. The OVX + CIA + YSJB group had a markedly greater BV, but a reduction in BS and the BS/BV ratio, than those in the OVX + CIA group (Figure 2).

## YSJB reduced osteoclast differentiation in inflamed joints

Osteoclasts are the only cells involved in bone resorption. We used TRACP staining to observe osteoclast differentiation in the synovial membrane and BM (Figure 3A). TRACP<sup>+</sup> osteoclasts were absent in the synovial membrane of rats in the sham group, but the BM contained a few osteoclasts. Compared with the sham group, CIA with/without OVX increased osteoclast differentiation significantly in the synovial membrane and BM. However, only in the BM, the OVX + CIA group showed significantly more osteoclasts than the CIA group. Moreover, YSJB treatment reduced the number of osteoclasts significantly in

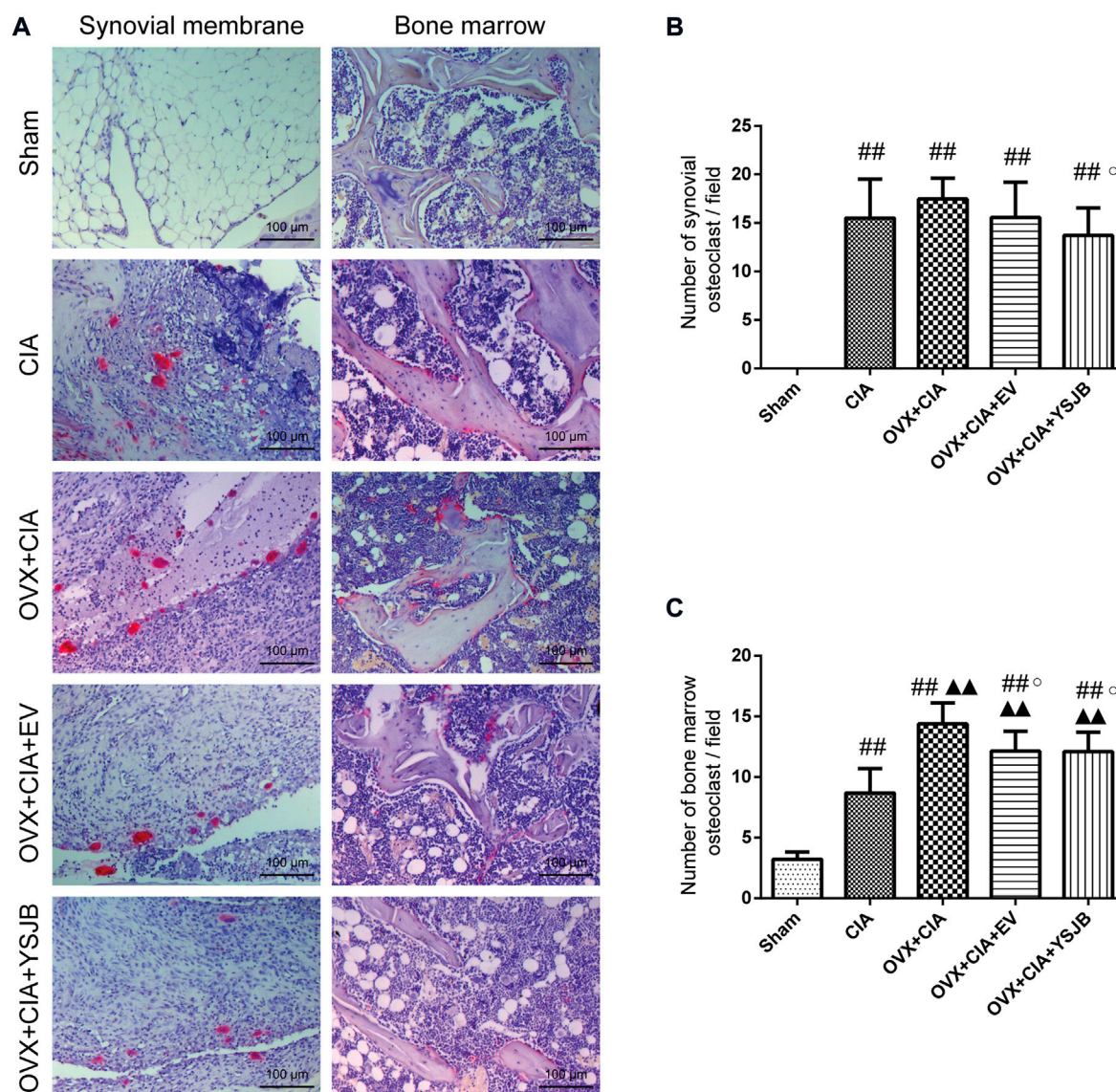


FIGURE 3

YSJB suppresses osteoclast differentiation in the synovial membrane and bone marrow of OVX + CIA rats. **(A)** Sections of ankle joints were stained with TRACP. **(B,C)** Evaluation of osteoclasts in the synovial membrane and bone marrow. Data are the mean  $\pm$  SD. # $p$  < 0.05, ## $p$  < 0.01 compared with the sham group. \* $p$  < 0.05, \*\* $p$  < 0.01 compared with the CIA group. ^ $p$  < 0.05, ^^ $p$  < 0.01 compared with the OVX + CIA group. ° $p$  < 0.05 compared with the OVX + CIA group.

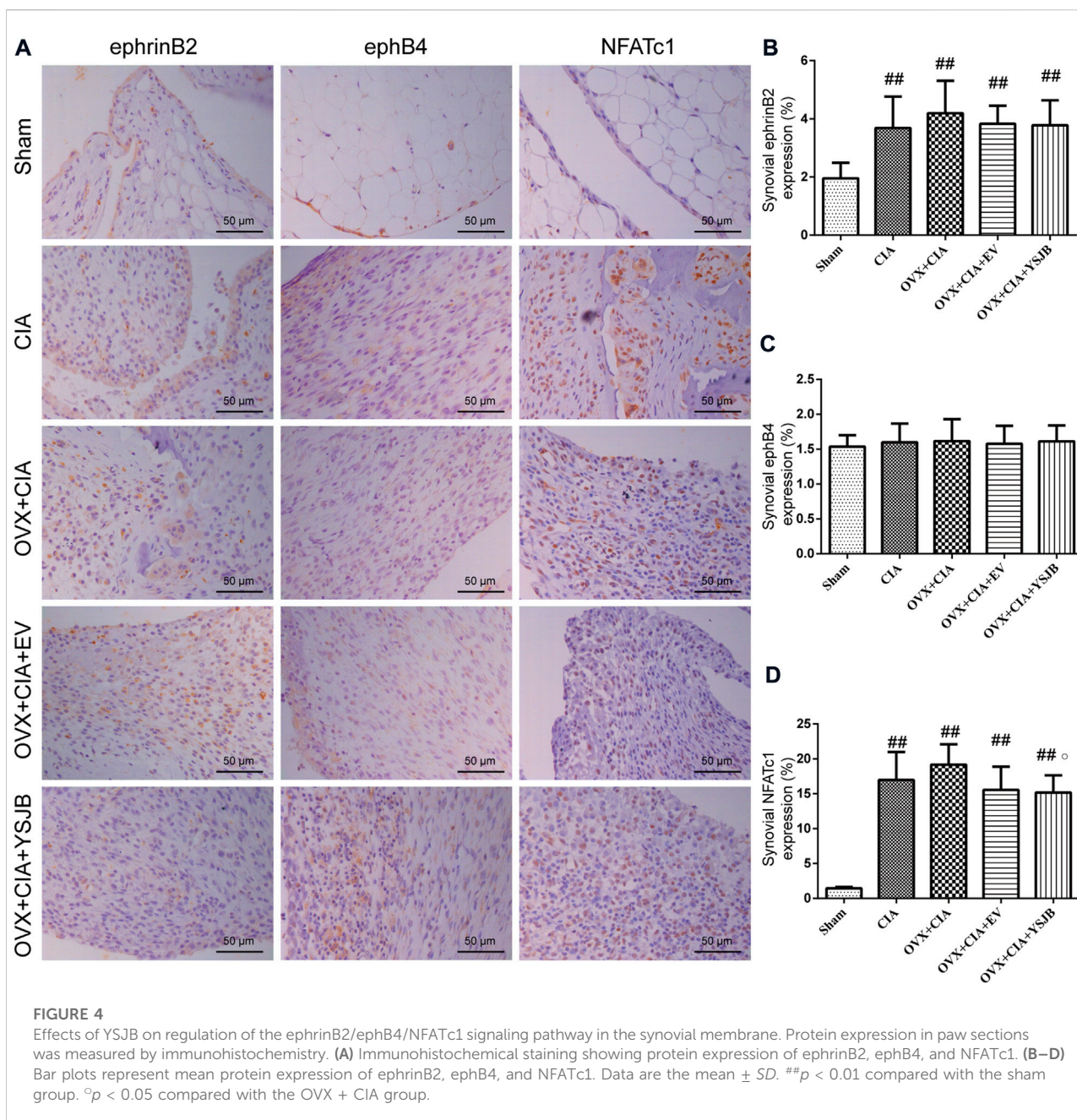
both regions, and EV treatment reduced only the number of osteoclasts in the BM (Figures 3B,C).

### Effects of YSJB on regulating the protein expression of ephrinB2, ephB4 and NFATc1 in the synovial membrane

We wished to ascertain if ephrinB2–ephB4 signaling was involved in the inhibitory effects of YSJB upon osteoclast differentiation. We measured the expression of ephrinB2 and

ephB4 as well as one osteoclastic transcription factor (NFATc1) in the synovium. Protein expression of ephrinB2, ephB4, and NFATc1 was measured in the synovial membrane of the joints by immunohistochemistry (Figure 4A). In the CIA, OVX + CIA, OVX + CIA + EV, and OVX + CIA + YSJB groups, the percentage of cells expressing ephrinB2 and NFATc1 was increased significantly (Figures 4B,D). In the synovial membrane, significant expression of ephrinB2 or NFATc1 was not observed in the EV group, but YSJB reduced NFATc1 expression significantly compared with that in the OVX + CIA group. No significant differences were found in ephB4 expression among groups (Figure 4C).



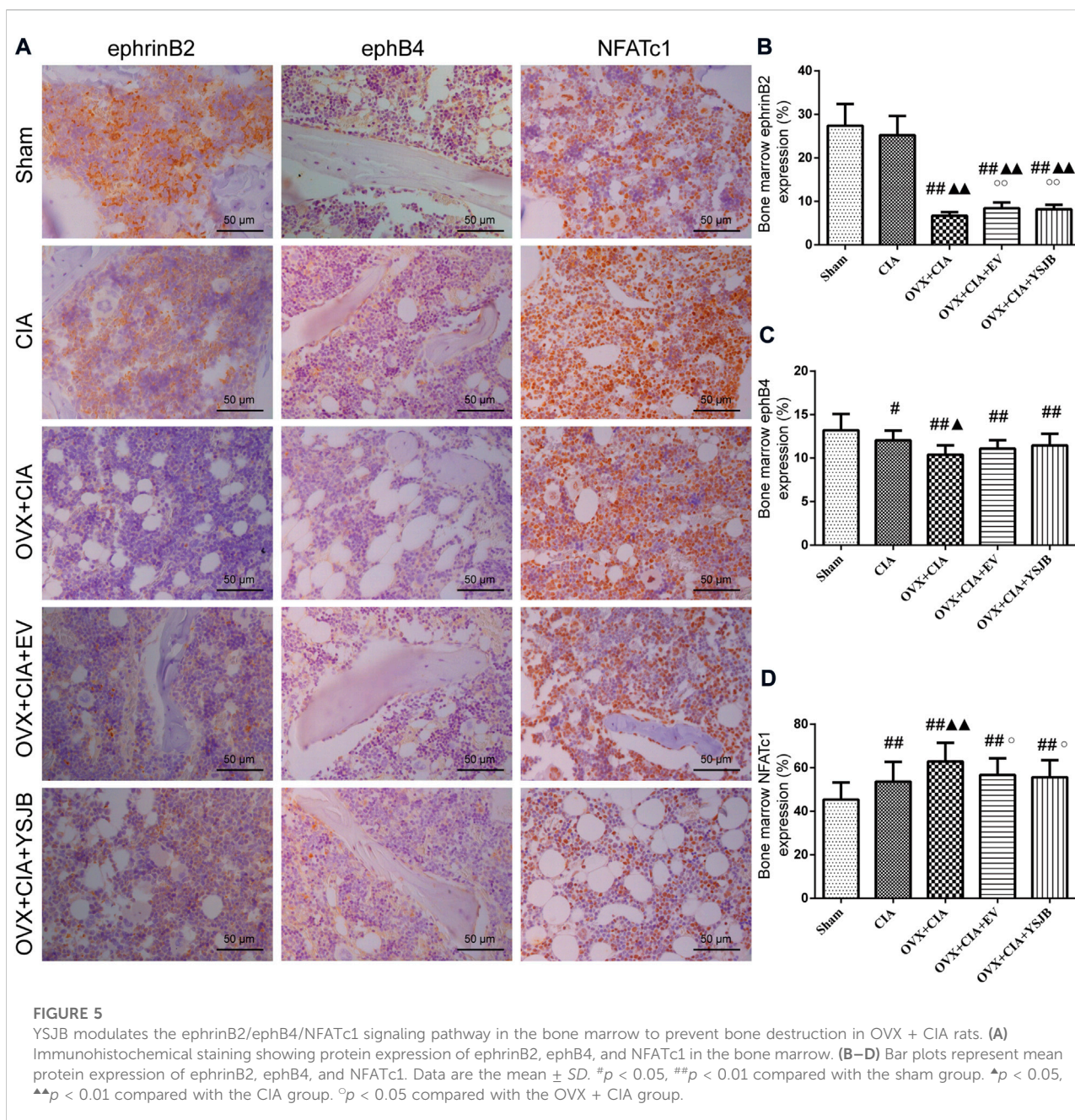


## YSJB regulates protein expression of ephrinB2 and NFATc1 in the BM

Based on the *in vivo* effects of YSJB upon osteoclast formation, we evaluated the effect of YSJB on regulation of the local protein expression of ephrinB2, ephB4, and NFATc1 in the BM (Figure 5A). In comparison with the sham group, the other four groups showed significantly downregulated ephB4 expression and upregulated NFATc1 expression in the BM. The OVX + CIA group, OVX + CIA + EV group, and OVX + CIA + YSJB group had reduced ephrinB2 expression compared with that in the sham group

(Figure 5B). The OVX + CIA + YSJB group, OVX + CIA + EV group, and OVX + CIA group had significantly downregulated expression of ephrinB2 compared with that in the CIA group. The OVX + CIA group showed lower ephB4 expression and higher NFATc1 expression than that in the CIA group in the BM. YSJB treatment and EV treatment increased ephrinB2 expression markedly, but also reduced NFATc1 expression significantly (Figures 5B,D). However, no significant differences were observed in ephB4 expression in the BM upon EV treatment or YSJB treatment when compared with that in the OVX + CIA group (Figure 5C).





## Discussion

We explored the protective effects of YSJB upon articular microstructure by inhibiting osteoclast differentiation in CIA rats under postmenopausal conditions. YSJB modulated protein expression of ephrinB2, ephB4, and NFATc1 in the synovial membrane and BM of OVX+CIA rats. Post-menopausal status in RA is related to considerable damage and disability, and early menopause is a risk factor for RA (Sammartano, 2012). Menopause is associated with worsening progression of functional decline. Women with RA during menopause had a worse disability of

function compared with women with RA before the menopause (Mollard et al., 2018).

Inflammatory arthritis in postmenopausal women may be a complex outcome associated with estrogen deficiency and the immune system (Sapir-Koren and Livshits, 2017). Epidemiological studies have suggested that RA incidence is increased in postmenopausal women, which may be associated with estrogen deficiency. Stojanovic et al. showed that postmenopausal women with RA had a prominent reduction in bone mineral density (Stojanovic et al., 2021). However, we did not observe significantly increased destruction of local bone in

OVX + CIA rats compared with CIA rats. Also, significant changes in the histology score were not observed in comparison with the CIA group, which could be attributed to the age of rats (the age at RA onset can affect the clinical picture and disease severity) (Banas et al., 2016). Heidari and Heidari (2014) concluded that BMD loss in postmenopausal-onset RA was not greater than that in premenopausal age-matched controls, which was possibly because the estrogen deficiency regulating immunologic reactions compensates for the negative effects of estrogen deprivation on bone mass in post-RA patients. The role of estrogen deficiency in RA progression has been explored in animal models in which OVX complicates CIA. A recent *in vivo* study indicated that ovariectomy upregulated the expression of inflammatory factors in CIA animals as well as aggravating erosion of trabecular bone (Ibáñez et al., 2011). Reduced estrogen levels during menopause can lead to the development of a proinflammatory pattern that leads to RA onset (Chakraborty et al., 2022).

Estrogen has been reported to delay arthritis progression and protect articular cartilage in rats suffering from arthritis (Engdahl et al., 2018; Li and Li, 2020; Hang et al., 2021), but hormone replacement may no longer be an option (Stubelius et al., 2011). EV has been used to treat and prevent osteoporosis in studies (Li et al., 2020; Petr, 2021). Early administration of EV can significantly inhibit expression of the markers of high bone turnover in surgically induced menopause in women (Vatrasreth et al., 2021). However, we showed that administration of EV (a sex hormone) elicited little protective effect upon RA progression.

YSJB has been shown to regulate inflammatory and immunomodulatory responses in experimental models of arthritis. Perera et al. (2010); Perera et al. (2011) reported that YSJB decreased prostaglandin levels and increased expression of the pro-apoptotic Bax in the synovium of adjuvant arthritis (AA) rats, and downregulated expression of tumor necrosis factor- $\alpha$ , interleukin (IL)-1 $\beta$  mRNA, and caspase-3 in synoviocytes. Previously, we showed that YSJB ameliorated bone loss and bone destruction in CIA rats, and that YSJB had a protective effect on the kidney deficiency induced by androgen deficiency in CIA rats (Zhao et al., 2012; Zhao et al., 2018). Here, we further explored the influence of YSJB on bone destruction in OVX + CIA rats as a model of premenopausal arthritis. YSJB treatment also reduced the histology score and arthritis index score of OVX + CIA rats by alleviating inflammatory-cell infiltration, cartilage and bone damage, and joint swelling. Moreover, YSJB exhibited a bone-protective effect according to micro-CT. Erosion of periarticular bone and bone destruction contribute considerably to RA pathogenesis. In RA, cartilage destruction accompanied by bone erosion in inflamed joints is related to increasing osteoclastogenesis. Osteoclasts are large, multinucleated, bone-resorbing cells derived from monocyte/macrophage progenitor cells. They

have key roles in the destruction and loss of bone. Their excessive resorption activities are involved in the bone destructive observed in RA (Nishioku et al., 2020).

We showed that upregulation of osteoclast formation leading to bone resorption could be enhanced by ovariectomy, and that osteoclasts were activated markedly after upregulation of the inflammatory response. Inflammation of synovial tissue is a common feature of RA: it causes pannus formation within a joint (leading to secondary articular cartilage and bone erosion) and results in irreversible joint damage and disability. Local inflammation is considered to increase osteoclast activity, which results in local bone loss (Prieto-Potin et al., 2015). Luukkonen et al. found that the proinflammatory stimulus of synovial fluid during RA drives monocyte differentiation towards osteoclastogenesis *in vitro* (Luukkonen et al., 2022). Perera et al. (2010); Perera et al. (2011) reported that YSJB decreased prostaglandin levels and increased expression of the pro-apoptotic Bax in the synovium of AA rats, and downregulated expression of TNF- $\alpha$ , IL-1 $\beta$  mRNA, and caspase-3 in synoviocytes. We observed osteoclast differentiation in synovial tissue. YSJB treatment to restore the upregulation of osteoclast numbers and expression of the essential osteoclastic transcription factor NFATc1 in the synovial membrane and BM of OVX + CIA group.

EphrinB2-ephB4 signaling has important regulatory roles in skeletal homeostasis *via* communication between osteoclasts and osteoblasts; ephrinB2 has a negative impact upon osteoclasts, whereas ephB4 has a positive effect on osteoblasts (Zhao et al., 2006). EphrinB2 ligand is expressed simultaneously on the osteoclast membranes and osteoblast membranes. It can be activated by the ephB4 receptor, which is expressed on the osteoblast membrane to inhibit osteoclast differentiation (Ge et al., 2020). Several studies have shown that ephrinB2 and ephB4 participate in various bone-related diseases (Shen et al., 2016; Valverde-Franco et al., 2016; Wu et al., 2016).

However, YSJB did not show a significantly altered effect on expression of ephrinB2 and ephB4 in synovial tissue. Kurowska et al. suggested that the BM should be taken into consideration when studying therapeutic interventions aimed at osteoclast activation in bone resorption in RA (Kurowska et al., 2021). Hence, we also, observed regulation of expression of ephrinB2 and ephB4 in the BM. Consistent with the findings of Kurowska et al. targeting osteoclasts in the BM may be efficacious treatment for postmenopausal inflammatory arthritis.

Variations in estrogen levels lead to differential regulation of protein expression, and their related signaling is directly/indirectly associated with RA pathogenesis. We found that expression of ephrinB2 and ephB4 was markedly lower in the BM, and that YSJB increased ephrinB2 expression significantly (but not ephB4 expression) in the BM. Osteoclasts in the BM were negatively correlated with ephrinB2 expression. In addition, we noted decreased expression of ephrinB2 and ephB4, but increased osteoclast differentiation and NFATc1 expression in the BM of rats



in the OVX + CIA group compared with the CIA group. Zhang et al. reported that enhancement of ephrinB2–ephrB4 signaling could inhibit osteoclastogenesis and prevent bone loss in OVX rats, and that knockdown of ephrinB2 expression reversed the inhibitory effect upon osteoclasts (Zhang et al., 2022). Huang et al. (2020) showed that modulating the balance of the ephB4–ephrinB2 axis could improve the characteristics of osteoporosis. EphB4–ephrinB2 signaling affects the osteoclastic factors RANK ligand/osteoprotegerin (Li et al., 2021). Differential outcomes of ephB4–ephrinB2 signaling may offer formidable challenges for the development of RA therapeutics. YSJB upregulated ephrinB2 expression significantly in the BM and downregulated NFATc1 expression in rats of OVX + CIA group. In this model of postmenopausal arthritis, YSJB administration improved arthritis progression and prevented bone destruction by reducing osteoclastogenesis and regulating the expression of ephrinB2, ephB4, and NFATc1 in the BM. Our results suggest that modulation by YSJB of ephrinB2 signaling in the BM (but not the synovium) ameliorates bone destruction in CIA. Further studies may characterize the precise mechanisms underlying the involvement of the ephrinB2–ephrB4 axis in the antiresorptive YSJB treatment of RA.

## Conclusion

YSJB exhibits a bone-protective effect and it may be a promising therapeutic strategy for alleviating bone destruction in arthritis under postmenopausal conditions. Moreover, one of the mechanisms is associated with the modulation of ephrinB2 signaling.

## Data availability statement

The raw data supporting the conclusions of this article will be made available by the corresponding author, without undue reservation.

## References

- Banas, T., Hajdyla-Banas, I., Pitynski, K., Nieweglowska, D., Juszczak, G., Ludwin, A., et al. (2016). Age at natural menopause in women on long-term methotrexate therapy for rheumatoid arthritis. *Menopause* 23 (10), 1130–1138. doi:10.1097/GME.0000000000000674
- Chakraborty, D., Sarkar, A., Mann, S., Agnihotri, P., Saquib, M., Malik, S., et al. (2022). Estrogen-mediated differential protein regulation and signal transduction in rheumatoid arthritis. *J. Mol. Endocrinol.* 69 (1), R25–r43. doi:10.1530/JME-22-0010
- Engdahl, C., Bondt, A., Harre, U., Raufer, J., Pfeifle, R., Camponeschi, A., et al. (2018). Estrogen induces St6gal1 expression and increases IgG sialylation in mice and patients with rheumatoid arthritis: A potential explanation for the increased risk of rheumatoid arthritis in postmenopausal women. *Arthritis Res. Ther.* 20 (1), 84. doi:10.1186/s13075-018-1586-z
- Ge, Y. W., Feng, K., Liu, X. L., Chen, H. F., Sun, Z. Y., Wang, C. F., et al. (2020). The recombinant protein EphB4-fc changes the T<sub>H</sub>1 particle-mediated imbalance of OPG/RANKL via EphrinB2/EphB4 signaling pathway and inhibits the release of

## Ethics statement

The animal study was reviewed and approved by Institute of Basic Theory of Traditional Chinese Medicine, China Academy of Chinese Medical Sciences.

## Author contributions

HX drafted the manuscript and conducted the experiments. LT analyzed the data and participated in discussions. JC participated in experiments. PZ and HZ revised the manuscript. HZ designed the manuscript and formulated the concept. All authors approved the final version of the manuscript.

## Funding

This study was supported by the National Natural Science Foundation of China (82074299).

## Conflict of interest

The authors declare that the research was conducted in the absence of any commercial or financial relationships that could be construed as a potential conflict of interest.

## Publisher's note

All claims expressed in this article are solely those of the authors and do not necessarily represent those of their affiliated organizations, or those of the publisher, the editors and the reviewers. Any product that may be evaluated in this article, or claim that may be made by its manufacturer, is not guaranteed or endorsed by the publisher.

proinflammatory factors *in vivo*. *Oxid. Med. Cell. Longev.* 2020, 1404915. doi:10.1155/2020/1404915

Hang, X., Zhang, Z., Niu, R., Wang, C., Yao, J., Xu, Y., et al. (2021). Estrogen protects articular cartilage by downregulating ASIC1a in rheumatoid arthritis. *J. Inflamm. Res.* 14, 843–858. doi:10.2147/JIR.S295222

Heidari, B., and Heidari, P. (2014). Bone mineral density loss in postmenopausal onset rheumatoid arthritis is not greater than premenopausal onset disease. *Casp. J. Intern. Med.* 5 (4), 213–218.

Huang, M., Wang, Y., and Peng, R. (2020). Icaritin alleviates glucocorticoid-induced osteoporosis through EphB4/ephrin-B2 Axis. *Evid. Based. Complement. Altern. Med.* 2020, 2982480. doi:10.1155/2020/2982480

Ibáñez, L., Alcaraz, M. J., Maicas, N., Guede, D., Caeiro, J. R., Koenders, M. I., et al. (2011). Up-regulation of the inflammatory response by ovariectomy in collagen-induced arthritis. effects of tin protoporphyrin IX. *J. Inflamm.* 34 (6), 585–596. doi:10.1007/s10753-010-9266-4

- Kim, J. S., Choi, M., Choi, J. Y., Kim, J. Y., Song, J. S., et al. (2020). Implication of the association of fibrinogen citrullination and osteoclastogenesis in bone destruction in rheumatoid arthritis. *J. Cells* 9 (12), E2720. doi:10.3390/cells9122720
- Kurowska, W., Slowinska, I., Krogulec, Z., Syrowka, P., and Maslinski, W. (2021). Antibodies to citrullinated proteins (ACPA) associate with markers of osteoclast activation and bone destruction in the bone marrow of patients with rheumatoid arthritis. *J. Clin. Med.* 10 (8), 1778. doi:10.3390/jcm10081778
- Kvien, T. K., Uhlig, T., Ødegård, S., and Heiberg, M. S. (2006). Epidemiological aspects of rheumatoid arthritis: The sex ratio. *Ann. N. Y. Acad. Sci.* 1069, 212–222. doi:10.1196/annals.1351.019
- Li, S., Cong, C., Liu, Y., Liu, X., Kluwe, L., Shan, X., et al. (2020). Tiao Geng decoction for treating menopausal syndrome exhibits anti-aging effects likely via suppressing ASK1/MKK7/JNK mediated apoptosis in ovariectomized rats. *J. Ethnopharmacol.* 261, 113061. doi:10.1016/j.jep.2020.113061
- Li, T., Wang, H., Liu, R., Wang, X., Huang, L., Wu, Z., et al. (2021). The role of EphB4/ephrinB2 signaling in root repair after orthodontically-induced root resorption. *Am. J. Orthod. Dentofac. Orthop.* 159 (3), e217–e232. doi:10.1016/j.ajodo.2020.07.035
- Li, X., and Li, M. (2020). Estrogen downregulates TAK1 expression in human fibroblast-like synoviocytes and in a rheumatoid arthritis model. *Exp. Ther. Med.* 20 (2), 1764–1769. doi:10.3892/etm.2020.8848
- Liu, H., Zhu, Y., Gao, Y., Qi, D., Zhao, L., Zhao, L., et al. (2020). NR1D1 modulates synovial inflammation and bone destruction in rheumatoid arthritis. *Cell Death Dis.* 11 (2), 129. doi:10.1038/s41419-020-2314-6
- Luukkainen, J., Huhtakangas, J., Palosaari, S., Tuukkanen, J., Vuolteenaho, O., and Lehenkari, P. (2022). Preliminary report: Osteoarthritis and rheumatoid arthritis synovial fluid increased osteoclastogenesis *in vitro* by monocyte differentiation pathway regulating cytokines. *Mediat. Inflamm.* 2022, 2606916. doi:10.1155/2022/2606916
- Matsuo, K. (2010). Eph and ephrin interactions in bone. *Adv. Exp. Med. Biol.* 658, 95–103. doi:10.1007/978-1-4419-1050-9\_10
- Matsuo, K., and Otaki, N. (2012). Bone cell interactions through eph/ephrin: Bone modeling, remodeling and associated diseases. *Cell adhesion. Migr.* 6 (2), 148–156. doi:10.4161/cam.20888
- Mollard, E., Pedro, S., Chakravarty, E., Clowse, M., Schumacher, R., and Michaud, K. (2018). The impact of menopause on functional status in women with rheumatoid arthritis. *Rheumatol. Oxf.* 57 (5), 798–802. doi:10.1093/rheumatology/kex526
- Nishioku, T., Kawamoto, M., Okizono, R., Sakai, E., Okamoto, K., and Tsukuba, T. (2020). Dimethyl fumarate prevents osteoclastogenesis by decreasing NFATc1 expression, inhibiting of erk and p38 MAPK phosphorylation, and suppressing of HMGB1 release. *Biochem. Biophys. Res. Commun.* 530 (2), 455–461. doi:10.1016/j.bbrc.2020.05.088
- Pennell, L. M., Galligan, C. L., and Fish, E. N. (2012). Sex affects immunity. *J. Autoimmun.* 38 (2–3), J282–J291. doi:10.1016/j.jaut.2011.11.013
- Perera, P. K., Li, Y., Peng, C., Fang, W., and Han, C. (2010). Immunomodulatory activity of a Chinese herbal drug Yi Shen Juan Bi in adjuvant arthritis. *Indian J. Pharmacol.* 42 (2), 65–69. doi:10.4103/0253-7613.64489
- Perera, P. K., Peng, C., Xue, L., Li, Y., and Han, C. (2011). *Ex vivo* and *in vivo* effect of Chinese herbal pill Yi Shen Juan Bi (YJB) on experimental arthritis. *J. Ethnopharmacol.* 134 (1), 171–175. doi:10.1016/j.jep.2010.11.065
- Petr, K. (2021). Estetrol and the possibilities of its clinical use[J]. *Ceska Gynekol.* 86 (3), 217–221. doi:10.48095/ccgc2021217
- Prieto-Potin, I., Largo, R., Roman-Blas, J. A., Herrero-Beaumont, G., and Walsh, D. A. (2015). Characterization of multinucleated giant cells in synovium and subchondral bone in knee osteoarthritis and rheumatoid arthritis. *BMC Musculoskelet. Disord.* 16, 226. doi:10.1186/s12891-015-0664-5
- Romanovsky, A. A. (2006). Microsomal prostaglandin E synthase-1, ephrins, and ephrin kinases as suspected therapeutic targets in arthritis: Exposed by "criminal profiling". *Ann. N. Y. Acad. Sci.* 1069, 183–194. doi:10.1196/annals.1351.016
- Sammaritano, L. R. (2012). Menopause in patients with autoimmune diseases. *Autoimmun. Rev.* 11 (6–7), A430–A436. doi:10.1016/j.autrev.2011.11.006
- Sapir-Koren, R., and Livshits, G. (2017). Postmenopausal osteoporosis in rheumatoid arthritis: The estrogen deficiency-immune mechanisms link. *Bone* 103, 102–115. doi:10.1016/j.bone.2017.06.020
- Shah, L., Elshaikh, A. O., Lee, R., Joy Mathew, C., Jose, M. T., and Cancarevic, I. (2020). Do menopause and aging affect the onset and progression of rheumatoid arthritis and systemic lupus erythematosus? *J. Cureus* 12 (10), e10944. doi:10.7759/cureus.10944
- Shen, L. L., Zhang, L. X., Wang, L. M., Zhou, R. J., Yang, C. Z., Zhang, J., et al. (2016). Disturbed expression of EphB4, but not EphrinB2, inhibited bone regeneration in an *in vivo* inflammatory microenvironment[J]. *Mediat. Inflamm.* 2016, 6430407. doi:10.1155/2016/6430407
- Stojanovic, A., Veselinovic, M., Draginic, N., Rankovic, M., Andjic, M., Bradic, J., et al. (2021). The influence of menopause and inflammation on redox status and bone mineral density in patients with rheumatoid arthritis. *Oxid. Med. Cell. Longev.* 2021, 9458587. doi:10.1155/2021/9458587
- Stubelius, A., Andréasson, E., Karlsson, A., Ohlsson, C., Tivesten, A., Islander, U., et al. (2011). Role of 2-methoxyestradiol as inhibitor of arthritis and osteoporosis in a model of postmenopausal rheumatoid arthritis. *Clin. Immunol.* 140 (1), 37–46. doi:10.1016/j.clim.2011.03.006
- Tazaki, Y., Sugitani, K., Ogai, K., Kobayashi, I., Kawasaki, H., Aoyama, T., et al. (2018). RANKL, Ephrin-Eph and Wnt10b are key intercellular communication molecules regulating bone remodeling in autologous transplanted goldfish scales. *Comp. Biochem. Physiol. A Mol. Integr. Physiol.* 225, 46–58. doi:10.1016/j.cbpa.2018.06.011
- Valverde-Franco, G., Lussier, B., Hum, D., Wu, J., Hamadjida, A., Dancause, N., et al. (2016). Cartilage-specific deletion of ephrin-B2 in mice results in early developmental defects and an osteoarthritis-like phenotype during aging *in vivo*. *Arthritis Res. Ther.* 18, 65. doi:10.1186/s13075-016-0965-6
- van der Woude, D., and van der Helm-van Mil, A. H. M. (2018). Update on the epidemiology, risk factors, and disease outcomes of rheumatoid arthritis. *Best. Pract. Res. Clin. Rheumatol.* 32 (2), 174–187. doi:10.1016/j.berh.2018.10.005
- Vatrasresth, J., Suwan, A., and Panyakhamlerd, K. (2021). Effects of early estradiol valerate administration on bone turnover markers in surgically induced menopausal women. *BMC Womens Health* 21 (1), 363. doi:10.1186/s12905-021-01508-w
- Wallenius, M., Skomsvoll, J. F., Koldingsnes, W., Rodevand, E., Mikkelsen, K., Kaufmann, C., et al. (2009). Comparison of work disability and health-related quality of life between males and females with rheumatoid arthritis below the age of 45 years. *Scand. J. Rheumatol.* 38 (3), 178–183. doi:10.1080/03009740802400594
- Wu, M., Ai, W., Chen, L., Zhao, S., and Liu, E. (2016). Bradykinin receptors and EphB2/EphrinB2 pathway in response to high glucose-induced osteoblast dysfunction and hyperglycemia-induced bone deterioration in mice. *Int. J. Mol. Med.* 37 (3), 565–574. doi:10.3892/ijmm.2016.2457
- Xia, Y., Fan, D., Li, X., Lu, X., Ye, Q., Xi, X., et al. (2021). Yi shen juan Bi pill regulates the bone immune microenvironment via the JAK2/STAT3 signaling pathway *in vitro*. *Front. Pharmacol.* 12, 746786. doi:10.3389/fphar.2021.746786
- Xiao, C., Zhou, J., He, Y., Jia, H., Zhao, L., Zhao, N., et al. (2009). Effects of triptolide from radix tripterygium wilfordii (leigongteng) on cartilage cytokines and transcription factor NF-kappaB: A study on induced arthritis in rats. *Chin. Med.* 4, 13. doi:10.1186/1749-8546-4-13
- Zhang, Y., Kou, Y., Yang, P., Rong, X., Tang, R., Liu, H., et al. (2022). ED-71 inhibited osteoclastogenesis by enhancing EphrinB2-EphB4 signaling between osteoclasts and osteoblasts in osteoporosis. *Cell. Signal.* 96, 110376. doi:10.1016/j.cellsig.2022.110376
- Zhao, C., Irie, N., Takada, Y., Shimoda, K., Miyamoto, T., Nishiwaki, T., et al. (2006). Bidirectional ephrinB2-EphB4 signaling controls bone homeostasis. *Cell Metab.* 4 (2), 111–121. doi:10.1016/j.cmet.2006.05.012
- Zhao, H., Li, J., He, X., Lu, C., Xiao, C., Niu, X., et al. (2012). The protective effect of yi shen juan bi pill in arthritic rats with castration-induced kidney deficiency. *Evid. Based. Complement. Altern. Med.* 2012, 102641. doi:10.1155/2012/102641
- Zhao, H., Xu, H., Zuo, Z., Wang, G., Liu, M., Guo, M., et al. (2018). Yi shen juan Bi pill ameliorates bone loss and destruction induced by arthritis through modulating the balance of cytokines released by different subpopulations of T cells. *Front. Pharmacol.* 9, 262. doi:10.3389/fphar.2018.00262



## OPEN ACCESS

## EDITED BY

Dongwei Zhang,  
Beijing University of Chinese Medicine,  
China

## REVIEWED BY

Lei Wan,  
Guangzhou University of Chinese  
Medicine, China  
Liu Haiquan,  
Huizhou Hospital of Guangzhou  
University of Chinese Medicine, China  
Dongfeng Zhao,  
Shanghai University of Traditional  
Chinese Medicine, China

## \*CORRESPONDENCE

Kang Liu,  
liukang1982@163.com  
Xiao-Lin Shi,  
xlshi-2002@163.com

<sup>†</sup>These authors have contributed equally  
to this work and share the first  
authorship

## SPECIALTY SECTION

This article was submitted to  
Experimental Pharmacology and Drug  
Discovery,  
a section of the journal  
Frontiers in Pharmacology

RECEIVED 15 July 2022

ACCEPTED 20 September 2022

PUBLISHED 11 October 2022

## CITATION

Yuan Y-F, Wang S, Zhou H, Tang B-B,  
Liu Y, Huang H, He C-J, Chen T-P,  
Fang M-H, Liang B-C, Mao Y-D-L,  
Qie F-Q, Liu K and Shi X-L (2022),  
Exploratory study of sea buckthorn  
enhancing QiangGuYin efficacy by  
inhibiting CKIP-1 and Notum activating  
the Wnt/ $\beta$ -catenin signaling pathway  
and analysis of active ingredients by  
molecular docking.  
*Front. Pharmacol.* 13:994995.  
doi: 10.3389/fphar.2022.994995

## COPYRIGHT

© 2022 Yuan, Wang, Zhou, Tang, Liu,  
Huang, He, Chen, Fang, Liang, Mao, Qie,  
Liu and Shi. This is an open-access  
article distributed under the terms of the  
[Creative Commons Attribution License  
\(CC BY\)](https://creativecommons.org/licenses/by/4.0/). The use, distribution or  
reproduction in other forums is  
permitted, provided the original  
author(s) and the copyright owner(s) are  
credited and that the original  
publication in this journal is cited, in  
accordance with accepted academic

# Exploratory study of sea buckthorn enhancing QiangGuYin efficacy by inhibiting CKIP-1 and Notum activating the Wnt/ $\beta$ -catenin signaling pathway and analysis of active ingredients by molecular docking

Yi-Feng Yuan<sup>1†</sup>, Shen Wang<sup>1†</sup>, Hang Zhou<sup>1†</sup>, Bin-Bin Tang<sup>1,2†</sup>,  
Yang Liu<sup>1</sup>, Hai Huang<sup>1</sup>, Cai-Jian He<sup>1</sup>, Tian-Peng Chen<sup>1</sup>,  
Mou-Hao Fang<sup>1</sup>, Bo-Cheng Liang<sup>2</sup>, Ying-De-Long Mao<sup>2</sup>,  
Feng-Qin Qie<sup>3</sup>, Kang Liu<sup>2\*</sup> and Xiao-Lin Shi<sup>2\*</sup>

<sup>1</sup>The Second School of Clinical Medicine, Zhejiang Chinese Medical University, Hangzhou, China, <sup>2</sup>The Second Affiliated Hospital of Zhejiang Chinese Medical University (Xinhua Hospital of Zhejiang Province), Hangzhou, China, <sup>3</sup>Yushi Health Research Institute, Tokyo, Japan

**Background:** Sea buckthorn (SBT) is a traditional Chinese medicine (TCM), rich in calcium, phosphorus, and vitamins, which can potentially prevent and treat osteoporosis. However, no research has been conducted to confirm these hypotheses. QiangGuYin (QGY) is a TCM compound used to treat osteoporosis. There is a need to investigate whether SBT enhances QGY efficacy.

**Objectives:** The aim of this study was to explore whether SBT enhances QGY efficacy by inhibiting CKIP-1 and Notum expression through the Wnt/ $\beta$ -catenin pathway. The study also aimed to explore the active components of SBT.

**Methods:** Experimental animals were divided into control, model, QGY, SBT, SBT + *Eucommia ulmoides* (EU), and SBT + QGY groups. After treatment, bone morphometric parameters, such as estrogen, PINP, and S-CTX levels, and Notum, CKIP-1, and  $\beta$ -catenin expression were examined. Screening of SBT active components was conducted by molecular docking to obtain small molecules that bind Notum and CKIP-1.

**Results:** The results showed that all the drug groups could elevate the estrogen, PINP, and S-CTX levels, improve femoral bone morphometric parameters, inhibit Notum and CKIP-1 expression, and promote  $\beta$ -catenin expression. The effect of SBT + EU and SBT + QGY was superior to the others. Molecular docking identified that SBT contains seven small molecules (folic acid, rhein, quercetin, kaempferol, mandenol, isorhamnetin, and ent-epicatechin) with potential effects on CKIP-1 and Notum.

**Conclusion:** SBT improves bone morphometric performance in PMOP rats by inhibiting CKIP-1 and Notum expression, increasing estrogen levels, and

activating the Wnt/ $\beta$ -catenin signaling pathway. Furthermore, SBT enhances the properties of QGY. Folic acid, rhein, quercetin, kaempferol, mandenol, isorhamnetin, and ent-epicatechin are the most likely active ingredients of SBT. These results provide insight into the pharmacological mechanisms of SBT in treating osteoporosis.

#### KEYWORDS

sea buckthorn, postmenopausal osteoporosis, Notum, CKIP-1, Wnt/ $\beta$ -catenin signaling pathway, molecular docking, QiangGuYin

## Introduction

Postmenopausal osteoporosis (PMOP) is the most common type of osteoporosis in women within 5–10 years of menopause and is characterized by estrogen deficiency, decreased bone mineral density, and impaired bone quality. PMOP is similar to primary osteoporosis regarding the imbalance in bone metabolism and a bias toward heightened bone resorption activity. Unique PMOP characteristics include a high bone turnover rate, that is, a high turnover type of bone metabolism. After the completion of each bone turnover, the residual resorption lacunae and unmineralized new bone exponentially increase in the high turnover state, and the corresponding indexes of bone metabolism also rise. QiangGuYin (QGY) is a compound developed by Prof. Xiaolin Shi to treat PMOP and is patented in China (Patent No. ZL200610053058.8). Several clinical studies have confirmed the efficacy of QGY in treating PMOP. QGY is highly effective in elevating bone mineral density, reducing the risk of falling, and alleviating osteoporotic pain (Shi, Liu, and Li, 2007; Shi et al., 2008, 2017; Xiao et al., 2019; Li et al., 2021; Mao et al., 2021; Hui et al., 2022). Herein, we evaluated the clinical efficacy of QGY for PMOP and hope to further enhance its efficacy.

Sea buckthorn (SBT) is a spiny nitrogen-fixing deciduous shrub cultivated worldwide for its nutritional and medicinal values. Fruits, seeds, and other parts of SBT are rich in vitamins A, B1, B12, C, E, K, and P, flavonoids, lycopene, carotenoids, and plant sterols. SBT is therapeutically important because it is rich in potent antioxidant substances. These molecules possess antioxidant, anticoagulant, anticancer, wound healing, anti-inflammatory, and radioprotective properties (Suryakumar and Gupta, 2011; Patel et al., 2012). Among them, antioxidant and anti-inflammatory effects inhibit or alleviate PMOP. Studies showed that SBT fatty acids significantly increase serum estrogen, insulin-like growth factor (IGF), transforming growth factor (TGF) levels, trabecular number, cortical bone thickness, and maximum bone stress resistance and improve the bone density in old female rats (Liu, Yuan, Guo, Wei, Zhao, Chen, et al., 2006; Liu, Yuan, Guo, Wei, Zhao, Kang, et al., 2006). Therefore, SBT has considerable potential in treating osteoporosis, and its efficacy, mechanism of action, and active ingredients

should be explored. At the same time, we explored whether SBT can enhance the efficacy of QGY.

Our previous study found that CKIP-1 regulates bone metabolism (Liu et al., 2018; Yang et al., 2018) and that QGY acts as an anti-osteoporosis agent by inhibiting CKIP-1 and Akt binding in osteoblasts, activating the Akt/mTOR signaling pathway, inhibiting cellular autophagy, promoting osteogenic differentiation, and promoting osteoporosis (Yuan et al., 2022). QGY also influences osteoblast differentiation through the Wnt/ $\beta$ -catenin pathway by affecting the expression of related miRNAs in the exostome of osteoclasts (Tang et al., 2020). Notum is a carboxyl esterase that catalyzes the deacetylation and inactivation of Wnts by inhibiting the Wnt signaling pathway (Kakugawa et al., 2015; Zhang et al., 2015). Therefore, animal experiments were used in this study to investigate the efficacy of SBT in treating PMOP and augmenting the efficacy of QGY. The mechanism through which SBT exerts its effect was also explored. The main active components in SBT that mediate its effects were identified by molecular docking.

## Materials and methods

### Ethics statement

The protocol for this study was approved by the Laboratory Animal Management and Ethics Committee of Zhejiang Chinese Medical University (Approval Number: IACUC-20220613-01). All animal experiments were conducted in accordance with the Guidelines for the Care and Use of NIH Laboratory Animals (NIH Publication No. 80–23, revised in 1978).

### Experimental animals

Mature female Sprague–Dawley (SD) rats ( $n = 34$ , 6 ~ 8-week-old,  $200 \pm 20$  g in weight) were purchased from the Experimental Animal Center of Hangzhou Medical College (production license no. SCXK 2019–0002, Hangzhou, China) and were provided with enough food and water. The rats were reared in a specific pathogen-free room at 20–25°C, with a relative humidity of  $60 \pm 5\%$ , and 12 h light/dark cycle.



## Preparation of medicines

SBT, *Eucommia ulmoides* (EU), and QGY were purchased from the Pharmaceutical Preparation Center of the Second Affiliated Hospital of Zhejiang Chinese Medical University. Each preparation was a 22.2 ml formulation containing a different combination of drugs. The SBT group is composed of 20 g of SBT, and the SBT + EU group comprised 20 g of SBT and 10 g of EU. The QGY group comprised 245 g of crude drugs, including 30 g of Astragali Radix, 30 g of Dipsaci Radix, 25 g of Lonicerae Japonicae Caulis, 25 g of Spatholobi Caulis, 20 g of Drynariae Rhizoma, 20 g of Chuanxiong Rhizoma, 20 g of Cervi Cornu Degelatinatum, 20 g of Vespae Nidus, 15 g of *Eucommia ulmoides*, 15 g of Gentianae Macrophyllae Radix, 15 g of Saposhnikovia Radix, and 10 g of Cinnamomi Cortex. The SBT + QGY group comprised 245 g of the crude drugs and 20 g of SBT.

## Grouping and treatment

A total of 34 rats were randomly divided into six groups: 1) control group (n = 4); 2) model group (n = 6); 3) SBT group (n = 6); 4) SBT + EU group (n = 6); 5) SBT + QGY group (n = 6); and 6) QGY group (n = 6). Except for the control group, all the other groups underwent bilateral oophorectomy. The rats were acclimatized for 10 weeks before receiving the treatments.

The corresponding drug was administered by gavage at a dose of 10 ml/kg twice daily. The rats in the normal control group and model group received physiological saline. The treatments lasted 6 weeks, after which the right femur bones of mice in each group were extracted for a micro-CT scan.

## Histomorphometric analysis

The rats were scanned from the hip region to the limb using an animal X-ray imaging system (Mikasa X-ray HF100HA, Mikasa, Japan) to measure the hip bone width and obtain macroscopic imaging of the lower limbs. Bone tissue analysis was conducted using a micro-CT imaging system (Micro-CT  $\mu$ CT100, SCANCO Medical, Sweden). The right femur sample was scanned at 14.8  $\mu$ m resolution. Trabecular bone regions of interest were selected for three-dimensional reconstruction. The parameters measured using the reconstructed images include bone mineral density (BMD), connectivity density (Conn.D.), bone mineral content (BMC), trabecular thickness (Tb.Th), trabecular number (Tb.N), bone volume fraction (BV/TV), and trabecular separation (Tb.Sp), which reflected the internal microarchitecture of the femur.

## Western blot analysis

To evaluate the effect of each drug on the expression of Notum and CKIP-1 and the regulation of the Wnt/ $\beta$ -catenin signaling pathway, the bone marrow of the right tibia was analyzed by Western blotting. The antibodies used include Notum (Notum rabbit antibody, dilution 1:1,000, Proteintech, Chicago, United States), CKIP-1 (CKIP-1 rabbit antibody, dilution 1:1,000, Proteintech, Chicago, United States), and  $\beta$ -catenin ( $\beta$ -catenin rabbit antibody, dilution 1:1,000, Proteintech, Chicago, United States). The mean normalized protein expression  $\pm$ S.D. was calculated from independent experiments. GAPDH (GAPDH polyclonal antibody, dilution 1:10,000, Proteintech, Chicago, United States) was used as the internal control.

## ELISA analysis

The estrogen level, bone turnover markers, C-terminal cross-linking telopeptide of type I collagen (S-CTX), and pro-collagen type I N-terminal propeptide (PINP) in the orbital blood of rats were measured using enzyme-linked immunosorbent assay (ELISA) analysis.

## Molecular docking of sea buckthorn

### Platform and software

Computational simulation and data processing were conducted using the Microsoft Windows 10 Professional operating system, whereas BIOVIA Discovery Studio 2019 (DS) was used for molecular docking research. Default settings were used except where specified.

## Receptor protein preparation

Notum (PDB ID: 4UZQ) and CKIP-1 (PDB ID: 3AA1) protein crystal models were derived from human-derived protein crystallization in the PDB database (<http://www.rcsb.org>). The amino acid sequences and protein space models of 4UZQ and 3AA1 were imported using the BLAST search module in DS, followed by both protein preparation and structure processing of protein crystallization. Water molecules and alternate conformations were removed, atomic names were standardized, and missing residues were restored through complementation to obtain a prototype of the actual structure.

## Determination of the protein active site

The crystal models of Notum and CKIP-1 proteins chosen here presented the corresponding ligands. For the 4UZQ protein model, the corresponding ligands were palmitoleic acid and 2-acetamido-2-deoxy-beta-D-glucopyranose. Palmitoleic acid has been validated as a Notum protein inhibitor, and palmitoleic acid has been used in several studies to search for the corresponding inhibitor. Thus, the active site was determined using the receptor residues within the 4UZQ palmitoleic acid range and expanded to 9 Å using the ligand expansion method. For the 3AA1 protein model, the identified ligand was 2-(n-morpholino)ethanesulfonic acid. The receptor residues in this range were chosen to determine the active site, and the ligand expanded to 9 Å.

## Preparation of small molecules

The small-molecule structure file of the SBT component with oral bioavailability (OB)  $\geq 30\%$  and drug resistance (DL)  $\geq 0.18$  was downloaded from the Traditional Chinese Medicine Systems Pharmacology Database and Analysis Platform (TCMSP). The three-dimensional structure of the small molecule was then downloaded from the TCMSP and loaded onto the DS docking software. Hydrogenation and energy optimization were performed using the CHARMM force field, and ligands were prepared and preserved for molecular docking as candidate small molecules.

## Molecular docking parameters

All molecular docking and screening in this study were performed using the CDOCKER function under the Dock Ligands module in DS. The target protein binding cavity's x, y, and z coordinate positions were 13.173522, 38.263435, and 29.118304 for 4UZQ and 20.999862, 4.295655, and -4.878816 for 3AA1, respectively. The post-cluster radius was adjusted to 0.5, and default settings were used for the remaining parameters to ensure diversity of docked conformations.

## ADMT property prediction

SBT small molecules were initially screened based on the CDOCKER ENERGY score of molecular docking. Only the top five small molecules were considered in the subsequent analyses. The ADMET module in DS was then used to predict the activity of these small-molecule compounds, including water solubility, blood-brain barrier retention, CYP2D6 binding, liver toxicity, intestinal uptake, and plasma protein binding.

## Statistical analysis

Statistical analysis was performed by GraphPad Prism 9.0 software (San Diego, CA, United States). Continuous normally distributed data are presented as mean  $\pm$  S.D., and differences between corresponding groups were analyzed using the Bonferroni's or Dunnett's *post hoc* test and one-way ANOVA.  $p < 0.05$  was considered statistically significant.

## Results

### Micro-CT analysis of the femur

PMOP was established in a rat model to understand the effects of SBT and QGY. After treatment, the rats were scanned radiographically from the hip to the lower limb (Figure 1A), and the region of interest on the femur was reconstructed in three dimensions (Figure 1B).

Compared to the human hip bone, X-ray scanning revealed that the rat hip bone was long and curved. Thus, the area with the most significant curvature was selected for width measurement. This study found that compared with the control, the hip in the model group was significantly wider ( $p < 0.001$ ), whereas the hip in all drug groups was significantly narrower ( $p < 0.001$ ) than that in the model group. Meanwhile, the hip reduction was most significant in the SBT + QGY group. The effect was comparable

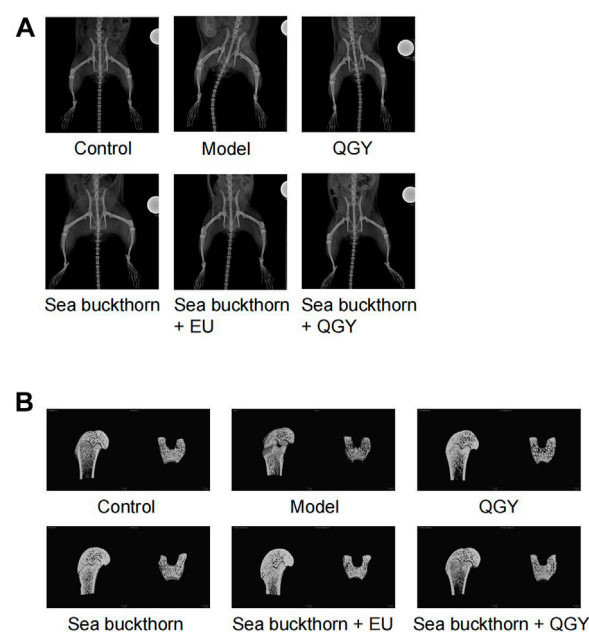


**FIGURE 1**  
X-ray images of the rat hip and 3D images of the region of interest of the femur. (A) X-ray images showing the rat hip. (B) 3D images of the region of interest of the femur.

for the QGY and SBT + EU groups. The SBT group displayed the least change (Figure 2A). The effect of SBT alone was inferior to the combination therapy groups, indicating that SBT enhanced the efficacy of QGY.

Three-dimensional reconstruction of the region of interest to the femoral head in rats revealed a significant decrease in BMD, BMC, BV/TV, Conn.D, Tb.N, and a significant increase in Tb.Sp in the model group, suggesting a successful PMOP induction. Compared to the model group, BMD, BMC, BV/TV, Conn.D, Tb.N, and Tb.Th in the drug groups showed almost a significant increase and a decrease in Tb. Sp. These results showed that the preparations containing SBT exerted a better effect than those without SBT (Figures 2B–H).

## ELISA analysis of estrogen, PINP, and S-CTX

Although the ELISA results showed that estrogen levels were significantly lower in the treatment group than those in the control group, they were still higher than those in the model group. The treatment can still effectively inhibit the decline of estrogen in rats. The findings also suggest that SBT + QGY was more effective in reducing estrogen levels than either medicine alone (Figure 3A).

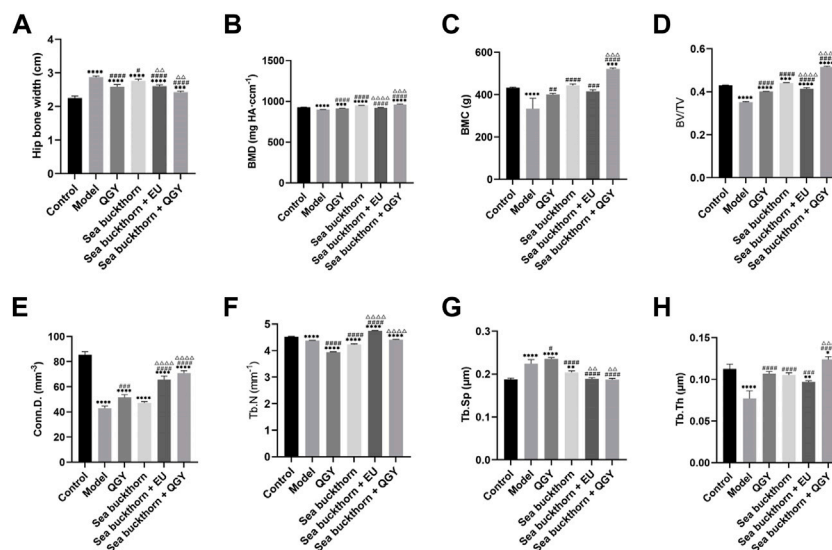
The concentration of bone turnover markers PINP and S-CTX was significantly higher in the model group than that in the control group, suggesting high bone metabolism in rats,

similar to PMOP. After treatment, the PINP concentration significantly decreased in the treatment groups except for the SBT group, which indicated that SBT alone had little effect on PINP. However, PINP reduction was higher in the SBT + QGY group than that in the QGY group (Figure 3C). This trend was also reflected in the expression of S-CTX (Figure 3B). This suggests that SBT enhances the efficacy of QGY, including inhibition of bone formation and bone absorption, but is more inclined to inhibit the latter.

## Western blot analysis of Notum, CKIP-1, and $\beta$ -catenin

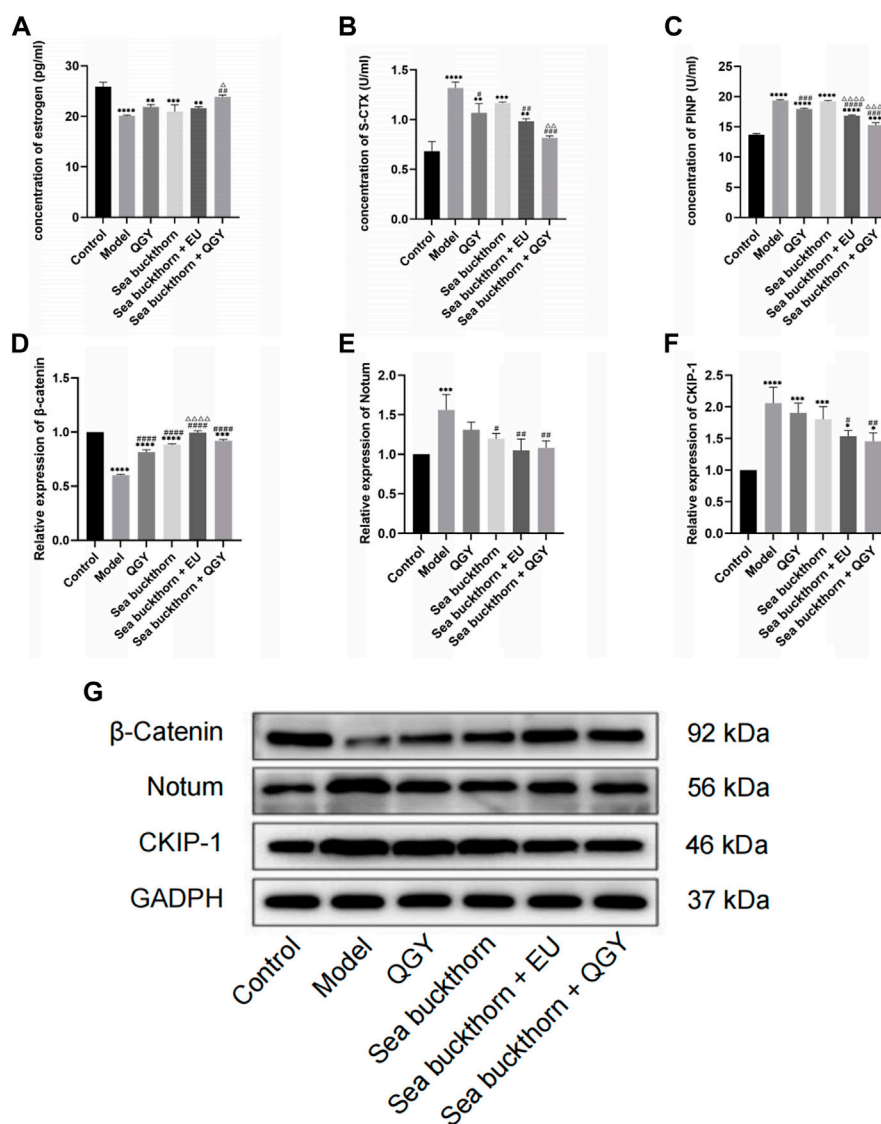
The effects of SBT on the expression of Notum and CKIP-1 and the regulation of the Wnt/ $\beta$ -catenin signaling pathway were assessed using the Western blot assay. Compared with the control group, SBT significantly decreased the expression of  $\beta$ -catenin but increased that of Notum and CKIP-1, all regulated *via* the Wnt/ $\beta$ -catenin signaling pathway. Inhibition of Notum and CKIP-1 expression is a common feature in PMOP.

This study found that all the drug groups suppressed the expression of Notum and CKIP-1 but promoted  $\beta$ -catenin expression (Figures 3D–G). Meanwhile, the effect of SBT + QGY was greater than that of either SBT or QGY alone, while the effect of SBT + EU was greater than that of either SBT or EU alone, further demonstrating that SBT inhibits osteoporosis. According to our results, SBT inhibits the expression of



**FIGURE 2**

Analytical results of micro-CT for bone morphometry. (A–H) Results of the hip bone width, BMD, BMC, BV/TV, Conn.D, Tb.N, Tb.Sp, and Tb.Th. \*, \*\*, \*\*\*, and \*\*\*\* show  $p < 0.05$ ,  $p < 0.01$ ,  $p < 0.001$ , and  $p < 0.0001$ , respectively, in comparison with the normal control group; #, ##, ###, and #### show  $p < 0.05$ ,  $p < 0.01$ ,  $p < 0.001$ , and  $p < 0.0001$ , respectively, in comparison with the PMOP model group;  $\Delta$ ,  $\Delta\Delta$ ,  $\Delta\Delta\Delta$ , and  $\Delta\Delta\Delta\Delta$  show  $p < 0.05$ ,  $p < 0.01$ ,  $p < 0.001$ , and  $p < 0.0001$ , respectively, in comparison with the QGY group.

**FIGURE 3**

(A–C) The levels of estrogen, S-CTX and PINP. (D–G) the expression of β-catenin, Notum, and CKIP-1. \*, \*\*, \*\*\*, and \*\*\*\*,  $p < 0.05$ ,  $p < 0.01$ ,  $p < 0.001$ , and  $p < 0.0001$ , respectively, in comparison with the normal control group; #, ##, ###, and ####,  $p < 0.05$ ,  $p < 0.01$ ,  $p < 0.001$ , and  $p < 0.0001$  respectively, in comparison with the PMOP model group; Δ, ΔΔ, ΔΔΔ, and ΔΔΔΔ,  $p < 0.05$ ,  $p < 0.01$ ,  $p < 0.001$ , and  $p < 0.0001$  respectively, in comparison with the QGY group.

Notum and CKIP-1 by activating the Wnt/β-catenin signaling pathway. SBT further enhances the anti-osteoporotic properties of QGY.

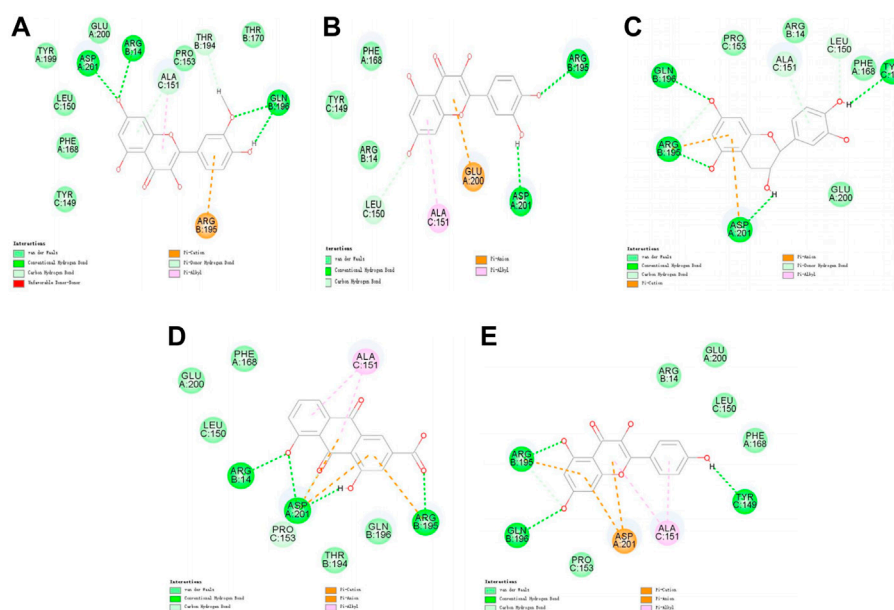
## Molecular docking of SBT

Molecular docking was performed on 33 prospective compounds with 4UZQ and 3AA1 receptors based on  $OB \geq 30\%$  and  $DL \geq 0.18$  (Table 1). The top five small molecules were

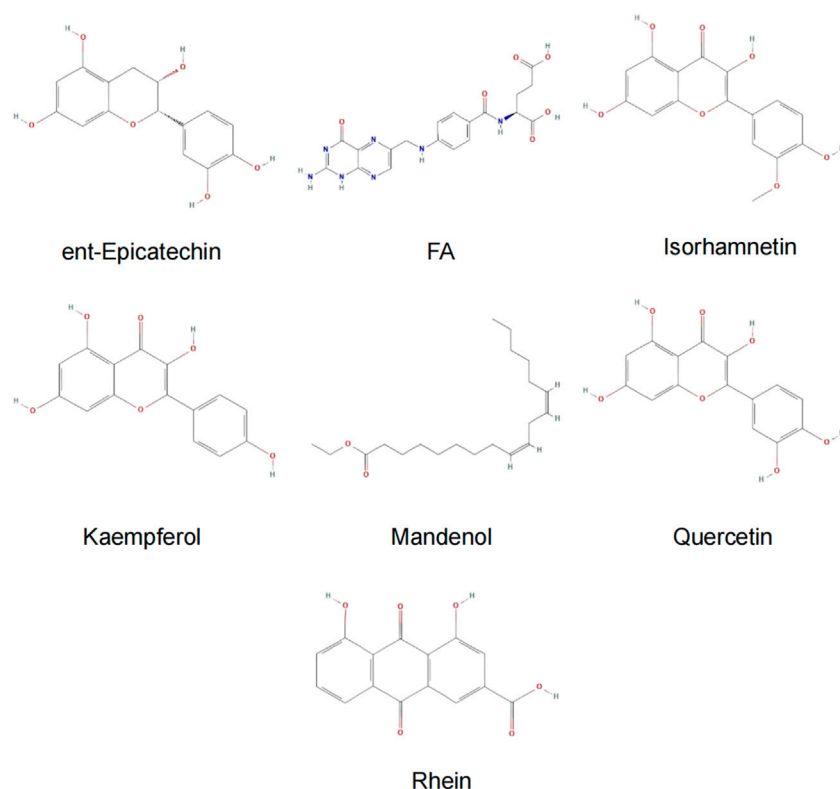
selected for each protein score based on the CDOCKER ENERGY score (Figures 4, 5; Tables 2, 3).

Among the 10 selected small molecules, three are repeated, namely, quercetin, rhein, and kaempferol (Figure 6). Folic acid and mandenol were unique to 4UZQ, while isorhamnetin and ent-epicatechin were unique to 3AA1. ADMET evaluation of the seven compounds showed that only folic acid, quercetin, and mandenol were absorbed into the human intestine, and folic acid and mandenol were less hepatotoxic. Mandenol binds to plasma protein more strongly than folic acid (Table 4).





**FIGURE 5**  
2D interaction map of Notum with selected small-molecule compounds. (A) Folic acid; (B) rhein; (C) quercetin; (D) kaempferol; (E) mandenol.

**FIGURE 6**

Active ingredients of sea buckthorn identified by virtual screening using molecular docking tools.

et al., 2021; Mao et al., 2021; Hui et al., 2022). Studies have also shown that QGY promotes bone formation and inhibits bone resorption (Wu et al., 2008; Wang, Wu, and Shi, 2016; Yao et al., 2016; Liu et al., 2018; Yang et al., 2018; Huang, Shi, and Deng, 2019; Liang et al., 2019; Yuan et al., 2022). Thus, we studied the effects of SBT, QGY, SBT + QGY, and SBT + EU. The SBT + EU group was particularly important because EU is an important herb in QGY that strengthens bones. Multiple pharmacological studies have confirmed that EU inhibits bone resorption but promotes bone formation (MEHL, 2011; Tan et al., 2014; Zhang et al., 2014; Cheng et al., 2019; Qi et al., 2019; Jian et al., 2020; Zhao et al., 2020).

## Sea buckthorn enhances QGY efficacy on bone morphological parameters in PMOP rats

Micro-CT can demonstrate the three-dimensional structure of the bone more intuitively, which could relieve the clinical efficacy of therapies. In the study, micro-CT analysis showed that QGY, SBT, and EU, either alone or in any combination, increased bone morphometric parameters such as BMD, BMC, BV/TV,

Conn.D, and Tb.Th. However, the Tb.N and Tb.Sp results were not anticipated. Intake of QGY and SBT decreased Tb.N, contrary to our expectations. Similarly, the increase in Tb.Sp was observed in the QGY group, which was also contrary to our expectation. But, SBT + QGY increased the Tb.N and decreased Tb.Sp, which is still in line with our expectations.

The bone metabolic index results revealed that S-CTX, an indicator of bone resorption, and PINP, a bone formation indicator, were both inhibited in the four treatment groups. The inhibition of S-CTX was higher in the SBT + QGY and SBT + EU groups than that in the QGY group, suggesting that SBT enhances the effect of QGY in inhibiting bone resorption and bone formation. We found that QGY significantly inhibited bone turnover, contrary to the previous studies. In the present study, the experiments were conducted for 6 weeks, whereas in other studies, the experiments were conducted for at least 2 months (Wang, Wu, and Shi, 2016; Yao et al., 2016; Huang, Shi, and Deng, 2019). Therefore, we speculate that QGY may inhibit bone turnover in the early stage of treatment. With regard to the degree of improvement in overall indicators, QGY effectively results in osteoporosis treatment, and SBT may improve its effect.

TABLE 1 A total of 33 components of sea buckthorn after initial screening from the TCMSP database.

No.	MOL ID	Chemical name	OB	DL
1	MOL001004	Pelargonidin	37.99	0.21
2	MOL010211	14,15-Dimethyl-alpha-sitosterol	43.14	0.78
3	MOL010212	14-Methyl-alpha-sitosterol	43.49	0.78
4	MOL010227	Canthaxanthine	41.59	0.56
5	MOL010228	Carotenoid	40.76	0.55
6	MOL010230	ST5330591	48.08	0.84
7	MOL010232	cis-Lycopene	45.51	0.54
8	MOL010234	Delta-carotene	31.80	0.55
9	MOL010240	Ergosta-7-en-3-beta-ol	38.76	0.83
10	MOL010241	Ergostenol	35.41	0.71
11	MOL010247	(2R,6S,7aR)-2-[(1E,3E,5E,7E,9E,11E,13E,15E)-16-[(1R,4R)-4-hydroxy-2,6,6-trimethyl-1-cyclohex-2-enyl]-1,5,10,14-tetramethylhexadeca-1,3,5,7,9,11,13,15-octaenyl]-2,4,4,7a-tetramethyl-6,7-Dihydro-5H-benzofuran-6-ol	57.88	0.53
12	MOL010248	Gamma-carotene	30.98	0.55
13	MOL001979	LAN	42.12	0.75
14	MOL010267	LYC	32.57	0.51
15	MOL010283	ZINC03831331	47.60	0.65
16	MOL001420	ZINC04073977	38.00	0.76
17	MOL001494	Mandenol	42.00	0.19
18	MOL001510	24-Epicampesterol	37.58	0.71
19	MOL002268	Rhein	47.07	0.28
20	MOL002588	(3S,5R,10S,13R,14R,17R)-17-[(1R)-1,5-dimethyl-4-methylenehexyl]-4,4,10,13,14-pentamethyl-2,3,5,6,7,11,12,15,16,17-decahydro-1H-cyclopenta [a]phenanthren-3-ol	42.37	0.77
21	MOL002773	Beta-carotene	37.18	0.58
22	MOL000354	Isorhamnetin	49.60	0.31
23	MOL000358	Beta-sitosterol	36.91	0.75
24	MOL000359	Sitosterol	36.91	0.75
25	MOL000422	Kaempferol	41.88	0.24
26	MOL000433	Folic acid	68.96	0.71
27	MOL000449	Stigmasterol	43.83	0.76
28	MOL000492	(+)-Catechin	54.83	0.24
29	MOL005100	5,7-Dihydroxy-2-(3-hydroxy-4-methoxyphenyl) chroman-4-one	47.74	0.27
30	MOL006756	Schottenol	37.42	0.75
31	MOL000073	Ent-epicatechin	48.96	0.24
32	MOL000953	CLR	37.87	0.68
33	MOL000098	Quercetin	46.43	0.28

TABLE 2 Top five ingredients scored after docking 3AA1 molecules with 33 compounds.

No.	MOL ID	Chemical name	InCHI Key	CDOCKER ENERGY
1	MOL000433	Folic acid	OVBPILPVIDEAO-LBPRGKRZSA-N	32.185
2	MOL002268	Rhein	FCDLCPWAQCPTKC-UHFFFAOYSA-N	31.788
3	MOL000098	Quercetin	REFJWTPEDVJJY-UHFFFAOYSA-N	22.012
4	MOL000422	Kaempferol	IYRMWMYZSQPKC-UHFFFAOYSA-N	21.700
5	MOL001494	Mandenol	FMMOAYVCKXGMF-MURFETPASA-N	18.008

TABLE 3 Top five ingredients scored after docking 4UZQ molecules with 33 compounds.

No.	MOL ID	Chemical name	InCHI Key	CDOCKER ENERGY
1	MOL000433	Folic acid	OVBPILPVIDEAO-LBPRGKRZSA-N	32.185
2	MOL002268	Rhein	FCDLCPWAQCPTKC-UHFFFAOYSA-N	31.788
3	MOL000098	Quercetin	REFJWTPEDVJJIY-UHFFFAOYSA-N	22.012
4	MOL000422	Kaempferol	IYRMWMYZSQPJKC-UHFFFAOYSA-N	21.700
5	MOL001494	Mandenol	FMMOAYVCKXGMF-MURFETPASA-N	18.008

TABLE 4 Results of ADMET screening.

No.	Chemical name	Molecular formula	Human intestinal absorptivity	Aqueous solubility (25°C)	Blood-brain barrier permeability	Cytochrome P450 2D6 inhibition	Hepatotoxicity	Plasma protein tuberculosis rate
1	Folic acid	C <sub>19</sub> H <sub>19</sub> N <sub>7</sub> O <sub>6</sub>	3	3	4	False	False	False
2	Rhein	C <sub>15</sub> H <sub>8</sub> O <sub>6</sub>	0	3	4	False	True	False
3	Quercetin	C <sub>15</sub> H <sub>10</sub> O <sub>7</sub>	1	3	4	False	True	False
4	Kaempferol	C <sub>15</sub> H <sub>10</sub> O <sub>6</sub>	0	3	3	False	True	False
5	Mandenol	C <sub>20</sub> H <sub>36</sub> O <sub>2</sub>	2	2	4	False	False	True
6	Isorhamnetin	C <sub>16</sub> H <sub>12</sub> O <sub>7</sub>	0	3	4	False	True	False
7	Ent-epicatechin	C <sub>15</sub> H <sub>14</sub> O <sub>6</sub>	0	3	4	False	True	False

Human intestinal absorptivity: 0–3 decreases in turn; water solubility (25°C): 0–6 increases in turn, and four is the best case; blood–brain barrier permeability: 0–5 decreases in turn; cytochrome P450 2D6 inhibition: true stands for inhibitory, and false for non-inhibitory; hepatotoxicity: true represents hepatotoxic, and false represents not hepatotoxic; plasma protein tuberculosis rate: true represents having high plasma protein binding, and false represents not having high plasma protein binding.

In clinical practice or other studies, the hip bone width has not been used in osteoporosis detection. In the present study, the hip bone was wider for rats in the model group than that in the control group, but the bone width decreased after treatment. This suggests that, unlike in humans, the hip bone may be an indicator of osteoporosis in rats. The hip bone was wider, but BMD, BMC, BV/TV, Conn.D, and Tb.Th were lower in the model rats, implying that degenerative bone changes may widen the hip joints of the rats.

### Sea buckthorn enhances QGY efficacy by inhibiting the expression of Notum and CKIP-1 and activating the Wnt/ $\beta$ -catenin signaling pathway

High estrogen levels and expression of  $\beta$ -catenin, Notum, and CKIP-1 were observed in all treatment groups, consistent with previous studies (Figures 3D–F). The inhibition of Notum and CKIP-1 was higher in the SBT + EU and SBT + QGY groups than that in the other groups. The activation of  $\beta$ -catenin was also higher in the SBT + EU and SBT + QGY groups than that in the other groups. Thus, we speculate that SBT activates the Wnt/ $\beta$ -

catenin signaling pathway by inhibiting Notum and CKIP-1 expression.

The Wnt/ $\beta$ -catenin signaling pathway regulates bone metabolic homeostasis and participates in skeletal growth, development, repair, and remodeling. Studies show that  $\beta$ -catenin promotes the proliferation and differentiation of osteoblasts and inhibits osteoclasts during bone formation *via* the Wnt signaling pathway (A.Maupin, J.Droscha, and O.Williams, 2013).  $\beta$ -Catenin regulates bone resorption and modulates bone formation, thus impacting bone mass.  $\beta$ -Catenin also regulates osteoblast and osteoclast formation during osteoblast differentiation (Chen and Long, 2013).

Estrogen is a steroid hormone that regulates bone tissue metabolism by modulating the physiological activity of osteoblasts and osteoclasts (Zhao et al., 2007; Pereira et al., 2015). Estrogen binds to the estrogen receptor (ER) on the cell membrane and plays a corresponding biological role. On the one hand, estrogen regulates osteoclast activity *via* the RANKL/RANK pathway and osteoblast activity *via* the ERK1/2 pathway. On the other hand, it promotes the differentiation of bone marrow mesenchymal stem cells into osteoblasts by activating the Wnt signaling pathway (Gao et al., 2013). Therefore, based on the increase in estrogen levels in all four

drug groups, we hypothesized that SBT and QGY activate the Wnt/ $\beta$ -catenin signaling pathway by increasing the production of estrogen and promoting bone formation *via* the RANKL/RANK/OPG axis. A recent study in rats has revealed that blocking the effects of estrogen on the hypothalamus increases the total bone mass by 500% and enhances the bone mechanical strength and mineral density throughout old age (Herber et al., 2019). In blood, estrogen promotes bone growth, but in the hypothalamus, it exerts an opposite effect. This study also showed us a new direction of anti-osteoporosis research.

Our research revealed that estrogen levels were significantly low, while CKIP-1 and Notum expression were significantly high in rats with PMOP. Further studies involving an estrogen production inhibition test are required to confirm the relationship between estrogen and CKIP-1, as well as Notum.

## Molecular docking screening identified seven potential active components that potentially affect CKIP-1 and Notum

Molecular docking identified seven small molecules in SBT, namely, folic acid, rhein, quercetin, mandenol, kaempferol, isosalmonetin, and ent-epicatechin that potentially affect CKIP-1 and Notum expression. Quercetin, kaempferol, and isorhamnetin are members of the flavonoid family, specifically known for their antioxidant, wound healing, lipid regulation, antihypertensive, and immunomodulatory properties (Gupta et al., 2006; Pang et al., 2008, 2008; Pandurangan, Bose and Banerji, 2011; Hou et al., 2017, 2017). Folic acid is an important nutrient that participates in the metabolism of genetic materials and proteins, affecting animal reproductive performance and secretion of bile in the pancreas (Savini et al., 2019; Sato, 2020). Mandenol is a fatty acid that regulates blood glucose and protects the retina (Bouras et al., 2017; Gao et al., 2017). Ent-epicatechin is a polyphenol with antioxidant properties that protect the liver (Maheshwari et al., 2011; Guo et al., 2017). In addition, rhein possesses antitumor, antiviral, anti-inflammatory, and antifibrotic properties (Xu et al., 2016; Ge et al., 2017; Tang et al., 2017; Wang et al., 2018). These seven small molecules, however, are only the calculated results of molecular docking, and whether they promote or inhibit CKIP-1 and Notum expression remains to be explored further.

According to the ADMET property prediction results, only folic acid, quercetin, and mandenol are absorbed in the human intestine. Still, quercetin is hepatotoxic, and mandenol has a higher tuberculosis rate of plasma proteins than folic acid (Table 4). Therefore, the results of the present study show that mandenol has a very high clinical application potential. But these results were generated *in silico*. Thus, further experiments are needed to validate them. Regarding limitations, the findings of this study were not validated using experimental studies.

## Conclusion

SBT improves bone morphometric performance in PMOP rats by inhibiting CKIP-1 and Notum expression, increasing estrogen levels, and activating the Wnt/ $\beta$ -catenin signaling pathway. Furthermore, SBT enhances the properties of QGY. Folic acid, rhein, quercetin, kaempferol, mandenol, isorhamnetin, and ent-epicatechin are the most likely active ingredients in SBT. These results provide insight into the pharmacological mechanisms of SBT in treating osteoporosis.

## Data availability statement

The original contributions presented in the study are included in the article/Supplementary Material; further inquiries can be directed to the corresponding authors.

## Ethics statement

The animal study was reviewed and approved by the Laboratory Animal Management and Ethics Committee of Zhejiang Chinese Medical University.

## Author contributions

X-LS and KL contributed in studying the design and coordination, acquisition of funding, and supervised the study. SW designed the validation experiments and revised the manuscript. Y-FY performed most of the experiments and statistical analysis and wrote the manuscript. HZ, B-BT, YL, HH, C-JH, T-PC, M-HF, B-CL, and Y-LM performed parts of the experiments. F-QQ provided help for the manuscript modification. All authors reviewed and approved the final manuscript.

## Funding

This study is funded by the National Natural Science Foundation of China (82074183; 81873129; 81803902; 81973884).

## Conflict of interest

The authors declare that the research was conducted in the absence of any commercial or financial relationships that could be construed as a potential conflict of interest.



## Publisher's note

All claims expressed in this article are solely those of the authors and do not necessarily represent those of their affiliated

## References

- Bouras, K., Kopsidas, K., Bariotakis, M., Kitsiou, P., Kapodistria, K., Agrogiannis, G., et al. (2017). Effects of dietary supplementation with Sea buckthorn (*hippophae rhamnoides* L.) seed oil on an experimental model of hypertensive retinopathy in wistar rats. *Biomed. Hub.* 2 (1), 1–12. doi:10.1159/000456704
- Chen, J., and Long, F. (2013).  $\beta$ -catenin promotes bone formation and suppresses bone resorption in postnatal growing mice. *J. Bone Min. Res.* 28 (5), 1160–1169. doi:10.1002/jbmr.1834
- Cheng, C.-F., Chien-Fu Lin, J., Tsai, F. J., Chen, C. J., Chiou, J. S., Chou, C. H., et al. (2019). Protective effects and network analysis of natural compounds obtained from *Radix dipsaci*, *Eucommiae cortex*, and *Rhizoma drynariae* against RANKL-induced osteoclastogenesis *in vitro*. *J. Ethnopharmacol.* 244, 112074. doi:10.1016/j.jep.2019.112074
- Gao, S., Guo, Q., Qin, C., Shang, R., and Zhang, Z. (2017). Sea buckthorn fruit oil extract alleviates insulin resistance through the PI3K/Akt signaling pathway in type 2 diabetes mellitus cells and rats. *J. Agric. Food Chem.* 65 (7), 1328–1336. doi:10.1021/acs.jafc.6b04682
- Gao, Y., Huang, E., Zhang, H., Wang, J., Wu, N., Chen, X., et al. (2013). Crosstalk between Wnt/ $\beta$ -catenin and estrogen receptor signaling synergistically promotes osteogenic differentiation of mesenchymal progenitor cells. *PLoS One* 8 (12), e82436. doi:10.1371/journal.pone.0082436
- Ge, H., Tang, H., Liang, Y., Wu, J., Yang, Q., Zeng, L., et al. (2017). Rhein attenuates inflammation through inhibition of NF- $\kappa$ B and NALP3 inflammasome *in vivo* and *in vitro*. *Drug Des. Devel Ther.* 11, 1663–1671. doi:10.2147/DDDT.S133069
- Guo, R., Chang, X., Guo, X., Brennan, C. S., Li, T., Fu, X., et al. (2017). Phenolic compounds, antioxidant activity, antiproliferative activity and bioaccessibility of Sea buckthorn (*Hippophae rhamnoides* L.) berries as affected by *in vitro* digestion. *Food Funct.* 8 (11), 4229–4240. doi:10.1039/c7fo00917h
- Gupta, A., Kumar, R., Pal, K., Singh, V., Banerjee, P. K., and Sawhney, R. C. (2006). Influence of sea buckthorn (*Hippophae rhamnoides* L.) flavone on dermal wound healing in rats. *Mol. Cell Biochem.* 290 (1–2), 193–198. doi:10.1007/s11010-006-9187-6
- Herber, C. B., Krause, W. C., Wang, L., Bayrer, J. R., Li, A., Schmitz, M., et al. (2019). Estrogen signaling in arcuate Kiss1 neurons suppresses a sex-dependent female circuit promoting dense strong bones. *Nat. Commun.* 10 (1), 163. doi:10.1038/s41467-018-08046-4
- Hou, D., Wang, D., Ma, X., Chen, W., Guo, S., and Guan, H. (2017). Effects of total flavonoids of *Hippophae rhamnoides* (L.) on cytotoxicity of NK92-M1 cells. *Int. J. Immunopathol. Pharmacol.* 30 (4), 353–361. doi:10.1177/0394632017736673
- Huang, J., Shi, X., and Deng, Z. (2019). Effect of qianggu yin combined with probiotics on osteoporotic fracture healing in rats. *Chin. J. Mod. Appl. Pharm.* 36 (07), 791–795. doi:10.13748/j.cnki.issn1007-7693.2019.07.004
- Hui, M., Wang, S., Zhong, R., Gong, J., Han, Z., and Shi, X. (2022). Clinical observation on osteoporosis belonging to kidney deficiency and blood stasis syndrome treated with QiangguYin (强骨饮) combined with electroacupuncture. *Chin. J. Traditional Med. Sci. Technol.* 29 (01), 73–75.
- Jian, G.-H., Su, B. Z., Zhou, W. J., and Xiong, H. (2020). Application of network pharmacology and molecular docking to elucidate the potential mechanism of *Eucommia ulmoides*-*Radix Achyranthis Bidentatae* against osteoarthritis. *BioData Min.* 13, 12. doi:10.1186/s13040-020-00221-y
- Kakugawa, S., Langton, P. F., Zebisch, M., Howell, S., Chang, T. H., Liu, Y., et al. (2015). Notum deacylates Wnt proteins to suppress signalling activity. *Nature* 519 (7542), 187–192. doi:10.1038/nature14259
- Li, S., Kang, S., Sun, J., Yuan, Y., Huang, X., Li, J., et al. (2021). Influence of qianggu yin on risk factors of falls in postmenopausal osteoporosis patients with kidney deficiency and blood stasis syndrome. *J. Guangzhou Univ. Traditional Chin. Med.* 38 (08), 1611–1616. doi:10.13359/j.cnki.gzxbcm.2021.08.014
- Liang, B., Li, M., Wang, J., Zhang, J., Mao, Y., and Shi, X. (2019). Study on the mechanism and targets of qiangguYin based on bioinformatics in postmenopausal osteoporosis treatment. *Chin. J. General Pract.* 17 (06), 909–914. doi:10.16766/j.cnki.issn.1674-4152.000823
- Lin, C., Fan, Y.-j., Mehl, C., Zhu, J.-j., Chen, H., Jin, L.-y., et al. (2011). *Eucommia ulmoides* Oliv. antagonizes H<sub>2</sub>O<sub>2</sub>-induced rat osteoblastic MC3T3-E1 apoptosis by inhibiting expressions of caspases 3, 6, 7, and 9. *J. Zhejiang Univ. Sci. B* 12 (01), 47–54. doi:10.1631/jzus.B1000057
- Liu, B., Yuan, B., Guo, X., Wei, X., Zhao, L., Chen, D., et al. (2006). Experimental study on the effect of tiangui gengnian capsule on the aged female rats osteoporosis. *Zhong Yao Cai* 29 (08), 803–806. doi:10.13863/j.issn1001-4454.2006.08.023
- Liu, B., Yuan, B., Guo, X., Wei, X., Zhao, L., Kang, J., et al. (2006). Experimental study on effect of tiangui gengnian soft capsule on aged female rats with osteoporosis. *Zhongguo Zhong Xi Yi Jie He Za Zhi* 26 (02), 135–139.
- Liu, Z., et al. (2018). Effect of yiqiwenjing prescription on osteoclasts apoptosis mediated by CKIP-1. *Chin. J. Traditional Med. Traumatology Orthop.* 26 (08), 14–17.
- Maheshwari, D. T., Yogendra Kumar, M. S., Verma, S. K., Singh, V. K., and Singh, S. N. (2011). Antioxidant and hepatoprotective activities of phenolic rich fraction of *Seabuckthorn* (*Hippophae rhamnoides* L.) leaves. *Food Chem. Toxicol.* 49 (9), 2422–2428. doi:10.1016/j.fct.2011.06.061
- Mao, Y., He, C., Chen, T., Fang, M., Zhou, H., and Shi, X. (2021). Clinical efficacy of yiqi wenjing decoction on treatment of osteoporosis. *Chin. J. Traditional Med. Traumatology Orthop.* 29 (08), 22–24.
- Maupin, A., Droscha, K. J., and Williams, O. (2013). A comprehensive overview of skeletal phenotypes associated with alterations in wnt/ $\beta$ -catenin signaling in humans and mice. *Bone Res.* 1 (01), 27–71. doi:10.4248/BR201301004
- Pandurangan, N., Bose, C., and Banerji, A. (2011). Synthesis and antioxygenic activities of seabuckthorn flavone-3-ols and analogs. *Bioorg Med. Chem. Lett.* 21 (18), 5328–5330. doi:10.1016/j.bmcl.2011.07.008
- Pang, X., Zhao, J., Zhang, W., Zhuang, X., Wang, J., Xu, R., et al. (2008). Antihypertensive effect of total flavones extracted from seed residues of *Hippophae rhamnoides* L. in sucrose-fed rats. *J. Ethnopharmacol.* 117 (2), 325–331. doi:10.1016/j.jep.2008.02.002
- Patel, C. A., Divakar, K., Santani, D., Solanki, H. K., and Thakkar, J. H. (2012). Remedial prospective of *hippophae rhamnoides* linn. (Sea buckthorn). *ISRN Pharmacol.* 2012, 1–6. doi:10.5402/2012/436857
- Pereira, C. S., Stringheta-Garcia, C. T., da Silva Xavier, L., Tirapeli, K. G., Pereira, A. A. F., Kayahara, G. M., et al. (2017). Llex paraguariensis decreases oxidative stress in bone and mitigates the damage in rats during perimenopause. *Exp. Gerontol.* 98, 148–152. doi:10.1016/j.exger.2017.07.006
- Pereira, F. M. B. G., Rodrigues, V. P., de Oliveira, A. E., Brito, L. M., and Lopes, F. F. (2015). Association between periodontal changes and osteoporosis in postmenopausal women. *Climacteric* 18 (2), 311–315. doi:10.3109/13697137.2014.966239
- Qi, S., Zheng, H., Chen, C., and Jiang, H. (2019). Du-zhong (*Eucommia ulmoides* Oliv.) cortex extract alleviates lead acetate-induced bone loss in rats. *Biol. Trace Elem. Res.* 187 (1), 172–180. doi:10.1007/s12011-018-1362-6
- Sato, K. (2020). Why is folate effective in preventing neural tube closure defects? *Med. Hypotheses* 134, 109429. doi:10.1016/j.mehy.2019.109429
- Savini, C., Yang, R., Savelyeva, L., Göckel-Krzikalla, E., Hotz-Wagenblatt, A., Westermann, F., et al. (2019). Folate repletion after deficiency induces irreversible genomic and transcriptional changes in human papillomavirus type 16 (HPV16)-immortalized human keratinocytes. *Int. J. Mol. Sci.* 20 (5), E1100. doi:10.3390/ijms20051100
- Shi, X., Zhu, Y., Ning, Y., Wu, L., Yu, S., and Liu, K. (2008). Investigation of the effect of qianggu drink on the TRACP5b of osteoporosis. *Chin. J. Traditional Med. Traumatology Orthop.* 16 (01), 25–27. doi:10.3969/j.issn.1005-0205.2007.02.004
- Shi, X., Liu, K., and Li, S. (2007). The clinical report about the curative effect of zi Ni qiang gu yin on 44 patients who suffered from osteoporosis. *Chin. J. Traditional Med. Traumatology Orthop.* 15(02), 9–10.
- Shi, Z.-Y., Zhang, X. G., Li, C. W., Liu, K., Liang, B. C., and Shi, X. L. Effect of traditional Chinese medicine product, QiangGuYin, on bone mineral density and bone turnover in Chinese postmenopausal osteoporosis *Evid. Based Complement. Altern. Med.* (2017), 2017. eCAM, 6062707. doi:10.1155/2017/6062707

- Suryakumar, G., and Gupta, A. (2011). Medicinal and therapeutic potential of Sea buckthorn (*Hippophae rhamnoides* L.). *J. Ethnopharmacol.* 138 (2), 268–278. doi:10.1016/j.jep.2011.09.024
- Tan, X.-L., Zhang, Y. H., Cai, J. P., Zhu, L. H., Ge, W. J., and Zhang, X. (2014). 5-(Hydroxymethyl)-2-furaldehyde inhibits adipogenic and enhances osteogenic differentiation of rat bone mesenchymal stem cells. *Nat. Prod. Commun.* 9 (4), 529–532. doi:10.1177/1934578x1400900427
- Tang, B., Liu, K., Wu, L., and Shi, X. (2020). Preliminary study of the effect of the strong-bone decoction on osteoblast differentiation by regulation of osteoclast-derived exosomes. *Chin. J. Osteoporos.* 26 (11), 1598–1603. doi:10.1016/j.prmcm.2022.100087
- Tang, N., Chang, J., Lu, H. C., Zhuang, Z., Cheng, H. L., Shi, J. X., et al. (2017). Rhein induces apoptosis and autophagy in human and rat glioma cells and mediates cell differentiation by ERK inhibition. *Microb. Pathog.* 113, 168–175. doi:10.1016/j.micpath.2017.10.031
- Wang, B., Wu, P., and Shi, X. (2016). Effect of Qianggu Yin (强骨饮, QGY) on bone microstructure in the ovariectomized osteoporosis rats. *J. Traditional Chin. Orthop. Traumatology* 28 (07), 6–9.
- Wang, Q.-W., Su, Y., Sheng, J. T., Gu, L. M., Zhao, Y., Chen, X. X., et al. (2018). Anti-influenza A virus activity of rhein through regulating oxidative stress, TLR4, Akt, MAPK, and NF- $\kappa$ B signal pathways. *PLoS One* 13 (1), e0191793. doi:10.1371/journal.pone.0191793
- Wu, L.-G., Chen, H., Shi, X., Liu, K., Xu, J., Mao, Y., et al. (2008). Effects of the principium of replenishing Qi and nourishing kidney deficiency on collum femoris of bone histomorphometry in ovariectomized rats. *Journal of Zhejiang Chinese Medical University Hangzhou China*, 36–37+40. doi:10.16466/j.issn1005-5509.2008.01.038
- Xiao, W., Wang, J., Chen, W., Mao, Y., Zhang, J., Liu, Z., et al. (2019). Clinical study on qiangguyin in preventing fall with osteoporosis. *Chin. J. Mod. Appl. Pharm.* 36 (14), 1797–1801. doi:10.13748/j.cnki.issn1007-7693.2019.14.014
- Xu, S., Lv, Y., Zhao, J., Wang, J., Wang, G., and Wang, S. (2016). The inhibitory effect of rhein on proliferation of high glucose-induced mesangial cell through cell cycle regulation and induction of cell apoptosis. *Pharmacogn. Mag.* 12 (2), S257–S263. doi:10.4103/0973-1296.182158
- Yang, Y., Liu, Z., Wang, J., Liu, K., and Shi, X. (2018). Effect of qiangguyin on rat osteoblasts in CKIP-1 overexpressing. *Chin. J. Traditional Med. Traumatology Orthop.* 26 (10), 1–5.
- Yao, J., Wang, B., Wu, P., Liu, K., and Shi, X. (2016). The effect of strengthening-bone receipt on the change of trabecular bone of fracture healing under micro-CT in rat osteoporotic model. *Chin. J. Osteoporos.* 22 (11), 1395–1398+1403.
- Yuan, Y., Sun, J., Zhou, H., Wang, S., He, C., Chen, T., et al. (2022). The effect of QiangGuYin on osteoporosis through the AKT/mTOR/autophagy signaling pathway mediated by CKIP-1. *Aging (Albany NY)* 14 (2), 892–906. doi:10.18632/aging.203848
- Zhang, R., Pan, Y. L., Hu, S. J., Kong, X. H., Juan, W., and Mei, Q. B. (2014). Effects of total lignans from *Eucommia ulmoides* barks prevent bone loss *in vivo* and *in vitro*. *J. Ethnopharmacol.* 155 (1), 104–112. doi:10.1016/j.jep.2014.04.031
- Zhang, X., Cheong, S. M., Amado, N. G., Reis, A. H., MacDonald, B. T., Zebisch, M., et al. (2015). Notum is required for neural and head induction via Wnt decylation, oxidation, and inactivation. *Dev. Cell* 32 (6), 719–730. doi:10.1016/j.devcel.2015.02.014
- Zhao, Q., Shao, J., Chen, W., and Li, Y. P. (2007). Osteoclast differentiation and gene regulation. *Front. Biosci.* 12, 2519–2529. doi:10.2741/2252
- Zhao, X., Wang, Y., Nie, Z., Han, L., Zhong, X., Yan, X., et al. (2020). *Eucommia ulmoides* leaf extract alters gut microbiota composition, enhances short-chain fatty acids production, and ameliorates osteoporosis in the senescence-accelerated mouse P6 (SAMP6) model. *Food Sci. Nutr.* 8 (9), 4897–4906. doi:10.1002/fsn3.1779



## OPEN ACCESS

## EDITED BY

Dongwei Zhang,  
Beijing University of Chinese Medicine,  
China

## REVIEWED BY

Liming Xue,  
Shanghai Municipal Center for Disease  
Control and Prevention, China  
Yong Ma,  
Nanjing University of Chinese Medicine,  
China

## \*CORRESPONDENCE

Ronghua Zhang,  
tzrh@jnu.edu.cn  
Huaqin Tian,  
13929969262@139.com  
Panpan Wang,  
wangpp@jnu.edu.cn

<sup>†</sup>These authors have contributed equally  
to this work and share first authorship

## SPECIALTY SECTION

This article was submitted to  
Experimental Pharmacology and Drug  
Discovery,  
a section of the journal  
Frontiers in Pharmacology

RECEIVED 12 August 2022

ACCEPTED 03 October 2022

PUBLISHED 12 October 2022

## CITATION

Li Y, Li L, Li X, Luo B, Ye Q, Wang H,  
Yang L, Zhu X, Han L, Zhang R, Tian H  
and Wang P (2022). A mechanistic  
review of chinese medicine polyphenols  
on bone formation and resorption.  
*Front. Pharmacol.* 13:1017538.  
doi: 10.3389/fphar.2022.1017538

## COPYRIGHT

© 2022 Li, Li, Luo, Ye, Wang, Yang,  
Zhu, Han, Zhang, Tian and Wang. This is  
an open-access article distributed  
under the terms of the [Creative  
Commons Attribution License \(CC BY\)](#).  
The use, distribution or reproduction in  
other forums is permitted, provided the  
original author(s) and the copyright  
owner(s) are credited and that the  
original publication in this journal is  
cited, in accordance with accepted  
academic practice. No use, distribution  
or reproduction is permitted which does  
not comply with these terms.

# A mechanistic review of chinese medicine polyphenols on bone formation and resorption

Yan Li<sup>1†</sup>, Lingyu Li<sup>2,3,4†</sup>, Xiaoyun Li<sup>4</sup>, Bingjie Luo<sup>4</sup>, Qianyun Ye<sup>1</sup>,  
Haoyu Wang<sup>1</sup>, Li Yang<sup>3,4</sup>, Xiaofeng Zhu<sup>1,3</sup>, Li Han<sup>3,5</sup>,  
Ronghua Zhang<sup>2,3,4\*</sup>, Huaqin Tian<sup>6\*</sup> and Panpan Wang<sup>2,3,5\*</sup>

<sup>1</sup>College of Traditional Chinese Medicine, Jinan University, Guangzhou, China, <sup>2</sup>Cancer Research Institute, Jinan University, Guangzhou, China, <sup>3</sup>Guangdong Provincial Key Laboratory of Traditional Chinese Medicine Informatization, Jinan University, Guangzhou, China, <sup>4</sup>College of Pharmacy, Jinan University, Guangzhou, China, <sup>5</sup>First Affiliated Hospital of Jinan University, Guangzhou, China, <sup>6</sup>Foshan Hospital of Traditional Chinese Medicine, Foshan, China

Bone reconstruction includes a steady state system of bone formation and bone absorption. This tight coupling requires subtle coordination between osteoblasts and osteoclasts. If this balance is broken, it will lead to bone mass loss, bone density reduction, and bone metabolic diseases, such as osteoporosis. Polyphenols in Chinese herbal medicines are active ingredients in plant extracts with high safety and few side effects, and they can play a role in affecting bone formation and bone resorption. Some of these have estrogen-like effects and can better target bone health in postmenopausal women. The purpose of this review is to provide comprehensive information on the mechanisms underlying the relationship between traditional Chinese medicine polyphenols and bone formation or bone resorption.

## KEYWORDS

Chinese herbal medicine, polyphenols, bone resorption, bone formation, osteoblast, osteoclast

## 1 Introduction

Bones are essential to the human body, providing structural support, protecting vital organs such as the bone marrow and brain, promoting blood production, and serving as a reservoir of minerals. From birth to death, bones are constantly reshaped to maintain critical functions and maintain constant changes in bone mass.

Bone remodeling is achieved through the tight coupling of bone resorption and bone formation, and this is closely related to the participation of osteoclasts and osteoblasts. Bone marrow-derived osteoclasts are responsible for the absorption of aged bone, and mesenchymal osteoblasts are responsible for the synthesis and mineralization of new bone. If this balance is broken, such as increased bone resorption that is not compensated for by a similar increase in bone formation, this will lead to bone mass loss, bone density reduction, and bone metabolic diseases, such as osteoporosis (Crotti et al., 2015). Bone remodeling is regulated by multiple local cytokines (e.g., platelet-derived growth factor (PDGF), insulin-like growth factor [IGF], beta tumor growth factor (TGF)), and systemic

hormones (growth hormones, parathyroid hormone (PTH), insulin, and oxytocin), vitamin D, energy metabolism (Karsenty and Khosla, 2022), and the regulation of multiple signaling pathways. Among these, Wnt, TGF $\beta$ , RANK/RANKL, and the M-CSF/C-FMS pathway regulate the differentiation and activity of osteoclasts. The Runt-associated transcription factor 2 (Runx 2), Osterix (Osx),  $\beta$ -catenin, activating transcription factor 4 (Atf 4), and the activating protein 1 (AP-1) family are the primary transcription factors involved in osteoblast differentiation (Chau et al., 2009; Soltanoff et al., 2009; Meyer et al., 2014). However, recent research suggests that positioned bone is also an important organ with paracrine and endocrine functions. Moreover, there is crosstalk between osteoblasts and osteoclasts that allow them to communicate and influence each other. The sympathetic nervous system (SNS) also has an effect on bone balance (Karsenty and Khosla, 2022).

For the past 3 decades, the mainstay of treatment for osteoporosis has been antiresorptive agents (e.g., bisphosphonates) that reduce fracture risk through continuous administration. However, some epidemiological studies have shown an association between long-term bisphosphonate therapy and atypical femoral fractures (AFF) (Shane et al., 2014). Therefore, these drugs are not suitable for long-term use for the treatment of bone-damaging diseases, and they may not be suitable as oral drugs either. In addition, long-term medication can cause problems such as gastrointestinal (GI) toxicity, weight loss, bone pain, low calcium levels (Lu et al., 2016; Gao et al., 2017; Grigg et al., 2017; Lange et al., 2017; Monda et al., 2017). Hence, potential new drugs are urgently needed to replace existing treatment strategies due to clinically adverse effects (Estell and Rosen, 2021).

Chinese herbal medicine has been used for many centuries. Polyphenols are the active ingredients extracted from Chinese herbal medicine. A polyphenol is a type of plant component that widely exists in plants and contains a variety of hydroxyphenols. They are important secondary metabolites in plants, with polyphenol structures. Polyphenols are primarily found in the bark, roots, shells, leaves, and fruits of plants. Polyphenols can be divided into flavonoids, phenolic acids, lignans, and stilbenes according to their structure. As bioactive molecules, polyphenols derived from Chinese herbal medicines have been shown to have many effects on human health by acting on different biological systems. Polyphenols have many physiological activities such as anti-osteoporosis, anti-oxidation, anti-infection, anti-tumor, and anti-atherosclerosis activities. In addition, a large number of studies have shown the effectiveness of polyphenols in the treatment of bone related diseases (Tao et al., 2016; Zou et al., 2016; Chen et al., 2017). Polyphenols can play a role in bone reconstruction by affecting bone formation and bone resorption. Polyphenols act on osteoclasts, osteoblasts and bone marrow mesenchymal stem cells, regulate several important signal pathways, and play a role in bone remodeling. In addition, these polyphenols are low cost and have fewer adverse

reactions. Therefore, they are more suitable for long-term use than synthetic drugs. Hence, their therapeutic potential would represent a new approach for future drug discovery and development based on polyphenol extracts from Chinese herbal medicines.

In this paper, the research progress of the specific mechanism of polyphenol compounds on bone formation and bone absorption is reviewed. This paper provides a theoretical basis for the basic research of polyphenol compounds on bone formation and bone absorption (Figures 1–3). In addition to the text of the polyphenols, we have summarized the main traditional Chinese medicine of polyphenols components (Table 1).

## 2.1 Flavonoids

### 2.1.1 Icariin

Icariin.

Icariin (ICA) is 8-isopentenyl flavonoid glycoside and is the most abundant flavonoid active ingredient in epimedium. Bone marrow stromal cells (BMSCs) are stem cells isolated from adult bone marrow that have the ability to differentiate into osteoblasts, chondrocytes, adipocytes, and myoblasts. Epimedium has the ability to promote bone formation and can promote the proliferation of bone marrow mesenchymal stem cells and the differentiation of osteoblasts. At the level of the epigenetic regulation mechanism, ICA can regulate the homeostasis between osteogenic and adipogenic differentiation of mesenchymal stem cells (MSCs) through ABCB1 promoter demethylation (Sun et al., 2015). Similarly, it can also conduct epigenetic modification through miRNA. For example, studies have shown that ICA regulates the levels of Mir-23a-3p and Mir-335-5p and regulates the downstream pathway, thus affecting the osteogenic differentiation of BMSCs (Zhang et al., 2021; Teng et al., 2022). In addition, up-regulating the expression of Mir-335-5p and inhibiting phosphatase and tensin homolog deleted on chromosome ten (PTEN) can improve the susceptibility of osteoporosis (OP), thus providing new strategies for the prevention and treatment of OP (Teng et al., 2022). ICA can promote osteogenic differentiation by regulating the BMP/Smads pathway, the BMA1-BMP2 signaling pathway, and the BMP-2/Smad 5/Runx two and WNT/ $\beta$ -catenin pathways in BMSCs (Gao et al., 2021; Zhang et al., 2021; Jiao et al., 2022). Epimedium promotes the migration of bone marrow mesenchymal stem cells *in vitro* and *in vivo* through the MAPK signaling pathway (Jiao et al., 2018). In addition, ICA can promote the *in-situ* proliferation and osteogenic differentiation of bone marrow mesenchymal stem cells, thus improving the curative effect of bone marrow mesenchymal stem cell transplantation in the treatment of OP (Gao et al., 2021).

ICA can promote the differentiation of osteoblasts and increase bone mineral density. Bone formation primarily

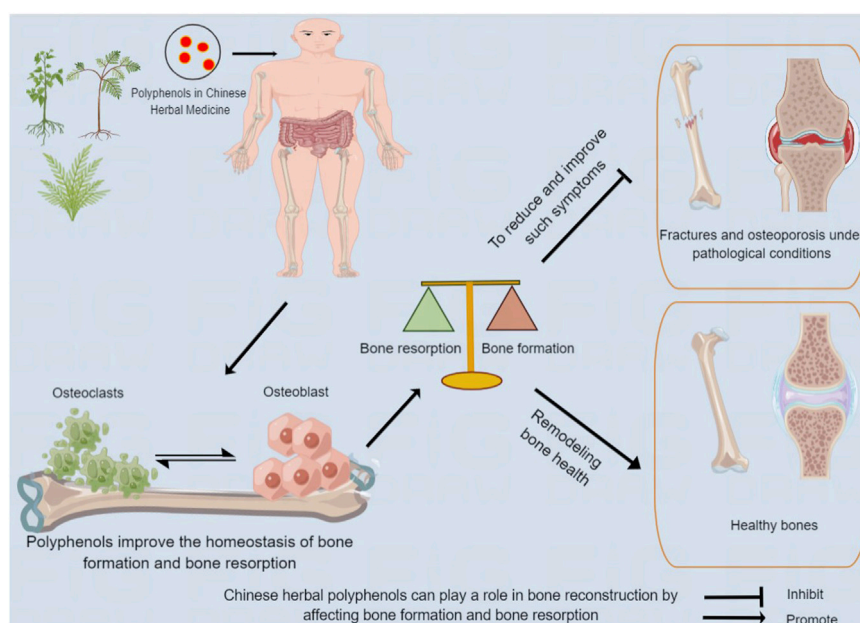


**FIGURE 1**

Chinese herbal polyphenols can play a role in bone reconstruction by affecting bone formation and bone resorption. After being absorbed in the gastrointestinal tract, Chinese medicine polyphenols act on human bones, and improve bone absorption and bone formation, contributing to bone remodeling and health, and reducing and improving adverse events.

promotes the synthesis and mineralization of the bone matrix through the proliferation and differentiation of osteoblasts that play important roles in bone formation and osteoporosis. ICA has an estrogen-like pharmacological activity that can stimulate the differentiation and mineralization of osteoblasts, regulate the differentiation of osteoclasts, inhibit the adipogenic trans-differentiation of osteoblasts, and increase the number of osteoblasts differentiated into mature osteoblasts through the ER-mediated pathway (Zhang et al., 2016). *In vivo*, icariin increases the peak bone mass of rats during the growing period. Osteoblasts respond to icariin through the activation of cAMP/PKA/CREB signals. After the cAMP/PKA/CREB signal was blocked, icariin-induced osteogenesis was inhibited. These results further support that icariin promotes bone formation through the activation of the cAMP/PKA/CREB pathway (Shi et al., 2017). Icariin can also improve OP by regulating the balance of the EphB 4/ephrin-B2 pathway (Huang et al., 2020). Interestingly, ICA can also prevent the iron overload induced reduction of Runx2, alkaline phosphatase, and osteopontin expression, thereby inhibiting iron-induced osteoblast apoptosis and promoting bone formation (Jing et al., 2019). In addition, some studies have shown that icariin might exert an osteoprotective effect by maintaining osteocyte viability and thereby regulating bone remodeling (Feng et al., 2013; Ho et al., 2018; Park et al., 2019).

ICA inhibits the formation of osteoclasts, and ICA inhibits the differentiation of pre-osteoclasts to osteoclasts. It also inhibits the expression of various genes involved in osteoclast formation and bone resorption (Zhang S. et al., 2017). Studies have shown that icariin can block osteoclast formation induced by MCF seven and MDA-MB-231 breast cancer cells by inhibiting the activation of NF- $\kappa$  B. In addition, icariin inhibits the expression of TRAF-6 stimulated by RANKL and then inhibits ERK phosphorylation, but it has no effect on the activation of p 38, JNK, and Akt (Kim et al., 2018). In addition, ICA can also prevent inflammatory bone loss. ICA inhibits the LPS-induced osteoclast formation process by inhibiting the activation of the p38 and JNK pathways (Hsieh et al., 2011).

In summary, ICA can prevent and treat osteoporosis by improving bone metabolism, promoting the differentiation of bone marrow mesenchymal stem cells, stimulating osteoblasts, and inhibiting osteoclast activity.

### 2.1.2 Bavachin

Bavachin (BA) is the extract of the Chinese medicine *Psoralea corylifolia*. BA may stimulate bone formation or have potential anti-osteoporosis activity (Wang et al., 2001). BA can obviously stimulate cell proliferation and promote the differentiation of osteoblasts. This function may be related to its characteristic structure, that is, the isoprene side chains connected in each of its molecular skeletons (Li et al., 2014).



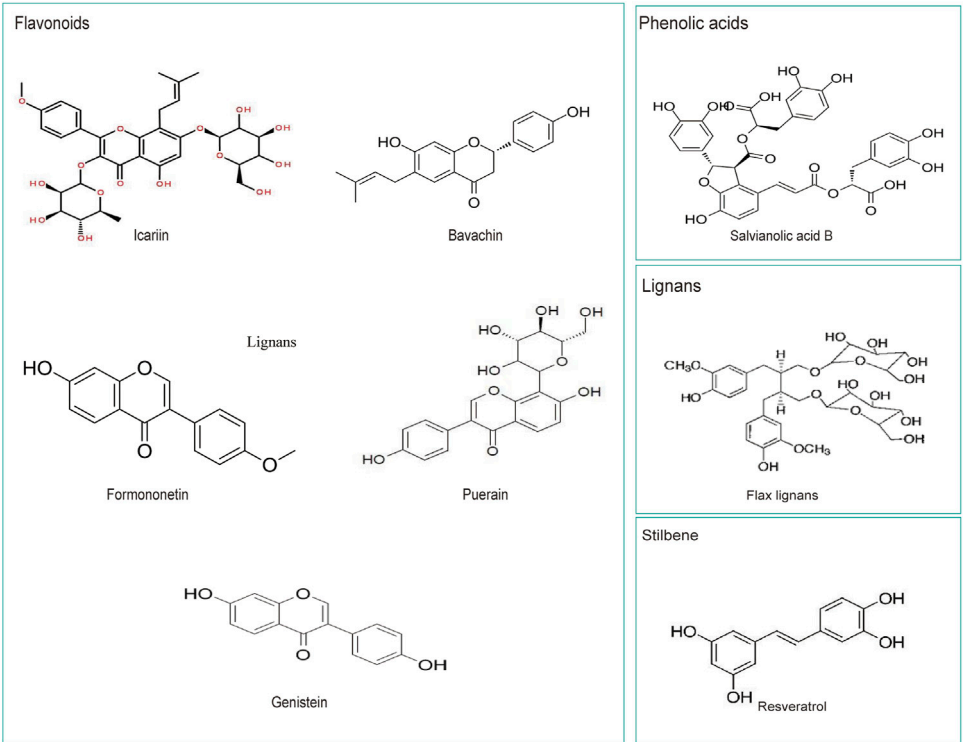


**FIGURE 2**  
The chemical structures of several widely studied polyphenols in Chinese herbal medicine.

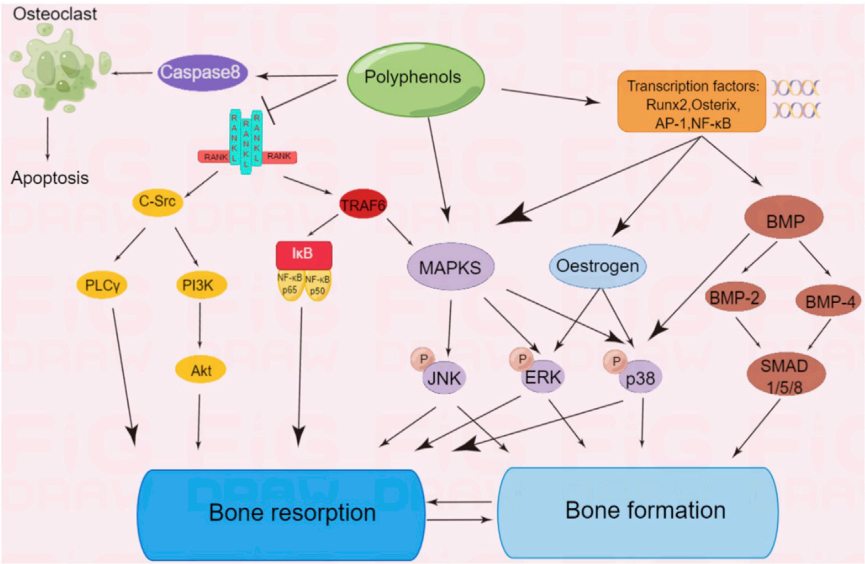


**FIGURE 3**  
Polyphenols regulate multiple signaling pathways of bone formation or bone resorption.

TABLE 1 List of Chinese herbal polyphenols connected with the mechanism of bone formation or resorption.

Traditional Chinese medicine	Polyphenols	Mechanism of action	References
Glycyrrhiza uralensis Fisch	Glabridin	Glabridin shows slightly positive effect on osteoporotically changed bone tissue. And glabridin inhibiting RANKL-induced activation of signaling molecules and subsequent transcription factors in osteoclast precursors	Kim et al. (2012); Klasik-Ciszewska et al. (2016)
Glycyrrhiza uralensis Fisch	Isoliquiritigenin (ILQ)	ILQ reduces bone resorption <i>in vivo</i> and osteoclast differentiation <i>in vitro</i> , by mechanisms likely differing from actions of ovarian hormones. In addition, ISL directly reduced RANKL-RANK-TRAF6 signaling pathway induced osteoclastogenesis	Zhu et al. (2012); Ji et al. (2018); Joyce et al. (2022)
Curcuma longa L.	Curcumin	Curcumin Modulates the Crosstalk Between Macrophages and Bone Mesenchymal Stem Cells to Ameliorate Osteogenesis. And curcumin enhanced the BMSC function for the proliferation and migration of articular chondrocytes, and anabolic gene expression of extracellular matrix in articular chondrocytes <i>in vitro</i> , and the generation of articular cartilage <i>in vivo</i> . And Curcumin reduced apoptosis and promoted osteogenesis under oxidative stress	Yang et al. (2020); Chen et al. (2021); Tan et al. (2021); Zhang et al. (2021a)
Taxillus sutchuenensis (Lecomte) Danser	Quercetin	Quercetin was shown to inhibit RANKL-mediated osteoclastogenesis, osteoblast apoptosis, oxidative stress and inflammatory response while promoting osteogenesis, angiogenesis, antioxidant expression, adipocyte apoptosis and osteoclast apoptosis. The possible underlying mechanisms involved are regulation of Wnt, NF- $\kappa$ B, Nrf2, SMAD-dependent, and intrinsic and extrinsic apoptotic pathways	Tsuji et al., 2009; Mariee et al., 2012; Xing et al., 2017; Fayed et al., 2019; Xu et al., 2019; Nani et al., 2021
Tripterygium wilfordii Hook. f.	Celastrol	Celastrol could regulate BM-MSCs fate and bone-fat balance in OP and skeletal aging by stimulating PGC-1 $\alpha$ . In addition, Celastrol inhibits glucocorticoid-induced osteoporosis in rat <i>via</i> the PI3K/AKT and Wnt signaling pathways. And Celastrol Attenuates RANKL-Induced Osteoclastogenesis <i>in vitro</i>	Xi et al., 2018; Li et al., 2020b; Xu et al., 2021
Zingiber officinale Roscoe	6-Gingerol	6-Gingerol Inhibits Inflammation-Associated Osteoclast Differentiation <i>via</i> Reduction of Prostaglandin E <sub>2</sub> Levels. And 6-Gingerol-stimulated osteoclast differentiation of bone marrow macrophages	Khan et al., 2012; Hwang et al., 2018; Zang et al., 2021
Lycium ruthenicum Murr	Anthocyanidin	Anthocyanins display their beneficial role on bone formation, including upregulating the osteoblastic genes, promoting the proliferation of osteoblasts and enhancing the mineral nodule formation	Li et al., 2017; Melough et al., 2017; Karunarathne et al., 2021; Liu et al., 2021
Rhodiola rosea L.	Salidroside	Salidroside improves bone histomorphology and prevents bone loss rats by regulating the OPG/RANKL Ratio, the HIF-1 $\alpha$ /VEGF signalling pathway, the Wnt/ $\beta$ -catenin signaling pathway	(Zheng et al., 2018; Guo et al., 2020; Li et al., 2021b)
Crocus sativus L.	Crocin	Anti-apoptotic effects, as well as osteoclast inhibition effects of crocin, have suggested it as a natural substance to treat osteoporosis and degenerative disease of bone and cartilage	Cao et al., 2014; Fu et al., 2017; Algandaby, (2019)
Reynoutria japonica Houtt	Polydatin	Polydatin improves osteogenic differentiation of human bone mesenchymal stem cells <i>via</i> BMP2-Wnt/ $\beta$ -catenin signaling pathway. In addition, Polydatin alleviates osteoporosis by enhancing the osteogenic differentiation of osteoblasts	Shen et al., 2020; Yuan et al., 2022
GALLA CHINENSIS	Epigallocatechin gallate (EGCG)	EGCG repressed new bone formation through Wnt/ $\beta$ -Catenin/COX-2 pathway. In addition, it may enhance bone defect healing <i>via</i> at least partly by the <i>de novo</i> bone formation of BMP-2	Lin et al., 2019; Zhang et al., 2021b
Davallia mariesii Moore ex Bak	Eriodictyol	Eriodictyol inhibits osteoclast differentiation and ovariectomy-induced bone loss <i>in vivo</i> . In addition, it Inhibits RANKL-Induced Osteoclast Formation and Function <i>Via</i> Inhibition of NFATc1 Activity	Lee et al., 2015; Song et al., 2016
Davallia mariesii Moore ex Bak	Naringenin	Naringenin promotes SDF-1/CXCR4 signaling pathway in BMSCs osteogenic differentiation. And naringenin is a Potential Anabolic Treatment for Bone Loss by Modulating Osteogenesis, Osteoclastogenesis, and Macrophage Polarization	Wang et al., 2021; Zhou et al., 2022

It has been shown that BA can reduce bone turnover by decreasing serum alkaline phosphatase, serum carboxy-terminal collagen crosslinks (CTX) levels, and the urine deoxypyridinoline (u-DPD)/creatinine ratio, and preventing OVX-induced urinary calcium and phosphorus excretion. Similarly, BA can reduce the contents of gamma-aminobutyric acid (GABA) and GABABRI in the femur, increase the bone mineral density, and reduce urinary calcium excretion, thus achieving the purpose of preventing and treating osteoporosis *in vivo* (Zhu et al., 2015).

BA may inhibit osteoclast differentiation through the NF- $\kappa$ B signaling pathway and the MAPK signaling pathway *in vitro* (Wei et al., 2022). BA treatment can inhibit osteoclast function and promote the up-regulation and down-regulation of the osteoclast marker gene, RANKL, and the osteoblast marker gene, OPG. Serum aminoterminal propeptide of type I procollagen (PINP) is widely considered as a biomarker for evaluating osteoblast activity (Hale et al., 2007). It was found that BA significantly improved the level of serum PINP. These results indicated that BA not only has estrogen-like effects, but also has beneficial effects on the function of osteoblasts. BA can prevent OVX-induced bone loss, but it does not affect uterine estrogen. This type of bone protection makes this a promising alternative to treat postmenopausal osteoporosis (PMOP) safely and effectively (Weng et al., 2015).

BA can achieve the purpose of anti-osteoporosis through a delicate balance of bone formation and bone resorption.

### 2.1.3 Formononetin

Formononetin (FO) is one of the primary isoflavones extracted from *Astragalus membranaceus*. Studies have shown that it can stimulate the formation of osteoblasts, thus increasing bone mass and improving the microstructure of bone. FO can regulate the expression of RANKL and OPG at the mRNA level, as well as related markers of osteogenic differentiation, thus promoting the mineralization potential of osteoblasts (Zaklos-Szyda et al., 2020). In addition, FO promoted bone regeneration in a mouse model of cortical bone defect in a manner similar to PTH and upregulated the expression of the predominant runt-related transcription factor 2 and osteocalcin (Singh et al., 2017). The research results showed that FO inhibited fat formation through the AMPK/ $\beta$ -catenin signal transduction pathway, thus improving the inverse relationship between osteoblasts and adipocytes and preventing obesity and bone loss induced by high-fat diets (Gautam et al., 2017).

FO can inhibit the activation of osteoclasts and plays an important role. Studies have shown that FO can inhibit the proliferation and differentiation of primary bone marrow mononuclear macrophages into osteoclasts and down-regulate the expression of proteins and genes related to the bone resorption function of osteoclasts, and this may be one of the mechanisms of FO in preventing and treating destruction and collapse in femoral head necrosis (Hong et al., 2020). FO

attenuates osteoclast differentiation and calcium loss by regulating the transcription factor, AP-1, in type I diabetic mice, and it is expected to be a prospective drug for the treatment of osteoporosis (Jing et al., 2022).

The immunomodulatory activity of formononetin can prevent OVX-induced bone loss. In addition, the generation of osteoclasts and apoptosis of osteoblasts induced by IL-17 are inhibited (Mansoori et al., 2016). FO can reduce the production of osteoclasts by inhibiting the activation of NF- $\kappa$ B, c-fos, and nuclear factors that activate the cytoplasmic one signal pathway induced by RANKL in T cells (Huh et al., 2014). FO also has estrogen-like effects that can inhibit bone loss caused by estrogen deficiency after menopause and improve the activity of alkaline phosphatase in OVX rats *in vivo* and *in vitro* (Ha et al., 2010).

In a word, FO can stimulate the formation of osteoblasts and inhibit the activation of osteoclasts.

### 2.1.4 Puerarin

Pueraria, originating from China, has a long history and is one of the most commonly used Chinese medicines in Asia. Due to its high isoflavone content, it has been widely used as a natural alternative to hormone replacement therapy for postmenopausal symptoms (Lee et al., 2021). Puerarin (PUE) is an isoflavone isolated from the pueraria root that is widely distributed in several organs related to aging, such as the hippocampus, femur, tibia, and mammary gland, after oral administration (Anukunwithaya et al., 2018). In addition to anti-inflammatory, antioxidant, and anti-diabetic effects (Xiao et al., 2011; Chen et al., 2018; Jeon et al., 2020), PUE also plays an important role in bone diseases such as OP. PUE can promote bone formation by influencing the expression of osteogenic related genes and promoting the formation of a mineralized matrix. PUE can significantly enhance alkaline phosphatase activity, mineralized matrix generation, and osteoblast-related protein expression levels. In addition, microCT imaging measurements demonstrated that PUE significantly promoted new bone formation (Yang et al., 2022). At the level of epigenetic modification, PUE regulates transcriptional expression related to bone formation through microRNA (Shan et al., 2018; Zhou et al., 2020). For example, PUE can regulate the up-regulation of Mir-155-3p to promote BMSCs differentiation and bone formation and increase bone mass in bone grafted rats.

Studies have shown that PUE also has a regulatory effect on bone resorption. PUE can down-regulate the mRNA levels of osteoclast marker genes CTR, CATH-K, NFATc1 and c-fos, indicating that PUE inhibits osteoclast cell function *in vitro* (Yang et al., 2019). *In vitro*, PUE attenuated bone resorption without impairing osteoclast viability and significantly prevented OVX-induced bone loss by inhibiting bone resorption without altering bone formation (Qiu et al., 2022). Furthermore, PUE inhibits RANKL-induced osteoclast activation, the bone resorption capacity, and

F-actin ring formation *in vitro* with an increase in the PUE concentration (Yang et al., 2019). PUE may play a protective role in osteoclast-related osteolytic diseases. *In vitro*, PUE prevented RANCL-induced osteoclast differentiation, bone resorption, and F-actin ring formation, reduced phosphorylation of p65, and prevented P65 translocation from the cytoplasm to the nucleus in a concentration-dependent manner. PUE also decreased the expression of osteoclast specific factors (Tang et al., 2020). *In vivo* experiments, PUE significantly inhibited bone resorption mediated wear particles in a skull bone resorption model (Yang et al., 2019).

PUE can also prevent cell apoptosis through the HDAC1/HDAC3 signaling pathway and regulate the expression of HIF-1 $\alpha$ , TIMP-3, and Bcl-2, thus playing an anti-osteoporosis role (Guo et al., 2019; Waqas et al., 2020). For osteoporosis, it also increases bone mass and inhibits osteoclast formation (Yang et al., 2018; Xiao et al., 2020). By enhancing osteogenesis and promoting bone formation, PUE also improves OVX-induced osteoporosis and lipid metabolism by regulating phospholipid metabolism and polyunsaturated fatty acid biosynthesis, thereby reducing adipogenic differentiation. In addition, activation of the Wnt pathway and inhibition of the PPAR $\gamma$  pathway promote adipogenesis in osteogenic differentiation of inactivated rat bone marrow mesenchymal stem cells (Li et al., 2022). For osteoporosis caused by postmenopausal estrogen deficiency, the results of a clinical trial showed that PUE was well tolerated for the short-term treatment of mild to severe menopausal symptoms in women. Kudzu root extract may benefit bone and cartilage health and may be a promising natural alternative to existing treatments for menopausal symptoms (Bihlet et al., 2021).

Recent studies have found that the microbiota plays an important role in regulating the skeletal microenvironment, thereby triggering anti-osteoporosis effects. Furthermore, intestinal microbiota can participate in the process of osteoporosis by inducing inflammatory reactions and changes in the autoimmune system. PUE treatment can improve the bone microenvironment and inhibit OVX-induced osteoporosis by regulating the release of short chain fatty acids (SCFAs) from intestinal flora and repairing the intestinal mucosal integrity (Li B. et al., 2020). In addition, serum pharmacokinetics suggest that pueraria root extract may undergo enterohepatic circulation (Mun et al., 2009).

### 2.1.5 Genistein

Genistein is a natural isoflavone compound found in legumes and dentate plants. It is a phytoestrogen that makes up more than 60% of soy isoflavones (Nazari-Khanamiri and Ghasemnejad-Berenji, 2021). Its pharmacological properties make it a potential drug for treating a variety of conditions including postmenopausal symptoms, cancer, and bone, brain, and heart disease (Nazari-Khanamiri and Ghasemnejad-Berenji, 2021).

It is well known that genistein has been shown to stimulate bone formation by osteoblasts and inhibit bone resorption by osteoclasts, thereby increasing bone mass (Yamaguchi, 2012). Genistein improves bone healing by triggering the estrogen receptor  $\alpha$ -mediated expression of osteogenesis-related genes and maturation of osteoblasts. The inhibition of ER expression was shown to immediately reduce the genistein-induced enhancement of mitochondrial energy production and osteoblast activation (Wu et al., 2020). Additionally, studies have shown that genistein promotes osteoblast differentiation and maturation by activating the ER, p38MAPK-Runx2, and NO/cGMP pathways and by inducing the osteoclastogenesis inhibitor, osteoprotegerin (OPG), and blocking the NF- $\kappa$ B signaling pathway, inhibiting osteoclast formation and bone resorption (Ming et al., 2013).

At the level of epigenetic modification, genistein counteracts NF- $\kappa$ B-induced osteoclast generation and downstream signaling by directly regulating the transcription of histone methyltransferases EzH2 and EzH1 (Kushwaha et al., 2022). Furthermore, there are clinical trials showing that supplementation with the dietary phytoestrogen genistein may be as effective as hormone replacement therapy in reducing bone loss associated with menopause without the associated bone loss side effects (Cotter and Cashman, 2003; Sansai et al., 2020). In this study, to improve the bioavailability of genistein and reduce its side effects, the nanofied formulation of genistein with Vitamin D was invented to enhance the therapeutic efficacy of the osteoporosis model *in vitro* and improve alkaline phosphatase activity and multinucleated giant cell formation (Kushwaha et al., 2022). If the bioavailability of genistein is improved, its future market development potential is huge.

## 2.2 Phenolic acids

### 2.2.1 Salvia B

*Salvia miltiorrhiza* Bunge, also known as *Salvia miltiorrhiza* Bunge, is often used in traditional Chinese medicine (TCM) in combination with other traditional Chinese medicines to treat bone diseases. Salvianolic acid B (Sal B) is a water-soluble phenolic compound isolated from *Salvia miltiorrhiza* Bunge in which the active ingredient in the water-soluble phenolic compound is greater than 50% (Cao et al., 2012). As a polyphenolic acid compound with seven phenolic hydroxyl groups, Sal B is one of the strongest natural antioxidants, and it is metabolized into salvianol *in vivo* (Chen et al., 2013; Tang et al., 2014).

It is worth noting that Sal B can also act on osteoblasts and induce bone marrow-derived mesenchymal stem cells to become osteoblasts. Studies have shown that Sal B and *Salvia miltiorrhiza* can induce osteogenic differentiation of rat bone marrow stromal cells by up-regulating the nitric oxide pathway (Zhang X. et al., 2017). In addition, Sal B can protect osteoblasts treated with

prednisolone acetate by stimulating the activity of osteoblasts and the expression of genes related to bone formation and differentiation. It can also increase the alkaline phosphatase (ALP) activity in osteoblasts and stimulate the expression of ALP, which is inhibited by prednisolone acetate, and up-regulate the expression of Runx2, Osx, OCN, IGF-I, Col-I, HO-I, mRNA, and protein expression (Qiao et al., 2019). For the first time, studies have shown that Sal B can target TAZ to promote osteogenesis and reduce adipogenesis by activating MEK-ERK signaling pathway, which provides evidence that Sal B can be used as a potential therapeutic agent for the management of bone diseases (Wang et al., 2019). Sal B can also play a cytoprotective role to inhibit the apoptosis of BMSCs by regulating H<sub>2</sub>O<sub>2</sub>-mediated ROS/MEK/ERK1/2 pathway (Lu et al., 2010). This indicated that Sal B had a protective effect on osteoblasts by stimulating osteoblast activity and the expression of genes related to bone formation and differentiation.

## 2.3 Lignans

### 2.3.1 Flax lignans

Flax lignans are phytonutrient extract of *Linum usitatissimum* L. Chemically, the C6-OH of the glucose of flax lignans is esterified to the carboxylic acid of hydroxymethylglutaric acid (Imran et al., 2015). Flax lignans in combination with low-dose estrogen treatment maximally prevents bone loss induced by oophorectomy (Sacco et al., 2009). However, its use alone has no effect on the bone mineral density content, and a clinical study showed no statistically significant difference in bone turnover markers between the treatment group and the placebo group (Alcorn et al., 2017). Flax lignans have no negative effects on bone strength and bone health in aged rats (Ward et al., 2001a). These studies indicate that supplementation with flaxseed may contribute to improving the bone properties of osteoporosis, and these predominantly protective effects may be attributed to flaxseed oil (predominantly ALA), not to the fractions of flax lignans (Ward et al., 2001b; Lucas et al., 2002; Cohen and Ward, 2005). Flax Lignans are characterized by anti-inflammatory, antioxidant, and neuroprotective properties (Watanabe et al., 2020; Asad et al., 2021; Wu et al., 2021).

## 2.4 Stilbenes

### 2.4.1 Resveratrol

Resveratrol (RES), a non-flavonoid polyphenolic organic compound and is a bioactive component in *Rhizoma Polygoni Cuspidati*. It is easily absorbed after oral administration and is excreted through the urine and feces after metabolism. A large number of experimental studies have shown that RES has antioxidant, anti-inflammatory, anti-cancer, and

cardiovascular and cerebrovascular protection effects (Biswas et al., 2020; Thaung Zaw et al., 2021; De Luca et al., 2022; Dzator et al., 2022; Mahjabeen et al., 2022).

Previous studies have shown that RES also plays an important role in protecting and promoting early bone metabolism and differentiation through a mechanism similar to genistein that promotes osteoblast-mediated bone formation and inhibits osteoclast-stimulated bone formation (Tou, 2015). RES increased the serum OPG, femoral SIRT1, and  $\beta$ -catenin expression and significantly decreased the NF- $\kappa$ B ligand receptor activator (RANKL) by stimulating SIRT1 expression and Wnt/ $\beta$ -catenin signaling. Finally, the bone mass of the femur increased and the bone mineral density significantly increased (Wang et al., 2022). In addition, RES can also protect bone cells from some physicochemical damage. For example, studies have shown that RES pretreatment for 30 min can significantly prevent cadmium-induced apoptosis and attenuate ERK1/2 and JNK signaling by regulating ERK1/2 and JNK signaling. It also produces cadmium-induced inhibition of osteogenic differentiation (Mei et al., 2021).

The aging of mesenchymal stem cells (MSCs) and the associated decline of osteogenic function lead to the disruption of the balance between bone formation and resorption, which is the key pathogenesis of osteoporosis during aging. Recent data has shown that RES can improve the osteogenic differentiation of senescent BMMSCs, and long-term intermittent applications can enhance bone formation and compensate for bone loss. The specific mechanism is that RES up-regulates Mitofilin, promotes the transcription of mitochondrial autonomous genes, and restores cell metabolism through mitochondrial function (Lv et al., 2018). Mitofilin, also known as the mitochondrial inner membrane protein (IMT) or Mic60, is a core component of the mitochondrial contact site and crista tissue system (MICOS) (Li et al., 2016; Tarasenko et al., 2017). Mitofilin is indispensable for mitochondrial homeostasis and osteogenesis in bone marrow mesenchymal stem cells (Chen et al., 2008; Pietilä et al., 2010). Mitofilin deficiency leads to aging and bone loss in BMMSC (George et al., 2011; Sahin et al., 2011).

Relevant clinical trials have also proved the efficacy and safety of RES. A clinical study conducted at the Aarhus University Hospital showed that high-dose RES supplements increased bone mineral density (BMD) and bone alkaline phosphatase in obese men, with positive effects on bones (Ornstrup et al., 2014). A 24-month RES (RESHAW) trial of healthy ageing in women showed that regular 75 mg resveratrol supplementation twice daily had the potential to slow bone loss in the lumbar spine and femoral neck, which is common at fracture sites in postmenopausal women without significant osteoporosis (Wong et al., 2020). However, a systematic review and meta-analysis showed that



RES supplements did not show any significant effect on BMD or serum bone markers (Li Q. et al., 2021). Therefore, further research utilizing better organized multicenter randomized trials is necessary so that physicians can provide more advice for clinical decision-making.

### 3 Conclusion

The incidence of bone metabolic diseases has been increasing annually. The imbalance of bone formation and absorption is an important mechanism of bone metabolism related diseases. Chinese herbal medicine has been used for thousands of years, among which polyphenols are an important active ingredient. This paper reviewed how polyphenols in Chinese herbal medicine can help bone reconstruction and improve bone metabolism by affecting the balance between bone formation and bone absorption. Generally speaking, regarding the beneficial effects of polyphenols in bone metabolic diseases, due to the lack of multi-center randomized trials in polyphenols in this field, it is considered necessary to conduct human trials, and further research can be conducted in this research field.

### Author contributions

All the authors listed in this article made direct and substantial contributions to the work and approved its publication.

### References

- Alcorn, J., Whiting, S., Viveky, N., Di, Y., Mansell, K., Fowler, S., et al. (2017). Protocol for a 24-week randomized controlled study of once-daily oral dose of flax lignan to healthy older adults. *JMIR Res. Protoc.* 6 (2), e14. doi:10.2196/resprot.6817
- Algendaby, M. M. (2019). Crocin attenuates metabolic syndrome-induced osteoporosis in rats. *J. Food Biochem.* 43 (7), e12895. doi:10.1111/jfbc.12895
- Anukunwithaya, T., Poo, P., Hunsakunachai, N., Rodsiri, R., Malaivijitnond, S., and Khemawoot, P. (2018). Absolute oral bioavailability and disposition kinetics of puerarin in female rats. *BMC Pharmacol. Toxicol.* 19 (1), 25. doi:10.1186/s40360-018-0216-3
- Asad, B., Khan, T., Gul, F. Z., Ullah, M. A., Drouet, S., Mikac, S., et al. (2021). Scarlet flax *Linum grandiflorum* (L.) *in vitro* cultures as a new source of antioxidant and anti-inflammatory lignans. *Molecules* 26 (15), 4511. doi:10.3390/molecules26154511
- Bihlet, A. R., Byrjalsen, I., Andersen, J. R., Simonsen, S. F., Mundbjerg, K., Helmer, B., et al. (2021). The efficacy and safety of multiple dose regimens of kudzu (pueraria lobata) root extract on bone and cartilage turnover and menopausal symptoms. *Front. Pharmacol.* 12, 760629. doi:10.3389/fphar.2021.760629
- Biswas, P., Dellanoce, C., Vezzoli, A., Mrakic-Spota, S., Malnati, M., Beretta, A., et al. (2020). Antioxidant activity with increased endogenous levels of vitamin C, E and A following dietary supplementation with a combination of glutathione and resveratrol precursors. *Nutrients* 12 (11), E3224. doi:10.3390/nu12113224
- Cao, P. C., Xiao, W. X., Yan, Y. B., Zhao, X., Liu, S., Feng, J., et al. (2014). Preventive effect of crocin on osteoporosis in an ovariectomized rat model. *Evid. Based. Complement. Altern. Med.* 2014, 825181. doi:10.1155/2014/825181
- Cao, W., Guo, X. W., Zheng, H. Z., Li, D. P., Jia, G. B., and Wang, J. (2012). Current progress of research on pharmacologic actions of salvianolic acid B. *Chin. J. Integr. Med.* 18 (4), 316–320. doi:10.1007/s11655-012-1052-8
- Chau, J. F., Leong, W. F., and Li, B. (2009). Signaling pathways governing osteoblast proliferation, differentiation and function. *Histol. Histopathol.* 24 (12), 1593–1606. doi:10.14670/HH-24.1593
- Chen, C. T., Shih, Y. R., Kuo, T. K., Lee, O. K., and Wei, Y. H. (2008). Coordinated changes of mitochondrial biogenesis and antioxidant enzymes during osteogenic differentiation of human mesenchymal stem cells. *Stem Cells* 26 (4), 960–968. doi:10.1634/stemcells.2007-0509
- Chen, C. Y., Li, H., Yuan, Y. N., Dai, H. Q., and Yang, B. (2013). Antioxidant activity and components of a traditional Chinese medicine formula consisting of *Crataegus pinnatifida* and *Salvia miltiorrhiza*. *BMC Complement. Altern. Med.* 13, 99. doi:10.1186/1472-6882-13-99
- Chen, S., Liang, H., Ji, Y., Kou, H., Zhang, C., Shang, G., et al. (2021). Curcumin modulates the crosstalk between macrophages and bone mesenchymal stem cells to ameliorate osteogenesis. *Front. Cell Dev. Biol.* 9, 634650. doi:10.3389/fcell.2021.634650
- Chen, X., Ren, S., Zhu, G., Wang, Z., and Wen, X. (2017). Emodin suppresses cadmium-induced osteoporosis by inhibiting osteoclast formation. *Environ. Toxicol. Pharmacol.* 54, 162–168. doi:10.1016/j.etap.2017.07.007
- Chen, X., Yu, J., and Shi, J. (2018). Management of diabetes mellitus with puerarin, a natural isoflavone from pueraria lobata. *Am. J. Chin. Med.* 46 (8), 1771–1789. doi:10.1142/s0192415x18500891
- Cohen, S. L., and Ward, W. E. (2005). Flaxseed oil and bone development in growing male and female mice. *J. Toxicol. Environ. Health. A* 68 (21), 1861–1870. doi:10.1080/15287390500226516
- Cotter, A., and Cashman, K. D. (2003). Genistein appears to prevent early postmenopausal bone loss as effectively as hormone replacement therapy. *Nutr. Rev.* 61 (10), 346–351. doi:10.1301/nr.2003.oct.346-351

### Funding

Our work was supported by Guangdong Provincial Key Laboratory of Traditional Chinese Medicine Informatization (2021B1212040007), the National Natural Science Foundation of China (81603342), National Key R&D Program of China 2018YFC2002500, Foshan “Summit Plan” of building high-level hospitals, and the Administration of Traditional Chinese Medicine of Guangdong Province (No. 20171074), Guangdong Provincial Bureau of Traditional Chinese Medicine (20221107), Natural Science Foundation of Guangdong Province (2022A1515012641).

### Conflict of interest

The authors declare that the research was conducted in the absence of any commercial or financial relationships that could be construed as a potential conflict of interest.

### Publisher's note

All claims expressed in this article are solely those of the authors and do not necessarily represent those of their affiliated organizations, or those of the publisher, the editors and the reviewers. Any product that may be evaluated in this article, or claim that may be made by its manufacturer, is not guaranteed or endorsed by the publisher.

- Crotti, T. N., Dharmapatri, A. A., Alias, E., and Haynes, D. R. (2015). Osteoimmunology: Major and costimulatory pathway expression associated with chronic inflammatory induced bone loss. *J. Immunol. Res.* 2015, 281287. doi:10.1155/2015/281287
- De Luca, A., Bellavia, D., Raimondi, L., Carina, V., Costa, V., Fini, M., et al. (2022). Multiple effects of resveratrol on osteosarcoma cell lines. *Pharm. (Basel)* 15 (3), 342. doi:10.3390/ph15030342
- Dzator, J. S. A., Howe, P. R. C., Coupland, K. G., and Wong, R. H. X. (2022). A randomised, double-blind, placebo-controlled crossover trial of resveratrol supplementation for prophylaxis of hormonal migraine. *Nutrients* 14 (9), 1763. doi:10.3390/nu14091763
- Estell, E. G., and Rosen, C. J. (2021). Emerging insights into the comparative effectiveness of anabolic therapies for osteoporosis. *Nat. Rev. Endocrinol.* 17 (1), 31–46. doi:10.1038/s41574-020-00426-5
- Fayed, H. A., Barakat, B. M., Elshaer, S. S., Abdel-Naim, A. B., and Menze, E. T. (2019). Antiosteoporotic activities of isoquercitrin in ovariectomized rats: Role of inhibiting hypoxia inducible factor-1 alpha. *Eur. J. Pharmacol.* 865, 172785. doi:10.1016/j.ejphar.2019.172785
- Feng, R., Feng, L., Yuan, Z., Wang, D., Wang, F., Tan, B., et al. (2013). Icaritin protects against glucocorticoid-induced osteoporosis *in vitro* and prevents glucocorticoid-induced osteocyte apoptosis *in vivo*. *Cell Biochem. Biophys.* 67 (1), 189–197. doi:10.1007/s12013-013-9533-8
- Fu, L., Pan, F., and Jiao, Y. (2017). Crocin inhibits RANKL-induced osteoclast formation and bone resorption by suppressing NF- $\kappa$ B signaling pathway activation. *Immunobiology* 222 (4), 597–603. doi:10.1016/j.imbio.2016.11.009
- Gao, J., Gao, C., Li, H., Wang, G. S., Xu, C., and Ran, J. (2017). Effect of zoledronic acid on reducing femoral bone mineral density loss following total hip arthroplasty: A meta-analysis from randomized controlled trials. *Int. J. Surg.* 47, 116–126. doi:10.1016/j.ijsu.2017.08.559
- Gao, J., Xiang, S., Wei, X., Yadav, R. I., Han, M., Zheng, W., et al. (2021). Icaritin promotes the osteogenesis of bone marrow mesenchymal stem cells through regulating sclerostin and activating the wnt/ $\beta$ -catenin signaling pathway. *Biomed. Res. Int.* 2021, 6666836. doi:10.1155/2021/6666836
- Gautam, J., Khedgikar, V., Kushwaha, P., Choudhary, D., Nagar, G. K., Dev, K., et al. (2017). Formononetin, an isoflavone, activates AMP-activated protein kinase/ $\beta$ -catenin signalling to inhibit adipogenesis and rescues C57BL/6 mice from high-fat diet-induced obesity and bone loss. *Br. J. Nutr.* 117 (5), 645–661. doi:10.1017/S0007114517000149
- George, S. K., Jiao, Y., Bishop, C. E., and Lu, B. (2011). Mitochondrial peptidase IMMP2L mutation causes early onset of age-associated disorders and impairs adult stem cell self-renewal. *Aging Cell* 10 (4), 584–594. doi:10.1111/j.1474-9726.2011.00686.x
- Grigg, A., Butcher, B., Khodr, B., Bajel, A., Hertzberg, M., Patil, S., et al. (2017). An individualised risk-adapted protocol of pre- and post transplant zoledronic acid reduces bone loss after allogeneic stem cell transplantation: Results of a phase II prospective trial. *Bone Marrow Transpl.* 52 (9), 1288–1293. doi:10.1038/bmt.2017.108
- Guo, C. J., Xie, J. J., Hong, R. H., Pan, H. S., Zhang, F. G., and Liang, Y. M. (2019). Puerarin alleviates streptozotocin (STZ)-induced osteoporosis in rats through suppressing inflammation and apoptosis via HDAC1/HDAC3 signaling. *Biomed. Pharmacother.* 115, 108570. doi:10.1016/j.biopha.2019.01.031
- Guo, Q., Yang, J., Chen, Y., Jin, X., Li, Z., Wen, X., et al. (2020). Salidroside improves angiogenesis-osteogenesis coupling by regulating the HIF-1 $\alpha$ /VEGF signalling pathway in the bone environment. *Eur. J. Pharmacol.* 884, 173394. doi:10.1016/j.ejphar.2020.173394
- Ha, H., Lee, H. Y., Lee, J. H., Jung, D., Choi, J., Song, K. Y., et al. (2010). Formononetin prevents ovariectomy-induced bone loss in rats. *Arch. Pharm. Res.* 33 (4), 625–632. doi:10.1007/s12272-010-0418-8
- Hale, L. V., Galvin, R. J., Risteli, J., Ma, Y. L., Harvey, A. K., Yang, X., et al. (2007). PINP: A serum biomarker of Bone formation in the rat. *Bone* 40 (4), 1103–1109. doi:10.1016/j.bone.2006.11.027
- Ho, M. X., Poon, C. C., Wong, K. C., Qiu, Z. C., and Wong, M. S. (2018). Icaritin, but not genistein, exerts osteogenic and anti-apoptotic effects in osteoblastic cells by selective activation of non-genomic ER $\alpha$  signaling. *Front. Pharmacol.* 9, 474. doi:10.3389/fphar.2018.00474
- Hong, Y. B., Jiang, H., Wang, J. W., Yu, P. F., and You, W. L. (2020). Experimental study on the inhibition of Formononetin on the differentiation of osteoclasts induced by RANKL. *Zhongguo Gu Shang* 33 (1), 64–70. doi:10.3969/j.issn.1003-0034.2020.01.012
- Hsieh, T. P., Sheu, S. Y., Sun, J. S., and Chen, M. H. (2011). Icaritin inhibits osteoclast differentiation and bone resorption by suppression of MAPKs/NF- $\kappa$ B regulated HIF-1 $\alpha$  and PGE(2) synthesis. *Phytomedicine* 18 (2–3), 176–185. doi:10.1016/j.phymed.2010.04.003
- Huang, M., Wang, Y., and Peng, R. (2020). Icaritin alleviates glucocorticoid-induced osteoporosis through EphB4/ephrin-B2 Axis. *Evid. Based. Complement. Altern. Med.* 2020, 2982480. doi:10.1155/2020/2982480
- Huh, J. E., Lee, W. I., Kang, J. W., Nam, D., Choi, D. Y., Park, D. S., et al. (2014). Formononetin attenuates osteoclastogenesis via suppressing the RANKL-induced activation of NF- $\kappa$ B, c-Fos, and nuclear factor of activated T-cells cytoplasmic 1 signaling pathway. *J. Nat. Prod.* 77 (11), 2423–2431. doi:10.1021/np500417d
- Hwang, Y. H., Kim, T., Kim, R., and Ha, H. (2018). The natural product 6-gingerol inhibits inflammation-associated osteoclast differentiation via reduction of prostaglandin E<sub>2</sub> levels. *Int. J. Mol. Sci.* 19 (7), E2068. doi:10.3390/ijms19072068
- Imran, M., Ahmad, N., Anjum, F. M., Khan, M. K., Mushtaq, Z., Nadeem, M., et al. (2015). Potential protective properties of flax lignan secoisolariciresinol diglucoside. *Nutr. J.* 14, 71. doi:10.1186/s12937-015-0059-3
- Jeon, Y. D., Lee, J. H., Lee, Y. M., and Kim, D. K. (2020). Puerarin inhibits inflammation and oxidative stress in dextran sulfate sodium-induced colitis mice model. *Biomed. Pharmacother.* 124, 109847. doi:10.1016/j.biopha.2020.109847
- Ji, B., Zhang, Z., Guo, W., Ma, H., Xu, B., Mu, W., et al. (2018). Isoliquiritigenin blunts osteoarthritis by inhibition of bone resorption and angiogenesis in subchondral bone. *Sci. Rep.* 8 (1), 1721. doi:10.1038/s41598-018-19162-y
- Jiao, F., Tang, W., Huang, H., Zhang, Z., Liu, D., Zhang, H., et al. (2018). Icaritin promotes the migration of BMSCs *in vitro* and *in vivo* via the MAPK signaling pathway. *Stem Cells Int.* 2018, 2562105. doi:10.1155/2018/2562105
- Jiao, F., Tang, W., Wang, J., Liu, D., Zhang, H., and Tang, D. (2022). Icaritin promotes the repair of bone marrow mesenchymal stem cells in rabbit knee cartilage defects via the BMP/Smad pathway. *Ann. Transl. Med.* 10 (12), 691. doi:10.21037/atm-22-2515
- Jing, W., Feng, L., Peng, K., Zhang, W., and Wang, B. (2022). Formononetin attenuates osteoclast differentiation and calcium loss by mediating transcription factor AP-1 in type I diabetic mice. *J. Biochem. Mol. Toxicol.* 36 (6), e23042. doi:10.1002/jbt.23042
- Jing, X., Du, T., Chen, K., Guo, J., Xiang, W., Yao, X., et al. (2019). Icaritin protects against iron overload-induced bone loss via suppressing oxidative stress. *J. Cell. Physiol.* 234 (7), 10123–10137. doi:10.1002/jcp.27678
- Joyce, K. M., Wong, C. P., Scriven, I. A., Olson, D. A., Doerge, D. R., Branscum, A. J., et al. (2022). Isoliquiritigenin decreases bone resorption and osteoclast differentiation. *Mol. Nutr. Food Res.* 66 (11), e2100974. doi:10.1002/mnfr.202100974
- Karsenty, G., and Khosla, S. (2022). The crosstalk between bone remodeling and energy metabolism: A translational perspective. *Cell Metab.* 34 (6), 805–817. doi:10.1016/j.cmet.2022.04.010
- Karunaratne, W., Molagoda, I. M. N., Lee, K. T., Choi, Y. H., Jin, C. Y., and Kim, G. Y. (2021). Anthocyanins isolated from *Hibiscus syriacus* L. attenuate lipopolysaccharide-induced inflammation and endotoxic shock by inhibiting the TLR4/MD2-mediated NF- $\kappa$ B signaling pathway. *Phytomedicine* 91, 153237. doi:10.1016/j.phymed.2020.153237
- Khan, K., Singh, A., Mittal, M., Sharan, K., Singh, N., Dixit, P., et al. (2012). [6]-Gingerol induces bone loss in ovary intact adult mice and augments osteoclast function via the transient receptor potential vanilloid 1 channel. *Mol. Nutr. Food Res.* 56 (12), 1860–1873. doi:10.1002/mnfr.201200200
- Kim, B., Lee, K. Y., and Park, B. (2018). Icaritin abrogates osteoclast formation through the regulation of the RANKL-mediated TRAF6/NF- $\kappa$ B/ERK signaling pathway in Raw264.7 cells. *Phytomedicine* 51, 181–190. doi:10.1016/j.phymed.2018.06.020
- Kim, H. S., Suh, K. S., Sul, D., Kim, B. J., Lee, S. K., and Jung, W. W. (2012). The inhibitory effect and the molecular mechanism of glabridin on RANKL-induced osteoclastogenesis in RAW264.7 cells. *Int. J. Mol. Med.* 29 (2), 169–177. doi:10.3892/ijmm.2011.822
- Klasik-Ciszewska, S., Kaczmarczyk-Sedlak, I., and Wojnar, W. (2016). Effect of glabridin and glycyrrhizic acid on histomorphometric parameters of bones in ovariectomized rats. *Acta Pol. Pharm.* 73 (2), 517–527.
- Kushwaha, A. C., Mohanbhai, S. J., Sardoiwala, M. N., Jaganathan, M., Karmakar, S., and Roy Choudhury, S. (2022). Nanoemulsified genistein and vitamin D mediated epigenetic regulation to inhibit osteoporosis. *ACS Biomater. Sci. Eng.* 8 (9), 3810–3818. doi:10.1021/acsbomaterials.2c00165
- Lange, U., Classen, K., Muller-Ladner, U., and Richter, M. (2017). Weekly oral bisphosphonates over 2 years prevent bone loss in cardiac transplant patients. *Clin. Transpl.* 31 (11), e13122. doi:10.1111/ctr.13122
- Lee, J., Noh, A. L., Zheng, T., Kang, J. H., and Yim, M. (2015). Eriodicyol inhibits osteoclast differentiation and ovariectomy-induced bone loss *in vivo*. *Exp. Cell Res.* 339 (2), 380–388. doi:10.1016/j.yexcr.2015.10.001
- Lee, M. R., Kim, B., Lee, Y., Park, S. Y., Shim, J. H., Chung, B. H., et al. (2021). Ameliorative effects of pueraria lobata extract on postmenopausal symptoms

through promoting estrogenic activity and bone markers in ovariectomized rats. *Evid. Based. Complement. Altern. Med.* 2021, 7924400. doi:10.1155/2021/7924400

Li, B., Liu, M., Wang, Y., Gong, S., Yao, W., Li, W., et al. (2020a). Puerarin improves the bone micro-environment to inhibit OVX-induced osteoporosis via modulating SCFAs released by the gut microbiota and repairing intestinal mucosal integrity. *Biomed. Pharmacother.* 132, 110923. doi:10.1016/j.biopha.2020.110923

Li, B., Wang, Y., Gong, S., Yao, W., Gao, H., Liu, M., et al. (2022). Puerarin improves OVX-induced osteoporosis by regulating phospholipid metabolism and biosynthesis of unsaturated fatty acids based on serum metabolomics. *Phytomedicine*. 102, 154198. doi:10.1016/j.phymed.2022.154198

Li, D., Wang, P., Luo, Y., Zhao, M., and Chen, F. (2017). Health benefits of anthocyanins and molecular mechanisms: Update from recent decade. *Crit. Rev. Food Sci. Nutr.* 57 (8), 1729–1741. doi:10.1080/10408398.2015.1030064

Li, H., Ruan, Y., Zhang, K., Jian, F., Hu, C., Miao, L., et al. (2016). Mic60/Mitofilin determines MICOS assembly essential for mitochondrial dynamics and mtDNA nucleoid organization. *Cell Death Differ.* 23 (3), 380–392. doi:10.1038/cdd.2015.102

Li, L., Wang, B., Li, Y., Li, L., Dai, Y., Lv, G., et al. (2020b). Celastrol regulates bone marrow mesenchymal stem cell fate and bone-fat balance in osteoporosis and skeletal aging by inducing PGC-1 $\alpha$  signaling. *Aging (Albany NY)* 12 (17), 16887–16898. doi:10.18632/aging.103590

Li, Q., Yang, G., Xu, H., Tang, S., and Lee, W. Y. (2021a). Effects of resveratrol supplementation on bone quality: A systematic review and meta-analysis of randomized controlled trials. *BMC Complement. Med. Ther.* 21 (1), 214. doi:10.1186/s12906-021-03381-4

Li, W. D., Yan, C. P., Wu, Y., Weng, Z. B., Yin, F. Z., Yang, G. M., et al. (2014). Osteoblasts proliferation and differentiation stimulating activities of the main components of *Fructus Psoraleae corylifoliae*. *Phytomedicine* 21 (4), 400–405. doi:10.1016/j.phymed.2013.09.015

Li, X. H., Chen, F. L., and Shen, H. L. (2021b). Salidroside promoted osteogenic differentiation of adipose-derived stromal cells through Wnt/ $\beta$ -catenin signaling pathway. *J. Orthop. Surg. Res.* 16 (1), 456. doi:10.1186/s13018-021-02598-w

Lin, S. Y., Kang, L., Chen, J. C., Wang, C. Z., Huang, H. H., Lee, M. J., et al. (2019). (-)-Epigallocatechin-3-gallate (EGCG) enhances healing of femoral bone defect. *Phytomedicine* 55, 165–171. doi:10.1016/j.phymed.2018.07.012

Liu, J., Zhou, H., Song, L., Yang, Z., Qiu, M., Wang, J., et al. (2021). Anthocyanins: Promising natural products with diverse pharmacological activities. *Molecules* 26 (13), 3807. doi:10.3390/molecules26133807

Lu, B., Ye, Z., Deng, Y., Wu, H., and Feng, J. (2010). MEK/ERK pathway mediates cytoprotection of salvianolic acid B against oxidative stress-induced apoptosis in rat bone marrow stem cells. *Cell Biol. Int.* 34 (11), 1063–1068. doi:10.1042/CBI20090126

Lu, H., Champlin, R. E., Popat, U., Pundole, X., Escalante, C. P., Wang, X., et al. (2016). Ibandronate for the prevention of bone loss after allogeneic stem cell transplantation for hematologic malignancies: A randomized-controlled trial. *Bonekey Rep.* 5, 843. doi:10.1038/bonekey.2016.72

Lucas, E. A., Wild, R. D., Hammond, L. J., Khalil, D. A., Juma, S., Daggy, B. P., et al. (2002). Flaxseed improves lipid profile without altering biomarkers of bone metabolism in postmenopausal women. *J. Clin. Endocrinol. Metab.* 87 (4), 1527–1532. doi:10.1210/jcem.87.4.8374

Lv, Y. J., Yang, Y., Sui, B. D., Hu, C. H., Zhao, P., Liao, L., et al. (2018). Resveratrol counteracts bone loss via mitofilin-mediated osteogenic improvement of mesenchymal stem cells in senescence-accelerated mice. *Theranostics* 8 (9), 2387–2406. doi:10.1016/j.thno.2018.07.012

Mahjabeen, W., Khan, D. A., and Mirza, S. A. (2022). Role of resveratrol supplementation in regulation of glucose hemostasis, inflammation and oxidative stress in patients with diabetes mellitus type 2: A randomized, placebo-controlled trial. *Complement. Ther. Med.* 66, 102819. doi:10.1016/j.ctim.2022.102819

Mansoori, M. N., Tyagi, A. M., Shukla, P., Srivastava, K., Dev, K., Chillara, R., et al. (2016). Methoxyisoflavones formononetin and isoflavone genistein inhibit the differentiation of Th17 cells and B-cell lymphopoiesis to promote osteogenesis in estrogen-deficient bone loss conditions. *Menopause* 23 (5), 565–576. doi:10.1097/GME.0000000000000646

Mariee, A. D., Abd-Allah, G. M., and El-Beshbishy, H. A. (2012). Protective effect of dietary flavonoid quercetin against lipemic-oxidative hepatic injury in hypercholesterolemic rats. *Pharm. Biol.* 50 (8), 1019–1025. doi:10.3109/13880209.2012.655424

Mei, W., Song, D., Wu, Z., Yang, L., Wang, P., Zhang, R., et al. (2021). Growth responses, accumulation, translocation and distribution of vanadium in tobacco and its potential in phytoremediation. *Ecotoxicol. Environ. Saf.* 214, 111297. doi:10.1016/j.ecoenv.2020.111297

Melough, M. M., Sun, X., and Chun, O. K. (2017). The role of AOPP in age-related bone loss and the potential benefits of berry anthocyanins. *Nutrients* 9 (7), E789. doi:10.3390/nu9070789

Meyer, M. B., Benkusky, N. A., and Pike, J. W. (2014). The RUNX2 cistrome in osteoblasts: Characterization, down-regulation following differentiation, and relationship to gene expression. *J. Biol. Chem.* 289 (23), 16016–16031. doi:10.1074/jbc.M114.552216

Ming, L. G., Chen, K. M., and Xian, C. J. (2013). Functions and action mechanisms of flavonoids genistein and icariin in regulating bone remodeling. *J. Cell. Physiol.* 228 (3), 513–521. doi:10.1002/jcp.24158

Monda, V., Lupoli, G. A., Messina, G., Peluso, R., Panico, A., Villano, I., et al. (2017). Improvement of bone physiology and life quality due to association of risedronate and anastrozole. *Front. Pharmacol.* 8, 632. doi:10.3389/fphar.2017.00632

Mun, J. G., Grannan, M. D., Lachcik, P. J., Reppert, A., Yousef, G. G., Rogers, R. B., et al. (2009). *In vivo* metabolic tracking of <sup>14</sup>C-radiolabelled isoflavones in kudzu (*Pueraria lobata*) and red clover (*Trifolium pratense*) extracts. *Br. J. Nutr.* 102 (10), 1523–1530. doi:10.1017/S000711450999047x

Nani, A., Murtaza, B., Sayed Khan, A., Khan, N. A., and Hichami, A. (2021). Antioxidant and anti-inflammatory potential of polyphenols contained in mediterranean diet in obesity: Molecular mechanisms. *Molecules* 26 (4), 985. doi:10.3390/molecules26040985

Nazari-Khanamiri, F., and Ghasemnejad-Berenji, M. (2021). Cellular and molecular mechanisms of genistein in prevention and treatment of diseases: An overview. *J. Food Biochem.* 45 (11), e13972. doi:10.1111/jfbc.13972

Ornstrup, M. J., Harsløf, T., Kjær, T. N., Langdahl, B. L., and Pedersen, S. B. (2014). Resveratrol increases bone mineral density and bone alkaline phosphatase in obese men: A randomized placebo-controlled trial. *J. Clin. Endocrinol. Metab.* 99 (12), 4720–4729. doi:10.1210/jc.2014-2799

Park, B. K., Lee, J. H., Seo, H. W., Oh, K. S., Lee, J. H., and Lee, B. H. (2019). Icarin protects against radiation-induced mortality and damage *in vitro* and *in vivo*. *Int. J. Radiat. Biol.* 95 (8), 1094–1102. doi:10.1080/09553002.2019.1589021

Pietilä, M., Lehtonen, S., Närhi, M., Hassinen, I. E., Leskelä, H. V., Aranko, K., et al. (2010). Mitochondrial function determines the viability and osteogenic potency of human mesenchymal stem cells. *Tissue Eng. Part C Methods* 16 (3), 435–445. doi:10.1089/ten.tec.2009.0247

Qiao, J., Liu, A., Liu, J., Guan, D., and Chen, T. (2019). Salvianolic acid B (Sal B) alleviates the decreased activity induced by prednisolone acetate on osteoblasts by up-regulation of bone formation and differentiation genes. *Food Funct.* 10 (9), 6184–6192. doi:10.1039/c9fo01246j

Qiu, Z., Li, L., Huang, Y., Shi, K., Zhang, L., Huang, C., et al. (2022). Puerarin specifically disrupts osteoclast activation via blocking integrin- $\beta$ 3 Pyk2/Src/Cbl signaling pathway. *J. Orthop. Transl.* 33, 55–69. doi:10.1016/j.jot.2022.01.003

Sacco, S. M., Jiang, J. M., Reza-Lopez, S., Ma, D. W., Thompson, L. U., and Ward, W. E. (2009). Flaxseed combined with low-dose estrogen therapy preserves bone tissue in ovariectomized rats. *Menopause* 16 (3), 545–554. doi:10.1097/gme.0b013e31818fc00a

Sahin, E., Colla, S., Liesa, M., Moslehi, J., Müller, F. L., Guo, M., et al. (2011). Telomere dysfunction induces metabolic and mitochondrial compromise. *Nature* 470 (7334), 359–365. doi:10.1038/nature09787

Sansai, K., Na Takuathung, M., Khatsri, R., Teekachunhatean, S., Hanprasertpong, N., and Koonrungsomboon, N. (2020). Effects of isoflavone interventions on bone mineral density in postmenopausal women: A systematic review and meta-analysis of randomized controlled trials. *Osteoporos. Int.* 31 (10), 1853–1864. doi:10.1007/s00198-020-05476-z

Shan, Z., Cheng, N., Huang, R., Zhao, B., and Zhou, Y. (2018). Puerarin promotes the proliferation and differentiation of MC3T3-E1 cells via microRNA-106b by targeting receptor activator of nuclear factor- $\kappa$ B ligand. *Exp. Ther. Med.* 15 (1), 55–60. doi:10.3892/etm.2017.5405

Shane, E., Burr, D., Abrahamsen, B., Adler, R. A., Brown, T. D., Cheung, A. M., et al. (2014). Atypical subtrochanteric and diaphyseal femoral fractures: Second report of a task force of the American society for bone and mineral research. *J. Bone Min. Res.* 29 (1), 1–23. doi:10.1002/jbmr.1998

Shen, Y. S., Chen, X. J., Wuri, S. N., Yang, F., Pang, F. X., Xu, L. L., et al. (2020). Polydatin improves osteogenic differentiation of human bone mesenchymal stem cells by stimulating TAZ expression via BMP2-Wnt/ $\beta$ -catenin signaling pathway. *Stem Cell Res. Ther.* 11 (1), 204. doi:10.1186/s13287-020-01705-8

Shi, W., Gao, Y., Wang, Y., Zhou, J., Wei, Z., Ma, X., et al. (2017). The flavonol glycoside icariin promotes bone formation in growing rats by activating the cAMP signaling pathway in primary cilia of osteoblasts. *J. Biol. Chem.* 292 (51), 20883–20896. doi:10.1074/jbc.M117.809517



- Singh, K. B., Dixit, M., Dev, K., Maurya, R., and Singh, D. (2017). Formononetin, a methoxy isoflavone, enhances bone regeneration in a mouse model of cortical bone defect. *Br. J. Nutr.* 117 (11), 1511–1522. doi:10.1017/S0007114517001556
- Soltanoff, C. S., Yang, S., Chen, W., and Li, Y. P. (2009). Signaling networks that control the lineage commitment and differentiation of bone cells. *Crit. Rev. Eukaryot. Gene Expr.* 19 (1), 1–46. doi:10.1615/critrevukargeneexpr.v19.i1.10
- Song, F., Zhou, L., Zhao, J., Liu, Q., Yang, M., Tan, R., et al. (2016). Eriodictyol inhibits RANKL-induced osteoclast formation and function via inhibition of NFATc1 activity. *J. Cell. Physiol.* 231 (9), 1983–1993. doi:10.1002/jcp.25304
- Sun, Z. B., Wang, J. W., Xiao, H., Zhang, Q. S., Kan, W. S., Mo, F. B., et al. (2015). Icarin may benefit the mesenchymal stem cells of patients with steroid-associated osteonecrosis by ABCB1-promoter demethylation: A preliminary study. *Osteoporos. Int.* 26 (1), 187–197. doi:10.1007/s00198-014-2809-z
- Tan, L., Cao, Z., Chen, H., Xie, Y., Yu, L., Fu, C., et al. (2021). Curcumin reduces apoptosis and promotes osteogenesis of human periodontal ligament stem cells under oxidative stress *in vitro* and *in vivo*. *Life Sci.* 270, 119125. doi:10.1016/j.lfs.2021.119125
- Tang, W., Xiao, L., Ge, G., Zhong, M., Zhu, J., Qin, J., et al. (2020). Puerarin inhibits titanium particle-induced osteolysis and RANKL-induced osteoclastogenesis via suppression of the NF- $\kappa$ B signaling pathway. *J. Cell. Mol. Med.* 24 (20), 11972–11983. doi:10.1111/jcmm.15821
- Tang, Y., Jacobi, A., Vater, C., Zou, X., and Stiehler, M. (2014). Salvianolic acid B protects human endothelial progenitor cells against oxidative stress-mediated dysfunction by modulating Akt/mTOR/4EBP1, p38 MAPK/ATF2, and ERK1/2 signaling pathways. *Biochem. Pharmacol.* 90 (1), 34–49. doi:10.1016/j.bcp.2014.04.008
- Tao, K., Xiao, D., Weng, J., Xiong, A., Kang, B., and Zeng, H. (2016). Berberine promotes bone marrow-derived mesenchymal stem cells osteogenic differentiation via canonical Wnt/ $\beta$ -catenin signaling pathway. *Toxicol. Lett.* 240 (1), 68–80. doi:10.1016/j.toxlet.2015.10.007
- Tarasenko, D., Barbot, M., Jans, D. C., Kroppen, B., Sadowski, B., Heim, G., et al. (2017). The MICOS component Mic60 displays a conserved membrane-bending activity that is necessary for normal cristae morphology. *J. Cell Biol.* 216 (4), 889–899. doi:10.1083/jcb.201609046
- Teng, J. W., Bian, S. S., Kong, P., and Chen, Y. G. (2022). Icarin triggers osteogenic differentiation of bone marrow stem cells by up-regulating miR-335-5p. *Exp. Cell Res.* 414 (2), 113085. doi:10.1016/j.yexcr.2022.113085
- Thaung Zaw, J. J., Howe, P. R., and Wong, R. H. (2021). Long-term effects of resveratrol on cognition, cerebrovascular function and cardio-metabolic markers in postmenopausal women: A 24-month randomised, double-blind, placebo-controlled, crossover study. *Clin. Nutr.* 40 (3), 820–829. doi:10.1016/j.clnu.2020.08.025
- Tou, J. C. (2015). Evaluating resveratrol as a therapeutic bone agent: Preclinical evidence from rat models of osteoporosis. *Ann. N. Y. Acad. Sci.* 1348 (1), 75–85. doi:10.1111/nyas.12840
- Tsuji, M., Yamamoto, H., Sato, T., Mizuha, Y., Kawai, Y., Taketani, Y., et al. (2009). Dietary quercetin inhibits bone loss without effect on the uterus in ovariectomized mice. *J. Bone Min. Metab.* 27 (6), 673–681. doi:10.1007/s00774-009-0088-0
- Wang, D., Li, F., and Jiang, Z. (2001). Osteoblastic proliferation stimulating activity of Psoralea corylifolia extracts and two of its flavonoids. *Planta Med.* 67 (8), 748–749. doi:10.1055/s-2001-18343
- Wang, N., Li, Y., Li, Z., Liu, C., and Xue, P. (2019). Sal B targets TAZ to facilitate osteogenesis and reduce adipogenesis through MEK-ERK pathway. *J. Cell. Mol. Med.* 23 (5), 3683–3695. doi:10.1111/jcmm.14272
- Wang, X., Lu, C., Chen, Y., Wang, Q., Bao, X., Zhang, Z., et al. (2022). Resveratrol promotes bone mass in ovariectomized rats and the SIRT1 rs7896005 SNP is associated with bone mass in women during perimenopause and early postmenopause. *Climacteric* 20 (7), 1–9. doi:10.1080/13697137.2022.2073809
- Wang, Y., Bai, S., Cheng, Q., Zeng, Y., Xu, X., and Guan, G. (2021). Naringenin promotes SDF-1/CXCR4 signaling pathway in BMSCs osteogenic differentiation. *Folia histochem. Cytobiol.* 59 (1), 66–73. doi:10.5603/FHC.a2021.0008
- Waqas, M., Qamar, H., Zhang, J., Yao, W., Li, A., Wang, Y., et al. (2020). Puerarin enhance vascular proliferation and halt apoptosis in thiram-induced avian tibial dyschondroplasia by regulating HIF-1 $\alpha$ , TIMP-3 and BCL-2 expressions. *Ecotoxicol. Environ. Saf.* 190, 110126. doi:10.1016/j.ecoenv.2019.110126
- Ward, W. E., Yuan, Y. V., Cheung, A. M., and Thompson, L. U. (2001a). Exposure to flaxseed and its purified lignan reduces bone strength in young but not older male rats. *J. Toxicol. Environ. Health.* A 63 (1), 53–65. doi:10.1080/152873901750128362
- Ward, W. E., Yuan, Y. V., Cheung, A. M., and Thompson, L. U. (2001b). Exposure to purified lignan from flaxseed (*Linum usitatissimum*) alters bone development in female rats. *Br. J. Nutr.* 86 (4), 499–505. doi:10.1079/bjn2001429
- Watanabe, Y., Ohata, K., Fukunoki, A., Fujimoto, N., Matsumoto, M., Nessa, N., et al. (2020). Antihypertensive and renoprotective effects of dietary flaxseed and its mechanism of action in deoxycorticosterone acetate-salt hypertensive rats. *Pharmacology* 105 (1–2), 54–62. doi:10.1159/000502789
- Wei, C., Zhu, X., Lu, J., Xia, C., and Li, W. (2022). Effects and mechanism of bavachin on osteoclast differentiation. *J. Chin. J. Osteoporos.* 28 (07), 942–947.
- Weng, Z. B., Gao, Q. Q., Wang, F., Zhao, G. H., Yin, F. Z., Cai, B. C., et al. (2015). Positive skeletal effect of two ingredients of Psoralea corylifolia L. on estrogen deficiency-induced osteoporosis and the possible mechanisms of action. *Mol. Cell. Endocrinol.* 417, 103–113. doi:10.1016/j.mce.2015.09.025
- Wong, R. H., Thaung Zaw, J. J., Xian, C. J., and Howe, P. R. (2020). Regular supplementation with resveratrol improves bone mineral density in postmenopausal women: A randomized, placebo-controlled trial. *J. Bone Min. Res.* 35 (11), 2121–2131. doi:10.1002/jbmr.4115
- Wu, G. J., Chen, J. T., Chong, Y. G., Chang, C. C., Liu, S. H., and Chen, R. M. (2020). Genistein improves bone healing via triggering estrogen receptor alpha-mediated expressions of osteogenesis-associated genes and consequent maturation of osteoblasts. *J. Agric. Food Chem.* 68 (39), 10639–10650. doi:10.1021/acs.jafc.0c02830
- Wu, Z., Wu, B., Lv, X., Xie, Y., Xu, S., Ma, C., et al. (2021). Serum lipidomics reveals the anti-inflammatory effect of flax lignans and sinapic acid in high-fat-diet mice. *J. Agric. Food Chem.* 69 (32), 9111–9123. doi:10.1021/acs.jafc.0c07291
- Xi, J., Li, Q., Luo, X., Wang, Y., Li, J., Guo, L., et al. (2018). Celastrol inhibits glucocorticoid-induced osteoporosis in rat via the PI3K/AKT and Wnt signaling pathways. *Mol. Med. Rep.* 18 (5), 4753–4759. doi:10.3892/mmr.2018.9436
- Xiao, C., Li, J., Dong, X., He, X., Niu, X., Liu, C., et al. (2011). Anti-oxidative and TNF- $\alpha$  suppressive activities of puerarin derivative (4AC) in RAW264.7 cells and collagen-induced arthritic rats. *Eur. J. Pharmacol.* 666 (1–3), 242–250. doi:10.1016/j.ejphar.2011.05.061
- Xiao, L., Zhong, M., Huang, Y., Zhu, J., Tang, W., Li, D., et al. (2020). Puerarin alleviates osteoporosis in the ovariectomy-induced mice by suppressing osteoclastogenesis via inhibition of TRAF6/ROS-dependent MAPK/NF- $\kappa$ B signaling pathways. *Aging (Albany NY)* 12 (21), 21706–21729. doi:10.18632/aging.103976
- Xing, L. Z., Ni, H. J., and Wang, Y. L. (2017). Quercitrin attenuates osteoporosis in ovariectomized rats by regulating mitogen-activated protein kinase (MAPK) signaling pathways. *Biomed. Pharmacother.* 89, 1136–1141. doi:10.1016/j.biopha.2017.02.073
- Xu, D., Hu, M. J., Wang, Y. Q., and Cui, Y. L. (2019). Antioxidant activities of quercetin and its complexes for medicinal application. *Molecules* 24 (6), E1123. doi:10.3390/molecules24061123
- Xu, Q., Chen, G., Xu, H., Xia, G., Zhu, M., Zhan, H., et al. (2021). Celastrol attenuates RANKL-induced osteoclastogenesis *in vitro* and reduces titanium particle-induced osteolysis and ovariectomy-induced bone loss *in vivo*. *Front. Pharmacol.* 12, 682541. doi:10.3389/fphar.2021.682541
- Yamaguchi, M. (2012). Nutritional factors and bone homeostasis: Synergistic effect with zinc and genistein in osteogenesis. *Mol. Cell. Biochem.* 366 (1–2), 201–221. doi:10.1007/s11010-012-1298-7
- Yang, C., Li, J., Zhu, K., Yuan, X., Cheng, T., Qian, Y., et al. (2019). Puerarin exerts protective effects on wear particle-induced inflammatory osteolysis. *Front. Pharmacol.* 10, 1113. doi:10.3389/fphar.2019.01113
- Yang, C., Zhu, K., Yuan, X., Zhang, X., Qian, Y., and Cheng, T. (2020). Curcumin has immunomodulatory effects on RANKL-stimulated osteoclastogenesis *in vitro* and titanium nanoparticle-induced bone loss *in vivo*. *J. Cell. Mol. Med.* 24 (2), 1553–1567. doi:10.1111/jcmm.14842
- Yang, X., Yang, Y., Zhou, S., Gong, X., Dai, Q., Zhang, P., et al. (2018). Puerarin stimulates osteogenic differentiation and bone formation through the ERK1/2 and p38-MAPK signaling pathways. *Curr. Mol. Med.* 17 (7), 488–496. doi:10.2174/1566524018666171219101142
- Yang, Y., Chen, D., Li, Y., Zou, J., Han, R., Li, H., et al. (2022). Effect of puerarin on osteogenic differentiation *in vitro* and on new bone formation *in vivo*. *Drug Des. devel. Ther.* 16, 2885–2900. doi:10.2147/dddt.S379794
- Yuan, Y., Feng, G., Yang, J., Yang, C., and Tu, Y. H. (2022). Polydatin alleviates osteoporosis by enhancing the osteogenic differentiation of osteoblasts. *Eur. Rev. Med. Pharmacol. Sci.* 26 (12), 4392–4402. doi:10.26355/eurrev\_202206\_29078
- Zaklos-Szyda, M., Budryn, G., Grzelczyk, J., Perez-Sanchez, H., and Zyzelewicz, D. (2020). Evaluation of isoflavones as bone resorption inhibitors upon interactions with receptor activator of nuclear factor- $\kappa$ B ligand (RANKL). *Molecules* 25 (1), 206. doi:10.3390/molecules25010206
- Zang, L., Kagotani, K., Nakayama, H., Bhagat, J., Fujimoto, Y., Hayashi, A., et al. (2021). 10-Gingerol suppresses osteoclastogenesis in RAW264.7 cells and zebrafish osteoporotic scales. *Front. Cell Dev. Biol.* 9, 588093. doi:10.3389/fcell.2021.588093

- Zhang, D., Fong, C., Jia, Z., Cui, L., Yao, X., and Yang, M. (2016). Icariin stimulates differentiation and suppresses adipocytic transdifferentiation of primary osteoblasts through estrogen receptor-mediated pathway. *Calcif. Tissue Int.* 99 (2), 187–198. doi:10.1007/s00223-016-0138-2
- Zhang, R., Zhang, Q., Zou, Z., Li, Z., Jin, M., An, J., et al. (2021a). Curcumin supplementation enhances bone marrow mesenchymal stem cells to promote the anabolism of articular chondrocytes and cartilage repair. *Cell Transpl.* 30, 963689721993776. doi:10.1177/0963689721993776
- Zhang, S., Feng, P., Mo, G., Li, D., Li, Y., Mo, L., et al. (2017a). Icariin influences adipogenic differentiation of stem cells affected by osteoblast-osteoclast co-culture and clinical research adipogenic. *Biomed. Pharmacother.* 88, 436–442. doi:10.1016/j.biopha.2017.01.050
- Zhang, S. L., Chen, Z. H., Lin, D. T., Yan, Q., Gao, F., and Lin, H. (2021b). Epigallocatechin gallate regulates inflammatory responses and new bone formation through Wnt/ $\beta$ -Catenin/COX-2 pathway in spondyloarthritis. *Int. Immunopharmacol.* 98, 107869. doi:10.1016/j.intimp.2021.107869
- Zhang, X. Y., Li, H. N., Chen, F., Chen, Y. P., Chai, Y., Liao, J. Z., et al. (2021). Icariin regulates miR-23a-3p-mediated osteogenic differentiation of BMSCs via BMP-2/Smad5/Runx2 and WNT/ $\beta$ -catenin pathways in osteonecrosis of the femoral head. *Saudi Pharm. J.* 29 (12), 1405–1415. doi:10.1016/j.jsps.2021.10.009
- Zhang, X., Zou, L., Li, J., Xu, B., Wu, T., Fan, H., et al. (2017b). Salviolic acid B and danshensu induce osteogenic differentiation of rat bone marrow stromal stem cells by upregulating the nitric oxide pathway. *Exp. Ther. Med.* 14 (4), 2779–2788. doi:10.3892/etm.2017.4914
- Zheng, H., Qi, S., and Chen, C. (2018). Salidroside improves bone histomorphology and prevents bone loss in ovariectomized diabetic rats by upregulating the OPG/RANKL ratio. *Molecules* 23 (9), 2398. doi:10.3390/molecules23092398
- Zhou, X., Zhang, Z., Jiang, W., Hu, M., Meng, Y., Li, W., et al. (2022). Naringenin is a potential anabolic treatment for bone loss by modulating osteogenesis, osteoclastogenesis, and macrophage polarization. *Front. Pharmacol.* 13, 872188. doi:10.3389/fphar.2022.872188
- Zhou, Y., Lian, H., Liu, K., Wang, D., Xiu, X., and Sun, Z. (2020). Puerarin improves graft bone defect through microRNA-155-3p-mediated p53/TNF- $\alpha$ /STAT1 signaling pathway. *Int. J. Mol. Med.* 46 (1), 239–251. doi:10.3892/ijmm.2020.4595
- Zhu, L., Wei, H., Wu, Y., Yang, S., Xiao, L., Zhang, J., et al. (2012). Licorice isoliquiritigenin suppresses RANKL-induced osteoclastogenesis *in vitro* and prevents inflammatory bone loss *in vivo*. *Int. J. Biochem. Cell Biol.* 44 (7), 1139–1152. doi:10.1016/j.biocel.2012.04.003
- Zhu, Z., Sheng, H., Lin, Z., Ding, X., and Liu, Y. (2015). Experimental study on the effect of bavachin on osteoporosis in ovariectomized rats. *J. Shaanxi Tradit. Chin. Med.* 36 (08), 1083–1084.
- Zou, Y. C., Yang, X. W., Yuan, S. G., Zhang, P., and Li, Y. K. (2016). Celastrol inhibits prostaglandin E2-induced proliferation and osteogenic differentiation of fibroblasts isolated from ankylosing spondylitis hip tissues *in vitro*. *Drug Des. devel. Ther.* 10, 933–948. doi:10.2147/DDDT.S97463





## OPEN ACCESS

## EDITED BY

Dongwei Zhang,  
Beijing University of Chinese Medicine,  
China

## REVIEWED BY

Lili Wang,  
Beijing University of Chinese Medicine,  
China  
Jian Wei,  
Liuzhou People's Hospital, China

## \*CORRESPONDENCE

Shuanglei Li,  
lslei66@126.com

<sup>†</sup>These authors share first authorship

## SPECIALTY SECTION

This article was submitted to  
Experimental Pharmacology and Drug  
Discovery,  
a section of the journal  
Frontiers in Pharmacology

RECEIVED 03 August 2022

ACCEPTED 31 October 2022

PUBLISHED 17 November 2022

## CITATION

Chen W, Jin X, Wang T, Bai R, Shi J,  
Jiang Y, Tan S, Wu R, Zeng S, Zheng H,  
Jia H and Li S (2022), Ginsenoside  
Rg1 interferes with the progression of  
diabetic osteoporosis by promoting  
type H angiogenesis modulating  
vasculogenic and osteogenic coupling.  
*Front. Pharmacol.* 13:1010937.  
doi: 10.3389/fphar.2022.1010937

## COPYRIGHT

© 2022 Chen, Jin, Wang, Bai, Shi, Jiang,  
Tan, Wu, Zeng, Zheng, Jia and Li. This is  
an open-access article distributed  
under the terms of the [Creative  
Commons Attribution License \(CC BY\)](#).  
The use, distribution or reproduction in  
other forums is permitted, provided the  
original author(s) and the copyright  
owner(s) are credited and that the  
original publication in this journal is  
cited, in accordance with accepted  
academic practice. No use, distribution  
or reproduction is permitted which does  
not comply with these terms.

# Ginsenoside Rg1 interferes with the progression of diabetic osteoporosis by promoting type H angiogenesis modulating vasculogenic and osteogenic coupling

Wenhui Chen<sup>1,2†</sup>, Xinyan Jin<sup>1†</sup>, Ting Wang<sup>1</sup>, Rui Bai<sup>1,3</sup>, Jun Shi<sup>4</sup>,  
Yunxia Jiang<sup>2</sup>, Simin Tan<sup>1</sup>, Ruijie Wu<sup>1</sup>, Shiqi Zeng<sup>1</sup>,  
Hongxiang Zheng<sup>1</sup>, Hongyang Jia<sup>1</sup> and Shuanglei Li<sup>2\*</sup>

<sup>1</sup>School of Graduate, Guangxi University of Chinese Medicine, Nanning, China, <sup>2</sup>Department of Endocrinology, The First Affiliated Hospital of Guangxi University of Chinese Medicine, Nanning, China,

<sup>3</sup>Faculty of Chinese Medicine Science, Guangxi University of Chinese Medicine, Nanning, China,

<sup>4</sup>School of Public Health and Management, Guangxi University of Chinese Medicine, Nanning, China

Ginsenoside Rg1 (Rg1) has been demonstrated to have antidiabetic and antiosteoporotic activities. The aim of this study was to investigate the protective effect of Rg1 against diabetic osteoporosis and the underlying mechanism. *In vitro*, we found that Rg1 increased the number of osteoprogenitors and alleviated high glucose (HG) induced apoptosis of osteoprogenitors by MTT assays and flow cytometry. qRT-PCR and western blot analysis suggested that Rg1 can also promote the secretion of vascular endothelial growth factor (VEGF) by osteoprogenitors and promote the coupling of osteogenesis and angiogenesis. Rg1 can also promote the proliferation of human umbilical vein endothelial cells (HUVECs) cultured in high glucose, enhance the angiogenic ability of endothelial cells, and activate the Notch pathway to promote endothelial cells to secrete the osteogenesis-related factor Noggin to regulate osteogenesis, providing further feedback coupling of angiogenesis and osteogenesis. Therefore, we speculated that Rg1 may have similar effects on type H vessels. We used the Goto-Kakizaki (GK) rat model to perform immunofluorescence staining analysis on two markers of type H vessels, Endomucin (Emcn) and CD31, and the osteoblast-specific transcription factor Osterix, and found that Rg1 stimulates type H angiogenesis and bone formation. *In vivo* experiments also demonstrated that Rg1 promotes VEGF secretion, activates the Noggin/Notch pathway, increases the level of coupling between type H vessels and osteogenesis, and improves the bone structure of GK rats. All of these data reveal that Rg1 is a promising candidate drug for treating diabetic osteoporosis as a potentially bioactive molecule that promotes angiogenesis and osteointegration coupling.

## KEYWORDS

type H vessels, Notch, Noggin, VEGF, diabetic osteoporosis, angiogenic-osteogenic coupling, ginsenoside Rg1

## 1 Introduction

Diabetes mellitus (DM)-induced osteoporosis is a systemic metabolic bone disease. It causes systemic bone loss and bone microstructure damage due to chronic long-term hyperglycemia, resulting in increased bone fragility, decreased bone strength, and fracture (Parizad et al., 2019). At present, it is generally recognized that the fracture risk of type 1 diabetes mellitus (T1DM) and type 2 diabetes mellitus (T2DM) patients is significantly increased (Moayeri et al., 2017), while the proportion of osteoporosis among patients with microvascular complications of T1DM is higher (Campos Pastor et al., 2000). In the setting of microvascular disease, T1DM patients have obvious progressive bone loss, and the loss of cancellous and cortical bone occurs earlier than in T1DM patients without microvascular disease and healthy people. T2DM patients with microangiopathy show typical age-related bone loss, which is most obvious in the cortical bone (Shanbhogue et al., 2017). At the same time, high-resolution peripheral bone quantitative CT (HR-pQCT) showed that when T1DM/T2DM was combined with microvascular lesions, the bone structure of the radius was damaged, but the pathological features of T1DM were trabecular damage and a thin cortex, while the pathological features of the T2DM radius were a thin and porous cortex with an intact trabecular bone (Shanbhogue et al., 2016). Regardless of T1DM or T2DM, there is bone cortex damage in the presence of microvascular disease. The Haversian system of the Bone Cortical Reconstruction Center is the pathway of blood vessels, and microvascular disease may lead to disorders of Haversian system reconstruction, which then affects bone cortex reconstruction. Therefore, diabetes osteoporosis may be a type of microvascular disease of diabetes.

Kusumbe et al. (2014) found bone microvessels with unique morphological and functional features in the bone system, which are called type H vessels and are characterized by high expression of the endothelial markers Emcn and CD31. There is evidence that type H vessels play an important role in bone formation, bone microstructure and the number of osteoprogenitors, and type H angiogenesis can occur simultaneously with osteogenesis (Ramasamy et al., 2014). Type H vessels make the vascular environment rich in factors that favor osteogenesis and stimulate proliferation and differentiation of osteoprogenitors in the bone marrow, thereby directing bone formation (Kusumbe et al., 2014; Ramasamy et al., 2014; Xu et al., 2018). Reductions in this type of vessel are closely associated with the loss of bone mass (L. Wang et al., 2017). In conclusion, type H vessels can not only mediate the growth of bone vessels, but also maintain the level of osteoprogenitors and couple angiogenesis with osteogenesis (Kusumbe et al., 2014; Ramasamy et al., 2014; H. Xie et al., 2014). A recent study showed that T1DM in mice can lead to overall abnormalities in the intraosseous vascular

system, especially type H vessels, resulting in uncoupling of angiogenesis and osteogenesis (X.-F. Hu et al., 2021). So we suspect that it may be a potential therapeutic target for high-glucose-induced bone loss.

Currently, several drugs used in clinical practice to treat osteoporosis, including bisphosphonates, estrogens, calcitonin, and denosumab, have good efficacy. However, they all achieve the therapeutic aim from the perspective of inhibiting bone resorption and fail to show beneficial effects on angiogenesis and bone formation, thus limiting their clinical application in bone loss caused by high glucose-induced microangiopathy.

Ginsenosides are the main active substances of *Panax ginseng*, *Panax quinquefolius*, and *Panax notoginseng* (Xiang et al., 2008; Kim et al., 2017). Ginsenoside Rg1 is one of the most effective components of ginsenoside. It can regulate cell proliferation, differentiation and regeneration and has anti-inflammatory, anti-apoptotic and other pharmacological activities (W. Xie et al., 2018). Previous studies have reported that ginsenoside Rg1 is able to intervene in glucose transport and disposal (C.-W. Wang et al., 2015), alter insulin secretion and bind to receptors to control blood glucose (J. Gu et al., 2013). Y. Gu et al. (2016) found that ginsenoside Rg1 could promote osteogenic differentiation of rBMSCs through BMP-2/SMAD signaling. *In vivo*, it can promote the transformation of fibrous callus into osteogenic callus and promote fracture healing in rats with tibial fracture. Another study showed that ginsenoside Rg1 is the main pro-angiogenic active component in ginseng and can increase the expression of VEGF to promote cerebral angiogenesis (Chen et al., 2019). These results suggest that ginsenoside Rg1, in addition to its anti-diabetic and anti-osteoporotic activities, also promotes angiogenesis. We therefore hypothesized that ginsenoside Rg1 may promote type H angiogenesis and interfere with angiogenic and osteogenic coupling, and reverse diabetes osteoporosis.

Increasing evidence suggests that some pathways are activated during angiogenic-osteogenic coupling, including the Notch pathway and the VEGF pathway (Ramasamy et al., 2014; Shen et al., 2021). Rg1 is closely related to these pathways and can treat a variety of diseases by regulating them (Ren et al., 2021), but studies on the treatment of diabetic osteoporosis have not been reported. Therefore, we carried out a study on the protective effect and potential mechanism of ginsenoside Rg1 on diabetic osteoporosis.

## 2 Materials and methods

### 2.1 Drugs and reagents

Ginsenoside Rg1 (purity  $\geq 98\%$ , molecular structural formula is shown in Supplementary Figure S1) was obtained from

Shanghai Tube Biological Co., Ltd. The MTT kit was obtained from Sigma (United States). Annexin V-FITC/PI kit was obtained from BestBio (Shanghai, China). PI kit and RIPA lysis buffer were obtained from Beyotime Biotechnology (Shanghai, China). The BCIP/NBT alkaline phosphatase chromogenic kit and Alizarin Red S staining kit were obtained from Solarbio (Beijing, China). SYBR Green I Master Mix and reverse transcription kit were obtained from Thermo (United States). Anti-VEGF antibody was obtained from Boster (Wuhan, China). Anti-NOG, anti-Notch1, anti-CD31 and anti-Osterix antibodies were obtained from Abcam (United Kingdom). Anti-Emcn antibody was obtained from Abbkine (Wuhan, China). Horseradish enzyme-labeled goat anti-rabbit IgG and horseradish enzyme-labeled goat anti-mouse IgG were obtained from ZSGB-Bio (Beijing, China). Anti-GAPDH antibody, fluorescein (FITC)-conjugated AffiniPure goat anti-rabbit IgG and Cy3-conjugated AffiniPure goat anti-mouse IgG were obtained from Proteintech (United States). Rabbit anti-CD73/PE conjugated antibody, rabbit anti-CD90/PE conjugated antibody, rabbit anti-CD14/FITC conjugated antibody and rabbit anti-CD19/FITC conjugated antibody were obtained from Bioss (Beijing, China).

## 2.2 Isolation, culture and identification of osteoprogenitors

Six-month-old SD rats were sacrificed, and both femurs were removed under aseptic conditions. After washing, cancellous bone was processed into 2–5 mm<sup>2</sup> fragments and then repeatedly washed with PBS. Bone tissues were transferred into culture dishes, and 7 ml DMEM containing 10% fetal bovine serum, 100 U/ml penicillin, 100 mg/ml streptomycin, and 2 ml glutamine was added. Bone tissues were incubated in a 37°C incubator containing 5% CO<sub>2</sub> for 4–6 days without changing the medium until a certain number of spindle-adherent cells appeared around the bone tissue under the microscope.

The first passage of osteoprogenitors was taken for identification by flow cytometry. CD73 and CD90 are markers of osteoprogenitors. At 80%–90% confluency, the osteoprogenitors were collected after treatment with trypsin. They were divided into two groups for identification. One group was treated with anti-CD73/PE antibody and anti-CD19/FITC antibody, and the other group was treated with anti-CD90/PE antibody and anti-CD14/FITC antibody and incubated in the dark at 4°C for 30 min. The control group was treated with nonspecific isotype antibody labeled with the same fluorescence. After incubation, the cells were washed twice with PBS, resuspended in 200 µl PBS, and detected by flow cytometry (BD-FACSVerse).

The results showed that the positive rate of CD73 and CD90 was 99.6% and 86.1%, respectively. Osteoprogenitors

lacked CD14 and CD19 expression, whereas CD19 and CD14 expression rates were 4.7% and 7.2%, indicating that the culture of osteoprogenitors was successful (Figure 1).

## 2.3 Culture of vascular endothelial cells

Human umbilical vein endothelial cells, a common cell type used for *in vitro* angiogenesis studies, were purchased from Wuxi Buhe Bio-Pharmaceutical Company. The cells were inoculated into 96-well culture plates at a density of  $5 \times 10^4$  cells/well for passage, and 100 µl of high-glucose DMEM was added (containing 10% fetal bovine serum, 0.1 mg/ml streptomycin and 100 U/ml penicillin). The cells were cultured at 37°C in a 5% CO<sub>2</sub> incubator. At 80%–90% confluence, the cells were treated with trypsin, replated for expansion and used for downstream experiments after 4 passages.

## 2.4 Exploration of the working concentration of ginsenoside Rg1 by MTT assay

After the osteoprogenitors grew, the cell concentration was adjusted to  $5 \times 10^4$  cells/mL and they were inoculated into 96-well culture plates and cultured overnight at 37°C in a 5% CO<sub>2</sub> incubator. Different concentrations of Rg1 were added to the cell culture wells the next day, and after 48 h of culture, 10 µl of MTT was added to each well and incubated for 3–4 h. The liquid in the wells was aspirated, 200 µl of DMSO (Invitrogen) was added, and the OD value was measured using a microplate reader (Thermo, MK3) at a wavelength of 492 nm. Using CurveExpert software, the working concentration of Rg1 was calculated to be 164.8 µM (Supplementary Table S1), and this concentration was used for the downstream experiments.

## 2.5 Proliferation of osteoprogenitors was measured by MTT assay

After the osteoprogenitors grew, the cell concentration was adjusted to  $5 \times 10^4$  cells/mL and they were inoculated into 96-well culture plates and cultured overnight at 37°C in a 5% CO<sub>2</sub> incubator. Osteoprogenitors were divided into four groups: the CON group (with 5.5 mmol/L glucose), HG group (with 32.8 mmol/L glucose), Rg1 group (with Rg1 concentration of 164.8 µM) and HG + Rg1 group (with 32.8 mmol/L glucose + Rg1 concentration of 164.8 µM). The culture conditions except for the culture medium were kept consistent across the groups. After incubation for 24 h, 48 h and 72 h, 10 µl MTT was added to the wells of each group and then incubated for 3–4 h. OD value was measured with a microplate reader at a wavelength

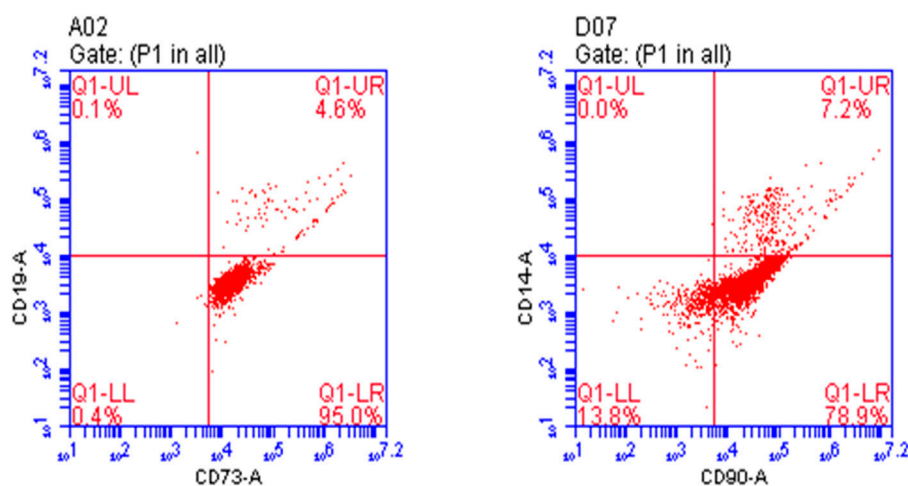


FIGURE 1

Identification of osteoprogenitors by flow cytometry.

of 492 nm after shaking the liquid for 10 min. The measured OD values were used for the analysis of cell viability.

## 2.6 Proliferation of HUVECs were measured by MTT assay

After the HUVECs grew, the cell concentration was adjusted to  $5 \times 10^4$  cells/mL and they were inoculated into 96-well culture plates and cultured overnight at 37°C in a 5% CO<sub>2</sub> incubator. The HUVECs were divided into three groups: the CON group (with 5.5 mmol/L glucose), HG group (with 32.8 mmol/L glucose), and HG + Rg1 group (with 32.8 mmol/L glucose + Rg1 concentration of 164.8 μM). The culture conditions except for the culture medium were kept consistent across the groups. After incubation for 24 h, 48 h and 72 h, 10 μl MTT was added to the wells of each group and then incubated for 3–4 h. OD value was measured with a microplate reader at a wavelength of 492 nm after shaking the liquid for 10 min. The measured OD values were used for the analysis of cell viability.

## 2.7 Flow cytometry detection of apoptosis of osteoprogenitors and HUVECs

Cells in each group were treated with trypsin without EDTA, and centrifuged at 1,500 rpm at room temperature for 5 min to collect cells. The cells were resuspended with PBS, then washed, and then 300 μl of 1× Binding Buffer suspension cells were added. Add 5 μl Annexin V-FITC, mix well, incubate in dark at room temperature for 15 min, and then stain with 10 μl PI.

Finally, flow cytometry was used for detection and FlowJo 7.6 software was used for analysis.

## 2.8 Alkaline phosphatase (ALP) and alizarin red s (ARS) staining

ALP and ARS staining of the osteoprogenitors was used to assess the effect of ginsenoside Rg1 on osteogenic differentiation. Briefly, osteoprogenitors were inoculated in 24-well plates after adjusting the cell concentration to  $1 \times 10^5$  cells/mL. The osteoprogenitors were divided into three groups according to different treatment methods: control group (with 1,640 medium (Hyclone)), inducer group (with osteogenic induction medium) and ginsenoside Rg1 + inducer group (with osteogenic induction medium + Rg1 concentration of 164.8 μM). Osteogenic induction medium contained 10% FBS, 2% penicillin–streptomycin, 0.01 μmol/L dexamethasone, 10 mmol/L β-glycerophosphate sodium, and 50 mg/L ascorbic acid. Proliferation of osteoprogenitors was observed daily under a microscope. ALP staining and activity assays were performed with a BCIP/NBT kit at 7 days after osteogenic induction, and mineral deposition was evaluated by Alizarin Red S staining at Day 14 of differentiation. Finally, ImageJ software was used for quantitative analysis.

## 2.9 Immunofluorescence staining

Osteoprogenitor samples from the above three groups were fixed in 4% paraformaldehyde and permeabilized with 0.1% Triton for 15 min. After blocking with 5% FBS for 1 h at

TABLE 1 Primer sequences used in the qRT-PCR assays.

Primer	Sequence (5'-3')
VEGF (RAT)-RT-F	GAGTATATCTTCAAGCCGTCCTGTGTG
VEGF (RAT)-RT-R	GTTCTATCTTCTTGGTCTGCATTCA
GAPDH (RAT)-RT-F	ACGACCCCTTCATTGACCTCAACTACA
GAPDH (RAT)-RT-R	GACATACTCAGCACCAGCATCACCCCA
Notch1 (RAT)-RT-F	ACAGTGCCGAGTGTGAGTGGGATGG
Notch1 (RAT)-RT-R	CAGGAAGTGGAAGGAGTTGTTGCGT
NOG (RAT)-RT-F	CCAGCACTATCTACACATCCGCCCA
NOG (RAT)-RT-R	GCGTCTCGTTCAGATCCTTCTCCTT
GAPDH (human)-RT-F	ATGGGGAAGGTGAAGGTCGGAGT
GAPDH (human)-RT-R	TAGTTGAGGTCAATGAAGGGGTC
Notch1 (human)-RT-F	GCAGCCTCAACATCCCTACAAGA
Notch1 (human)-RT-R	CCCACGAAGAAGCAGAAGCACAAG
NOG (human)-RT-F	CTTTTGCCGCGCTACGTGAAG
NOG (human)-RT-R	TCGGAAATGATGGGGTACTGGA

room temperature, the cells were incubated overnight at 4°C with anti-Osterix antibody (1:1,000). Subsequently, cells were washed three times with PBS and incubated for 1 h with FITC-conjugated Affinipure Goat Anti-Rabbit IgG (1:200). Incubate with Hoechst (Beyotime Biotechnology, Shanghai, China) for 15 min at room temperature in the dark. Finally, fluorescence signals were collected using a fluorescence microscope (OLYMPUS, IX71, Japan).

## 2.10 Quantitative real-time polymerase chain reaction analysis

Total RNA of bone tissue or cells was extracted with TRIzol reagent (Invitrogen). cDNA was obtained from total RNA using a Reverse Transcription Kit. Next, qRT-PCR was performed using SYBR Green qPCR Master Mix. Relative gene expression was calculated using the  $2^{-\Delta\Delta C_t}$  method, and GAPDH was used as a reference for normalization. The real-time PCR primer sequences are shown in Table 1.

## 2.11 Western blot analysis

Total proteins were obtained with RIPA lysis buffer (Beyotime, Shanghai, China) supplemented with phenylmethanesulfonyl fluoride. After centrifugation at  $12,000 \times g$  for 10 min, the supernatant was extracted. Proteins were resolved by 10% SDS-PAGE and transferred to PVDF membranes (Millipore, United States) by electroblotting. Blocking was performed with 5% skimmed milk for 2 h at 37°C followed by incubation with anti-NOG, anti-Notch1, anti-VEGF (1:1000) and anti-GAPDH (1:5000) antibodies

overnight at 4°C. After washing three times with TBST solution, the blots were incubated with the secondary antibodies (goat anti-mouse IgG and goat anti-rabbit IgG, 1:5000) conjugated to horseradish peroxidase for 1 h at 37°C. An appropriate amount of ECL luminescence solution (Beijing Dingguo) was added to the membrane, and images were taken using an integrated chemiluminescence instrument (ChemiScope 5300 Pro).

## 3 Animals and treatments

### 3.1 Animals and experimental design

GK rats are a polygenic non obese diabetic rat model developed by selection from Wistar rats. It is characterized by impaired glucose-stimulated insulin secretion, fasting hyperglycemia and insulin resistance, which are very similar to the development of type 2 diabetes in humans. Moreover, it was found that the bone mineral density (BMD) of the femur and fifth lumbar vertebra in 6-month-old GK rats were lower than that in normal control Wistar rats, and the bone formation indicator osteocalcin (OCN) was significantly reduced, and the bone absorption indicator tartrate resistant acid phosphatase (TRAP) activity was significantly increased, suggesting that GK rats have osteopenia and an increased risk of fracture (Zhang et al., 2009). GK rats provide a good animal model for studying the pathogenesis and preventive measures of diabetic osteoporosis.

A total of 20 female 4-month-old GK rats purchased from Covance Laboratory Animal Co., Ltd. were used in this study. They were divided into two groups by random number table: the GK rat model group and the GK rat + Rg1 group, with 10 rats in each group. Another 10 Wistar rats of the same age were used as the blank control group. A standard laboratory diet was fed to all rats with *ad libitum* access to feed and water. The GK rats + Rg1 group were intragastrically administered Rg110 mg/kg/d, and the blank control group and the GK rats group were intragastrically administered an equal volume of normal saline. Micro-computed tomography (micro-CT) examination was performed before Rg1 treatment in Wistar group and GK group for reference. After 12 weeks of treatment, all three groups of rats underwent micro-CT examination, bone tissue morphometric analysis, qRT-PCR analysis (same method as Section 2.10), and western blot analysis (same method as Section 2.11). All experimental procedures were approved by the Animal Ethics and Experimental Safety Committee of Guangxi University of Traditional Chinese Medicine.

### 3.2 Micro-CT analysis

The dissected tibiae were soaked in tissue fixative and then analyzed with a micro-CT Skyscan 1176 (Skyscan, Aartselaar, Belgium). The scanner was set to a voltage of 50 kV, a current of



800  $\mu$ A, and a resolution of 12  $\mu$ m per pixel. Three-dimensional image reconstruction was performed with N-Recon software, and three-dimensional analysis was performed with CT-AN software to measure bone volume/total volume (BV/TV), trabecular thickness (Tb. Th), trabecular number (Tb. N), trabecular separation (Tb. Sp), structure model index (SMI) and BMD in each group.

### 3.3 Histological analysis

For histological analysis, after sacrificing the rats, the proximal metaphysis of the tibia of the right hind limb (approximately 1/3 of the total length) was taken, and the tibial samples were fixed in 4% paraformaldehyde solution for 24 h. They were decalcified in 7% EDTA for 2 weeks, dehydrated through graded ethanol of an increasing concentration, and then embedded in paraffin. The samples were cut into 5- $\mu$ m-thick sections, deparaffinized, and rehydrated. Hematoxylin staining (Shanghai Zhanyun Chemical Co., Ltd.) was performed for 5 min followed by washing with distilled water, sections were then stained with eosin (Shanghai Zhanyun Chemical Co., Ltd.) for 2–8 s, dehydrated with absolute ethanol, added with neutral gum, and sealed. Finally, it was observed under a microscope.

### 3.4 Immunofluorescence staining

Tibial specimens were fixed in 10% formaldehyde, washed in water, then dehydrated in ethanol, embedded in paraffin, and samples were sectioned, deparaffinized in xylene, and rehydrated. Tibial specimens were incubated in 3% H<sub>2</sub>O<sub>2</sub>/PBS for 10 min to quench endogenous peroxidase activity. After antigen retrieval in trisodium citrate buffer at 95°C for 5 min and blocking with 5% BSA for 15 min, the sections were incubated with anti-CD31 antibody, anti-Emcn antibody (1:200) and anti-Osterix antibody (1:1000) at 4°C overnight. After washing with PBS, the corresponding rabbit secondary antibody or mouse secondary antibody (1:200) was added and incubated for 1 h. Finally, the slides were mounted after staining with Hoechst and observed under a microscope.

## 4 Statistical analysis

All data are presented as the mean  $\pm$  standard deviation (SD). Data were analyzed using GraphPad Prism 9.0 software (GraphPad Software, United States). Two-tailed Student's t-test was used for comparison between two groups, and Tukey's multiple comparison test was performed after one-way analysis of variance (ANOVA) for multiple groups. The differences were judged to be statistically significant when  $p < 0.05$ .

## 5 Results

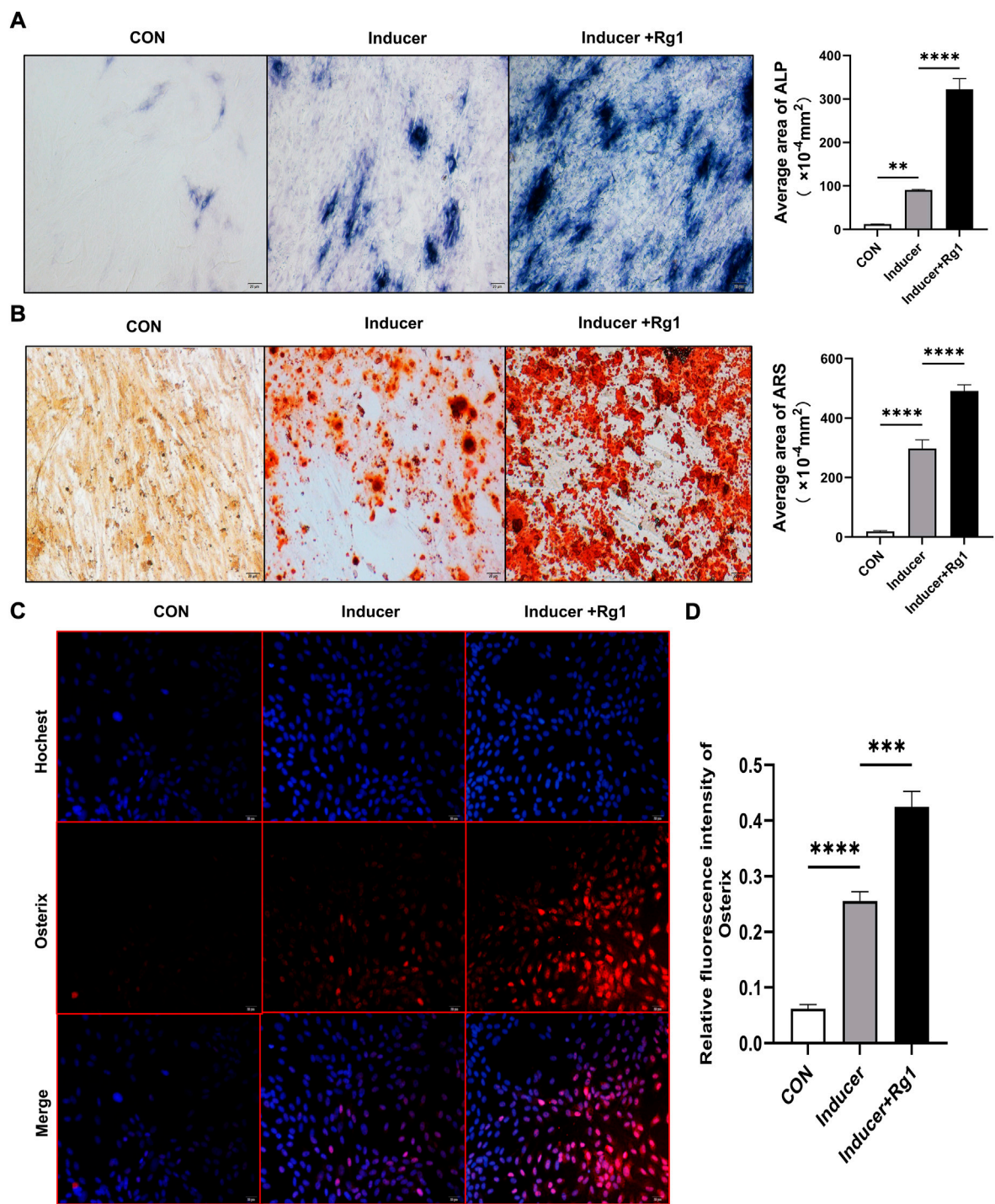
### 5.1 Ginsenoside Rg1 promotes osteogenic differentiation of osteoprogenitors

To evaluate the role of Rg1 in bone formation *in vitro*, we isolated and cultured osteoprogenitors and carried out osteogenic differentiation experiments. The results of the ALP staining (Figure 2A) showed that ALP in the control group without osteogenic inducer basically did not stain, and there was no significant osteogenic differentiation. In the Inducer group, the ALP staining was intense, and osteogenic potential was enhanced. ALP staining was further enhanced in cells cotreated with Rg1 and inducer. ALP-positive cells were significantly increased, and osteogenic induction showed the most significant effect. ARS staining showed similar results (Figure 2B), with significant staining and enhanced osteogenic potential in the Inducer group compared with the control group. Compared with the Inducer group, ARS staining was more obvious in the Inducer + Rg1 group, indicating that the number of calcium nodules was increased and the osteogenic potential was significantly enhanced.

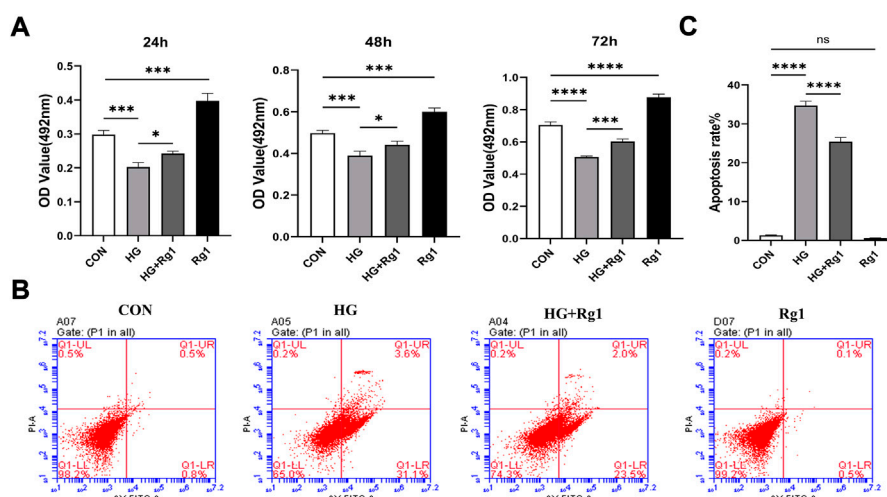
Osterix is well-known to be an osteoblast-specific transcription factor that is mostly densely distributed around type H vessels and plays an important role in osteoblast differentiation, maturation and activity (Ramazzotti et al., 2019). The Osterix gene is a signature gene for osteoblast lineage formation. We used immunofluorescence staining to detect its expression level to further evaluate the role of Rg1 in promoting bone differentiation. The results showed (Figures 2C,D) that Osterix expression levels were low in the control group and increased after addition of the inducer. Compared with the Inducer group, the Inducer + Rg1 group had significantly increased Osterix expression levels and promoted osteogenic differentiation of cells to a greater extent.

### 5.2 Ginsenoside Rg1 can promote (under high glucose exposure) osteoprogenitor proliferation and inhibit osteoprogenitor apoptosis

Osterix + osteoprogenitors give rise to osteoblasts and osteocytes (Kusumbe et al., 2014), and their recruitment plays an important role in bone tissue regeneration and remodeling. Lower numbers of osteoprogenitors in the bone marrow stroma may impede osteoblast generation and bone formation and compromise bone mass and healing (Weinberg et al., 2014). To investigate the effect of Rg1 on the proliferation and apoptosis of osteoprogenitors, we first detected the proliferation of osteoprogenitors treated with Rg1 for 24 h, 48 h, and 72 h by MTT assays. The results (Figure 3A) showed that the proliferation of osteoprogenitors was similar in the three time



**FIGURE 2** Ginsenoside Rg1 can promote osteogenic differentiation of osteoprogenitors. **(A)** ALP staining and quantitative analysis in CON group, Inducer group and Inducer + Rg1 group. **(B)** Alizarin red staining and quantitative analysis in CON group, Inducer group and Inducer + Rg1 group. **(C)** Immunofluorescence staining of Osterix in the CON group, Inducer group and Inducer + Rg1 group. **(D)** Quantification of the mean relative levels of Osterix in osteoprogenitors in each group. Scale bar: 20  $\mu\text{m}$ . Data are presented as the mean  $\pm$  SD. \* $p < 0.05$ , \*\* $p < 0.01$ , \*\*\* $p < 0.001$ , \*\*\*\* $p < 0.0001$ , NS: not significant. The above experiments were independently performed three times.

**FIGURE 3**

Ginsenoside Rg1 can promote (under high glucose exposure) osteoprogenitor proliferation and inhibit apoptosis. (A) MTT assays were used to assess the proliferation of osteoprogenitors by OD values in each group at 24 h, 48 h, and 72 h. (B) Flow cytometry was used to detect the apoptosis of osteoprogenitors in each group at 48 h. (C) The apoptosis rate of the osteoprogenitors in each group at 48 h. Data are presented as the mean  $\pm$  SD. \* $p < 0.05$ , \*\* $p < 0.01$ , \*\*\* $p < 0.001$ , \*\*\*\* $p < 0.0001$ , NS: not significant. The above experiments were independently performed three times.

periods, and the addition of Rg1 significantly promoted cell proliferation under normal culture conditions. Compared with the control group, cell proliferation was significantly inhibited in high glucose culture, but when Rg1 was added to high glucose culture, the inhibition of cell proliferation significantly improved. The effect was most apparent at 48 h and the cells reached confluence at 72 h, so 48 h was selected for the subsequent experiments. Previous experiments have shown that the number of osteoprogenitors is significantly decreased in aged and ovariectomized mice (Kusumbe et al., 2014; L. Wang et al., 2017) and our study demonstrated that a similar situation also occurs during bone formation under high glucose exposure. As shown by flow cytometry (Figures 3B,C), compared with the control group, the apoptosis rate of osteoprogenitors was significantly increased under high glucose culture and significantly decreased when Rg1 was added under high glucose culture.

### 5.3 Ginsenoside Rg1 promotes the secretion of vascular endothelial growth factor from high glucose-exposed osteoprogenitors and regulates angiogenesis

In addition to playing an important role in osteogenesis, osteoprogenitors are also a vital source of VEGF. Hu and Olsen found that the osteoblastic lineage (including osteoprogenitors, preosteoblasts, and mature osteoblasts) is an important source of VEGF at the site of injury in cortical bone defects (K. Hu and

Olsen, 2017). VEGF is one of the most important angiogenic factors and it is essential for vascular homeostasis (Olsson et al., 2006; Li et al., 2013). In this regard, we investigated VEGF secretion by osteoprogenitors before and after Rg1 treatment. The results of the qRT-PCR and western blot experiments suggested a common trend (Figures 4A,B). The addition of Rg1 under normal conditions significantly increased intracellular VEGF expression levels. The expression of VEGF was much lower in the high glucose group compared to the control group, but it was raised when Rg1 was given to the high glucose culture. Osteoblastic lineage can guide vascular sprouting through high secretion of VEGF and promote the generation of new blood vessels (Gerber et al., 1999; K. Hu and Olsen, 2016). New blood vessels remove metabolic waste products, increase the supply of oxygen, nutrients, and minerals required for osteogenesis, and may recruit osteoprogenitors to the site of injury, further supporting angiogenesis and osteogenesis through positive feedback loops.

### 5.4 Ginsenoside Rg1 enhanced the proliferation ability of HUVECs exposed to high glucose and promoted their secretion of the osteogenesis-related factors Notch1 and Noggin

Angiogenesis involves endothelial cell (EC) proliferation and, in most developing and regenerating organs, the emergence of endothelial sprouts from preexisting vessels (Wacker and Gerhardt, 2011). To explore the effect of Rg1 on angiogenesis,

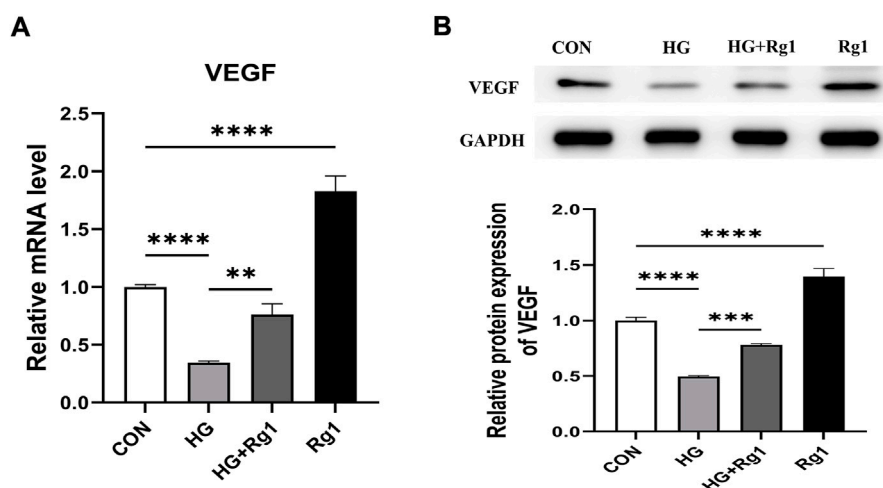


FIGURE 4

Ginsenoside Rg1 promotes VEGF secretion from osteoprogenitors. (A) qRT-PCR was used to detect the expression level of VEGF mRNA in osteoprogenitors in each group. (B) Western blotting was used to detect the expression level of VEGF protein in osteoprogenitors in each group. The housekeeping gene GAPDH served as an internal control. Data are presented as the mean  $\pm$  SD. \* $p < 0.05$ , \*\* $p < 0.01$ , \*\*\* $p < 0.001$ , \*\*\*\* $p < 0.0001$ , NS: not significant. The above experiments were independently performed three times.

we examined the effect of Rg1 on the proliferation of HUVECs by MTT assay. According to the experimental findings (Figure 5A), the cell proliferation trend of each group was approximately the same at three time points: 24 h, 48 h, and 72 h. Compared with the control group, high glucose significantly inhibited HUVECs proliferation, but when Rg1 was added, the inhibitory effect of glucose on cell proliferation was alleviated. Rg1 improved cell proliferation inhibition induced by high glucose most significantly at 72 h, so 72 h was used in the subsequent experiments. Flow cytometry further showed that high glucose accelerated apoptosis of HUVECs, while Rg1 significantly alleviated EC apoptosis induced by high glucose (Figures 5B,C).

A large body of evidence suggests that vascular ECs have a significant impact on osteogenic regulation (Ramasamy et al., 2016a). Noggin is a mediator secreted by ECs. It is involved in the regulation of osteoblast function and can promote the proliferation and differentiation of osteoblast progenitor cells as well as the maturation and hypertrophy of chondrocytes. Noggin is positively regulated by Notch signaling (Ramasamy et al., 2014). Notch signaling is a critical component of molecular crosstalk linking angiogenesis, vascular secretory signaling, and osteogenesis (Kusumbe et al., 2014; Ramasamy et al., 2014). It not only plays a decisive role in the differentiation and function of osteoblast lineage cells, but also promotes the proliferation and angiogenesis of EC in mouse long bones (Ramasamy et al., 2014; Ballhause et al., 2021). Notch1 is one of the receptors for Notch. Notch1 signaling positively impacts the fracture healing process (Novak et al., 2020), and inhibition of Notch1 reduces the proliferation and differentiation of

osteoblasts (Ann et al., 2011; Zanotti and Canalis, 2014). To further test the effect of Rg1 on ECs, we examined the levels of Notch1 and Noggin in HUVECs. qRT-PCR (Figure 5D) showed that high glucose inhibited Notch1 and NOG mRNA secretion by HUVECs compared with the control group, and the expression levels of Notch1 and NOG mRNA were significantly increased after the addition of Rg1. The western blot assays for Notch1 and Noggin protein levels expressed in HUVECs showed the same trend (Figure 5E). Thus, we believe that Rg1 can promote the proliferation of vascular ECs exposed to high glucose through activating Notch signaling, which has a positive effect on angiogenesis *in vitro*. Under the stimulation of Notch signaling, Rg1 can further promote ECs to secrete the osteogenic-related factor Noggin, which is conducive to osteogenesis.

## 5.5 Ginsenoside Rg1 can improve bone loss and microstructural deterioration in GK rats

To investigate the effect of Rg1 on high glucose-induced bone loss *in vivo*, we used micro-CT to analyze tibiae from GK rats. Micro-CT scans showed that cancellous bone mass was significantly reduced in GK rats compared with Wistar rats (Figures 6A,B), but bone loss was reduced in GK rats treated with Rg1 (Figures 6C,D). Quantitative microstructural analysis also showed that Rg1 treatment for 12 weeks prevented high glucose-induced bone loss, as shown by increased BV/TV, BMD, and Tb. N, and decreased



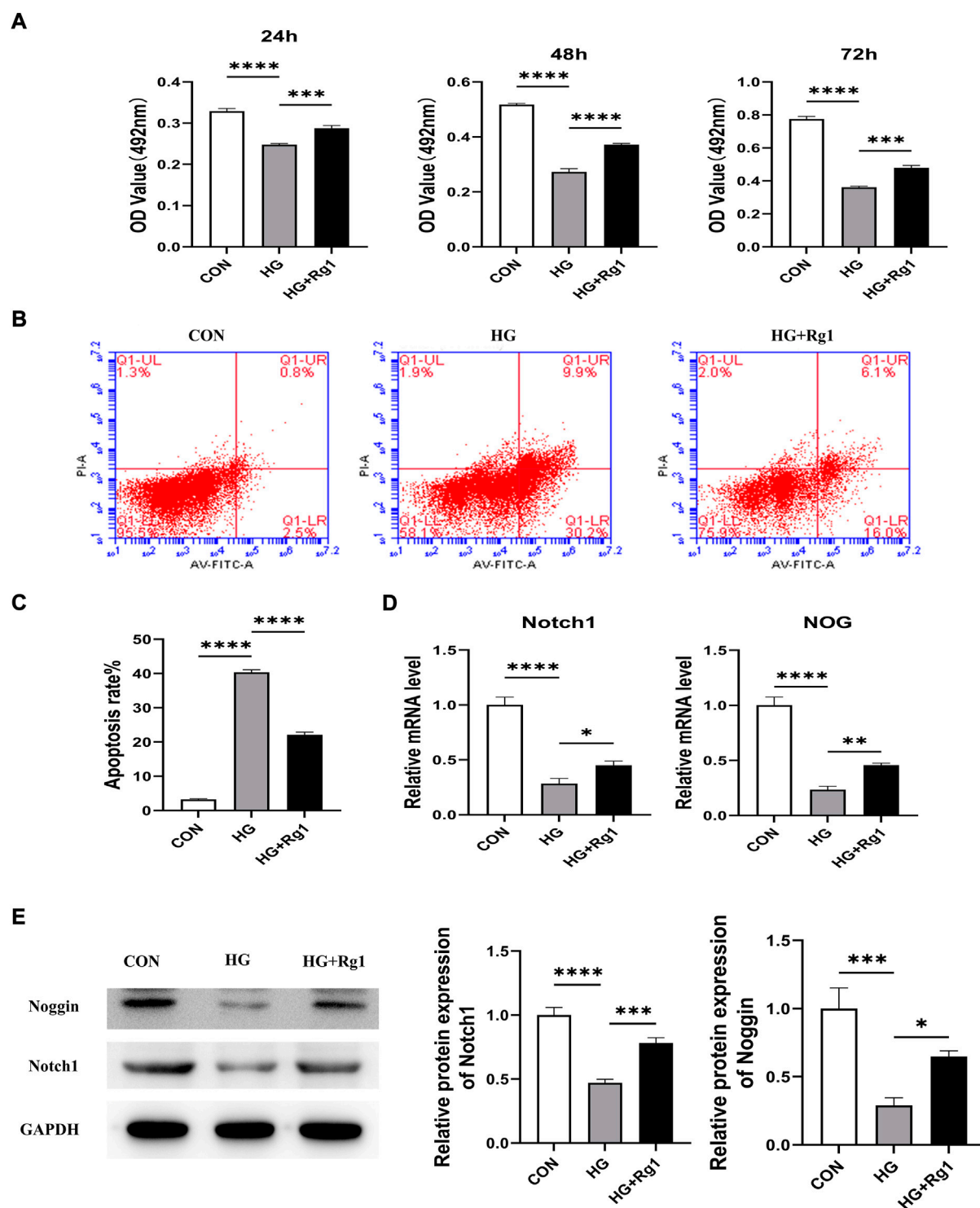
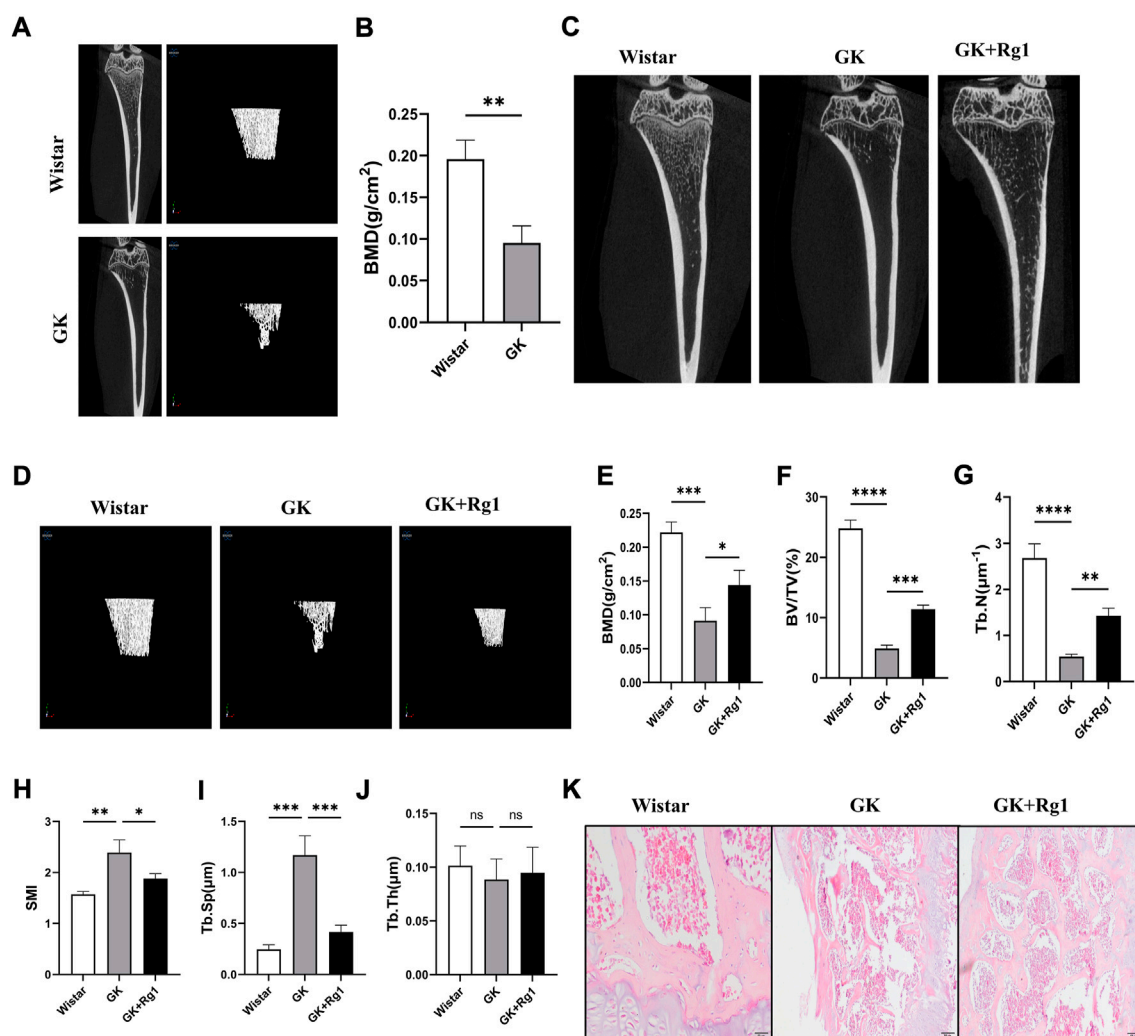


FIGURE 5

Ginsenoside Rg1 promotes the proliferation of HUVECs and their secretion of Notch1 and Noggin in high glucose culture. (A) MTT assays were used to detect the proliferation of HUVECs by the OD values in each group at 24 h, 48 h, and 72 h. (B) Flow cytometry was used to detect the apoptosis of HUVECs in each group at 72 h. (C) The apoptosis rate of HUVECs in each group at 72 h. (D) qRT-PCR was used to detect the levels of the Notch1 and NOG mRNA expressed by HUVECs in each group. (E) Western blotting was used to detect the levels of the Notch1 and Noggin protein secreted by the HUVECs in each group. The housekeeping gene GAPDH served as an internal control. Data are presented as the mean  $\pm$  SD. \* $p < 0.05$ , \*\* $p < 0.01$ , \*\*\* $p < 0.001$ , \*\*\*\* $p < 0.0001$ , NS: not significant. The above experiments were independently performed three times.





**FIGURE 6**

Ginsenoside Rg1 could ameliorate bone mass reduction and microstructural damage in GK rats. (A) Micro-CT images of the tibiae of Wistar and GK rats before treatment. (B) BMD of the tibia of Wistar and GK rats before treatment. (C) Two-dimensional micro-CT images of the tibia of rats in each group after 12 weeks of treatment. (D) Three-dimensional micro-CT images of the trabecular bone of rats in each group after 12 weeks of treatment. (E–J) Quantitative analysis of BMD (E), BV/TV (F), Tb.N (G), SMI (H), Tb.Sp (I), and Tb.Th (J) in the proximal tibia of rats in each group after 12 weeks of treatment. (K) H&E staining of the tibial metaphysis in each group. Scale bar: 50 μm. Data are presented as the mean ± SD. \* $p < 0.05$ , \*\* $p < 0.01$ , \*\*\* $p < 0.001$ , \*\*\*\* $p < 0.0001$ , NS: not significant.  $n = 3$ . H&E staining experiments were performed independently three times.

Tb.Sp and SMI in the GK + Rg1 group compared with the GK group (Figures 6E–I). Among them, the Tb.Th index was not significantly different before and after Rg1 treatment (Figure 6J), which may be related to the compensatory increase in trabecular thickness during severe osteoporosis. The H&E staining results further demonstrated the therapeutic effect of Rg1. Compared with Wistar rats, GK model rats had sparse bone tissue, microarchitecture damage, bone thinning, trabecular bone reduction, and an enlarged bone marrow cavity, and after Rg1 treatment, the bone tissue structure became tight, the trabecular bone increased, and the bone marrow cavity decreased (Figure 6K).

## 5.6 Ginsenoside Rg1 promoted the formation of type H vessels and bone formation in GK rats, and increased the expression levels of VEGF, Noggin, and Notch1 in bone tissue

We have demonstrated with the above *in vitro* experiments that Rg1 enhances the angiogenic ability of ECs and promotes the upregulation of angiogenesis-related factor (VEGF) expression, indicating that Rg1 may play a potential role in type H angiogenesis, so we verified this conjecture *in vivo* in GK rats. Immunofluorescence staining showed that CD31 and Emcn

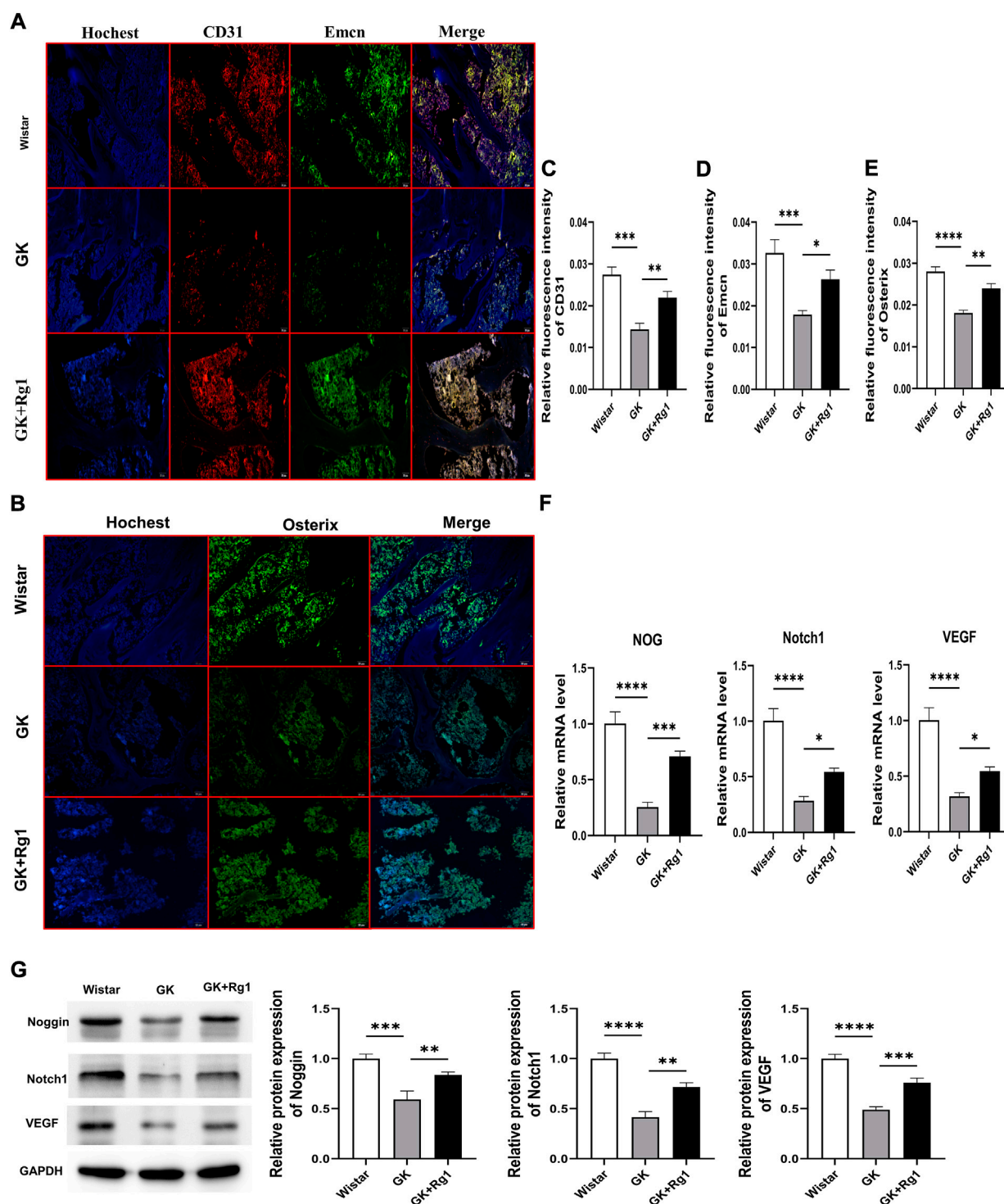


FIGURE 7

Ginsenoside Rg1 promotes type H angiogenesis and osteogenesis related factor secretion in GK rats. (A) Immunofluorescence staining images of CD31 and Emcn in bone tissue of GK rats in each group. (B) Osterix immunofluorescence staining images in bone tissue of GK rats in each group. (C–E) Quantification of the mean relative levels of CD31 (C), Emcn (D), and Osterix (E) in bone tissue of GK rats in each group. (F) qRT-PCR was used to detect the expression levels of the NOG, Notch1, and VEGF mRNA in the bone tissue of GK rats in each group. (G) Western blotting was used to detect the protein expression levels of Noggin, Notch1, and VEGF in the bone tissue of GK rats in each group. The housekeeping gene GAPDH served as an internal control. Data are expressed as the mean  $\pm$  SD. Scale bar: 20  $\mu$ m \* $p$  < 0.05, \*\* $p$  < 0.01, \*\*\* $p$  < 0.001, \*\*\*\* $p$  < 0.0001, NS: not significant.  $n$  = 3. The above experiments were independently performed three times.

expression was significantly reduced and that the abundance of type H vessels was impaired in GK rats compared to the Wistar rats (Figures 7A,C,D). At the same time, we also found decreased expression levels of osteoblast-specific transcription factor (Osterix) in the bone tissue of GK rats (Figures 7B,E). However, CD31, Emcn, and Osterix expression levels all increased after 12 weeks of Rg1 treatment (Figures 7A–E). This suggests that Rg1 promotes type H angiogenesis accompanied with bone formation.

Previous studies have shown that both type H angiogenesis and osteogenesis are closely related to VEGF, Notch1, and Noggin (Ramasamy et al., 2014; Fu et al., 2020; Shen et al., 2021). We also found that Rg1 could increase the levels of angiogenesis and osteogenesis by promoting the secretion of the above factors under high glucose exposure *in vitro*. Therefore, we analyzed the expression levels of Notch1, Noggin, and VEGF in bone tissues of GK rats by qRT-PCR and western blotting. qRT-PCR analysis showed that Notch1, VEGF, and NOG mRNA expression levels were significantly decreased in the bone tissue of GK rats and significantly increased after Rg1 treatment (Figure 7F). The western blot analysis was consistent with the trends in the qRT-PCR data (Figure 7G). This suggests that Rg1 plays an active role in osteogenesis by promoting type H angiogenesis through activation of the VEGF/Notch/Noggin pathway under high glucose exposure.

## 6 Discussion

Bone is a connective tissue rich in large blood vessels and capillaries, and the vascular network can act as a structural template for bone as well as regulate bone mass changes (Y. Peng et al., 2020; Tomlinson and Silva, 2013). The vascular system of bone is essential for bone growth, remodeling, and fracture healing. Angiogenesis is a prerequisite for the healing of skeletal conditions such as fractures and defects (Maes, 2013; Ramasamy et al., 2016b). Vascular injury is a major contributor to many organ dysfunctions caused by diabetes, which are referred to as diabetic vascular complications (Beckman and Creager, 2016; Antonopoulos et al., 2021). Previous studies on diabetic bone vessels have focused on the relationship between vascular injury and abnormal hematopoiesis in the bone marrow, and little attention has been given to the potential association between the bone vascular system and bone mass lesions (Fajardo, 2017; Shanbhogue et al., 2017). However, there is increasing evidence that microangiopathy has direct deleterious effects on bone (Oikawa et al., 2010; J. Peng et al., 2016). Type H vessels are specialized capillary subtypes that have been shown to couple angiogenesis and osteogenesis in rodents and humans (L. Wang et al., 2017). They are located in the bone marrow near the growth plate and represent the critical component of the metabolically specialized bone microenvironment with the privilege of obtaining nutrients

and oxygen, thereby promoting the growth potential of peripheral perivascular cells (Ellis et al., 2011; Kusumbe et al., 2014; Langen et al., 2017; H. Xie et al., 2014). It has been proposed that human type H vessels are sensitive biomarkers of bone mass and early indicators of bone loss (L. Wang et al., 2017).

It is increasingly recognized that changes in bone mass coincide with the number of type H vessels in aging and ovariectomized (OVX) mice as well as in elderly and postmenopausal osteoporotic individuals (Kusumbe et al., 2014; L. Wang et al., 2017; Xu et al., 2018; Zhao et al., 2012). Recently, it has been shown that osteoblasts may lose the support and regulation of type H vessels when the bone vascular system is affected by metabolic disorders in diabetes, resulting in osteogenic disorders and increased bone fragility (X.-F. Hu et al., 2021). Our results also showed that CD31<sup>+</sup> and Emcn-labeled type H vessels were significantly sparse in the bone tissue of diabetic rats, and cytological experiments also confirmed that vascular ECs exposed to high glucose had decreased proliferation and increased apoptosis. At the same time, the bone density of diabetic rats decreased significantly, the bone structure was destroyed significantly, and osteogenesis reflected by Osterix labeling decreased. The deterioration of cancellous bone that we observed in GK rats is similar to the findings of other investigators (Y. Liang et al., 2019), suggesting that type H vascular injury during diabetes may be associated with reduced bone mass and osteogenesis. In view of the effect of high glucose on type H vessels and the effect of type H vessels on bone regeneration, we believe that promoting type H angiogenesis may be an ideal strategy to prevent diabetic bone loss.

Among the more than 30 different ginsenosides, ginsenoside Rg1 is one of the most abundant and active components (Radad et al., 2004). Rg1 promotes osteogenic differentiation of a variety of cells. Rg1 treatment upregulated the transcription of osteogenic genes to promote osteogenic differentiation in human dental pulp stem cells and altered gene expression profiles (P. Wang et al., 2014). Wang et al. found that Rg1 activates Nrf2 signaling to regulate osteogenic differentiation of bone marrow mesenchymal stem cells and protects the osteogenic lineage (Hou et al., 2022; P. Wang et al., 2012). Rg1 also inhibited osteoclast differentiation and maturation and reduced destruction of articular cartilage in collagen-induced arthritis mice (Y. Gu et al., 2014). Rg1 treatment has positive effects in both fracture models and ovariectomy-induced osteoporosis rat models (Gong et al., 2006; Y. Gu et al., 2016). However, no studies have been published to date on the protective effect of Rg1 in diabetes-induced osteoporosis.

We investigated the ability of Rg1 to promote type H angiogenesis. Angiogenesis involves the proliferation and migration of ECs, as well as eventual capillary tube formation and the upregulation of some angiogenesis-related factors *in vivo* (Ucuzian et al., 2010). We used HUVECs to determine whether

Rg1 could promote vascular EC proliferation. The MTT assay and flow cytometry showed that Rg1 treatment significantly increased EC proliferation and inhibited EC apoptosis induced by high glucose, suggesting that Rg1 can promote angiogenesis. VEGF is one of the major regulators of vascular growth. It has the capacity to control crucial stages of angiogenesis, including the proliferation and migration of ECs (Blázquez et al., 2004). Overexpression of VEGF and its receptors promotes angiogenesis, and inhibition of VEGF blocks angiogenesis (Ferrara, 2004). In this study, we found that high glucose increased the apoptosis of osteoprogenitors, inhibited VEGF secretion from osteoprogenitors, and hindered angiogenesis. However, VEGF gene and VEGF protein levels were significantly increased in osteoprogenitors treated with Rg1 compared with the control group. This is consistent with other investigators reporting that ginsenoside Rg1 promotes VEGF synthesis and thus promotes angiogenic activity (Leung et al., 2006; Chen et al., 2019). We therefore hypothesized that Rg1 has the same effect on type H vessels. *In vivo*, we performed immunofluorescence analysis of CD31 and Emcn. The results showed that CD31 and Emcn expression levels were increased after 12 weeks of Rg1 treatment compared with the GK rat group, verifying the effect of Rg1 on promoting type H angiogenesis.

Notch signaling has been reported to be involved in type H angiogenesis (Kusumbe et al., 2014; Ramasamy et al., 2014). Activation of Notch signaling in bone ECs promotes EC proliferation in the columns of type H vessels and increases the abundance of type H vessels (Ramasamy et al., 2014). Notch signaling also controls the release of the vascular secretory factor Noggin. On the one hand, Noggin stimulates the differentiation of osteoprogenitors, affects trabecular bone mass, and growth plate morphology. On the other hand, Noggin promotes the maturation and hypertrophy of chondrocytes, thereby affecting angiogenesis through VEGF-A expression in hypertrophic chondrocytes (Ramasamy et al., 2014). VEGF is involved in bone formation in addition to angiogenesis (Yang et al., 2012). Loss of VEGF-A expression in osteoprogenitors inhibited their differentiation into mature osteoblasts, resulting in reduced bone density (Liu et al., 2012). Previous studies have also shown that VEGF, in addition to increasing the activity of ECs and promoting angiogenesis, directly enhances the recruitment and differentiation of osteogenic progenitor cells, thereby regulating the morphogenesis of the growth plate and promoting fracture healing (Mayr-Wohlfart et al., 2002; Keramaris et al., 2008). In conclusion, the VEGF/Notch/Noggin pathway emphasizes the coupling between angiogenesis and osteogenesis, reflecting communication between ECs and osteocytes. This in-depth understanding of the role of angiogenesis-osteogenic coupling in the bone microenvironment may aid in the development of new diagnostic biomarkers and therapies to treat bone lesions, such as osteoporosis or osteonecrosis.

EC-specific inactivation of Notch signaling through inactivation of Dll4 or Rbpj, which encodes RBP-J $\kappa$ , an essential mediator of Notch-induced gene transcription, leads to a reduction in angiogenesis, loss of type H vasculature, and reduced bone formation (Ramasamy et al., 2014). Deficiency of Notch activity also significantly decreases Noggin expression by vascular endothelium, resulting in impaired osteogenic and chondrocyte differentiation function in mice (Ramasamy et al., 2014). Another study showed that the reduction of type H vessels and the reduction of serum VEGF and Noggin levels in hindlimb-unloading (HU) mice were parallel to bone loss (S. Liang et al., 2021). We also found that high glucose inhibited the expression of Notch1, Noggin and VEGF in GK rats, which was more intuitively reflected by the decreased expression levels of CD31, Emcn and Osterix in the bone tissue of GK rats. These results suggest that high glucose may affect angiogenic osteogenic coupling by inhibiting the VEGF/Notch/Noggin pathway and ultimately accelerate osteoporosis. All the above data indicate that Rg1 plays a role through VEGF/Notch/Noggin pathway. However, other factors that may be involved in the preventive effect of rg1 on high glucose-induced bone loss, except VEGF, Notch1, and Noggin, remain to be elucidated. We will conduct more in-depth studies of Rg1 in the future including experiments in toxicology.

In conclusion, the findings of this study suggest that Rg1 plays an active role in diabetic osteoporosis by positively regulating the Notch pathway, stimulating VEGF and Noggin signaling, reversing the damage inflicted by high-glucose exposure on osteoprogenitors and ECs, promoting the secretion of factors related to angiogenesis and bone formation, increasing the number of type H blood vessels, and enhancing the coupling between angiogenesis and osteogenesis. To our knowledge, this is the first study to report that Rg1 can interfere with the progression of diabetic osteoporosis by promoting type H angiogenesis and modulating vasculogenic and osteogenic coupling, expanding the therapeutic range of Rg1. Finally, these findings from cytology and animal models need to be validated in human samples, and clinical analysis of human bone specimens should be performed in the future.

## Data availability statement

The original contributions presented in the study are included in the article/Supplementary Material; further inquiries can be directed to the corresponding author.

## Ethics statement

The animal study was reviewed and approved by the Animal Ethic Committee of the Guangxi University of Traditional Chinese Medicine.



## Author contributions

The concept of the study was provided by WC and SL. WC, SL, and XJ participated in the design of the study protocol. Animal procedures were performed by JS, ST, HJ, and RW. Cell experiments were performed by TW, YJ, SZ, and HZ. Data acquisition was performed by RB, TW, and YJ. Statistical analysis was performed by XJ, JS, YJ, and RB. The manuscript was drafted by WC and XJ. SL and WC supervised the experiments and provided funding. All authors read and approved the final manuscript.

## Funding

This research was funded by the Guangxi Natural Science Foundation Project (No. 2019GXNSFAA185041, No. 2020GXNSFAA297193), the National Natural Science Foundation of China (No. 81860784) and the Guangxi Key Laboratory of Basic Research in Traditional Chinese Medicine Funded Project (No. K201137905).

## References

- Ann, E.-J., Kim, H.-Y., Choi, Y.-H., Kim, M.-Y., Mo, J.-S., Jung, J., et al. (2011). Inhibition of Notch1 signaling by Runx2 during osteoblast differentiation. *J. Bone Min. Res.* 26 (2), 317–330. doi:10.1002/jbmr.227
- Antonopoulos, A. S., Siasos, G., Oikonomou, E., Goulipoulos, N., Konsola, T., Tsigkou, V., et al. (2021). Arterial stiffness and microvascular disease in type 2 diabetes. *Eur. J. Clin. Invest.* 51 (2), e13380. doi:10.1111/eci.13380
- Ballhause, T. M., Jiang, S., Baranowsky, A., Brandt, S., Mertens, P. R., Froesch, K.-H., et al. (2021). Relevance of Notch signaling for bone metabolism and regeneration. *Int. J. Mol. Sci.* 22 (3), 1325. doi:10.3390/ijms22031325
- Beckman, J. A., and Creager, M. A. (2016). Vascular complications of diabetes. *Circ. Res.* 118 (11), 1771–1785. doi:10.1161/CIRCRESAHA.115.306884
- Blázquez, C., González-Feria, L., Alvarez, L., Haro, A., Casanova, M. L., and Guzmán, M. (2004). Cannabinoids inhibit the vascular endothelial growth factor pathway in gliomas. *Cancer Res.* 64 (16), 5617–5623. doi:10.1158/0008-5472.CAN-03-3927
- Campos Pastor, M. M., López-Ibarra, P. J., Escobar-Jiménez, F., Serrano Pardo, M. D., and García-Cervigón, A. G. (2000). Intensive insulin therapy and bone mineral density in type 1 diabetes mellitus: A prospective study. *Osteoporos. Int.* 11 (5), 455–459. doi:10.1007/s001980070114
- Chen, J., Zhang, X., Liu, X., Zhang, C., Shang, W., Xue, J., et al. (2019). Ginsenoside Rg1 promotes cerebral angiogenesis via the PI3K/Akt/mTOR signaling pathway in ischemic mice. *Eur. J. Pharmacol.* 856, 172418. doi:10.1016/j.ejphar.2019.172418
- Ellis, S. L., Grassinger, J., Jones, A., Borg, J., Camenisch, T., Haylock, D., et al. (2011). The relationship between bone, hemopoietic stem cells, and vasculature. *Blood* 118 (6), 1516–1524. doi:10.1182/blood-2010-08-303800
- Fajardo, R. J. (2017). Is diabetic skeletal fragility associated with microvascular complications in bone? *Curr. Osteoporos. Rep.* 15 (1), 1–8. doi:10.1007/s11914-017-0341-8
- Ferrara, N. (2004). Vascular endothelial growth factor: Basic science and clinical progress. *Endocr. Rev.* 25 (4), 581–611. doi:10.1210/er.2003-0027
- Fu, R., Lv, W.-C., Xu, Y., Gong, M.-Y., Chen, X.-J., Jiang, N., et al. (2020). Endothelial ZEB1 promotes angiogenesis-dependent bone formation and reverses osteoporosis. *Nat. Commun.* 11 (1), 460. doi:10.1038/s41467-019-14076-3
- Gerber, H. P., Vu, T. H., Ryan, A. M., Kowalski, J., Werb, Z., and Ferrara, N. (1999). VEGF couples hypertrophic cartilage remodeling, ossification and angiogenesis during endochondral bone formation. *Nat. Med.* 5 (6), 623–628. doi:10.1038/9467
- Gong, Y.-S., Chen, J., Zhang, Q.-Z., and Zhang, J.-T. (2006). Effect of 17beta-oestradiol and ginsenoside on osteoporosis in ovariectomised rats. *J. Asian Nat. Prod. Res.* 8 (7), 649–656. doi:10.1080/10286020500246063
- Gu, J., Li, W., Xiao, D., Wei, S., Cui, W., Chen, W., et al. (2013). Compound K, a final intestinal metabolite of ginsenosides, enhances insulin secretion in MIN6 pancreatic  $\beta$ -cells by upregulation of GLUT2. *Fitoterapia* 87, 84–88. doi:10.1016/j.fitote.2013.03.020
- Gu, Y., Fan, W., and Yin, G. (2014). The study of mechanisms of protective effect of Rg1 against arthritis by inhibiting osteoclast differentiation and maturation in CIA mice. *Mediat. Inflamm.* 2014, 305071. doi:10.1155/2014/305071
- Gu, Y., Zhou, J., Wang, Q., Fan, W., and Yin, G. (2016). Ginsenoside Rg1 promotes osteogenic differentiation of rBMSCs and healing of rat tibial fractures through regulation of GR-dependent BMP-2/SMAD signaling. *Sci. Rep.* 6, 25282. doi:10.1038/srep25282
- Hou, J., Wang, L., Wang, C., Ma, R., Wang, Z., Xiao, H., et al. (2022). Ginsenoside Rg1 reduces oxidative stress via Nrf2 activation to regulate age-related mesenchymal stem cells fate switch between osteoblasts and adipocytes. *Evid. Based. Complement. Altern. Med.* 2022, 1411354. doi:10.1155/2022/1411354
- Hu, K., and Olsen, B. R. (2016). Osteoblast-derived VEGF regulates osteoblast differentiation and bone formation during bone repair. *J. Clin. Invest.* 126 (2), 509–526. doi:10.1172/JCI82585
- Hu, K., and Olsen, B. R. (2017). Vascular endothelial growth factor control mechanisms in skeletal growth and repair. *Dev. Dyn.* 246 (4), 227–234. doi:10.1002/dvdy.24463
- Hu, X.-F., Xiang, G., Wang, T.-J., Ma, Y.-B., Zhang, Y., Yan, Y.-B., et al. (2021). Impairment of type H vessels by NOX2-mediated endothelial oxidative stress: Critical mechanisms and therapeutic targets for bone fragility in streptozotocin-induced type 1 diabetic mice. *Theranostics* 11 (8), 3796–3812. doi:10.7150/thno.50907
- Keramiris, N. C., Calori, G. M., Nikolaou, V. S., Schemitsch, E. H., and Giannoudis, P. V. (2008). Fracture vascularity and bone healing: A systematic review of the role of VEGF. *Injury* 39 (2), S45–S57. doi:10.1016/S0020-1383(08)70015-9
- Kim, J. H., Yi, Y.-S., Kim, M.-Y., and Cho, J. Y. (2017). Role of ginsenosides, the main active components of Panax ginseng, in inflammatory responses and diseases. *J. Ginseng Res.* 41 (4), 435–443. doi:10.1016/j.jgr.2016.08.004
- Kusumbe, A. P., Ramasamy, S. K., and Adams, R. H. (2014). Coupling of angiogenesis and osteogenesis by a specific vessel subtype in bone. *Nature* 507 (7492), 323–328. doi:10.1038/nature13145

## Conflict of interest

The authors declare that the research was conducted in the absence of any commercial or financial relationships that could be construed as a potential conflict of interest.

## Publisher's note

All claims expressed in this article are solely those of the authors and do not necessarily represent those of their affiliated organizations, or those of the publisher, the editors and the reviewers. Any product that may be evaluated in this article, or claim that may be made by its manufacturer, is not guaranteed or endorsed by the publisher.

## Supplementary material

The Supplementary Material for this article can be found online at: <https://www.frontiersin.org/articles/10.3389/fphar.2022.1010937/full#supplementary-material>



- Langen, U. H., Pitulescu, M. E., Kim, J. M., Enriquez-Gasca, R., Sivaraj, K. K., Kusumbe, A. P., et al. (2017). Cell-matrix signals specify bone endothelial cells during developmental osteogenesis. *Nat. Cell Biol.* 19 (3), 189–201. doi:10.1038/ncb3476
- Leung, K. W., Pon, Y. L., Wong, R. N. S., and Wong, A. S. T. (2006). Ginsenoside-Rg1 induces vascular endothelial growth factor expression through the glucocorticoid receptor-related phosphatidylinositol 3-kinase/Akt and beta-catenin/T-cell factor-dependent pathway in human endothelial cells. *J. Biol. Chem.* 281 (47), 36280–36288. doi:10.1074/jbc.M606698200
- Li, S., Haigh, K., Haigh, J. J., and Vasudevan, A. (2013). Endothelial VEGF sculpts cortical cytoarchitecture. *J. Neurosci.* 33 (37), 14809–14815. doi:10.1523/JNEUROSCI.1368-13.2013
- Liang, S., Ling, S., Du, R., Li, Y., Liu, C., Shi, J., et al. (2021). The coupling of reduced type H vessels with unloading-induced bone loss and the protection role of *Panax quinquefolium* saponin in the male mice. *Bone* 143, 115712. doi:10.1016/j.bone.2020.115712
- Liang, Y., Liu, Y., Lai, W., Du, M., Li, S., Zhou, L., et al. (2019). 1, 25-Dihydroxy vitamin D3 treatment attenuates osteopenia, and improves bone muscle quality in Goto-Kakizaki type 2 diabetes model rats. *Endocrine* 64 (1), 184–195. doi:10.1007/s12020-019-01857-5
- Liu, Y., Berendsen, A. D., Jia, S., Lotinun, S., Baron, R., Ferrara, N., et al. (2012). Intracellular VEGF regulates the balance between osteoblast and adipocyte differentiation. *J. Clin. Invest.* 122 (9), 3101–3113. doi:10.1172/JCI61209
- Maes, C. (2013). Role and regulation of vascularization processes in endochondral bones. *Calcif. Tissue Int.* 92 (4), 307–323. doi:10.1007/s00223-012-9689-z
- Mayr-Wohlfart, U., Waltenberger, J., Hausser, H., Kessler, S., Günther, K.-P., Dehio, C., et al. (2002). Vascular endothelial growth factor stimulates chemotactic migration of primary human osteoblasts. *Bone* 30 (3), 472–477. doi:10.1016/s8756-3282(01)00690-1
- Moayeri, A., Mohamadpour, M., Mousavi, S. F., Shirzadpour, E., Mohamadpour, S., and Amraei, M. (2017). Fracture risk in patients with type 2 diabetes mellitus and possible risk factors: A systematic review and meta-analysis. *Ther. Clin. Risk Manag.* 13, 455–468. doi:10.2147/TCRM.S131945
- Novak, S., Roeder, E., Sinder, B. P., Adams, D. J., Siebel, C. W., Grcevic, D., et al. (2020). Modulation of Notch1 signaling regulates bone fracture healing. *J. Orthop. Res.* 38 (11), 2350–2361. doi:10.1002/jor.24650
- Oikawa, A., Siragusa, M., Quaini, F., Mangialardi, G., Katara, R. G., Caporali, A., et al. (2010). Diabetes mellitus induces bone marrow microangiopathy. *Arterioscler. Thromb. Vasc. Biol.* 30 (3), 498–508. doi:10.1161/ATVBAHA.109.200154
- Olsson, A.-K., Dimberg, A., Kreuger, J., and Claesson-Welsh, L. (2006). VEGF receptor signalling—in control of vascular function. *Nat. Rev. Mol. Cell Biol.* 7 (5), 359–371. doi:10.1038/nrm1911
- Parizad, N., Baghi, V., Karimi, E. B., and Ghanei Gheshlagh, R. (2019). The prevalence of osteoporosis among Iranian postmenopausal women with type 2 diabetes: A systematic review and meta-analysis. *Diabetes Metab. Syndr.* 13 (4), 2607–2612. doi:10.1016/j.dsx.2019.07.036
- Peng, J., Hui, K., Hao, C., Peng, Z., Gao, Q. X., Jin, Q., et al. (2016). Low bone turnover and reduced angiogenesis in streptozotocin-induced osteoporotic mice. *Connect. Tissue Res.* 57 (4), 277–289. doi:10.3109/03008207.2016.1171858
- Peng, Y., Wu, S., Li, Y., and Crane, J. L. (2020). Type H blood vessels in bone modeling and remodeling. *Theranostics* 10 (1), 426–436. doi:10.7150/tno.34126
- Radad, K., Gille, G., Moldzio, R., Saito, H., and Rausch, W.-D. (2004). Ginsenosides Rb1 and Rg1 effects on mesencephalic dopaminergic cells stressed with glutamate. *Brain Res.* 1021 (1), 41–53. doi:10.1016/j.brainres.2004.06.030
- Ramasamy, S. K., Kusumbe, A. P., Itkin, T., Gur-Cohen, S., Lapidot, T., and Adams, R. H. (2016a). Regulation of hematopoiesis and osteogenesis by blood vessel-derived signals. *Annu. Rev. Cell Dev. Biol.* 32, 649–675. doi:10.1146/annurev-cellbio-111315-124936
- Ramasamy, S. K., Kusumbe, A. P., Schiller, M., Zeuschner, D., Bixel, M. G., Milia, C., et al. (2016b). Blood flow controls bone vascular function and osteogenesis. *Nat. Commun.* 7, 13601. doi:10.1038/ncomms13601
- Ramasamy, S. K., Kusumbe, A. P., Wang, L., and Adams, R. H. (2014). Endothelial Notch activity promotes angiogenesis and osteogenesis in bone. *Nature* 507 (7492), 376–380. doi:10.1038/nature13146
- Ramazzotti, G., Fiume, R., Chiarini, F., Campana, G., Ratti, S., Billi, A. M., et al. (2019). Phospholipase C- $\beta$ 1 interacts with cyclin E in adipose-derived stem cells osteogenic differentiation. *Adv. Biol. Regul.* 71, 1–9. doi:10.1016/j.abior.2018.11.001
- Ren, T.-T., Yang, J.-Y., Wang, J., Fan, S.-R., Lan, R., and Qin, X.-Y. (2021). Ginsenoside Rg1 attenuates cadmium-induced neurotoxicity *in vitro* and *in vivo* by attenuating oxidative stress and inflammation. *Inflamm. Res.* 70 (10–12), 1151–1164. doi:10.1007/s00011-021-01513-7
- Shanhoghe, V. V., Hansen, S., Frost, M., Brixen, K., and Hermann, A. P. (2017). Bone disease in diabetes: Another manifestation of microvascular disease? *Lancet. Diabetes Endocrinol.* 5 (10), 827–838. doi:10.1016/S2213-8587(17)30134-1
- Shanhoghe, V. V., Hansen, S., Frost, M., Jørgensen, N. R., Hermann, A. P., Henriksen, J. E., et al. (2016). Compromised cortical bone compartment in type 2 diabetes mellitus patients with microvascular disease. *Eur. J. Endocrinol.* 174 (2), 115–124. doi:10.1530/EJE-15-0860
- Shen, J., Sun, Y., Liu, X., Zhu, Y., Bao, B., Gao, T., et al. (2021). EGFL6 regulates angiogenesis and osteogenesis in distraction osteogenesis via Wnt/ $\beta$ -catenin signaling. *Stem Cell Res. Ther.* 12 (1), 415. doi:10.1186/s13287-021-02487-3
- Tomlinson, R. E., and Silva, M. J. (2013). Skeletal blood flow in bone repair and maintenance. *Bone Res.* 1 (4), 311–322. doi:10.4242/BR201304002
- Ucuzian, A. A., Gassman, A. A., East, A. T., and Greisler, H. P. (2010). Molecular mediators of angiogenesis. *J. Burn Care Res.* 31 (1), 158–175. doi:10.1097/BCR.0b013e3181c7ed82
- Wacker, A., and Gerhardt, H. (2011). Endothelial development taking shape. *Curr. Opin. Cell Biol.* 23 (6), 676–685. doi:10.1016/j.ccb.2011.10.002
- Wang, C.-W., Su, S.-C., Huang, S.-F., Huang, Y.-C., Chan, F.-N., Kuo, Y.-H., et al. (2015). An essential role of cAMP response element binding protein in ginsenoside Rg1-mediated inhibition of Na<sup>+</sup>/Glucose cotransporter 1 gene expression. *Mol. Pharmacol.* 88 (6), 1072–1083. doi:10.1124/mol.114.097352
- Wang, L., Zhou, F., Zhang, P., Wang, H., Qu, Z., Jia, P., et al. (2017). Human type H vessels are a sensitive biomarker of bone mass. *Cell Death Dis.* 8 (5), e2760. doi:10.1038/cddis.2017.36
- Wang, P., Wei, X., Zhang, F., Yang, K., Qu, C., Luo, H., et al. (2014). Ginsenoside Rg1 of *Panax ginseng* stimulates the proliferation, odontogenic/osteogenic differentiation and gene expression profiles of human dental pulp stem cells. *Phytomedicine* 21 (2), 177–183. doi:10.1016/j.phymed.2013.08.021
- Wang, P., Wei, X., Zhou, Y., Wang, Y.-P., Yang, K., Zhang, F.-J., et al. (2012). Effect of ginsenoside Rg1 on proliferation and differentiation of human dental pulp cells *in vitro*. *Aust. Dent. J.* 57 (2), 157–165. doi:10.1111/j.1834-7819.2012.01672.x
- Weinberg, E., Maymon, T., Moses, O., and Weinreb, M. (2014). Streptozotocin-induced diabetes in rats diminishes the size of the osteoprogenitor pool in bone marrow. *Diabetes Res. Clin. Pract.* 103 (1), 35–41. doi:10.1016/j.diabres.2013.11.015
- Xiang, Y.-Z., Shang, H.-C., Gao, X.-M., and Zhang, B.-L. (2008). A comparison of the ancient use of ginseng in traditional Chinese medicine with modern pharmacological experiments and clinical trials. *Phytother. Res.* 22 (7), 851–858. doi:10.1002/ptr.2384
- Xie, H., Cui, Z., Wang, L., Xia, Z., Hu, Y., Xian, L., et al. (2014). PDGF-BB secreted by preosteoclasts induces angiogenesis during coupling with osteogenesis. *Nat. Med.* 20 (11), 1270–1278. doi:10.1038/nm.3668
- Xie, W., Zhou, P., Sun, Y., Meng, X., Dai, Z., Sun, G., et al. (2018). Protective effects and target network analysis of ginsenoside Rg1 in cerebral ischemia and reperfusion injury: A comprehensive overview of experimental studies. *Cells* 7 (12), E270. doi:10.3390/cells7120270
- Xu, R., Yallowitz, A., Qin, A., Wu, Z., Shin, D. Y., Kim, J.-M., et al. (2018). Targeting skeletal endothelium to ameliorate bone loss. *Nat. Med.* 24 (6), 823–833. doi:10.1038/s41591-018-0020-z
- Yang, Y.-Q., Tan, Y.-Y., Wong, R., Wenden, A., Zhang, L.-K., and Rabie, A. B. M. (2012). The role of vascular endothelial growth factor in ossification. *Int. J. Oral Sci.* 4 (2), 64–68. doi:10.1038/ijos.2012.33
- Zanotti, S., and Canalis, E. (2014). Notch1 and Notch2 expression in osteoblast precursors regulates femoral microarchitecture. *Bone* 62, 22–28. doi:10.1016/j.bone.2014.01.023
- Zhang, L., Liu, Y., Wang, D., Zhao, X., Qiu, Z., Ji, H., et al. (2009). Bone biomechanical and histomorphometrical investment in type 2 diabetic Goto-Kakizaki rats. *Acta Diabetol.* 46 (2), 119–126. doi:10.1007/s00592-008-0068-1
- Zhao, Q., Shen, X., Zhang, W., Zhu, G., Qi, J., and Deng, L. (2012). Mice with increased angiogenesis and osteogenesis due to conditional activation of HIF pathway in osteoblasts are protected from ovariectomy induced bone loss. *Bone* 50 (3), 763–770. doi:10.1016/j.bone.2011.12.003



## OPEN ACCESS

## EDITED BY

Xiaofeng Zhu,  
Jinan University, China

## REVIEWED BY

Dipranjan Laha,  
National Institutes of Health (NIH),  
United States  
Manjinder Singh,  
Chitkara University, India  
Takuma Matsubara,  
Kyushu Dental University, Japan

## \*CORRESPONDENCE

Guoqing Tan,  
yxkmt@hotmail.com  
Zhanwang Xu,  
xzw6001@163.com

## SPECIALTY SECTION

This article was submitted to  
Experimental Pharmacology  
and Drug Discovery,  
a section of the journal  
Frontiers in Pharmacology

RECEIVED 20 July 2022

ACCEPTED 08 November 2022

PUBLISHED 18 November 2022

## CITATION

Li Z, Li D, Su H, Xue H, Tan G and Xu Z  
(2022), Autophagy: An important target  
for natural products in the treatment of  
bone metabolic diseases.  
*Front. Pharmacol.* 13:999017.  
doi: 10.3389/fphar.2022.999017

## COPYRIGHT

© 2022 Li, Li, Su, Xue, Tan and Xu. This is  
an open-access article distributed  
under the terms of the [Creative  
Commons Attribution License \(CC BY\)](#).  
The use, distribution or reproduction in  
other forums is permitted, provided the  
original author(s) and the copyright  
owner(s) are credited and that the  
original publication in this journal is  
cited, in accordance with accepted  
academic practice. No use, distribution  
or reproduction is permitted which does  
not comply with these terms.

# Autophagy: An important target for natural products in the treatment of bone metabolic diseases

Zhichao Li<sup>1</sup>, Dandan Li<sup>2</sup>, Hui Su<sup>1</sup>, Haipeng Xue<sup>3</sup>, Guoqing Tan<sup>3\*</sup>  
and Zhanwang Xu<sup>3\*</sup>

<sup>1</sup>First College of Clinical Medicine, Shandong University of Traditional Chinese Medicine, Jinan, China, <sup>2</sup>College of Integrated Traditional Chinese and Western Medicine, Hebei University of Chinese Medicine, Shijiazhuang, China, <sup>3</sup>Department of Orthopedics, Affiliated Hospital of Shandong University of Traditional Chinese Medicine, Jinan, China

Bone homeostasis depends on a precise dynamic balance between bone resorption and bone formation, involving a series of complex and highly regulated steps. Any imbalance in this process can cause disturbances in bone metabolism and lead to the development of many associated bone diseases. Autophagy, one of the fundamental pathways for the degradation and recycling of proteins and organelles, is a fundamental process that regulates cellular and organismal homeostasis. Importantly, basic levels of autophagy are present in all types of bone-associated cells. Due to the cyclic nature of autophagy and the ongoing bone metabolism processes, autophagy is considered a new participant in bone maintenance. Novel therapeutic targets have emerged as a result of new mechanisms, and bone metabolism can be controlled by interfering with autophagy by focusing on certain regulatory molecules in autophagy. In parallel, several studies have reported that various natural products exhibit a good potential to mediate autophagy for the treatment of metabolic bone diseases. Therefore, we briefly described the process of autophagy, emphasizing its function in different cell types involved in bone development and metabolism (including bone marrow mesenchymal stem cells, osteoblasts, osteocytes, chondrocytes, and osteoclasts), and also summarized research advances in natural product-mediated autophagy for the treatment of metabolic bone disease caused by dysfunction of these cells (including osteoporosis, rheumatoid joints, osteoarthritis, fracture nonunion/delayed union). The objective of the study was to identify the function that autophagy serves in metabolic bone disease and the effects, potential, and challenges of natural products for the treatment of these diseases by targeting autophagy.

## KEYWORDS

autophagy, natural products, bone metabolism, osteoporosis, rheumatoid arthritis, osteoarthritis, fracture nonunion/delayed union

## Introduction

The bone acts as the primary structural component of the human body, which serves the functions of providing structural support, protection and movement, mineral storage, hematopoiesis, hormone secretion, and cognitive regulation. The supposedly robust and static bone tissue is dynamically remodeled continuously and regularly to carry out these intricate duties (Hadjidakis and Androulakis, 2006). This is necessary for microfracture recovery, the maintenance of calcium homeostasis, and the adaptation of the bone to different stresses (Sims and Gooi, 2008). Any imbalance in this process can cause disturbances in bone metabolism, leading to the development of many bone diseases such as osteoporosis (OP), osteoarthritis (OA), rheumatoid arthritis (RA), and fracture nonunion/delayed union, which can seriously impair patients' quality of life and possibly put their lives in danger (Wang S. et al., 2020). Although various drugs have helped to reduce pain, restore bone strength, prevent bone deformities, and maintain daily activities to some extent, they have always had less satisfactory drawbacks, such as the inability to reverse the disease, high costs, restrictions on long-term drug use, and side effects (Ruderman, 2012; Sugiyama et al., 2015; Hunter and Bierma-Zeinstra, 2019). As a result, the current treatment strategy for these common metabolic bone diseases is largely conservative. Researchers have never stopped looking for novel medications, but the creation of new medications must be supported by a thorough comprehension of the disease mechanisms.

Autophagy provides a new perspective for understanding metabolic bone disease, which is an intracellular survival mechanism critical for cellular function (Kuma and Mizushima, 2010). Autophagy is constitutive as well as adaptive; under normal physiological conditions, basal levels of autophagy help remove damaged and malfunctioning cellular components and maintain basic energy homeostasis, whereas, under various stress conditions (especially nutritional deficiencies), upregulation of autophagy generates energy to maintain metabolism by providing additional nutrients from the recovered cellular components (Kim and Lee, 2014; Li et al., 2020b). The role of this mechanism transcends a single cell type or tissue and extends to the entire organism. Autophagy is the fundamental process that maintains cellular and organismal homeostasis (Dikic and Elazar, 2018). Novel therapeutic targets have emerged as a result of new mechanisms, and altering autophagy by focusing on certain regulatory molecules in autophagy can affect a number of disease processes (Al-Bari et al., 2021). Thus, autophagy is a crucial pharmacological target for drug development and therapeutic intervention in a variety of diseases, including bone metabolic disorders. More intriguingly, natural compounds derived from plants, animals, and microorganisms have been demonstrated to have the ability to influence autophagy through a variety of

mechanisms, and as a result, may be crucial in the prevention or treatment of metabolic bone disease, implying the emergence of alternative drugs with lower costs, fewer side effects, and longer-term applications (Luk et al., 2020; Zheng H. et al., 2020; Mueller et al., 2021).

In this review, we provided a review of the current knowledge on the role of autophagy in bone metabolism disorders, to explore the potential relationship between autophagy and bone metabolism disorders. To serve as a resource for future studies, we also presented an overview of the functions and mechanisms of natural compounds that have been suggested to control autophagy in the treatment of prevalent metabolic bone disease in recent years.

## Initiation and regulation of autophagy

Mammals have so far been classified as having three different types of autophagy: chaperone-mediated autophagy (CMA), micro-autophagy, and macro-autophagy (Mizushima and Komatsu, 2011). This paper focuses on macro-autophagy, henceforth referred to as autophagy. Autophagy is influenced by multiple signaling pathways, of which the most widely studied are the phosphoinositide3 kinase (PI3K)/protein kinase B (Akt) and 5' AMP-activated protein kinase pathways. Together, these pathways converge on the mammalian target of rapamycin (mTOR). mTOR recruits various proteins to form two distinct complexes, mTORC1, and mTORC2. mTORC1 is involved in the regulation of autophagy and is a recognized negative regulator of autophagy (Jung et al., 2010; Chen X. D. et al., 2020). Autophagy is a highly conserved process that typically consists of several phases, including initiation, nucleation, elongation, maturation, and degradation (Yin et al., 2016; Markaki and Tavernarakis, 2020). The UNC-51-like kinase (ULK1) complex (which is composed of ULK1, ATG101, ATG13 and FAK family kinase-interacting protein of 200 kDa (FIP200), *etc.*) is activated and recruits the class 3 PI3K complex (which is composed of vacuolar protein sorting (Vps) 15, Vps34, ATG14 and Beclin1, *etc.*) to the autophagy initiation site to form an isolated membrane. autophagy-related protein (Atg) seven then binds the Atg12-Atg5-Atg16 complex and microtubule-associated protein one light chain 3 (LC3) I with phosphatidylethanolamine (PE) to produce LC3 II (Rabinowitz and White, 2010). LC3 II modifies the expanding phagophore to participate in cargo recognition and recruitment (Li et al., 2020a). The phagophore eventually enlarges and closes to form an autophagosome, a double membrane structure (Ravikumar et al., 2010). After maturing into the autophagolysosome, which is made up of the autophagosome and lysosome, acidic proteases break down the autophagolysosome and its contents into amino acids, lipids, nucleotides, and energy for cellular recycling (Ravikumar et al., 2010) (Figure 1).

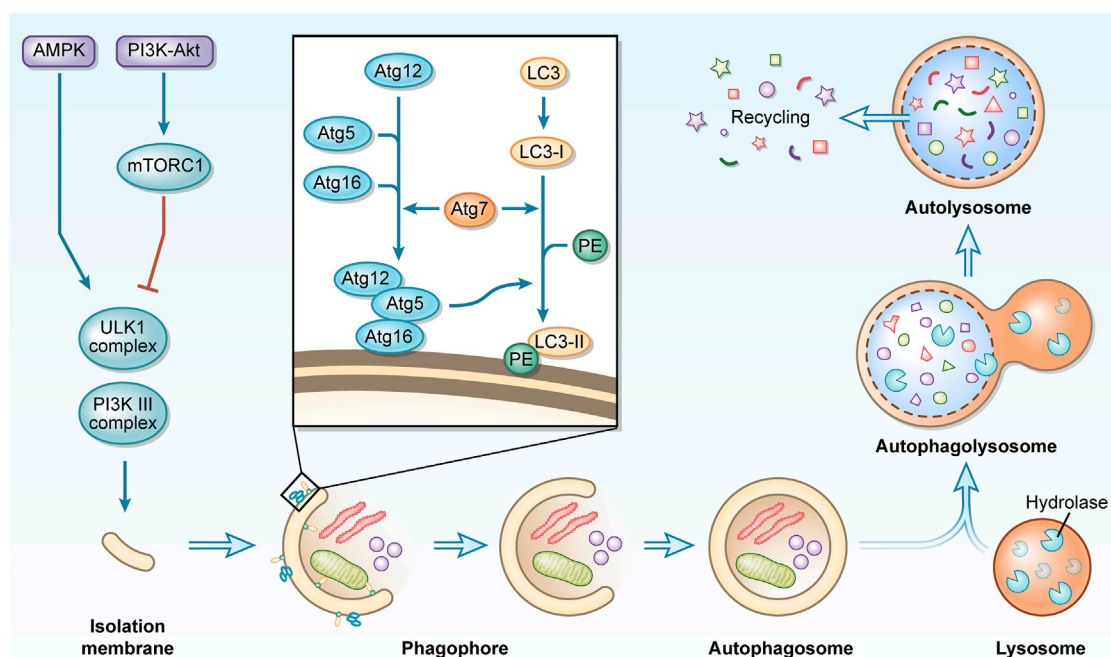


FIGURE 1

A concise description of the macro-autophagy process. During macro-autophagy, cellular components are sequestered in autophagosomes and transported to lysosomes for degradation to achieve recycling use.

## Autophagy in bone metabolism

As an active metabolic tissue, bone undergoes a continuous remodeling cycle. Cells of different lineages perform specific skeletal functions, with osteoblasts and chondrocytes from bone marrow mesenchymal stem cells (BMSCs) shaping bone for maximum adaptability and osteoclasts of the monocyte/macrophage lineage resorbing large surfaces of predominantly cancellous bone to maintain mineral homeostasis (Zaidi, 2007). This complex mechanism of simultaneous activation couples bone formation and bone resorption, carefully balancing the development and maintenance of bone size, shape, and integrity (Boyle et al., 2003; Zaidi, 2007). Osteocytes, which are descended from osteoblasts, operate as sensors embedded in the matrix and may translate mechanical stimuli into biochemical signals (Palumbo and Ferretti, 2021). With the cyclic nature of autophagy and the continuous remodeling of bone tissue, and the levels of basal autophagy found to be present in all bone-related cells, it is reasonable to assume that autophagy plays an important role in bone homeostasis.

## Autophagy in BMSCs

Autophagy participates in fundamental processes such as stem cell quiescence, self-renewal, differentiation, and

pluripotency by regulating cell remodeling, and metabolism, and as an important mechanism of quality control (Boya et al., 2018). Adult stem cells known as BMSCs are pluripotent and may differentiate into a variety of cell types, including osteoblasts, adipocytes, chondrocytes, and neurons, etc (Chen et al., 2018). Autophagy in BMSCs is activated in response to environmental induction and hormones, which are essential for the survival, anti-aging, and differentiation of BMSCs. Early activation of autophagy can effectively inhibit apoptosis in BMSCs under conditions of hypoxia (28), serum deprivation (Zhang et al., 2012), oxidative stress (Song et al., 2014; Fan et al., 2019), inflammatory environments (Yang et al., 2016), highly saturated fatty acid environments (Liu et al., 2018), radiation (Alessio et al., 2015), and glucocorticoids administration (Wang et al., 2015). When exposed for an excessively long or severe period, this defense mechanism causes a switch from protective to destructive autophagy, which appears to depend on the intensity and duration of the stressful environment (Hu et al., 2019).

We concentrate on the function of autophagy in the osteogenic differentiation of BMSCs since specialized differentiation of BMSCs, such as differentiation to neurons (Li et al., 2016) or adipocytes (Song et al., 2015), needs the participation of autophagy. Undifferentiated BMSCs tend to accumulate large amounts of undegraded autophagic vacuoles with limited autophagic conversion, which continues to increase



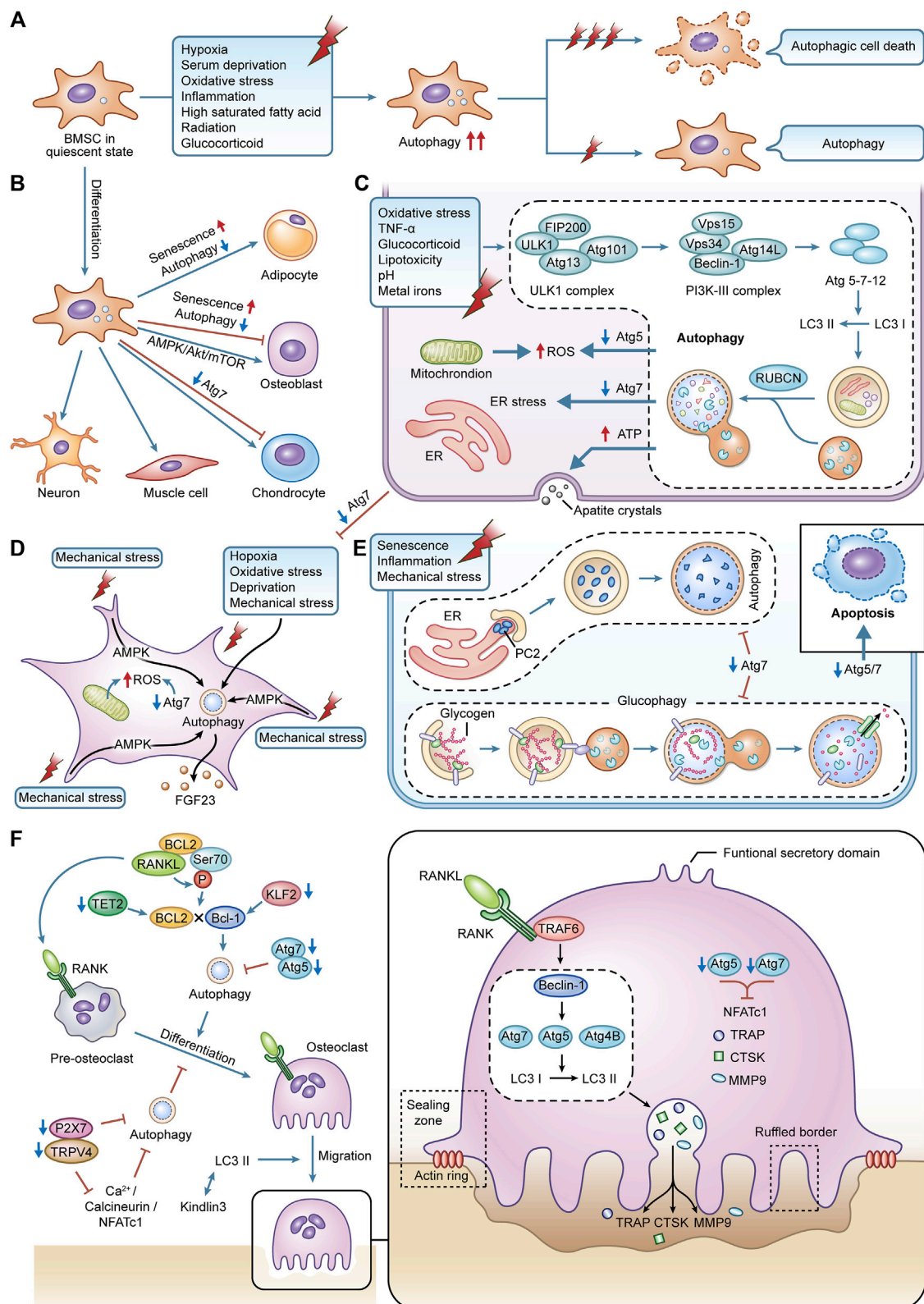


FIGURE 2

The effects of autophagy in various bone cell. (A) autophagy in BMSCs is activated during cellular differentiation, responding to external stress.

(B) the specialized differentiation process in BMSCs is modified by autophagy. (C) autophagy in osteoblasts is activated caused by the stimulation of (Continued)



**FIGURE 2 (Continued)**

external stress. It can maintain redox balance within osteoblasts and affect the cellular mineralization and differentiation process. **(D)** terminally differentiated osteocytes can maintain lifespan and adapt to harsh environments *via* autophagy. The interaction between autophagy and mechanical stress is critical for the functions of osteocytes. **(E)** autophagy is an essential part of BMSCs differentiating into chondrocytes. Autophagy can regulate the secretion of type II collagen. Glycophagy can supply energy for chondrocytes. **(F)** the differentiation, migration, and bone resorption functions of osteoclasts are supported by autophagy.

when osteogenic differentiation is initiated (Nuschke et al., 2014), which may be driven by elevated bioenergetic needs. Autophagy provides the morphology and structure required to support osteogenic differentiation, the energy required for metabolic remodeling and anabolic precursors (Ceccariglia et al., 2020), which is also reflected in the dependence of autophagy on 5' AMP-activated protein kinase (AMPK)/Akt/mTOR signaling early in osteogenic differentiation (Pantovic et al., 2013), and inhibition of autophagy would significantly inhibit the osteogenic differentiation capacity of BMSCs. Furthermore, the efficiency of the autophagic process is decreased with age (Wu et al., 2009), which for BMSCs is frequently reflected in an imbalance of osteogenic and lipogenic differentiation, leading to bone loss and fat accumulation (Moerman et al., 2004). Inhibition of autophagy can put young BMSCs into a relatively senescent state, predisposing them to lipogenic differentiation. In contrast, the autophagy activator rapamycin reverses this property, which may be due to the correlation between the regulation of autophagy on reactive oxygen species (ROS) levels and the expression of P53 (a regulator of senescence) (Ma et al., 2018), suggesting that reasonable maintenance of autophagy levels would be beneficial for the prevention of aging and rejuvenation of BMSCs (Yang et al., 2018; Kondrikov et al., 2020) (Figures 2A,B).

## Autophagy in osteoblasts

Osteoblasts are the primary constructors of bone, and these cells deposit bone matrix through continuous synthesis and resection activities (Yin et al., 2019). Deletion of autophagy-related genes impairs autophagy and negatively affects osteoblast activity and function. Increased susceptibility to oxidative stress damage and suppression of osteoblast proliferation and differentiation result from the deletion of Atg5 (Weng et al., 2018). Specific knockdown of Atg7 induces endoplasmic reticulum (ER) stress during bone development and remodeling stages thereby promoting apoptosis in osteoblasts (Li H. et al., 2018), and this deletion, if present early in the differentiation of the osteoblast lineage, can even affect the transition of osteoblasts to osteocytes and disrupt the formation and maintenance of the osteocyte network, so severely that more than 50% of mice with Atg7 knockdown will fracture as a result (Piemontese et al., 2016).

At the same time, autophagy facilitates the survival of osteoblasts under various stressful environments. Through the ER stress pathway, early activation of autophagy in osteoblasts can successfully reduce intracellular ROS levels and remove damaged mitochondria, counteracting the damage brought on by oxidative stress (Li D. Y. et al., 2017). This protective effect is equally beneficial in alleviating osteoblast apoptosis induced by toxic stimuli such as tumor necrosis factor- $\alpha$  (TNF- $\alpha$ ) (Zheng L. W. et al., 2020), glucocorticoids (Wang et al., 2019), lipotoxicity (Al Saeedi et al., 2020), acidity (Zhang et al., 2017), and metal ions (Xu G. et al., 2021; Liu et al., 2021).

Osteoblasts are dedicated mineralized cells, and the presence of double-membrane autophagosomes containing apatitic pinpoint-like structures was found in primary osteoblast cell lines, suggesting that intracellular mineralization, one of the mechanisms of mineralization, may be mediated by autophagy, with autophagosomes acting as carriers of the secretion of mineralization (Nollet et al., 2014). This shift from a low steady state to a high autophagic flux may be designed to meet the high-energy demands of active osteoblasts during mineralization, thus promoting a high synthesis of secreted proteins and the removal of misfolded bone matrix proteins. In contrast, the deletion of Atg7 and Beclin1 significantly reduces the mineralization efficiency of osteoblast cell lines (Nollet et al., 2014). Osteoblast proliferation to mineralization is inhibited when FIP200 (a component of the complex that initiates autophagosome formation) is specifically deleted (Liu et al., 2013). In contrast, deletion of RUBCN (a negative regulator gene of autophagosome-lysosome fusion) leads to enhanced osteoblast differentiation and mineralization and elevated expression of key transcription factors related to osteoblast function such as Runx2 and Bglap/Osteocalcin, which may be achieved through accelerated autophagic degradation of the intracellular structural domain of NOTCH (Yoshida et al., 2022) (Figure 2C).

## Autophagy in osteocytes

Organelle recycling is required to give nourishment and adapt to the new environment as a result of the major changes in the spatial location and morphology of cells during the transition of osteoblasts to osteocytes (Dallas and Bonewald, 2010). Considering that those mature osteocytes are terminally differentiated cells that do not actively divide, intracellular

degradation mechanisms are required to protect them from undergoing cell death (Stroikin et al., 2005). However, because of their lengthy longevity, they must be able to endure conditions with low oxygen, high levels of oxidative stress, nutrient deprivation, and constant mechanical stress. This biological evidence highlights autophagy as a potential mechanism to ensure the survival of osteocytes in their unique microenvironment. Osteocyte resistance to oxidative stress and hypoxia-induced cell death is naturally facilitated by osteocytes' higher autophagic activity than osteoblasts (Zahm et al., 2011; Kurihara et al., 2021). The oxidative stress in the bones of young mice climbs to elderly levels when Atg7 is lacking, and this causes skeletal abnormalities that are comparable to those brought on by aging (Onal et al., 2013).

The osteocytes are mechanoreceptive cells, which mediate the adaptive response to bone loading, perceive mechanical forces and translate them into graded structures as well as ensure metabolic changes (Qin et al., 2020). Mechanical loading is a specific and potent stimulus for osteocytes, which improves bone strength and inhibits defects in bone aging (Klein-Nulend et al., 2012). Autophagy is highly sensitive to the changes in mechanical stress in slime mold and mammalian cells (King et al., 2011). Periodic mechanical stretching alters the size and shape of osteocytes and promotes the network development of osteocytes, which is associated with upregulated autophagy (Inaba et al., 2017). Fluid shear stress-induced autophagy in osteocytes *in vitro* promotes osteocyte survival by preserving adenosine triphosphate (ATP), which is an adaptive response of osteocytes to mechanical stress (Zhang et al., 2018). Furthermore, the interaction between autophagy and mechanical tension is essential for regulating the secretory capacity of osteocytes, and mechanical tension can activate autophagy and enhance the secretion of fibroblast growth factor-23 (FGF23) (a homeostatic regulator within mineralization and phosphate) in osteocytes *via* AMPK signaling, thereby promoting the development and formation of osteoblasts (Xu H. et al., 2021) (Figure 2D).

## Autophagy in chondrocytes

Most bones develop by endochondral ossification. Apoptosis of chondrocytes, calcification of the mesenchyme, new bone deposition, and longitudinal development of the diaphysis are all ongoing processes that occur in the cartilage growth plate at the confluence of the epiphysis and the diaphysis. The cartilage growth plate is mainly composed of chondrocytes and extracellular matrix (ECM). Chondrocyte proliferation, differentiation, hypertrophy, and ECM formation are essential for skeletal development and linear growth (Berendsen and Olsen, 2015). Autophagy is required for the conversion of mesenchymal stem cells to proliferating chondrocytes, as reflected by the completion of a multi-step differentiation process from mesenchymal condensation to

calcification during normal ATDC5 cell culture, whereas COL2A1 expression is completely blocked during the culture of Atg7-deficient ATDC5 cells (Wang X. J. et al., 2021). Even if the transformation can be completed, deletion of Atg5 or Atg7 in the chondrocyte will also result in decreased chondrocyte proliferation and higher apoptosis, as well as related growth retardation and shorter bone length in mice (Vuppalapati et al., 2015; Wang X. J. et al., 2021). At the same time, due to the vascularization of the growth plate, chondrocytes grow in a hypoxic and nutrient-deficient environment. It is also necessary to rely on autophagosomes to selectively wrap glycogen in the chondrocytes so that the glycogen is catabolized to glucose to provide energy, which is known as glycophagy (Vuppalapati et al., 2015; Ueno and Komatsu, 2017).

On the other hand, functional cartilage requires the homeostasis of chondrocytes and the integrity of cartilage ECM (Luo et al., 2019). Autophagy regulates the secretion of type II collagen, which is a major component of cartilage ECM, and deletion of Atg7 would result in type II procollagen not being transported and remaining within the ER (Cinque et al., 2015). Under the stresses of aging, inflammation and mechanical stimulation, increased apoptosis, decreased ECM production and excessive activation of proteases in chondrocytes contribute to the degeneration of cartilage and the destruction of the joint microarchitecture, leading to the development of diseases such as OA and RA. Contrarily, increased autophagy in chondrocytes can reduce the progression of these disorders by influencing intracellular metabolic processes, demonstrating the benefits of autophagy on chondrocyte survival and prevention of cartilage deterioration (Tian et al., 2021) (Figure 2E).

## Autophagy in osteoclasts

Hematopoietic cell-derived mononuclear osteoclast precursors are drawn to resorption sites where they combine to become terminally differentiated multinucleated osteoclasts (Montaseri et al., 2020). The alternating between migration and phases of bone resorption as well as considerable phenotypic alterations show that they are extremely mobile (Roy and Roux, 2020). After adhering to the area of bone resorption, osteoclasts undergo cytoskeletal reorganization and polarization, leading to the formation of a series of membrane domains such as the sealing zone, ruffled border, basolateral domain and functional secretory domain, which work together to complete the osteolysis process when osteoclasts lyse bone tissue (Georgess et al., 2014). The sealing zone, formed by a dense arrangement of actin-rich podosomes, forms a unique microenvironment between the cells and the bone surface. The transient reabsorption complex, which consists of actin rings and a ruffled border, is sealed off from the extracellular fluid in this region to form an absorption lacuna (Saltel et al., 2008). The ruffled border is formed by the fusion of acid-donating vesicles, which release hydrolases such as

cathepsin K (CTSK), matrix metalloproteinase9 (MMP9), and tartrate-resistant acidic phosphatase (TRAP), and is the site truly responsible for bone resorption (Saltel et al., 2008). This fusion process takes place in the sealing zone, where several intracellular membranes are moved to create lengthy folds resembling fingers. Furthermore, in the non-resorption/migration state of osteoclasts, the relaxed osteoclasts undergo depolarization as they switch from the sealing zone to the podosome belts (Ory et al., 2008).

Autophagy is essential for osteoclast differentiation, migration and maintenance of bone resorption function. The receptor activator of nuclear factor- $\kappa$ B (NF- $\kappa$ B) (RANK)/receptor activator of NF- $\kappa$ B ligand (RANKL)/osteoprotegerin system mediates the process of osteoclast differentiation involving a series of signaling molecules, and the calcium signaling pathway Ca<sup>2+</sup>/calcineurin/nuclear factor of activated T-cell c1 (NFATc1), as one of the key pathways, can be mediated by Ca<sup>2+</sup>-permeable channels such as transient receptor potential vanilloid 4 (TRPV4) or P2X7 receptor (P2X7R). On the other hand, by inhibiting autophagy and Ca<sup>2+</sup>/calcineurin/NFATc1 signaling, suppression of either TRPV4 or P2X7R prevents osteoclast differentiation (Cao et al., 2019; Ma et al., 2022). The expression of Atg5, Atg7, Atg4B, and Beclin1 is increased in RANKL-stimulated bone marrow macrophages, and inhibition of Beclin1 will significantly reduce RANKL-mediated Atg activation and osteoclast differentiation (Arai et al., 2019). Meanwhile, after RANKL stimulation, the ubiquitin ligase tumor necrosis factor receptor-associated factor 6 (TRAF6) is recruited to RANK, thereby initiating Atg and subsequent osteoclasts differentiation at an early stage by mediating Beclin1 ubiquitination (Arai et al., 2019). In addition, RANKL can promote osteoclastogenesis *via* the B-cell lymphoma 2 (BCL2)/Beclin1 pathway, and the mechanism may be related to the fact that RANKL induces Beclin1-dependent protective autophagy by promoting BCL2 phosphorylation at the Ser70 site in osteoclast precursors (Ke et al., 2019; Ke et al., 2022). The tet methylcytosine dioxygenase 2 (TET2)/Beclin1 or kruppel-like factor 2 (KLF2)/Beclin1 autophagy-related pathways have also been shown to promote osteoclastogenesis (Laha et al., 2019; Yang et al., 2022). Deletion of Atg5 or Atg7 would also impede autophagy, which would result in a reduction in osteoclast differentiation and the expression of osteoclast markers such as NFATc1, TRAP, CTSK, and MMP9 (Lin et al., 2016; Chen W. et al., 2021).

One of the key components of the osteoclast's exercise of bone resorption is migration over the bone matrix. Podosome rings undergo continuous and rapid assembly disassembly and drive osteoclast migration by exerting traction on the bone surface (Georgess et al., 2014). kindlin3 is an important bridging protein in the podosome, and downregulation of autophagy due to the deletion of LC3 II would enhance the interaction between kindlin3 and integrins, thereby inhibiting the breakdown of the abandoned podosome rings and leading to the disassembly of the actin cytoskeleton and impaired migration

of osteoclasts (Zhang Y. et al., 2020). For optimal resorption of the bone matrix, osteoclasts require lysosomal transport and fusion to produce fold-edge boundaries and gaps for acidic resorption (Na et al., 2020). The fusion of lysosomes with the border of the fold is similar to the fusion of lysosomes with autophagosomes, suggesting that autophagy proteins are involved in regulating lysosomal localization and the release of reabsorbed molecules (Dawodu et al., 2018). Atg5, Atg7, and Atg4B, together with LC3, which is necessary for the formation of actin rings and the release of tissue proteinase K, are required for the construction of the edge of the fold (DeSelm et al., 2011; Chung et al., 2012) (Figure 2F).

## CMA and micro-autophagy in bone

As with macro-autophagy, CMA similarly responds to nutrient deficiency (Cuervo et al., 1995), oxidative stress (Kaushik and Cuervo, 2006), hypoxia (Hubbi et al., 2013), genotoxic (Park et al., 2015) and other stimuli. Unlike macro-autophagy, CMA does not utilize autophagosomes, chaperone HSC70 and cochaperones deliver protein cargoes containing specific KFERQ-like sequences directly to the lysosome, where they are then transported *via* lysosome-associated membrane protein type 2A (LAMP2A) translocation system is transferred into the lysosome (Sahu et al., 2011; Akel et al., 2022). Compared to the wild type, vertebral cancellous bone mass was significantly lower in LAMP2A and LAMP2C global knockout mice, which was associated with increased osteoclastogenesis due to increased RANKL expression (Akel et al., 2022). BMSCs also exhibited higher CMA activity during osteogenic differentiation, this trend promotes the transition of BMSCs to OBs while inhibiting the potential of BMSCs to differentiate into lipogenic cells and chondrocytes (Gong et al., 2021). Downregulation of LAMP2A in BMSCs is also closely associated with impaired osteogenic differentiation during aging (Gong et al., 2021). Furthermore, leptin affects CMA-mediated expression of megalin (lipoprotein-related protein 2, a key receptor for 25(OH)D3 entry into BMSCs) by inhibiting the levels of LAMP2A and HSC70, thereby increasing the utilization of 25(OH)D3 by BMSCs and making 25(OH)D3-induced enhanced osteogenic differentiation potential of BMSCs, which also suggests that CMA is essential for the role of vitamin D in bone health (He et al., 2021).

During microautophagy, lysosomes and late endosomes capture a small amount of surrounding cytoplasm through membrane protrusion and invagination and degrade it in the endolysosomal lumen (Sahu et al., 2011). In mammalian cells, the exact mechanisms of microautophagy regulation remain largely elusive, with only studies exploring the association of dysfunctional microautophagy with various neurodegenerative diseases (e.g., Alzheimer's disease, Parkinson's disease, and amyotrophic lateral sclerosis) and cancer, the knowledge that

may open a new window for the use of microautophagy in the skeletal domain (Wang L. et al., 2022).

## Mitophagy in bone

Lemaster first defined “mitochondrial autophagy” to emphasize the non-random nature of the mitochondrial autophagic process (Lemasters, 2005). This selective autophagy process mediates mitochondrial quality control by removing damaged mitochondria and coordinating the dynamic balance between mitochondrial and cellular energy requirements (Liang et al., 2020). Similarly, this activity plays an important role in bone cells to mediate the homeostasis of bone metabolism. An increase in mitochondrial mass implies an accumulation of damaged mitochondria and requires a corresponding mitochondrial autophagic activity to maintain a good mitochondrial mass. The induction of mitochondrial autophagy eliminates damaged and unnecessary mitochondria from dental pulp stem cells and preserves healthy mitochondria, which promotes their differentiation into osteoblasts (Maity et al., 2022). During TNF- $\alpha$ -induced osteoblast senescence, the impaired bone anabolic activity can be ameliorated by restoring mitochondrial dysfunction and promoting mitochondrial autophagy (Lu et al., 2022). Furthermore, *in vitro* estrogen administration also promoted mitochondrial autophagy to some extent, which effectively increased osteoblast activity and promoted their proliferation (Sun et al., 2018). Interestingly, just like autophagy, the role played by mitochondrial autophagy seems to depend on the spatiotemporal location of the cell. In high-glucose-treated osteoblasts, mitochondrial autophagy accelerates their osteogenic dysfunction, and pharmacological and genetic inhibition of mitochondrial autophagy can effectively rescue osteoblast differentiation and mineralization (Zhao et al., 2020). The PTEN-induced putative kinase 1 (PINK1)/Parkin pathway is a key player in regulating mitochondrial homeostasis and the most important player in mitochondrial autophagy (Ploumi et al., 2017). For osteoclasts, the mitochondrial deacetylase sirtuin 3 promotes mitochondrial metabolism and mitochondrial autophagy in osteoclasts by deacetylating PINK1, which in turn promotes osteoclast differentiation. Thus, although osteoclast progenitors from sirtuin 3-deficient aged mice are able to differentiate into osteoclasts, however, these differentiated cells exhibit impaired polykaryon formation and resorption activity, further emphasizing the importance of mitochondrial autophagy regulation in bone cells and its contribution to skeletal disease (Ling et al., 2021).

## Natural product-targeted autophagy for the treatment of metabolic bone disease

The growing body of research connecting autophagy and bone metabolic hints at the possibility of treating metabolic bone

disease by inhibiting autophagy. Natural materials derived from natural plants and animals, minerals and their processed products are characterized by novel and diverse structures, better activity and less toxic side effects, and are a “treasure trove” for the development of drugs and nutrients (Li et al., 2021). With the increasing use of natural products, a variety of natural compounds have been screened as effective modulators of autophagy. Importantly, several of these natural compounds can cure metabolic bone disease by targeting autophagy through a number of distinct modes of action. The discovery and research of natural compounds that control autophagy now focus mostly on autophagy inducers and inhibitors because of the dual nature of autophagy during bone metabolism. The regulatory function of these natural products in OP, RA, OA, and fracture nonunion/delayed union is highlighted in this section through activation or inhibition of autophagy.

## Osteoporosis

The majority of patients with OP are unaware that they have this sneaky illness, which is defined by decreased bone density, degeneration of the microarchitecture of bone tissue, increased skeletal fragility, and an increased risk of fractures, including hip, spine, and wrist fractures (Sánchez-Riera et al., 2010). The pathogenesis of this most common skeletal disease is based on an imbalance in the activity of osteoblasts and osteoclasts during bone metabolism (Zaidi, 2007). OP is classified as primary or secondary OP, and the former includes postmenopausal OP and senile OP. Due to diverse underlying causes and rates of development, autophagy has distinct functions in the various OP. In the early stage of the postmenopausal OP, estrogen decreases and bone metabolism has a high-conversion pattern, at this time osteoclastic bone resorption is enhanced and exceeds bone formation, and autophagy plays a more important role in bone resorption (Li et al., 2020b). Progressively lower levels of autophagy in osteocytes with aging are thought to be the underlying cause of bone loss (Chen et al., 2014), and defective autophagy in BMSCs due to aging will also lead to an imbalance in osteogenic and lipogenic differentiation. Bone conversion is delayed in the advanced stages of senile OP or postmenopausal OP (Ma et al., 2018). The predominant pathogenesis of secondary OP, such as the most prevalent glucocorticoid-induced OP, is characterized by impaired osteogenic differentiation, increased osteoblast and osteocyte apoptosis, and prolonged osteoclast lifespan, which results in reduced bone formation and early massive bone loss (Jia et al., 2006; Wang T. et al., 2020). While autophagy plays a role in promoting osteoclastic bone resorption and maintaining the survival of osteoblasts as well as osteocytes, this is usually dependent on glucocorticoid dose and duration of treatment and is regulated by systemic metabolism (Chen et al., 2014). Furthermore, in the disturbed bone microenvironment caused by



oxidative stress or inflammation, damaging apoptosis of bone cells and enhanced osteoclast activity are the main causes of bone loss, and the level of autophagy often depends on the changes in the microenvironment and the severity of the stress.

Based on our current review, the mechanisms of action of natural products that target autophagy for the treatment of OP can be divided into four groups: promoting autophagy to encourage osteogenic differentiation of BMSCs and osteoblast mineralization, inhibiting autophagy to prevent the differentiation of osteoclasts, inhibiting autophagy to prevent apoptosis in bone cells, and raising the level of protective autophagy in stressful environments. Leonurine, the active ingredient of *Leonurus japonicus*, promotes the proliferation of BMSCs in SD rats, upregulates the gene and protein levels of Atg5, Atg7, and LC3, and promotes the differentiation of BMSCs toward osteoblasts through activation of autophagy that depends on the PI3K/Akt/mTOR pathway (Zhao et al., 2021). Icaritin is an important active ingredient in *Epimedium brevicornum* and is mainly metabolized to Icaritin after ingestion. Icaritin reduces ovariectomy (OVX)-induced osteoclast formation in OP mice and promotes osteogenic differentiation by enhancing autophagy in BMSCs (Liang et al., 2019). Similar to osthole, a key component of *Cnidium monnieri* and *Angelica pubescens*, osthole is a coumarin derivative that alleviates OP symptoms in OVX mice by preserving autophagy and encouraging osteogenic differentiation of BMSCs (Zheng et al., 2019). Arbutin, a natural hydroquinone glycoside abundant in plants such as *Vaccinium*, *Asteraceae* and *Ericaceae*, promotes bone formation by activating autophagy to promote osteoblast differentiation and mineralization and attenuate dexamethasone-induced bone mass and loss of trabecular bone structure (Zhang et al., 2021a). In addition, Ginsenoside Rg3, an extract of *Panax ginseng*, significantly attenuated OVX-induced weight gain, decreased bone mineral density and histological alterations in femoral tissue in rats. And *in vitro*, it significantly enhances AMPK signaling, autophagy, osteogenic differentiation and mineralization, inhibits mTOR signaling, and attenuates OVX-induced osteoporosis (Zhang X. et al., 2020).

Kaempferol, a natural flavonol, exists in large quantities as a dietary substance in fruits and vegetables such as tea, citrus fruits and cauliflower, and is also widely distributed in medicinal herbs such as *Bauhinia microstachya*, *Chromolaena odorata* and *Ardisia japonica* (Bangar et al., 2022). Concentrations of Kaempferol above 50  $\mu$ M inhibit RANKL-induced osteoclast differentiation and formation of resorption pits in RAW 264.7 cells, with the mechanism being related to degradation of p62/SQSTM1 (autophagy-related scaffold protein) to inhibit autophagy and activate apoptosis (Kim et al., 2018). Ursolic acid, a pentacyclic triterpene found mainly in the Lamiaceae family, ameliorates OVX-induced osteoporosis in rats by blocking the autophagic process, reducing the expression of the major transcription factor and NFATc1 affecting osteoclast

formation and the activity of the inhibitor of NF- $\kappa$ B kinase/NF- $\kappa$ B of its upstream pathway (Zheng H. et al., 2020).

Autophagy may be a major self-protective mechanism for osteocytes in response to excess glucocorticoids (Li et al., 2020b). Enhanced autophagy in osteocytes treated with low doses of glucocorticoids acts as anti-apoptotic self-protection (Wang T. et al., 2020), therefore, activation of appropriate levels of autophagy to protect osteocytes from apoptosis is a promising strategy to combat glucocorticoid-induced OP and glucocorticoid-associated osteonecrosis of the femoral head. Pinocembrin, a natural flavonoid compound isolated from *compositae* and propolis, attenuates dexamethasone-induced active damage and apoptosis in mice with long bone cell Y4 by inhibiting PI3K/Akt/mTOR signaling to activate autophagy (Wang X. Y. et al., 2020). It is also important to activate autophagy in osteoblasts to maintain cellular activity and prevent apoptosis. The bisbenzylisoquinoline alkaloid fangchinoline, which is obtained from the roots of *Stephania tetrandra*, shares the same structural features as tetrandrine (Zhang et al., 2021b). Fangchinoline administration dramatically lowers osteoblast apoptosis in prednisolone-induced osteoporosis rats by triggering autophagy, improves altered microstructural parameters in rat vertebrae, and avoids bone loss (Zhu W. et al., 2019). Similarly, iridoid glycoside Aucubin, which is abundant in *Eucommia ulmoides*, and monoterpene glucoside Paeoniflorin, which is abundant in the roots of *Paeonia lactiflora*, can enhance autophagy via AMPK and Akt/mTOR signaling pathways, respectively, to prevent glucocorticoid-induced apoptosis in osteoblasts, thereby effectively reducing OP symptoms (Yang et al., 2021; Yue et al., 2021). Another mechanism strongly linked to OP is the NF- $\kappa$ B signaling, which when activated promotes osteoclast activation and creation whereas when inactivated encourages osteoblast differentiation *in vitro* and bone formation *in vivo* (Nandy et al., 2018). In contrast, Timosaponin B-II, a component of the major steroidal saponin of *Anemarrhena asphodeloides*, attenuates high glucose-induced oxidative stress and osteoblast apoptosis by inhibiting the mTOR/NF- $\kappa$ B pathway to activate autophagy (Wang N. et al., 2021).

Oxidative stress is a key mechanism leading to the uncoupling of osteoclast and osteoblast functions in OP (Domazetovic et al., 2017), which may be brought on by excessive ROS production and then brings on OP (Baek et al., 2010). In age-induced oxidative stress, the excessive production of ROS impairs the proliferation and osteogenic differentiation of BMSCs, blocks the maturation of osteoblast precursors and induces apoptosis by inhibiting osteoblast mineralization (Coipeau et al., 2009; Cervellati et al., 2014). Contrarily, it is now generally accepted that the degree of autophagy is inversely connected with oxidative stress and that activating autophagy lowers oxidative stress damage and apoptosis while inhibiting autophagy would increase oxidative stress in osteoblasts (Li D. Y. et al., 2017). Other studies have shown that the damage caused by



TABLE 1 Natural products for the treatment of OP by targeting autophagy.

Natural products	Activation/inhibition of autophagy	Autophagy-Related Mode of Action	Effect of treatment	References
Icariin	Activation	P62, Beclin1, LC3	Promotes BMSCs osteogenic differentiation and inhibits osteoclast formation	Liang et al. (2019)
osthole	Activation	Beclin1, LC3	Promotes BMSCs osteogenic differentiation	Zheng et al. (2019)
Arbutin	Activation	Atg7, P62, Beclin1, LC3	Promotes osteoblast differentiation and mineralization	Zhang et al. (2021a)
Ginsenoside Rg3	Activation	P62, Beclin1, LC3, AMPK/mTOR	Promotes osteoblast differentiation and mineralization	Zhang X. et al. (2020)
Kaempferol	Inhibition	Atg5, P62, Beclin1, LC3	Inhibits osteoclast differentiation and promotes apoptosis	Kim et al. (2018)
Ursolic acid	Inhibition	P62, LC3, NF-κB	Inhibits osteoclast formation	Zheng H. et al. (2020)
Pinocembrin	Activation	P62, Beclin1, LC3, PI3K/Akt/mTOR	Inhibits osteocytes apoptosis	Wang X. Y. et al. (2020)
Fangchinoline	Activation	Atg5, Beclin1, LC3	Inhibits osteoblast apoptosis	Zhu W. et al. (2019)
aucubin	Activation	Beclin1, LC3, AMPK	Inhibits osteoblast apoptosis	Yue et al. (2021)
Paeoniflorin	Activation	Beclin1, LC3, Akt/mTOR	Inhibits osteoblast apoptosis	Yang et al. (2021)
Timosaponin B-II	Activation	Beclin1, LC3, mTOR/NF-κB	Antagonizes oxidative stress damage and inhibits osteoblast apoptosis	Wang N. et al. (2021)
Curculigoside	Activation	p62, Beclin1, LC3	Antagonizes oxidative stress damage and promotes osteoblast mineralization	Zhang et al. (2019)
Monotropein	Activation	Beclin1, LC3, Akt/mTOR	Antagonizes oxidative stress damage and inhibits osteoblast apoptosis	Shi et al. (2020)
isoliquritigenin	Activation	Atg5, Beclin1, LC3, NF-κB	Improves inflammatory response and inhibits osteoclast differentiation	Liu et al. (2016)

oxidative stress to osteoblasts can be mitigated by the early initiation of autophagy (Yin et al., 2019). Moreover, activation of autophagic activity also reduces apoptosis in osteocytes under high oxidative stress (Manolagas and Parfitt, 2010). The phenolic glycoside Curculigoside, which is abundant in *Curculigo orchioides*, inhibits phosphorylation of Forkhead box O1 (FOXO1), an upstream protein of antioxidant enzymes, and increases the expression of FOXO1 in osteoblasts with iron overload, thereby increasing the levels of antioxidant enzymes and LC3, promoting osteoblast autophagy and mineralization, and inhibiting oxidative damage caused by iron overload (Zhang et al., 2019). Similarly, monotropein, an iridoid glycoside extracted from the roots of *Morinda officinalis*, similarly inhibits H<sub>2</sub>O<sub>2</sub>-induced reactive oxygen species production in osteoblasts, enhances autophagy-mediated antioxidant effects via the Akt/mTOR pathway, and guards against oxidative stress in osteoblasts (Shi et al., 2020).

The upregulation of systemic inflammation is an important mechanism in the aging process, often referred to as inflammatory aging (Flynn et al., 2019). The ongoing stimulation of inflammatory pathways in bone tissue, such as NF-κB signaling, throughout this process has a number of detrimental impacts on the preservation of bone mass, including the suppression of osteoblast development and mineralization and aberrant activation of osteoclast activity (Park et al., 2007; Chang et al., 2009). The current study

suggests that autophagy is closely related to inflammation in the development of OP. For example, the inflammatory factor TNF-α induces increased expression of ATG7 and Beclin1 in arthritis models (Lin et al., 2013), and low concentrations of interleukin (IL) 17A activates autophagy via the c-Jun amino-terminal kinase (JNK) pathway, thereby promoting osteoclast differentiation and bone resorption activity (Ke et al., 2018). Therefore, reconciling inflammation with autophagy levels would be beneficial to inhibit osteoclast activity and bone resorption. For instance, autophagy is in charge of osteoclast development and enhanced activity in lipopolysaccharide-induced inflammatory bone loss (Chen L. et al., 2020). Extracts of *Glycyrrhiza* root isoliquiritigenin can inhibit RANKL-induced NF-κB expression and nuclear translocation, and suppress the expression of LC3 II and Beclin1 *in vitro*. And by drastically decreasing NF-κB-dependent autophagy of osteoclast precursors and consequently limiting osteoclast development, it may be able to treat lipopolysaccharide-induced inflammatory bone deterioration (Liu et al., 2016) (Table 1; and Figure 3).

## Rheumatoid arthritis

RA is characterized by progressive inflammation and destruction of bone and cartilage in the affected joint, which

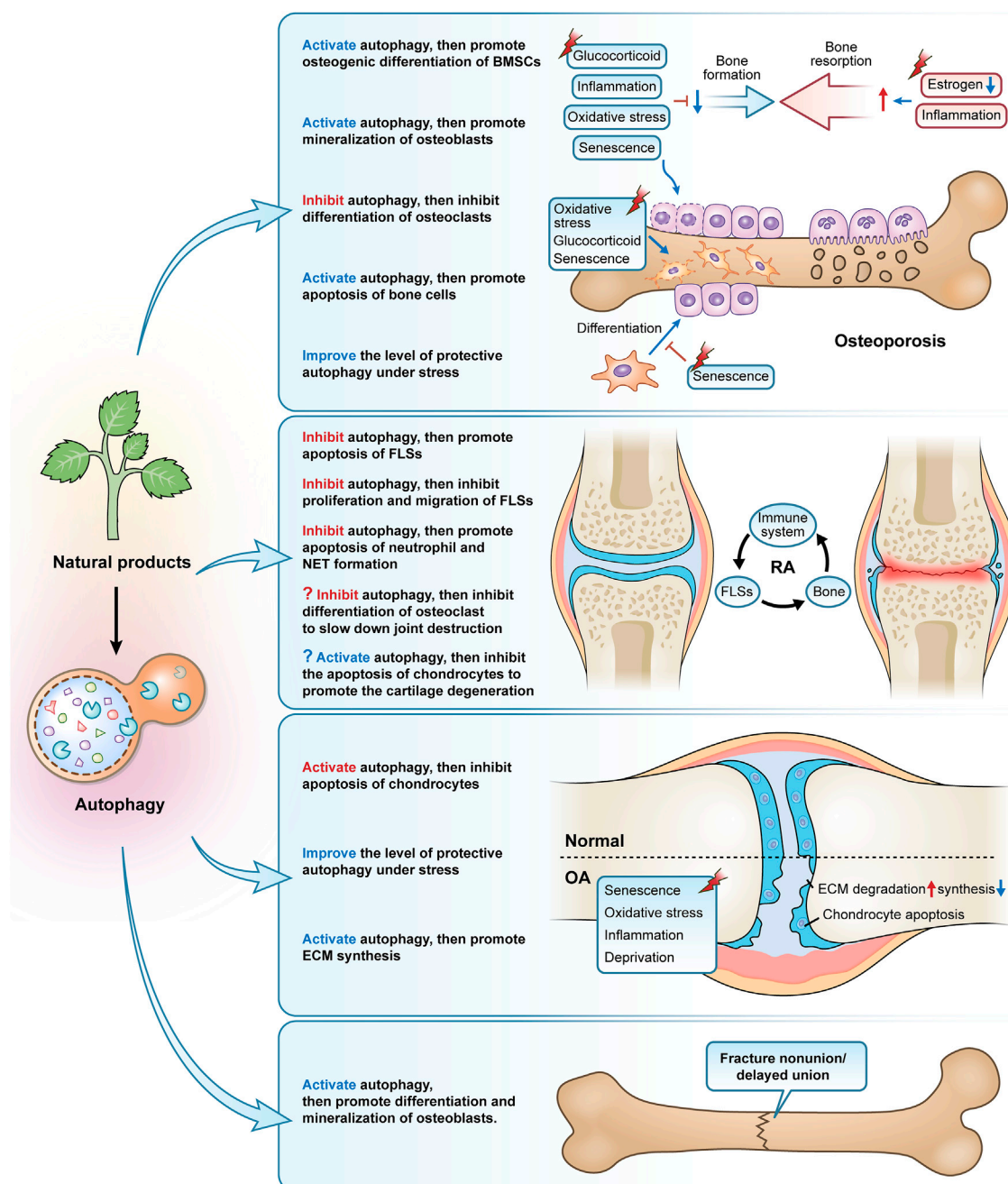


FIGURE 3

The primary modes and mechanisms of natural products targeting autophagy to regulate bone metabolism disorders. Natural products, used as autophagy activators or inhibitors, can effectively control osteoporosis, rheumatoid arthritis, osteoarthritis, and fracture nonunion/delayed union.

essentially depends on the interaction between the immune system, fibroblast-like synoviocytes (FLSs) and bone (Komatsu and Takayanagi, 2022). The immune system promotes the tissue-destroying properties of FLSs and influences the function of bone cells, such as increased bone resorption by osteoclasts (Komatsu and Takayanagi, 2022).

With its capacity to produce inflammatory mediators such as matrix-degrading enzymes, cytokines, and chemokines, FLSs are thought to play a significant role in the pathogenesis of RA, ultimately leading to the destruction of bone and cartilage (Karami et al., 2020). By preventing excessive immune cell activation and cytokine generation, the proper operation of

the apoptotic program can reduce inflammation (Vomero et al., 2018). However, studies have found a reduced rate of apoptosis and apoptotic mediators of FLSs in RA, suggesting that these cells are resistant to apoptosis (Firestein et al., 1995). Activation of autophagy was shown to be an important pathway of the anti-apoptosis of FLSs in RA, this can be explained by the fact that autophagy is a cellular pro-survival mechanism and high levels of autophagy in FLSs, although the detailed mechanism between autophagy and apoptosis remains to be elucidated (Shin et al., 2010). Baicalin and Silibinin are two different flavonoid compounds from the dried roots of *Scutellaria baicalensis* and *Silybum marianum*, respectively, both of which can induce apoptosis and reduce inflammation by inhibiting autophagy in RA FLSs (Tong et al., 2018; Chen X. et al., 2022). Similarly, Oridonin, a kaurene-type diterpenoid isolated from *Rabdosia rubescens*, and Daphnetin, a coumarin derivative widely distributed in the thymelaeaceae family, also have the ability to inhibit the autophagy of RA FLSs and thus inhibit proliferation and induce apoptosis (Deng et al., 2020; He et al., 2020). Triptolide, a significant epoxy diterpene lactone derived from *Tripterygium wilfordii*, prevents cell migration and preserves the redox status of RA FLSs by preventing autophagy (Xie et al., 2019). The cytokine IL 21, a key immunomodulator, invokes a variety of immunomodulatory functions in RA including FLSs proliferation, the differentiation of T-cell subsets, and B-cell activation, and induces autophagy in adjuvant arthritis (AA)-FLSs through a PI3K/Akt-dependent manner (Niu et al., 2010; Dinesh and Rasool, 2019). In contrast, Berberine, an isoquinoline alkaloid (Zhu et al., 2022) widely distributed in the Berberidaceae, Papaveraceae, Menispermaceae, Ranunculaceae, and other botanical families, inhibits IL 21/IL 21R-mediated autophagy of AA-FLSs, inhibits the proliferation of a subpopulation of CD4<sup>+</sup> T cells (T helper lymphocyte 17 (Th17)), and induces cellular differentiation of another subpopulation of CD4<sup>+</sup> T cells (regulatory T lymphocyte (Treg)) that are suppressive of RA, thereby restoring an immune imbalance of Th17/Treg (Dinesh and Rasool, 2019). Additionally, excessive levels of pro-inflammatory cytokines cause neutrophils and activated macrophages to secrete ROS, which is then created by mitochondria to the extent of 90% (Zhang et al., 2016). Resveratrol, a non-flavonoid polyphenolic compound from *Vitis*, can lead to the accumulation of ROS by inhibiting autophagy, which in turn induces mitochondrial dysfunction and leads to apoptosis in FLSs (Cao et al., 2018).

Immune cells of various subtypes have a role in the development and progression of RA. As well as having a phenotype of delayed apoptosis and releasing high amounts of degradative enzymes and reactive oxygen species, activated neutrophils can also induce autoimmunity and worsen tissue damage by forming neutrophil extracellular traps (NETs) (Cascão et al., 2010; Khandpur et al., 2013). Several natural products, including Andrographolide, a diterpene compound derived from *Andrographis paniculata*, quercetin, a flavonoid

compound derived from various vegetables and fruits, and Emodin, an anthraquinone derivative widely found in herbs such as *Rheum palmatum*, *Polygonum cuspidatum*, and *Cassiae semen*, exhibit effects of inhibiting the autophagy of neutrophils, promoting apoptosis and inhibiting NETs formation (Li X. et al., 2019; Zhu M. et al., 2019; Yuan et al., 2020) (Table 2; Figure 3).

We concentrate further on how autophagy contributes to RA joint degeneration. First, the secretion of pro-inflammatory factors and RANKL in FLSs allow osteoclast differentiation to be induced and bone resorption to be activated. The activation of autophagy is demonstrated by the high expression of Beclin1 and Atg7 in osteoclasts of human RA, while overexpression of Beclin1 induces osteoclastogenesis and significantly enhances their resorptive capacity (Lin et al., 2013). In the Atg7-deficient RA mice model, inhibition of autophagy reduces the number of osteoclasts and resists TNF- $\alpha$ -induced bone erosion (Lin et al., 2013). Similar to this, in bone marrow mononuclear cells from RA mice caused by K/BxN serum, there is a dramatically increased expression of autophagy-related genes such as Beclin1, Atg7, and LC3 II, and the production of autophagic vesicles is greatly enhanced during osteoclast differentiation (Laha et al., 2019).

Secondly, one of the primary factors contributing to the degeneration and loss of articular cartilage in RA is thought to be the apoptosis of articular chondrocytes. The autophagy inhibitor 3-MA increases joint inflammation and cartilage damage and induces chondrocyte apoptosis in rats with AA, whereas the autophagy activator Rapamycin reduces joint inflammation and chondrocyte apoptosis, suggesting that autophagy activation ameliorates damage to chondrocytes in AA rats by inhibiting apoptosis (Zhou et al., 2019). The accumulation of large amounts of acid in the synovial fluid is one of the important pathological features of RA, and elevated acid has been found in synovial biopsies of patients with early RA (Chang et al., 2005). Extracellular acidification causes chondrocytes to undergo apoptosis through the action of acid-sensitive ion channel 1a (ASIC1a), which is a crucial factor in the destruction of articular cartilage in RA (Xie et al., 2018). Contrarily, several studies have shown that estrogen protects articular cartilage from acidosis-induced damage by encouraging the breakdown of the ASIC1a protein. This is related to the fact that estrogen increases autophagy in chondrocytes to some extent, which in turn encourages the breakdown of the ASIC1a protein, which is reliant on the autophagy-lysosome pathway (Xie et al., 2018; Song et al., 2020; Su et al., 2021). However, we would like to ask, in the treatment of RA, should we choose to inhibit autophagy to attenuate osteoclast differentiation and bone resorption, or should we choose to promote autophagy to protect chondrocyte apoptosis and cartilage metabolism and repair? Does this rely on various RA triggers, phases, or the activation of autophagy brought on by various substances and signals? Nevertheless, RA can be treated by regulating autophagy

TABLE 2 Natural products for the treatment of RA by targeting autophagy.

Natural products	Activation/inhibition of autophagy	Autophagy-Related Mode of Action	Effect of treatment	References
Baicalin	Inhibition	Beclin1, Atg5, Atg7, Atg12, LC3	Promotes FLSs apoptosis and reduces inflammatory response	<a href="#">Chen X. et al. (2022)</a>
Silibinin	Inhibition	Beclin1, LC3, NF-κB, SIRT1	Promotes FLSs apoptosis and reduces inflammatory response	<a href="#">Tong et al. (2018)</a>
Oridonin	Inhibition	Beclin1, LC3, Atg5	Inhibits FLSs proliferation and promotes apoptosis	<a href="#">He et al. (2020)</a>
Daphnetin	Inhibition	Beclin1, LC3, Atg5, Akt/mTOR	Inhibits FLSs proliferation and promotes apoptosis	<a href="#">Deng et al. (2020)</a>
Triptolide	Inhibition	Beclin1, LC3, PI3K/Akt	Inhibits FLSs migration and maintains redox homeostasis	<a href="#">Xie et al. (2019)</a>
Berberine	inhibition	Beclin1, LC3, Atg5	Restores Th17/Treg immune imbalance	<a href="#">Dinesh and Rasool, (2019)</a>
Resveratrol	Inhibition	LC3, Atg5	Induces mitochondrial dysfunction and promotes FLSs apoptosis	<a href="#">Cao et al. (2018)</a>
Andrographolide	Inhibition	P62, Beclin1, LC3, PAD4	Promotes neutrophil apoptosis and inhibits NETs formation	<a href="#">Li X. et al. (2019)</a>
Quercetin	Inhibition	Beclin1, LC3, Atg5	Promotes neutrophil apoptosis and inhibits NETs formation	<a href="#">Yuan et al. (2020)</a>
Emodin	Inhibition	Beclin1, LC3, Atg5	Promotes neutrophil apoptosis and inhibits NETs formation	<a href="#">Zhu M. et al. (2019)</a>

in a cell-specific manner. But despite the fact that we have not yet discovered any studies on the pertinent natural products that interfere in the treatment of RA by focusing on autophagy in osteoclasts or chondrocytes, we do think that this may be an intriguing area for future investigation ([Figure 3](#)).

Osteoarthritis

OA is the most common degenerative joint disease, manifested by articular cartilage erosion, synovial inflammation, osteoid formation, and subchondral osteosclerosis ([Hunter and Bierma-Zeinstra, 2019](#)). The most severe degenerative alterations among them are found in articular cartilage, which is intimately connected to the metabolic imbalance and abnormal apoptosis of chondrocytes due to aging or overuse of cartilage ([Fujii et al., 2022](#)). Therefore, modulating chondrocyte behavior and thus restoring homeostasis of articular cartilage is a central theme in the study of OA ([van der Kraan, 2012](#)). It is debatable whether OA causes an increase or decrease in the amount of autophagy. An earlier study has demonstrated that ULK1, Beclin1, and LC3 proteins are expressed in articular chondrocytes of both humans and mice and are reduced in aging or surgery-induced OA as well as increased apoptosis of chondrocytes ([Caramés et al., 2010](#)). Another study from the same time period, however, found increased expression of LC3 and Beclin1 in OA chondrocytes, particularly when the chondrocytes were experiencing nutritional stress and catabolism, and this study attributed this differential result to the different locations of the collected samples of OA cartilage ([Sasaki et al., 2012](#)). A recent study explained this issue in

a targeted manner by observing changes in autophagy in different weight-bearing states and at different stages of OA, and it was observed that autophagy was stronger in weight-bearing areas than in the non-weight-bearing areas and was stronger in the 4-week group than in the 10-week group, in other words, autophagy was differentially expressed in different stages of OA, with stronger expression in the early stages of OA and diminishing expression as the disease progressed ([Zhang et al., 2022](#)). In any case, however, these results demonstrate that autophagy is a protective process for maintaining homeostasis in the cartilage. Therefore, starting with chondrocyte autophagy and activating the autophagy activity of chondrocytes can effectively reverse the state of autophagic failure and provide an effective way to prevent and treat OA degeneration.

Currently, most studies based on natural products for the treatment of OA have been conducted by inducing autophagy in cartilage, and these products include the saponin Astragaloside IV from *Astragalus membranaceus* ([Liu et al., 2017](#)), polyphenol curcumin from *Curcuma longa* ([Li X. et al., 2017](#); [Chen T. et al., 2021](#); [Yao et al., 2021](#); [Jin et al., 2022](#)), coumarins isopsoralen from *Psoralea corylifolia* seeds ([Chen Z. et al., 2020](#)), Icariin ([Mi et al., 2018](#); [Tang et al., 2021a](#)), furocoumarin Columbianetin from the root of *Radix Angelicae Pubescentis* ([Chen W. et al., 2022](#)), glucosilxanthone mangiferin from in various parts of *Mangifera indica* ([Li Y. et al., 2019](#)), flavonoid baicalin from the root of *Scutellaria baicalensis* ([Li Z. et al., 2020](#)), polyphenolic compound chlorogenic acid from coffee and plants such as *Lonicera japonica* ([Zada et al., 2021](#)), polyphenol anthocyanidin delphinidin from various brightly colored fruits and vegetables ([Lee et al., 2020](#)), polyphenol tannin punicalagin from the peel of *Punica granatum* ([Kong](#)

TABLE 3 Natural products for the treatment of OA by targeting autophagy.

Natural products	Activation/ inhibition of autophagy	Autophagy-Related Mode of Action	Effect of treatment	References
Astragaloside IV	Activation	P62, LC3	Inhibits chondrocyte apoptosis	Liu et al. (2017)
Curcumin	Activation	P62, Beclin1, LC3, ERK1/2, NF- $\kappa$ B, miR-34a, Akt/mTOR, AMPK/PINK1/Parkin	Inhibits chondrocyte apoptosis and inflammatory signal transduction and maintains mitochondrial homeostasis	Li X. et al. (2017), Chen T. et al. (2021), Yao et al. (2021), Jin et al. (2022)
Isopsoralen	Activation	P62, LC3, LAMP1	Inhibits chondrocyte apoptosis	Chen Z. et al. (2020)
Icariin	Activation	Atg5, Atg7, LC3, NF- $\kappa$ B, PI3K/AKT/mTOR	Reduces inflammatory response and inhibits chondrocyte apoptosis	Mi et al., 2018; Tang et al. (2021a)
Columbianetin	Activation	P62, Beclin1, LC3	Reduces inflammatory response and inhibits chondrocyte apoptosis	Chen W. et al. (2022)
Mangiferin	Activation	Atg5, p62, LC3, LAMP2, AMPK/mTOR	Antagonizes oxidative stress damage and inhibits chondrocyte apoptosis and ECM degradation	Li Y. et al. (2019)
Baicalin	Activation	Beclin1, LC3, miR-766-3p/AIFM1	Inhibits chondrocyte apoptosis and ECM degradation	Li Z. et al. (2020)
Chlorogenic acid	Activation	P62, LC3	Antagonizes oxidative stress and inhibits chondrocyte apoptosis	Zada et al. (2021)
Delphinidin	Activation	Nrf2, NF- $\kappa$ B, LC3	Antagonizes oxidative stress and inhibits chondrocyte apoptosis	Lee et al. (2020)
Punicalagin	Activation	Atg12-5, LC3, Beclin1, ULK1, p62, LAMP2	Antagonizes oxidative stress damage and inhibits chondrocyte apoptosis and ECM degradation	Kong et al. (2020)
Lycopene	Activation	MAPK, PI3K/Akt/NF- $\kappa$ B, Beclin1, LC3, mTOR	Reduces inflammatory response, antagonizes oxidative stress damage, increases chondrocyte proliferation and inhibits apoptosis	Wu et al. (2021)
Sinensetin	Activation	P62, Beclin1, LC3, AMPK/mTOR	Antagonizes oxidative stress damage, inhibits chondrocyte apoptosis and ECM degradation	Zhou et al. (2021)
Glabridin	Activation	Beclin1, Atg5, LC3, mTOR	Antagonizes oxidative stress damage, inhibits apoptosis and promoting ECM synthesis	Dai et al. (2021)
Saikosaponin D	Activation	PI3k/Akt/mTOR, NF- $\kappa$ B	Reduces inflammatory response, antagonizes oxidative stress damage, inhibits apoptosis, and promotes ECM synthesis	Jiang et al. (2020)
(-)-Epigallocatechin 3-gallate	Activation	P62, Beclin1, LC3, mTOR	Reduces inflammatory response, delays cartilage degeneration, and inhibits chondrocyte apoptosis and ECM degradation	Huang et al. (2020)
Rhoifolin	Activation	Atg12-5, P62, LC3, Beclin1, P38/JNK, PI3K/AKT/mTOR	Reduces inflammatory response and inhibits ECM degradation	Yan et al. (2021)
Quercetin	Activation	TSC2/RHBE/mTOR	Promotes chondrocyte viability, inhibits apoptosis, and promotes ECM synthesis	Lv et al. (2022)
Shikonin	Activation	P62, LC3, Beclin1	Restores the balance between chondrocyte anabolism and catabolism	Wang A. et al. (2022)

et al., 2020), natural carotenoid compound Lycopene from bright red-orange fruits and vegetables such as *Lycopersicon esculentum* (Wu et al., 2021), polymethoxylated flavonoid Sinensetin from citrus fruits (Zhou et al., 2021), isoflavonoid glabridin from the root of *Glycyrrhiza glabra* (Dai et al., 2021), triterpenoid saponin compound saikosaponin D from *Bupleurum falcatum* (Jiang et al., 2020), polyphenols (-)-Epigallocatechin 3-gallate from green tea (Huang et al., 2020), flavonoid rhoifolin from *Rhus succedanea* (Yan et al., 2021), quercetin (Lv et al., 2022), and naphthoquinone compound Shikonin from the root of *Lithospermum erythrorhizon* (Wang A. et al., 2022). Because of the large number, we have summarized in the table the specific mechanisms involved in these studies. Inhibiting chondrocyte

apoptosis, regulating the metabolic balance of ECM synthesis and degradation, and re-establishing the disturbed microenvironment within the cartilage are all ways that these medications affect the autophagic process of chondrocytes in OA caused by various triggers (aging, inflammatory factors, oxidative stress, oxygen-glucose deprivation, and serum deprivation) (Table 3; Figure 3).

## Fracture nonunion/delayed union

Despite the strong self-healing ability of bone tissue, about 5–10% of patients still experience problems with fracture healing



(Nelson et al., 2003). LC3 II is upregulated in bone tissue after internal fixation in a rat femoral fracture model and positively correlates with the number of cells positive for Proliferating cell nuclear antigen (a key protein for osteoblast proliferation) (Zhou et al., 2015). Systemic administration of rapamycin-induced autophagy in a rat femur fracture model, significantly promoting mineralization, formation, and remodeling of bone scabs and the expression of proliferating cell nuclear antigen and vascular endothelial growth factor (Yang et al., 2015). It has also been demonstrated that AMPK activation accelerates the healing of fractures by increasing autophagy, which improves osteoblast differentiation and mineralization (Li G. et al., 2018). Autophagy, therefore, presents a possible therapeutic target for the clinical treatment of fracture nonunion/delayed union given the significant role it plays in bone development and bone mineralization. However, there are focused research on medications, particularly those involving natural compounds, that monitor and target autophagy using fracture nonunion or delayed union models (only two items).  $\beta$ -Ecdysterone, a polyhydroxylated steroid hormone found mainly in *Achyranthes bidentata* and *Cyanotis arachnoidea*, activates autophagy by inhibiting PI3K/Akt/mTOR signaling pathway in femoral tissue of rats with femoral fractures, promoting osteoblast differentiation and mineralization, inhibiting apoptosis, and accelerating fracture healing (Tang et al., 2021b). Similarly, curcumin-treated rat femur fracture osteoblasts exhibited rapid fracture healing and autophagy activation, whereas the rate of fracture healing was noticeably slowed in the presence of curcumin plus 3-MA (Li Y. et al., 2018) (Figure 3).

## Conclusion and prospects for the future

The orderly conduct of bone metabolic processes and the maintenance of homeostasis in bone depend on the coordinated cooperation of multiple cell types, which requires the proper functioning of BMSCs, osteoblasts, osteocytes, osteoclasts and chondrocytes. It has been established through investigation of certain autophagy-related gene knockdowns that autophagy is crucial to the maintenance of these cell types' functional integrity. Consequently, increasing autophagy may be a key therapeutic focus for treating metabolic bone disease. Meanwhile, recent studies have reported the therapeutic role of natural products as inducers or inhibitors of autophagy in various diseases, including diseases caused by various disorders of bone metabolism, such as OP, RA, OA, and fracture nonunion/delayed union.

Despite the surprising results, there are still some challenges that have not been overcome and are inevitable to be addressed. On the one hand, both bone metabolism and autophagy are dynamic processes, with different metabolic bone diseases and affected bone cells, various disease stages, varying trigger intensities and durations, and different degrees of inhibition

or activation of autophagy in different individuals. This undoubtedly increases the demand for precise regulation of autophagy. We must be cautious when identifying autophagic "defects" and determining the "positive or negative" functions performed by autophagy before we seek to restore cellular viability by the elimination of cellular damage *via* autophagy. For example, excessive activation may result in increased secondary mineral deposition and bone fragility even if impaired autophagic activity in osteocytes is linked to decreased bone mass and slowed bone turnover (Li et al., 2020b). For many skeletal tissues with low cell numbers and extended lifespans, excessive induction of autophagy may accelerate apoptosis and senescence thereby exacerbating the disease state (Shapiro et al., 2014). Another illustration is the transformation of early activated protective autophagy into destructive autophagy with ongoing or increased stress, which necessitates an accurate measurement of the spatiotemporal location and autophagic state of the afflicted cells. Therefore, there is no consensus on the therapeutic potential of autophagy. The stage of autophagy should be included in follow-up research, and it is necessary to build a dynamic observation system of autophagy under various illness phases in order to standardize and unify follow-up investigations. The close association between bone cells in particular calls for increased specific targeting of autophagy, which requires us to identify the level of autophagy in the main affected bone cells in different metabolic bone diseases; for example, bone resorption by osteoclasts and bone formation by osteoblasts both require autophagic activity, which requires us to choose between inhibition or activation of autophagy.

On the other hand, to cope with the need for precise autophagic regulation, it is necessary to continuously figure out the effective dose of natural products, early and late administration, specific targeting of different cells, precise regulation and range maintenance of autophagic levels, and differential responses of different individuals. The bioavailability of many natural compounds is constrained by features including poor absorption, quick metabolism, and rapid elimination (Rahman et al., 2020). As a result, it may be advantageous to structurally alter natural products based on the control of autophagy to enhance their targeting, efficacy, and safety. Also, the development and utilization of nanocarriers may be effective in improving the stability, solubility, and sustainability of natural products, as demonstrated by excellent precedents such as the treatment of ischemia-reperfusion with curcumin and the promotion of nerve recovery with resveratrol (Kalani et al., 2016; Fan et al., 2020). Furthermore, translation to clinical application is a difficult threshold to cross in the short term, and although some natural products have shown promising results in clinical trials for the treatment of skeletal disorders, it has not been elucidated whether their effects are associated with autophagy. A recent randomized, placebo-controlled trial in middle-aged adults investigated the role of Urolithin A, a natural compound produced by intestinal flora following ingestion of pomegranate, berries and nuts, in

improving muscle performance by promoting mitochondrial autophagy, which may inform subsequent clinical studies of natural products modulating autophagy in the treatment of skeletal disorders (Singh et al., 2022).

Finally, although we have reviewed studies on the regulation of autophagy by natural products to treat common metabolic bone diseases, more metabolic bone diseases should be included, such as osteolysis, Paget disease of bone, and osteogenesis imperfecta, and there is still a paucity of studies on natural products in the treatment of these diseases, and the role of autophagy in these diseases is obscure. What's more, it is anticipated that more pertinent mechanisms will be discovered, leading to an increase in the validity of the theoretical underpinnings and options for natural product-targeted autophagy in the treatment of various metabolic bone diseases. In any case, the regulation of autophagy is thought to be an exciting strategy for drug development.

## Author contributions

ZL was responsible for the collection, collation of data, and writing of the original manuscript. DL, HS, and HX were accountable for collection of data. GT and ZX were responsible for concept development and manuscript revision. All authors reviewed and accepted the final version of the manuscript.

## References

- Akel, N., MacLeod, R. S., Berryhill, S. B., Laster, D. J., Dimori, M., Crawford, J. A., et al. (2022). Loss of chaperone-mediated autophagy is associated with low vertebral cancellous bone mass. *Sci. Rep.* 12 (1), 3134. doi:10.1038/s41598-022-07157-9
- Al Saedi, A., Myers, D. E., Stupka, N., and Duque, G. (2020). 1, 25(OH)(2)D(3) ameliorates palmitate-induced lipotoxicity in human primary osteoblasts leading to improved viability and function. *Bone* 141, 115672. doi:10.1016/j.bone.2020.115672
- Al-Bari, M., Ito, Y., Ahmed, S., Radwan, N., Ahmed, H. S., and Eid, N. (2021). Targeting autophagy with natural products as a potential therapeutic approach for cancer. *Int. J. Mol. Sci.* 22 (18), 9807. doi:10.3390/ijms22189807
- Alessio, N., Del, G. S., Capasso, S., Di Bernardo, G., Cappabianca, S., Cipollaro, M., et al. (2015). Low dose radiation induced senescence of human mesenchymal stromal cells and impaired the autophagy process. *Oncotarget* 6 (10), 8155–8166. doi:10.18632/oncotarget.2692
- Arai, A., Kim, S., Goldshteyn, V., Kim, T., Park, N. H., Wang, C. Y., et al. (2019). Beclin1 modulates bone homeostasis by regulating osteoclast and chondrocyte differentiation. *J. Bone Min. Res.* 34 (9), 1753–1766. doi:10.1002/jbmr.3756
- Baek, K. H., Oh, K. W., Lee, W. Y., Lee, S. S., Kim, M. K., Kwon, H. S., et al. (2010). Association of oxidative stress with postmenopausal osteoporosis and the effects of hydrogen peroxide on osteoclast formation in human bone marrow cell cultures. *Calcif. Tissue Int.* 87 (3), 226–235. doi:10.1007/s00223-010-9393-9
- Bangar, S. P., Chaudhary, V., Sharma, N., Bansal, V., Ozogul, F., and Lorenzo, J. M. (2022). Kaempferol: A flavonoid with wider biological activities and its applications. *Crit. Rev. Food Sci. Nutr.*, 1–25. doi:10.1080/10408398.2022.2067121
- Berendsen, A. D., and Olsen, B. R. (2015). Bone development. *Bone*. 80, 14–18. doi:10.1016/j.bone.2015.04.035
- Boya, P., Codogno, P., and Rodriguez-Muela, N. (2018). Autophagy in stem cells: Repair, remodelling and metabolic reprogramming. *Development* 145 (4), dev146506. doi:10.1242/dev.146506
- Boyle, W. J., Simonet, W. S., and Lacey, D. L. (2003). Osteoclast differentiation and activation. *Nature* 423 (6937), 337–342. doi:10.1038/nature01658
- Cao, B., Dai, X., and Wang, W. (2019). Knockdown of TRPV4 suppresses osteoclast differentiation and osteoporosis by inhibiting autophagy through Ca(2+) -calcineurin-NFATc1 pathway. *J. Cell. Physiol.* 234 (5), 6831–6841. doi:10.1002/jcp.27432
- Cao, W., Zhang, J., Wang, G., Lu, J., Wang, T., and Chen, X. (2018). Reducing-autophagy derived mitochondrial dysfunction during resveratrol promotes fibroblast-like synovial cell apoptosis. *Anat. Rec.* 301 (7), 1179–1188. doi:10.1002/ar.23798
- Caramés, B., Taniguchi, N., Otsuki, S., Blanco, F. J., and Lotz, M. (2010). Autophagy is a protective mechanism in normal cartilage, and its aging-related loss is linked with cell death and osteoarthritis. *Arthritis Rheum.* 62 (3), 791–801. doi:10.1002/art.27305
- Cascão, R., Rosário, H. S., Souto-Carneiro, M. M., and Fonseca, J. E. (2010). Neutrophils in rheumatoid arthritis: More than simple final effectors. *Autoimmun. Rev.* 9 (8), 531–535. doi:10.1016/j.autrev.2009.12.013
- Ceccariglia, S., Cargnoni, A., Silini, A. R., and Parolini, O. (2020). Autophagy: A potential key contributor to the therapeutic action of mesenchymal stem cells. *Autophagy* 16 (1), 28–37. doi:10.1080/15548627.2019.1630223
- Cervellati, C., Bonaccorsi, G., Cremonini, E., Romani, A., Fila, E., Castaldini, M. C., et al. (2014). Oxidative stress and bone resorption interplay as a possible trigger for postmenopausal osteoporosis. *Biomed. Res. Int.* 2014, 569563. doi:10.1155/2014/569563
- Chang, J., Wang, Z., Tang, E., Fan, Z., McCauley, L., Franceschi, R., et al. (2009). Inhibition of osteoblastic bone formation by nuclear factor-kappaB. *Nat. Med.* 15 (6), 682–689. doi:10.1038/nm.1954
- Chang, X., Yamada, R., and Yamamoto, K. (2005). Inhibition of antithrombin by hyaluronic acid may be involved in the pathogenesis of rheumatoid arthritis. *Arthritis Res. Ther.* 7 (2), R268–R273. doi:10.1186/ar1487

## Funding

This work was supported by the National Natural Science Foundation of China (No. 82174410), Natural Science Foundation of Shandong Province (ZR202011050051), Natural Science Foundation of Shandong Province (ZR2020MH362) and the Construction Project of Inheritance Studio of National Famous Old Chinese Medicine Experts [Chinese Medicine Education Letter (2022) grant No. 75].

## Conflict of interest

The authors declare that the research was conducted in the absence of any commercial or financial relationships that could be construed as a potential conflict of interest.

## Publisher's note

All claims expressed in this article are solely those of the authors and do not necessarily represent those of their affiliated organizations, or those of the publisher, the editors and the reviewers. Any product that may be evaluated in this article, or claim that may be made by its manufacturer, is not guaranteed or endorsed by the publisher.

- Chen, K., Yang, Y. H., Jiang, S. D., and Jiang, L. S. (2014). Decreased activity of osteocyte autophagy with aging may contribute to the bone loss in senile population. *Histochem. Cell Biol.* 142 (3), 285–295. doi:10.1007/s00418-014-1194-1
- Chen, X., He, Y., and Lu, F. (2018). Autophagy in stem cell biology: A perspective on stem cell self-renewal and differentiation. *Stem Cells Int.* 2018, 9131397. doi:10.1155/2018/9131397
- Chen, L., Yang, Y., Bao, J., Wang, Z., Xia, M., Dai, A., et al. (2020a). Autophagy negative-regulating wnt signaling enhanced inflammatory osteoclastogenesis from pre-OCs in vitro. *Biomed. Pharmacother.* 126, 110093. doi:10.1016/j.biopha.2020.110093
- Chen, X. D., Tan, J. L., Feng, Y., Huang, L. J., Zhang, M., and Cheng, B. (2020b). Autophagy in fate determination of mesenchymal stem cells and bone remodeling. *World J. Stem Cells* 12 (8), 776–786. doi:10.4252/wjsc.v12.i8.776
- Chen, T., Zhou, R., Chen, Y., Fu, W., Wei, X., Ma, G., et al. (2021). Curcumin ameliorates IL-1 $\beta$ -induced apoptosis by activating autophagy and inhibiting the NF- $\kappa$ B signaling pathway in rat primary articular chondrocytes. *Cell Biol. Int.* 45 (5), 976–988. doi:10.1002/cbin.11541
- Chen, W., Xian, G., Gu, M., Pan, B., Wu, X., Ye, Y., et al. (2021). Autophagy inhibitors 3-MA and LY294002 repress osteoclastogenesis and titanium particle-stimulated osteolysis. *Biomater. Sci.* 9 (14), 4922–4935. doi:10.1039/d1bm00691f
- Chen, W., Zheng, H., Zhang, X., Xu, Y., Fu, Z., Ji, X., et al. (2022a). Columbianetin alleviates lipopolysaccharides (LPS)-induced inflammation and apoptosis in chondrocyte through activation of autophagy by inhibiting serum and glucocorticoid-induced protein kinase 1 (SGK1) expression. *Bioengineered* 13 (2), 4051–4062. doi:10.1080/21655979.2022.2032970
- Chen, X., Wang, Y., Cai, J., Wang, S., Cheng, Z., Zhang, Z., et al. (2022b). Anti-inflammatory effect of baicalin in rats with adjuvant arthritis and its autophagy-related mechanism. *Technol. Health Care.* 30 (S1), 191–200. doi:10.3233/THC-228018
- Chen, Z., Li, C., Qian, Y. H., Fu, Y., and Feng, Z. M. (2020c). Enhancement of autophagy flux by isoprosalen ameliorates interleukin-1 $\beta$ -stimulated apoptosis in rat chondrocytes. *J. Asian Nat. Prod. Res.* 22 (2), 179–192. doi:10.1080/10286020.2018.1537265
- Chung, Y. H., Yoon, S. Y., Choi, B., Sohn, D. H., Yoon, K. H., Kim, W. J., et al. (2012). Microtubule-associated protein light chain 3 regulates cdc42-dependent actin ring formation in osteoclast. *Int. J. Biochem. Cell Biol.* 44 (6), 989–997. doi:10.1016/j.biocel.2012.03.007
- Cinque, L., Forrester, A., Bartolomeo, R., Svelto, M., Venditti, R., Montefusco, S., et al. (2015). FGF signalling regulates bone growth through autophagy. *Nature* 528 (7581), 272–275. doi:10.1038/nature16063
- Coipeau, P., Rosset, P., Langonne, A., Gaillard, J., Delorme, B., Rico, A., et al. (2009). Impaired differentiation potential of human trabecular bone mesenchymal stromal cells from elderly patients. *Cytotherapy* 11 (5), 584–594. doi:10.1080/14653240903079385
- Cuervo, A. M., Knecht, E., Terlecky, S. R., and Dice, J. F. (1995). Activation of a selective pathway of lysosomal proteolysis in rat liver by prolonged starvation. *Am. J. Physiol.* 269, C1200–C1208. doi:10.1152/ajpcell.1995.269.5.C1200
- Dai, J., Zhang, Y., Chen, D., Chen, D., Li, X., Wang, J., et al. (2021). Glabridin inhibits osteoarthritis development by protecting chondrocytes against oxidative stress, apoptosis and promoting mTOR mediated autophagy. *Life Sci.* 268, 118992. doi:10.1016/j.lfs.2020.118992
- Dallas, S. L., and Bonewald, L. F. (2010). Dynamics of the transition from osteoblast to osteocyte. *Ann. N. Y. Acad. Sci.* 1192, 437–443. doi:10.1111/j.1749-6632.2009.05246.x
- Dawodu, D., Patecki, M., Hegermann, J., Dumler, I., Haller, H., and Kiyan, Y. (2018). OxLDL inhibits differentiation and functional activity of osteoclasts via scavenger receptor-A mediated autophagy and cathepsin K secretion. *Sci. Rep.* 8 (1), 11604. doi:10.1038/s41598-018-29963-w
- Deng, H., Zheng, M., Hu, Z., Zeng, X., Kuang, N., and Fu, Y. (2020). Effects of Daphnetin on the autophagy signaling pathway of fibroblast-like synoviocytes in rats with collagen-induced arthritis (CIA) induced by TNF- $\alpha$ . *Cytokine* 127, 154952. doi:10.1016/j.cyto.2019.154952
- DeSelm, C. J., Miller, B. C., Zou, W., Beatty, W. L., van Meel, E., Takahata, Y., et al. (2011). Autophagy proteins regulate the secretory component of osteoclastic bone resorption. *Dev. Cell* 21 (5), 966–974. doi:10.1016/j.devcel.2011.08.016
- Dikic, I., and Elazar, Z. (2018). Mechanism and medical implications of mammalian autophagy. *Nat. Rev. Mol. Cell Biol.* 19 (6), 349–364. doi:10.1038/s41580-018-0003-4
- Dinesh, P., and Rasool, M. (2019). Berberine mitigates IL-21/IL-21r mediated autophagic influx in fibroblast-like synoviocytes and regulates Th17/treg imbalance in rheumatoid arthritis. *Apoptosis* 24 (7–8), 644–661. doi:10.1007/s10495-019-01548-6
- Domazetovic, V., Marcucci, G., Iantomasi, T., Brandi, M. L., and Vincenzini, M. T. (2017). Oxidative stress in bone remodeling: Role of antioxidants. *Clin. Cases Min. Bone Metab.* 14 (2), 209–216. doi:10.11138/ccmbm/2017.14.1.209
- Fan, P., Yu, X. Y., Xie, X. H., Chen, C. H., Zhang, P., Yang, C., et al. (2019). Mitophagy is a protective response against oxidative damage in bone marrow mesenchymal stem cells. *Life Sci.* 229, 36–45. doi:10.1016/j.lfs.2019.05.027
- Fan, Y., Li, Y., Huang, S., Xu, H., Li, H., and Liu, B. (2020). Resveratrol-primed exosomes strongly promote the recovery of motor function in SCI rats by activating autophagy and inhibiting apoptosis via the PI3K signaling pathway. *Neurosci. Lett.* 736, 135262. doi:10.1016/j.neulet.2020.135262
- Firestein, G. S., Yeo, M., and Zvaifler, N. J. (1995). Apoptosis in rheumatoid arthritis synovium. *J. Clin. Invest.* 96 (3), 1631–1638. doi:10.1172/JCI118202
- Flynn, M. G., Markofski, M. M., and Carrillo, A. E. (2019). Elevated inflammatory status and increased risk of chronic disease in chronological aging: Inflamm-aging or inflamm-inactivity. *Aging Dis.* 10 (1), 147–156. doi:10.14336/AD.2018.0326
- Fujii, Y., Liu, L., Yagasaki, L., Inotsume, M., Chiba, T., and Asahara, H. (2022). Cartilage homeostasis and osteoarthritis. *Int. J. Mol. Sci.* 23 (11), 6316. doi:10.3390/ijms23116316
- Georgess, D., Machuca-Gayet, I., Blangy, A., and Jurdic, P. (2014). Podosome organization drives osteoclast-mediated bone resorption. *Cell Adh. Migr.* 8 (3), 191–204. doi:10.4161/cam.27840
- Gong, Y., Li, Z., Zou, S., Deng, D., Lai, P., Hu, H., et al. (2021). Vangl2 limits chaperone-mediated autophagy to balance osteogenic differentiation in mesenchymal stem cells. *Dev. Cell* 56 (14), 2103–2120.e9. doi:10.1016/j.devcel.2021.06.011
- Hadjidakis, D. J., and Androulakis, I. I. (2006). Bone remodeling. *Ann. N. Y. Acad. Sci.* 1092, 385–396. doi:10.1196/annals.1365.035
- He, Q., Qin, R., Glowacki, J., Zhou, S., Shi, J., Wang, S., et al. (2021). Synergistic stimulation of osteoblast differentiation of rat mesenchymal stem cells by leptin and 25(OH)D(3) is mediated by inhibition of chaperone-mediated autophagy. *Stem Cell Res. Ther.* 12 (1), 557. doi:10.1186/s13287-021-02623-z
- He, S. D., Huang, S. G., Zhu, H. J., Luo, X. G., Liao, K. H., Zhang, J. Y., et al. (2020). Oridonin suppresses autophagy and survival in rheumatoid arthritis fibroblast-like synoviocytes. *Pharm. Biol.* 58 (1), 146–151. doi:10.1080/13880209.2020.1711783
- Hu, C., Zhao, L., Wu, D., and Li, L. (2019). Modulating autophagy in mesenchymal stem cells effectively protects against hypoxia- or ischemia-induced injury. *Stem Cell Res. Ther.* 10 (1), 120. doi:10.1186/s13287-019-1225-x
- Huang, H. T., Cheng, T. L., Ho, C. J., Huang, H. H., Lu, C. C., Chuang, S. C., et al. (2020). Intra-articular injection of (-)-Epigallocatechin 3-gallate to attenuate articular cartilage degeneration by enhancing autophagy in a post-traumatic osteoarthritis rat model. *Antioxidants (Basel)* 10 (1), E8. doi:10.3390/antiox10010008
- Hubbi, M. E., Hu, H., KshitizAhmed, I., Levchenko, A., and Semenza, G. L. (2013). Chaperone-mediated autophagy targets hypoxia-inducible factor-1A (Hif-1A) for lysosomal degradation. *J. Biol. Chem.* 288 (15), 10703–10714. doi:10.1074/jbc.M112.414771
- Hunter, D. J., and Bierma-Zeinstra, S. (2019). Osteoarthritis. *Lancet* 393 (10182), 1745–1759. doi:10.1016/S0140-6736(19)30417-9
- Inaba, N., Kuroshima, S., Uto, Y., Sasaki, M., and Sawase, T. (2017). Cyclic mechanical stretch contributes to network development of osteocyte-like cells with morphological change and autophagy promotion but without preferential cell alignment in rat. *Biochem. Biophys. Rep.* 11, 191–197. doi:10.1016/j.bbrep.2017.04.018
- Jia, D., O'Brien, C. A., Stewart, S. A., Manolagas, S. C., and Weinstein, R. S. (2006). Glucocorticoids act directly on osteoclasts to increase their life span and reduce bone density. *Endocrinology* 147 (12), 5592–5599. doi:10.1210/en.2006-0459
- Jiang, J., Meng, Y., Hu, S., Botchway, B., Zhang, Y., and Liu, X. (2020). Saikosaponin D: A potential therapeutic drug for osteoarthritis. *J. Tissue Eng. Regen. Med.* 14 (8), 1175–1184. doi:10.1002/term.3090
- Jin, Z., Chang, B., Wei, Y., Yang, Y., Zhang, H., Liu, J., et al. (2022). Curcumin exerts chondroprotective effects against osteoarthritis by promoting AMPK/PINK1/Parkin-mediated mitophagy. *Biomed. Pharmacother.* 151, 113092. doi:10.1016/j.biopha.2022.113092
- Jung, C. H., Ro, S. H., Cao, J., Otto, N. M., and Kim, D. H. (2010). MTOR regulation of autophagy. *FEBS Lett.* 584 (7), 1287–1295. doi:10.1016/j.febslet.2010.01.017
- Kalani, A., Chaturvedi, P., Kamat, P. K., Maldonado, C., Bauer, P., Joshua, I. G., et al. (2016). Curcumin-loaded embryonic stem cell exosomes restored neurovascular unit following ischemia-reperfusion injury. *Int. J. Biochem. Cell Biol.* 79, 360–369. doi:10.1016/j.biocel.2016.09.002
- Karami, J., Masoumi, M., Khorramdelazad, H., Bashiri, H., Darvishi, P., Sereshki, H. A., et al. (2020). Role of autophagy in the pathogenesis of rheumatoid arthritis:

Latest evidence and therapeutic approaches. *Life Sci.* 254, 117734. doi:10.1016/j.lfs.2020.117734

Kaushik, S., and Cuervo, A. M. (2006). Autophagy as a cell-repair mechanism: Activation of chaperone-mediated autophagy during oxidative stress. *Mol. Asp. Med.* 27 (5–6), 444–454. doi:10.1016/j.mam.2006.08.007

Ke, D., Fu, X., Xue, Y., Wu, H., Zhang, Y., Chen, X., et al. (2018). IL-17A regulates the autophagic activity of osteoclast precursors through RANKL-JNK1 signaling during osteoclastogenesis *in vitro*. *Biochem. Biophys. Res. Commun.* 497 (3), 890–896. doi:10.1016/j.bbrc.2018.02.164

Ke, D., Ji, L., Wang, Y., Fu, X., Chen, J., Wang, F., et al. (2019). JNK1 regulates RANKL-induced osteoclastogenesis via activation of a novel bcl-2-beclin-1-autophagy pathway. *Faseb J.* 33 (10), 11082–11095. doi:10.1096/fj.201802597RR

Ke, D., Yu, Y., Li, C., Han, J., and Xu, J. (2022). Phosphorylation of BCL2 at the Ser70 site mediates RANKL-induced osteoclast precursor autophagy and osteoclastogenesis. *Mol. Med.* 28 (1), 22. doi:10.1186/s10020-022-00449-w

Khandpur, R., Carmona-Rivera, C., Vivekanandan-Giri, A., Gizinski, A., Yalavarthi, S., Knight, J. S., et al. (2013). NETs are a source of citrullinated autoantigens and stimulate inflammatory responses in rheumatoid arthritis. *Sci. Transl. Med.* 5 (178), 178ra40–178r. doi:10.1126/scitranslmed.3005580

Kim, C. J., Shin, S. H., Kim, B. J., Kim, C. H., Kim, J. H., Kang, H. M., et al. (2018). The effects of kaempferol-inhibited autophagy on osteoclast formation. *Int. J. Mol. Sci.* 19 (1), E125. doi:10.3390/ijms19010125

Kim, K. H., and Lee, M. S. (2014). Autophagy--A key player in cellular and body metabolism. *Nat. Rev. Endocrinol.* 10 (6), 322–337. doi:10.1038/nrendo.2014.35

King, J. S., Veltman, D. M., and Insall, R. H. (2011). The induction of autophagy by mechanical stress. *Autophagy* 7 (12), 1490–1499. doi:10.4161/auto.7.12.17924

Klein-Nulend, J., Bacabac, R. G., and Bakker, A. D. (2012). Mechanical loading and how it affects bone cells: The role of the osteocyte cytoskeleton in maintaining our skeleton. *Eur. Cell. Mater.* 24, 278–291. doi:10.22203/ecm.v024a20

Komatsu, N., and Takayanagi, H. (2022). Mechanisms of joint destruction in rheumatoid arthritis - immune cell-fibroblast-bone interactions. *Nat. Rev. Rheumatol.* 18 (7), 415–429. doi:10.1038/s41584-022-00793-5

Kondrikov, D., Elmansi, A., Bragg, R. T., Mobley, T., Barrett, T., Eisa, N., et al. (2020). Kynurenine inhibits autophagy and promotes senescence in aged bone marrow mesenchymal stem cells through the aryl hydrocarbon receptor pathway. *Exp. Gerontol.* 130, 110805. doi:10.1016/j.exger.2019.110805

Kong, J., Wang, J., Gong, X., Zheng, X., and Chen, T. (2020). Punicalagin inhibits tert-butyl hydroperoxide-induced apoptosis and extracellular matrix degradation in chondrocytes by activating autophagy and ameliorates murine osteoarthritis. *Drug Des. devel. Ther.* 14, 5521–5533. doi:10.2147/DDDT.S282932

Kuma, A., and Mizushima, N. (2010). Physiological role of autophagy as an intracellular recycling system: With an emphasis on nutrient metabolism. *Semin. Cell Dev. Biol.* 21 (7), 683–690. doi:10.1016/j.semcdb.2010.03.002

Kurihara, M., Mukudai, Y., Watanabe, H., Asakura, M., Abe, Y., Houri, A., et al. (2021). Autophagy prevents osteocyte cell death under hypoxic conditions. *Cells Tissues Organs* 210 (5–6), 326–338. doi:10.1159/000519086

Laha, D., Deb, M., and Das, H. (2019). KLF2 (Krüppel-Like factor 2 [lung]) regulates osteoclastogenesis by modulating autophagy. *Autophagy* 15 (12), 2063–2075. doi:10.1080/15548627.2019.1596491

Lee, D. Y., Park, Y. J., Song, M. G., Kim, D. R., Zada, S., and Kim, D. H. (2020). Cytoprotective effects of delphinidin for human chondrocytes against oxidative stress through activation of autophagy. *Antioxidants (Basel)* 9 (1), E83. doi:10.3390/antiox9010083

Lemasters, J. J. (2005). Selective mitochondrial autophagy, or mitophagy, as a targeted defense against oxidative stress, mitochondrial dysfunction, and aging. *Rejuvenation Res.* 8 (1), 3–5. doi:10.1089/rej.2005.8.3

Li, B., Duan, P., Li, C., Jing, Y., Han, X., Yan, W., et al. (2016). Role of autophagy on bone marrow mesenchymal stem-cell proliferation and differentiation into neurons. *Mol. Med. Rep.* 13 (2), 1413–1419. doi:10.3892/mmr.2015.4673

Li, D. Y., Yu, J. C., Xiao, L., Miao, W., Ji, K., Wang, S. C., et al. (2017a). Autophagy attenuates the oxidative stress-induced apoptosis of Mc3T3-E1 osteoblasts. *Eur. Rev. Med. Pharmacol. Sci.* 21 (24), 5548–5556. doi:10.26355/eurrev\_201712\_13991

Li, X., Feng, K., Li, J., Yu, D., Fan, Q., Tang, T., et al. (2017b). Curcumin inhibits apoptosis of chondrocytes through activation ERK1/2 signaling pathways induced autophagy. *Nutrients* 9 (4), E414. doi:10.3390/nu9040414

Li, G., Chen, L., and Chen, K. (2018a). Curcumin promotes femoral fracture healing in a rat model by activation of autophagy. *Med. Sci. Monit.* 24, 4064–4072. doi:10.12659/MSM.908311

Li, H., Li, D., Ma, Z., Qian, Z., Kang, X., Jin, X., et al. (2018b). Defective autophagy in osteoblasts induces endoplasmic reticulum stress and causes remarkable bone loss. *Autophagy* 14 (10), 1726–1741. doi:10.1080/15548627.2018.1483807

Li, Y., Su, J., Sun, W., Cai, L., and Deng, Z. (2018c). AMP-activated protein kinase stimulates osteoblast differentiation and mineralization through autophagy induction. *Int. J. Mol. Med.* 41 (5), 2535–2544. doi:10.3892/ijmm.2018.3498

Li, X., Yuan, K., Zhu, Q., Lu, Q., Jiang, H., Zhu, M., et al. (2019a). Andrographolide ameliorates rheumatoid arthritis by regulating the apoptosis-NETosis balance of neutrophils. *Int. J. Mol. Sci.* 20 (20), E5035. doi:10.3390/ijms20205035

Li, Y., Wu, Y., Jiang, K., Han, W., Zhang, J., Xie, L., et al. (2019b). Mangiferin prevents TBHP-induced apoptosis and ECM degradation in mouse osteoarthritic chondrocytes via restoring autophagy and ameliorates murine osteoarthritis. *Oxid. Med. Cell. Longev.* 2019, 8783197. doi:10.1155/2019/8783197

Li, X., He, S., and Ma, B. (2020a). Autophagy and autophagy-related proteins in cancer. *Mol. Cancer* 19 (1), 12. doi:10.1186/s12943-020-1138-4

Li, X., Xu, J., Dai, B., Wang, X., Guo, Q., and Qin, L. (2020b). Targeting autophagy in osteoporosis: From pathophysiology to potential therapy. *Ageing Res. Rev.* 62, 101098. doi:10.1016/j.arr.2020.101098

Li, Z., Cheng, J., and Liu, J. (2020). Baicalin protects human OA chondrocytes against IL-1 $\beta$ -induced apoptosis and ECM degradation by activating autophagy via MiR-766-3p/AIFM1 Axis. *Drug Des. devel. Ther.* 14, 2645–2655. doi:10.2147/DDDT.S255823

Li, Y. Q., Zhang, F., Yu, L. P., Mu, J. K., Yang, Y. Q., Yu, J., et al. (2021). Targeting PINK1 using natural products for the treatment of human diseases. *Biomed. Res. Int.* 2021, 4045819. doi:10.1155/2021/4045819

Liang, K. X., Kristiansen, C. K., Mostafavi, S., Vatne, G. H., Zantigh, G. A., Kianian, A., et al. (2020). Disease-specific phenotypes in ipsc-derived neural stem cells with polg mutations. *EMBO Mol. Med.* 12 (10), e12146. doi:10.15252/emmm.202012146

Liang, X., Hou, Z., Xie, Y., Yan, F., Li, S., Zhu, X., et al. (2019). Icarin promotes osteogenic differentiation of bone marrow stromal cells and prevents bone loss in OVX mice via activating autophagy. *J. Cell. Biochem.* 120 (8), 13121–13132. doi:10.1002/jcb.28585

Lin, N. Y., Beyer, C., Giessl, A., Kireva, T., Scholtyssek, C., Uderhardt, S., et al. (2013). Autophagy regulates TNF $\alpha$ -mediated joint destruction in experimental arthritis. *Ann. Rheum. Dis.* 72 (5), 761–768. doi:10.1136/annrheumdis-2012-201671

Lin, N. Y., Chen, C. W., Kagwiria, R., Liang, R., Beyer, C., Distler, A., et al. (2016). Inactivation of autophagy ameliorates glucocorticoid-induced and ovariectomy-induced bone loss. *Ann. Rheum. Dis.* 75 (6), 1203–1210. doi:10.1136/annrheumdis-2015-207240

Ling, W., Krager, K., Richardson, K. K., Warren, A. D., Ponte, F., Aykin-Burns, N., et al. (2021). Mitochondrial Sirt3 contributes to the bone loss caused by aging or estrogen deficiency. *Jci Insight* 6 (10), 146728. doi:10.1172/jci.insight.146728

Liu, F., Fang, F., Yuan, H., Yang, D., Chen, Y., Williams, L., et al. (2013). Suppression of autophagy by FIP200 deletion leads to osteopenia in mice through the inhibition of osteoblast terminal differentiation. *J. Bone Min. Res.* 28 (11), 2414–2430. doi:10.1002/jbmr.1971

Liu, S., Zhu, L., Zhang, J., Yu, J., Cheng, X., and Peng, B. (2016). Anti-osteoclastogenic activity of isoliquiritigenin via inhibition of NF- $\kappa$ B-dependent autophagic pathway. *Biochem. Pharmacol.* 106, 82–93. doi:10.1016/j.bcp.2016.03.002

Liu, J., Meng, Q., Jing, H., and Zhou, S. (2017). Astragaloside IV protects against apoptosis in human degenerative chondrocytes through autophagy activation. *Mol. Med. Rep.* 16 (3), 3269–3275. doi:10.3892/mmr.2017.6980

Liu, Y., Wang, N., Zhang, S., and Liang, Q. (2018). Autophagy protects bone marrow mesenchymal stem cells from palmitate-induced apoptosis through the ROS-JNK/p38 MAPK signaling pathways. *Mol. Med. Rep.* 18 (2), 1485–1494. doi:10.3892/mmr.2018.9100

Liu, P., Cui, Y., Liu, M., Xiao, B., Zhang, J., Huang, W., et al. (2021). Protective effect of mitophagy against aluminum-induced MC3T3-E1 cells dysfunction. *Chemosphere* 282, 131086. doi:10.1016/j.chemosphere.2021.131086

Lu, Z. F., Jiang, L., Lesani, P., Zhang, W. J., Li, N., Luo, D., et al. (2022). Nicotinamide mononucleotide alleviates osteoblast senescence induction and promotes bone healing in osteoporotic mice. *J. Gerontol. A Biol. Sci. Med. Sci.* glac175. doi:10.1093/gerona/glac175

Luk, H. Y., Appell, C., Chyu, M. C., Chen, C. H., Wang, C. Y., Yang, R. S., et al. (2020). Impacts of green tea on joint and skeletal muscle health: Prospects of translational nutrition. *Antioxidants (Basel)* 9 (11), E1050. doi:10.3390/antiox911050

Luo, P., Gao, F., Niu, D., Sun, X., Song, Q., Guo, C., et al. (2019). The role of autophagy in chondrocyte metabolism and osteoarthritis: A comprehensive research review. *Biomed. Res. Int.* 2019, 5171602. doi:10.1155/2019/5171602

Lv, S., Wang, X., Jin, S., Shen, S., Wang, R., and Tong, P. (2022). Quercetin mediates TSC2-RHEB-mTOR pathway to regulate chondrocytes autophagy in knee osteoarthritis. *Gene* 820, 146209. doi:10.1016/j.gene.2022.146209



- Ma, Y., Qi, M., An, Y., Zhang, L., Yang, R., Doro, D. H., et al. (2018). Autophagy controls mesenchymal stem cell properties and senescence during bone aging. *Aging Cell* 17 (1), e12709. doi:10.1111/ace1.12709
- Ma, Y., Di, R., Zhao, H., Song, R., Zou, H., and Liu, Z. (2022). P2X7 receptor knockdown suppresses osteoclast differentiation by inhibiting autophagy and Ca(2+)/calcineurin signaling. *Mol. Med. Rep.* 25 (5), 160. doi:10.3892/mmr.2022.12677
- Maity, J., Barthels, D., Sarkar, J., Prateeksha, P., Deb, M., Rolph, D., et al. (2022). Ferutinin induces osteoblast differentiation of dpSCs via induction of Klf2 and autophagy/mitophagy. *Cell Death Dis.* 13 (5), 452. doi:10.1038/s41419-022-04903-9
- Manolagas, S. C., and Parfitt, A. M. (2010). What Old means to bone. *Trends Endocrinol. Metab.* 21 (6), 369–374. doi:10.1016/j.tem.2010.01.010
- Markaki, M., and Tavernarakis, N. (2020). Autophagy mechanisms and roles: Recent advances and implications. *Febs J.* 287 (23), 5024–5026. doi:10.1111/febs.15573
- Mi, B., Wang, J., Liu, Y., Liu, J., Hu, L., Panayi, A. C., et al. (2018). Icariin activates autophagy via down-regulation of the NF- $\kappa$ B signaling-mediated apoptosis in chondrocytes. *Front. Pharmacol.* 9, 605. doi:10.3389/fphar.2018.00605
- Mizushima, N., and Komatsu, M. (2011). Autophagy: Renovation of cells and tissues. *Cell* 147 (4), 728–741. doi:10.1016/j.cell.2011.10.026
- Moerman, E. J., Teng, K., Lipschitz, D. A., and Lecka-Czernik, B. (2004). Aging activates adipogenic and suppresses osteogenic programs in mesenchymal marrow stroma/stem cells: The role of PPAR- $\gamma$  transcription factor and TGF- $\beta$ /BMP signaling pathways. *Aging Cell* 3 (6), 379–389. doi:10.1111/j.1474-9728.2004.00127.x
- Montaseri, A., Giampietri, C., Rossi, M., Riccioli, A., Del, F. A., and Filippini, A. (2020). The role of autophagy in osteoclast differentiation and bone resorption function. *Biomolecules* 10 (10), E1398. doi:10.3390/biom10101398
- Mueller, A. L., Payandeh, Z., Mohammadkhani, N., Mubarak, S., Zakeri, A., Alagheband, B. A., et al. (2021). Recent advances in understanding the pathogenesis of rheumatoid arthritis: New treatment strategies. *Cells* 10 (11), 3017. doi:10.3390/cells10113017
- Na, W., Lee, E. J., Kang, M. K., Kim, Y. H., Kim, D. Y., Oh, H., et al. (2020). Aesculetin inhibits osteoclastic bone resorption through blocking ruffled border formation and lysosomal trafficking. *Int. J. Mol. Sci.* 21 (22), E8581. doi:10.3390/ijms21228581
- Nandy, A., Lin, L., Velentzas, P. D., Wu, L. P., Baehrecke, E. H., and Silverman, N. (2018). The NF- $\kappa$ B factor relish regulates Atg1 expression and controls autophagy. *Cell Rep.* 25 (8), 2110–2120. doi:10.1016/j.celrep.2018.10.076
- Nelson, F. R., Brighton, C. T., Ryaby, J., Simon, B. J., Nielson, J. H., Lorch, D. G., et al. (2003). Use of physical forces in bone healing. *J. Am. Acad. Orthop. Surg.* 11 (5), 344–354. doi:10.5435/00124635-200309000-00007
- Niu, X., He, D., Zhang, X., Yue, T., Li, N., Zhang, J. Z., et al. (2010). IL-21 regulates Th17 cells in rheumatoid arthritis. *Hum. Immunol.* 71 (4), 334–341. doi:10.1016/j.humimm.2010.01.010
- Nollet, M., Santucci-Darmanin, S., Breuil, V., Al-Sahlane, R., Cros, C., Topi, M., et al. (2014). Autophagy in osteoblasts is involved in mineralization and bone homeostasis. *Autophagy* 10 (11), 1965–1977. doi:10.4161/auto.36182
- Nuschke, A., Rodrigues, M., Stolz, D. B., Chu, C. T., Griffith, L., and Wells, A. (2014). Human mesenchymal stem cells/multipotent stromal cells consume accumulated autophagosomes early in differentiation. *Stem Cell Res. Ther.* 5 (6), 140. doi:10.1186/scrt530
- Onal, M., Piemontese, M., Xiong, J., Wang, Y., Han, L., Ye, S., et al. (2013). Suppression of autophagy in osteocytes mimics skeletal aging. *J. Biol. Chem.* 288 (24), 17432–17440. doi:10.1074/jbc.M112.444190
- Ory, S., Brazier, H., Pawlak, G., and Blangy, A. (2008). Rho GTPases in osteoclasts: Orchestrators of podosome arrangement. *Eur. J. Cell Biol.* 87 (8–9), 469–477. doi:10.1016/j.ejcb.2008.03.002
- Palumbo, C., and Ferretti, M. (2021). The osteocyte: From “prisoner” to “orchestrator”. *J. Funct. Morphol. Kinesiol.* 6 (1), 28. doi:10.3390/jfmk6010028
- Pantovic, A., Krstic, A., Janjetovic, K., Kocic, J., Harhaji-Trajkovic, L., Bugarski, D., et al. (2013). Coordinated time-dependent modulation of AMPK/Akt/mTOR signaling and autophagy controls osteogenic differentiation of human mesenchymal stem cells. *Bone* 52 (1), 524–531. doi:10.1016/j.bone.2012.10.024
- Park, B. K., Zhang, H., Zeng, Q., Dai, J., Keller, E. T., Giordano, T., et al. (2007). NF- $\kappa$ B in breast cancer cells promotes osteolytic bone metastasis by inducing osteoclastogenesis via GM-CSF. *Nat. Med.* 13 (1), 62–69. doi:10.1038/nm1519
- Park, C., Suh, Y., and Cuervo, A. M. (2015). Regulated degradation of chk1 by chaperone-mediated autophagy in response to dna damage. *Nat. Commun.* 6, 6823. doi:10.1038/ncomms7823
- Piemontese, M., Onal, M., Xiong, J., Han, L., Thostenson, J. D., Almeida, M., et al. (2016). Low bone mass and changes in the osteocyte network in mice lacking autophagy in the osteoblast lineage. *Sci. Rep.* 6, 24262. doi:10.1038/srep24262
- Ploumi, C., Daskalaki, I., and Tavernarakis, N. (2017). Mitochondrial biogenesis and clearance: A balancing act. *Febs J.* 284 (2), 183–195. doi:10.1111/febs.13820
- Qin, L., Liu, W., Cao, H., and Xiao, G. (2020). Molecular mechanosensors in osteocytes. *Bone Res.* 8, 23. doi:10.1038/s41413-020-0099-y
- Rabinowitz, J. D., and White, E. (2010). Autophagy and metabolism. *Science* 330 (6009), 1344–1348. doi:10.1126/science.1193497
- Rahman, H. S., Othman, H. H., Hammadi, N. I., Yeap, S. K., Amin, K. M., Abdul, S. N., et al. (2020). Novel drug delivery systems for loading of natural plant extracts and their biomedical applications. *Int. J. Nanomed.* 15, 2439–2483. doi:10.2147/IJN.S227805
- Ravikumar, B., Sarkar, S., Davies, J. E., Futter, M., Garcia-Arencibia, M., Green-Thompson, Z. W., et al. (2010). Regulation of mammalian autophagy in physiology and pathophysiology. *Physiol. Rev.* 90 (4), 1383–1435. doi:10.1152/physrev.00030.2009
- Roy, M., and Roux, S. (2020). Rab GTPases in osteoclastic bone resorption and autophagy. *Int. J. Mol. Sci.* 21 (20), E7655. doi:10.3390/ijms21207655
- Ruderman, E. M. (2012). Overview of safety of non-biologic and biologic DMARDs. *Rheumatol. Oxf.* 51, i37–i43. doi:10.1093/rheumatology/kes283
- Sahu, R., Kaushik, S., Clement, C. C., Cannizzo, E. S., Scharf, B., Follenzi, A., et al. (2011). Microautophagy of cytosolic proteins by late endosomes. *Dev. Cell* 20 (1), 131–139. doi:10.1016/j.devcel.2010.12.003
- Saltel, F., Chabadel, A., Bonnelye, E., and Jurdic, P. (2008). Actin cytoskeletal organisation in osteoclasts: A model to decipher transmigration and matrix degradation. *Eur. J. Cell Biol.* 87 (8–9), 459–468. doi:10.1016/j.ejcb.2008.01.001
- Sánchez-Riera, L., Wilson, N., Kamalaraj, N., Nolla, J. M., Kok, C., Li, Y., et al. (2010). Osteoporosis and fragility fractures. *Best. Pract. Res. Clin. Rheumatol.* 24 (6), 793–810. doi:10.1016/j.berh.2010.10.003
- Sasaki, H., Takayama, K., Matsushita, T., Ishida, K., Kubo, S., Matsumoto, T., et al. (2012). Autophagy modulates osteoarthritis-related gene expression in human chondrocytes. *Arthritis Rheum.* 64 (6), 1920–1928. doi:10.1002/art.34323
- Shapiro, I. M., Layfield, R., Lotz, M., Settembre, C., and Whitehouse, C. (2014). Boning up on autophagy: The role of autophagy in skeletal biology. *Autophagy* 10 (1), 7–19. doi:10.4161/auto.26679
- Shi, Y., Liu, X. Y., Jiang, Y. P., Zhang, J. B., Zhang, Q. Y., Wang, N. N., et al. (2020). Monotropin attenuates oxidative stress via akt/mTOR-mediated autophagy in osteoblast cells. *Biomed. Pharmacother.* 121, 109566. doi:10.1016/j.biopha.2019.109566
- Shin, Y. J., Han, S. H., Kim, D. S., Lee, G. H., Yoo, W. H., Kang, Y. M., et al. (2010). Autophagy induction and CHOP under-expression promotes survival of fibroblasts from rheumatoid arthritis patients under endoplasmic reticulum stress. *Arthritis Res. Ther.* 12 (1), R19. doi:10.1186/ar2921
- Sims, N. A., and Gooi, J. H. (2008). Bone remodeling: Multiple cellular interactions required for coupling of bone formation and resorption. *Semin. Cell Dev. Biol.* 19 (5), 444–451. doi:10.1016/j.semcdb.2008.07.016
- Singh, A., D’Amico, D., Andreux, P. A., Fouassier, A. M., Blanco-Boise, W., Evans, M., et al. (2022). Urolithin A improves muscle strength, exercise performance, and biomarkers of mitochondrial health in a randomized trial in middle-aged adults. *Cell Rep. Med.* 3 (5), 100633. doi:10.1016/j.xcrm.2022.100633
- Song, C., Song, C., and Tong, F. (2014). Autophagy induction is a survival response against oxidative stress in bone marrow-derived mesenchymal stromal cells. *Cytotherapy* 16 (10), 1361–1370. doi:10.1016/j.jcyt.2014.04.006
- Song, B. Q., Chi, Y., Li, X., Du, W. J., Han, Z. B., Tian, J. J., et al. (2015). Inhibition of notch signaling promotes the adipogenic differentiation of mesenchymal stem cells through autophagy activation and PTEN-PI3K/AKT/mTOR pathway. *Cell. Physiol. Biochem.* 36 (5), 1991–2002. doi:10.1159/000430167
- Song, S. J., Tao, J. J., Li, S. F., Qian, X. W., Niu, R. W., Wang, C., et al. (2020). 17 $\beta$ -Estradiol attenuates rat articular chondrocyte injury by targeting ASIC1a-mediated apoptosis. *Mol. Cell. Endocrinol.* 505, 110742. doi:10.1016/j.mce.2020.110742
- Stroik, Y., Dalen, H., Brunk, U. T., and Terman, A. (2005). Testing the “garbage” accumulation theory of ageing: Mitotic activity protects cells from death induced by inhibition of autophagy. *Biogerontology* 6 (1), 39–47. doi:10.1007/s10522-004-7382-y
- Su, J. W., Li, S. F., Tao, J. J., Xu, Y. Y., Wang, K., Qian, X. W., et al. (2021). Estrogen protects against acidosis-mediated articular chondrocyte injury by promoting ASIC1a protein degradation. *Eur. J. Pharmacol.* 908, 174381. doi:10.1016/j.ejphar.2021.174381



- Sugiyama, T., Kim, Y. T., and Oda, H. (2015). Osteoporosis therapy: A novel insight from natural homeostatic system in the skeleton. *Osteoporos. Int.* 26 (2), 443–447. doi:10.1007/s00198-014-2923-y
- Sun, X., Yang, X., Zhao, Y., Li, Y., and Guo, L. (2018). Effects of 17 $\beta$ -estradiol on mitophagy in the murine Mc3T3-E1 osteoblast cell line is mediated via G protein-coupled estrogen receptor and the erk1/2 signaling pathway. *Med. Sci. Monit.* 24, 903–911. doi:10.12659/msm.908705
- Tang, Y., Li, Y., Xin, D., Chen, L., Xiong, Z., and Yu, X. (2021a). Icarin alleviates osteoarthritis by regulating autophagy of chondrocytes by mediating PI3K/AKT/mTOR signaling. *Bioengineered* 12 (1), 2984–2999. doi:10.1080/21655979.2021.1943602
- Tang, Y., Mo, Y., Xin, D., Xiong, Z., Zeng, L., Luo, G., et al. (2021b). Regulation of osteoblast autophagy based on PI3K/AKT/mTOR signaling pathway study on the effect of B-ecdysterone on fracture healing. *J. Orthop. Surg. Res.* 16 (1), 719. doi:10.1186/s13018-021-02862-z
- Tian, Z., Zhang, X., and Sun, M. (2021). Phytochemicals mediate autophagy against osteoarthritis by maintaining cartilage homeostasis. *Front. Pharmacol.* 12, 795058. doi:10.3389/fphar.2021.795058
- Tong, W. W., Zhang, C., Hong, T., Liu, D. H., Wang, C., Li, J., et al. (2018). Silibinin alleviates inflammation and induces apoptosis in human rheumatoid arthritis fibroblast-like synoviocytes and has a therapeutic effect on arthritis in rats. *Sci. Rep.* 8 (1), 3241. doi:10.1038/s41598-018-21674-6
- Ueno, T., and Komatsu, M. (2017). Autophagy in the liver: Functions in health and disease. *Nat. Rev. Gastroenterol. Hepatol.* 14 (3), 170–184. doi:10.1038/nrgastro.2016.185
- van der Kraan, P. M. (2012). Osteoarthritis year 2012 in review: Biology. *Osteoarthr. Cartil.* 20 (12), 1447–1450. doi:10.1016/j.joca.2012.07.010
- Vomero, M., Barbati, C., Colasanti, T., Perricone, C., Novelli, L., Ceccarelli, F., et al. (2018). Autophagy and rheumatoid arthritis: Current knowledges and future perspectives. *Front. Immunol.* 9, 1577. doi:10.3389/fimmu.2018.01577
- Vuppalapati, K. K., Boudierlique, T., Newton, P. T., Kaminsky, V. O., Wehtje, H., Ohlsson, C., et al. (2015). Targeted deletion of autophagy genes Atg5 or Atg7 in the chondrocytes promotes caspase-dependent cell death and leads to mild growth retardation. *J. Bone Min. Res.* 30 (12), 2249–2261. doi:10.1002/jbmr.2575
- Wang, L., Fan, J., Lin, Y. S., Guo, Y. S., Gao, B., Shi, Q. Y., et al. (2015). Glucocorticoids induce autophagy in rat bone marrow mesenchymal stem cells. *Mol. Med. Rep.* 11 (4), 2711–2716. doi:10.3892/mmr.2014.3099
- Wang, L., Heckmann, B. L., Yang, X., and Long, H. (2019). Osteoblast autophagy in glucocorticoid-induced osteoporosis. *J. Cell. Physiol.* 234 (4), 3207–3215. doi:10.1002/jcp.27335
- Wang, S., Deng, Z., Ma, Y., Jin, J., Qi, F., Li, S., et al. (2020a). The role of autophagy and mitophagy in bone metabolic disorders. *Int. J. Biol. Sci.* 16 (14), 2675–2691. doi:10.7150/ijbs.46627
- Wang, T., Liu, X., and He, C. (2020b). Glucocorticoid-induced autophagy and apoptosis in bone. *Apoptosis* 25 (3–4), 157–168. doi:10.1007/s10495-020-01599-0
- Wang, X. Y., Gong, L. J., Huang, J. M., Jiang, C., and Yan, Z. Q. (2020c). Pinocembrin alleviates glucocorticoid-induced apoptosis by activating autophagy via suppressing the PI3K/Akt/mTOR pathway in osteocytes. *Eur. J. Pharmacol.* 880, 173212. doi:10.1016/j.ejphar.2020.173212
- Wang, L., Klionsky, D. J., and Shen, H. M. (2022a). The emerging mechanisms and functions of microautophagy. *Nat. Rev. Mol. Cell Biol.* doi:10.1038/s41580-022-00529-z
- Wang, A., Fang, S., Zhong, L., Lu, M., Zhou, H., Huang, W., et al. (2022b). Shikonin, a promising therapeutic drug for osteoarthritis that acts via autophagy activation. *Int. Immunopharmacol.* 106, 108563. doi:10.1016/j.intimp.2022.108563
- Wang, N., Xu, P., Wu, R., Wang, X., Wang, Y., Shou, D., et al. (2021). Timosaponin BI improved osteoporosis caused by hyperglycemia through promoting autophagy of osteoblasts via suppressing the mTOR/NF $\kappa$ B signaling pathway. *Free Radic. Biol. Med.* 171, 112–123. doi:10.1016/j.freeradbiomed.2021.05.014
- Wang, X. J., Tian, W., Xu, W. W., Lu, X., Zhang, Y. M., Li, L. J., et al. (2021). Loss of autophagy causes increased apoptosis of tibial plateau chondrocytes in Guinea pigs with spontaneous osteoarthritis. *Cartilage* 13, 796S–807S. doi:10.1177/19476035211044820
- Weng, Y. M., Ke, C. R., Kong, J. Z., Chen, H., Hong, J. J., and Zhou, D. S. (2018). The significant role of ATG5 in the maintenance of normal functions of Mc3T3-E1 osteoblast. *Eur. Rev. Med. Pharmacol. Sci.* 22 (5), 1224–1232. doi:10.26355/eurrev\_201803\_14462
- Wu, J. J., Quijano, C., Chen, E., Liu, H., Cao, L., Fergusson, M. M., et al. (2009). Mitochondrial dysfunction and oxidative stress mediate the physiological impairment induced by the disruption of autophagy. *Aging (Albany NY)* 1 (4), 425–437. doi:10.18632/aging.100038
- Wu, Z., Zhang, X., Li, Z., Wen, Z., and Lin, Y. (2021). Activation of autophagy contributes to the protective effects of Lycopene against oxidative stress-induced apoptosis in rat chondrocytes. *Phytother. Res.* 35 (7), 4032–4045. doi:10.1002/ptr.7127
- Xie, Y. Y., Li, Y., Zhou, R. P., Dai, B. B., Qian, Y. J., Wu, X. S., et al. (2018). Effects of autophagy on acid-sensing ion channel 1A-mediated apoptosis in rat articular chondrocytes. *Mol. Cell. Biochem.* 443 (1–2), 181–191. doi:10.1007/s11010-017-3223-6
- Xie, C., Jiang, J., Liu, J., Yuan, G., and Zhao, Z. (2019). Triptolide suppresses human synovial cell MH7A cells mobility and maintains redox balance by inhibiting autophagy. *Biomed. Pharmacother.* 115, 108911. doi:10.1016/j.biopha.2019.108911
- Xu, G., Li, X., Zhu, Z., Wang, H., and Bai, X. (2021a). Iron overload induces apoptosis and cytoprotective autophagy regulated by ROS generation in mc3t3-E1 cells. *Biol. Trace Elem. Res.* 199 (10), 3781–3792. doi:10.1007/s12011-020-02508-x
- Xu, H., Xia, M., Sun, L., Wang, H., and Zhang, W. B. (2021b). Osteocytes enhance osteogenesis by autophagy-mediated FGF23 secretion under mechanical tension. *Front. Cell Dev. Biol.* 9, 782736. doi:10.3389/fcell.2021.782736
- Yan, J., Ni, B., Sheng, G., Zhang, Y., Xiao, Y., Ma, Y., et al. (2021). Rhoifolin ameliorates osteoarthritis via regulating autophagy. *Front. Pharmacol.* 12, 661072. doi:10.3389/fphar.2021.661072
- Yang, G. E., Duan, X., Lin, D., Li, T., Luo, D., Wang, L., et al. (2015). Rapamycin-induced autophagy activity promotes bone fracture healing in rats. *Exp. Ther. Med.* 10 (4), 1327–1333. doi:10.3892/etm.2015.2660
- Yang, R., Ouyang, Y., Li, W., Wang, P., Deng, H., Song, B., et al. (2016). Autophagy plays a protective role in tumor necrosis factor- $\alpha$ -induced apoptosis of bone marrow-derived mesenchymal stem cells. *Stem Cells Dev.* 25 (10), 788–797. doi:10.1089/scd.2015.0387
- Yang, M., Wen, T., Chen, H., Deng, J., Yang, C., and Zhang, Z. (2018). Knockdown of insulin-like growth factor 1 exerts a protective effect on hypoxic injury of aged BM-MSCs: Role of autophagy. *Stem Cell Res. Ther.* 9 (1), 284. doi:10.1186/s13287-018-1028-5
- Yang, L., Liu, S., Mu, S., Guo, R., Zhou, L., and Fu, Q. (2021). Paeoniflorin attenuates dexamethasone-induced apoptosis of osteoblast cells and promotes bone formation via regulating AKT/mTOR/Autophagy signaling pathway. *Evid. Based. Complement. Altern. Med.* 2021, 6623464. doi:10.1155/2021/6623464
- Yang, C., Tao, H., Zhang, H., Xia, Y., Bai, J., Ge, G., et al. (2022). TET2 regulates osteoclastogenesis by modulating autophagy in OVX-induced bone loss. *Autophagy*, 1–13. doi:10.1080/15548627.2022.2048432
- Yao, J., Liu, X., Sun, Y., Dong, X., Liu, L., and Gu, H. (2021). Curcumin-alleviated osteoarthritic progression in rats fed a high-fat diet by inhibiting apoptosis and activating autophagy via modulation of MicroRNA-34a. *J. Inflamm. Res.* 14, 2317–2331. doi:10.2147/JIR.S312139
- Yin, Z., Pascual, C., and Klionsky, D. J. (2016). Autophagy: Machinery and regulation. *Microb. Cell* 3 (12), 588–596. doi:10.15698/mic2016.12.546
- Yin, X., Zhou, C., Li, J., Liu, R., Shi, B., Yuan, Q., et al. (2019). Autophagy in bone homeostasis and the onset of osteoporosis. *Bone Res.* 7, 28. doi:10.1038/s41413-019-0058-7
- Yoshida, G., Kawabata, T., Takamatsu, H., Saita, S., Nakamura, S., Nishikawa, K., et al. (2022). Degradation of the NOTCH intracellular domain by elevated autophagy in osteoblasts promotes osteoblast differentiation and alleviates osteoporosis. *Autophagy* 18, 2323–2332. doi:10.1080/15548627.2021.2017587
- Yuan, K., Zhu, Q., Lu, Q., Jiang, H., Zhu, M., Li, X., et al. (2020). Quercetin alleviates rheumatoid arthritis by inhibiting neutrophil inflammatory activities. *J. Nutr. Biochem.* 84, 108454. doi:10.1016/j.jnutbio.2020.108454
- Yue, C., Jin, H., Zhang, X., Li, W., Wang, D., Tong, P., et al. (2021). Aucubin prevents steroid-induced osteoblast apoptosis by enhancing autophagy via AMPK activation. *J. Cell. Mol. Med.* 25 (21), 10175–10184. doi:10.1111/jcmm.16954
- Zada, S., Pham, T. M., Hwang, J. S., Ahmed, M., Lai, T. H., Elashkar, O., et al. (2021). Chlorogenic acid protects human chondrocyte C28/I2 cells from oxidative stress-induced cell death through activation of autophagy. *Life Sci.* 285, 119968. doi:10.1016/j.lfs.2021.119968
- Zahm, A. M., Bohensky, J., Adams, C. S., Shapiro, I. M., and Srinivas, V. (2011). Bone cell autophagy is regulated by environmental factors. *Cells Tissues Organs* 194 (2–4), 274–278. doi:10.1159/000324647
- Zaidi, M. (2007). Skeletal remodeling in health and disease. *Nat. Med.* 13 (7), 791–801. doi:10.1038/nm1593
- Zhang, Q., Yang, Y. J., Wang, H., Dong, Q. T., Wang, T. J., Qian, H. Y., et al. (2012). Autophagy activation: A novel mechanism of atorvastatin to protect mesenchymal stem cells from hypoxia and serum deprivation via AMP-activated protein kinase/mammalian target of rapamycin pathway. *Stem Cells Dev.* 21 (8), 1321–1332. doi:10.1089/scd.2011.0684

- Zhang, J., Song, X., Cao, W., Lu, J., Wang, X., Wang, G., et al. (2016). Autophagy and mitochondrial dysfunction in adjuvant-arthritis rats treatment with resveratrol. *Sci. Rep.* 6, 32928. doi:10.1038/srep32928
- Zhang, Z., Lai, Q., Li, Y., Xu, C., Tang, X., Ci, J., et al. (2017). Acidic pH environment induces autophagy in osteoblasts. *Sci. Rep.* 7, 46161. doi:10.1038/srep46161
- Zhang, B., Hou, R., Zou, Z., Luo, T., Zhang, Y., Wang, L., et al. (2018). Mechanically induced autophagy is associated with ATP metabolism and cellular viability in osteocytes *in vitro*. *Redox Biol.* 14, 492–498. doi:10.1016/j.redox.2017.10.021
- Zhang, Q., Zhao, L., Shen, Y., He, Y., Cheng, G., Yin, M., et al. (2019). Curculigoside protects against excess-iron-induced bone loss by attenuating akt-FoxO1-dependent oxidative damage to mice and osteoblastic MC3T3-E1 cells. *Oxid. Med. Cell. Longev.* 2019, 9281481. doi:10.1155/2019/9281481
- Zhang, X., Huang, F., Chen, X., Wu, X., and Zhu, J. (2020a). Ginsenoside Rg3 attenuates ovariectomy-induced osteoporosis via AMPK/mTOR signaling pathway. *Drug Dev. Res.* 81 (7), 875–884. doi:10.1002/ddr.21705
- Zhang, Y., Cui, Y., Wang, L., and Han, J. (2020b). Autophagy promotes osteoclast podosome disassembly and cell motility through the interaction of Kindlin3 with LC3. *Cell. Signal.* 67, 109505. doi:10.1016/j.cellsig.2019.109505
- Zhang, Y., Li, M., Liu, Z., and Fu, Q. (2021a). Arbutin ameliorates glucocorticoid-induced osteoporosis through activating autophagy in osteoblasts. *Exp. Biol. Med.* 246 (14), 1650–1659. doi:10.1177/15353702211002136
- Zhang, Y., Wang, S., Chen, Y., Zhang, J., Yang, J., Xian, J., et al. (2021b). Fangchinoline inhibits human esophageal cancer by transactivating ATF4 to trigger both noxa-dependent intrinsic and DR5-dependent extrinsic apoptosis. *Front. Oncol.* 11, 666549. doi:10.3389/fonc.2021.666549
- Zhang, S. L., Zhang, K. S., Wang, J. F., Wang, Y. C., Zhang, H., Tang, C., et al. (2022). Corresponding changes of autophagy-related genes and proteins in different stages of knee osteoarthritis: An animal model study. *Orthop. Surg.* 14 (3), 595–604. doi:10.1111/os.13057
- Zhao, W., Zhang, W., Ma, H., and Yang, M. (2020). Nipa2 regulates osteoblast function by modulating mitophagy in type 2 diabetes osteoporosis. *Sci. Rep.* 10 (1), 3078. doi:10.1038/s41598-020-59743-4
- Zhao, B., Peng, Q., Poon, E., Chen, F., Zhou, R., Shang, G., et al. (2021). Leonurine promotes the osteoblast differentiation of rat BMSCs by activation of autophagy via the PI3K/Akt/mTOR pathway. *Front. Bioeng. Biotechnol.* 9, 615191. doi:10.3389/fbioe.2021.615191
- Zheng, X., Yu, Y., Shao, B., Gan, N., Chen, L., and Yang, D. (2019). Osthole improves therapy for osteoporosis through increasing autophagy of mesenchymal stem cells. *Exp. Anim.* 68 (4), 453–463. doi:10.1538/expanim.18-0178
- Zheng, H., Feng, H., Zhang, W., Han, Y., and Zhao, W. (2020a). Targeting autophagy by natural product ursolic acid for prevention and treatment of osteoporosis. *Toxicol. Appl. Pharmacol.* 409, 115271. doi:10.1016/j.taap.2020.115271
- Zheng, L. W., Wang, W. C., Mao, X. Z., Luo, Y. H., Tong, Z. Y., and Li, D. (2020b). TNF- $\alpha$  regulates the early development of avascular necrosis of the femoral head by mediating osteoblast autophagy and apoptosis via the P38 MAPK/NF- $\kappa$ B signaling pathway. *Cell Biol. Int.* 44 (9), 1881–1889. doi:10.1002/cbin.11394
- Zhou, Q., Luo, D., Li, T., Liu, Z., Zou, W., Wang, L., et al. (2015). Bone fracture in a rat femoral fracture model is associated with the activation of autophagy. *Exp. Ther. Med.* 10 (5), 1675–1680. doi:10.3892/etm.2015.2752
- Zhou, R., Zhu, F., Wu, X., Song, S., Chen, Y., Zhu, C., et al. (2019). Effects of autophagy on apoptosis of articular chondrocytes in adjuvant arthritis rats. *J. Cell. Mol. Med.* 23 (11), 7879–7884. doi:10.1111/jcmm.14629
- Zhou, W., Shi, Y., Wang, H., Yu, C., Zhu, H., and Wu, A. (2021). Sinensetin reduces osteoarthritis pathology in the tert-butyl hydroperoxide-treated chondrocytes and the destabilization of the medial meniscus model mice via the AMPK/mTOR signaling pathway. *Front. Pharmacol.* 12, 713491. doi:10.3389/fphar.2021.713491
- Zhu, M., Yuan, K., Lu, Q., Zhu, Q., Zhang, S., Li, X., et al. (2019a). Emodin ameliorates rheumatoid arthritis by promoting neutrophil apoptosis and inhibiting neutrophil extracellular trap formation. *Mol. Immunol.* 112, 188–197. doi:10.1016/j.molimm.2019.05.010
- Zhu, W., Ding, W., Shang, X., Zhu, D., and Dai, X. (2019b). Fangchinoline promotes autophagy and inhibits apoptosis in osteoporotic rats. *Med. Sci. Monit.* 25, 324–332. doi:10.12659/MSM.912624
- Zhu, W. Q., Wu, H. Y., Sun, Z. H., Guo, Y., Ge, T. T., Li, B. J., et al. (2022). Current evidence and future directions of berberine intervention in depression. *Front. Pharmacol.* 13, 824420. doi:10.3389/fphar.2022.824420

## Glossary

<b>OP</b> osteoporosis	<b>MMM9</b> matrix metalloproteinase nine
<b>OA</b> osteoarthritis	<b>TRAP</b> tartrate-resistant acidic phosphatase
<b>RA</b> rheumatoid arthritis	<b>NF-<math>\kappa</math>B</b> nuclear factor- $\kappa$ B
<b>CMA</b> chaperone-mediated autophagy	<b>RANK</b> receptor activator of NF- $\kappa$ B
<b>PI3K</b> phosphoinositide3 kinase	<b>RANKL</b> receptor activator of NF- $\kappa$ B ligand
<b>Akt</b> protein kinase B	<b>NFATc1</b> nuclear factor of activated T-cell c1
<b>AMPK</b> 5' AMP-activated protein kinase	<b>TRPV4</b> transient receptor potential vanilloid four
<b>mTOR</b> mammalian target of rapamycin	<b>P2X7R</b> P2X7 receptor
<b>mTORC</b> mammalian target of rapamycin complex	<b>TRAF6</b> tumor necrosis factor receptor-associated factor 6
<b>ULK1</b> UNC-51-like kinase	<b>BCL2</b> B-cell lymphoma two
<b>FIP200</b> FAK family kinase-interacting protein of 200 kDa	<b>TET2</b> tet methylcytosine dioxygenase 2
<b>Vps</b> vacuolar protein sorting	<b>KLF2</b> kruppel-like factor 2
<b>Atg</b> autophagy-related protein	<b>LAMP2A</b> lysosome-associated membrane protein type 2A
<b>LC3</b> microtubule-associated protein one light chain three	<b>PINK1</b> PTEN-induced putative kinase one
<b>PE</b> phosphatidylethanolamine	<b>OVX</b> ovariectomy
<b>BMSCs</b> bone marrow mesenchymal stem cells	<b>FOXO1</b> Forkhead box O1
<b>ROS</b> oxygen species	<b>IL</b> interleukin
<b>ER</b> endoplasmic reticulum	<b>JNK</b> c-Jun amino-terminal kinase
<b>TNF-<math>\alpha</math></b> tumor necrosis factor-alpha	<b>FLSs</b> fibroblast-like synoviocytes
<b>ATP</b> adenosine triphosphate	<b>AA</b> adjuvant arthritis
<b>FGF23</b> fibroblast growth factor-23	<b>Th17</b> T helper lymphocyte 17
<b>ECM</b> extracellular matrix	<b>Treg</b> regulatory T lymphocyte
<b>PC2</b> type II procollagen	<b>NETs</b> neutrophil extracellular traps
<b>CTSK</b> cathepsin K	<b>ERK</b> extracellular signal-regulated kinases
	<b>PINK1</b> PTEN-induced putative kinase one
	<b>LAMP</b> lysosomal associated membrane protein



## OPEN ACCESS

## EDITED BY

Xiaofeng Zhu,  
Jinan University, China

## REVIEWED BY

Zhiguo Zhang,  
Institute of Basic Theory (China Academy  
of Chinese Medical Sciences), China  
Xinhua Qu,  
Shanghai Jiao Tong University, China  
Larissa G. Pinto,  
King's College London, United Kingdom

## \*CORRESPONDENCE

Ren Xu,  
xuren526@xmu.edu.cn  
Feng Xu,  
xufenghou@163.com  
Gang Rui,  
reigang@163.com  
Mengyu Zhou,  
zhoumengyu@gxmu.edu.cn

<sup>†</sup>These authors have contributed equally  
to this work

## SPECIALTY SECTION

This article was submitted to  
Experimental Pharmacology and Drug  
Discovery,  
a section of the journal  
Frontiers in Pharmacology

RECEIVED 17 August 2022

ACCEPTED 03 November 2022

PUBLISHED 06 January 2023

## CITATION

Wu Z, Li X, Chen X, He X, Chen Y,  
Zhang L, Li Z, Yang M, Yuan G, Shi B,  
Chen N, Li N, Feng H, Zhou M, Rui G,  
Xu F and Xu R (2023), Phosphatidyl  
Inositol 3-Kinase (PI3K)-Inhibitor  
CDZ173 protects against LPS-  
induced osteolysis.  
*Front. Pharmacol.* 13:1021714.  
doi: 10.3389/fphar.2022.1021714

## COPYRIGHT

© 2023 Wu, Li, Chen, He, Chen, Zhang,  
Li, Yang, Yuan, Shi, Chen, Li, Feng, Zhou,  
Rui, Xu and Xu. This is an open-access  
article distributed under the terms of the  
[Creative Commons Attribution License](https://creativecommons.org/licenses/by/4.0/)  
(CC BY). The use, distribution or  
reproduction in other forums is  
permitted, provided the original author(s)  
and the copyright owner(s) are credited  
and that the original publication in this  
journal is cited, in accordance with  
accepted academic practice. No use,  
distribution or reproduction is permitted  
which does not comply with these terms.

# Phosphatidyl Inositol 3-Kinase (PI3K)-Inhibitor CDZ173 protects against LPS-induced osteolysis

Zuoxing Wu<sup>1,2,3†</sup>, Xuedong Li<sup>4†</sup>, Xiaohui Chen<sup>1,2,3†</sup>, Xuemei He<sup>2†</sup>,  
Yu Chen<sup>2</sup>, Long Zhang<sup>2</sup>, Zan Li<sup>5</sup>, Mengyu Yang<sup>2</sup>, Guixin Yuan<sup>2</sup>,  
Baohong Shi<sup>2</sup>, Ning Chen<sup>6</sup>, Na Li<sup>1,2,3</sup>, Haotian Feng<sup>7</sup>,  
Mengyu Zhou<sup>8\*</sup>, Gang Rui<sup>1\*</sup>, Feng Xu<sup>9\*</sup> and Ren Xu<sup>1,2,3,10\*</sup>

<sup>1</sup>Department of Orthopedic Surgery, The First Affiliated Hospital of Xiamen University, School of Medicine, Xiamen University, Xiamen, China, <sup>2</sup>The First Affiliated Hospital of Xiamen University-ICMRS Collaborating Center for Skeletal Stem Cell, School of Medicine, Xiamen University, Xiamen, China, <sup>3</sup>Fujian Provincial Key Laboratory of Organ and Tissue Regeneration, School of Medicine, Xiamen University, Xiamen, China, <sup>4</sup>Department of Medical Laboratory, The Fourth Affiliated Hospital of Guangxi Medical University, Liuzhou, China, <sup>5</sup>Department of Sports Medicine, Xiangya Hospital, Central South University, Changsha, China, <sup>6</sup>Department of Endocrinology, Zhongshan Hospital (Xiamen), Fudan University, Xiamen, China, <sup>7</sup>Inner Mongolia Dairy Technology Research Institute Co. Ltd., Hohhot, China, <sup>8</sup>Department of Dentistry, The First Affiliated Hospital of Guangxi Medical University, Nanning, China, <sup>9</sup>Department of Subject Planning, Ninth People's Hospital Shanghai, Jiaotong University School of Medicine, Shanghai, China, <sup>10</sup>Research Centre for Regenerative Medicine, Guangxi Key Laboratory of Regenerative Medicine, Guangxi Medical University, Nanning, China

A major complication of a joint replacement is prosthesis loosening caused by inflammatory osteolysis, leading to the revision of the operation. This is due to the abnormal activation of osteoclast differentiation and function caused by periprosthetic infection. Therefore, targeting abnormally activated osteoclasts is still effective for treating osteolytic inflammatory diseases. CDZ173 is a selective PI3K inhibitor widely used in autoimmune-related diseases and inflammatory diseases and is currently under clinical development. However, the role and mechanism of CDZ173 in osteoclast-related bone metabolism remain unclear. The possibility for treating aseptic prosthesis loosening brought on by inflammatory osteolysis illness can be assessed using an LPS-induced mouse cranial calcium osteolysis model. In this study, we report for the first time that CDZ173 has a protective effect on LPS-induced osteolysis. The data show that this protective effect is due to CDZ173 inhibiting the activation of osteoclasts *in vivo*. Meanwhile, our result demonstrated that CDZ173 had a significant inhibitory effect on RANKL-induced osteoclasts. Furthermore, using the hydroxyapatite resorption pit assay and podosomal actin belt staining,

**Abbreviations:** ALP, Alkaline phosphatase; AR, Alizarin red; BMMs, Bone marrow macrophages; BMSc, Bone mesenchymal stem cells; BV/TV, Bone volume/tissue volume; CCK8, Cell counting kits 8; CTSK, Cathepsin K; DC-STAMP, Dendritic cell-specific transmembrane protein; H&E, Hematoxylin-Eosin; IκBα, B cell inhibitory factor α; LPS, Lipopolysaccharide; M-CSF, Macrophage colony-stimulating factor; MMP9, Matrix metalloproteinase 9; μCT, Microcomputed tomography; NC, Nitrocellulose; NFATc1, Nuclear factor of activated T-cell cytoplasmic 1; OC, Osteoclast; PMSF, Phosphatase inhibitor and phenylmethylsulfonyl fluoride; RANKL, Receptor activator of nuclear factor-κB ligand; RANK, Receptor activator of nuclear factor-κB; Tb. Sp, Trabecular bone separation; Tb.Th, Trabecular thickness; TLR4, Toll-like receptor 4; TRAF6, Tumor necrosis factor receptor-associated factor 6; TRAP, Tartrate-resistant acid phosphatase.



respectively, the inhibitory impact of CDZ173 on bone resorption and osteoclast fusion of pre-OC was determined. In addition, staining with alkaline phosphatase (ALP) and alizarin red (AR) revealed that CDZ173 had no effect on osteoblast development *in vitro*. Lastly, CDZ173 inhibited the differentiation and function of osteoclasts by weakening the signal axis of PI3K-AKT/MAPK-NFATc1 in osteoclasts. In conclusion, our results highlight the potential pharmacological role of CDZ173 in preventing osteoclast-mediated inflammatory osteolysis and its potential clinical application.

#### KEYWORDS

Osteoclast, CDZ173, Osteolysis, PI3K, MAPK

## Introduction

Osteoclasts and osteoblasts work together to maintain the integrity and health of bone tissue through a dynamic equilibrium in the metabolism of bone tissue (Rossi et al., 2019; Zhan et al., 2019). Osteolysis is a pathological condition characterized by bone loss and osteopenia caused by excessive activation of osteoclasts or reduction of osteoblasts. The diseases associated with it include osteoporosis, aseptic prosthesis loosening, periodontitis, and so on (Mbalaviele et al., 2017; Gao et al., 2022). Osteoclasts are the only multinucleated macrophages with bone resorption function in the body, which play a key role in bone development, reconstruction, and repair (Mediero and Cronstein, 2013; Yu et al., 2021). Joint replacement been extensively used to treat joint pain and joint instability caused by severe trauma, osteoarthritis and osteoporotic fractures (Wu et al., 2019; Zhou et al., 2020). However, aseptic loosening and periprosthetic infection leading to inflammatory osteolysis are still common complications of joint replacement, resulting in a high incidence rate and a decline in functional prognosis (Ren et al., 2011; Zhu et al., 2016). A primary reason for these inflammatory responses is that the excessive activation of osteoclasts induced by bacterial endotoxin pollution or bacterial endotoxin on implant-derived wear particles eventually leads to the loss of bone around the prosthesis (Han et al., 2020). Therefore, drug development targeting osteoclasts remains an effective means to prevent periprosthetic osteolysis.

From the hematopoietic stem cell lineage, osteoclasts are differentiated from mononuclear macrophages. Receptor activator of nuclear factor- $\kappa$ B ligand (RANKL) and macrophage colony-stimulating factor (M-CSF) play two important roles in osteoclast differentiation (Kim et al., 2020; Honma et al., 2021; Udagawa et al., 2021). As a member of the tumor necrosis factor superfamily, RANKL is a type II homotrimeric transmembrane protein that is mainly produced by osteoblasts and stromal cells in the form of surface proteins or secreted factors. RANK is a protein receptor highly expressed on the surface of osteoclasts. In the process of osteoclast maturation, the combination of RANKL and RANK will recruit some factors

such as molecules like necrosis factor receptor-associated factor 6 (TRAF6) and Src tyrosine kinase. This recruitment will then activate downstream PI3K-AKT, NF- $\kappa$ B, and MAPK (An et al., 2019; Xin et al., 2020; Ma et al., 2021), thereby inducing the activation of the nuclear factor of activated T-cell cytoplasmic 1 (NFATc1), resulting in the subsequent expression of osteoclast-specific genes *DC-STAMP*, *MMP9*, *TRAP* and *CTSK* (Yang et al., 2019; Xin et al., 2020).

Lipopolysaccharide (LPS), a crucial part of Gram-negative bacteria's cell membrane and a key biological agent thought to be responsible for inflammatory bone loss (Xing et al., 2011). Importantly, triggering an inflammatory response cascade can lead to the development of osteoclasts and an increase in bone loss. As a result, LPS can stimulate osteoclasts to activate NF- $\kappa$ B and MAPK signaling pathways by attaching to the pattern recognition receptor toll-like receptor (TLR4) (Shao et al., 2019; Fang et al., 2021). Simultaneously, LPS can induce systemic inflammatory responses and promote the production of osteoclast-related factors, such as TNF- $\alpha$ , MCSF, etc., ultimately promoting the excessive activation of osteoclasts and bone loss (Wang et al., 2019). Therefore, developing drugs capable of inhibiting LPS-induced osteolysis remains a significant goal in preventing periprosthetic infection and inflammatory local bone destruction in aseptic joint loosening.

CDZ173 is a highly selective inhibitor of PI3K (Hoegenauer et al., 2017). In previous clinical studies, oral CDZ173 can effectively reduce lymphocyte proliferation dose-dependently to improve immune-related diseases (Rao et al., 2017). Systemic lupus erythematosus and rheumatoid arthritis are two examples of autoimmune disorders that can be made worse by activating the PI3K pathway. The development of CDZ173, as a potent and specific inhibitor of PI3K, has also been focused on investigating its benefits in the above diseases (Hoegenauer et al., 2017; Rao et al., 2017; Jamee et al., 2020). Meanwhile, studies have shown that CDZ173 can effectively inhibit the production of antigen-specific antibodies and alleviate disease symptoms in a rat collagen-induced arthritis model (Hoegenauer et al., 2017). However, the role of CDZ173 in osteolytic inflammatory diseases and osteoclasts has not been elucidated. Given the extensive research on CDZ173 in various

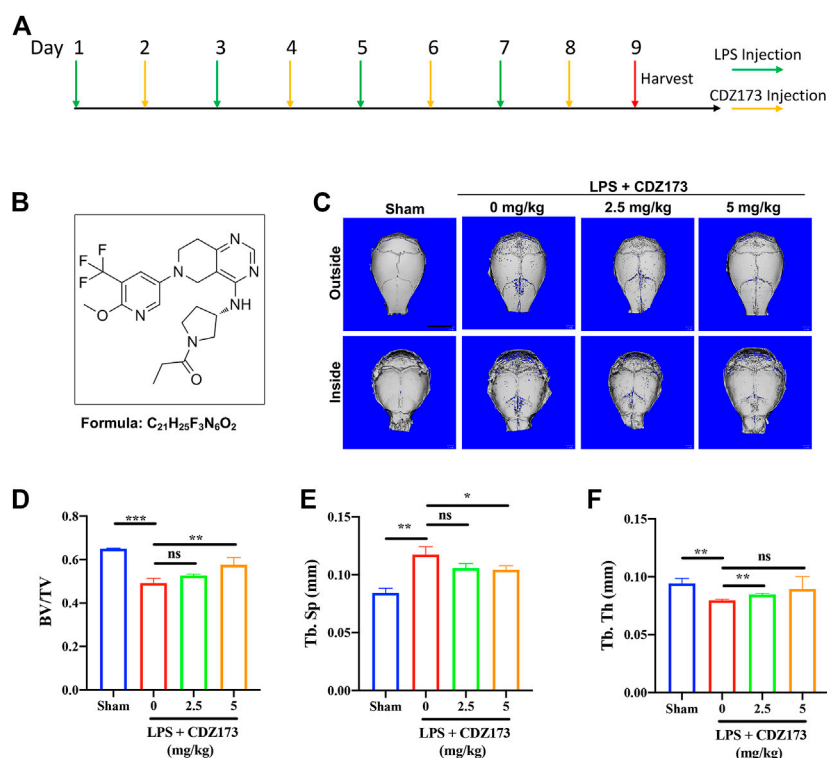


FIGURE 1

CDZ173 protected against titanium LPS-induced osteolysis of the mouse calvaria. (A) The timeline of the animal model. (B) Chemical structure of CDZ173. (C) Three-dimensional reconstructed micro-CT images of calvarial tissue from the Sham, PBS vehicle, and CDZ173 treated groups. (D) Bone volume to tissue volume (BV/TV, %) histomorphometric analysis (E) bone trabecular thickness (F) number of treatment group bone porosity (scale bar = 5 mm) (\* $p < 0.05$ , \*\* $p < 0.01$ , \*\*\* $p < 0.001$ ).

immune diseases and its therapeutic potential in clinical trials, we explored the effect of CDZ173 on LPS-induced inflammatory bone loss and analyzed its specific cellular and molecular mechanisms.

## Materials and methods

### Reagents

CDZ173 (purity >98% Figure 1A) was purchased from Selleck Co., LTD. (Shanghai, China). Recombinant M-CSF and RANKL mice were obtained from R&D Systems (Minneapolis, MN, United States). LPS was purchased from Sigma Chemical (Co.St.Louis, MO, United States). Promega (Madison, WI, United States) provided cell counting kits (CCK8). Tartrate-resistant acid phosphatase (TRAP) staining kits were obtained from Sigma Aldrich (St Louis, MO, United States). Antibodies for PI3K, phospho-PI3K, AKT, phospho-AKT, ERK, phospho-ERK, JNK, phospho-JNK, p38, phospho-p38, NF- $\kappa$ B p65, anti-phospho-NF- $\kappa$ B p65,  $\beta$ -Actin were obtained from Cell Signalling Technology (Boston, MA,

United States). Antibodies for NFATc1 were obtained from Santa Cruz Biotechnology (Dallas, TX, United States), and antibodies for c-Fos were obtained from Abcam Technology (Cambridge, United Kingdom).

### Mice model

We randomly divided 32 healthy male C57BL/6J mice (6–8 weeks old) into 4 groups, namely the Sham group, LPS group, Low-Dose (2.5 mg/kg) group, and High-Dose (5 mg/kg) group, resulting in 8 mice in each group. After the start of the experiment, LPS was injected subcutaneously *via* the sagittal line of the skull in LPS group, low-dose (2.5 mg/kg) and high-dose (5 mg/kg) mice on the first, third, fifth and seventh day respectively, with the dose of 5 mg/kg LPS; On the second, fourth, sixth and eighth days, the mice in the low dose group (2.5 mg/kg) and the high dose group (5 mg/kg) were injected 2.5 mg/kg and 5 mg/kg CDZ173 through the sagittal line skin of the skull, respectively. Mice in the Sham group and LPS group were injected with the same amount of normal saline at the same

position. Mice were slaughtered after the experiment on the ninth day, and their heads were removed before being preserved in 4% paraformaldehyde for 48 h and analyzed using microcomputed tomography (CT) and tissue sectioning.

## Micro-CT scanning and histological

The mouse skull specimens fixed with 4% FPA were scanned by high-resolution  $\mu$ CT. The set parameters were: voltage 50 kV and current 500 kV  $\mu$  A. Scanning range: 2 cm  $\times$  2 cm, scanning layer thickness 10  $\mu$ m. After scanning (Skyscan 1,272; Skyscan; Aartselaar, Belgium), three-dimensional reconstruction was performed with the nrecon software, and ctan software was used to analyze and compare the relevant parameters of reconstructed bone tissue, including bone volume fraction (BV/TV), trabecular bone separation (Tb. Sp), and trabecular bone porosity. The cranial bone samples after  $\mu$ CT scanning were placed in 10% EDTA and decalcified at room temperature for 4 weeks. 5  $\mu$ m sections were taken for Hematoxylin-Eosin (H&E) and Tartrate-resistant acid phosphatase (TRAP) activity staining. Hematoxylin-eosin staining is one of the most commonly used staining methods in paraffin section technology. The hematoxylin staining solution was alkaline, which mainly stained the chromatin in the nucleus and the nucleic acid in the cytoplasm with violet blue. Eosin is an acidic dye that mainly makes the cytoplasm and extracellular matrix components red. We observed the degree of bone destruction by H&E staining. Tartrate-resistant acid phosphatase (TRAP) staining here mainly explores the relative abundance of osteoclasts in bone tissue. Osteomeasure (Osteomeasure, LA, United States) was used to determine the number of osteoclast positive cells (TRAP + Cell Number) and the ratio of osteoclast to bone tissue contact surface (OC.S/BS) in each sample.

## Cell culture and CCK8 cell proliferation assay

In the first step, we obtained bone marrow monocyte/macrophages (BMMs) from long bone in 6–8-week-old male C57BL/6 mice. BMMs were grown in a humidified incubator at 37°C and 5% CO<sub>2</sub> using a complete medium consisting of a-MEM supplemented with 10% (v/v) FBS, 1% (w/v) penicillin/streptomycin, and 30 ng/ml M-CSF. The CCK8 assay evaluated the effect of CDZ173 on the proliferation of BMMs cells. BMMs were seeded into a 96-well plate at a density of  $6 \times 10^3$  cells/well in full -MEM with 30 ng/ml M-CSF for 24 h. After that, the cells were incubated with the stated doses of CDZ173 (0–20  $\mu$ M) for the remaining 48 h. Subsequently, we added 10  $\mu$ l/well CCK8 buffer to each well according to the instructions and at 37°C for 2 hours. The TriStar2 LB 942 multi-mode microplate reader was used to measure the absorbance at 450 nm (Bio-Tek Instruments, Winooski, VT, United States).

TABLE 1 The primer sets used are as follows.

TRACP	Forward: 5'-TGTGGCCATCTTTATGCT-3' Reverse: 5'-GTCATTTCTTTGGGCTT-3'
DC-STAMP	Forward: 5'-TCTGCTGTATCGGCTCATCTC-3' Reverse: 5'-ACTCCTTGGGTTCTTGCTT-3'
MMP-9	Forward: 5'-CGTGTCTGGAGATTCGACTTGA-3' Reverse: 5'-TTGGAACTCACACGCCAGA-3'
CTSK	Forward: 5'-AGGCGGCTCTATATGACCACTG-3' Reverse: 5'-TCTTCAGGGCTTCTCGTTC-3'
C-fos	Forward: 5'-CCAGTCAAGAGCATCAGCAA-3' Reverse: 5'-AAGTAGTGCAGCCCGAGTA-3'
NFATc1	Forward: 5'-GGTGCTGTCTGGCCATAACT-3' Reverse: 5'-GAAACGCTGGTACTGGCTTC-3'
$\beta$ -actin	Forward: 5'-TCTGCTGGAAGGTGGACAGT-3' Reverse: 5'-CCTCTATGCCAACACAGTGC-3'

## Osteoclast formation assay *in vitro*

To observe whether CDZ173 affects the differentiation of osteoclasts, M-CSF-dependent BMMs were seeded at a density of  $6 \times 10^3$  cells per well in 96-well plates that contained full -MEM. To confirm that the cells adhered properly, they were placed there for an entire night. BMMs were simulated by employing a concentration of RANKL equal to 30 ng/ml in conjunction with an incremental doubling of CDZ173 (from 1.25, 2.5, and 5.0  $\mu$ M, dose-dependent effect). The M-CSF, RANKL, and CDZ173-containing culture medium was changed every 2 days to promote the development of mature, multinucleated OCs. Detection of Tartrate-resistant acid phosphatase (TRAP) activity involved staining for the protein after cells were fixed in 4% paraformaldehyde for 15–20 min.

## Real-time PCR analysis

In order to explore the expression of particular OC genes at the conclusion of OC formation following the application of CDZ173, real-time PCR was utilized. The same reagents and settings for the real-time PCR apparatus were used as were described in the prior literature for the extraction of cell RNA (Li et al., 2020). Table 1 shows the related primer sets.

## Bone resorption pit assay

In the beginning, BMMs were plated at a density of  $1 \times 10^5$  cells per well into 6-well plates that contained a-MEM complete media. They were then subjected to the culture of an extra 30 ng/ml of RANKL until mature osteoclasts developed. Mature

osteoclasts were isolated and then cultured for an additional 2 days in hydroxyapatite-coated 96-well plates (Corning, United States) containing varying doses of CDZ173. Lastly, the mature OCs were dissolved in 10% sodium hypochlorite for 15 min, followed by two washes in phosphate-buffered saline (PBS), and finally drying. Light microscopic images were captured for each well, and pit areas were quantified using ImageJ. BMM cells were implanted into 6-well plates containing  $\alpha$ -MEM complete medium at a density of  $1 \times 10^5$  cells/well under 30 ng/ml RANKL and 30 ng/ml M-CSF culture until mature osteoclasts appeared on the third or fourth day.

## Podosome belt formation assay

To induce the development of fully functional, multinucleated OC, BMMs ( $8 \times 10^3$  cells/well) were seeded into 96-well plates and grown in complete  $\alpha$ -MEM media with M-CSF (30 ng/ml), RANKL (30 ng/ml), and CDZ173 (1.25, 2.5, and 5 M). On day six, cells were washed, fixed with 4% paraformaldehyde, and permeabilized with 100 ml of 0.1% Triton X-100 in each well for 5 min. Nonspecific immunoreactivity was blocked with the 3% BSA in PBS. Podosome belts were stained by washing the cells and then incubating them with rhodamine-conjugated phalloidin for 1 h in a dark environment. Following this, the cells were washed with PBS a total of three times, and then counterstained with DAPI for a period of 5 minutes. After that, images were obtained through the employment of a fluorescent microscope (Leica, Germany).

## Osteoblastogenesis assay

We obtained bone mesenchymal stem cells (BMSc) from the long bone in 4–6-week-old male C57BL/6 mice. BMSc were grown in a humidified incubator at 37°C and 5% CO<sub>2</sub> using a complete medium consisting of  $\alpha$ -MEM supplemented with 10% (v/v) FBS, 1% (w/v) penicillin/streptomycin. To induce osteoblast differentiation, the grown BMSc ( $5 \times 10^4$  cells/well) were seeded in 48-well plates and cultured in osteogenic medium (50  $\mu$ g/ml ascorbic acid, 5 mM glycerol phosphate) with or without different concentrations of CDZ173. The culture medium was changed every other day, ALP staining was performed after 7 days of differentiation, and AR staining was performed after 21 days of differentiation.

## Western blotting

The molecular mechanism through which CDZ173 inhibits osteoclasts was analyzed by using western blotting. BMMs were

plated at a density of  $1.5 \times 10^5$  cells/well in 6-well dishes. BMMs adhered overnight and were stimulated with RANKL for 0 (no stimulation), 5, 10, 20, 30, or 60 min after pretreatment with 5  $\mu$ M CDZ173 or a vehicle control. The whole cells were then extracted in RIPA lysis buffer containing phosphatase inhibitor and phenylmethylsulfonyl fluoride (PMSF) for 30 min to obtain total proteins. Subsequently, an electronic imprinting device separated the proteins using SDS-PAGE gel and transferred them to a nitrocellulose (NC) membrane. The membrane was then sealed in 5% skimmed milk for 1 h and then incubated overnight at 4°C with specific primary antibodies: PI3K(1:1,000), phospho-PI3K(1:500), AKT (1:1,000), phospho-AKT (1:500), ERK (1:1,000), phospho-ERK (1:1,000) (1:500), JNK(1:1,000), phospho-JNK(1:500), p38 (1:1,000), phospho-p38 (1:500), NF- $\kappa$ B p65 (1:1,000), anti-phospho-NF- $\kappa$ B p65 (1:500),  $\beta$ -Actin (1:1,000), NFATc1 (1:100) and c-Fos(1:1,000). The next day, the membrane was washed three times with TBS containing 1% Tween for 5 minutes and then incubated with a fluorescent secondary antibody for 1 h. Finally, the membrane was washed three times with TBST, visualized with image quantia-4000 imaging system (GE Healthcare, Chicago, Illinois, United States), and the results were analyzed using the ImageJ software.

## Statistical analysis

Data was illustrated either as means  $\pm$  standard deviation (SD), or the representative one with all independent triplicates. Statistical analysis among or within groups was conducted by one-way ANOVA tests using SPSS 19.0 software (SPSS Inc., United States). \* $p < 0.05$ , \*\* $p < 0.01$ , \*\*\* $p < 0.001$  was regarded as statistical significance.

## Results

### CDZ173 protected LPS-Induced calvarial osteolysis by inhibiting osteoclast activation *in vivo*

CDZ173 (Figure 1B), a selective PI3K inhibitor, has been used to treat immune diseases and arthritis (Hoegenauer et al., 2017). At the same time, it can alleviate blood-related tumors by inhibiting the PI3K-AKT signaling pathway (Hoegenauer et al., 2017; Rao et al., 2017). To explore the potential of CDZ173 (Figure 1B) to protect joint prosthesis loosening, we established a model of skull osteolysis induced by LPS to simulate bone loss caused by inflammation *in vivo*. Subsequently, we injected LPS and CDZ173 (2.5 mg/kg and 5 mg/kg) subcutaneously into the sagittal suture of the head in mice. Compared with the sham group, micro-CT showed an extensive bone loss in the calvaria of mice after LPS injection



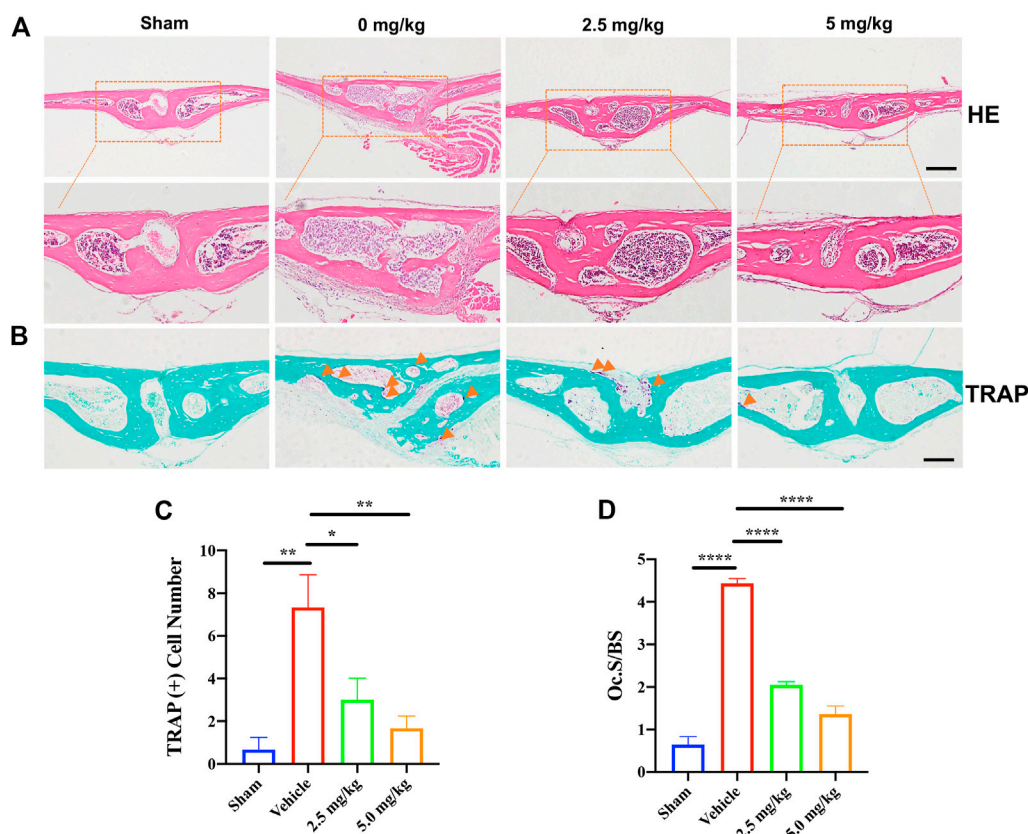


**FIGURE 2**

H&E and TRAP staining were performed on the calvarial tissue collected from the Sham, PBS vehicle, and CDZ173 treated groups. Representative images of calvaria stained with H&E(A) and TRAP(B), histological assessment of (C–D), and number of osteoclasts per field of tissue (TRAP<sup>+</sup> Number) and (Oc.S/BS) in sections were shown (scale bar = 500  $\mu$ M) (\* $p$  < 0.05, \*\* $p$  < 0.01, \*\*\*\* $p$  < 0.0001).

(Figure 1C). Compared with the LPS group, the mice treated with CDZ173 had reduced bone loss in the skull, and the recovery of bone volume/tissue volume (BV/TV) and trabecular bone separation (Tb. Sp) in the high dose (5.0 mg/kg) group was better than that in the low dose (2.5 mg/kg) group (Figures 1C–E). In terms of the bone morphological parameters, trabecular thickness (Tb. Th), there appeared to be a trend of recovery in the high-dose (5.0 mg/kg) group compared with the LPS group, although there was no significant difference due to the larger standard (Figure 1F).

Histological H&E staining further confirmed the protective effect of CDZ173 on LPS-induced bone erosion (Figure 2A). Additionally, histological TRAP staining and quantification showed that the number of osteoclasts on the bone surface was significantly reduced in the low-dose CDZ173 group ( $p$  = 0.0147) and the high-dose CDZ173 group ( $p$  = 0.0039) compared with the LPS group (Figures 2B,C), and the ratio of osteoclast surface to bone contact surface was also significantly reduced in the low-dose

( $p$  < 0.0001) and high-dose ( $p$  < 0.0001) CDZ173 groups (Figure 2D). Therefore, our data show that CDZ173 alleviates LPS-induced calvarial loss in mice by inhibiting the over-activation of osteoclasts *in vivo*.

### CDZ173 inhibited RANKL-induced osteoclast differentiation and had no toxic effect on BMMs *in vitro*

We previously determined the protective effect of CDZ173 on local calvarial osteolysis by inhibiting the activation of osteoclasts *in vivo*. Next, we explored the protective effect of CDZ173 on LPS-induced osteolysis *in vitro*. First, we evaluated the toxic effect of CDZ173 on BMMs using the CCK8 assay. As shown in Figure 3A, CDZ173 did not have any toxic effect on BMMs when the concentration of CDZ173 was below 10  $\mu$ M. At the same time, we found that CDZ173 inhibited the number and size of osteoclasts under different concentrations (1.25, 2.5, and

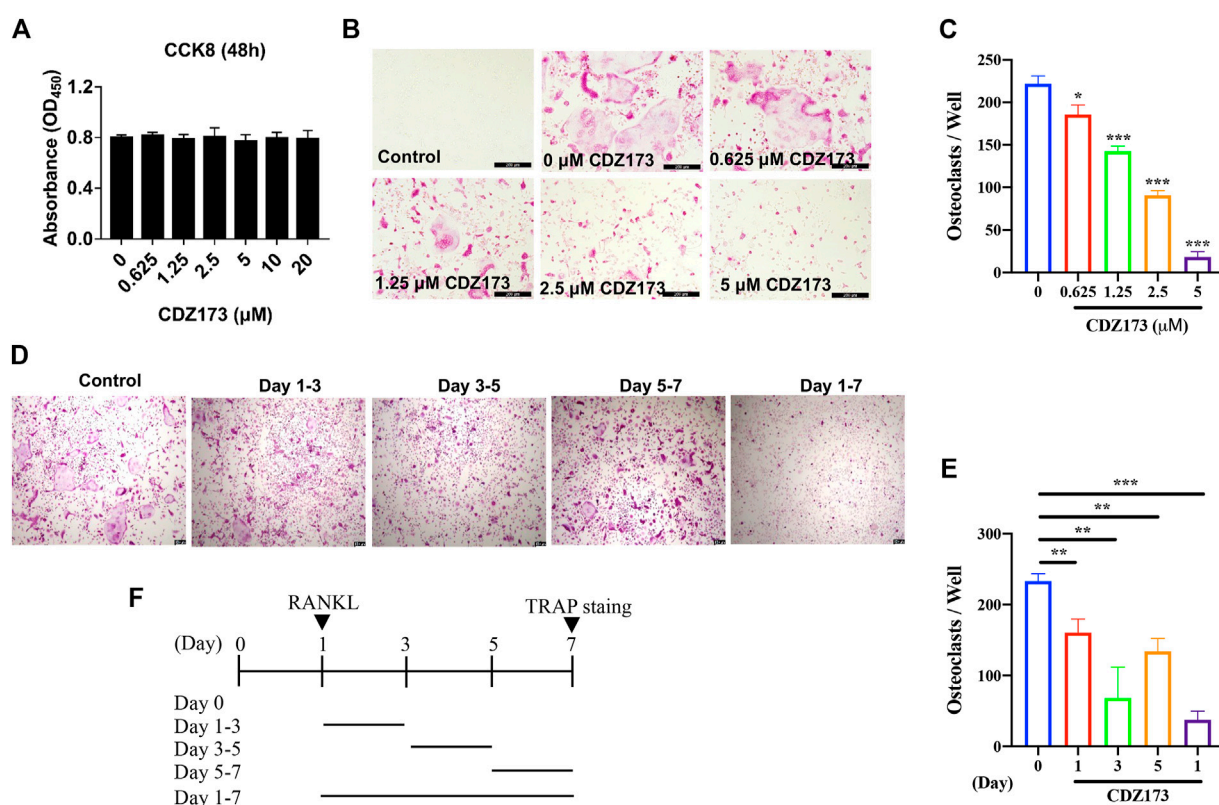


FIGURE 3

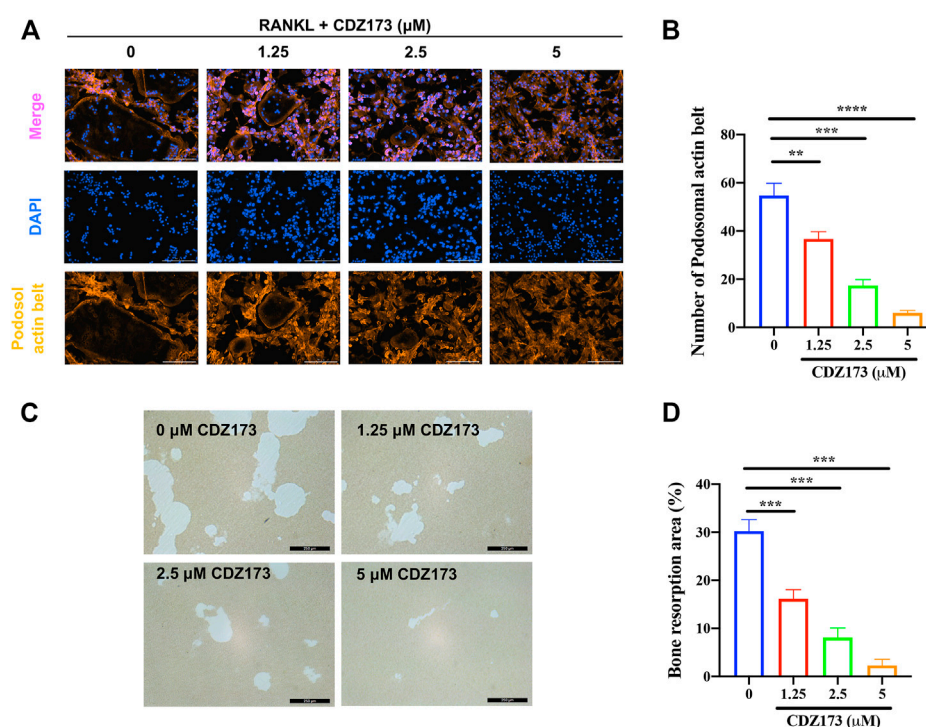
CDZ173 inhibited RANKL-induced OC formation without cytotoxic effects *in vitro*. (A) BMMs were treated with indicated concentrations of CDZ173 for 48 h and tested by CCK-8 assays. (B) BMMs were given the relevant doses of CDZ173, M-CSF (30 ng/ml), and RANKL (30 ng/ml) over the course of 5 days. After that, the cells were stained for TRAP after being fixed with 4% paraformaldehyde (scale bar = 200 μm). (C) The number of TRAP positive multinucleated OC (nuclei >3) were quantified (n = 3). (D–F) TRAP positive BMMs after the treatment with 5 μM CDZ173 for the indicated days during OC formation (scale bar = 100 μm). (E) The number of TRAP positive multinucleated OC (nuclei >3) were quantified (n = 3) (\**p* < 0.05, \*\**p* < 0.01, \*\*\**p* < 0.001).

5 μM) by RANKL-induced BMMs osteoclast differentiation in a dose-dependent manner, with the most significant inhibitory effect at 5 μM, where osteoclast number decreased by about 90 percent (Figures 3B,C). To further explore at which stage CDZ173 inhibited osteoclasts, we set up the effect of CDZ173 on osteoclasts at different time gradients. We found that CDZ173 inhibited osteoclasts through TRAP staining and quantitative analysis. The best inhibitory effect is in the middle stage of cell differentiation (Figures 3D–F). Taken together, we identified that CDZ173 inhibited osteoclast differentiation by disrupting RANKL-induced metaphase signaling in BMMs.

## CDZ173 inhibited bone resorption and podosomal actin belt formation

Both the development of the podosomal actin belt and the resorption of bone tissue are necessary preconditions for the

actualization of osteoclast function (Tan et al., 2017; Qiu et al., 2022). At the same time, in the above osteoclast differentiation TRAP staining experiment, we found that the osteoclasts generated following treatment with CDZ173 were noticeably smaller in comparison to those that had not been treated. As a result, we investigated this morphological shift further by labeling the podosomal actin belt with immunofluorescence. The podosomal actin belt is organized into a narrow actin band that surrounds one dormant nonpolarized osteoclast. This band serves to demarcate the boundaries of a single osteoclast. This feature can determine changes in osteoclast size, indicating impaired precursor cell fusion (Wang et al., 2019). Notably, as the concentration of CDZ173 increased, the number of podosomal belts decreased in a concentration-dependent manner compared with the control group, especially at a CDZ173 concentration of (5 μM), the number of podosomal actin belts decreased most significantly (Figures 4A,B). Next, we investigated the effect of CDZ173 on the bone

**FIGURE 4**

CDZ173 inhibited bone resorption and osteoclast fusion *in vitro* (A) BMMs were stimulated for 5 days with M-CSF (30 ng/ml) and RANKL (30 ng/ml) in the absence or presence of indicated concentrations of CDZ173, then fixed and immunostained for podosomeal actin belt. The representative image of the podosomal actin belt (Orange) in osteoclasts was captured by an immunofluorescence microscope. The nuclei (blue) were counterstained with DAPI (scale bar = 200 μM). (B) The number of podosomal actin belts in each group was quantified. (C) Mature OC were placed in hydroxyapatite-coated plates and treated for 24 h with 5 μM CDZ173. Attached cells were removed and micrographs of bone resorption pits were taken under a light microscope (scale bar = 250 μM). (D) The proportion of bone resorption area in total bone resorption area was quantified by ImageJ software (\*\* $p < 0.01$ , \*\*\* $p < 0.001$ , \*\*\*\* $p < 0.0001$ ).

resorption function of osteoclasts. As shown in Figures 4C,D, apatite absorption lacunae were reduced in size by CDZ173 in a concentration-dependent manner. Compared with the control group, the hydroxyapatite absorption lacunae after treatment with CDZ173 with a concentration of 5 μM decreased by nearly 30%. These findings imply that CDZ173 blocks the osteoclast function of RANKL-induced BMMs.

## CDZ173 inhibited osteoclast-specific gene expression

Osteoclast-specific genes are up-regulated during RANKL-induced osteoclast formation (Zhou et al., 2015; Krieger et al., 2020). These genes include transcription factors c-Fos and NFATc1 in the osteoclast nucleus, dendritic cell-specific transmembrane protein (DC-STAMP), matrix metalloproteinase 9 (MMP 9), tartrate resistant acid phosphatase (Trap), and cathepsin K (CTSK) involved in absorption function. Therefore, we detected the effect of CDZ173 on osteoclast-specific genes by quantitative

fluorescence PCR. We identified that CDZ173 inhibited their expression in a dose-dependent manner (Figures 5A–F). Therefore, osteoclast development was suppressed and osteoclast-specific gene expression was decreased by CDZ173 *in vitro*.

## CDZ173 does not affect osteoblast differentiation and mineralization

We identified that CDZ173 protects LPS-induced local osteolysis by inhibiting the overactivation of osteoclasts. Therefore, we verified the effect of CDZ173 on osteoblasts by culturing osteoblasts *in vitro*. First, the toxic effects of CDZ173 (0, 10, 5, 2.5, and 1.25 μM) on BMSCs at different doses were determined using the CCK-8 reagent. The results showed that CDZ173 below 20 μM had no significant effect on the proliferation of BMSCs (Figure 6A). To explore the impact of CDZ173 on osteoblast formation, we carried out experiments of BMSC-induced osteoblast differentiation. BMSCs were cultured in an osteogenic induction medium, and different doses of CDZ173 (0, 1.25, 2.5, and 5 μM) were added for intervention. ALP and AR

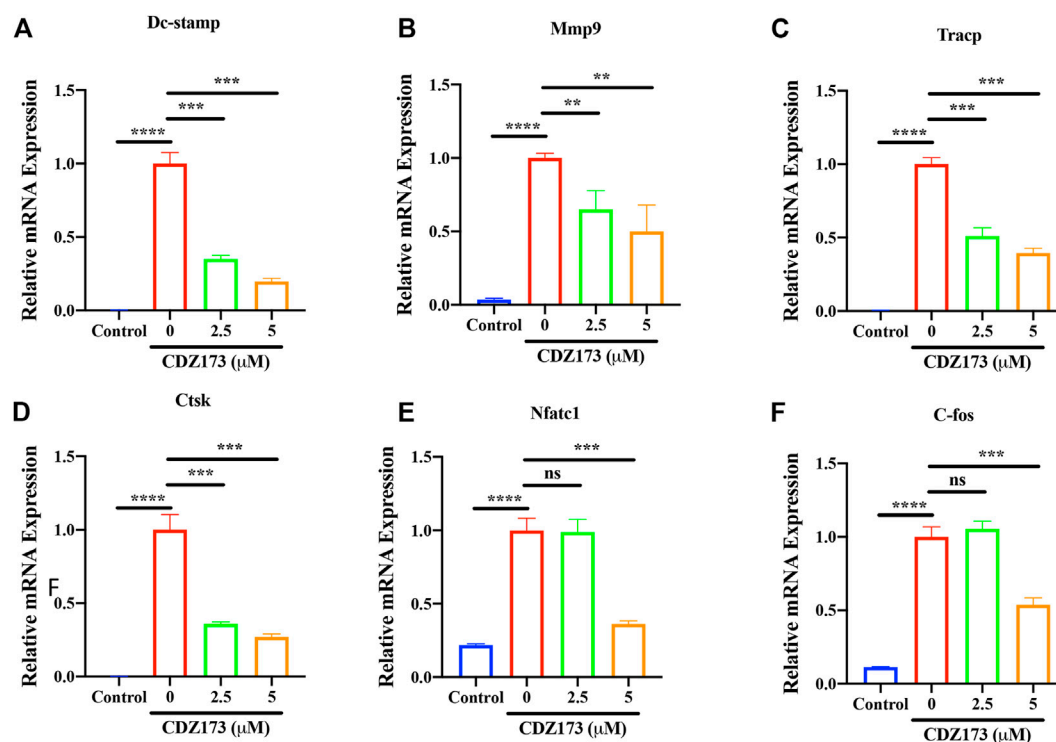


FIGURE 5

CDZ173 suppressed RANKL-induced expression of OC-Specific genes. BMMs were stimulated with M-CSF (30 ng/ml), and RANKL (30 ng/ml) in the absence or presence of indicated concentrations of CDZ173 for 5 days to form multinucleated TRAP positive OCs. Specific primers were used to perform real-time PCR for OC related genes (A) *Dc-stamp*, (B) *Mmp-9*, (C) *Trap*, (D) *Ctsk*, (E) *Nfatc1* and (F) *C-fos*. Gene expression levels of *Dc-stamp*, *Mmp9*, *Trap*, *Ctsk*, *Nfatc1* and *C-fos* were expressed relative to control group (\*\* $p < 0.01$ , \*\*\* $p < 0.001$ , \*\*\*\* $p < 0.0001$ ).

staining were performed on the cells after 7 and 21 days of culture, respectively (Figures 6B,C). The results demonstrated that CDZ173 had no appreciable impact on osteoblast differentiation and mineralization.

### CDZ173 inhibits osteoclast development by inhibiting PI3K-AKT and MAPKs signaling pathways

To further clarify the potential molecular mechanism of CDZ173 involved in osteoclast differentiation and function, we first detected the PI3K-AKT classical signaling pathway of RANKL-induced osteoclast formation. After BMMs were stimulated by RANKL, western blot analysis demonstrated that the phosphorylation levels of PI3K and AKT increased significantly, reaching the peak at 5 and 10 min, respectively. However, after treatment with CDZ173, the phosphorylation levels of PI3K and AKT decreased significantly, while there was no significant change in total protein (Figures 7A,C). Previous research has demonstrated a critical function for the three main MAPK subfamilies (JNK, ERK, and p38) in osteoclast activity

and development (Fang et al., 2020). At the same time, our western blot results showed that the phosphorylation of ERK, JNK, and p38 increased significantly under the stimulation of RANKL, and all three peaked in 10 min. However, after treatment with CDZ173, the phosphorylation of ERK and JNK decreased but had no impact on the phosphorylation of p38 (Figures 7A,D–F). We also observed the effect of CDZ173 on NF- $\kappa$ B. CDZ173 did not affect B cell inhibitory factor  $\alpha$  (I $\kappa$ B $\alpha$ ) degradation or p65 phosphorylation (Figures 7A,G,H), suggesting that CDZ173 does not affect NF- $\kappa$ B in the early signaling of the osteoclast process. These results demonstrated that CDZ173 attenuates osteoclast formation by inhibiting the binding of PI3K-AKT and MAPK signals.

### CDZ173 inhibits the transcription factors NFATc1 and c-fos in the osteoclast nucleus to weaken osteoclast differentiation

During osteoclast development, activation of the PI3K-AKT, NF- $\kappa$ B, and MAPK signaling cascades are critical for efficient



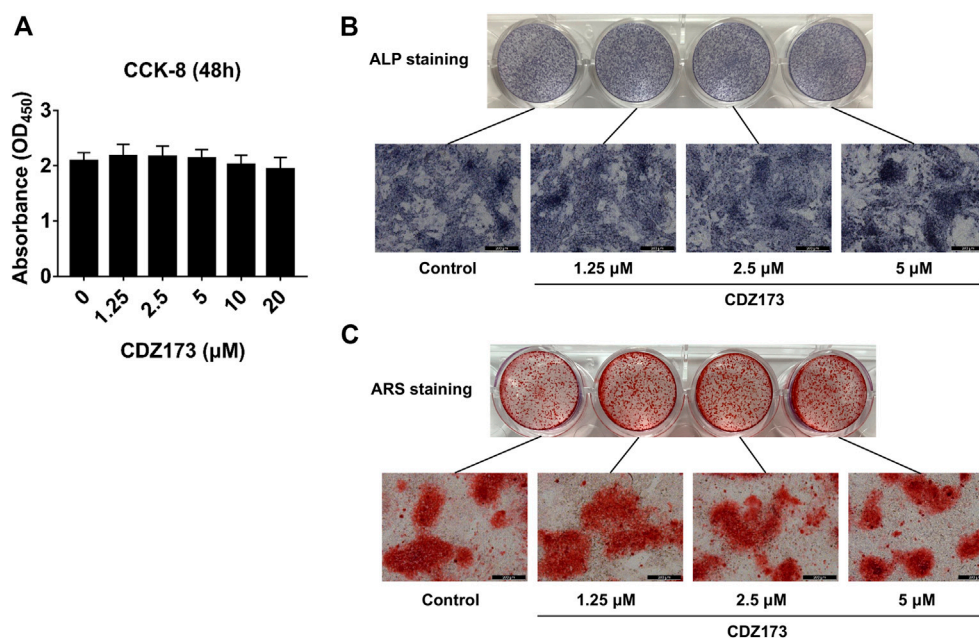


FIGURE 6

CDZ173 did not affect the differentiation and mineralization of osteoblasts. (A) For 48 h, BMSCs were exposed to the stated doses of CDZ173 before being evaluated using CCK-8 assays. (B) ALP staining in the absence or presence of CDZ173 (1.25, 2.5, and 5 µM) for 7 days (scale bar = 200 µM). (C) Alizarin Red S in the absence or presence of CDZ173 (1.25, 2.5, and 5 µM) for 21 days (scale bar = 200 µM).

activation of downstream nuclear transcription factors such as c-Fos and NFATc1, which is a direct downstream transcription factor of c-Fos target (Lin et al., 2020; Kim et al., 2021). As a crucial distal transcription factor, NFATc1 regulates the transcription of many osteoclast marker genes and promotes the formation, fusion, and resorption of osteoclasts. Our earlier results determined that CDZ173 affects the osteoclasts early signaling pathways MAPK and PI3K-AKT. Therefore, the role of CDZ173 in the late development of osteoclasts was observed with these added investigations. Our findings revealed that the expression of transcription factor NFATc1 in the nucleus of osteoclasts peaked on the third day, and the expression of c-Fos peaked on the fifth day (Figure 8A). In contrast, the expression of NFATc1 and c-Fos were significantly down-regulated in the group treated with CDZ173 (Figures 8B,C). The above results indicated that the blockade of early PI3K-AKT, ERK, and JNK signaling pathways by CDZ173 effectively inhibited the induction and transcriptional activities of c-Fos and NFATc1 proteins, thereby contributing to the anti-osteoclast effect of CDZ173 small molecules (Figure 9).

## Discussion

Osteoclasts are responsible for resorbing bone matrix, in which osteoblasts differentiate into osteocytes (Udagawa et al., 2021). Thus, the mutually beneficial interaction of these 2 cells

ensures that the structural integrity of skeletal tissue is kept in the best possible condition (Mediero and Cronstein, 2013). However, when osteoclasts are overactivated and gradually become dominant, bone resorption is more substantial than bone formation, leading to osteolytic diseases, including rheumatoid arthritis, periodontitis, aseptic sterility after joint replacement, and bone loss induced by prosthesis loosening (Zhu et al., 2021; Gao et al., 2022). Notably, joint replacement is still the most direct and effective surgery for patients with advanced bone disease. However, aseptic prosthesis loosening brought on by inflammatory osteolysis carried by postoperative periprosthetic infection is one of the main causes of joint replacement failure. It is still a difficulty faced by clinicians that also brings pain to patients and increases their economic burden (Liu et al., 2022). Bacterial endotoxin, which contaminates prostheses, has been identified as a significant factor in osteolysis caused by debris, as it enhances wear particle reactivity and its pro-inflammatory effects (Kandahari et al., 2016). Studies have shown that prosthetic loosening wear particles and bacterial product-related inflammatory responses activate the immune system to secrete pro-osteoclastogenic cytokines (Kandahari et al., 2016). This process enhances osteoclast recruitment and activity, ultimately promoting the dominance of bone resorption in bone metabolism, resulting in bone destruction in the periprosthetic area (Kandahari et al., 2016; Yan et al., 2018). Therefore, modulating abnormal osteoclast activity is an effective strategy to prevent inflammatory bone loss.

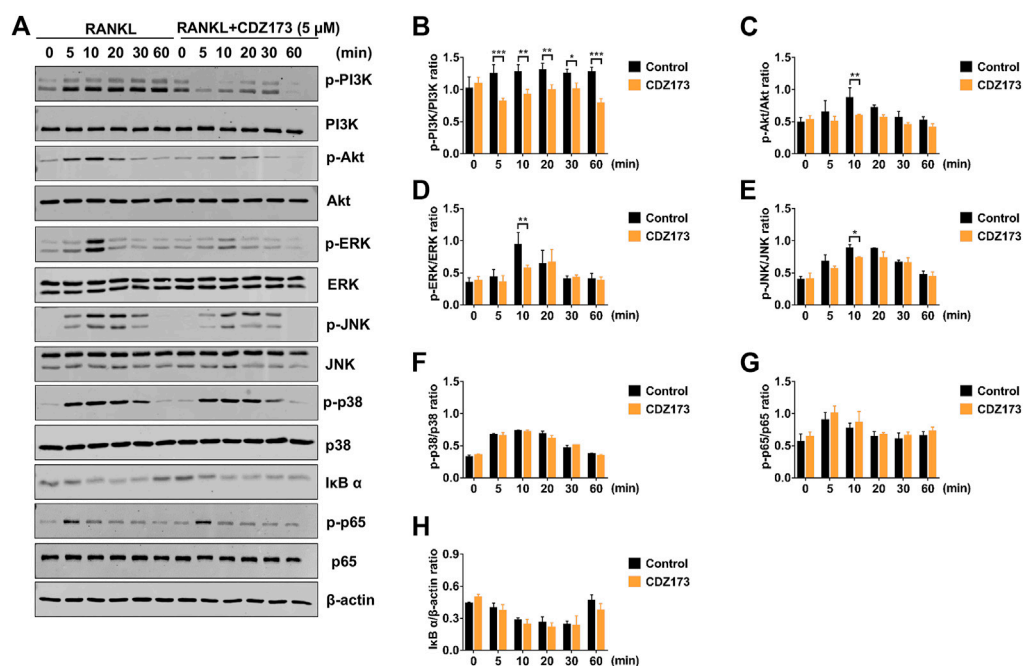


FIGURE 7

CDZ173 suppressed RANKL-induced PI3K-AKT and MAPKs but not NF- $\kappa$ B signaling pathways. (A) BMMs were pretreated for 4 h with or without 5 mM CDZ173, then stimulated for the given durations with RANKL (30 ng/ml). Cells were lysed, total proteins were extracted and subjected to western blot analysis using specific antibodies against p-PI3K, total PI3K, p-Akt, total Akt, p-ERK, total ERK, p-JNK, total JNK, p-p38, total p38, p-p65, total p65 and I $\kappa$ B $\alpha$ . Antibody against  $\beta$ -actin was used as internal loading control. The relative densitometry of protein bands for (B) p-PI3K/total PI3K, (C) p-AKT/total Akt, (D) p-ERK/total ERK, (E) p-JNK/total JNK, (F) p-p38/total p38, (G) p-p65/total p65, and (H) I $\kappa$ B $\alpha$ / $\beta$ -actin were quantified using ImageJ ( $n = 3$ ). (\* $p < 0.05$ , \*\* $p < 0.01$ , \*\*\* $p < 0.001$ ).

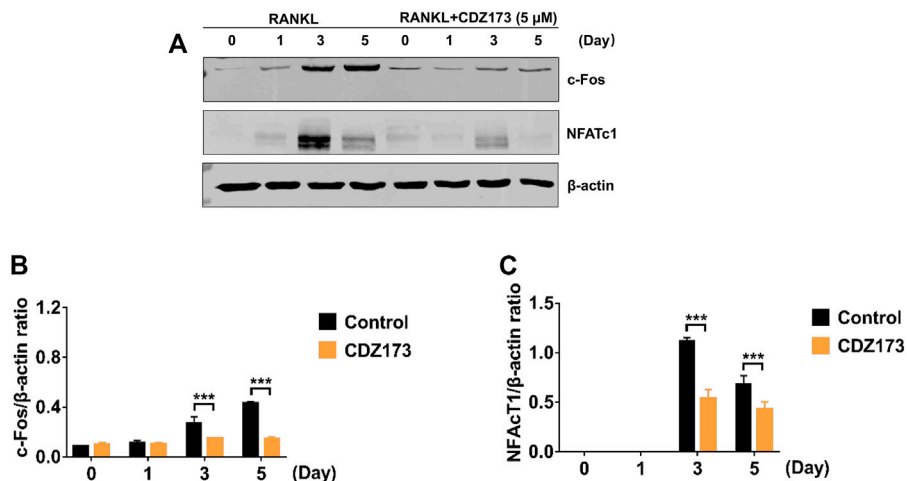


FIGURE 8

CDZ173 inhibited RANKL induced C-fos and NFATc1 transcriptional activity. (A) BMMs cultured with M-CSF(30 ng/ml) and RANKL (30 ng/ml) absence or presence of 5  $\mu$ M CDZ173 for 1, 3 or 5 days were lysed and total cellular protein extracts were subjected to western blot analysis using specific antibodies to NFATc1, c-Fos and  $\beta$ -actin. The relative densitometry of protein bands for (B) c-Fos and (C) NFATc1 against  $\beta$ -actin were quantified using ImageJ ( $n = 3$ ) (\*\* $p < 0.001$ ).

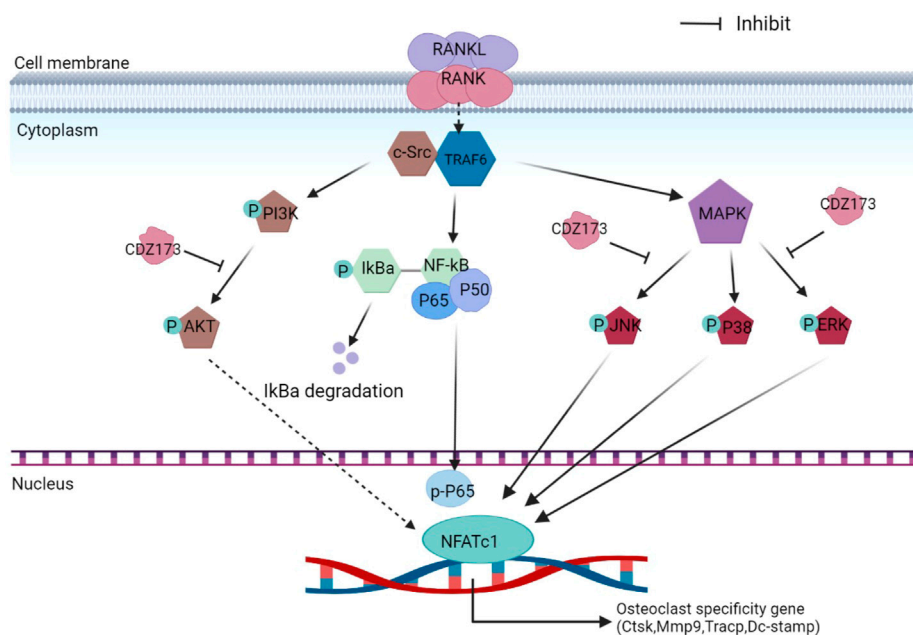


FIGURE 9

Schematic diagram of the suppressing influence of CDZ173 on the formation of osteoclasts.

Added compounds have been studied or developed for treating osteolytic diseases, including calcitonin, cathepsin-K inhibitors, bisphosphonates, anti-RANKL antibodies, and some Chinese herbal medicines (Miller, 2009; Kuritani et al., 2018; Wu et al., 2019). However, in some cases, there is still a risk of severe side effects, including the presence of cardiovascular events and nephrotoxicity. As a potent PI3K-selective small molecule inhibitor with suitable properties and efficacy, CDZ173 can be used as a therapeutic agent for immune-mediated diseases and is currently in clinical trials for APDS and primary Sjögren's syndrome (Rao et al., 2017; Jamee et al., 2020). In addition, oral CDZ173 has effectively decreased lymphocyte proliferation in clinical experimental studies (Rao et al., 2017). Furthermore, CDZ173 effectively inhibited the production of antigen-specific antibodies and alleviated disease symptoms in a rat collagen-induced arthritis model (Hoegenauer et al., 2017). These results indicate that CDZ173 has excellent anti-inflammatory properties, although it is unknown whether CDZ173 participates in inflammatory osteolysis. In the present study, we employed LPS to induce local osteolysis in the mice calvaria to mimic inflammation-induced bone loss disease. Micro-CT results showed that compared with the vehicle group, the BV/TV in the CDZ173-treated drug group was significantly increased, and the porosity also decreased, indicating a significant improvement in CDZ173 bone loss. At the same time, the TRAP staining of histological sections showed that the osteoclasts in the drug group were significantly reduced after CDZ173 treatment compared with the vehicle

group. Therefore, we demonstrate that the protective effect of CDZ173 against LPS-induced calvarial bone loss is by inhibiting osteoclast activation *in vivo*.

Osteoclasts play a central role in forming and regulating bone mass and are the main resorbing cells of bone (Boyce, 2013; Meng et al., 2022). The initial process of bone resorption is the attachment of osteoclasts to the bone matrix, resulting in polarization followed by a fold of the cytoplasm and membrane into the ruffled edge, which attaches to the bone surface and secretes H<sup>+</sup> through the proton pump on the ruffled edge (Takayanagi, 2021). The extracellular environment becomes acidified from these steps, thereby degrading the minerals of bone tissue, and its secreted cathepsin K degrades the bone matrix (Roodman, 1991; Takayanagi, 2021). Our *in vitro* osteoclast differentiation experiments showed that CDZ173 inhibited osteoclast differentiation in a concentration-dependent manner, and CDZ173 significantly inhibited the expression of osteoclast-specific genes. Then, we investigated the effect of CDZ173 on the resorption function of osteoclasts using bone-mimicking hydroxyapatite cell plates. The results showed that the bone resorption area of hydroxyapatite plates treated with CDZ173 was significantly reduced, suggesting that CDZ173 could inhibit the function of osteoclasts that lead to absorbing bone matrix. Meanwhile, we performed immunofluorescence staining experiments on the osteoclast podosomal actin belt, and the results found that the size of the podosomal actin belt was significantly reduced after CDZ173 treatment. At the same time, our ALP and AR

staining conclusively confirmed that CDZ173 does not affect osteoblasts *in vitro*.

RANKL is extremely important during osteoclastogenesis. Its combination with cognate receptor RANK recruits the adaptor protein TRAF6 to rapidly trigger a series of downstream signaling events, mainly NF- $\kappa$ B, MAPK, and PI3K-AKT, that drive osteoclast precursor cells to differentiate and fuse into multinucleated giant cells and subsequently exert bone resorption (An et al., 2019; Xin et al., 2020). Results have shown that PI3K-AKT signaling is essential in osteoclast differentiation and survival (Xin et al., 2020; Zhao et al., 2020). Briefly, the RANKL-RANK interaction can activate PI3K signaling molecules, which activate AKT to promote its phosphorylation to p-AKT, thereby activating the PI3K-AKT signaling pathway to enhance the expression of NFATc1 and nuclear export (Xin et al., 2020). Collectively, these steps promote the inhibition of osteoclast differentiation (Xin et al., 2020). A previous study showed that the inhibition of PI3K-AKT by the PI3K inhibitor LY294002 reduced osteoclast formation and attenuated the expression of the NFATc1 transcription factor (Zhao et al., 2020), suggesting that the PI3K-AKT-NFATc1 signaling axis is essential for RANKL-induced osteoclastogenesis. CDZ173 is a selective small-molecule PI3K inhibitor (Hoegenauer et al., 2017). To study how CDZ173 regulates osteoclast formation, we performed western blot experiments to analyze its effects on PI3K-AKT, NF- $\kappa$ B, and MAPK signaling pathways. First, we applied western blotting to detect whether CDZ173 affected the phosphorylation status of PI3K and AKT. The results in western blot analysis indicated that CDZ173 treatment significantly improved RANKL-induced activation of the PI3K-AKT pathway.

When RANKL is stimulated, the classic signaling pathways in osteoclasts that respond include NF- $\kappa$ B and MAPK (An et al., 2019; Guo et al., 2020). However, our protein band analysis results indicated that CDZ173 responded to RANKL stimulation but did not inhibit the activation of NF- $\kappa$ B. Treatment of cells with CDZ173 did not affect I $\kappa$ B $\alpha$  degradation, p65 phosphorylation, and NF- $\kappa$ B transcriptional activity. This indicated that the effect of CDZ173 on the formation of RANKL-stimulated osteoclasts was not achieved by acting on the NF- $\kappa$ B signaling pathway. Activation of three MAPK signaling pathways, JNK, p38, and ERK, is important in efficiently stimulating osteoclastogenesis. Notably, the ability of monocyte precursors produced from JNK1 or ERK1 mutant mice to develop into the osteoclast lineage is diminished (He et al., 2011; Sadangi et al., 2020). Furthermore, ERK is essential for osteoclast survival and cell polarity maintenance during bone resorption. JNK signaling is essential for controlling osteoclast development, differentiation, and apoptosis. In contrast, p38 signaling is mainly involved in osteoclast production rather than activity. In the current investigation, we discovered that CDZ173 strongly decreased the activation of ERK and JNK signaling, but had no discernible impact on the activation of p38. Additionally, CDZ173 dramatically reduced the expression of c-Fos and NFATc1 according to our western blotting results, and our RT-PCR results similarly

demonstrated that CDZ173 administration greatly reduced c-Fos and NFATc1 mRNA expression. The above results suggest that CDZ173 affects the formation of osteoclasts by inhibiting the activation of transcription factors c-Fos and NFATc1.

Collectively, we determined that CDZ173 attenuated LPS-induced calvarial bone loss and demonstrated this protective effect *in vitro* and *in vivo* due to CDZ173 inhibiting osteoclast activation without affecting osteoblast activation. Meanwhile, we demonstrated that CDZ173 inhibited osteoclast differentiation by downregulating the expression of Dc-stamp, Trap/Acp5, Mmp-9, and Ctsk genes by inhibiting RANKL-activated PI3K-AKT, ERK, and JNK signaling pathways *in vitro*. Combining the pharmacokinetics and safety evaluation of CDZ173 in clinical concept studies and the potential of CDZ173 for the treatment of immune diseases, we believe that CDZ173 is a promising drug for the treatment of osteoclast-mediated bone loss disease in the clinic.

## Data availability statement

The original contributions presented in the study are included in the article/Supplementary Material, further inquiries can be directed to the corresponding authors.

## Ethics statement

The animal study was reviewed and approved by Ethics Committee of the Xiamen University.

## Author contributions

All authors listed have made a substantial, direct, and intellectual contribution to the work and approved it for publication.

## Funding

This work was supported in part by National Key R&D Program of China (2020YFA0112900 to RX), National Natural Science Foundation of China (81972034, 92068104 to RX and 82002262 to NL) and Natural Science Foundation of Fujian Province (2022J06003 to RX).

## Acknowledgments

The authors thank AiMi Academic Services ([www.aimieditor.com](http://www.aimieditor.com)) for the English language editing and review services. The authors acknowledged all the members of our laboratory for the help. ZW, XL, XC, XH, NL, YC, LZ, ZL, BS, MY, GY, NC, and HF, carried out experiments, analyzed the data and GR prepared the



figures; ZW wrote the main manuscript, MZ, FX, and RX designed the study and revised the manuscript. All authors reviewed the manuscript.

## Conflict of interest

HF was employed by the Inner Mongolia Dairy Technology Research Institute Co. Ltd.

The authors declare that the research was conducted in the absence of any commercial or financial relationships that could be construed as a potential conflict of interest.

## References

- An, Y., Zhang, H., Wang, C., Jiao, F., Xu, H., Wang, X., et al. (2019). Activation of ROS/MAPKs/NF- $\kappa$ B/NLRP3 and inhibition of efferocytosis in osteoclast-mediated diabetic osteoporosis. *FASEB J. official Publ. Fed. Am. Soc. Exp. Biol.* 33, 12515–12527. doi:10.1096/fj.201802805RR
- Boyce, B. F. (2013). Advances in the regulation of osteoclasts and osteoclast functions. *J. Dent. Res.* 92, 860–867. doi:10.1177/0022034513500306
- Fang, C., He, M., Li, D., and Xu, Q. (2021). YTHDF2 mediates LPS-induced osteoclastogenesis and inflammatory response via the NF- $\kappa$ B and MAPK signaling pathways. *Cell. Signal.* 85, 110060. doi:10.1016/j.cellsig.2021.110060
- Fang, Q., Zhou, C., and Nandakumar, K. S. (2020). Molecular and cellular pathways contributing to joint damage in rheumatoid arthritis. *Mediat. Inflamm.* 2020, 3830212. doi:10.1155/2020/3830212
- Gao, X., Ge, J., Zhou, W., Xu, L., and Geng, D. (2022). IL-10 inhibits osteoclast differentiation and osteolysis through MEG3/IRF8 pathway. *Cell. Signal.* 95, 110353. doi:10.1016/j.cellsig.2022.110353
- Guo, J., Ren, R., Sun, K., Yao, X., Lin, J., Wang, G., et al. (2020). PERK controls bone homeostasis through the regulation of osteoclast differentiation and function. *Cell Death Dis.* 11, 847. doi:10.1038/s41419-020-03046-z
- Han, B., Geng, H., Liu, L., Wu, Z., and Wang, Y. (2020). GSH attenuates RANKL-induced osteoclast formation *in vitro* and LPS-induced bone loss *in vivo*. *Biomed. Pharmacother. = Biomedicine Pharmacother.* 128, 110305. doi:10.1016/j.biopha.2020.110305
- He, Y., Staser, K., Rhodes, S. D., Liu, Y., Wu, X., Park, S.-J., et al. (2011). Erk1 positively regulates osteoclast differentiation and bone resorptive activity. *PLoS one* 6, e24780. doi:10.1371/journal.pone.0024780
- Hoegenauer, K., Soldermann, N., Zécri, F., Strang, R. S., Graveleau, N., Wolf, R. M., et al. (2017). Discovery of CDZ173 (leniolisib), representing a structurally novel class of PI3K delta-selective inhibitors. *ACS Med. Chem. Lett.* 8, 975–980. doi:10.1021/acsmchemlett.7b00293
- Honma, M., Ikebuchi, Y., and Suzuki, H. (2021). Mechanisms of RANKL delivery to the osteoclast precursor cell surface. *J. Bone Min. Metab.* 39, 27–33. doi:10.1007/s00774-020-01157-3
- Jamee, M., Moniri, S., Zaki-Dizaji, M., Olbrich, P., Yazdani, R., Jadidi-Niaragh, F., et al. (2020). Clinical, immunological, and genetic features in patients with activated PI3K $\delta$  syndrome (APDS): A systematic review. *Clin. Rev. Allergy Immunol.* 59, 323–333. doi:10.1007/s12016-019-08738-9
- Kandahari, A. M., Yang, X., Laroche, K. A., Dighe, A. S., Pan, D., and Cui, Q. (2016). A review of UHMWPE wear-induced osteolysis: The role for early detection of the immune response. *Bone Res.* 4, 16014. doi:10.1038/boneres.2016.14
- Kim, I., Kim, J. H., Kim, K., Seong, S., Lee, K.-B., and Kim, N. (2021). IRF2 enhances RANKL-induced osteoclast differentiation via regulating NF- $\kappa$ B/NFATc1 signaling. *BMB Rep.* 54, 482–487. doi:10.5483/BMBRep.2021.54.9.070
- Kim, J.-M., Lin, C., Stavre, Z., Greenblatt, M. B., and Shim, J.-H. (2020). Osteoblast-osteoclast communication and bone homeostasis. *Cells* 9, E2073. doi:10.3390/cells9092073
- Krieger, N. S., Chen, L., Becker, J., DeBoyace, S., Wang, H., Favus, M. J., et al. (2020). Increased osteoclast and decreased osteoblast activity causes reduced bone mineral density and quality in genetic hypercalciuric stone-forming rats. *JBM plus* 4, e10350. doi:10.1002/jbm4.10350
- Kuritani, M., Sakai, N., Karakawa, A., Isawa, M., Chatani, M., Negishi-Koga, T., et al. (2018). Anti-mouse RANKL antibodies inhibit alveolar bone destruction in periodontitis model mice. *Biol. Pharm. Bull.* 41, 637–643. doi:10.1248/bpb.b18-00026
- Li, S., Liu, Q., Wu, D., He, T., Yuan, J., Qiu, H., et al. (2020). PKC- $\delta$  deficiency in B cells displays osteopenia accompanied with upregulation of RANKL expression and osteoclast-osteoblast uncoupling. *Cell Death Dis.* 11, 762. doi:10.1038/s41419-020-02947-3
- Lin, Y., Gu, Y., Zuo, G., Jia, S., Liang, Y., Qi, M., et al. (2020). [Zoledronate regulates osteoclast differentiation and bone resorption in high glucose through p38 MAPK pathway]. *Nan fang yi ke da xue xue bao = J. South. Med. Univ.* 40, 1439–1447. doi:10.1212/j.issn.1673-4254.2020.10.09
- Liu, X., Diao, L., Zhang, Y., Yang, X., Zhou, J., Mao, Y., et al. (2022). Piperlongumine inhibits titanium particles-induced osteolysis, osteoclast formation, and RANKL-induced signaling pathways. *Int. J. Mol. Sci.* 23, 2868. doi:10.3390/ijms23052868
- Ma, Y., Ran, D., Zhao, H., Song, R., Zou, H., Gu, J., et al. (2021). Cadmium exposure triggers osteoporosis in duck via P2X7/PI3K/AKT-mediated osteoblast and osteoclast differentiation. *Sci. Total Environ.* 750, 141638. doi:10.1016/j.scitotenv.2020.141638
- Mbalaviele, G., Novack, D. V., Schett, G., and Teitelbaum, S. L. (2017). Inflammatory osteolysis: A conspiracy against bone. *J. Clin. Invest.* 127, 2030–2039. doi:10.1172/JCI93356
- Mediero, A., and Cronstein, B. N. (2013). Adenosine and bone metabolism. *Trends Endocrinol. Metab.* 24, 290–300. doi:10.1016/j.tem.2013.02.001
- Meng, X., Zhang, W., Lyu, Z., Long, T., and Wang, Y. (2022). ZnO nanoparticles attenuate polymer-wear-particle induced inflammatory osteolysis by regulating the MEK-ERK-COX-2 axis. *J. Orthop. Transl.* 34, 1–10. doi:10.1016/j.jot.2022.04.001
- Miller, P. D. (2009). Denosumab: anti-RANKL antibody. *Curr. Osteoporos. Rep.* 7, 18–22. doi:10.1007/s11914-009-0004-5
- Qiu, Z., Li, L., Huang, Y., Shi, K., Zhang, L., Huang, C., et al. (2022). Puerarin specifically disrupts osteoclast activation via blocking integrin- $\beta$ 3 Pyk2/Src/Cbl signaling pathway. *J. Orthop. Transl.* 33, 55–69. doi:10.1016/j.jot.2022.01.003
- Rao, V. K., Webster, S., Dalm, V. A. S. H., Šedivá, A., van Hagen, P. M., Holland, S., et al. (2017). Effective “activated PI3K $\delta$  syndrome”-targeted therapy with the PI3K $\delta$  inhibitor leniolisib. *Blood* 130, 2307–2316. doi:10.1182/blood-2017-08-801191
- Ren, P.-G., Irani, A., Huang, Z., Ma, T., Biswal, S., and Goodman, S. B. (2011). Continuous infusion of UHMWPE particles induces increased bone macrophages and osteolysis. *Clin. Orthop. Relat. Res.* 469, 113–122. doi:10.1007/s11999-010-1645-5
- Roodman, G. D. (1991). Osteoclast differentiation. *Crit. Rev. Oral Biol. Med.* 2, 389–409. doi:10.1177/10454411910020030601
- Rossi, F., Tortora, C., Punzo, F., Bellini, G., Argenziano, M., Di Paola, A., et al. (2019). The endocannabinoid/endovanilloid system in bone: From osteoporosis to osteosarcoma. *Int. J. Mol. Sci.* 20, E1919. doi:10.3390/ijms20081919
- Sadangi, S., Mohanty, A., Paichha, M., and Samanta, M. (2020). Molecular characterization and expression analysis of two crucial MAPKs- jnk1 and erk1 as cellular signal transducers in Labeo rohita in response to PAMPs stimulation and pathogenic invasion. *J. Fish. Biol.* 96, 580–589. doi:10.1111/jfb.14244

The reviewer XQ declared a shared affiliation with the author FX at the time of review.

## Publisher's note

All claims expressed in this article are solely those of the authors and do not necessarily represent those of their affiliated organizations, or those of the publisher, the editors and the reviewers. Any product that may be evaluated in this article, or claim that may be made by its manufacturer, is not guaranteed or endorsed by the publisher.

Shao, S., Fu, F., Wang, Z., Song, F., Li, C., Wu, Z.-X., et al. (2019). Diosmetin inhibits osteoclast formation and differentiation and prevents LPS-induced osteolysis in mice. *J. Cell. Physiol.* 234, 12701–12713. doi:10.1002/jcp.27887

Takayanagi, H. (2021). RANKL as the master regulator of osteoclast differentiation. *J. Bone Min. Metab.* 39, 13–18. doi:10.1007/s00774-020-01191-1

Tan, Z., Cheng, J., Liu, Q., Zhou, L., Kenny, J., Wang, T., et al. (2017). Neohesperidin suppresses osteoclast differentiation, bone resorption and ovariectomized-induced osteoporosis in mice. *Mol. Cell. Endocrinol.* 439, 369–378. doi:10.1016/j.mce.2016.09.026

Udagawa, N., Koide, M., Nakamura, M., Nakamichi, Y., Yamashita, T., Uehara, S., et al. (2021). Osteoclast differentiation by RANKL and OPG signaling pathways. *J. Bone Min. Metab.* 39, 19–26. doi:10.1007/s00774-020-01162-6

Wang, J., Chen, G., Zhang, Q., Zhao, F., Yu, X., Ma, X., et al. (2019). Phillyrin attenuates osteoclast formation and function and prevents LPS-induced osteolysis in mice. *Front. Pharmacol.* 10, 1188. doi:10.3389/fphar.2019.01188

Wu, Z., Wu, H., Li, C., Fu, F., Ding, J., Shao, S., et al. (2019). Daphnetin attenuates LPS-induced osteolysis and RANKL mediated osteoclastogenesis through suppression of ERK and NFATc1 pathways. *J. Cell. Physiol.* 234, 17812–17823. doi:10.1002/jcp.28408

Xin, Y., Liu, Y., Liu, D., Li, J., Zhang, C., Wang, Y., et al. (2020). New function of RUNX2 in regulating osteoclast differentiation via the AKT/NFATc1/CTSK Axis. *Calcif. Tissue Int.* 106, 553–566. doi:10.1007/s00223-020-00666-7

Xing, Q., de Vos, P., Faas, M. M., Ye, Q., and Ren, Y. (2011). LPS promotes pre-osteoclast activity by up-regulating CXCR4 via TLR-4. *J. Dent. Res.* 90, 157–162. doi:10.1177/0022034510379019

Yan, Z., Tian, X., Zhu, J., Lu, Z., Yu, L., Zhang, D., et al. (2018). Metformin suppresses UHMWPE particle-induced osteolysis in the mouse calvaria by promoting polarization of macrophages to an anti-inflammatory phenotype. *Mol. Med.* 24, 20. doi:10.1186/s10020-018-0013-x

Yang, Y., Chung, M. R., Zhou, S., Gong, X., Xu, H., Hong, Y., et al. (2019). STAT3 controls osteoclast differentiation and bone homeostasis by regulating NFATc1 transcription. *J. Biol. Chem.* 294, 15395–15407. doi:10.1074/jbc.RA119.010139

Yu, W., Zhong, L., Yao, L., Wei, Y., Gui, T., Li, Z., et al. (2021). Bone marrow adipogenic lineage precursors promote osteoclastogenesis in bone remodeling and pathologic bone loss. *J. Clin. Invest.* 131, 140214. doi:10.1172/JCI140214

Zhan, Y., Liang, J., Tian, K., Che, Z., Wang, Z., Yang, X., et al. (2019). Vindoline inhibits RANKL-induced osteoclastogenesis and prevents ovariectomy-induced bone loss in mice. *Front. Pharmacol.* 10, 1587. doi:10.3389/fphar.2019.01587

Zhao, H., Sun, Z., Ma, Y., Song, R., Yuan, Y., Bian, J., et al. (2020). Antiosteoclastic bone resorption activity of osteoprotegerin via enhanced AKT/mTOR/ULK1-mediated autophagic pathway. *J. Cell. Physiol.* 235, 3002–3012. doi:10.1002/jcp.29205

Zhou, L., Song, F., Liu, Q., Yang, M., Zhao, J., Tan, R., et al. (2015). Berberine sulfate attenuates osteoclast differentiation through RANKL induced NF-κB and NFAT pathways. *Int. J. Mol. Sci.* 16, 27087–27096. doi:10.3390/ijms16125998

Zhou, Z., Chen, X., Chen, X., Qin, A., Mao, Y., Pang, Y., et al. (2020). PP121 suppresses RANKL-Induced osteoclast formation *in vitro* and LPS-Induced bone resorption *in vivo*. *Exp. Cell Res.* 388, 111857. doi:10.1016/j.yexcr.2020.111857

Zhu, F., Wang, J., Ni, Y., Yin, W., Hou, Q., Zhang, Y., et al. (2021). Curculigoside protects against titanium particle-induced osteolysis through the enhancement of osteoblast differentiation and reduction of osteoclast formation. *J. Immunol. Res.* 2021, 5707242. doi:10.1155/2021/5707242

Zhu, X., Gao, J., Ng, P. Y., Qin, A., Steer, J. H., Pavlos, N. J., et al. (2016). Alexidine dihydrochloride attenuates osteoclast formation and bone resorption and protects against LPS-induced osteolysis. *J. Bone Min. Res.* 31, 560–572. doi:10.1002/jbmr.2710



## OPEN ACCESS

## EDITED BY

Dongwei Zhang,  
Beijing University of Chinese Medicine,  
China

## REVIEWED BY

Dhanachandra Singh Khuraijam,  
Cleveland Clinic, United States  
Zhen-lin Zhang,  
Shanghai Jiao Tong University, China  
Jirong Ge,  
Fujian Academy of Traditional Chinese  
Medicine, China

## \*CORRESPONDENCE

Peng Duan,  
✉ 1347911177@163.com

## SPECIALTY SECTION

This article was submitted to Experimental  
Pharmacology and Drug Discovery,  
a section of the journal  
Frontiers in Pharmacology

RECEIVED 07 August 2022

ACCEPTED 28 December 2022

PUBLISHED 10 January 2023

## CITATION

Yang Z, Xuan S, Li W, Hu W, Tu P and  
Duan P (2023), Clinical application of the  
fracture risk assessment tool in the general  
population and its correlation with bone  
turnover markers.  
*Front. Pharmacol.* 13:1013483.  
doi: 10.3389/fphar.2022.1013483

## COPYRIGHT

© 2023 Yang, Xuan, Li, Hu, Tu and Duan.  
This is an open-access article distributed  
under the terms of the [Creative Commons  
Attribution License \(CC BY\)](https://creativecommons.org/licenses/by/4.0/). The use,  
distribution or reproduction in other  
forums is permitted, provided the original  
author(s) and the copyright owner(s) are  
credited and that the original publication in  
this journal is cited, in accordance with  
accepted academic practice. No use,  
distribution or reproduction is permitted  
which does not comply with these terms.

# Clinical application of the fracture risk assessment tool in the general population and its correlation with bone turnover markers

Zhi Yang<sup>1</sup>, Shu Xuan<sup>2</sup>, Weihong Li<sup>1</sup>, Wan Hu<sup>1</sup>, Ping Tu<sup>1</sup> and  
Peng Duan<sup>1\*</sup>

<sup>1</sup>Department of Endocrinology and Metabolism, The Third Hospital of Nanchang, Nanchang, China, <sup>2</sup>School of Physical Education, Liaoning Normal University, Dalian, China

**Objective:** To compare the risk of osteoporotic fractures between the urban and urban-rural fringe populations in southern China and to explore the effect of bone turnover markers on fracture risk.

**Methods:** Epidemiological investigations were conducted in the urban and urban-rural fringe areas of southern China in June 2018. Residents aged 40 years and over who signed informed consent forms were included. Physical examination and questionnaire collection were completed. Bone turnover markers (BTMs) including osteocalcin (OC) and beta cross-linked C-telopeptide of type 1 collagen ( $\beta$ -CTX) were tested. Bone mineral density (BMD) of the femoral neck and lumbar vertebrae 1–4 were measured using dual energy X-ray absorptiometry. Fracture risk assessment tool (FRAX) values were calculated to show the probability of major osteoporotic fracture (PMOF) and probability of hip fracture (PHF) over the next 10 years.

**Results:** A total of 1,051 participants were included in this study, including 553 in the urban areas and 498 in the urban-rural fringe areas. The average PMOF and PHF were 3.4 (2.3–5.4) % and .6 (.3–1.5) %, respectively. Compared with that in the urban populations, the femoral neck BMD in the urban-rural fringe populations was lower and FRAX values were generally higher, especially for women. FRAX values in various populations were mainly negatively correlated with lumbar and femoral neck BMD and were positively correlated with  $\beta$ -CTX; meanwhile, only PHF was negatively correlated with OC. After adjusting for sex, elevated  $\beta$ -CTX levels significantly increased the risk of high PMOF in various populations and increased the risk of high PHF in the urban-rural fringe populations. In particular, the risks of increased PMOF and PHF could increase by as much as 33 times and 19.5 times, respectively, in the urban-rural fringe areas.

**Conclusion:** The urban-rural fringe populations in Southern China may be at risk of osteoporotic fracture. In addition to being related to BMD, the FRAX value also correlates with some BTMs. Combining FRAX with BMD, and BTMs may better predict the fracture risk.

## KEYWORDS

osteoporotic fracture, fracture risk assessment tool, bone mineral density, bone turnover markers, the urban areas, the urban-rural fringe areas

## Introduction

One osteoporotic fracture occurs every 3 s worldwide. The latest epidemiological results on mainland China have revealed that, in the population aged  $\geq 40$  years, the prevalence of osteoporosis was 5.0% among men and 20.6% among women, and the prevalence of vertebral fractures was 10.5% and 9.7% among men and women, respectively. In the past 5 years, the prevalence of clinical fractures was 4.1% among men and 4.2% among women (Wang et al., 2021). These findings suggest that prevention of osteoporotic fractures should be emphasized at present. The fracture risk assessment tool (FRAX), recommended by the World Health Organization, has become popular worldwide. The FRAX is a computer-based algorithm that calculates the probability of a major osteoporotic fracture (PMOF) and the probability of a hip fracture (PHF) over the next 10 years (John et al., 2018). PMOF mainly includes clinical spine, forearm, hip or shoulder fractures. FRAX is most commonly used in patients with at least one clinical risk factor for osteoporotic fractures and is especially suitable for those who have never had a fracture in the past but have reduced bone mass.

However, the FRAX algorithm has several limitations. For example, it is only applicable to people aged 40–90 years and is not suitable for those who have been diagnosed with osteoporosis or treated for it, or patients suffering from fragility fractures. However, one of the advantages of FRAX is that the femoral neck bone mineral density (BMD) can be optionally input into the calculation model. This enables the FRAX to be used as a simple or self-screening tool for the general population. Therefore, it can be widely used in families, communities, or primary medical centers where BMD testing conditions are not available. In most areas, a PMOF  $\geq 20\%$  or PHF  $\geq 3\%$  indicates a high risk of osteoporotic fracture, which can be used as intervention thresholds to initiate anti-osteoporosis treatment. These thresholds are also recommended by the Diagnosis and Treatment Guidelines for Osteoporosis in China (Chinese Society of Osteoporosis and Bone Mineral Research, 2017).

Osteoporosis and osteoporotic fractures are associated with many environmental factors. With rapid urbanization in China, the living conditions and quality of life of citizens have greatly improved. It is worth noting that people's physical activity has gradually decreased, likely due to the change from heavy farm work to easy housework, and even a sedentary lifestyle. Changes in lifestyle inevitably lead to subtle changes in the characteristics of osteoporosis and its fractures. This cross-sectional study was conducted in two districts of Nanchang City, Jiangxi Province, Southern China. First, the Xihu District is located in the central area of Nanchang City. Urban residents have stable jobs and incomes, limited physical activities, complete social medical security, and rampant chronic diseases. Second, Qingshanhu District is located in an urban-rural fringe area. With the expansion of the urban scale in recent years, residents in the urban-rural fringe are no longer engaged in agricultural labor, and their lifestyle has changed dramatically, thus leading to an increase in chronic diseases.

Based on the difference between the urban populations and urban-rural fringe populations, this study aimed to compare the application characteristics of FRAX in the two populations, and add BMD and bone turnover markers (BTMs) for analysis, in order to better predict fracture risk.

## Materials and methods

The study was conducted in accordance with the Declaration of Helsinki (revised in 2013). The study protocol was approved by the ethics committee of the Third Hospital of Nanchang. Written informed consent was obtained from all the participants. This study is from the cooperation project of the International Osteoporosis Foundation (IOF) in China (IOFCJO-D001).

### Study design

This cross-sectional study was conducted in June 2018. First, we carried out this study in eight community health service centers (Nanpu, Shizi Street, Shengjinta, and Chaoyang communities in Xihu District, Jingdong Town, Hufang Town, Tangshan town, and Shanghai Road in Qingshanhu District), immediately trained researchers and prepared materials. Second, recruitment methods included posting advertisements on bulletin boards and WeChat groups as well as recruitment *via* telephone appointments. Third, all participants obtained full informed consent in the health service centers. Residents received an appointment form after confirming their identity and signing an informed consent form. Finally, residents provided their informed consent, appointment form, and ID card to the investigation site for registration and health examinations.

### Study population

The inclusion criteria were Han residents, aged 40–90 years old, regardless of sex, who voluntarily participated and signed informed consent. The exclusion criteria included people under the age of 40 or over 90, pregnant or lactating women, people with blood system diseases or X-ray allergy, people who refused any on-site examination, or those who refused to go to the hospital to check BMD. Finally, 1,051 participants were enrolled in the study, including 553 in the Xihu District and 498 in the Qingshanhu District.

### Questionnaire survey

The questionnaire mainly included the clinical risk factors used to calculate the FRAX values, such as name, age, sex, menopausal age of women, previous fracture (yes or no), parent fractured hip (yes or no), current smoking (yes or no), glucocorticoids use (yes or no), rheumatoid arthritis (yes or no), secondary osteoporosis (yes or no), and alcohol consumption of three or more units per day (yes or no).

### Physical examination

Trained researchers measured blood pressure, height, weight, and waist circumference at the survey site. Blood pressure was measured using five electronic sphygmomanometers (Omron, Kyoto, Japan) in a calm sitting position. Three standard measurements were carried out with an interval of at least 1 min, and the average of three measurements was taken for analysis. The height and weight of each participant were measured with calibrated instruments,



accurate to .1 cm and .1 kg respectively. Body mass index (BMI) was calculated using the following formula:  $BMI = \text{weight (kg)}/\text{height}^2 (\text{m}^2)$ . Waist circumference was measured with a soft ruler around the abdomen horizontally, accurate to .1 cm.

## Sample testing

Participants were required to take an oral glucose tolerance test (OGTT) on site after 8–10 h of fasting. However, those who had been diagnosed with diabetes or were taking antidiabetic drugs would be exempt from the OGTT. Fasting blood glucose (FBG), two-hour postprandial blood glucose (2hBG), blood urea nitrogen (BUN), serum creatinine (SCr), total cholesterol (CHOL), triglycerides (TG), high-density lipoprotein cholesterol (HDL-C), and low-density lipoprotein cholesterol (LDL-C) levels were measured using the same autoanalyzer (Roche, Basel, Switzerland). Biochemical indicators of bone metabolism were also measured, such as serum calcium (Ca) and phosphorus (P) levels (5,800, Beckman Coulter, California, United States), as well as serum 25-hydroxyvitamin D (25(OH)D), osteocalcin (OC), and beta-cross-linked C-telopeptide of type 1 collagen ( $\beta$ -CTX) concentrations (COBAS E602, Roche, Basel, Switzerland). OC and  $\beta$ -CTX are BTMs, that reflect bone formation and bone resorption, respectively.

Estimated glomerular filtration rate (eGFR) was calculated using the Chronic Kidney Disease Epidemiology Collaboration equation. According to the 1999 World Health Organization diagnostic criteria, glucose metabolism can be divided into normal glucose tolerance, prediabetes, and diabetes. According to the National Cholesterol Education Program (NCEP) Expert Panel on Detection, Evaluation, and Treatment of High Blood Cholesterol in Adults (Adult Treatment Panel III) criteria, dyslipidemia was defined as CHOL  $\geq 6.22$  mmol/L, HDL-C  $< 1.04$  mmol/L, LDL-C  $\geq 4.14$  mmol/L, and/or TG  $\geq 2.26$  mmol/L.

## BMD measurement

According to the appointment time arranged at the investigation site, the participants took their ID card and the appointment form to the Third Hospital of Nanchang for BMD examination, which was completed within 3 months. The BMD of the femoral neck and lumbar vertebrae 1–4 was measured using dual energy X-ray absorptiometry (DXA) (Medilink, Montpellier, France).

## FRAX assessment

By clicking on the website: <http://www.shef.ac.uk/FRAX>, and then selecting the language Chinese simplified, we entered the FRAX model to evaluate the fracture risk of people. After inputting the 11 clinical risk factors collected in the questionnaire, we selected BMD as “DMS/Medilink” and input the femoral neck BMD in item 12. Finally, on clicking the calculate button, we obtained the values of PMOF and PHF over the next 10 years.

## Statistical analyses

All trained persons input the questionnaires, BMD results, and FRAX values into the EpiData software (Odense, Denmark). After a

double-check, it was combined with the downloaded blood test results to form the final database.

All analyses were performed using the SAS 9.1 software (North Carolina, United States). Categorical variables are presented as numbers (proportions). Continuous variables are presented as means  $\pm$  standard deviations (SD) or medians (interquartile ranges), and all non-normally distributed data were logarithmically transformed. Student's t-test and chi-squared test were used to compare the means and proportions of residents in the two different districts. Spearman's correlation analysis and stepwise regression analysis were used to evaluate the correlation between FRAX values, and BMD, and BTMs. Logistic regression analysis was used to assess the effect of BTMs on fracture risks. The difference was statistically significant with  $p$ -value  $< .05$ .

## Results

### Characteristics of population

The mean age of the study population was  $59 \pm 8$  years. Of the participants, 76.2% were women, of which 84.6% were menopausal, and the mean menopausal age was  $49 \pm 4$  years. The prevalence of previous fractures, diabetes, and dyslipidemia were 19.9%, 13.8%, and 29.2%, respectively (Table 1).

Compared with the urban-rural fringe populations, the urban populations had a larger waist circumference (both in men and women), and more participants consumed three or more units of alcohol daily.

There were no differences in glucose metabolism and lipid metabolism; however, more people in the urban-rural fringe had decreased eGFR ( $< 90$  mL/min/1.73 m<sup>2</sup>) (Table 1).

### Comparison of BMD and FRAX values

The mean BMD of lumbar vertebrae 1–4 in all participants was  $.78 \pm .15$  g/cm<sup>2</sup> and that of the femoral neck was  $.77 \pm .13$  g/cm<sup>2</sup>. The average PMOF and PHF were 3.4 (2.3–5.4)% and .6 (.3–1.5)%, respectively.

There was no sex difference in the lumbar BMD between the two districts. The femoral neck BMD of urban-rural fringe females was lower than that of urban females (urban female:  $.76 \pm .12$  g/cm<sup>2</sup>, urban-rural fringe female:  $.73 \pm .12$  g/cm<sup>2</sup>,  $p = .002$ ), however, there was no difference in males (Table 2).

It was found that the 10-year probabilities of fractures in the urban-rural fringe areas were generally higher than those in the urban areas. However, these differences were mainly observed in females. The PMOF was 3.4 (2.4–5.1)% in urban females and 4.0 (2.6–6.7)% in urban-rural fringe females ( $p = .0003$ ), and the PHF was .5 (.2–1.2)% in urban females and .7 (.3–2.0)% in urban-rural fringe females ( $p < .0001$ ), respectively (Table 2).

### Comparison of biochemical indicators of bone metabolism

As a bone metabolism regulating hormone, the mean level of 25(OH)D in the whole population was  $54.63 \pm 16.74$  nmol/L. Serum

**TABLE 1 Comparison of population characteristics between the urban and urban-rural fringe areas.**

Variables	The whole population	The urban populations (1)	The urban-rural fringe populations (2)	p-value (1 vs. 2)
Numbers	1051	553	498	—
Age (years)	59 ± 8	58 ± 7	61 ± 9	<.0001
Female (n,%)	801 (76.2%)	429 (77.6%)	372 (74.7%)	.25
Postmenopausal women (n,%)	678 (84.6%)	362 (84.4%)	316 (84.9%)	.83
Menopausal age (years)	49 ± 4	49 ± 4	49 ± 4	.10
BMI (kg/m <sup>2</sup> )	24.06 ± 3.14	23.91 ± 3.11	24.24 ± 3.17	.10
Waist circumference (cm)				
Female	81.4 ± 9.3	83.2 ± 8.3	79.4 ± 10.0	<.0001
Male	85.8 ± 9.1	87.2 ± 8.3	84.4 ± 9.8	.02
Systolic pressure (mmHg)	126 (114–142)	126 (113–140)	127 (115–143)	.11
Diastolic pressure (mmHg)	78 ± 11	78 ± 11	78 ± 11	.30
Current smoking (n, %)	103 (10.4%)	48 (9.0%)	55 (12.1%)	.25
Alcohol consumption of three or more units per day (n, %)	136 (13.8%)	83 (15.5%)	53 (11.7%)	.007
Previous fracture (n, %)	209 (19.9%)	99 (17.9%)	110 (22.1%)	.09
Parent fractured hip (n, %)	115 (10.9%)	64 (11.6%)	51 (10.2%)	.49
Glucocorticoids use (n, %)	18 (1.7%)	9 (1.63%)	9 (1.81%)	.82
Rheumatoid arthritis (n, %)	91 (8.7%)	35 (6.3%)	56 (11.2%)	.005
Secondary osteoporosis (n, %)	36 (3.4%)	15 (2.7%)	21 (4.2%)	.18
FBG (mmol/L)	5.40 (4.96–5.90)	5.60 (5.28–6.07)	5.09 (4.65–5.60)	<.0001
2hBG (mmol/L)	6.74 (5.70–8.15)	6.74 (5.74–7.98)	6.73 (5.49–8.35)	.27
Glucose metabolism (n, %)				.82
Normal glucose tolerance	651 (61.9%)	341 (66.6%)	310 (62.25%)	
Prediabetes	255 (24.3%)	138 (25.0%)	117 (23.5%)	
Diabetes	145 (13.8%)	74 (13.4%)	71 (14.3%)	
BUN (mmol/L)	4.84 (4.07–5.76)	4.79 (4.10–5.72)	4.87 (4.07–5.79)	.63
SCr (μmol/L)	58 (49–68)	52 (45–61)	63 (57–75)	<.0001
eGFR (mL/min/1.73 m <sup>2</sup> )	129 (110–154)	147 (126–171)	115 (101–129)	<.0001
eGFR <90 mL/min/1.73 m <sup>2</sup> (n, %)	72 (7.3%)	18 (3.4%)	54 (11.9%)	<.0001
CHOL (mmol/L)	5.07 (4.48–5.70)	5.32 (4.68–5.97)	4.87 (4.29–5.41)	<.0001
HDL-C (mmol/L)	1.49 ± .36	1.55 ± .41	1.41 ± .29	<.0001
LDL-C (mmol/L)	2.91 (2.48–3.38)	2.98 (2.55–3.55)	2.80 (2.38–3.25)	<.0001
TG (mmol/L)	1.37 (.97–1.95)	1.33 (.94–1.93)	1.42 (1.01–1.96)	.05
Dyslipidemia (n, %)	302 (29.2%)	168 (31.3%)	134 (27.0%)	.13

BMI, body mass index; FBG, fasting blood glucose; 2hBG, two-hour postprandial blood glucose; BUN, blood urea nitrogen; SCr, serum creatinine; eGFR, estimated glomerular filtration rate; CHOL, total cholesterol; HDL-C, high-density lipoprotein cholesterol; LDL-C, low-density lipoprotein cholesterol; TG, triglycerides.

Ca and P, both biochemical markers, were 2.31 (2.23–2.38) and 1.04 (.92–1.15) mmol/L, respectively. The average levels of OC and  $\beta$ -CTX were 11.20 (9.00–14.60) and .22 (.16–.31) ng/mL, respectively.

In female participants, higher 25(OH)D and lower serum P concentrations were found in the urban-rural fringe areas than

those in the urban areas. For both males and females, the levels of serum Ca and the bone resorption marker  $\beta$ -CTX in the urban-rural fringe were lower than those in the urban areas. As a marker of bone formation, OC showed no difference between the two different areas (Table 3).

**TABLE 2 Comparison of BMD and FRAX values between the urban and urban-rural fringe females and males.**

Variables		The urban populations	The urban-rural fringe populations	<i>p</i> -value
Lumbar BMD (g/cm <sup>2</sup> )	All	.78 ± .15	.80 ± .15	.05
	Female	.76 ± .14	.77 ± .15	.10
	Male	.85 ± .15	.87 ± .15	.42
femoral neck BMD (g/cm <sup>2</sup> )	All	.78 ± .13	.75 ± .13	.0008
	Female	.76 ± .12	.73 ± .12	.002
	Male	.82 ± .15	.79 ± .13	.10
PMOF (%)	All	3.3 (2.3–5.0)	3.6 (2.5–6.1)	.002
	Female	3.4 (2.4–5.1)	4.0 (2.6–6.7)	.0003
	Male	2.9 (1.9–4.7)	2.9 (1.9–4.3)	.72
PHF (%)	All	.6 (.3–1.2)	.8 (.3–1.9)	<.0001
	Female	.5 (.2–1.2)	.7 (.3–2.0)	<.0001
	Male	.7 (.3–1.7)	.9 (.4–1.6)	.44

BMD, bone mineral density; FRAX, fracture risk assessment tool; PMOF, probability of a major osteoporotic fracture; PHF, probability of hip fracture; Lumbar BMD, was the BMD, of lumbar vertebrae 1–4.

**TABLE 3 Comparison of biochemical indicators of bone metabolism between the urban and urban-rural fringe females and males.**

Variables		The urban populations	The urban-rural fringe populations	<i>p</i> -value
25(OH)D (nmol/L)	All	52.60 ± 15.55	56.78 ± 17.69	<.0001
	Female	50.24 ± 14.26	53.95 ± 15.21	.0006
	Male	60.38 ± 17.08	65.17 ± 21.52	.06
Ca (mmol/L)	All	2.34 (2.28–2.40)	2.27 (2.15–2.35)	<.0001
	Female	2.34 (2.28–2.40)	2.27 (2.16–2.35)	<.0001
	Male	2.33 (2.27–2.39)	2.27 (2.14–2.35)	<.0001
P (mmol/L)	All	1.05 (.94–1.16)	1.03 (.90–1.13)	.04
	Female	1.08 (.98–1.18)	1.06 (.94–1.14)	.04
	Male	.96 (.85–1.05)	.92 (.83–1.07)	.82
OC (ng/mL)	All	11.20 (9.10–14.70)	14.40 (11.30–18.35)	.46
	Female	12.20 (9.60–15.1)	11.90 (9.40–15.20)	.40
	Male	9.55 (8.00–11.60)	9.90 (7.90–11.90)	.74
β-CTX (ng/mL)	All	.24 (.16–.34)	.20 (.15–.27)	<.0001
	Female	.24 (.17–.35)	.21 (.15–.27)	<.0001
	Male	.22 (.16–.33)	.18 (.14–.25)	.0004

25(OH)D, 25-hydroxyvitamin D; Ca, calcium; P, phosphorus; OC, osteocalcin; β-CTX, beta cross-linked C-telopeptide of type 1 collagen. 25(OH)D was bone metabolism regulating hormone, Ca and P were biochemical markers, OC, and β-CTX, were bone turnover markers.

## Correlation of FRAX values with BMD and BTMs

Spearman's correlation analysis and stepwise regression analysis were performed, with PMOF and PHF as dependent variables and lumbar BMD, femoral neck BMD, 25(OH)D, Ca, P, OC, and β-CTX as independent variables.

The results in the whole population suggested that PMOF was negative correlated with lumbar and femoral neck BMD and serum

Ca levels and was positively correlated with β-CTX. Meanwhile, PHF was negatively correlated with lumbar and femoral neck BMD, Ca, P, and OC, and positively correlated with 25(OH)D and β-CTX (Table 4).

In urban residents, it was verified that PMOF was still negatively correlated with lumbar and femoral neck BMD and was positively correlated with β-CTX. PHF was mostly negatively correlated with femoral neck BMD, P, and OC and was positively correlated with 25(OH)D and β-CTX (Table 5).

**TABLE 4 Spearman's correlation and stepwise regression analysis of BMD and BTMs associated with FRAX values in the whole population.**

Variables	Log PMOF				Log PHF			
	r	p-value	$\beta$	p-value	r	p-value	$\beta$	p-value
Lumbar BMD	-.92881	<.0001	-.24909	<.0001	-1.77831	<.0001	-.20207	.02
femoral neck BMD	-1.40352	<.0001	-1.14035	<.0001	-3.46985	<.0001	-3.35254	<.0001
25(OH)D	-.00106	.03			.00025184	.79	.0028	<.0001
Log Ca	-.50715	.049	-.6541	.0008	-.63647	.20	-.80704	.01
Log P	.26713	.02			-.09657	.22	-.4259	.003
Log OC	.24826	<.0001			.28631	.005	-.28767	.0003
Log $\beta$ -CTX	.20441	<.0001	.1078	.0007	.3295	<.0001	.28542	<.0001

**TABLE 5 Spearman's correlation and stepwise regression analysis of BMD and BTMs associated with FRAX values in the urban populations.**

Variables	Log PMOF				Log PHF			
	r	p-value	$\beta$	p-value	r	p-value	$\beta$	p-value
Lumbar BMD	-.87381	<.0001	-.17321	.01	-1.78078	<.0001		
femoral neck BMD	-1.29793	<.0001	-1.12035	<.0001	-3.47346	<.0001	-3.47492	<.0001
25(OH)D	-.00062731	.37			.00020021	.88	.00234	.002
Log Ca	-.09876	.88			-.69853	.58		
Log P	.36015	.02			-.13979	.64	-.55791	.001
Log OC	.36784	<.0001			.46207	.001	-.25806	.009
Log $\beta$ -CTX	.23765	<.0001	.0734	.04	.39484	<.0001	.2746	<.0001

**TABLE 6 Spearman's correlation and stepwise regression analysis of BMD and BTMs associated with FRAX values in the urban-rural fringe populations.**

Variables	Log PMOF				Log PHF			
	r	p-value	$\beta$	p-value	r	p-value	$\beta$	p-value
Lumbar BMD	-1.04519	<.0001	-.39863	<.0001	-1.88396	<.0001	-.33024	.02
femoral neck BMD	-1.55624	<.0001	-1.18325	<.0001	-3.42995	<.0001	-3.25238	<.0001
25(OH)D	-.00174	.01			-.00041299	.75		
Log Ca	-.38825	.22	-.74778	.002	-.03454	.95		
Log P	.21618	.19			.03064	.92		
Log OC	.14386	.06			.16162	.26	-.45505	.0007
Log $\beta$ -CTX	.22383	.0004	.21629	.0005	.39610	.001	.4088	.0003

In the urban-rural fringe areas, we found that PMOF was negatively correlated with BMD and Ca and was positively correlated with  $\beta$ -CTX. PHF was negatively correlated with BMD and OC was positively correlated with  $\beta$ -CTX (Table 6).

In summary, FRAX values in various populations were mainly negatively correlated with lumbar and femoral neck BMD and were positively correlated with  $\beta$ -CTX. In addition, PHF and OC were negatively correlated in all participants.

## Effect of BTMs on fracture risks

Further logistic regression analysis was performed to evaluate the effect of BTMs on FRAX values. The dependent variable was increased fracture risk. However, only .4% of the participants reached the threshold level of PMOF  $\geq 20\%$ , and 10.7% reached a PHF  $\geq 3\%$ . Instead, we uniformly defined the increased risk as the FRAX values reaching the upper 1/3 of PMOF or PHF. The independent variables



**TABLE 7 Odds ratios for having increased PMOF by different BTMs after adjusting for sex.**

Variables	Increased PMOF					
	The whole population		The urban populations		The urban-rural fringe populations	
	OR (95% CI)	<i>p</i> -value	OR (95% CI)	<i>p</i> -value	OR (95% CI)	<i>p</i> -value
25(OH)D	.990 (.981–.999)	.04	.990 (.977–1.003)	.12	.984 (.970–.998)	.03
Ca	.603 (.334–1.089)	.09	.157 (.017–1.415)	.10	2.093 (.901–4.860)	.09
P	1.533 (.525–3.759)	.35	1.891 (.524–6.827)	.33	.442 (.116–1.685)	.23
OC	1.026 (.989–1.065)	.16	1.018 (.966–1.073)	.51	.976 (.925–1.030)	.38
$\beta$ -CTX	3.976 (1.066–14.831)	.04	5.802 (1.071–31.444)	.04	34.024 (2.642–438.133)	.007

OR, odds ratio; CI, confidence interval. The thresholds of increased PMOF, were higher than 4.6% in the whole population, higher than 4.2% in the urban populations, and higher than 5.0% in the urban-rural fringe populations. All models were adjusted for sex.

**TABLE 8 Odds ratios for having increased PHF by different BTMs after adjusting for sex.**

Variables	Increased PHF					
	The whole population		The urban populations		The urban-rural fringe populations	
	OR (95% CI)	<i>p</i> -value	OR (95% CI)	<i>p</i> -value	OR (95% CI)	<i>p</i> -value
25(OH)D	.994 (.986–1.003)	.22	1.002 (.989–1.015)	.78	.989 (.976–1.022)	.11
Ca	.707 (.392–1.274)	.25	.234 (.026–2.143)	.20	1.133 (.519–2.473)	.75
P	1.085 (.443–2.653)	.86	1.322 (.358–4.880)	.68	.805 (.221–2.935)	.74
OC	1.027 (.990–1.065)	.16	1.060 (1.005–1.118)	.03	.989 (.938–1.044)	.69
$\beta$ -CTX	3.685 (.994–13.654)	.05	4.904 (.906–26.553)	.07	20.484 (1.707–245.826)	.02

The thresholds of increased PHF, were higher than 1.1% in the whole population, higher than .9% in the urban populations, and higher than 1.4% in the urban-rural fringe populations. All models were adjusted for sex.

were 25(OH)D, Ca, P, OC, and  $\beta$ -CTX levels. Based on the different prevalence and characteristics of osteoporosis in men and women, all the models were adjusted for sex.

First, the thresholds of increased PMOF were higher than 4.6% in the whole population, higher than 4.2% in the urban areas, and higher than 5.0% in the urban-rural fringe areas. In various populations, elevated  $\beta$ -CTX levels significantly increased the risk of major osteoporotic fractures, and even increased the risk by up to 33 times in the urban-rural fringe areas [odds ratios (ORs), 95% confidence intervals (CIs) = 3.976 (1.066–14.831), 5.802 (1.071–31.444), and 34.024 (2.642–438.133) in the whole population and urban and urban-rural fringe populations, respectively]. However, OC levels had no statistical effect on high PMOF. In addition, among other markers, only elevated 25(OH)D levels slightly reduced the risk of high PMOF by 1%–1.6% in the whole population and urban-rural fringe populations (Table 7).

Moreover, the thresholds of increased PHF were higher than 1.1% in the whole population, higher than .9% in the urban areas, and higher than 1.4% in the urban-rural fringe areas. After adjustment for sex,  $\beta$ -CTX was no longer significant for high PHF in the overall and urban populations. However, it is worth mentioning that the increase in  $\beta$ -CTX dramatically increased this risk by nearly 19.5 times in the urban-rural fringe areas [OR (95% CI) = 20.484 (1.228–16.471)],

suggesting that  $\beta$ -CTX is extremely important for the early warning of this population (Table 8).

## Discussion

According to the degree of BMD reduction, low bone mass is usually defined as 1–2.5 SD lower than the average peak bone mass of healthy adults of the same sex and race. There are many people with low bone mass in China, who fall into the high-risk group for the development of osteoporosis. Epidemiological data revealed that the prevalence of low bone mass in China is 32.9% in people aged 40–49 years, including 31.2% in the urban areas and 33.9% in the rural areas, and is 46.4% in people over 50 years of age, including 45.4% in the urban areas and 46.9% in the rural areas (Chinese Society of Osteoporosis and Bone Mineral Research, 2019). This report suggests that there are more people with low bone mass in rural China, and the risk of osteoporosis tends to be higher. The latest survey confirms this finding (Wang et al., 2021). The prevalence of osteoporosis was higher in the rural areas (22.3%) than that in the urban areas (17.3%) ( $p < .001$ ) among females, and the prevalence of vertebral fracture was significantly higher among males in the rural areas (11.8%) than that in the urban areas (8.2%) ( $p = .008$ ). In the past 5 years, the prevalence of clinical fractures in the urban and rural areas

was similar, both among males and females. In addition, rural residence has become a new risk factor (other factors include well-known factors such as female sex, older age, lower BMI, smoking, etc.), which is significantly associated with lower BMD in the lumbar spine (L1 to L4). With the promotion of new rural construction and urban expansion, the urban-rural fringe areas have become a new focus, with particular interest being paid to the disease characteristics of the population. In other words, with a sharp decline in physical activity, a gradually urbanized lifestyle, and a fast-growing economy, residents in the urban-rural fringe areas are more likely to suffer from various chronic non-communicable diseases without knowing.

Consistent with the above epidemiological findings, this study showed that the average femoral neck BMD of urban-rural fringe residents was lower than that of urban residents, suggesting that the urban-rural fringe populations, especially females, might be a potential contributor to osteoporosis. According to the comparison between the groups, central obesity, alcohol consumption, high FBG and cholesterol levels were more common in the urban areas, and people in the urban-rural fringe areas seemed to be healthier. However, in the case of no difference in fracture history between the groups, bone and joint discomfort was more obvious in the urban-rural fringe populations (such as more self-reported rheumatoid arthritis), which indirectly reflected that they might be in the stage of low bone mass or pre-osteoporosis. However, this is insufficient. We did not collect information on diets rich in calcium and vitamin D supplementation, outdoor activity time, or frequency of falls, resulting in no comparison of more osteoporosis risk factors between the two groups. In addition, these two results deserve public attention. First, the calculated probability of osteoporotic fracture in the urban-rural fringe participants (mainly females) was generally higher than that of urban residents. It is urgent to strengthen the early screening and intervention of osteoporosis in the urban-rural fringe areas and to improve the prevention and control of osteoporosis in primary health institutions. Second, our results showed that FRAX values were generally at a relatively low level in the general population, and the number of people with PMOF  $\geq 20\%$  or PHF  $\geq 3\%$  was very small. Does this mean that our population is not at a high risk of osteoporosis fractures? Alternatively, does this mean that the FRAX value has no significance in predicting fractures? Probably not. Although affected by multiple comorbidities, FRAX can significantly discriminate the fracture risk of non-dialysis patients with chronic kidney disease, especially major osteoporotic fractures (Whitlock et al., 2019). In another study (Wu et al., 2022), 51.8% of 164 hemodialysis patients had a high risk of fractures according to the FRAX threshold. It was also found that a high risk of fractures based on FRAX was independently associated with all-cause mortality. However, the FRAX thresholds are not compatible between countries and regions. FRAX is also believed to underestimate the fracture probability in some cases, such as in individuals with prior fractures (Wu et al., 2014). Therefore, more factors need to be combined with FRAX to assess the risk. On the one hand, we defined the upper 1/3 of the FRAX value as a high risk of fracture, and on the other hand, we integrated BMD and BTMs into fracture risk assessment.

Stepwise regression analysis confirmed that FRAX fracture probability was negatively correlated not only with femoral neck BMD (included in the algorithm) but also with lumbar BMD. Therefore, BMD of any traditional load-bearing bone should be considered. At the same time, the FRAX value combined with

BMD is superior to clinical risk factors or isolated BMD in predicting fractures (Wu et al., 2014), therefore, it may be prudent to combine the BMD of the lumbar vertebrae and femoral neck with the FRAX calculation. In addition, BTMs are another osteoporosis factors used in this study, including the bone formation marker OC and the bone resorption marker  $\beta$ -CTX. Stepwise regression analysis revealed that FRAX fracture probability was positively correlated with  $\beta$ -CTX, and PHF was additionally negatively correlated with OC in different populations. Through logistic regression analysis, we further observed that the increase in  $\beta$ -CTX levels significantly increased the risk of high PMOF in all models and increased the risk of high PHF in the urban-rural fringe populations, regardless of sex. No effect of OC was observed. At present, BTMs are not included in the FRAX algorithm, and official claims that BTMs predict fractures independently of BMD are uncertain. It was found to be independent in some studies (Gerdhem et al., 2004; Meier et al., 2005; Yoon and Yu, 2018), but not in all studies (Garnero et al., 2002; Bauer et al., 2009; Vilaca et al., 2017; Han et al., 2022). There is an inherent negative correlation between BTMs and BMD (either the femoral neck or lumbar vertebrae BMD). With the increase in age and the decline in estrogen levels in postmenopausal women, bone turnover becomes stronger (Jia and Cheng, 2022). Our study also found that BTMs and BMD could enter the multiple stepwise regression equation and had an impact on FRAX fracture risk. However, we did not observe any effect of BTMs independently of BMD. Therefore, whether the association between BTMs and fracture risk is affected by BMD cannot be determined, and BTMs cannot be included in the FRAX calculation as a risk factor (McCloskey et al., 2011).

Nevertheless, International Osteoporosis Foundation and International Federation of Clinical Chemistry and Laboratory Medicine (IOF-IFCC) points out that BTMs, especially bone resorption markers, have a certain practicability in predicting fractures. However, it is difficult to draw a clear conclusion because various BTMs were measured, different fracture sites were included, and the groupings of BTMs were inconsistent in previous studies (Vasikaran et al., 2011). Our study also found that the correlation analysis results of multiple biochemical indicators of bone metabolism were inconsistent. Compared with bone formation markers and other biochemical indicators, the correlation between the bone resorption marker  $\beta$ -CTX and fracture risk was clearer, which was consistent with the results of previous studies (Vasikaran et al., 2011). In addition, elevated  $\beta$ -CTX levels could significantly increase the risk of osteoporotic fractures by nearly 20–35 times in the urban-rural fringe areas, although the average  $\beta$ -CTX levels in males and females in this area were not high. These figures suggest that the increase in  $\beta$ -CTX would make the urban-rural fringe populations extremely vulnerable to osteoporosis and fractures. Therefore, after screening high-risk participants for fractures by FRAX, attention should be paid to the examination of  $\beta$ -CTX and BMD, which will contribute to the timeliness and effectiveness of early intervention.

In our study, OC was negatively correlated with PHF in all populations; however, we did not identify the effect of OC levels on the high fracture risk. IOF-IFCC recommends serum type I procollagen amino-terminal peptide (s-PINP) as the preferred bone formation marker (Vasikaran et al., 2011); however, OC is not only a bone formation marker but also an important metabolically active hormone involved in regulating glucose and lipid metabolism (Fukumoto and Martin, 2009; Magni et al., 2016; Dirckx et al.,

2019; Cipriani et al., 2020). Recent study found that low OC levels in circulation increase the risk of incident diabetes and diabetic kidney disease (DKD) (Ye et al., 2022). As a representative metabolic disease, diabetes is a prominent risk factor for osteoporosis and related fractures. Therefore, some scholars believe that diabetes is not sufficiently included in the FRAX algorithm (Chinese Society of Osteoporosis and Bone Mineral Research, 2017). In brief, OC is negatively correlated with PHF (although not strong enough) and also plays an endocrine role of bone in metabolic diseases (Ye et al., 2022); therefore, it can be hypothesized that low OC levels may generate additional predictive values under dual exposure.

In summary, IOF-IFCC recognizes the role of BTMs in the management of osteoporosis and believes that BTMs have good application prospects for fracture prediction and treatment monitoring (McCloskey et al., 2011). However, the popularity of BTMs testing in China is not sufficient and may become an area of interest in the future. In addition, our current evidence also suggests that it is necessary to combine FRAX with BMD and BTMs for a more ideal fracture prediction. The main limitation was the insufficient number of males recruited for the study, which may be due to the relatively low prevalence of osteoporosis in the male population, leading to their unwillingness to complete BMD measurements in hospital. Therefore, the difference in various parameters among men may not be accurately observed because of the insufficient proportions.

## Conclusion

In this study, the probability of a major osteoporotic fracture and hip fracture in the urban-rural fringe populations (especially females) within 10 years was higher than that in the urban populations, suggesting that urban-rural fringe residents in southern China may be at risk of osteoporosis and related fractures. In addition to being related to BMD, the FRAX value also correlates with some BTMs. For example, OC levels were negatively correlated with the probability of hip fracture and high  $\beta$ -CTX levels significantly increased the risk of osteoporotic fractures, especially in the urban-rural fringe populations. Therefore, we need to combine FRAX with BMD and BTMs to better predict the risk of fracture.

## Data availability statement

The raw data supporting the conclusion of this article will be made available by the authors, without undue reservation.

## References

- Bauer, D. C., Garnero, P., Harrison, S. L., Cauley, J. A., Eastell, R., Ensrud, K. E., et al. (2009). Biochemical markers of bone turnover, hip bone loss, and fracture in older men: The MrOS study. *J. Bone. Min. Res.* 24 (12), 2032–2038. doi:10.1359/jbmr.090526
- Chinese Society of Osteoporosis and Bone Mineral Research (2019). Epidemiological results of osteoporosis in China and the results of “healthy bones” special action. *Chin. J. Osteoporos. Bone. Min. Res.* 12 (3), 317–318. doi:10.3969/j.issn.1674-2591.2019.04.001
- Chinese Society of Osteoporosis and Bone Mineral Research (2017). Guidelines for diagnosis and management of primary osteoporosis (2017). *Chin. J. Osteoporos.* 10 (5), 413–443. doi:10.3969/j.issn.1006-7108.2019.03.001
- Cipriani, C., Colangelo, L., Santori, R., Renella, M., Mastrantonio, M., Minisola, S., et al. (2020). The Interplay between bone and glucose metabolism. *Front. Endocrinol. (Lausanne)*. 11, 122. doi:10.3389/fendo.2020.00122
- Dirckx, N., Moorers, M. C., Clemens, T. L., and Riddle, R. C. (2019). The role of osteoblasts in energy homeostasis. *Nat. Rev. Endocrinol.* 15 (11), 651–665. doi:10.1038/s41574-019-0246-y
- Fukumoto, S., and Martin, T. J. (2009). Bone as an endocrine organ. *Trends. Endocrinol. Metab.* 20 (5), 230–236. doi:10.1016/j.tem.2009.02.001
- Garnero, P., Cloos, P., Sornay-Rendu, E., Qvist, P., and Delmas, P. D. (2002). Type I collagen racemization and isomerization and the risk of fracture in postmenopausal women: The OFELY prospective study. *J. Bone. Min. Res.* 17 (5), 826–833. doi:10.1359/jbmr.2002.17.5.826
- Gerdhem, P., Ivaska, K. K., Alatalo, S. L., Halleen, J. M., Hellman, J., Isaksson, A., et al. (2004). Biochemical markers of bone metabolism and prediction of fracture in elderly women. *J. Bone. Min. Res.* 19 (3), 386–393. doi:10.1359/JBMR.0301244

## Ethics statement

The studies involving human participants were reviewed and approved by the ethics committee of the Third Hospital of Nanchang. The patients/participants provided their written informed consent to participate in this study.

## Author contributions

All authors critically reviewed the manuscript and contributed to conception, design and implementation of the protocol. ZY, PD, and PT had involved in drafting the manuscript or revising it critically.

## Funding

This work was supported by the Key Research and Development Programs of Jiangxi Province (Nos 20171BBG70058 and 20171ACH80002), the National Natural Science Foundation of China (No. 81760153), the Science and Technology Support Project of Nanchang City (No (2020)133), and the Science and Technology Plan Project of Health Commission of Jiangxi Provincial (No 202311273).

## Acknowledgments

The authors thank the field workers for their contribution and the participants for their cooperation.

## Conflict of interest

The authors declare that the research was conducted in the absence of any commercial or financial relationships that could be construed as a potential conflict of interest.

## Publisher's note

All claims expressed in this article are solely those of the authors and do not necessarily represent those of their affiliated organizations, or those of the publisher, the editors and the reviewers. Any product that may be evaluated in this article, or claim that may be made by its manufacturer, is not guaranteed or endorsed by the publisher.

- Han, M. S., Lee, G. J., Lee, S. K., Lee, J. K., and Moon, B. J. (2022). Clinical application of bone turnover markers in treating osteoporotic vertebral compression fractures and their role in predicting fracture progression. *Med. Baltim.* 101 (32), e29983. doi:10.1097/MD.00000000000029983
- Jia, L., and Cheng, M. (2022). Correlation analysis between risk factors, BMD and serum osteocalcin, CatheK, PINP,  $\beta$ -crosslaps, TRAP, lipid metabolism and BMI in 128 patients with postmenopausal osteoporotic fractures. *Eur. Rev. Med. Pharmacol. Sci.* 26, 7955–7959. doi:10.26355/eurrev\_202211\_30147
- John, A. K., Helena, J., Nicholas, C. H., and Eugene, V. M. (2018). A brief history of FRAX. *Arch. Osteoporos.* 13 (1), 118. doi:10.1007/s11657-018-0510-0
- Magni, P., Macchi, C., Sirtori, C. R., and Romanelli, M. M. C. (2016). Osteocalcin as a potential risk biomarker for cardiovascular and metabolic diseases. *Clin. Chem. Lab. Med.* 54 (10), 1579–1587. doi:10.1515/cclm-2015-0953
- McCloskey, E. V., Vasikaran, S., and Cooper, C. (2011). Position development conference Members Official positions for FRAX® clinical regarding biochemical markers from joint official positions development conference of the international society for clinical densitometry and international osteoporosis foundation on FRAX®. *J. Clin. Densitom.* 14 (3), 220–222. doi:10.1016/j.jocd.2011.05.008
- Meier, C., Nguyen, T. V., Center, J. R., Seibel, M. J., and Eisman, J. A. (2005). Bone resorption and osteoporotic fractures in elderly men: The dubbo osteoporosis epidemiology study. *J. Bone. Min. Res.* 20 (4), 579–587. doi:10.1359/JBMR.041207
- Vasikaran, S., Eastell, R., Bruyère, O., Foldes, A. J., Garnero, P., Griesmacher, A., et al. (2011). Markers of bone turnover for the prediction of fracture risk and monitoring of osteoporosis treatment: A need for international reference standards. *Osteoporos. Int.* 22 (2), 391–420. doi:10.1007/s00198-010-1501-1
- Vilaca, T., Gossiel, F., and Eastell, R. (2017). Bone turnover markers: Use in fracture prediction. *J. Clin. Densitom.* 20 (3), 346–352. doi:10.1016/j.jocd.2017.06.020
- Wang, L., Yu, W., Yin, X., Cui, L., Tang, S., Jiang, N., et al. (2021). Prevalence of osteoporosis and fracture in China: The China osteoporosis prevalence study. *JAMA. Netw. Open.* 4 (8), e2121106. doi:10.1001/jamanetworkopen.2021.21106
- Whitlock, R. H., Leslie, W. D., Shaw, J., Rigatto, C., Thorlacius, L., Komenda, P., et al. (2019). The Fracture Risk Assessment Tool (FRAX®) predicts fracture risk in patients with chronic kidney disease. *Kidney. Int.* 95 (2), 447–454. doi:10.1016/j.kint.2018.09.022
- Wu, C. H., McCloskey, E. V., Lee, J. K., Itabashi, A., Prince, R., Yu, W., et al. (2014). Consensus of official position of IOF/ISCD FRAX initiatives in Asia-Pacific region. *J. Clin. Densitom.* 17 (1), 150–155. doi:10.1016/j.jocd.2013.06.002
- Wu, P. Y., Chen, S. C., Lin, Y. C., Chen, P. C., Chuang, W. S., Huang, Y. C., et al. (2022). Role of fracture risk assessment tool and bone turnover markers in predicting all-cause and cardiovascular mortality in hemodialysis patients. *Front. Med. (Lausanne)*. 9, 891363. doi:10.3389/fmed.2022.891363
- Ye, X., Yu, R., Jiang, F., Hou, X., Wei, L., Bao, Y., et al. (2022). Osteocalcin and risks of incident diabetes and diabetic kidney disease: A 4.6-year prospective cohort study. *Diabetes. Care.* 45 (4), 830–836. doi:10.2337/dc21-2113
- Yoon, B. H., and Yu, W. (2018). Clinical utility of biochemical marker of bone turnover: Fracture risk prediction and bone healing. *J. Bone. Metab.* 25 (2), 73–78. doi:10.11005/jbm.2018.25.2.73



# Frontiers in Pharmacology

Explores the interactions between chemicals and living beings

The most cited journal in its field, which advances access to pharmacological discoveries to prevent and treat human disease.

## Discover the latest Research Topics

[See more →](#)

### Frontiers

Avenue du Tribunal-Fédéral 34  
1005 Lausanne, Switzerland  
[frontiersin.org](https://frontiersin.org)

### Contact us

+41 (0)21 510 17 00  
[frontiersin.org/about/contact](https://frontiersin.org/about/contact)

